Improving the discrimination of primary and secondary sources of organic aerosol : use of molecular markers and different approaches

Deepchandra Srivastava

THÈSE PRÉSENTÉE

POUR OBTENIR LE GRADE DE

DOCTEUR DE L'UNIVERSITÉ DE BORDEAUX

ÉCOLE DOCTORALE DES SCIENCES CHIMIQUES

PREPAREE A

L'INSTITUT NATIONAL DE L'ENVIRONNEMENT INDUSTRIEL ET DES RISQUES (INERIS)

Par Deepchandra SRIVASTAVA

Improving the discrimination of primary and secondary sources of organic aerosol: use of molecular markers and different approaches

Sous la direction de : Eric VILLENAVE
(co-direction de : Emilie PERRAUDIN)

Soutenue le 26 avril 2018

Membres du jury :

Mme RIFFAULT Véronique, Professeure, IMT Lille-Douai	Rapportrice
M. WENGER John, Professeur, University College Cork, Ireland	Rapporteur
Mme D'ANNA Barbara, Directrice de recherche, LCE, Marseille	Examinatrice
Mme GROS Valerie, Directrice de recherche, LSCE	Examinatrice
M. EL-HADDAD Imad, Chercheur, PSI	Examinateur
M. ALBINET Alexandre, Ingénieur, INERIS	Responsable de thèse
M. FAVEZ Olivier, Ingénieur, INERIS	Responsable de thèse
Mme PERRAUDIN Emilie, Maître de conférences, Université de Bordeaux	Co-encadrante de thèse
M. VILLENAVE Eric, Professeur, Université de Bordeaux	Directeur de thèse

UMR CNRS EPOC Environnements et Paléoenvironnements Océaniques et Continentaux

The important thing is not to stop questioning.

Curiosity has its own reason for existing.

Albert Einstein

Résumé

Les particules en suspension (ou aérosols) représentent aujourd'hui la classe de polluants atmosphériques la plus préoccupante en matière de santé publique et d'impact environnemental. De par la multiplicité de leurs sources d'émissions et/ou de leurs processus de formation dans l'atmosphère, elles ont une composition chimique complexe et leurs origines sont insuffisamment documentées. Une meilleure compréhension de ces phénomènes demeure essentielle à l'amélioration des outils de modélisation ainsi qu'à l'élaboration de politiques publiques efficaces.

Parmi les différentes familles de particules atmosphériques, les aérosols organiques (AO) font actuellement l'objet d'une attention particulière de la part de la communauté scientifique. Ils sont émis directement dans l'atmosphère (on parle alors d'AOP, pour aérosols organiques primaires), ou issus de processus de conversion gaz-particules (on parle alors d'AOS, pour aérosol organiques secondaires). AOP et AOS peuvent avoir des origines anthropiques ou biogéniques. L'objectif de ce travail de thèse était d'acquérir une meilleure connaissance de l'origine des AO à l'aide de marqueurs organiques moléculaires prélevés sur filtres et par couplage avec des données issues de mesures in-situ par spectrométrie de masse.

Une première étape de ce travail de thèse a consisté à réaliser une étude bibliographique sur les différentes approches d'étude de sources d'AO mises en œuvre au sein de la communauté internationale au cours des dix dernières années. Les méthodologies les plus souvent utilisées incluent les outils statistiques de type modèles récepteurs (e.g., *Chemical Mass Balance* (CMB) et *Positive Matrix Factorization* (PMF)), et les méthodes dites *EC-tracer* et *SOA-tracer*. Environ 200 études réalisées principalement en Europe, Amérique du Nord et Chine à l'aide de ces méthodologies ont pu être analysées et comparées. Chacune de ces méthodologies présentent ses propres avantages ainsi que des biais spécifiques, mais les résultats obtenus

indiquent une bonne cohérence globale pour la différenciation entre AOP et AOS au sein de la fraction organique des aérosols, en particulier lors de la période printemps-été (Figure 1). Des différences plus marquées sont observées en hiver, suggérant notamment la nécessité d'une meilleure prise en compte des émissions anthropiques liées à la combustion de biomasse (pour le chauffage). L'utilisation de nouveaux traceurs de sources moléculaires devraient permettre d'affiner la compréhension des phénomènes mis en jeux.

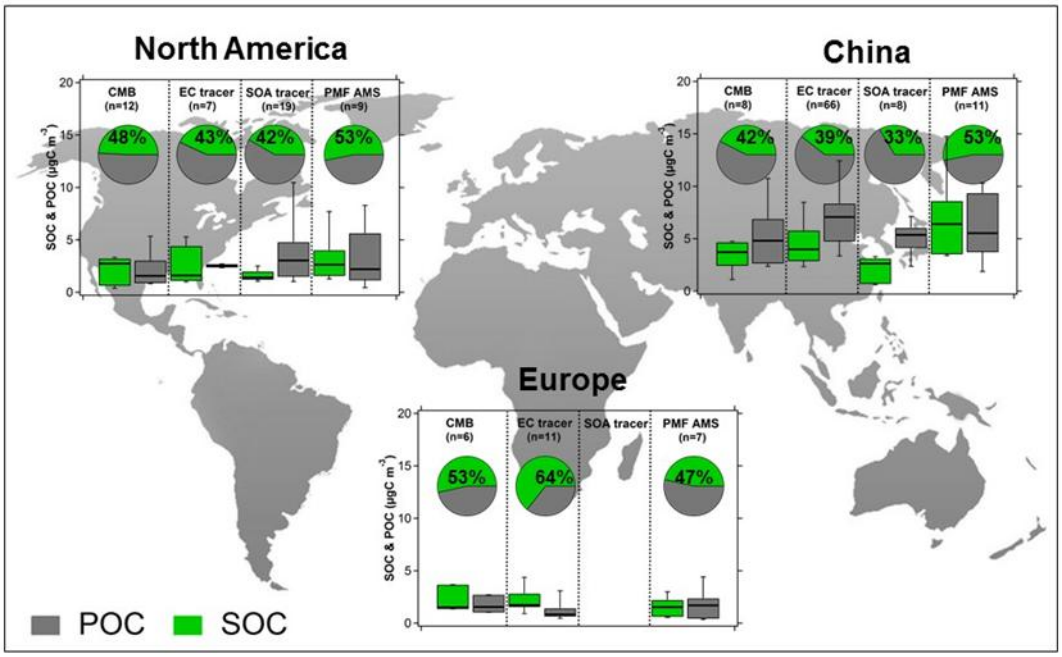

Figure 1: *Comparaison de résultats présentés dans la littérature scientifique pour la différenciation entre AOP et AOS au sein de la fraction fine des particules sur la période printemps-été (sites de fond urbain et péri-urbain) à l'aide des 4 méthodologies d'étude de sources les plus fréquemment utilisées en Europe, Amérique du Nord et Chine.*

La deuxième étape de la thèse était donc focalisée sur l'analyse chimique aussi complète que possible d'échantillons représentatifs de deux milieux urbains français. Les jeux de données obtenus ont ensuite été exploités par application de la méthode PMF. Ce travail expérimental a été basé sur deux campagnes de prélèvements réalisées à Grenoble (site urbain) au cours de l'année 2013 et dans la région parisienne (site péri-urbain du SIRTA, 25 km au sud-ouest de

Paris) lors d'un intense épisode de pollution aux particules (PM) observé en Mars 2015. Une caractérisation chimique étendue (de 139 à 216 espèces quantifiées) a été réalisée et l'utilisation de marqueurs moléculaires primaires et secondaires clés dans la PMF a permis de déconvoluer de 9 à 11 sources différentes de PM_{10} (respectivement à Grenoble et au SIRTA, Figures 2 et 3) incluant aussi bien des sources classiques (combustion de biomasse, trafic, poussières, sels de mer, nitrate et espèces inorganiques secondaires) que des sources non communément résolues telles que AO biogéniques primaires (spores fongiques et débris de plantes), AO secondaires (AOS) biogéniques (marin, oxydation de l'isoprène) et AOS anthropiques (oxydation des hydrocarbures aromatiques polycycliques (HAP) et/ou des composés phénoliques). En outre, le jeu de données obtenu pour la région parisienne à partir de prélèvements sur des pas de temps courts (4 h) a permis d'obtenir une meilleure compréhension des profils diurnes et des processus chimiques impliquées.

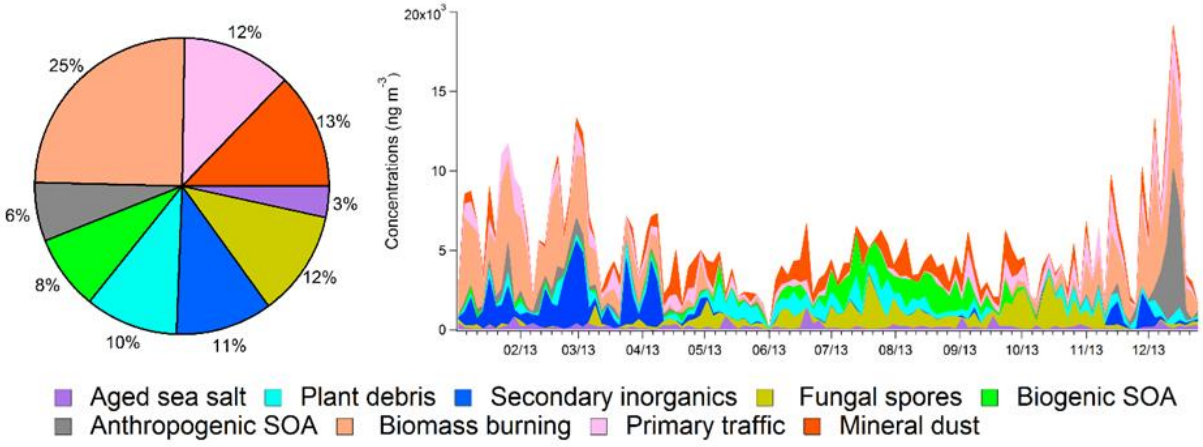

Figure 2: *Contributions moyennes (à gauche) et évolutions temporelles (à droite) des différents facteurs de sources de l'AO identifiés par PMF pour le site de fond urbain de Grenoble au cours de l'année 2013.*

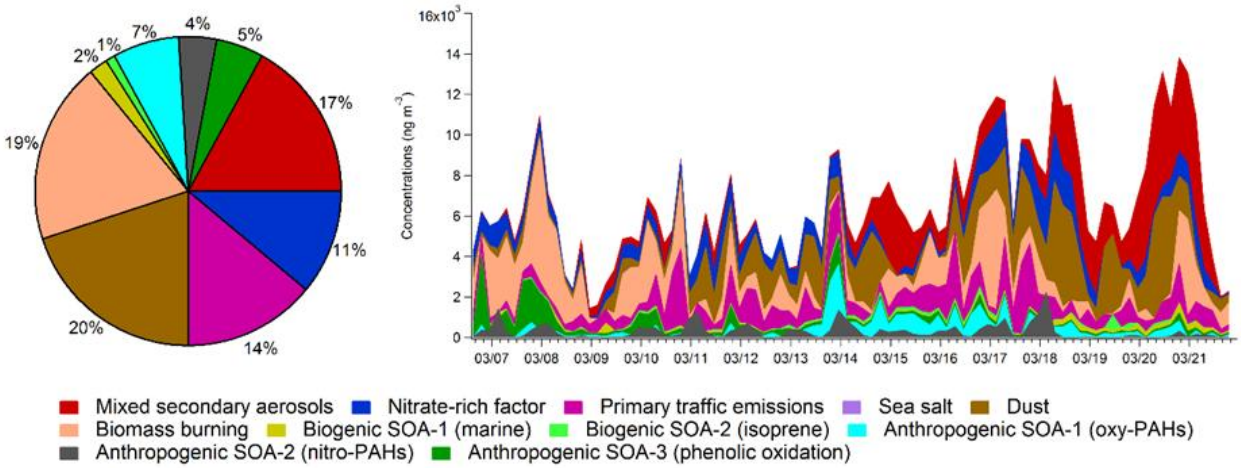

Figure 3. *Contributions moyennes (à gauche) et évolutions temporelles (à droite) des différents facteurs de sources de l'AO identifiés par PMF pour le site de fond péri-urbain du SIRTA lors de l'épisode de pollution aux particules de mars 2015.*

Les résultats obtenus pour le site du SIRTA ont pu être comparés à ceux issus d'autres techniques de mesures (en temps réel, ACSM (aerosol chemical speciation monitor) et analyse AMS (aerosol mass spectrometer) en différée) et/ou d'autres méthodes de traitement de données (méthodes traceur EC (elemental carbon) et traceur AOS). Un bon accord a été obtenu entre toutes les méthodes en termes de séparation des fractions primaires et secondaires (Figures 4 et 5).

L'identification des facteurs liés aux émissions primaires du trafic et de la combustion de biomasse a été confirmée par leurs profils diurnes. Ceux-ci sont comparables d'une méthodologie à l'autre avec cependant quelques problèmes de mélange dans le cas des analyses PMF basées sur les spectres de masse aérosol. Pour les facteurs AOS individuels, le facteur mélange d'aérosols secondaires obtenu à partir de la PMF appliquée sur les données chimiques filtres montre une très bonne corrélation avec les facteurs AO très oxydés déterminés à partir des analyses des données de spectrométrie de masse aérosol. Ces résultats suggèrent une origine commune de ces facteurs.

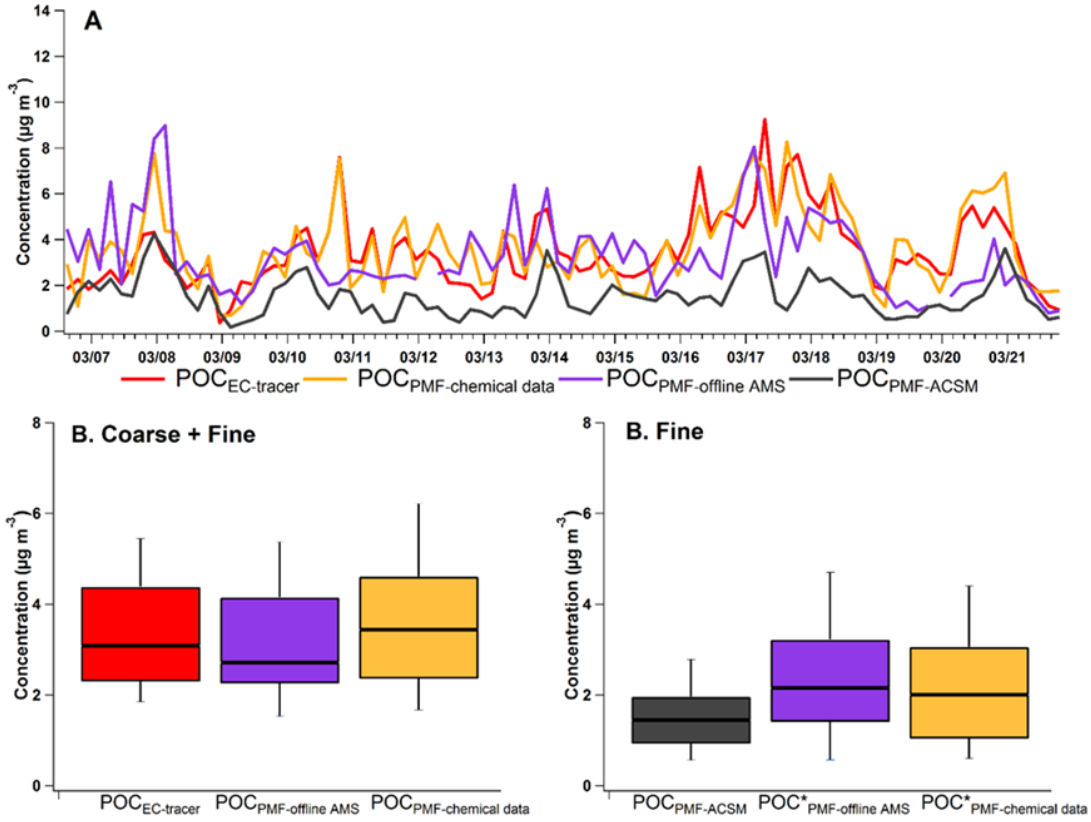

Figure 4: *Comparaison des concentrations totales carbone organique primaire (POC) estimées à partir de différentes méthodologies. A (figure du haut) : séries temporelles. B (figures du bas) : Boites à moustaches indiquant la valeur minimum, le premier quantile, la valeur médiane, le troisième quantile et la valeur maximum. POC*$_{PMF\text{-}chemical\ data}$: PMF basée sur les données chimiques filtres sans la part issus des poussières ; POC*$_{PMF\text{-}offline\ AMS}$: PMF basée sur les données offline AMS sans le facteur SCOA.*

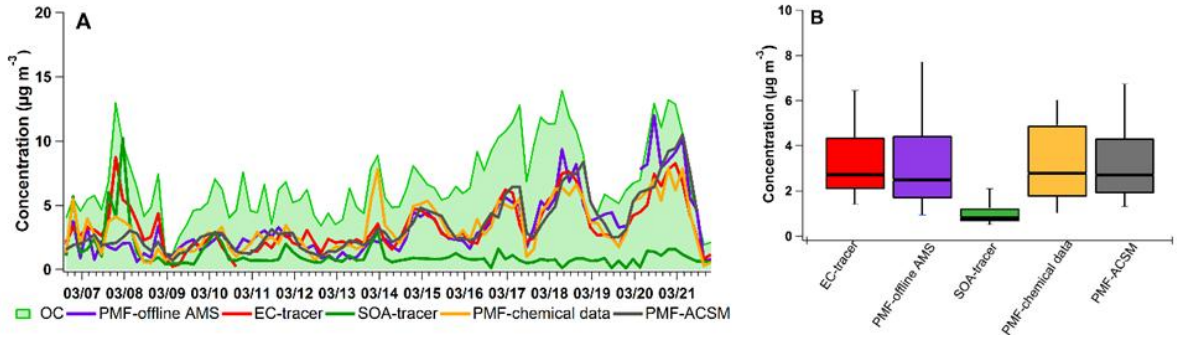

Figure 5: *Comparaison des concentrations totales en carbone organique secondaire (SOC) estimées à partir de différentes méthodologies. A (figure du haut) : séries temporelles. B (figures du bas) : Boites à moustaches indiquant la valeur minimum, le premier quantile, la valeur médiane, le troisième quantile et la valeur maximum.*

Cependant, aucune des approches utilisées n'a permis une identification complète des mécanismes spécifiques de formation et/ou des précurseurs gazeux responsables de cette fraction de l'AOS (qui représente ici environ 25% de l'AO total dans les PM_{10}). En particulier, pour la méthode *SOA-tracer*, même si la contribution secondaire de la combustion de biomasse a été prise en compte, la quantité totale d'AOS observée lors de l'épisode de pollution à longue distance est largement sous-estimée probablement en lien avec des espèces non prises en compte telles que les organonitrates ou organosulfates.

Ainsi, une nouvelle approche d'étude des sources de l'AO a été développée en combinant les mesures en temps réel (ACSM) et celles sur filtres (marqueurs moléculaires organiques) et en utilisant un script de synchronisation des données. Cette méthodologie a été appliquée aux données issues de la campagne réalisée en mars 2015 au SIRTA. L'analyse PMF combinée a été mise en œuvre sur la matrice de données unifiée, conduisant à l'obtention de 10 facteurs de source d'AO, dont 3 facteurs primaires et 7 facteurs secondaires (Figure 6). La cohérence de cette nouvelle méthodologie a été étudiée en comparant les résultats obtenus avec ceux issus de l'analyse PMF des données ACSM. Les résultats montrent une très bonne concordance pour les deux fractions, primaires et secondaires. Cette nouvelle méthode a permis l'identification claire de près de la moitié de la masse totale d'AOS (75% de OA) observée au cours de la campagne de prélèvements. Les facteurs secondaires identifiés ont été classés selon leur état d'oxydation, sources et/ou précurseurs d'AOS. Au final, environ 28% de la fraction totale semble liée à l'AOS anthropique (4 facteurs AOS) en lien avec les sources de combustion telles que la combustion de biomasse et les émissions issues du trafic routier.

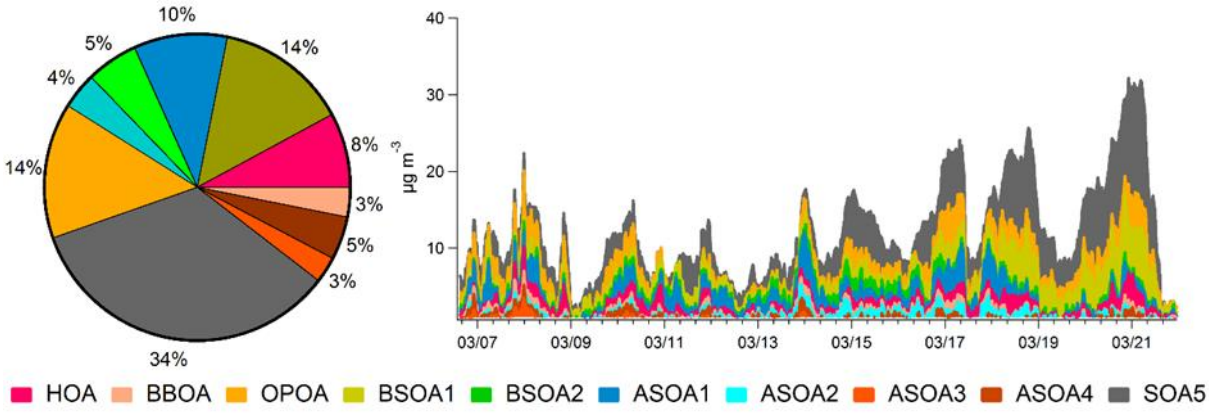

Figure 6: *Contributions moyennes (gauche) et évolution temporelle (droite) des différentes sources d'AO identifiées à Paris-SIRTA, France (Mars 2015). HOA : émissions primaires trafic ; BBOA : combustion de biomasse OA ; OPOA : AO primaire oxydé; BSOA-1 : AOS biogénique 1 (marin enrichi); BSOA-2 : AOS biogénique 2 (oxydation de l'isoprène); ASOA-1 : AOS anthropique 1 (HAP oxygénés) ; ASOA-2 : AOS anthropique 2 (HAP nitrés) ; ASOA-3: AOS anthropique 3 (oxydation des composés phénoliques); ASOA-4 : AOS anthropique 4 (oxydation du toluène) et SOA-5 (AOS 5).*

Les résultats obtenus ont aussi mis en évidence que 4 facteurs AO étaient liés aux émissions de la combustion de biomasse avec 2 sources primaires (AO combustion de biomasse (BBOA) et AOP oxydé (OPOA)) et 2 facteurs secondaires (en lien avec l'oxydation des composés phénoliques et du toluène). Chose intéressante, 80% du BBOA primaire semble être en fait de l'OPOA. L'AOS anthropique lié à l'oxydation des HAP (caractérisé par les nitro-HAP), toluène et les composés phénoliques, a montré des variations diurnes particulières avec des fortes concentrations au cours de la nuit indiquant un rôle majeur de la chimie nocturne. L'établissement d'un lien direct entre MO-OOA (OA oxygéné plus oxydé) ou LO-OOA (OA oxygéné moins oxydé), issus de l'analyse PMF des données ACSM, avec une source donnée est finalement très difficile à faire. Les résultats obtenus ont montré que l'OOA plus oxydé est probablement associé à des sous-produits d'oxydation ultimes alors que l'OOA moins oxydé n'est pas représentatif d'une source ou un processus chimique unique. Cependant, comparé aux

approches plus traditionnelles, cette nouvelle approche permet d'obtenir une meilleure compréhension des processus chimiques liés aux différentes sources de l'AO.

Mots clés : Chimie atmosphérique, Aérosols organiques, Marqueurs moléculaires, *Positive Matrix Factorization* (PMF)

Acknowledgements

First and foremost, I would like to acknowledge my sincere gratitude to Alex, Olivier, Eric and Emilie for giving me the opportunity to pursue my dreams. My most special thanks go to Alex and Olivier, with whom I have learnt all the new aspects of atmospheric sciences. Our trips to conferences, workshops and meeting, and long discussions (with 100+ slides) not have only helped me to evolve as a good researcher but their constant aid and suggestions have given me courage to believe and present myself in a better way. My list of questions has never bothered them, on the contrary they have always appreciated my curiosity. I would like to thank both for guarding each step of my career in the last years, and helping me to discover new things. The point where I have reached today in my career it would have not been possible without their guidance and unparalleled support, thank you so much for everything (from prefecture to articles). My sincere thanks also go to Eric and Emilie, for their thoughtful suggestions and discussions on skype, have helped me to learn something new always. The knowledge I got over our discussions and support during the China trip with Eric, was unforgettable, that has helped me to learn more about my field, thanks a lot. I would also like to thank Eric for taking care of the things at the university. I am also thankful to Emilie for sharing some good discussions during EAC and PhD day at Bordeaux and email exchanges we had. I would also like to give thanks to the members of the jury for agreeing to judge this work in a limited time. I am really thankful to Véronique RIFFAULT, John WENGER, Barbara D'ANNA, Valerie GROS, and Imad EL-HADDAD for their remarks, corrections, kindness and the exchanges that we had.

I am also very thankful to Kaspar and Imad for their help for the offline AMS analyses. The support I received especially from Kaspar to understand offline AMS data was incredible. Kaspar's constant help and input to make me understand the different stages of the offline AMS PMF analyses via whatsapp chats, phone calls and skype meetings have really made my way

much easier. His constant support during AAAR and EAC, had kept me motivated to find the mystery behind some unresolved things (i.e. WSOC). I also wanted to thank Dr. Philip K. Hopke, Uwayemi Sofowote and Jean-Eudes Petit (J-E) for their remarkable help in the understanding of ME-2 script. The discussions linked to error calculation, application of the constraints, and many more.., kept the research flow to move smoothly and never allowed stress to win over. I wanted to especially thank J-E, without whom this ME-2 work should not have reached to its final stage. Our discussion over ME-2, his warm hospitality in Reims, and ZeFir graphs (still feel they are the hottest ones), and PMF discussions (long running chapter), everything was amazing.

I would also like to thank the people from the lab (RESA). Firstly, a special and big thanks to Jérôme, without whom my GC analysis could have never happened, his constant support and lessons have made my GC path easier. Also, he never got bored with my questions, and the troubles I often had while running GC. The training he provided me on the sample preparation, sample analysis, troubleshooting, everything linked to instrumentation, have helped to set up a solid base for my analytical knowledge what I own today. Secondly, Francois, it was always delightful to have discussion with him. I still remember when I had a lot of issue related to TDU, he often used to come to discuss. Third one goes to Herve, Claudine, Nicolas, Serguei, Faustina, Jean-Pierre, Azziz and Ahmad, thank you so much for helping me out always.

I would like to thank people from my building, Florence, Jean, Sabastien, Anne-Sophie, Aline, Jessica, Valerie, Marie, Cecile, Nathalie, Celine, Benedicte, Nathalie, Robin, Vincent, Sylvie, Fabrice, Marion, Serge, Warda and Isaline. With all of them I never felt that I am living thousand miles away from home, every morning was wonderful in the lab including delicious cakes upstairs sometimes, thank you everyone. I particularly would like to thank Francois Gautier, the information provided by him on French culture has made my stay amicable. I would

also like to acknowledge the help I got from Caroline, Eva and Marc Durif linked to administrative purposes, for taking care of the things which was not always easy.

I would like to thank Tanguy, first friend of mine, I think I can say that after my arrival in France. Our discussions on science, politics (European + South China sea + US), religions and philosophy have really broadened my views on both aspects science as well as on social side. I am also good in football and Rugby now, ops not in playing just for the knowledge because of our discussions. I would also like to say thank to Patric Bodu for his support for all the graphical abstracts, all of them are simply great. I am also thankful to Florian for some nice discussions on SOA formation.

My heartily thanks for the members of my office, Yunjiang and Grazia. The time I had in my office it was beyond expectation, it was amazing. Discussions on ACSM datasets with Yunjiang and chemistry with Grazia, were always overwhelming, and helped further to enhance my basics on the things which I was not aware so much before. Apart from that, our funny chats over the topics where we had to explain to Yunjiang always, have also increased my humour as I was very bad in that initially. I am really thankful to you guys for being there through the highs and lows of PhD life. I am also thankful to Camille, new member of my office, successor of my office desk, her delightful nature and wonderful smile, have kept my stress level at the bottom during the last months of thesis.

I would like to thank Helene and Daniel, for making my life easier in France and for sharing some good time together. Thank you so much for dealing with all the letters and emails I received as my French level was initially zero. Apart from that, thank you Daniel for telling me about the things in the lab during my initial days and Helene for showing me the fish brain for the first time, and teaching me French in the starting days during lunch at the canteen. A big thanks to my group of friends, those have given some charm and cherish memories to my PhD period including the ones mentioned before. Thank you so much, Younes (king), Adrien

(barbecue king), Manoj, Neeraj, Audrey, Elenora, Lei, Nihal and Clementine. I am also thankful to Anitha for good Indian food and some nice evenings. I would never forget our trip to Fécamp (3 GB of pictures in 3 days), Amiens (dancing **), Brussels (Yunjiang*), Switzerland (coca cola project invention), and many more, thank you so much for giving the opportunity to have a balanced work life. I would also like to thank Julie, Julien, Vincent, Marta, Martin, Valentin, Clemence, Quentin, Ibtihel and Victor for sharing some good time together. Thank you so much guys, for the madness, and the good moments whether in the lab or outside we shared. A big thanks to all the other people at INERIS, including people at canteen, accueil, bibliothèque, DSI, ECOT lab, and Christine Couverchel for their generous behaviour and help.

I am also thankful to Sophie for the friendship, the good times we shared on skype to discuss about Iron Man (Grenoble Fe conc.), her unconditional support for everything whether it is linked to papers, PhD manuscript, PAHs or on GC unconventional problems. I am pretty sure Google is going to complain for our long Gmail chats. I am also thankful to Julien from Bordeaux for the good time we had in China.

My PhD journey is incomplete without acknowledging my family, their everlasting support, faith and unconditional love, have given me the inspiration to live my passion, my work. Even I am so far from the home but they never let me think a bit of it, my passion is more important for them rather than the distance, thank you so much for having immense trust on me. I am also thankful to my friends from India and abroad for their support since last couple of years. Then there are some fictional characters, without them I don't think I can survive. Thank you so much Sheldon, Sherlock, Michael Scolfield, Dr. House and Mr. Robot, you guys were always there and made me happy as much as you can. Finally, at last I would like to thank my laptops (LP-1003171 & LB-1004604), I know we were good companions, and we proved it at the end bravo!!.

Table of Contents

Chapter I

General introduction and objectives of the Thesis

1.1. Context

The impact of particulate matter (PM) on air quality, and so on human health, is now well recognized. A growing number of studies are notably confirming its influence on the occurrence of respiratory and cerebrovascular diseases, as well as heart attacks and other cardiovascular issues (Kelly and Fussell, 2015; Lippmann et al., 2013; Quan et al., 2010). The implementation of action plans to accurately reduce PM concentration levels in ambient air relies on sound knowledge of their origins. However, the scientific community and public powers are still facing PM source apportionment issues due to the multiplicity of their emission sources and the complexity of their (trans)-formation processes in the atmosphere.

Within the complex airborne particle mixture, organic matter represents a large fraction of the total mass of fine aerosols (from 20 to 90 % in the low troposphere) (Kanakidou et al., 2005; Kroll and Seinfeld, 2008). Organic aerosols (OA) also correspond to the most challenging and ambiguous chemical species in terms of molecular composition, sources, and formation processes. As other atmospheric particles, OA are commonly distinguished according to their introduction mode in the particulate phase. Organic compounds directly emitted in the particulate phase in ambient air are defined as primary organic aerosol (POA). Particulate organic species originating from the oxidation reactions of (semi-) volatile organic compounds (VOCs, SVOCs) and mass transfer processes of their by-products into the aerosol, either via homogeneous or heterogeneous mechanisms, form the secondary organic aerosol (SOA) (Hallquist et al., 2009). The distribution between POA and SOA strongly depends on the location and the season. If POA emissions could eventually be controlled once elucidated, SOA, influenced by biogenic/anthropogenic VOC emissions and by atmospheric photochemistry, are more difficult to regulate. A better knowledge on their origins are though fundamental as they

may constitute about 80 to 90 % of the total OA in some locations (Carlton et al., 2009; Zhang et al., 2011) (Figure I.1).

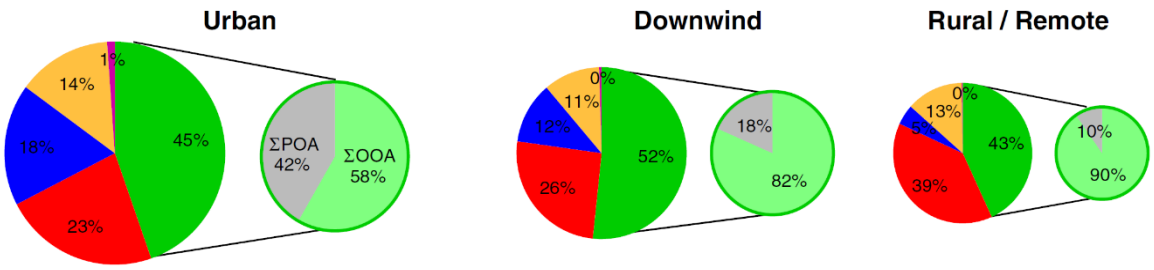

Figure I.1. *Average PM_1 composition. Pink: chloride; Yellow: ammonium, Blue: nitrate; Red: sulfate; Green: organic; Light green: oxygenated organic aerosol (OOA); Grey: primary organic aerosol (POA). Adapted from Zhang et al. (2011).*

A better understanding of OA sources and/or their formation processes is also crucial for the optimization of chemistry-transport models which are still commonly unable to accurately simulate various OA fractions, and especially SOA (Ciarelli et al., 2016) (Figure I.2).

Such issues of current models notably lead to a poor air quality forecast during specific pollution events, such as those related to high loadings of biomass burning emissions. They also participate to significant uncertainties within near-term climate models, which do not fully take OA into account (Belis et al., 2013).

Epidemiological studies show a clear link between increased mortality and enhanced concentrations of ambient aerosols. The chemical and physical properties of aerosol particles causing health effects are still unclear. Recent studies have shown that a significant amount of SOA (major fraction of OA as shown before) may induce potential health risk (Baltensperger et al., 2008; Kramer et al., 2016; Tuet et al., 2017). Particularly, PAHs (polycyclic aromatic hydrocarbons) derivatives (oxy- and nitro-PAHs) are probably more mutagenic than their

parent PAHs as they act as direct mutagens (Baltensperger et al., 2008; Durant et al., 1996; Kramer et al., 2016; Pedersen et al., 2005; Rosenkranz and Mermelstein, 1985; Tuet et al., 2017). Furthermore, some of these compounds are suspected to be carcinogenic and have been recently classified in the 2A (probably carcinogenic to human) and 2B (possibly carcinogenic to human) groups by IARC (International Agency for Research on Cancer, IARC, 2013, IARC, 2012). Therefore, investigating the sources of such compounds can be a key tool to assess health risks for humans exposed to airborne pollutants.

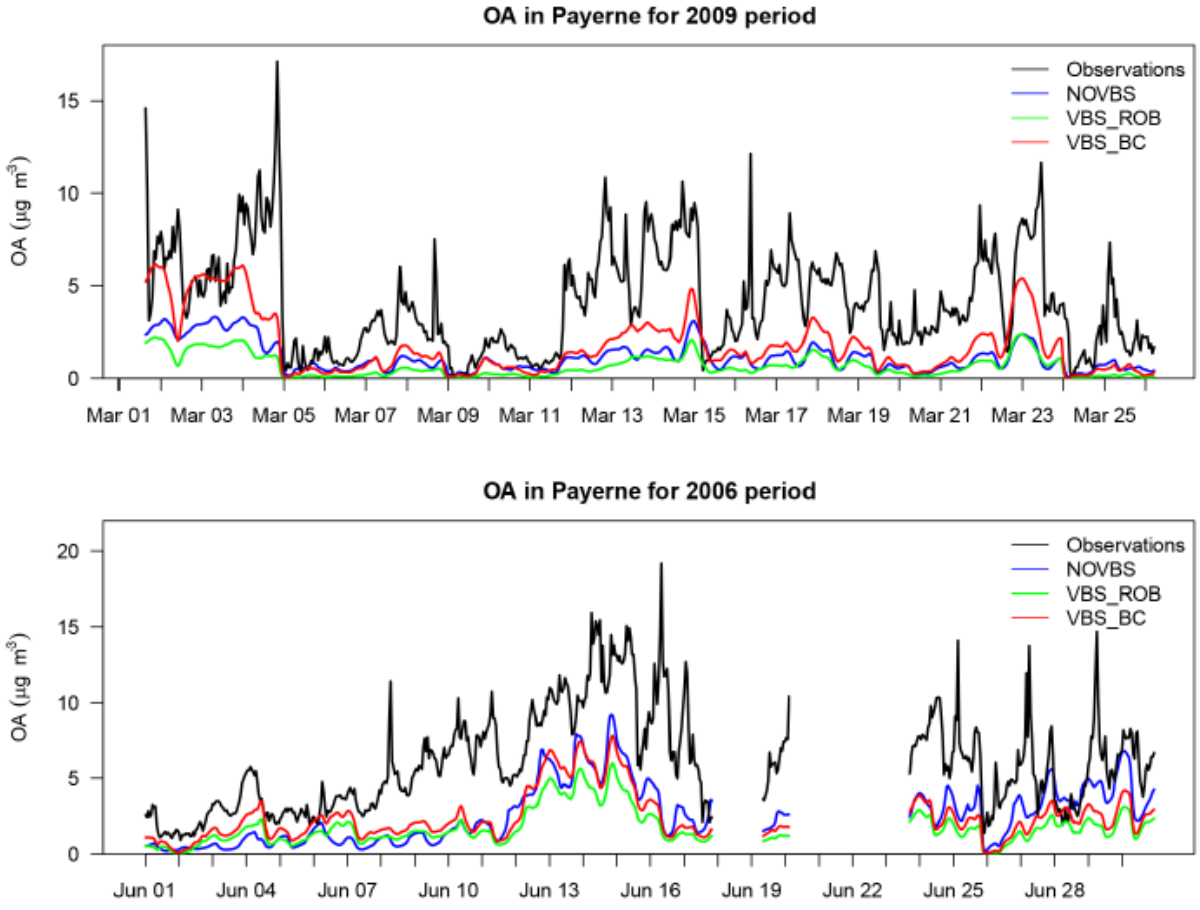

Figure I.2. *Comparison of OA simulation by three currently used European Chemistry Transport Models to measurements at a Swiss rural background site in March 2009 and June 2006. Adapted from Ciarelli et al. (2016).*

Several source apportionment methodologies have been developed during the last decades. These methods are generally based on the monitoring data, emission inventories (i.e., dispersion models) and statistical evaluations (i.e., receptor models) (Gray et al., 1986; Grosjean, 1984; Kleindienst et al., 2007; Paatero, 1997; Paatero and Tapper, 1994; Turpin and Huntzicker, 1995; Watson et al., 1990). However, only few of these approaches (e.g., SOA-tracer method, positive matrix factorization (PMF)) can provide direct information on the secondary sources based on the chemical speciation of molecular markers (Kleindienst et al., 2007; Kleindienst et al., 2010; Shrivastava et al., 2007; Zhang et al., 2009). The latter species should have a high degree of source specificity and be relatively stable in the atmosphere, to allow gaining insights into aerosol sources and the underlying mechanisms of SOA formation and/or ageing (Schauer et al., 1996). Recently, considerable progress has been made in the molecular characterization of individual SOA constituents from the photooxidation of biogenic and anthropogenic VOCs that can serve as markers for SOA characterization, such as markers from isoprene oxidation, 2-methyltetrols (i.e., the diastereoisomers, 2-methylthreitol and 2-methylerythritol) and 2-methylglyceric acid. These markers have already been used in receptor models (i.e., PMF) to provide deep insight into OA fractions (Heo et al., 2013; Hu et al., 2010; Jaeckels et al., 2007; Shrivastava et al., 2007; Zhang et al., 2009). It appears that the use of molecular markers has the unique advantage of distinguishing SOA contributions from different VOC precursor classes (Figure I.3). Filter-based markers often rely on rather weak time-resolution (typically 24 h), making it difficult to isolate fast transformation processes. Thus, there are still significant gaps in our knowledge which places limitations on our ability to investigate SOA origins.

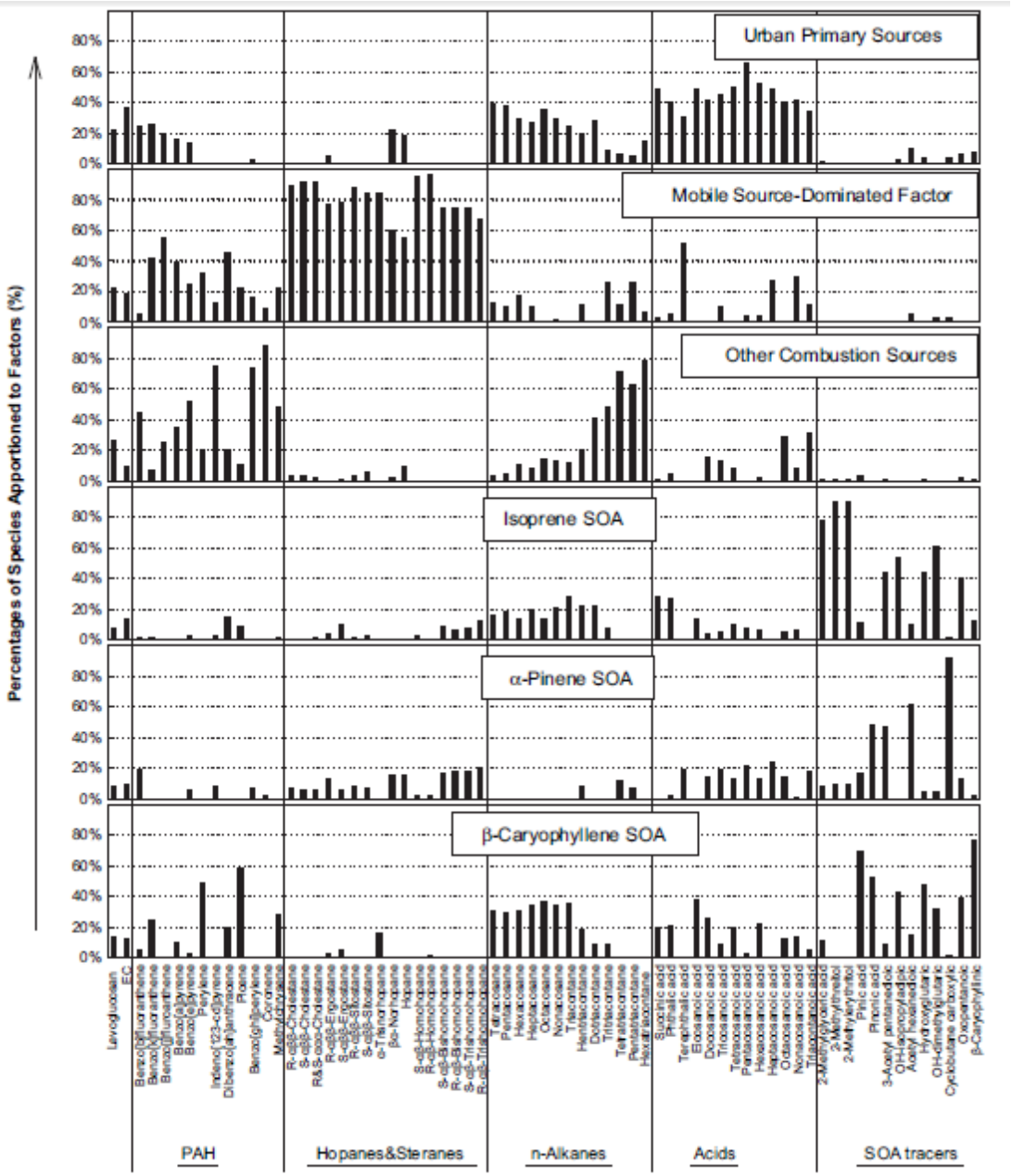

***Figure I.3**. Distribution of molecular markers among identified factors in OA source apportionment using PMF model. Adapted from Zhang et al. (2009).*

On the other hand, for about 15 years, the use of online instrumentation for aerosol chemical characterization (i.e., AMS (aerosol mass spectrometer), ACSM (aerosol chemical speciation monitor)) has successfully improved the real-time measurements of particulate organic fractions. PMF analysis conducted on OA mass spectra further improved the differentiation of

OA factors (Lanz et al., 2007; Ulbrich et al., 2009; Zhang et al., 2011). The evolution of OA in the atmosphere is assessed to follow progressive oxidation steps from fresh to highly aged OA associated with a change of chemical functionalities, volatility, and oxidation state (Ng et al., 2010; Sun et al., 2011). The various OA factors retrieved from PMF analysis are then differentiated according to these properties, which might be roughly attributed to either primary or secondary fractions. However, such a discrimination remains relatively uncertain due to the non-specific nature of the measured mass fragments.

In this context, scientific efforts have still to be undertaken to get a better understanding of OA origins, considering as far as possible the whole complexity and variability of the involved processes. Combining different datasets from several measurement set-ups to refine the source apportionment of OA, and notably secondary ones, might help to achieve this goal.

1.2. Objectives of the PhD Thesis

The main goal of this experimental PhD work is to investigate methodologies dedicated to the source apportionment of POA and SOA fractions. These objectives can be described according to the three following questions:

1) How well does current and commonly-used OA source apportionment approaches agree to each other?
2) Which "novel" organic molecular markers could help a better discrimination between primary/secondary and/or biogenic/anthropogenic origins?
3) Can we improve the data treatment of OA mass spectra using some of these specific markers?

1.3. Strategy of the PhD Thesis and organization of the manuscript

To achieve these objectives, the present work has been designed in four main steps:

The first step involved a review on the different approaches currently used to apportion SOA fractions. Here, it has been chosen to mainly focus on SOA, rather than POA, as this fraction is probably the most challenging and is currently subject to on-going methodological developments. Benefits as well as drawbacks and specific issues of the considered approaches are discussed and compared. This review also offered the opportunity to summarise results obtained from a large set of studies conducted in different regions across the world.

The second step included the chemical analysis of a wide variety of molecular organic markers, notably including primary and secondary PAHs, anhydrosugars, cellulose combustion products, odd number higher alkanes, methanesulfonic acid (MSA), and various SOA markers related to the oxidation of isoprene, α-pinene, toluene, and phenolic compounds. These measurements were performed on filter samples collected during two field campaigns: a one year (2013)

campaign at a background urban site in Grenoble (France, Alpine region), and a short-term intensive campaign conducted in the Paris area at SIRTA during a PM pollution event (March 2015). Both of these datasets were enriched with inorganic and metallic species measurements, and then subjected to PMF analysis.

The third step corresponded to the comparison of results obtained from various source apportionment approaches (namely, PMF, EC- tracer method, and SOA-tracer method) applied to different datasets (extended chemical data, ACSM measurements, and offline AMS analysis) obtained from the intensive Paris campaign.

The fourth step relied on an attempt to develop a novel source apportionment methodology to refine the understanding of the various OA sources. In this last step, PMF was carried out with time synchronization using the multilinear engine (ME-2) algorithm on the combined dataset including OA ACSM mass spectra and specific primary and secondary organic molecular markers.

The plan of the present manuscript is basically following the order of these steps, half of the chapters being directly presented in the form of articles already published, or to be submitted soon. The next (and second) chapter is devoted to the review paper dedicated to commonly and widely used SOA source apportionment approaches **(Article I**). The third chapter describes the experimental work conducted during this thesis, including information on sampling sites, on the used instrumentation, and on the procedures developed/ improved for the analysis of organic molecular markers. The fourth chapter presents the results linked to the use of key organic molecular markers into PMF analysis applied to the Grenoble and Paris datasets **(Articles II and III**). The fifth chapter corresponds to the article related to the comparison of results obtained from different common methodologies applied to the Paris datasets **(Article IV)**. The sixth chapter deals with the development of a synergic approach to refine OA source

apportionment by combining off-line and on-line measurements **(Article V)**. Finally, the seventh chapter corresponds to major conclusions and perspectives linked to this work.

Due to the structure of this manuscript and the inclusion of articles already submitted or nearly submitted to different journals, references are separately provided in a dedicated subsection within each chapter.

References

Baltensperger, U., Dommen, J., Alfarra, M. R., Duplissy, J., Gaeggeler, K., Metzger, A., Facchini, M. C., Decesari, S., Finessi, E., Reinnig, C., Schott, M., Warnke, J., Hoffmann, T., Klatzer, B., Puxbaum, H., Geiser, M., Savi, M., Lang, D., Kalberer, M., Geiser, T., 2008. Combined determination of the chemical composition and of health effects of secondary organic aerosols: the POLYSOA project. J Aerosol Med Pulm Drug Deliv. 21, 145-54.

Belis, C. A., Karagulian, F., Larsen, B. R., Hopke, P. K., 2013. Critical review and meta-analysis of ambient particulate matter source apportionment using receptor models in Europe. Atmos. Environ. 69, 94-108.

Carlton, A. G., Wiedinmyer, C., Kroll, J. H., 2009. A review of Secondary Organic Aerosol (SOA) formation from isoprene. Atmos. Chem. Phys. 9, 4987-5005.

Ciarelli, G., Aksoyoglu, S., Crippa, M., Jimenez, J.-L., Nemitz, E., Sellegri, K., Äijälä, M., Carbone, S., Mohr, C., O'Dowd, C., 2016. Evaluation of European air quality modelled by CAMx including the volatility basis set scheme. Atmos. Chem. Phys. 16, 10313-10332.

Durant, J. L., Busby, W. F., Lafleur, A. L., Penman, B. W., Crespi, C. L., 1996. Human cell mutagenicity of oxygenated, nitrated and unsubstituted polycyclic aromatic hydrocarbons associated with urban aerosols. Mutation Research/Genetic Toxicology. 371, 123-157.

Gray, H. A., Cass, G. R., Huntzicker, J. J., Heyerdahl, E. K., Rau, J. A., 1986. Characteristics of atmospheric organic and elemental carbon particle concentrations in Los Angeles. Environ. Sci. Technol. 20, 580-589.

Grosjean, D., 1984. Particulate carbon in Los Angeles air. Sci. Total Environ. 32, 133-45.

Hallquist, M., Wenger, J., Baltensperger, U., Rudich, Y., Simpson, D., Claeys, M., Dommen, J., Donahue, N., George, C., Goldstein, A., 2009. The formation, properties and impact of secondary organic aerosol: current and emerging issues. Atmos. Chem. Phys. 9, 5155-5236.

Heo, J., Dulger, M., Olson, M. R., McGinnis, J. E., Shelton, B. R., Matsunaga, A., Sioutas, C., Schauer, J. J., 2013. Source apportionments of $PM_{2.5}$ organic carbon using molecular marker Positive Matrix Factorization and comparison of results from different receptor models. Atmos. Environ. 73, 51-61.

Hu, D., Bian, Q., Lau, A. K. H., Yu, J. Z., 2010. Source apportioning of primary and secondary organic carbon in summer $PM_{2.5}$ in Hong Kong using positive matrix factorization of secondary and primary organic tracer data. J. Geophys. Res.-Atmos. 115,

IARC, 2012. Some Chemical Present in Industrial and Consumer Products, Food and Drinking-Water Vol. 101 (868 pp. https://monographs.iarc.fr/ENG/Monographs/vol101/mono101.pdf).

IARC, 2013. Diesel and Gasoline Engine Exhausts and Some Nitroarenes Vol. 105 (714 pp.https://monographs.iarc.fr/ENG/Monographs/vol105/mono105.pdf).

Jaeckels, J. M., Bae, M.-S., Schauer, J. J., 2007. Positive matrix factorization (PMF) analysis of molecular marker measurements to quantify the sources of organic aerosols. Environ. Sci. Technol. 41, 5763-5769.

Kanakidou, M., Seinfeld, J., Pandis, S., Barnes, I., Dentener, F., Facchini, M., Dingenen, R. V., Ervens, B., Nenes, A., Nielsen, C., 2005. Organic aerosol and global climate modelling: a review. Atmos. Chem. Phys. 5, 1053-1123.

Kelly, F. J., Fussell, J. C., 2015. Air pollution and public health: emerging hazards and improved understanding of risk. Environ. Geochem. Health. 37, 631-649.

Kleindienst, T. E., Jaoui, M., Lewandowski, M., Offenberg, J. H., Lewis, C. W., Bhave, P. V., Edney, E. O., 2007. Estimates of the contributions of biogenic and anthropogenic hydrocarbons to secondary organic aerosol at a southeastern US location. Atmos. Environ. 41, 8288-8300.

Kleindienst, T. E., Lewandowski, M., Offenberg, J. H., Edney, E. O., Jaoui, M., Zheng, M., Ding, X., Edgerton, E. S., 2010. Contribution of Primary and Secondary Sources to Organic Aerosol and $PM_{2.5}$ at SEARCH Network Sites. J. Air Waste Manage. Assoc. 60, 1388-1399.

Kramer, A. J., Rattanavaraha, W., Zhang, Z., Gold, A., Surratt, J. D., Lin, Y.-H., 2016. Assessing the oxidative potential of isoprene-derived epoxides and secondary organic aerosol. Atmos. Environ. 130, 211-218.

Kroll, J. H., Seinfeld, J. H., 2008. Chemistry of secondary organic aerosol: Formation and evolution of low-volatility organics in the atmosphere. Atmos. Environ. 42, 3593-3624.

Lanz, V. A., Alfarra, M. R., Baltensperger, U., Buchmann, B., Hueglin, C., Szidat, S., Wehrli, M. N., Wacker, L., Weimer, S., Caseiro, A., 2007. Source attribution of submicron organic aerosols during wintertime inversions by advanced factor analysis of aerosol mass spectra. Environ. Sci. Technol. 42, 214-220.

Lippmann, M., Chen, L., Gordon, T., Ito, K., Thurston, G., 2013. National Particle Component Toxicity (NPACT) Initiative: integrated epidemiologic and toxicologic studies of the health effects of particulate matter components. Research Report (Health Effects Institute). 5-13.

Ng, N. L., Canagaratna, M. R., Zhang, Q., Jimenez, J. L., Tian, J., Ulbrich, I. M., Kroll, J. H., Docherty, K. S., Chhabra, P. S., Bahreini, R., Murphy, S. M., Seinfeld, J. H., Hildebrandt, L., Donahue, N. M., DeCarlo, P. F., Lanz, V. A., Prévôt, A. S. H., Dinar, E., Rudich, Y., Worsnop, D. R., 2010. Organic aerosol components observed in Northern Hemispheric datasets from Aerosol Mass Spectrometry. Atmos. Chem. Phys. 10, 4625-4641.

Paatero, P., 1997. Least squares formulation of robust non-negative factor analysis. Chemom. Intell. Lab. Syst. 37, 23-35.

Paatero, P., Tapper, U., 1994. Positive matrix factorization: A non-negative factor model with optimal utilization of error estimates of data values. Environmetrics. 5, 111-126.

Pedersen, D. U., Durant, J. L., Taghizadeh, K., Hemond, H. F., Lafleur, A. L., Cass, G. R., 2005. Human Cell Mutagens in Respirable Airborne Particles from the Northeastern United States. 2. Quantification of Mutagens and Other Organic Compounds. Environ. Sci. Technol. 39, 9547-9560.

Quan, C., Sun, Q., Lippmann, M., Chen, L.-C., 2010. Comparative effects of inhaled diesel exhaust and ambient fine particles on inflammation, atherosclerosis, and vascular dysfunction. Inhalation Toxicol. 22, 738-753.

Rosenkranz, H. S., Mermelstein, R., 1985. The genotoxicity, metabolism and carcinogenicity of nitrated polycyclic aromatic hydrocarbons. Journal of Environmental Science and Health. Part C: Environmental Carcinogenesis Reviews. 3, 221-272.

Schauer, J. J., Rogge, W. F., Hildemann, L. M., Mazurek, M. A., Cass, G. R., Simoneit, B. R., 1996. Source apportionment of airborne particulate matter using organic compounds as tracers. Atmos. Environ. 30, 3837-3855.

Shrivastava, M. K., Subramanian, R., Rogge, W. F., Robinson, A. L., 2007. Sources of organic aerosol: Positive matrix factorization of molecular marker data and comparison of results from different source apportionment models. Atmos. Environ. 41, 9353-9369.

Sun, Y. L., Zhang, Q., Schwab, J. J., Demerjian, K. L., Chen, W. N., Bae, M. S., Hung, H. M., Hogrefe, O., Frank, B., Rattigan, O. V., Lin, Y. C., 2011. Characterization of the sources and processes of organic and inorganic aerosols in New York city with a high-resolution time-of-flight aerosol mass apectrometer. Atmos. Chem. Phys. 11, 1581-1602.

Tuet, W. Y., Chen, Y., Xu, L., Fok, S., Gao, D., Weber, R. J., Ng, N. L., 2017. Chemical oxidative potential of secondary organic aerosol (SOA) generated from the photooxidation of biogenic and anthropogenic volatile organic compounds. Atmos. Chem. Phys. 17, 839-853.

Turpin, B. J., Huntzicker, J. J., 1995. Identification of secondary organic aerosol episodes and quantitation of primary and secondary organic aerosol concentrations during SCAQS. Atmos. Environ. 29, 3527-3544.

Ulbrich, I. M., Canagaratna, M. R., Zhang, Q., Worsnop, D. R., Jimenez, J. L., 2009. Interpretation of organic components from Positive Matrix Factorization of aerosol mass spectrometric data. Atmos. Chem. Phys. 9, 2891-2918.

Watson, J. G., Robinson, N. F., Chow, J. C., Henry, R. C., Kim, B., Pace, T., Meyer, E. L., Nguyen, Q., 1990. The USEPA/DRI chemical mass balance receptor model, CMB 7.0. Environ. Softw. 5, 38-49.

Zhang, Q., Jimenez, J. L., Canagaratna, M. R., Ulbrich, I. M., Ng, N. L., Worsnop, D. R., Sun, Y., 2011. Understanding atmospheric organic aerosols via factor analysis of aerosol mass spectrometry: a review. Anal. Bioanal. Chem. 401, 3045-3067.

Zhang, Y., Sheesley, R. J., Schauer, J. J., Lewandowski, M., Jaoui, M., Offenberg, J. H., Kleindienst, T. E., Edney, E. O., 2009. Source apportionment of primary and secondary organic aerosols using positive matrix factorization (PMF) of molecular markers. Atmos. Environ. 43, 5567-5574.

Chapter II

State of the art of SOA estimation methodologies

Article I

Comparison of methodologies based on measurement data to apportion Secondary Organic Carbon (SOC) in $PM_{2.5}$: a review of recent studies

To be submitted for publication in Atmospheric Environment

Comparison of methodologies based on measurement data to apportion secondary organic Carbon (SOC) in $PM_{2.5}$: a review of recent studies

D. Srivastava[1, 2,3], O. Favez[1, *], E. Perraudin[2,3], E. Villenave[2,3], A. Albinet[1, *]

[1]INERIS, Parc Technologique Alata, BP 2, 60550 Verneuil-en-Halatte, France

[2]CNRS, EPOC, UMR 5805 CNRS, 33405 Talence, France

[3]Université de Bordeaux, EPOC, UMR 5805 CNRS, 33405 Talence, France

[*] Correspondence to: alexandre.albinet@gmail.com; alexandre.albinet@ineris.fr; olivier.favez@ineris.fr

Abstract

Secondary organic aerosol (SOA) accounts for a significant fraction of airborne particulate matter. A detailed characterization of SOA is required to evaluate its impact on air quality and climate change. Despite the substantial amount of research studies done during these last decades, the estimation of the SOA fraction remains difficult due to the complexity of the physicochemical processes involved. Several methodologies have been developed to perform a quantitative and predictive assessment of the SOA amount. The selection of the appropriate approach is a major research challenge for the atmospheric science community. This review summarizes the current knowledge on the different secondary organic carbon (SOC) estimation methodologies commonly used: EC tracer method, chemical mass balance (CMB), SOA tracer method, radiocarbon (^{14}C) measurement and positive matrix factorization (PMF). The principles, limitations and challenges of each of the methodologies are discussed. A comprehensive -although not exhaustive- summary of results obtained on SOC estimates, for different regions across the world, during the last decade is proposed. The studies comparing directly the performances of the different methodologies are also reviewed. A comparison of the results on SOC contributions and concentrations obtained worldwide based on the different methodologies and under similar conditions (i.e. geographical and seasonal ones) is also done. Finally, the research needs on SOC apportionment are identified.

Keywords: Aerosols; Particulate matter; SOA; SOC; Source apportionment.

1 Introduction and objectives

Organic matter (OM) constitutes a major fraction, approximately 20-60% of fine airborne particles (Docherty et al., 2008). Besides their abundance, the ambient composition of atmospheric particulate organic matter (POM) remains poorly understood due its chemical complexity and large measurement uncertainties (Goldstein and Galbally, 2007; Turpin et al., 2000).

Atmospheric POM has both primary (directly emitted) and secondary (formed in the atmosphere) sources, which can be either natural or anthropogenic. Primary biogenic aerosols include pollen, bacteria, fungal and fern spores, viruses, and fragments of plants (Després et al., 2007; Simoneit and Mazurek, 1982). Such particles belong mainly to the coarse aerosol fraction and their global emissions on Earth reach up 1000 Tg yr^{-1} (Jaenicke, 2005). Anthropogenic primary sources include fuel combustion from transportation (road, rail, air and sea), energy production, biomass burning, industrial processes, waste disposal, cooking and agriculture activities (Querol et al., 2007; Seinfeld and Pandis, 2006). Emitted particles are mainly associated with the fine aerosol fraction and a global emission rate of about 50 Tg yr^{-1} has been estimated for anthropogenic POM (Kanakidou et al., 2005; Volkamer et al., 2006).

Secondary particles are formed in the atmosphere by gas-particle conversion processes such as nucleation, condensation and heterogeneous multiphase chemical reactions (Carlton et al., 2009; Zhang et al., 2007; Ziemann and Atkinson, 2012). The contribution of secondary organic aerosol (SOA) to POM reaches up to 80% under certain atmospheric conditions (Carlton et al., 2009). Most of organic aerosols (OA) in urban and rural atmospheres are speculated to be secondary in nature but their exact chemical composition remains uncertain (Shrivastava et al., 2007; Zhang et al., 2007; Zhao et al., 2013). Both biogenic and anthropogenic gaseous emission sources contribute to the SOA production (Carlton et al., 2009; Griffin et al., 1999). Air quality models have still difficulties to reproduce the observed particulate matter (PM) concentration

levels due to a poor illustration of the OA fractions, primary and notably secondary, reinforcing the need for improving the knowledge on SOA formation processes and on their contribution to total OA (Ciarelli et al., 2016a; Hallquist et al., 2009; Tsigaridis et al., 2014).

As defined, secondary organic carbon (SOC) is not directly emitted, and is present in the particulate phase along with primary OC (POC). In addition to the difficulties to chemically characterize POM due to its high complexity and diversity, there is a real challenge to identify relevant criteria to distinguish POC from SOC. A clear information on SOC formation and a right approach to apportion SOC are highly needed to apply efficient air quality strategies.

Several data treatment methodologies have been developed in the last decades to evaluate the contribution of SOC to total OM or PM. Offline methods, usually based on filter measurements, together with emission inventories data, include elemental carbon (EC) -tracer approach (Gray et al., 1986; Grosjean, 1984; Turpin and Huntzicker, 1995), statistical receptor models such as chemical mass balance (CMB) (Watson et al., 1990) or positive matrix factorization (PMF) (Paatero, 1997; Paatero and Tapper, 1994; Shrivastava et al., 2007; Zhang et al., 2009b), SOA-tracer method (Kleindienst et al., 2007), radiocarbon (^{14}C) measurements (Gelencsér et al., 2007; Liu et al., 2014; Szidat et al., 2009), water soluble organic carbon (WSOC)-based method (Weber et al., 2007) and regression approaches (Blanchard et al., 2008). Moreover, thanks to recent advances in online aerosol mass spectrometry (AMS) (DeCarlo et al., 2006; Jayne et al., 2000), real time measurements of aerosol chemical composition has improved the knowledge on OA sources over the last 15 years, and successfully enforced to classify their primary and secondary origins (Sun et al., 2011; Xu et al., 2014).

Among all the methods mentioned above, CMB and EC-tracer methodologies are the most commonly used worldwide. Increase in the use of AMS combined to PMF data analysis as well as SOA-tracer method, filter PMF approach and ^{14}C measurements is also noticeable, due to

their unique feature to establish direct connections between different SOA fractions and the nature of their precursors and/or their formation processes (El Haddad et al., 2011; Gelencsér et al., 2007; Hu et al., 2010; Kleindienst et al., 2010; Kourtchev et al., 2008). The present paper aims at presenting a comprehensive -although not exhaustive- summary of results obtained worldwide on SOC estimates during the last decade. After a brief synthesis of the current knowledge on SOA precursor emission inventories, the principles, limitations and challenges of each of the five methods mentioned above are discussed. The results obtained from each of these different methodologies are documented for different regions across the world (America, Asia, Europe and Middle East). The studies comparing directly the performances of the different methodologies are then reviewed and a comparison of the results obtained worldwide under similar conditions (i.e. geographical and seasonal ones) is also done. Finally, the research needs on SOC apportionment are finally identified and discussed.

2 Major sources of SOA precursors: current knowledge from emission inventories

SOA is formed in the atmosphere by oxidation reactions of hydrocarbons leading to the generation of volatile or non-volatile compounds involved in gas phase oxidation processes to form new particles either by nucleation or through condensation on pre-existing particles (Nozière et al., 2015; Zhao et al., 2013). Global SOA production from biogenic volatile organic compounds (BVOCs) ranges from 2.5 to 44.5 Tg yr^{-1}, whereas the global SOA production from anthropogenic VOCs (AVOCs) ranges from 3 to 25 Tg yr^{-1} (Tsigaridis and Kanakidou, 2007; Volkamer et al., 2006). The major classes of SOA precursors are volatile and semi volatile- alkanes, alkenes, aromatic hydrocarbons, and oxygenated compounds (Figure 1).

Biogenic SOA precursors are mostly alkenes; with ~50% isoprene and ~40% monoterpenes, the rest being other reactive alkenes, such as sesquiterpenes, oxygenated and unidentified VOCs

(Ziemann and Atkinson, 2012). Isoprene and monoterpenes have always been associated with a major fraction of total BVOC emissions. Isoprene has the largest global atmospheric emissions of all the non-methane VOCs, estimated to be 500 Tg yr^{-1}, with a range of 440-600 Tg yr^{-1} (Guenther et al., 2006). Despite low SOA yield, it contributes to about 4.6 Tg yr^{-1} to SOA mass (Tsigaridis and Kanakidou, 2007). The production of SOA from photo-oxidation of terpenes is speculated to make up 13-24 TgC yr^{-1} from global emission of monoterpenes of about 140 Tg yr^{-1} (Guenther et al., 1995). Other terpenoid compounds, such as sesquiterpenes, have lower emission than isoprene or monoterpenes, with a global emission of 26 TgC yr^{-1} (Acosta Navarro et al., 2014). However, they may contribute significantly to SOA formation because they are very reactive and show high secondary aerosol formation yields (Griffin et al., 1999). BVOCs come also largely from the oceans, particularly dimethylsulfide (DMS), which is oxidized into methane sulfonic acid aerosol (MSA) (Kettle and Andreae, 2000). Other identified marine SOA components are dicarboxylic acids (Kawamura and Sakaguchi, 1999), dimethyl- and dimethylammonium salts (Facchini et al., 2008; Hallquist et al., 2009). Also estimations showed that the global production of SOA from marine isoprene is insignificant in comparison to terrestrial sources (Arnold et al., 2009).

Anthropogenic SOA precursor emissions consist of ~40% alkanes, ~10% alkenes, and ~20% aromatics (trimethylbenzenes, xylenes and toluene), the remaining part being oxygenated and unidentified compounds (Ziemann and Atkinson, 2012). Most of the anthropogenic SOA are formed from the oxidation of substituted monoaromatic compounds and long-chain alkenes (Odum et al., 1997; Weber et al., 2007) emitted from sources such as fossil fuel burning, vehicle emissions, biomass burning, solvent use and evaporation (Chen et al., 2010a; Johnson et al., 2006; Kleeman et al., 2007; Marta and Manuel, 2010; Tkacik et al., 2012) . Global emission of aromatic compounds is about 18.8 Tg yr^{-1} (Henze et al., 2008) and result in an estimated range of SOA production of 2–12 Tg yr^{-1} (Henze et al., 2008). The oxidation of evaporated primary

OA (POA) vapours has also been observed as a potential source of SOA in the atmosphere (Robinson et al., 2007; Shen et al., 2015; Zhao et al., 2014b). Approximately 16 TgC yr^{-1} (9–23 TgC yr^{-1}) of the traditional POA could remain permanently in the condensed phase, while 19 TgC yr^{-1} (5–33 TgC yr^{-1}) undergo gas-phase oxidation before re-condensing onto pre-existing particles (Donahue et al., 2009; Hallquist et al., 2009). POA includes compounds with lower volatilities than traditional SOA precursors, such as long chain *n*-alkanes, polycyclic aromatic hydrocarbons (PAHs), and large alkenes, and therefore partitioned in the atmosphere between the gaseous and particulate phases. PAHs have been identified as a major component in emissions from diesel engines and wood burning sources (Schauer et al., 1999, 2001). Photooxidation of these compounds in the gas phase has been shown to yield high molecular weight oxygenated compounds (Sasaki et al., 1997; Wang et al., 2007), which may partition into the particle phase and lead to significant SOA formation (Mihele et al., 2002). PAHs are estimated to yield 3–5 times more SOA than light aromatic compounds and account for up to 54% of the total SOA from oxidation of diesel emissions, representing a potentially large source of urban SOA (Chan et al., 2009; Srivastava et al., 2018b; Zhang, 2012) Other anthropogenic precursors lead also to the formation of SOA notably, phenolic compounds and furans largely emitted by biomass burning (Bruns et al., 2016; Yee et al., 2013) and could account significantly to the SOA formed in winter periods.

Finally, on a global scale, BVOC emissions are expected to be one order of magnitude greater than those of anthropogenic VOCs (Seinfeld and Pandis, 1998). Isoprene has the largest global emission (3-5 times higher than monoterpenes) resulting in a probably dominant SOA production on a global scale. At regional and urban scales, anthropogenic sources are also believed to account for a significant fraction of SOA (Chen et al., 2010a; Foster and Caradonna, 2003; Kleeman et al., 2007; Rutter et al., 2014; Volkamer et al., 2006) with similar order of magnitude as biogenic SOA. However, it should be noted that estimations presented in this

section remain highly uncertain due to possible biases from model simulations based on data from laboratory oxidation experiments. A better understanding of the complex physicochemical mechanisms involved in the SOA formation is still required to better evaluate SOA fluxes. This notably implies further field/laboratory studies and subsequent relevant methodologies for the estimation of SOA fraction. Some of these methodologies are described and compared in the following sections.

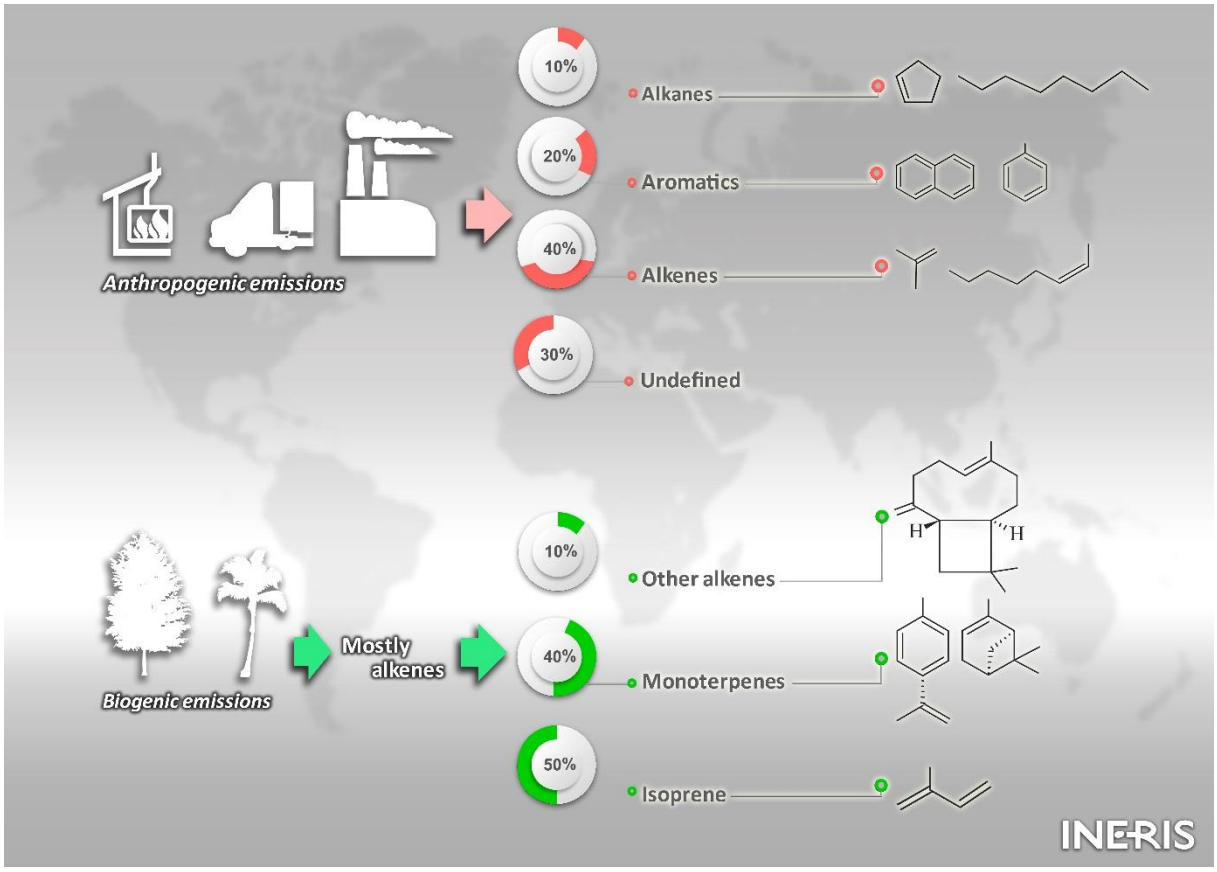

Figure 1. Distribution of the major classes of SOA precursors (adapted from Ziemann and Atkinson, 2012).

3 Description of the main approaches to apportion SOC fraction

This section proposes a comprehensive, although not exhaustive, review on recent applications of the most commonly used methods for SOC estimation from field measurements

with a presentation and discussion of their principles, limitations and challenges. The review proposed here concerns the studies reported from 2006 to 2016, focusing then on the most recent information available on SOC estimations. Only annual data and those related to the spring-summer period are considered. Data availability and statistical representativeness of all the world regions explain this choice. Besides, due to enhanced biogenic emissions and photo-chemical activities, the spring-summer period is the most favourable to observe high SOA concentrations.

As a first limitation, it should be noted that all offline filter-based methods may suffer from sampling artifacts leading to the overestimation and/or underestimation of atmospheric concentrations of the target compounds. On one hand, sorption of gas species on the filter or formation of secondary compounds by chemical reactions on the collection support between particulate compounds and atmospheric oxidants (O_3, NO_x, OH) induce an overestimation of particulate phase concentrations (positive artifact). On the other hand, volatilization of particulate compounds collected on the filter or chemical degradation due to reactions between collected compounds and atmospheric oxidants lead to an underestimation of particulate phase concentrations (negative artifact). These artifacts are highly dependent on temperature, compound vapour pressures and sampling flow rates (Albinet et al., 2010; Ding et al., 2002; Goriaux et al., 2006; Mader and Pankow, 2001; McDow and Huntzicker, 1990; Subramanian et al., 2004; Tsapakis and Stephanou, 2003; Turpin et al., 1994; Turpin et al., 2000).

3.1 EC-tracer method

3.1.1 Principle

The EC-tracer method is an extensively used approach since the 80s (Castro et al., 1999; Chu, 2005; Gray et al., 1986; Grosjean, 1984; Lim and Turpin, 2002; Pachon et al., 2010; Saffari et al., 2016; Saylor et al., 2006; Turpin and Huntzicker, 1995; Yu et al., 2004).

The main advantage of this method is to use only ambient measurements of OC and EC, which are readily available. Since EC and primary OC are mostly emitted by the same combustion sources (either modern or fossil fuel), EC can be used as a tracer for primary combustion generated OC (Gray et al., 1986; Strader et al., 1999; Turpin and Huntzicker, 1995). The ratio of ambient concentrations of particulate OC to EC includes information about the extent of SOC formation. Ambient OC/EC ratios larger than those specific to primary emissions illustrate SOA formation. In this method, OC primary can be expressed as in Equation (1).

$$[OC]_p = \left[\frac{OC}{EC}\right]_p [EC] + [OC]_{non-comb.} \quad (1)$$

The SOC fraction can be estimated using the following Equation (2).

$$[OC]_s = [OC] - [OC]_p \quad (2)$$

where [OC] is the measured total OC concentration, $[OC]_p$ is the POC concentration, $[OC/EC]_p$ represents the ratio of OC to EC concentrations for the primary sources affecting the site of interest, and $[OC]_{non\text{-}comb.}$ is the non-combustion contribution to the POC (Cabada et al., 2004; Strader et al., 1999; Turpin and Huntzicker, 1995), [EC] is the measured EC concentration, and $[OC]_S$ is the SOA contribution to the total OC. Sources of $[OC]_{non\text{-}comb.}$ include cooking activities, soil and road re-suspended PM, biogenic sources (i.e., plant detritus, resuspension of other biogenic material), etc. (Cabada et al., 2004; Plaza et al., 2006; Saylor et al., 2006). All of these parameters are time-dependent which means, substantially influenced by meteorological conditions and emission scenarios (Gray et al., 1986; Plaza et al., 2006). Details regarding the calculation of $[OC/EC]_p$ and $[OC]_{non\text{-}comb.}$ are provided in the supplementary material (SM).

3.1.2 Limitations and challenges

As detailed in the SM, ambient [OC/EC] ratios significantly fluctuate with time and locations and the EC-tracer method may suffer from major issues linked to the choice of constant values used in Equation (1). The assumption of constant primary $[OC/EC]_p$ and $[OC]_{non\text{-}comb.}$ values, assumed to be representative of the period of the study, may not be fully relevant. In particular, day to day $[OC/EC]_p$ values are function of the nature of the emission sources, the meteorological conditions and the influence of atmospheric pollutant transport, leading to significant uncertainties (Cabada et al., 2004; Strader et al., 1999). Therefore, a constant ratio might not be appropriate for the application of the EC-tracer method on a long-term basis, such as yearly timescale (Lonati et al., 2007; Yuan et al., 2006b). In addition, the application of the EC tracer method is not straight forward to data collected in cold periods. During these periods, data sets must be thoroughly examined to determine the days when secondary formation of particulate OC is expected to be negligible. Usually, parameters used for the determination of "primary emission predominance" conditions are low solar radiation, low temperature and low O_3 concentration levels, and/or occurrence of high NO and low NO_2 concentrations. Based on these criteria, (Lonati et al., 2007) obtained a $[OC/EC]_p$ ratio of 9.5, for the subset of data collected in Milan (Italy) during several cold seasons. However, this value seemed too high to be assumed as representative of primary ratio compared to previously reported values in several other studies (Strader et al., 1999; Turpin and Huntzicker, 1995; Yang et al., 2005). This result suggested that the selection of a constant $[OC/EC]_p$ value may not be adequate under all meteorological conditions. Besides$[OC/EC]_p$, the estimation of $[OC]_{non\text{-}comb.}$ is another important parameter in the application of the EC tracer method. $[OC]_{non\text{-}comb.}$ is usually assumed to be small (Chu, 2005) or negligible (Favez et al., 2008; Lim and Turpin, 2002) and often estimated by the intercept of the regression line of Equation (1). This lead to artificially higher values of SOC especially for the smaller values of EC (Saylor et al., 2006). Emission inventories

can also be used to estimate both, $[OC/EC]_p$ and $[OC]_{non\text{-}comb}$, parameters, but the accuracy of this approach, especially for $[OC]_{non\text{-}comb}$, is questionable.

Under the significant influence of local sources (e.g., wood combustion), with higher OC and lower EC emission rates, higher values of [OC/EC], not necessarily due to the existence of SOC derived from photochemical reactions, may be observed (Na et al., 2004). Consequently, qualitative estimation of SOC using [OC/EC] ratios should be applied only after a careful inspection of local sources of OC and EC. Moreover, the presence of a significant fraction of semi-VOCs (SVOCs) in the aerosol could induce significant variations of the [OC/EC] ratio, depending on the change in ambient air temperature (Castro et al., 1999). For instance, an increase of temperature from winter to summer would result in a decrease of the minimum [OC/EC] ratio due to the evaporation of primary SVOCs at higher temperatures in summer.

Another issue arises from the EC/OC analysis. The most commonly used thermal protocols are NIOSH (National Institute for Occupational Safety and Health), IMPROVE (Interagency Monitoring of PROtected Visual Environment) and EUSAAR 2 (European Supersites for Atmospheric Aerosol Research) (Birch and Cary, 1996; Cavalli et al., 2010; Chow et al., 2007; Chow et al., 1993). They differ mostly in their temperature programs and optical correction types for charring based on transmittance or reflectance. The three protocols are comparable for total carbon (TC) concentrations but the results can vary significantly concerning EC-OC split (Chiappini et al., 2014; Karanasiou et al., 2015; Wu et al., 2016). Moreover, depending on the protocol used, very low EC loading can be difficult to measure, for instance in the case of samples from remote locations.

In addition to the above limitations, it should also be noted that a variety of linear regression techniques and simple slope estimators can also show considerable variation in the [OC/EC] ratio. For instance, significant difference have been witnessed in SOC estimates made for

several Mexican cities in different studies (Mancilla et al., 2015; Martinez et al., 2012; Stone et al., 2008), as well as other locations around the world, and the selection of the approach to calculate [OC/EC] ratio is probably one of the main reason explaining the differences observed. Details on the use of different regression techniques and associated issues are provided in the SM.

In general, several authors indicated a $[OC/EC]_p$ ratio of approximately 2, used then as a threshold for interpreting ratios exceeding this value as an indicator of the presence of SOA (Gray et al., 1986; Strader et al., 1999; Turpin and Huntzicker, 1995; Turpin et al., 1991; Yang et al., 2005). Higher $[OC/EC]_p$ ratios may be due to the different approaches adopted to determine the dominant primary emission period by taking the above-mentioned conditions into account though there is no way to avoid the contribution of secondary formation processes. To account for the limitations of the EC-tracer method, several authors proposed to estimate the method uncertainties considering the EC/OC measurement and the assumptions inherent to the EC tracer method itself. Lim and Turpin (2002) suggested a value of ±10% of uncertainty in the SOC estimation while Pachon et al. (2010) estimated uncertainties of about of 80% on SOC values in winter and 47% in summer.

All of these results further suggest the strong need of a standard procedure to select primary [OC/EC] ratio and $[OC]_{non\text{-}comb.}$.

3.1.3 Review of recent studies based on the EC-tracer method

Figure A1 synthesizes the locations of the studies discussed in this section. Detailed references about these results are given in Tables A2 and A3 in the SM. It is important to note that no data (or very few) are displayed here for Africa, Oceania, Central Asia, Russia, Central and South America. This does not imply that no EC tracer studies have been conducted so far at these

places but rather means that they fall outside the specific criteria of this review ($PM_{2.5}$ fraction and studies from 2006 to 2016).

3.1.3.1 Studies in America

Seasonal and regional variations of SOA have been examined thoroughly over the North American continent using the EC-tracer method (Day et al., 2015; Docherty et al., 2008; Dreyfus et al., 2009; Kleindienst et al., 2010; Mancilla et al., 2015; Murillo et al., 2013; Pachon et al., 2010; Polidori et al., 2006; Saffari et al., 2016; Saylor et al., 2006; Seguel A et al., 2009; Sunder Raman et al., 2008; Toro Araya et al., 2014; Vega et al., 2010; Yu et al., 2007). Overall, annual SOC levels ranged from 1.1 to 2.7 µgC m^{-3}, contributing to 27-70% of $PM_{2.5}$ OC (Figure 2; Table A2). The highest contributions (~63% on average) were obtained for rural locations, while at urban sites contributions were in the range of 30 to 50%. SOC estimates in warm period in the USA obtained from the literature showed that 29-43% (1.0-1.8 µgC m^{-3}) of $PM_{2.5}$ OC was secondary, with the highest contribution (43%, 1.2 µgC m^{-3}) at a rural location (Centreville) (Figure 3, Table A3).

Few examples of SOC estimations are also available in Central and South America (Mancilla et al., 2015; Murillo et al., 2013; Seguel A et al., 2009; Toro Araya et al., 2014; Vega et al., 2010) (Figure 2). The annual average SOC contribution was approximately 57% and reached up to 87% of $PM_{2.5}$ OC in Mexico (Mancilla et al., 2015) (Figure 2, Table A2). Some other previous studies showed lower SOA contributions (Martinez et al., 2012; Stone et al., 2008), though the estimations were not carried out using the same approach. In Santiago, Chile, no significant differences have been observed between the annual and spring-summer SOC contributions (annual: 29±6% and spring-summer: 31±6%) (Toro Araya et al., 2014). These

results reflect that SOC may be a significant contributor to fine OC through the year as well as in the warm period due to favourable meteorological conditions.

3.1.3.2 Studies in Europe and the Middle East

Similarly to the American continent, SOC estimates using the EC tracer method has been extensively performed throughout Europe (Błaszczak et al., 2016; Favez et al., 2007; Grivas et al., 2012; Harrison and Yin, 2008; Khan et al., 2016; Laongsri and Harrison, 2013; Lonati et al., 2007; Mirante et al., 2014; Pant et al., 2014; Paraskevopoulou et al., 2014; Pietrogrande et al., 2016; Plaza et al., 2006; Samara et al., 2014; Wagener et al., 2014; Yubero et al., 2015). The annual and spring-summer average of SOC levels varied in the range 1.6-4.9 µgC m^{-3} and 0.90-4.4 µgC m^{-3}, contributing to 36-73% and 41-84% of $PM_{2.5}$ OC, respectively (Figures 2 and 3, Tables A2 and A3). As expected, in warmer periods, SOC contributed at higher rates to $PM_{2.5}$ OC than annually at all locations (61% on average), with the highest contribution observed in Milan (84%, 4.4 µgC m^{-3}). Surprisingly, the annual and spring-summer SOC contributions to $PM_{2.5}$ OC at both, urban and rural background sites in Birmingham did not show the expected pattern of higher contribution in summer than winter. This has been also spotted in other studies from other continents where data obtained did not show a strong SOC seasonality (i.e. Pittsburgh, USA, (Polidori et al., 2006)). These results suggest that a lower mixing layer height in winter favours SOC precursor stagnation, then SOC formation and notably anthropogenic SOA (Srivastava et al., 2018b). Processes that can also contribute to SOC formation are the adsorption of semi-volatile OCs onto existing solid particles and the dissolution of soluble gases that can undergo reactions on particles (Odum et al., 1996; Pandis et al., 1992).

The number of monitoring studies are limited in the Middle East region. The estimation of SOC contribution at 11 sites in Palestine (Nablus, East Jerusalem and Hebron), Jordan (Amman, Aqaba, Rahma and Zarka) and Israel (West Jerusalem, Eilat, Tel Aviv and Haifa) have been reported recently (Abdeen et al., 2014). The average SOC levels at all sites, excluding East Jerusalem and Nablus, were about 2.7 µgC m^{-3}, corresponding to a contribution of 55% to the $PM_{2.5}$ OC. Results suggested that the significant formation of SOA at urban locations was due to the gas/particle conversion of gaseous hydrocarbon precursors and reinforced the importance of identifying SOA precursors for effective reduction of aerosol loadings (Abdeen et al., 2014).

3.1.3.3 Studies in Asia

The environmental behaviour of particulate bound SOC has been investigated in Asia in places such as Korea, Japan, Taiwan, China and India (Batmunkh et al., 2011; Choi et al., 2012; Chou et al., 2010; Ichikawa et al., 2015; Khan et al., 2010; Kim et al., 2012; Park and Cho, 2011) (Figures 2 and 3; Tables A2 and A3).

The annual and spring-summer SOC levels at urban locations of Korea varied in the range 1.1-4.6 µgC m^{-3} to 1.1-5.7 µgC m^{-3}, contributing to 15-57% and to 45-83% of $PM_{2.5}$ OC, respectively. In the case of Japan and Taiwan, the annual and spring-summer SOC, at urban and suburban locations, accounted for >35% of $PM_{2.5}$ OC.

Carbonaceous aerosol in China has drawn special attention in recent years due to the very high PM and SOA concentration levels observed notably during haze events (Guo et al., 2014; Han et al., 2015; Huang et al., 2014; Lee, 2015; Sui et al., 2015; Tian et al., 2016; Zheng et al., 2015). All in all, the annual and spring-summer SOC levels varied in the range 2.5-23.9 µgC m^{-3} to 1.8-12.2 µgC m^{-3}, contributing to 25-63% and 21-67% of $PM_{2.5}$ OC, respectively (Cao et al., 2007; Cheng et al., 2012; Ding et al., 2012; Duan et al., 2007; Fan et al., 2016; Feng et

al., 2013; Feng et al., 2009; Gu et al., 2010; Hu et al., 2012; Huang et al., 2012; Ji et al., 2016; Lai et al., 2016; Li et al., 2015a; Li and Bai, 2009; Lin et al., 2009; Lv et al., 2016; Niu et al., 2013; Qiao et al., 2016; Tao et al., 2009; Wang et al., 2016a; Wu and Yu, 2016; Yao et al., 2016; Yu et al., 2006; Zhang et al., 2013; Zhang et al., 2011a; Zhang et al., 2012; Zhou et al., 2016; Zhou et al., 2014) (Figures 2 and 3). SOC estimations were especially performed in the Sichuan basin, one of the most populated region in China (about 100 million people) (Chen et al., 2014). The annual average SOC levels were 5.1, 4.5 and 11.4 µgC m^{-3} in Chengdu, Neijing and Chongqing, respectively, contributing to 27%, 25% and 34% of $PM_{2.5}$ OC levels. The SOC fractions shown in this study were very homogeneous and significantly lower than in previous studies using the EC tracer method, i.e. about 40% reported by Cao et al. (2007) and 57% by Zhang et al. (2008) in several urban regions of China. The rapid urbanization and industrialization of the region had significantly modified the emissions in the ambient air inducing a difference in the EC/OC ratios observed and preventing the availability of a stable $[OC/EC]_p$ in the EC tracer method. Besides, to understand the secondary processes in rural and mountainous areas of South and North China, measurements were conducted at Mount Heng and Mount Tai (Wang et al., 2012b; Zhou et al., 2012). High contributions of SOC to $PM_{2.5}$ OC (61-67%) were observed in spring-summer period indicating the influence of long-range transport of carbonaceous aerosol from PRD (Pearl River Delta) and eastern China, highly urbanized and industrialized regions, at Mount Heng and the presence of high SOA loading in the North China Plain. In both cases, the occurrence of in-cloud SOA formation and the role of heterogeneous chemistry was highlighted.

As in China, air quality monitering in India is being undertaken more rigorously than ever due to the very high PM concentration levels observed (Hooda et al., 2016; Joseph et al., 2012; Kumar et al., 2016; Pant et al., 2015; Pipal and Gursumeeran Satsangi, 2015; Rengarajan et al., 2011; Safai et al., 2014; Sudheer et al., 2015). The annual SOC levels varied in the range 6.0-

26.4 µgC m^{-3}, contributing to 42-58% of $PM_{2.5}$ OC in major urban cities such as New Delhi, Gurgoan, Ahmedabad, Pune and Mumbai (Figure 2; Table A2). Significant seasonal patterns have been observed at all of these locations with the highest SOC contribution noticed at Pune in summer (70%). Results were consistent with another study conducted at Pune by Pipal and Gursumeeran Satsangi, (2015), which showed higher effective carbon ratio values (ECR, defined as the ratio of SOC to the sum of POC and EC) in summer, indicating the larger formation of SOC in warm period (Safai et al., 2014). At a high-altitude site (Mount Abu) in western India, studies have shown very low SOC concentrations (0.8 µgC m^{-3}) with a contribution of about 51% to $PM_{2.5}$ OC (Kumar et al., 2016).

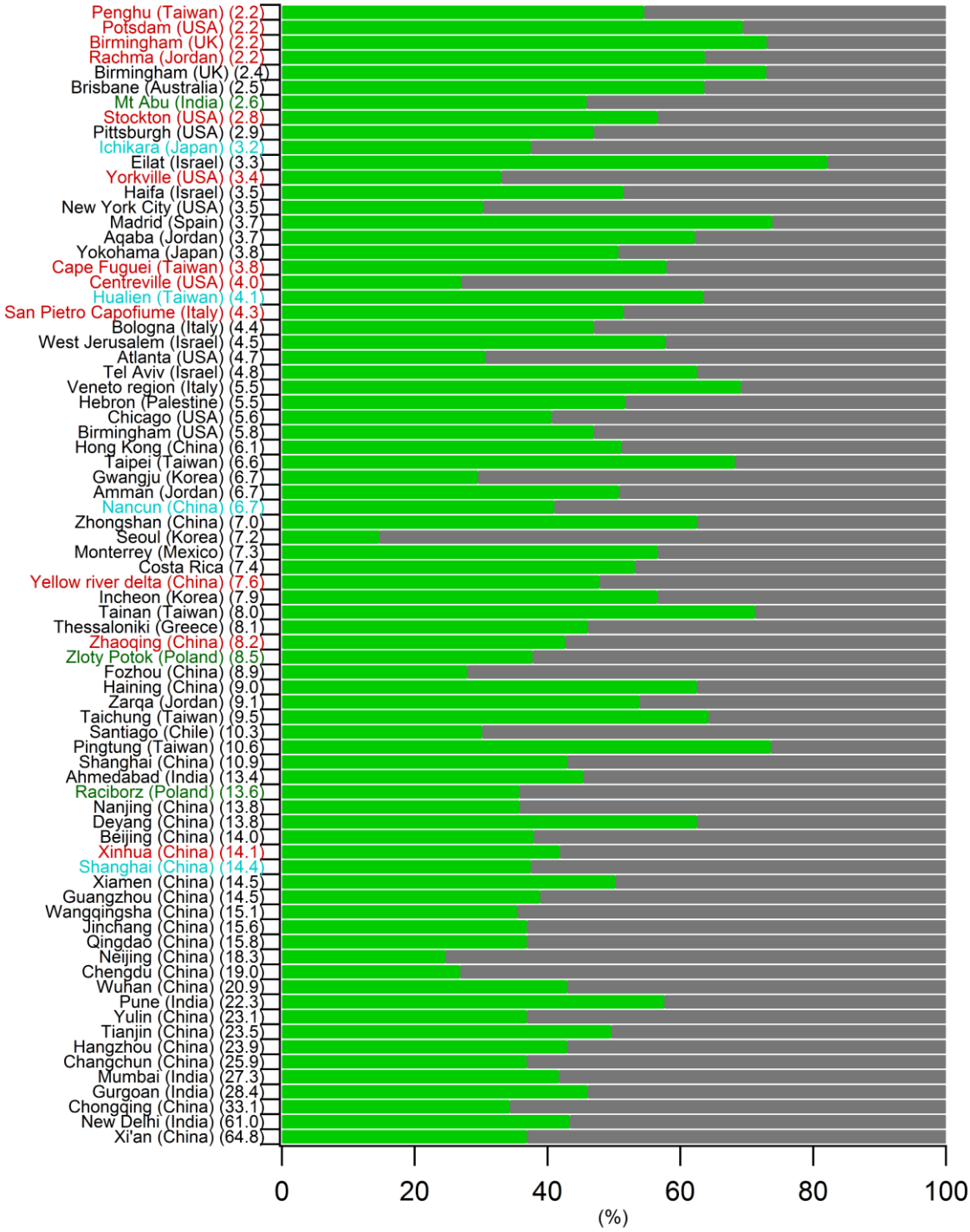

Figure 2. Annual SOC (green) and POC (grey) contributions to $PM_{2.5}$ OC estimated using the EC tracer method for all the monitored sites from 2006 to 2016. Results are presented in increasing order of OC concentration levels (µgC m^{-3}). In black, urban sites; in blue, suburban sites; in red, rural sites and in green, remote sites.

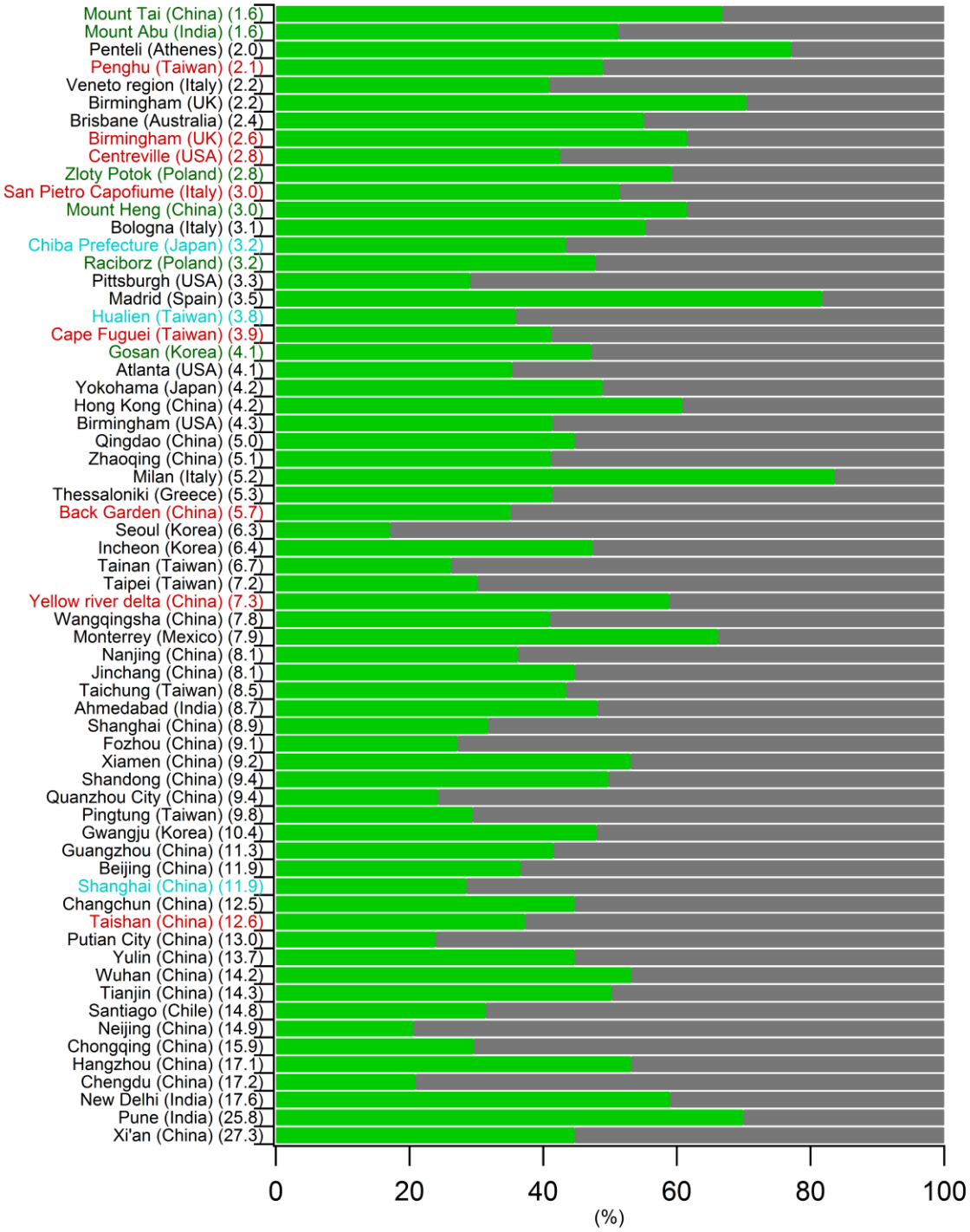

Figure 3. Spring-summer SOC (green) and POC (grey) contributions to $PM_{2.5}$ OC estimated using the EC tracer method for all the monitored sites from 2006 to 2016. Results are presented in increasing order of OC concentration levels (µgC m^{-3}). In black, urban sites; in blue, suburban sites; in red, rural sites and in green, remote sites.

3.2 Chemical Mass balance (CMB)

3.2.1 Introduction

As for other source-receptor models, in CMB, ambient concentrations of chemical species are expressed as the sum of the products of source compositions and contributions (Watson et al., 1990). CMB is based on an effective-variance least square approach to establish a balance between the source and the receptor site and finally to estimate the source contributions (Schauer et al., 1996; Watson et al., 1984; Watson et al., 2002). Fingerprints of the source emissions (source profiles) are used to calculate the atmospheric concentrations of the chemical species i at the receptor site *k*, C_{ik}, as follows (Equation (3)):

$$C_{ik} = \sum_j a_{ik} S_{kj} \qquad (3)$$

where, a_{ik} is the relative concentration of the chemical species *i* in the OC emissions from the source *j*, and S_{kj} is the contribution to OC from the source *j* at the receptor site *k*. The source profile abundances (i.e. the mass fraction of a chemical species in the emissions from each source type) and the receptor concentrations, with appropriate uncertainty estimates, are the input data of the model. The conservative nature of the chemical species with no significant removal through dry and wet depositions and/or degradation/formation by chemical reactions over time during the transport from the source to the receptor is one of the major assumptions considered in this model (Li et al., 2003). Another assumption is the non colinear nature of the source profiles (Watson et al., 2002). In addition, the number of species must be larger than the number of sources to produce significant results.

As the CMB applied to OC using molecular markers (Table B1) only considers primary sources, the OC not apportioned (un-apportioned OC) refers to SOC. SOC is then defined as the difference between the measured OC concentration and the aggregated OC concentration

from all primary sources resolved by CMB. The OC concentration obtained from all primary sources is referred as source contribution estimates (SCEs) (Equation (4)):

$$\boldsymbol{SOC = Measured\ OC - \sum SCEs\ (Primary\ sources)} \qquad (4)$$

CMB is successfully applied if source profiles consistent with the measurements performed at the receptor locations are used. Source profiles are the mass abundances of the chemical species in source emissions and are regarded as a category of sources rather than individual emitters (Watson et al., 2001; Watson et al., 2002). Relevant source profiles should be used as an input to evaluate correct SCEs, otherwise it can lead to ambiguity in the obtained results and could be considered as a major limitation of this method.

3.2.2 Limitations and challenges

Several factors make the use of CMB analysis strenuous. OC is not necessarily completely fitted by the model as markers and source profiles for SOC do not exist in all the cases.

The selection of appropriate source profiles is one of the critical steps to obtain a good fit between the CMB model results and PM total concentrations. Such profiles are generated using emission samples from a range of emitters of a particular source category which are analysed to determine their chemical composition and identify specific molecular source markers (Watson et al., 2002) (Table B1).They are then used for the identification and the quantification of the contributions of the different sources to PM. To a large extent, the CMB model results rely on the accuracy of the source profiles used as an input. However, in the absence of locally relevant source profiles, the SCEs can be prone to produce erroneous results. While the typical components of any source profiles are found to be more-or-less similar, the relative mass abundances vary with specific feature locations and emitter characteristics. Thus, the use of

different combinations of source profiles in CMB can provide statistically valid but completely different solutions. Generation of SOC source profiles is difficult due to the complex chemistry of SOA formation and the diversity of its composition (Bullock et al., 2008). Therefore, the major challenge for the real SOC estimation from CMB faces the lack of SOC profiles (Guo et al., 2012; Stone et al., 2009).

As already explained before, the difference between the measured OC and the sum of all apportioned primary sources is usually attributed to SOC. However, this approach presents a major issue when unknown primary sources contribute significantly to OC or are missed out in the available source profiles. In that case, SOC estimation using CMB could be overestimated or underestimated.

As specified in the preamble of this section, sampling artifacts could also influence the results obtained using CMB, alhough El Haddad et al. (2011) showed that sampling artifacts appeared to marginally influence the amount of un-apportioned OC.

Another important issue is the stability in the atmosphere of the molecular markers used (e.g. Table B1). Currently all the source-receptor models used in the source apportionment studies assume that marker compounds are chemically stable in the atmosphere (and so called tracer compounds) (Schauer et al., 1996). However, their photodegradation could occur in the atmosphere and may cause an underestimation of the contributions of sources, especially in summer (Robinson et al., 2007). As an example, levoglucosan has been for a long time used as the specific molecular marker of biomass burning aerosol, based on its high emission factors and assumed chemical stability (Simoneit et al., 1999). Recent studies showed that significant atmospheric chemical degradation of levoglucosan could occur on a timescale similar to that of atmospheric transport and deposition (Hennigan et al., 2010; Kessler et al., 2010; Mochida et al., 2010; Zhao et al., 2014a). This could induce an underestimation in the contribution of the

biomass burning source in the source apportionment results whatever the source-receptor model used.

3.2.3 Review of recent studies based on CMB approach

Figure B1 shows a summary of the application of CMB in source apportionment studies performed worldwide. Detailed references about all the results considered here are presented in Tables B2 and B3. Note that, even if many studies exist, no data or very few are displayed for Africa, Oceania, East and South-East Asia, Russia, Central and South America, because they fall outside the specific criteria of this review ($PM_{2.5}$ fraction and studies from 2006 to 2016).

3.2.3.1 Studies in North America

CMB has been used extensively in the USA to apportion the SOC fraction in $PM_{2.5}$ (Chen et al., 2010b; Hasheminassab et al., 2013; Heo et al., 2013; Ke et al., 2007; Lee et al., 2008b; Minguillón et al., 2008; Pachon et al., 2010; Sheesley et al., 2007; Shirmohammadi et al., 2016; Stone et al., 2008; Subramanian et al., 2007; Subramoney et al., 2013; Zheng et al., 2007; Zheng et al., 2014).

For all the different sampling type locations studied, annual SOC contributions presented an extremely wide range of values with SOC contributions to $PM_{2.5}$ OC from 2 to 67% and concentrations from 0.0 to 4.6 µgC m^{-3} (Figure 4, Table B2). All the urban locations showed SOC contributions >33% while rural and remote sites could show both, very low SOC contributions like in Northern and Southern Minnesota (2%) or quite high contributions like in Texas and Centreville (63%) with both, low and high OC concentration levels (from 0.8 to 6.3 µgC m^{-3}). Authors showed that Minnesota is often downwind of major Midwest regional

sources (from Illinois, Wisconsin, Iowa and Missouri) in summer and could be also influenced by local coal-fired electricity generation emissions explaining probably the low SOC amounts observed (Chen et al., 2010b).

During the warm period, the observed SOC contributions and concentrations at all the urban locations ranged from 21 to 79% and 0.7 to 2.8 µgC m^{-3}, respectively (Figure 5; Table B3). Biogenic SOA, from isoprene and pinene precursors, accounted as an important SOA source in the eastern USA where up to 80% land is covered by forests for instance in the south (Carlton et al., 2016; Ding et al., 2008b; Sareen et al., 2017; Xu et al., 2018; Zhang et al., 2018). In summer period when abundant biogenic VOC emissions exist, the favourable atmospheric conditions lead to high SOA formation.

3.2.3.2 Studies in Europe and the Middle East

CMB studies to apportion the SOC fraction in $PM_{2.5}$ in Europe are only few (Daher et al., 2012; El Haddad et al., 2009; El Haddad et al., 2011; Favez et al., 2010; Pant et al., 2014; Perrone et al., 2012; Pirovano et al., 2015; Yin et al., 2010).

The average annual SOC contributions to $PM_{2.5}$ OC ranged from 10 to 44% in London, Birmingham and Milan (urban and rural sites) and were in the concentration ranges of 0.7 to 1.2 µgC m^{-3} (Daher et al., 2012; Pant et al., 2014; Yu et al., 2006) (Figure 4, Table B2). Higher CMB SOC estimates were observed in the warm period, 33-78% (1.4-3.7 µgC m^{-3}) with the highest contribution (78%) at Marseille (France) and the lowest (33%) at Milan (Italy) (El Haddad et al., 2011; Perrone et al., 2012) (Figure 5, Table B3). Interestingly, at Summit (Greenland, Denmark), a remote site far from any biogenic or anthropogenic sources and activities, the SOC contribution reported was about 95%. These results highlight the long range transport and SOA formation until high latitude regions (von Schneidemesser et al., 2009).

The Middle East also witnesses a lack of studies to estimate the SOC fraction in $PM_{2.5}$ using CMB (Hamad et al., 2015; von Schneidemesser et al., 2010a; von Schneidemesser et al., 2010b). The annual SOC concentrations reported in the literature were in the range 1.4-5.5 µgC m^{-3}, contributing to about 42-67% of $PM_{2.5}$ OC (1.8-5.5 µgC m^{-3}) for sites located in Jordan, Palestine, Iraq and Israel (Figure 4, Table B2). For the spring-summer period, data are only available for West Jerusalem (Israel) and East Jerusalem (Palestine) with similar SOC contributions and concentrations to the annual average; 39% (1.9 µgC m^{-3}) and 48% (2.5 µgC m^{-3}) of $PM_{2.5}$ OC, respectively (Figure 5, Table B3). These results showed that SOA formation in the Middle East is significant in the region year-round. The intensity of the sunlight and high temperatures would result in a high reaction rate of SOA precursors and, in combination with drier conditions (lower wet deposition), would induce a larger SOA formation (von Schneidemesser et al., 2010a).

3.2.3.3 Studies in Asia

In the Asian continent, several studies have been performed during the last decade and notably in China (Huang and Wang, 2014; Kong et al., 2010; Lee et al., 2008a; Li et al., 2013; Li et al., 2012; Miller-Schulze et al., 2011; Shi et al., 2011; Stone et al., 2010a; Villalobos et al., 2015; Wang et al., 2016b; Wu et al., 2015; Zheng et al., 2006a; Zheng et al., 2006b; Zheng et al., 2011).

The annual and spring-summer SOC concentrations in Asia were in the ranges 0.7-7.7 µgC m^{-3} and 0.8-4.8 µgC m^{-3}, respectively, accounting for 12%-67% and 11%-80% of SOC in $PM_{2.5}$ OC, respectively (Figures 4 and 5; Tables B2 and B3).

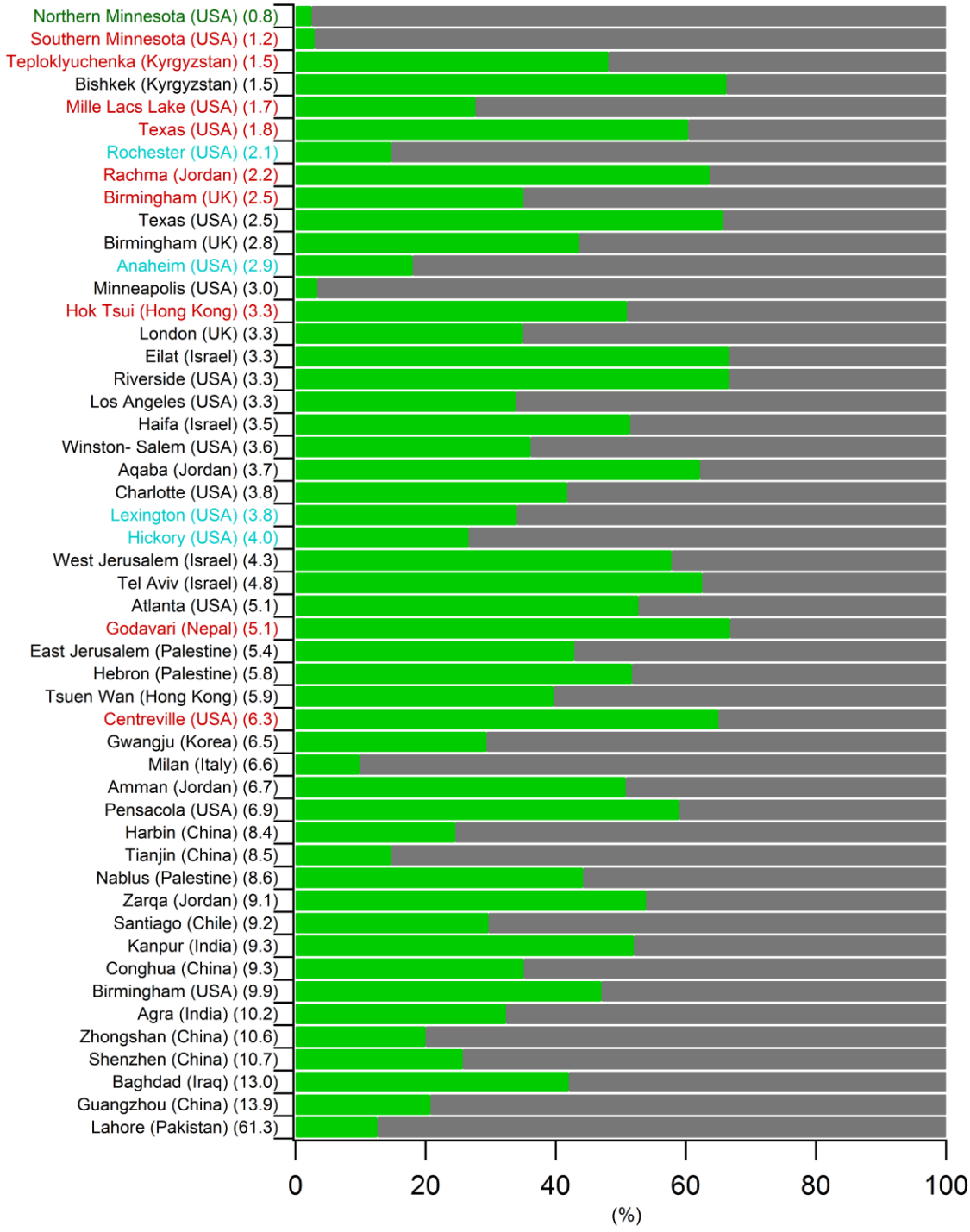

Figure 4. Annual SOC (green) and POC (grey) contributions to $PM_{2.5}$ OC using CMB for all the monitored sites from 2006 to 2016. Results are presented in increasing order of OC concentration levels (µgC m^{-3}). In black, urban sites; in blue, suburban sites; in red, rural sites and in green, remote sites.

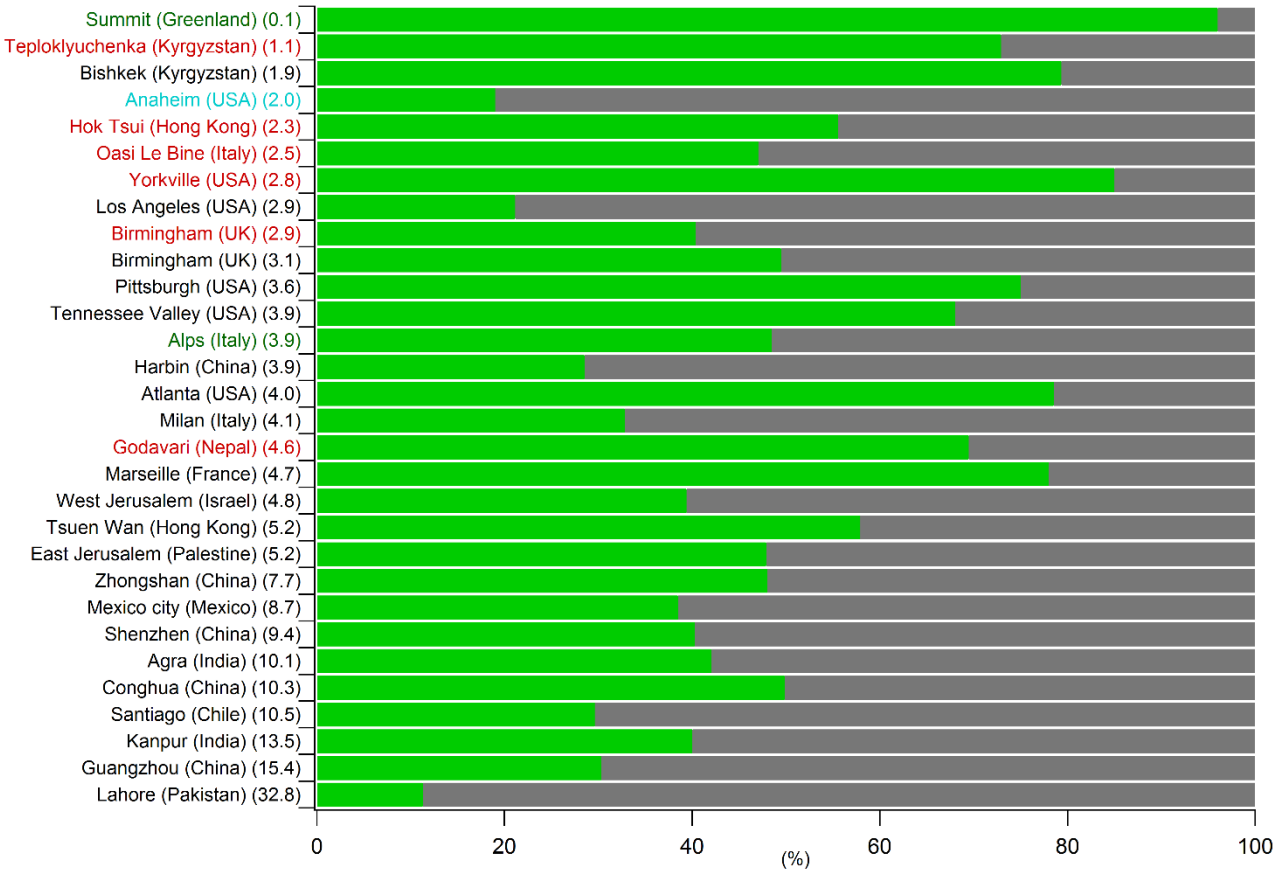

Figure 5. Spring-summer SOC (green) and POC (grey) contributions to $PM_{2.5}$ OC using CMB for all the monitored sites from 2006 to 2016. Results are presented in increasing order of OC concentration levels (µgC m^{-3}). In black, urban sites; in blue, suburban sites; in red, rural sites and in green, remote sites.

Only two sites have been investigated in Central Asia at Bishkek and Teploklyuchenka, in Kyrgyzstan where large SOC contributions (> 72%) were observed in summer period and at both sites (urban and rural). In India (Kanpur, Agra), Pakistan (Lahore) and Korea (Gwangju), the annual SOC concentrations were in the range 1.9-7.7 µgC m^{-3} corresponding to SOC contributions of about 32% (Miller-Schulze et al., 2011; Stone et al., 2010a; Villalobos et al., 2015). In China, the annual SOC concentrations were in the range 1.2-3.3 µgC m^{-3} and

contributions about 14% to 50% of $PM_{2.5}$ OC (Figure 4). Interestingly, SOC concentrations at the rural site Hok Tsui in Hong Kong showed a SOC contribution larger than 50% throughout the year (Zheng et al., 2006b). As expected, during the warm period the SOC concentrations and contributions were higher (4.8 µgC m^{-3} and >50% of $PM_{2.5}$ OC) (Figure 5).

3.3 SOA-tracer method

3.3.1 Introduction

The SOA-tracer method was developed by Kleindienst et al. (2007) to estimate the SOA contributions from several biogenic and anthropogenic hydrocarbon precursors to ambient OC concentrations using a series of organic molecular compounds (tracer or marker compounds, see section 3.2.2). For each hydrocarbon precursor, tracer compounds were first identified and measured during irradiation experiments performed in a smog chamber in the presence of NO_x. The SOA mass fraction, $f_{SOA,hc}$, defined as the ratio of the sum of the organic tracer concentrations to the mass concentration of aerosol formed in the smog chamber, is equal to the total SOA concentration in this case (Equation (5)).

$$f_{SOA,hc} = \frac{\sum_i [tr]_i}{[SOA]} \qquad (5)$$

with $[tr_i]$, the mass concentration of the tracer i in µg m^{-3}. EC/OC measurements were performed to determine SOC concentrations and then to convert the SOA mass fractions into SOC mass fractions $f_{soc,hc}$ using SOA/SOC mass ratios Equation (6).

$$f_{SOC,hc} = f_{SOA,hc} \frac{[SOA]}{[SOC]} \qquad (6)$$

Laboratory experiments were conducted to determine SOC mass fractions for isoprene, α-pinene, β-caryophyllene, and toluene. Details of the laboratory generated SOC mass fractions

are provided in SM (Table C1). All the other details about the smog chamber experiments are well described in Kleindienst et al. (2007).

3.3.2 Limitations and challenges

The main advantage of the SOA-tracer approach lies in the direct attribution of SOC concentrations and contributions to specific gaseous organic precursors. However, the method suffers also of several limitations.

Mass fractions, calculated considering the sum of tracer compounds, have been determined from single hydrocarbon smog chamber irradiations under varying SOA precursor and NO_x concentrations. Due to the complexity of atmospheric photooxidation chemical mechanisms, the wide range of organic and inorganic compounds present in the atmosphere, and the myriad of possible actual meteorological and photochemical conditions, considerable error may be associated with the use of a single-value mass fraction for each precursor. The main systematic error is probably the representativeness of smog chamber processes compared to those occurring in the atmosphere with differences in relative humidity, precursor and particulate matter concentrations, nature and oxidant concentrations, and irradiation conditions. Thus, the mass fractions derived from chamber experiments may be different from ambient air conditions. This has already been noticed when the SOA tracer method was applied for the first time to ambient air samples collected at Research Triangle Park, North Carolina (Kleindienst et al., 2007). Errors in the results were estimated to about 25% for isoprene, 48% for α-pinene, 22% for β-caryophyllene, and 33% for the toluene SOA mass fractions, respectively.

As defined, a tracer should be stable in the atmosphere (Simoneit et al., 1999). However, as already specified before in section 3.2.2., one of the most important limitation is related to the stability of these molecules in the atmosphere and in this case the term marker would be more

appropriate. The atmospheric lifetimes for the SOA tracers (markers) have been theoretically estimated based on their volatility (Nozière et al., 2015). The exact values are only available for few of them (e.g. cis-pinonic acid ~2.1-3.3 days and MBTCA (3-methyl-1,2,3-butanetricarboxylic acid) ~1.2 days) (Kostenidou et al., 2017; Lai et al., 2015).

Molecular tracer species are not necessarily produced from single precursors but could originated from the oxidation of other molecules. For instance, α-pinene SOA tracer compounds have been also observed in laboratory as by-products from the oxidation of β-pinene and d-limonene (Jaoui et al., 2005). Thus, the estimation of α-pinene derived SOC contribution may also contain some contributions from such other monoterpenes. Similarly, Kleindienst et al. (2007) also showed that toluene SOA tracer could also be formed from the photo-oxidation of xylenes.

So far, the main limitation of the method is probably due to the limited number of SOA tracers identified for specific known gaseous organic precursors and to the SOA/SOC data available in the literature. For instance, toluene is the only anthropogenic VOC considered in the SOA tracer method. Laboratory studies have shown considerable SOA yields from several aromatic compound VOCs, such as xylenes, ethyl-benzene, ethyl-toluene, trimethyl-benzenes, benzene (Martín-Reviejo and Wirtz, 2005; Odum et al., 1997; Ye et al., 2017). Currently, there is a lack of SOA tracer compounds for these precursors (Yee et al., 2013). In addition, recent research showed that the semi-volatile (SVOCs) and intermediate-volatility organic compounds (IVOCs) including cyclic, linear, branched alkanes, PAHs…, are important classes of SOA precursors (Chan et al., 2009; Kleindienst et al., 2012; Lamkaddam et al., 2017; Lim and Ziemann, 2005; Lim and Ziemann, 2009; Riva et al., 2015; Robinson et al., 2007; Schilling Fahnestock et al., 2015; Shakya and Griffin, 2010; Tkacik et al., 2012). SVOCs and IVOCs are abundant in gasoline- and diesel-powered vehicle exhausts as well as other anthropogenic sources (e.g. biomass burning), but little is known about their molecular composition and no

SOA markers with proper SOC mass fractions have been reported for such classes of compounds.

Phenol, cresols, furans and methoxy-phenols account for a significant fraction of pollutants emitted by biomass burning. The oxidation of these compounds is likely to form SOA, contributing significantly to OA loadings in the atmosphere (Bruns et al., 2016; Iinuma et al., 2010; Yee et al., 2013). Therefore, neglecting SOA derived from biomass burning would also underestimate the SOC fraction, especially in winter when this source of energy is largely used.

Besides, the presence of organosulfate compounds, a class of organic compounds reported to be formed from the oxidation of aromatic and polyaromatic compounds, isoprene, and monoterpenes in the presence of acidic sulfate seed particles (Iinuma et al., 2007; Riva et al., 2015; Surratt et al., 2007), could account for a significant fraction of total SOC but they are not yet included in the SOA tracer method. Similarly, no marker compounds have been identified to account for the organonitrate fraction that constitutes a significant part of OA in urban environments (Kiendler-Scharr et al., 2016).

In addition, the tracer-based approach does not consider SOA formed through cloud processing. For instance, glyoxal and methylglyoxal can partition into cloud droplets and yield SOA through in-cloud formation of carboxylic acids (e.g. glyoxylic, glycolic and oxalic acids) and subsequent cloud evaporation (Lim and Ziemann, 2005). In-cloud production is not represented in the laboratory-derived SOA mass fraction from any already studied precursor. Thus, SOA production in the real atmosphere could be higher than the one estimated using mass fractions proposed by Kleindienst et al. (2007).

Another issue is related to the quantification of these markers in PM samples. Most of the SOA tracers of well-known atmospheric biogenic and anthropogenic VOC precursors such as isoprene, monoterpenes, sesquiterpenes, and toluene are not commercially available. In that scenario, proxy compounds have been used more than often (Hu et al., 2008; Kleindienst et al.,

2007; Kleindienst et al., 2010). The lack of authentic standards critically implies a bias in the quantification of these species. It has been already noticed by Hu et al. (2008) in Hong Kong. The quantification uncertainty caused by using different surrogates other than ketopinic acid (surrogate for all tracer compounds to derive mass fractions of SOA tracers in the SOA tracer method by Kleindienst et al. (2007)) was estimated to be within a factor of 3. The use of different surrogate standards could be another reason for observing large uncertainties in the SOC estimation. Several research groups have resorted to synthesize these compounds. However, the synthesis remains a quite expensive and/or a time-consuming task. Only very recently, a few papers from our group have reported the use of authentic standards commercially available or synthesized on purpose by worldwide suppliers (Srivastava et al., 2018a; Srivastava et al., 2018b).

Finally, compared to other available methods, the SOA tracer method is presently the only approach which procures individual SOA contribution from different precursors. However, further laboratory and field evaluations of the method, for predicting SOC contributions, are needed to improve it and consider a large variety of SOA precursors.

3.3.3 Review of recent studies based on the SOA-tracer method

The SOA tracer approach has been applied in many studies across the world including several sites in the USA (Jayarathne et al., 2016; Kleindienst et al., 2007; Kleindienst et al., 2010; Lewandowski et al., 2008; Lewandowski et al., 2013; Offenberg et al., 2011; Offenberg et al., 2007; Rutter et al., 2014; Stone et al., 2010b; Stone et al., 2009), the Canadian Arctic (Fu et al., 2009a; Fu et al., 2013; Hu et al., 2013), Europe (El Haddad et al., 2011; Kourtchev et al., 2009; Kourtchev et al., 2011; Kourtchev et al., 2008), and Asia (Ding et al., 2016; Ding et al., 2014; Ding et al., 2012; Feng et al., 2013; Fu et al., 2016; Fu and Kawamura, 2011; Fu et al.,

2010; Fu et al., 2012; Fu et al., 2009b; Guo et al., 2012; Hu et al., 2010; Hu et al., 2008; Liu et al., 2014; Shen et al., 2015; Yang et al., 2016) (Figure 6).

Note that, the annual SOC estimates are only available for a few sites in the USA and China. The analysis and the quantification of all the SOA tracers needed to apply the SOA tracer method for the SOC estimation are a difficult and a time labour task and could explain the limited number of available results in the literature. Figure 6 shows the results obtained over the world in the $PM_{2.5}$ fraction only for the spring-summer period. Detailed references about all the results considered here are presented in Tables C2 and C3. Total SOC discussed below represents the sum of $SOC_{isoprene}$, $SOC_{\alpha\text{-pinene}}$, $SOC_{\beta\text{-caryophyllene}}$ and $SOC_{toluene}$.

3.3.3.1 Studies in North America

The annual SOC contributions observed at Bondville, Northbrook, Research Triangle Park (RTP), Cincinnati, Detroit, East St. Louis in the USA varied in the range 8-53%. SOC concentrations from the different precursors ranged from 0.2 to 0.9 µgC m^{-3} for isoprene, from 0.1-0.3 µgC m^{-3} for α-pinene, from 0.1-0.2 µgC m^{-3} for β-caryophyllene and from 0.2-0.3 µgC m^{-3} for toluene (Kleindienst et al., 2007; Lewandowski et al., 2008; Offenberg, 2011).

In the spring-summer period, the average SOC levels in the USA including urban, suburban, rural and remote locations varied in the range 0.2-2.6 µgC m^{-3}, contributing to 5-98% to $PM_{2.5}$ OC (Figure 6). Among the urban and suburban locations, Northbrook exhibited the highest SOC contribution (61%) and Bakersfield showed the lowest one (5%). Rural and remote sites (Medina, Bondville, RTP) showed that more than 60% of OC is from secondary origin.

This large local emission source may have a strong influence on SOA formation nearby downwind locations, including St. Louis. Besides, isoprene at other urban locations also presents high emission levels.

Results obtained at all the sites located in Eastern USA (Atlanta, Birmingham and Pensacola, East St Louis), have shown that α-pinene (59% of total SOC) and isoprene (26% of total SOC) SOAs were the main SOC contributors even at urban and suburban locations. Model simulations, as mentioned in section 3.2.3.1, have shown significant emissions of isoprene and monoterpene in the Eastern part of the North American continent (Guenther et al., 2006; Hantson et al., 2017; Heald et al., 2008; Lathiere et al., 2006). The land surface in there is characterized by rolling or hilly terrain with heavy vegetation, mainly consisting of mixed coniferous (mainly loblolly pines) and deciduous (mainly oak and hickory) forests. Then, during spring and summer, the biogenic emissions drive the production of SOA and specific experiments have been performed in the region to also understand the effects of anthropogenic pollution on biogenic SOA formation (Budisulistiorini et al., 2015; Carlton et al., 2016; Zhang et al., 2018). Finally, in highly urbanized and industrialised cities such as Mexico, Detroit, Cleveland, Riverside and Pasadena, $SOC_{toluene}$ appeared as a major contributor to total SOC (40 to 80%).

3.3.3.2 Studies in Europe

Only few studies have been performed in Europe and only biogenic SOC was accounted. Anthropogenic SOC was unfortunately neither measured nor detected. The average SOC in Europe ranged from 2% to 12 % (0.02-0.49 µgC m^{-3}) of $PM_{2.5}$ OC (Figure 6). It is worth noting that at all European sites, $SOC_{isoprene}$ contributions were largely lower than the sites monitored in North America due to the large isoprene emissions in the USA. Monoterpene emissions are dominant in Europe and account on average from 40% to 60% of total emitted VOCs (Steinbrecher et al., 2009). The remaining fraction is dominated by isoprene and other VOCs. This fact can be easily observed at Marseille (France), where $SOC_{\alpha\text{-pinene}}$ contributed to 3.5% of

total OC while $SOC_{isoprene}$ contribution was only about 0.6%. At remote or rural sites, Julich (Germany) and K-puszta (Hungary), the contribution of both isoprene and α-pinene SOC were similar.

3.3.3.3 Studies in Asia

In Asia, several studies have been conducted in India, Japan but especially in China (Figure 6). Studies conducted at urban and suburban background sites in Shanghai showed average annual SOC contributions of about 3% corresponding to SOC concentrations of about 0.3 µgC m^{-3} (Feng et al., 2013).

In the spring-summer period, the average SOC concentrations at urban sites in Beijing, Shanghai, Hong Kong and Wangqingsha (PRD) were 3.3, 0.6, 3.0 and 3.1 µgC m^{-3}, respectively. Results from all urban and suburban locations highlighted the major contributions of $SOC_{isoprene}$ (20-50%) and $SOC_{toluene}$ (50-80%) to total SOC except at Hong Kong where $SOC_{\alpha\text{-pinene}}$ (48%) and $SOC_{\beta\text{- caryophyllene}}$ (33%) were dominant. The very high urbanization and industrialization of these cities explain such $SOC_{toluene}$ contributions as well as the very high isoprene emissions in North Eastern China (Zhang et al., 2017). In Hong Kong, the observation of larger amounts of SOC attributable to monoterpenes rather than isoprene is consistent with high emissions of monoterpenes in the region (Hu et al., 2008), in addition to the higher SOA formation yields from monoterpene oxidation (Griffin et al., 1999). The only study conducted in India at Mumbai (Fu et al., 2016) showed a very minor contribution of SOC to fine OC of about 2% equivalent to SOC concentration of 0.47 µgC m^{-3}. Authors suggested that high ambient temperatures and relative humidity in tropical regions may affect the SOA yields, gas/particle partitioning, and aging processes explaining such low SOC contributions observed (Fu et al., 2016). Similarly, only one study has been performed in Japan so far at a rural site in

Hokkaido (Fu and Kawamura, 2011). The SOC contribution to total OC was about 16% (0.69 µgC m^{-3}) and mainly due to $SOC_{isoprene}$.

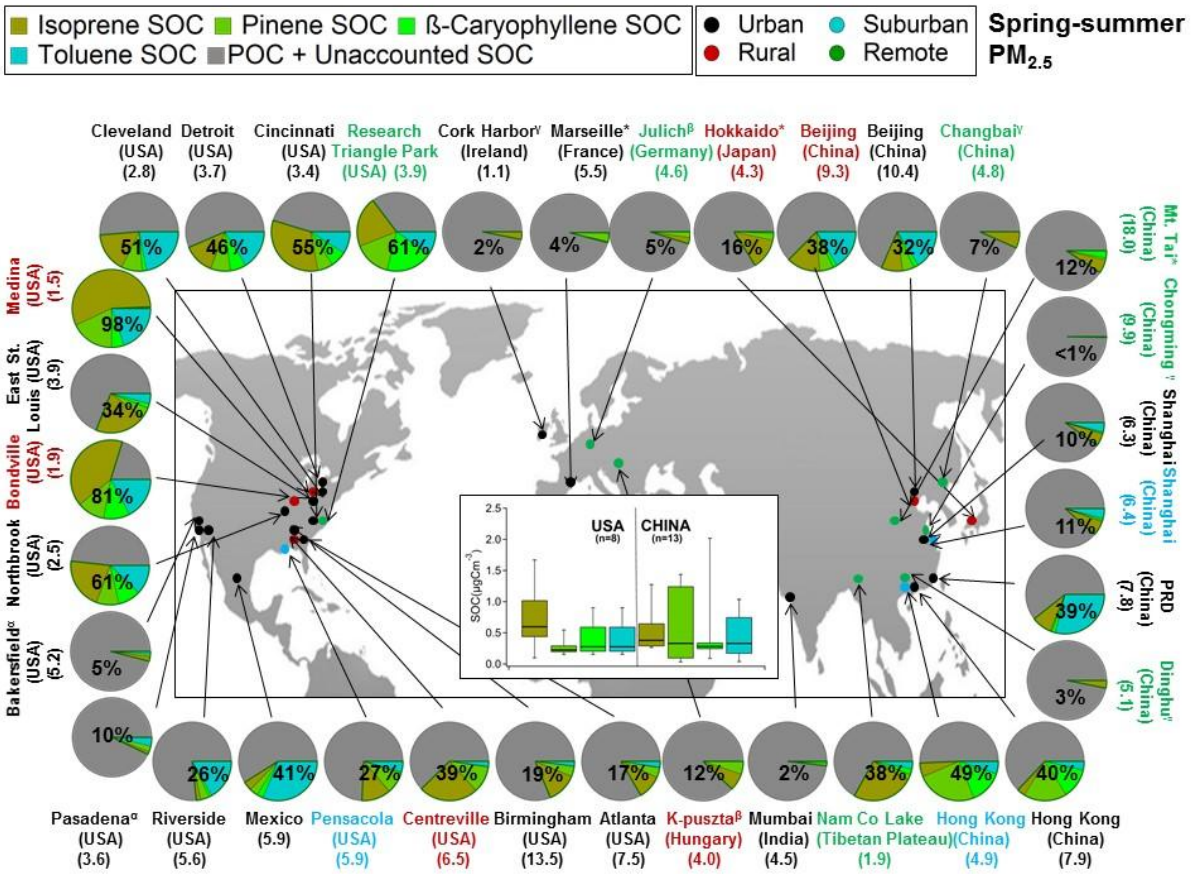

Figure 6. Spring-summer SOC contributions to $PM_{2.5}$ OC over the world for all the monitored sites from 2006 to 2016 using the SOA tracer method. OC concentrations (µgC m^{-3}) for each site are indicated into brackets. Box-plots represent the SOC concentrations (µgC m^{-3}) for USA and China. The number of data points considered is presented into brackets. * Toluene SOC was not reported at these locations. α β-caryophyllene SOC was not reported at these locations. β Toluene SOC and β-caryophyllene SOC were not reported at these locations. γ Only isoprene SOC was reported at these locations.

Finally, several studies have been performed at remote sites in China and on the Tibetan Plateau. Overall, very low SOC contributions to total OC were observed (1-12%) except at the

Tibetan plateau where SOC contribution observed in spring-summer period was about 38% with very low total OC concentrations (1.90 µgC m^{-3}) while, on annual basis, the contribution was about 13% (Shen et al., 2015). At other locations in China, total OC was significantly higher (4.8-18 µgC m^{-3}) and probably impacted by direct emissions explaining the low SOC contributions observed.

3.4 Positive Matrix Factorization (PMF) (including AMS data analysis)

3.4.1 Introduction

As other receptor models, the goal of PMF is to solve the chemical mass balance between the measured chemical species concentrations and source profiles as a linear combination of factors *p*, species profile *F* of each source, and the amount of mass *G* contributing to each individual sample (Equation (7)):

$$x_{ij} = \sum_{k=1}^{p} G_{ik} F_{kj} + E_{ij} \quad (7)$$

where x_{ij} represents the measured data for species *j* in sample *i*, and E_{ij} represents the residual of each sample/species not fitted by the model.

Thus, PMF is a multivariate factor analysis tool that decomposes the matrix *x* (*n*×*m)*, where *n* is the number of samples and *m* is the number of chemical species, into both matrices, factor contributions *G* (*n*×*p*) and factor profiles *F* (*p*×m), that need to be ascribed to a specific source.

The best model solution is obtained by minimizing the function Q (Equation. (8)):

$$Q = \sum_i \sum_j \left(\frac{e_{ij}}{s_{ij}}\right)^2 \quad (8)$$

where s_{ij} represents the measurement uncertainty of each data point. The Q value can be used to determine the optimal number of factors. The theoretical Q value should be approximately

equal to a value of $n \times m$, the number of values in the data matrix or the degree of freedom of the datum in the data set.

PMF does not rely on information from the correlation matrix but utilizes a point-by-point least squares minimization scheme and differs from the other factor analysis models such as principal comment analysis (PCA) by the property to consider standard deviations of observed data values and to introduce the constraint of non-negativity of all the factor matrices G and F to get physically meaningful solutions. The input data matrix contains the measured species concentrations and their corresponding uncertainties. One of the main features of the PMF results is their quantitative nature. It is then possible to obtain the composition of the sources determined by the model (Paatero, 1997; Paatero and Tapper, 1994). This is the distinctive advantage of PMF over other multivariate factor analysis approaches.

An estimation of the data uncertainties could be performed using known concentrations and the limit of detection values. The estimation of uncertainties is calculated using Equations (3) (Polissar et al., 1998):

$$\sigma_{ij} = \begin{cases} \frac{5}{6} LD_j & \text{if } X_{ij} < LD_j \\ \sqrt{(LD_j)^2 + (CV_j X_{ij})^2 + (aX_{ij})^2} & \text{if } X_{ij} \geq LD_j \end{cases} \quad (9)$$

where LD_j is the detection limit for compound j (defined as the lowest concentrations of the compound that can be measured with a signal to noise ratio of 3), CV_j is the coefficient of variation for compound j (calculated as the standard deviation of repeated analyses divided by the mean value of the repeated analyses), and a is a factor that could be applied to account for additional sources of uncertainty (Gianini et al., 2012).

Alternatively, the PMF program can compute heuristic error estimates, s_{ij}, for each x_{ij} based on the data point on its analytical error. This is done by means of three codes within the model (Sara et al., 2009).

3.4.2 Limitations and challenges

PMF has been widely applied to apportion the sources of PM based on speciation data from filter measurements such as OC, EC, major ions, and metals. However, many of these species are not source specific making difficult to link PMF factors with aerosol sources and to fully describe the OA. In such cases, SOC was calculated by summing OC fractions in sulfate and nitrate PMF factors or individually (Ke et al., 2008; Lee et al., 2008b; Pachon et al., 2010; Yuan et al., 2006a). Few studies also reported the use of species such as WSOC and humic-like substances (HuLiS) to characterize SOC (Qiao et al., 2016). By comparison, molecular organic markers (tracers) are highly source-class specific and provide a definitive link between factors and source classes. Molecular markers for SOA and POA can be directly included in the PMF model providing an insight into the primary–secondary split of OA sources (Heo et al., 2013; Hu et al., 2010; Jaeckels et al., 2007; Miyazaki et al., 2012b; Shrivastava et al., 2007; Srivastava et al., 2018a; Srivastava et al., 2018b; Wang et al., 2012a). The effectiveness of the method depends on the molecular markers used. In addition, and as already mentioned in sections 3.2.2 and 3.3.2, both the stability of molecular markers in the atmosphere and their limited number for known precursors of SOA, can hamper the PMF filter based source apportionment. Finally, as PMF analysis requires a larger number of samples (>100) in order to get a statistically robust solution, it has not been extensively performed to apportion OA sources based on filter measurements.

Filter samplings rely on measurements performed over several hours to days, making it difficult to capture the fast-atmospheric chemical processes related to OA. By comparison, online aerosol chemical characterization techniques, such as AMS, are faster, less labour intensive and allow the quantitatively determination of non-refractory PM with high time resolution (Allan et al., 2004; Jayne et al., 2000; Jimenez et al., 2003; Ng et al., 2010; Zhang et al., 2011b; Zhang et al., 2005). Several types of OA from the mass spectra obtained can be

apportioned by applying PMF to AMS/ACSM data. The oxygenated fraction of OA (OOA) identified by PMF-AMS is usually associated with SOA (Sun et al., 2011). This OOA fraction is commonly sub-divided in low oxidized (LO-OOA) and more oxidized (MO-OOA) or low volatile (LV-OOA) and semi-volatile (SV-OOA) OOAs (Ng et al., 2010). By comparison to filter based PMF with SOA markers, the explicit characterization of OOA is not possible with PMF-AMS because the mass fragmentation obtained is not specific. In some cases, detailed analyses have been done and highlighted additional sub-SOA fractions such as IEPOX-SOA, biogenic SOA from isoprene epoxydiols, or marine SOA using the entire mass spectrum measured by time of flight-AMS (TOF-AMS) (Budisulistiorini et al., 2013; Chang et al., 2011; Hu et al., 2015; Zhang et al., 2017). In addition, as for all mass spectrometry techniques, the interpretation of mass spectra from natural samples can be complicated by several interferences (Jayne et al., 2000). Other factors identified using PMF-AMS such as hydrocarbon-like OA (HOA), which in urban areas shows correspondence with fossil fuel POA, could potentially include other primary sources such as biomass burning (BBOA), cooking-like organic aerosol (COA) and also OOA (Lanz et al., 2007; Zhang et al., 2005). Besides, in some cases, OOA may also include contributions from biomass burning or other primary OA sources (Salcedo et al., 2006). Such instrumentation provides results with quite low uncertainties for both the aerosol chemical characterization and the apportionment of the different OA fractions including SOA (about 6%) (Crenn et al., 2015; Fröhlich et al., 2015a). The cost and complex maintenance requirements of the AMS make its deployment impractical for long-term monitoring. Consequently, most available datasets are often limited to a few weeks of measurements. This hinders the determination of the regional and seasonal aerosol characteristics and the identification of changes in the pollution trends representing a significant limitation for the atmospheric chemistry model validation and for the evaluation of the air quality policies. For these reasons, the aerosol chemical speciation monitor (ACSM) has been developed for routine

monitoring purposes allowing a similar discrimination of OA sources but with low resolution mass spectrometry (Fröhlich et al., 2015b; Fröhlich et al., 2013; Ng et al., 2011; Petit et al., 2017; Petit et al., 2015).

To extend the spatial and temporal coverage of AMS measurements, the application of the AMS to nebulized water extracts of filter samples has been developed (offline AMS) (Bozzetti et al., 2017; Daellenbach et al., 2016; Daellenbach et al., 2017). This approach facilitates the investigation of specific events and can extend the measurements to the PM_{10} or coarse aerosol fraction while it is not possible using online AMS or ACSM instrumentation (aerosol size range from 40 to 800 nm) (Bozzetti et al., 2016; Bozzetti et al., 2017; Daellenbach et al., 2017).

3.4.3 Review of recent studies based on the PMF approach

3.3.3.4 PMF-filter based studies

Only few studies have reported in the literature the use of filter based PMF for the estimation of SOC in the $PM_{2.5}$ fraction. These annual based studies covered a wide geographical region in North America but not for the rest of the world (only in Hong Kong and Shanghai, China) (Table D1). As mentioned before, PMF analysis is usually performed using "traditional" speciation data and the use of specific POA and SOA molecular markers is still rare (including for other aerosol fractions like PM_{10}) (Feng et al., 2013; Heo et al., 2013; Hu et al., 2010; Jaeckels et al., 2007; Miyazaki et al., 2012a; Shrivastava et al., 2007; Srivastava et al., 2018a; Srivastava et al., 2018b; Wang et al., 2012a; Zhang et al., 2009a; Zhang et al., 2009b).

Overall, the SOC in the USA ranged from 12% to 57 % (0.1-0.9 µgC m^{-3}) of $PM_{2.5}$ OC and 24 to 66% (0.7-6.8 µgC m^{-3}), in Hong Kong and Shanghai. In some cases, SOA contributions from anthropogenic and biogenic sources have not been differentiated by PMF (Hu et al., 2010)

especially when no molecular markers have been used (SOA based on nitrate or sulfate factors) (Lee et al., 2008b; Pachon et al., 2010).

The biogenic SOA fraction was apportioned by using SOA markers from the oxidation of isoprene (2-methylglyceric acid, 2-methylthreitol, 2-methylerythritol and C5-alkene triols) (Kleindienst et al., 2007), α-pinene (MBTCA, pinonic acid, norpinonic acid, pinic acid, 3-(2-hydroxy-ethyl)-2,2-dimethylcyclobutane-carboxylic acid and 3-acetyl-hexanedioic acid, 3-hydroxyglutaric acid, 2-hydroxy-4,4-dimethylglutaric acid) and β-caryophyllene (β-caryophyllinic acid) (Heo et al., 2013; Hu et al., 2010; Jaoui et al., 2007; Shrivastava et al., 2007; Wang et al., 2012a; Zhang et al., 2009b). Shrivastava et al. (2007) have observed that biogenic SOA contributed to more than 50% of the summertime OC in Pittsburgh (USA). Similarly, results also showed the relative average contributions of isoprene SOC, α-pinene SOC and β-caryophyllene SOC in the midwestern USA were 20%, 5% and 19% of $PM_{2.5}$ OC, respectively (Zhang et al., 2009b). In other PMF studies, the biogenic SOA factor followed the same pattern with high contributions during the warm period (Heo et al., 2013; Wang et al., 2012a).

Anthropogenic SOA fraction was mostly characterized in filter based PMF analysis using di- or tri-carboxylic aliphatic or aromatic carboxylic acids (e.g. 1,2-benzenedicarboxylic acid, 1,3-benzenedicarboxylic acid, 4-methyl-1,2-benzenedicarboxylic acid, benzene tricarboxylic acid, benzene tetracarboxylic acid, phthalic acid, succinic acid, 2,3-dihdroxy-4-oxopentanoic acid (DHOPA)) and phthalates (Feng et al., 2013; Heo et al., 2013; Hu et al., 2010; Jaeckels et al., 2007; Zhang et al., 2009a) but also very recently, in the PM_{10} fraction, using oxy-PAHs, nitro-PAHs or methlynitrocatechols (Srivastava et al., 2018a; Srivastava et al., 2018b).

3.3.3.5 PMF-AMS based studies

By comparison to filter based PMF, extensive studies on PMF-AMS have been reported by many authors in the literature with an estimate of the SOC contributions and concentrations in PM_1 (OOA factor). Several previous papers already reviewed the results obtained worldwide (Jimenez et al., 2009; Xu et al., 2014; Zhang et al., 2007; Zhang et al., 2011b). Here, the overall average SOC distribution has been obtained by compiling results, only for the spring-summer, from these review papers and from some other recent papers (Crippa et al., 2014; Crippa et al., 2013a; Huang et al., 2010; Jimenez et al., 2009; Li et al., 2015b; Sun et al., 2011; Xu et al., 2015; Zhang et al., 2007) (Figure 7). Detailed references about all the results considered for PMF-AMS SOC estimates are presented in Table D2.

3.3.3.5.1 Studies in North America

In North America (including Mexico), the average spring-summer SOC concentrations in urban locations ranged from 1.3 to 3.2 µgC m^{-3} contributing to 33-74% of PM_1 OC. The possible sources for the OOA observed in these studies included SOA (from either anthropogenic or biogenic precursors), the oxidation of HOA, and/or BBOA (Jimenez et al., 2009; Zhang et al., 2007). SOC contributions to PM_1 OC at rural/remote locations were significantly larger and about 67-91% corresponding to SOC concentrations in the range 0.4-2.8 µgC m^{-3}. As explained before (sections 3.2.3.1 and 3.3.3.1) biogenic emissions of SOA precursors (isoprene and monoterpenes) play a major role in the SOC concentrations observed in the spring-summer period especially at rural/remote locations (Budisulistiorini et al., 2015; Carlton et al., 2016; Guenther et al., 2006; Hantson et al., 2017; Heald et al., 2008; Lathiere et al., 2006; Zhang et al., 2018).

3.3.3.5.2 Studies in Europe

The studies to apportion the SOC fraction using PMF-AMS performed in Europe cover a wide geographical area providing a good overview of the SOC distribution over this continent. The average SOC estimates in warm period varied at urban locations (or urban downwind) in the range 0.6-4.1 µgC m^{-3}, contributing to about 27-83% of PM_1 OC, with the highest contribution at Zurich (Switzerland) (83%) and the lowest at Edinburgh (UK) (26%). Lanz et al. (2007) suggested that the OOA should not be always equated to SOA in places where the direct emission of oxygenated aerosol species from sources like biomass burning, charbroiling, cooking etc., are dominant. For instance, OOA in Zurich in summer were also composed of a significant amount of primary emissions (Lanz et al., 2007). Thus, the inclusion of oxidized primary particles in OAA cannot be ruled out and could cause an elevated SOA contribution under certain circumstances.

Several rural, remote and altitude sites have also been investigated in Europe using AMS or ACSM measurements. SOC concentrations in such locations ranged from 2.1 to 4.0 µgC m^{-3} corresponding to SOC contributions to PM_1 OC of about 46 to 93%. In such cases, the highest SOC concentrations observed (>3.5 µgC m^{-3}) in Hyytiälä (Finland), Jungfraujoch (Switzerland), Payerne (Switzerland), Finokalia (Greece) and Melpitz (Germany) corresponded also to the highest SOC contributions (>74%) indicating the long range transport of air masses with strong oxidation processes leading to the formation of high amount of SOA (Crippa et al., 2014).

3.3.3.5.3 Studies in Asia

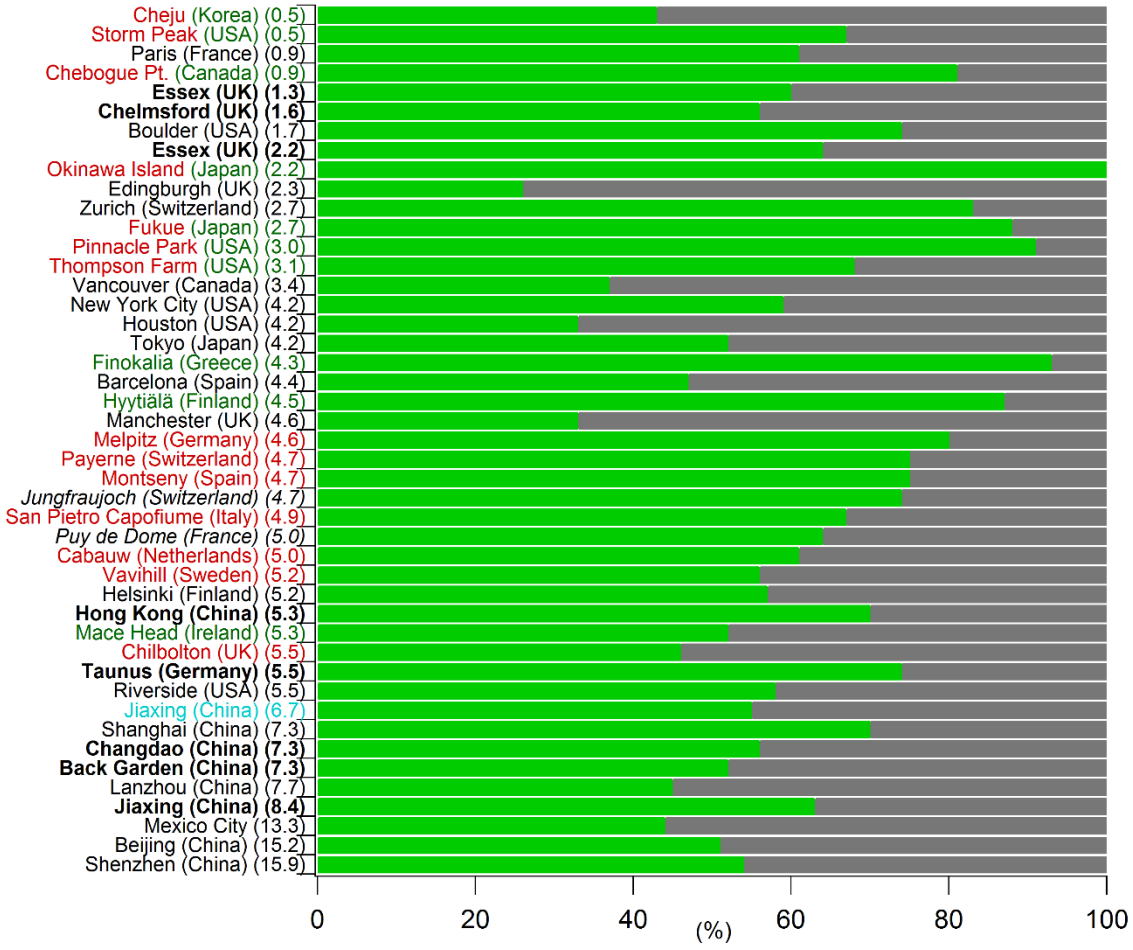

Figure 7. Spring-summer SOC (green) and POC (grey) contributions to PM_1 OC using PMF-AMS (AMS or ACSM) for all the monitored sites reference in Table D2. Results are presented in increasing order of OC concentration levels (µgC m^{-3}). In black, urban sites; in blue, suburban sites; in red, rural sites; in green, remote sites; in italic, high altitude sites and in bold, urban downwind sites.

In Asia, SOC concentrations at urban and suburban sites (or urban downwind) ranged from 2.2 (Tokyo, Japan) to 8.7 µgC m^{-3} (Shenzhen, China) corresponding to SOC contributions to PM_1 OC of about 45-73%. Higher SOC concentrations were observed in China in link with the

growing industrialization of this country and large VOCs emission from anthropogenic activities (Huang et al., 2010; Jimenez et al., 2009; Li et al., 2015b; Xu et al., 2014; Zhang et al., 2007). At rural/remote locations SOC concentrations observed were in the range 0.2 to 2.4 µgC m^{-3} for sites located in Japan and Korea with contributions from 43% and up to 100% in Okinawa Island (Japan) which is located to about 400-500 km from the Chinese coasts and the main Japanese island (Jimenez et al., 2009; Zhang et al., 2007). Long range transport could explain such SOC contributions observed (Zhang et al., 2007).

3.5 ^{14}C (radiocarbon) measurements

3.5.1 Introduction

Besides the use of specific organic marker species, isotopic abundances can also help to discriminate OA sources. The study of radiocarbon (^{14}C) itself does not allow the direct discrimination of SOC and POC but combined with another SOC apportionment method, it gives an insight for the distinction between the fossil fuel and the non-fossil fuel SOC origins.

^{14}C is present in small amount in living (or contemporary) materials but at approximately constant level and it is nearly absent in fossil fuels, which are much older than the ^{14}C half-life of about 5730 years. In addition, radiocarbon remains in its original state throughout chemical processes. Thus, a radiocarbon measurement provides a unique possibility of distinguishing quantitatively the relative contributions of both, fossil and contemporary carbon sources (Hildemann et al., 1994). The radiocarbon content of a carbonaceous sample is expressed as the fraction of "modern carbon" (f_M) based on the $^{14}C/^{12}C$ ratio observed in the atmospheric CO_2 of the year 1950, as a reference, following Equation (11) (Stuiver and Polach, 1977).

$$f_M = \frac{\left({}^{14}C/{}^{12}C \right)_{sample}}{\left({}^{14}C/{}^{12}C \right)_{AD1950}} \quad (11)$$

Values of f_M range from 0, for fossil sources, to values larger than 1, for contemporary sources. The f_M value for contemporary sources exceeds unity due to the atmospheric nuclear weapon tests in the 1950s and 1960s that significantly increased the radiocarbon content of the atmosphere (Levin et al., 2010). The term "modern carbon" only refers to measurements relative to the 1950 standard, and the terms "contemporary" or "non-fossil," and "fossil" carbon refer to quantities after correction.

Based on this specificity, carbon isotope data have been used in several studies to estimate the fossil fuel and contemporary (non-fossil) contributions to SOC by combining results from different SOC apportionment methodologies such CMB and EC tracer method with radiocarbon measurements. None of the other methodologies used and detailed here can do so far something similar except the SOA-tracer method. However, as specified previously in section 3.3.2, the lack of SOA tracer compounds for many precursors does not allow a complete description and discrimination of anthropogenic and biogenic SOCs. Thus, ^{14}C data can be useful to improve such discrimination and to understand the evolution mechanism of biogenic SOC, assumed as equivalent to the non-fossil fraction during the warm periods, and fossil SOC, which is still missing using other methodologies.

3.5.2 Limitations and challenges

First, the radiocarbon analysis requires large sample quantities to be quantitative and reproducible. In addition, this kind of analysis is quite expensive and then difficult to be performed routinely.

Second, emissions from nuclear power plants and incinerators of waste medical or biological products, containing ^{14}C used as a radioactive tracer, can significantly bias the estimated f_M. This could induce an overestimation of the true proportion of contemporary carbon. Such cases have been reported previously, suggesting that a ^{14}C contamination is uncommon but not impossible and could impact about 10% of the PM sampling sites (Buchholz et al., 2013). The occasional artificially inflated value of the modern carbon fraction needs to be always considered sincerely because its extent is not predictable.

Finally, another common problem is the true estimation of the biogenic fraction. ^{14}C measurements allow only the discrimination of fossil from non-fossil emissions. As both sources contribute to the contemporary carbon fraction, biomass burning emissions, which are mostly anthropogenic, cannot be separated from biogenic emissions using this methodology. The contemporary fraction is then considered as representative of the biogenic fraction only in summer. However, it can be also influenced by biomass burning emissions in case of forest fires or green waste burning.

3.5.3 Review of recent studies based on ^{14}C measurements

The application, across the world, of ^{14}C measurements, in combination with another methodology to determine SOC has been reported in the literature only in a limited number of studies for the spring-summer period (Ding et al., 2008a; El Haddad et al., 2013; El Haddad et al., 2011; Gelencsér et al., 2007; Gilardoni et al., 2011; Liu et al., 2016; Morino et al., 2015; Schichtel et al., 2008; Szidat et al., 2009) (Figure 8). To the best of our knowledge data on an annual basis do not exist. Details about all the results considered here are presented in Table E1.

3.5.3.1 Studies in North America

Overall, the application of radiocarbon measurements in the USA has been done at sites, including urban, suburban, rural and remote locations, with SOC concentrations in the range of 0.3 to 5.2 µgC m^{-3}, contributing to more than 40% of $PM_{2.5}$ OC (Ding et al., 2008a; Schichtel et al., 2008).

Very high contributions of $SOC_{contemporary}$ have been observed at all sites (about 72% of total SOC on average, 50-100% equivalent to 0.3-3.7 µgC m^{-3}). As explained before, $SOC_{contemporary}$ could account from both, biogenic and biomass burning sources. As the contribution from biomass burning was probably negligible in such periods of the year (except during forest fire events (Kaulfus et al., 2017; Roy et al., 2018)), these results suggested that $SOC_{contemporary}$ could mostly be attributed to biogenic sources. Moreover, at rural locations, the estimated contemporary SOC was even higher and varied from 82 to 99%. As mentioned in sections 3.2.3.1 and 3.3.3.1, significant emissions of isoprene and monoterpene in the Eastern part of the USA, and then formation of biogenic SOA, have been reported (Budisulistiorini et al., 2015; Carlton et al., 2016; Guenther et al., 2006; Hantson et al., 2017; Heald et al., 2008; Lathiere et al., 2006; Zhang et al., 2018).

$SOC_{fossil\ fuel}$ exhibited high contributions at all urban and suburban sites (in the range 12 to 54% of total SOC equivalent to 0.0-2.6 µgC m^{-3}). This contrasted with results obtained at rural locations where $SOC_{fossil\ fuel}$ accounted for about 7% of total SOC on average (3-18% equivalent to 0.0-0.7 µgC m^{-3}). These results showed the importance of fossil carbon emissions on the formation of SOA in urban environment.

3.5.3.2 Studies in Europe

In Europe, the average SOC contributions to $PM_{2.5}$ OC at sites where radiocarbon measurements have been also performed, were larger than 21% and up to 80% of $PM_{2.5}$ OC with a concentration range of 0.7-4.7 µgC m^{-3} (El Haddad et al., 2013; El Haddad et al., 2011; Gelencsér et al., 2007; Gilardoni et al., 2011). The average SOC levels observed for contemporary and fossil fractions were in the range 0.6-3.4 µgC m^{-3} and 0.1-1.3 µgC m^{-3}. Results showed that for all site typologies, SOC from non-fossil sources ($SOC_{contemporary}$) was dominant in the warm period (72-95% of total SOC) with slight to moderate contributions of fossil SOC (5-28% of total SOC). Note that, in Gotebörg (Sweden), no contemporary SOC was reported.

The site to site contributions of contemporary SOC were consistent with the wide geographical area covered across south-central Europe (Gelencsér et al., 2007). Rural and remote sites showed very high $SOC_{contemporary}$ contributions related most probably to biogenic SOA. High contribution of SOC_{fossil} (28% of total SOC, 1.3 µgC m^{-3}) was noticed in the Po Valley (Italy) known to be highly impacted by anthropogenic activities from the surroundings urban and industrialized areas. In addition, it has been shown that the concentrations of biogenic SOA observed in warm periods were also enhanced by anthropogenic primary emissions (Gilardoni et al., 2011). Both urban locations investigated showed SOC_{fossil} contributions of about 15 to 21% of total SOC.

3.5.3.3 Studies in Asia

In Asia, only two studies have been performed, and only in China, using ^{14}C measurements for SOC apportionment purposes. SOC contributions and concentrations levels at both urban

locations investigated were about 50% of $PM_{2.5}$ OC; 3.7-3.9 µgC m^{-3} (Beijing) and 59% of $PM_{2.5}$ OC; 2.0-4.1 µgC m^{-3} (Guangzhou), respectively (Liu et al., 2016; Morino et al., 2015).

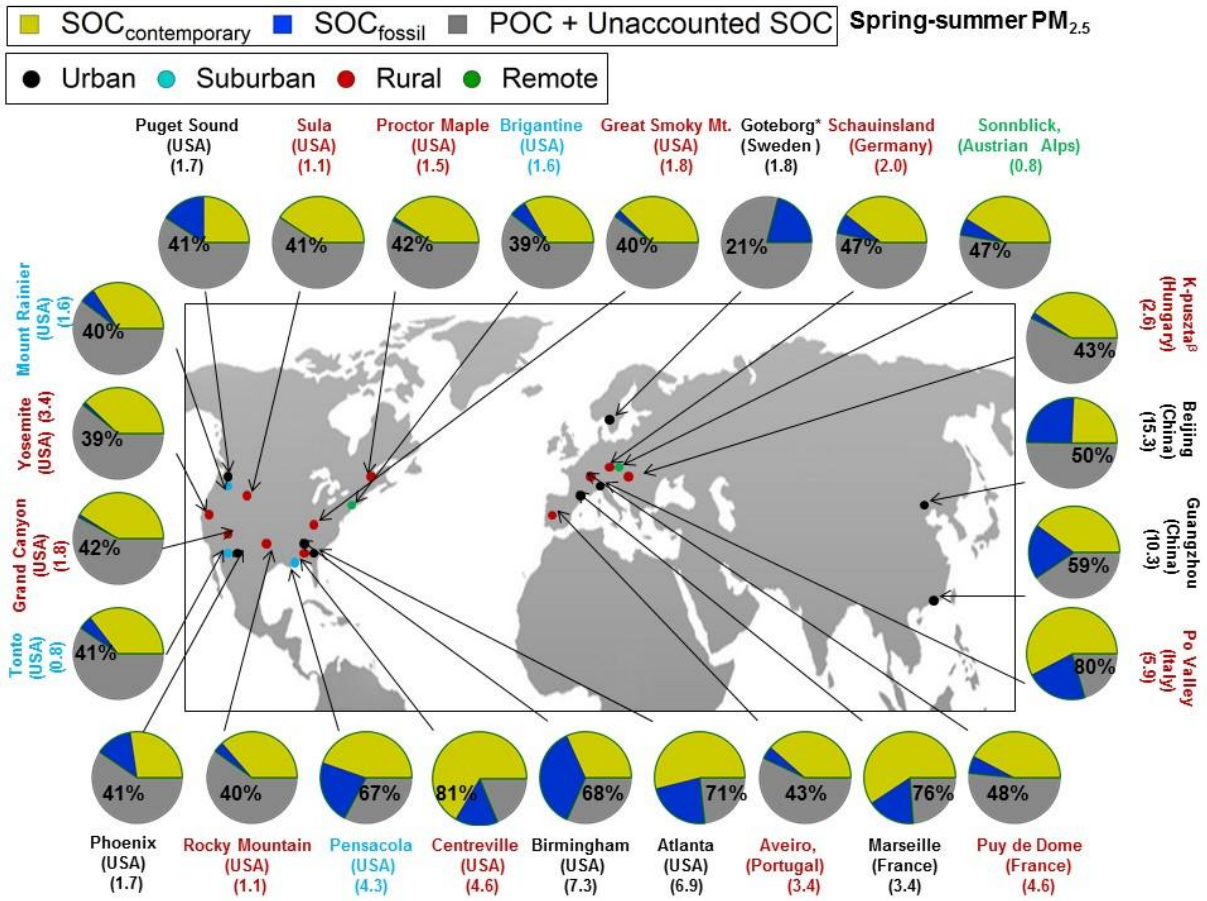

Figure 8. Spring-summer SOC contributions to $PM_{2.5}$ OC over the world for all the monitored sites from 2006 to 2016 using ^{14}C (Radiocarbon) measurements. OC concentrations (µgC m^{-3}) for each site are indicated into brackets. * Contemporary SOC was not reported.

On one hand, the differences observed in SOC composition between both sites (49 vs 67% of total SOC, Beijing and Guangzhou, respectively) may be linked to the differences of climate and land cover. In spring, the land of North China (Beijing) is bare and trees are still leafless, whereas, in South China (Guangzhou) lush vegetation is present emitting large VOC quantities including species such as isoprene, α-pinene, β-caryophyllene, etc, which are good biogenic

SOA precursors (Liu et al., 2016). On the other hand, the higher SOC_{fossil} contributions observed in Beijing (51% of total SOC) than in Guangzhou (33% of total SOC) was probably due that the primary anthropogenic emissions in this megalopolis. In addition, the differences in meteorological conditions between both cities may be another reason to explain such different SOC compositions.

4 Review of the studies comparing directly different methodologies

The above discussions highlight the advantages and limitations of the different methodologies usually used to estimate SOC. They have been applied worldwide showing many interesting features in terms of the influence of site typology, SOA precursor origins, SOC seasonality, etc. If the differences observed on the SOC contributions and concentrations can be related to the geographical origins and/or the meteorological conditions, they can also be linked to the uncertainties of the methodologies applied themselves. There are only few examples available in the literature where these methodologies have been compared thoroughly. This section summarizes the results reported in the literature where CMB, EC tracer method, SOA tracer method and/or PMF approach have been directly compared (Table 1).

Table 1. List of the studies reporting a direct comparison of SOC contributions evaluated using different methodologies.
Filter based PMF: √; PMF-AMS: √√; Filter based PMF and PMF-AMS: √√√;

Locations	Sampling periods	Methodologies				Main conclusions	References
		EC-tracer	CMB	SOA-tracer	PMF		
Pittsburgh, Pennsylvania (USA)	Annual (July 2001 - July 2002)	X	X			Good agreement (r^2=0.71, slope=0.75). Better in summer (r^2=0.81, slope=0.91) than in winter (r^2=0.45, slope=0.75).	(Subramanian et al., 2007)
London, Birmingham, Birmingham (UK) *	Summer (June – August 2010)	X	X			SOC estimates were in broad agreement (urban sites, r^2=0.70-0.92, slope=0.80-0.92; rural site, r^2=0.69-0.92, slope=0.73-0.88).	(Pant et al., 2014)
Atlanta, Birmingham, Centreville, Yorkville (USA)	Annual (January 2000 - December 2002)		X		√[1]	Lower SOC estimates using PMF. Good correlation between SOC estimates using CMB and EC tracer method (CMB vs EC, r=0.67-0-.84; CMB vs PMF, r=0.58-0.74; EC vs PMF, r=0.40-0.78). Comparable SOC levels (CMB vs EC) at urban sites while at rural sites, larger SOC levels estimated using CMB.	(Lee et al., 2008b)
Atlanta (USA)	Summer/Winter (February 1999 - December 2007)	X	X		√[1]	Higher SOC estimates using CMB especially in winter. CMB vs EC vs PMF: summer: 2.0±0.9 vs 1.5±1.4 vs 1.4±0.8 µg m^{-3}; winter 1.8±1.0 vs 0.8±2.0 vs 0.9±0.9 µg m^{-3}. The highest uncertainty were obtained using the EC tracer method. The PMF uncertainties were significantly higher than the uncertainties in the CMB method.	(Pachon et al., 2010)
Pittsburgh (USA)	Annual (July 2001 - August 2002)	X	X		√√√[1,2]	All methods (EC tracer, CMB, PMF-filter and PMF-AMS) provided the same seasonal pattern with more SOA in summer than in winter. Summer, EC tracer vs other approaches: 55-70 vs 30-40% SOC in $PM_{2.5}$ OC; winter, CMB vs other approaches: 50 vs 10% SOC in $PM_{2.5}$ OC. PMF-filter vs CMB: Non-winter: r^2=0.55, slope=0.72; in winter, poor correlation and low slope.	(Shrivastava et al., 2007)
Riverside (USA)	Summer (July - August 2005)	X	X		√√	SOA estimates were consistent for all the methods. Diurnal cycles of SOA/OA ratios were similar with maximum ratios observed during the early afternoon. However, the EC-tracer method apportioned SOA slightly differently throughout the evening/night.	(Docherty et al., 2008)
Birmingham, Centreville, Atlanta (USA)	Spring/Summer (August 2003 - August 2005)	X		X		For Atlanta, SOC estimates were similar (EC vs SOA tracer: spring: 1.4 vs 1.3 µg m^{-3}; summer: 1.2 vs 1.4 µg m^{-3}). For Birmingham and Centreville the differences were significantly larger (on average, 1.8 vs 2.8 µg m^{-3}; 1.2 vs 2.7 µg m^{-3}, respectively).	(Kleindienst et al., 2010)
Wangqingsha, Pearl River Delta (China)	Summer (August – September 2008), Fall-Winter (November – December 2008)	X		X		Good agreement in summer (r=0.57, slope=0.91, EC vs SOA tracer SOC: 3.2 vs 3.1 µg m^{-3}) and better than in fall-winter (EC vs SOA tracer SOC: 6.7 vs 2.0 µg m^{-3}). The minimum OC/EC ratio could be not representative of $(OC/EC)_p$ in winter season (biomass burning impacted). In fall-winter, other SOA precursors ("non-traditional" SOA) were probably significant but not considered in the SOA tracer method.	(Ding et al., 2012)
Marseille (France)	Summer (June - July 2008)		X	X		Both methods followed different temporal trends (only biogenic SOC was considered for the SOA tracer method) (r^2=0.18). CMB vs SOA tracer: 2.1-8.5 vs 0.0-0.6 µg m^{-3}.	(El Haddad et al., 2011)
Hong Kong, (China)	Summer (July – August 2006)		X	X	√[1+2]	SOC estimates showed very similar time evolutions throughout the sampling period. The average SOC from CMB, PMF-filter and SOA tracer method were: 7.8, 6.8 and 5.0 µg m^{-3} during high pollution episodes (regional transport) and 1.2, 0.7 and 0.5 µg m^{-3} under the influence of local emissions (local days).	(Hu et al., 2010)

[1]SOC based on sulfate and nitrate factors; [2] SOC factors based on SOA molecular markers; * underlined: rural sites; *italic: suburban sites*; normal: urban sites.

Detroit, Cincinnati, East St. Louis, Northbrook, Bondville (USA)	Annual (March 2004 - February 2005)			X	√[2]	SOA estimates were highly consistent except for few months with high secondary contributions (r^2=0.76, slope=1.01). Underestimation by PMF when the secondary contributions were very low.	(Zhang et al., 2009b)
Shanghai (China)[#] 2 sites: 1 urban + *1 suburban*	Winter (January 2010, January 2011)/Spring (April - May 2010)/Summer (July 2010)/Autumn (October – November 2010)	X		X	√[1+2]	SOA contributions might be underestimated with the SOA tracer method (only terpenes and aromatic compounds considered). EC vs SOA: fall-winter: 2.8-8.8 vs 0.1-0.4 µg m^{-3}; spring-summer 1.5-2.2 vs 0. 1-0.6 µg m^{-3}. PMF (2.1-2.8 µg m^{-3}) with no variation: a large part of the SOC was associated with nitrate and sulfate but not with the measured SOA tracers. SOA tracer and PMF-filter SOC estimates were significantly correlated (r^2=0.68). As commercial standards for many of the tracers are not available, large uncertainty in the quantification of the SOA tracers.	(Feng et al., 2013)
Atlanta (USA)	Summer (July - August 2001)/Winter (January 2002)		X		√[1]	Good correlation between SOC estimates (CMB vs PM, r^2=0.43-0.50, slope= 3.2-7.4). Larger SOC estimates using CMB may be due to the unresolved primary OC that would attribute to the CMB (high bias) and the SOA from the resolved primary sources that have not been included in the PMF SOA (low bias).	(Ke et al., 2008)
Hong Kong (China) 10 sites: 9 urbans + 1 traffic	1998-2002	X			√[1]	The SOC estimates by the EC tracer method were consistently higher than PMF method. Overestimation by 70–212% for the summer samples and by 4–43% for the winter samples. The overestimation by the EC tracer method resulted from the inability of obtaining a single OC/EC ratio that represented a mixture of primary sources varying in time and space.	(Yuan et al., 2006b)
Mexico City (Mexico)	Spring (March 2006)		X		√√	Better agreement using CMB estimates corrected from PMF LOA factor (local low nitrogen OA): 49% ($PM_{2.5}$ OC) vs 46% (PM_1 OC); r^2=0.40, slope=1.01.	(Aiken et al., 2009)
Guangzhou (China)	Summer (July 2006)	X			√√	Good correlation between SOC and OOA from PMF (r^2=0.60) but low regression slope (0.31) indicating that there was a substantial amount of noncarbon elements (e.g. O, N) in OOA.	(Hu et al., 2012)
Jiaxing, Yangtze River Delta (China)	Summer (July 2015)/Winter (December 2015)	X			√√	Good agreement in summer with similar time trends (PMF vs EC tracer: 7.2 vs 6.8 µg m^{-3}). In winter, strong biomass burning events led to overestimate SOA using the EC tracer method (3.9 vs 7.0 µg m^{-3}).	(Huang et al., 2013)
Beijing (China)	Fall (November 2013)	X			√√	SOC estimates obtained using EC tracer method were consistent with those from PMF (r^2=0.69) with very similar concentration levels.	(Ji et al., 2016)

4.1 EC-tracer vs CMB

The direct comparison between CMB and EC tracer method has been performed in 6 studies (Docherty et al., 2008; Lee et al., 2008b; Pachon et al., 2010; Pant et al., 2014; Shrivastava et al., 2007; Subramanian et al., 2007) (Table 1).

Overall, a good agreement, in terms of both correlations and absolute concentrations, between both methodologies has been observed in summer while the differences in winter were significantly larger. As explained before (section 3.1.2), the determination of $[OC/EC]_p$ in the EC tracer method might be challenging in winter due to the significant influence of local primary emissions. On the opposite, as observed in Pittsburgh, under the influence of regional air mass with high SOA background concentration levels, $[OC/EC]_p$ and/or the intercept used in the EC-tracer method may be overestimated leading to an underestimation of the SOC concentrations (Shrivastava et al., 2007; Subramanian et al., 2007). The impact of the determination of $[OC/EC]_p$ has been also observed for the study of the SOC diurnal cycles in Riverside. The reported diurnal cycles were similar using both EC tracer and CMB, methodologies (and PMF too) but slightly higher SOA/OA ratios have been observed throughout the evening/night using the EC-tracer method. This probably resulted from lower $[OC/EC]_p$ estimated during the night due to reduced diesel traffic at that time (Docherty et al., 2008). Overall, CMB approach seemed to overestimate SOC by comparison to the EC tracer method and again especially in cold period. The overestimation could be due to the significant contributions to OC of unknown and/or unresolved primary sources (e.g. cooking activities and natural gas combustion) then accounted as SOC (Lee et al., 2008b) (see section 3.2.2). Besides, SOC estimates seemed comparable at urban sites while larger SOC estimates made by CMB were observed at rural sites (Lee et al., 2008b). Again, the estimation of $[OC/EC]_p$ is quite challenging especially in remote locations which are far from the primary sources (see section 3.1.2). Finally, higher uncertainties have been noticed using the EC tracer method and can be

explained by the different approaches used for the estimation of $[OC/EC]_p$ (Docherty et al., 2008; Pachon et al., 2010).

4.2 SOA-tracer vs other methodologies (EC-tracer, CMB and PMF-filter)

The comparison of SOC evaluated using the SOA tracer method with other methodologies such as the EC tracer method, CMB and PMF has been reported in few studies (Ding et al., 2012; El Haddad et al., 2011; Feng et al., 2013; Hu et al., 2010; Kleindienst et al., 2010; Zhang et al., 2009b) (Table 1).

Results obtained with the SOA tracer approach agreed well with the other methodologies. However, the SOA tracer method tended to underestimate the SOC concentrations. As explained before (section 3.3.2), the number of SOA tracers and so, of SOA precursors, considered in the method is limited. This is especially true for anthropogenic SOA precursors (only toluene SOA is considered) explaining that the agreement observed was better in summer (Ding et al., 2012; Kleindienst et al., 2010), with a stronger biogenic SOA impact, than in fall-winter (Ding et al., 2012; Feng et al., 2013). SOA derived from biomass burning in such periods could be significant but is not considered in the "traditional" SOA tracer method. Besides, the accuracy of both CMB and EC tracer methodologies, could be affected by the local primary sources in winter (see sections 2.1.2, 3.2.2 and 4.1). However, the agreement between the SOA tracer method with CMB could be also weak even in summer when only biogenic SOA tracers are considered, highlighting the importance of anthropogenic SOA precursors even in warm period (El Haddad et al., 2011; Feng et al., 2013; Hu et al., 2010). The comparisons made with PMF-filter were quite consistent (Zhang et al., 2009b). It is also worth to note that when the secondary contributions were very low, the PMF-filter method underestimated the SOC concentrations, by comparison with the SOA tracer. This may be due to the non-linearity of the yield curve or errors introduced by PMF-filter because of the error structure of data at these

very low levels (Zhang et al., 2009b). Finally, large uncertainties in the SOA tracer method could be linked to the fact that the quantification of the SOA markers was not achieved with the use of authentic standards (Feng et al., (2013), section 3.3.2).

4.3 PMF vs other methodologies (EC-tracer, CMB)

There are several examples in the literature where the PMF-filter (Feng et al., 2013; Hu et al., 2010; Ke et al., 2008; Lee et al., 2008b; Pachon et al., 2010; Shrivastava et al., 2007; Yuan et al., 2006b; Zhang et al., 2009b) or PMF-AMS (Aiken et al., 2009; Docherty et al., 2008; Hu et al., 2012; Huang et al., 2013; Ji et al., 2016; Lee et al., 2008b; Shrivastava et al., 2007) methodologies have been compared with the CMB and/or EC tracer methods (Table 1).

A good agreement between PMF, for both PMF-filter and PMF-AMS, and the other methodologies, has been usually observed with significant correlations and similar SOC estimates. As seen before, both CMB and EC tracer methods tended to overestimate SOC, notably in winter period, due to the inherent limitations of both methodologies when the sampling site is locally influenced by primary emissions (Feng et al., 2013; Huang et al., 2013; Ke et al., 2008; Lee et al., 2008b; Pachon et al., 2010; Shrivastava et al., 2007; Yuan et al., 2006b) (see sections 2.1.2, 3.2.2 and 4.1).

The impact of local sources has been highlighted by Aiken et al. (2009) who observed, in spring in Mexico, a better agreement between CMB and PMF-AMS after subtracting the local low nitrogen OA fraction (LOA) from the non-apportioned OC, assumed to be SOC, obtained initially with CMB. In addition, the difference between PMF-AMS and the EC tracer method could also be significant even in summer when a substantial amount of non-carbon elements (i.e. O, N) were probably included in the OOA (Hu et al., 2012). However, the good agreement between PMF-AMS and the other methodologies was supported by the fact that nice

correlations (r^2=0.9) and regression slopes (0.8-0.9) were usually obtained between POC and HOA (in summer season) (Aiken et al., 2009; Hu et al., 2012; Zhang et al., 2005).

SOC estimated from the PMF-filter approach was generally lower than that from the CMB or EC tracer methodologies (Lee et al., 2008b; Shrivastava et al., 2007; Yuan et al., 2006b). PMF could over-attribute OC to certain factors because the model fits the measured OC while CMB only fits the molecular marker data. This occurred if markers for some important categories of OC (typically SOC ones) were not included in the PMF model. (Shrivastava et al., 2007). Without the use of SOA markers, SOC was apportioned based on the OC content of the nitrate and sulfate factors (see section 3.4.3) and the results obtained could not provide further information on SOC because of the colinearity of OC sources (Pachon et al., 2010). As mentioned before for the SOA tracer method (section 3.3.2), the identification of new molecular markers from other SOA precursors is strongly needed and would allow a better description of the SOC associated with nitrate and sulfate factors (Feng et al., 2012).

Finally, the different SOC apportionment approaches provide consistent results and they can achieve the same conclusions especially in the warm period. A good SOC apportionment may be more difficult to achieve when the influence of local (anthropogenic) emissions, like in the cold period, is significant (EC tracer method and CMB) or due to the lack of SOA molecular markers to account SOA from, notably, anthropogenic precursors and/or sources (SOA tracer method and PMF-filter).

5 Comparison based on the overall picture obtained from the review of recent studies

The above discussions show that results obtained using different SOC apportionment methodologies are comparable under certain conditions. Thus, a comparison of the SOC estimates obtained worldwide, and reviewed before, is proposed in this section. To get

comparable results, only urban and suburban locations are considered and both, annual and spring-summer SOC estimates are discussed.

5.1 Comparison of the annual SOC estimates obtained worldwide

A comparison of annual SOC estimates obtained in North America, Europe, the Middle East, India and China using CMB and EC tracer method is presented on Figure 9 (data from Tables A2 and B2). Results from other methodologies are not included due to the lack of data points on annual scale.

Overall, SOC estimates evaluated using the EC tracer method are always higher than the ones obtained with CMB whatever the geographical region considered. In North America, the agreement observed is quite good but the differences are particularly significant for Europe and China where a factor of about 2, in terms of both contributions and concentrations, between both methodologies can be seen. Similarly, in India, a factor of 2 can be observed but only for SOC concentrations. Both estimated SOC contributions are quite similar in this case. Previous discussions have already accentuated the fact that the selection of $[OC/EC]_p$ is quite challenging in cold period (fall-winter) under the influence of local primary sources (notably biomass burning) leading to an overestimation of SOC (see sections 3.1.2 and 4). This is particularly true for Europe, China where biomass burning for residential heating, and to a lesser extent, for cooking purposes in China and India, is one of the major sources of OA in winter (Chen et al., 2017; Denier van der Gon et al., 2015; Fountoukis et al., 2014; Gelencsér et al., 2007; Viana et al., 2015). Interestingly, the SOC estimates in the Middle East using CMB and EC tracer method are very similar. The stable climate and meteorological conditions through the year with no proper heating period explain such observations with low bias then more consistency between both methodologies.

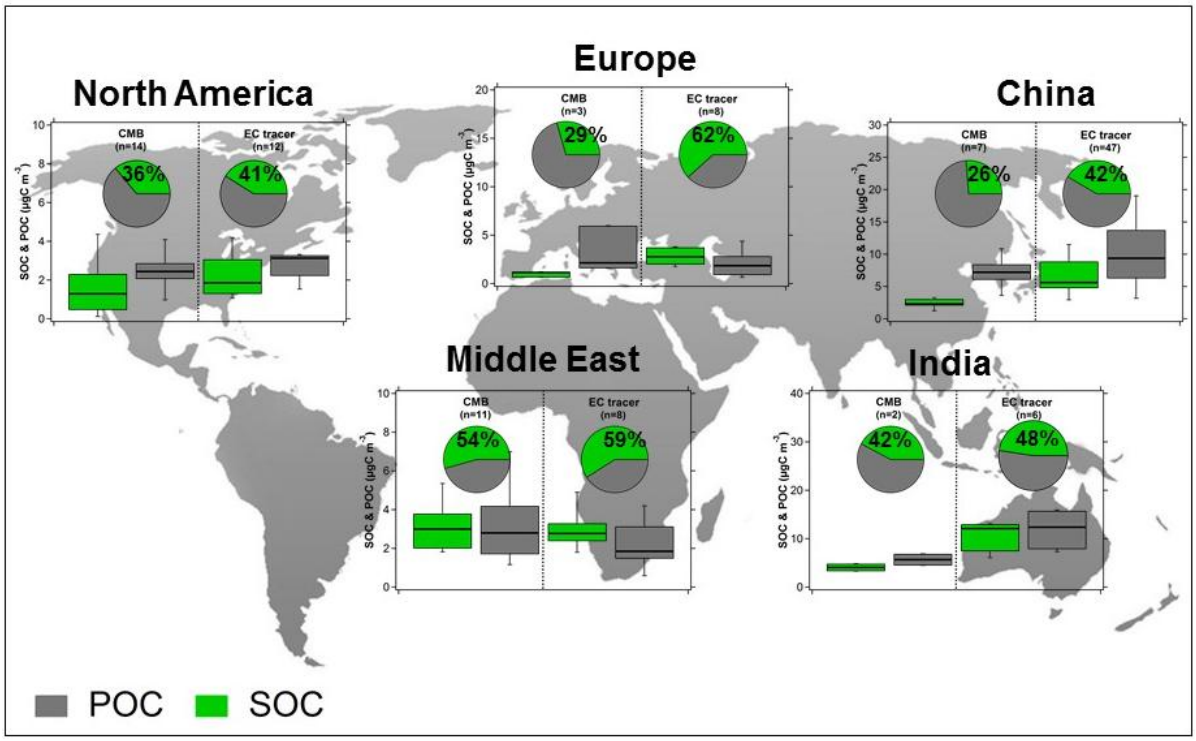

Figure 9. Comparison of annual SOC estimates ($PM_{2.5}$) obtained using CMB and EC tracer method for North America, Europe, the Middle East, India and China. Only urban and suburban locations are included. Box-plots show the SOC and POC concentrations (µgC m^{-3}) for each continent and each method. Into brackets, number of data points considered.

Despite the limitations of both methodologies (see sections 3.1.2, 3.2.2 and 4), clear patterns can be observed with annual SOC, and POC, concentration levels comparable in India and China and twice higher than the ones estimated in the other regions of the world. These results agree with modelling evaluations in terms of both annual SOA concentration levels and world distribution (Hodzic et al., 2016). They also highlight the significant influence of anthropogenic SOA in the developing countries (Hodzic et al., 2016; Huang et al., 2014). It seems more difficult to conclude in terms of SOC contributions due the inherent limitations of both methodologies especially when the cold period is also considered. A probably better overview can be made based on spring-summer SOC estimates only, and as presented below.

5.2 Comparison of the spring-summer SOC estimates obtained worldwide

The comparison of SOC estimates obtained for the spring-summer period in North America, Europe and China using CMB, EC tracer, SOA tracer and PMF-AMS methodologies is presented on Figure 10 (data from Tables A3, B3, C3 and D2). The results from the SOA tracer method are not included for Europe to avoid any kind of false representation because only biogenic SOC has been accounted in the studies reviewed. The results from ^{14}C measurements are also not included because they arise from other methodologies such as EC tracer or CMB.

When focusing on the warm period, a good agreement can be seen between all methodologies for both SOC contributions and average SOC concentrations. However, the SOA tracer method tends to underestimate the SOC estimates and it is particularly obvious for China. The rapid urbanization and industrialization in China have led to high emission of anthropogenic SOA precursors (Huang et al., 2014). However, and as detailed before (sections 3.3.2 and 4.2), only one anthropogenic marker (DHOPA) from toluene photooxidation is accounted for the SOA tracer method to estimate the SOA from anthropogenic sources. SOC from the oxidation of numerous other VOC and SVOC/IVOCS (i.e. alkanes, PAHs, furans, phenolic compounds) is not considered using such methodology. It is true that the biogenic emissions of isoprenoids (including both isoprene and monoterpenes) are significantly larger than the emissions of anthropogenic VOCs in China during daytime in summer (Tie et al., 2006). Nevertheless, several studies have also shown a high regional background of anthropogenic VOCs in summer that could lead to significant secondary SOA formation (Feng et al., 2013; Guo et al., 2012) explaining the observed SOC underestimation using the SOA tracer method. Besides, biogenic emissions, including SOA precursors such as isoprene and monoterpenes, significantly impact the organic loading during summer in North America (Budisulistiorini et al., 2015; Carlton et al., 2016; Guenther et al., 2006; Hantson et al., 2017; Heald et al., 2008; Lathiere et al., 2006; Zhang et al., 2018) (sections 3.2.3.1 and 3.3.3.1 and

3.5.3.1). As seen before, the biogenic SOA fraction is well documented in the SOA tracer method (see section 3.3) explaining the comparable SOC estimates obtained with the other methodologies for North America.

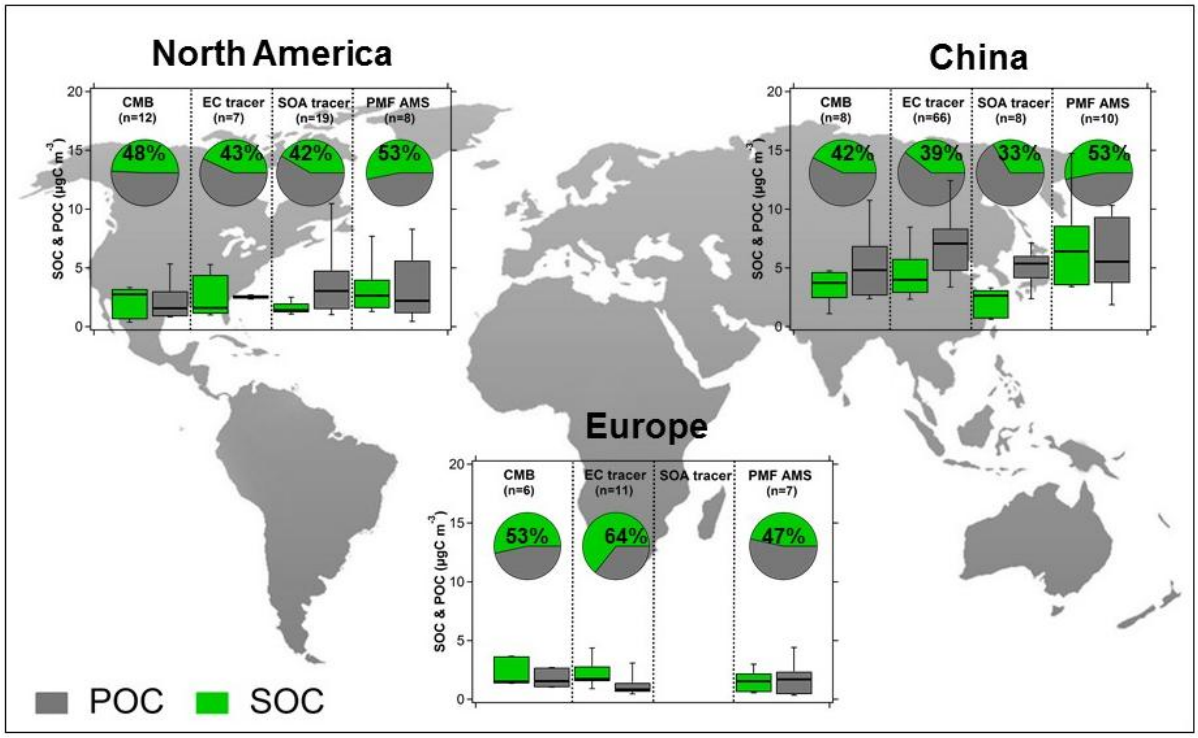

Figure 10. Comparison of spring-summer SOC estimates obtained using CMB, EC tracer method, SOA tracer method ($PM_{2.5}$) and PMF-AMS (PM_1) for North America, Europe and China. Only urban and suburban locations are included. Box-plots show the SOC and POC concentrations (µgC m^{-3}) for each continent and each method. Into brackets, number of data points considered.

Finally, the SOC contributions to $PM_{2.5}$ or PM_1 OC in spring-summer period are comparable in all the regions considered and in the range 39-64% (excluding the SOA tracer method for China). Average spring-summer SOC concentration ranges are similar in North America and Europe (1-3 µgC m^{-3}) and are significantly higher in China (4-6 µgC m^{-3}). The relatively good consistency between the different methodologies in North America, for both SOC concentration levels and contributions, may suggest that forest fire events, which are usually episodic in

summer, are not a major contributor to SOA, although they could play an important role on the PM concentration levels (Kaulfus et al., 2017; Roy et al., 2018). Biogenic SOA should dominate in such seasons. It is also worth to note the wide range of SOC concentrations observed in China notably from the PMF-AMS results. This country experiences recurrent severe haze pollution events even in summer time, with fine PM reaching very high concentration levels across many cities (Du et al., 2011; Huang et al., 2014) and SOA is a significant contributor to such PM concentrations (Huang et al., 2014; Lee, 2015). Thus, these specific events, especially characterized using AMS/ACSM instrumentation, could explain, to a certain extent, the observed variability of SOC concentrations in China.

6 Conclusion and future implications

This review has discussed the results reported on SOC estimates obtained by different methodologies in previous studies. Although the SOC estimates are method dependent, the results reviewed here confirm that SOC constitutes a significant fraction of OC.

The different methodologies to apportion SOC witness a certain number of uncertainties but they finally provide quite consistent results especially in the warm period (spring-summer). The selection of the appropriate methodology should be done very carefully because each approach has its own advantages and disadvantages.

As it requires only the determination of the concentrations of EC and OC, the EC tracer method is clearly the easiest methodology to use. This method gives a very good estimation of SOC, however, it is also strongly limited in winter due to the difficulty to estimate without any ambiguity primary OC. CMB also provides SOC concentrations and contributions in good agreement with the other approaches. The lack of emission profiles for uncommon and thus un-apportioned sources inducing an overestimation of SOC, is the principal limitation of this methodology. This is especially the case when the sampling site is strongly affected by local emissions sources. The current development of emission profile databases, such as SPECIATE

or SPECIEUROPE, is of great value to get the appropriate input to the CMB model for each case study and to finally get a better evaluation of SOC (Pernigotti et al., 2016; Simon et al., 2010). In combination with such methodologies, the use of radiocarbon measurements (^{14}C) may provide detailed information on the SOC origins and can be helpful to improve the understanding of the atmospheric processes involved. Nevertheless, the main limitations are related to the analytical costs and the amount of material required. Thus, this methodology is difficult to be implemented routinely to get a more detailed estimation of SOC. Similarly, PMF-AMS (or PMF-ACSM) provides a good estimation of SOC with low uncertainty, together with additional information about the SOA oxidation state and/or the volatility range. As mentioned before, detailed analyses can highlight additional sub-SOA fractions such as IEPOX-SOA or marine SOA (Budisulistiorini et al., 2013; Chang et al., 2011; Crippa et al., 2013b; Hu et al., 2015; Zhang et al., 2017). More sub-SOA factors are then expected but they are difficult to be resolved due to the non-specific nature of the mass fragments obtained. Only a detailed chemical characterization at the molecular level and the use of key species, i.e. molecular markers, allows to get a definitive link between SOC content and SOA sources. Both the SOA tracer method and PMF-filter, with or without the use of molecular markers (based on nitrate and sulfate factors in such a case), are in good agreement with the other SOC apportionment methodologies, especially in the warm period in the case of the SOA tracer method. The lack of markers for several SOA sources or SOA precursors, notably to account for anthropogenic SOA, together with the SOA/SOC mass ratio data, are probably the main limitations of such methodologies. Additionally, an evaluation of the stability of the molecular markers is strongly needed (Nozière et al., 2015).

The full discrimination and comprehension of OA sources are still difficult to achieve due to the complexity and the variability of the processes involved. By comparison to AMS, the recent development of new instrumentation provides an on-line aerosol chemical

characterization at the molecular level which, combined with PMF analysis, allows a better description of the OA and SOA sources. The shortcomings of low time resolution with filter measurements can be overcome using this kind of instruments to elucidate more information about the chemical processes involved. Such instrumentations include, for instance, TAG-AMS (thermal desorption aerosol gas chromatograph-AMS) (Williams et al., 2010; Williams et al., 2014; Zhang et al., 2016), EESI-TOF-MS (extractive electrospray ionization-time of flight-MS) (Doezema et al., 2012; Gallimore et al., 2017; Gallimore and Kalberer, 2013; Slowik et al., 2017; Stefenelli et al., 2017), or different inlets associated to PTR-MS (proton-transfer reaction-MS) or CIMS (chemical ionization MS) such as FIGAERO (filter inlet for gases and aerosols) (Lopez-Hilfiker et al., 2014), CHARON (chemical analysis of aerosol online) or thermo-desorption (TD) systems (Eichler et al., 2015; Gkatzelis et al., 2017; Holzinger et al., 2010; Salvador et al., 2016), which have been successfully applied to apportion SOC in details. However, these instruments are still costly and only appropriate for short term studies.

In parallel, like in the case of ^{14}C measurements, several authors have reported the combination of different datasets from several measurement systems to refine the source apportionment of SOA using PMF. Slowik et al. (2010) were the first ones to combine the AMS and PTR-MS data measurements, highlighting the capability of PMF to resolve more SOA (OOA) factors and improving the interpretations of their sources and photochemical processes (Crippa et al., 2013a; Slowik et al., 2010). This kind of approach has been explored in other studies, with the combination of AMS or ACSM data with other measurements, such as ambient and thermally denuded OA spectra (TD-PMF-AMS) (Docherty et al., 2011), by merging high resolution mass spectra of organic and inorganic aerosols from AMS measurements (McGuire et al., 2014; Sun et al., 2012) or combining offline AMS data and organic markers or ^{14}C measurements (Huang et al., 2014; Vlachou et al., 2017). In addition, the combination of PMF-ACSM outputs with inorganic species and black carbon (BC) measurements (Petit et al., 2014)

or ACSM mass spectra with metal concentrations (Sofowote et al., 2018), allowed the source apportionment of PM rather than only OA. This further suggests that a combination of approaches could enhance the understanding about subtler differences existing in OA and SOA content by accounting for different measurements.

Finally, all of these improvements in the understanding of SOA sources and formation will facilitate to bridge the existing gap between atmospheric models and field measurements (Aksoyoglu et al., 2011; Bessagnet et al., 2016; Ciarelli et al., 2016b; Ciarelli et al., 2017).

Acknowledgements

The authors wish to thank the French Ministry of Environment (MTES) for its financial support and Patrick Bodu for the design of the figures.

References

Abdeen, Z., Qasrawi, R., Heo, J., Wu, B., Shpund, J., Vanger, A., Sharf, G., Moise, T., Brenner, S., Nassar, K., Saleh, R., Al-Mahasneh, Q.M., Sarnat, J.A., Schauer, J.J., 2014. Spatial and Temporal Variation in Fine Particulate Matter Mass and Chemical Composition: The Middle East Consortium for Aerosol Research Study. Sci. World J. 2014, 878704.

Acosta Navarro, J.C., Smolander, S., Struthers, H., Zorita, E., Ekman, A.M., Kaplan, J., Guenther, A., Arneth, A., Riipinen, I., 2014. Global emissions of terpenoid VOCs from terrestrial vegetation in the last millennium. J. Geophys. Res.-Atmos. 119, 6867-6885.

Aiken, A.C., Salcedo, D., Cubison, M.J., Huffman, J.A., DeCarlo, P.F., Ulbrich, I.M., Docherty, K.S., Sueper, D., Kimmel, J.R., Worsnop, D.R., Trimborn, A., Northway, M., Stone, E.A., Schauer, J.J., Volkamer, R.M., Fortner, E., de Foy, B., Wang, J., Laskin, A., Shutthanandan, V., Zheng, J., Zhang, R., Gaffney, J., Marley, N.A., Paredes-Miranda, G., Arnott, W.P., Molina, L.T., Sosa, G., Jimenez, J.L., 2009. Mexico City aerosol analysis during MILAGRO using high resolution aerosol mass spectrometry at the urban supersite (T0) – Part 1: Fine particle composition and organic source apportionment. Atmos. Chem. Phys. 9, 6633-6653.

Aksoyoglu, S., Keller, J., Barmpadimos, I., Oderbolz, D., Lanz, V., Prévôt, A., Baltensperger, U., 2011. Aerosol modelling in Europe with a focus on Switzerland during summer and winter episodes. Atmos. Chem. Phys 11, 7355-7373.

Albinet, A., Papaiconomou, N., Estager, J., Suptil, J., Besombes, J.-L., 2010. A new ozone denuder for aerosol sampling based on an ionic liquid coating. Anal. Bioanal. Chem. 396, 857-864.

Allan, J.D., Delia, A.E., Coe, H., Bower, K.N., Alfarra, M.R., Jimenez, J.L., Middlebrook, A.M., Drewnick, F., Onasch, T.B., Canagaratna, M.R., 2004. A generalised method for the extraction of chemically resolved mass spectra from Aerodyne aerosol mass spectrometer data. J. Aerosol Sci. 35, 909-922.

Arnold, S., Spracklen, D., Williams, J., Yassaa, N., Sciare, J., Bonsang, B., Gros, V., Peeken, I., Lewis, A., Alvain, S., 2009. Evaluation of the global oceanic isoprene source and its impacts on marine organic carbon aerosol. Atmos. Chem. Phys. 9, 1253-1262.

Batmunkh, T., Kim, Y.J., Lee, K.Y., Cayetano, M.G., Jung, J.S., Kim, S.Y., Kim, K.C., Lee, S.J., Kim, J.S., Chang, L.S., An, J.Y., 2011. Time-Resolved Measurements of PM2.5 Carbonaceous Aerosols at Gosan, Korea. J. Air Waste Manage. Assoc. 61, 1174-1182.

Bessagnet, B., Pirovano, G., Mircea, M., Cuvelier, C., Aulinger, A., Calori, G., Ciarelli, G., Manders, A., Stern, R., Tsyro, S., García Vivanco, M., Thunis, P., Pay, M.T., Colette, A., Couvidat, F., Meleux, F., Rouïl, L., Ung, A., Aksoyoglu, S., Baldasano, J.M., Bieser, J., Briganti, G., Cappelletti, A., D'Isidoro, M., Finardi, S., Kranenburg, R., Silibello, C., Carnevale, C., Aas, W., Dupont, J.C., Fagerli, H., Gonzalez, L., Menut, L., Prévôt, A.S.H., Roberts, P., White, L., 2016. Presentation of the EURODELTA III intercomparison exercise – evaluation of the chemistry transport models' performance on criteria pollutants and joint analysis with meteorology. Atmos. Chem. Phys. 16, 12667-12701.

Birch, M.E., Cary, R.A., 1996. Elemental carbon-based method for occupational monitoring of particulate diesel exhaust: methodology and exposure issues. Analyst 121, 1183-1190.

Blanchard, C.L., Hidy, G.M., Tanenbaum, S., Edgerton, E., Hartsell, B., Jansen, J., 2008. Carbon in southeastern U.S. aerosol particles: Empirical estimates of secondary organic aerosol formation. Atmos. Environ. 42, 6710-6720.

Błaszczak, B., Rogula-Kozłowska, W., Mathews, B., Juda-Rezler, K., Klejnowski, K., Rogula-Kopiec, P., 2016. Chemical Compositions of PM2.5 at Two Non-Urban Sites from the Polluted Region in Europe. Aerosol. Air Qual. Res. 16, 2333-2348.

Bozzetti, C., Daellenbach, K.R., Hueglin, C., Fermo, P., Sciare, J., Kasper-Giebl, A., Mazar, Y., Abbaszade, G., El Kazzi, M., Gonzalez, R., Shuster-Meiseles, T., Flasch, M., Wolf, R., Křepelová, A., Canonaco, F., Schnelle-Kreis, J., Slowik, J.G., Zimmermann, R., Rudich, Y., Baltensperger, U., El Haddad, I., Prévôt, A.S.H., 2016. Size-Resolved Identification, Characterization, and Quantification of Primary Biological Organic Aerosol at a European Rural Site. Environ. Sci. Technol. 50, 3425-3434.

Bozzetti, C., El Haddad, I., Salameh, D., Daellenbach, K.R., Fermo, P., Gonzalez, R., Minguillón, M.C., Iinuma, Y., Poulain, L., Elser, M., Müller, E., Slowik, J.G., Jaffrezo, J.L., Baltensperger, U., Marchand, N., Prévôt, A.S.H., 2017. Organic aerosol source apportionment by offline-AMS over a full year in Marseille. Atmos. Chem. Phys. 17, 8247-8268.

Bruns, E.A., El Haddad, I., Slowik, J.G., Kilic, D., Klein, F., Baltensperger, U., Prévôt, A.S.H., 2016. Identification of significant precursor gases of secondary organic aerosols from residential wood combustion. Sci. Rep. 6, 27881.

Buchholz, B.A., Fallon, S.J., Zermeño, P., Bench, G., Schichtel, B.A., 2013. Anomalous elevated radiocarbon measurements of PM2.5. Nucl. Instrum. Methods Phys. Res., Sect. B 294, 631-635.

Budisulistiorini, S., Li, X., Bairai, S., Renfro, J., Liu, Y., Liu, Y., McKinney, K., Martin, S., McNeill, V., Pye, H., 2015. Examining the effects of anthropogenic emissions on isoprene-derived secondary organic aerosol formation during the 2013 Southern Oxidant and Aerosol Study (SOAS) at the Look Rock, Tennessee ground site. Atmos. Chem. Phys. 15, 8871-8888.

Budisulistiorini, S.H., Canagaratna, M.R., Croteau, P.L., Marth, W.J., Baumann, K., Edgerton, E.S., Shaw, S.L., Knipping, E.M., Worsnop, D.R., Jayne, J.T., Gold, A., Surratt, J.D., 2013. Real-Time Continuous Characterization of Secondary Organic Aerosol Derived from Isoprene Epoxydiols in Downtown Atlanta, Georgia, Using the Aerodyne Aerosol Chemical Speciation Monitor. Environ. Sci. Technol. 47, 5686-5694.

Cabada, J.C., Pandis, S.N., Subramanian, R., Robinson, A.L., Polidori, A., Turpin, B., 2004. Estimating the Secondary Organic Aerosol Contribution to PM2.5 Using the EC Tracer Method Special Issue of Aerosol Science and Technology on Findings from the Fine Particulate Matter Supersites Program. Aerosol Sci. Technol. 38, 140-155.

Cao, J., Lee, S., Chow, J.C., Watson, J.G., Ho, K., Zhang, R., Jin, Z., Shen, Z., Chen, G., Kang, Y., 2007. Spatial and seasonal distributions of carbonaceous aerosols over China. J. Geophys. Res.-Atmos. 112.

Carlton, A., Jimenez, J., Ambrose, J., Brown, S., Baker, K., Brock, C., Cohen, R., Edgerton, S., Farkas, C., Farmer, D., 2016. The Southeast Atmosphere Studies (SAS): Coordinated Investigation and Discovery to Answer Critical Questions About Fundamental Atmospheric Processes. Bull. Am. Meteorol. Soc.

Carlton, A.G., Wiedinmyer, C., Kroll, J.H., 2009. A review of Secondary Organic Aerosol (SOA) formation from isoprene. Atmos. Chem. Phys. 9, 4987-5005.

Castro, L.M., Pio, C.A., Harrison, R.M., Smith, D.J.T., 1999. Carbonaceous aerosol in urban and rural European atmospheres: estimation of secondary organic carbon concentrations. Atmos. Environ. 33, 2771-2781.

Cavalli, F., Viana, M., Yttri, K., Genberg, J., Putaud, J.-P., 2010. Toward a standardised thermal-optical protocol for measuring atmospheric organic and elemental carbon: the EUSAAR protocol. Atmos. Meas. Tech. 3, 79-89.

Chan, A.W.H., Kautzman, K.E., Chhabra, P.S., Surratt, J.D., Chan, M.N., Crounse, J.D., Kürten, A., Wennberg, P.O., Flagan, R.C., Seinfeld, J.H., 2009. Secondary organic aerosol formation from photooxidation of naphthalene and alkylnaphthalenes: implications for oxidation of intermediate volatility organic compounds (IVOCs). Atmos. Chem. Phys. 9, 3049-3060.

Chang, R.Y.W., Leck, C., Graus, M., Müller, M., Paatero, J., Burkhart, J.F., Stohl, A., Orr, L.H., Hayden, K., Li, S.M., Hansel, A., Tjernström, M., Leaitch, W.R., Abbatt, J.P.D., 2011. Aerosol composition and sources in the central Arctic Ocean during ASCOS. Atmos. Chem. Phys. 11, 10619-10636.

Chen, J., Li, C., Ristovski, Z., Milic, A., Gu, Y., Islam, M.S., Wang, S., Hao, J., Zhang, H., He, C., Guo, H., Fu, H., Miljevic, B., Morawska, L., Thai, P., Lam, Y.F., Pereira, G., Ding, A., Huang, X., Dumka, U.C., 2017. A review of biomass burning: Emissions and impacts on air quality, health and climate in China. Sci. Total Environ. 579, 1000-1034.

Chen, J., Ying, Q., Kleeman, M.J., 2010a. Source apportionment of wintertime secondary organic aerosol during the California regional PM10/PM2.5 air quality study. Atmos. Environ. 44, 1331-1340.

Chen, L.-W.A., Watson, J.G., Chow, J.C., DuBois, D.W., Herschberger, L., 2010b. Chemical mass balance source apportionment for combined PM2.5 measurements from US non-urban and urban long-term networks. Atmos. Environ. 44, 4908-4918.

Chen, Y., Xie, S., Luo, B., Zhai, C., 2014. Characteristics and origins of carbonaceous aerosol in the Sichuan Basin, China. Atmos. Environ. 94, 215-223.

Cheng, Y., He, K.-b., Duan, F.-k., Du, Z.-y., Zheng, M., Ma, Y.-l., 2012. Characterization of carbonaceous aerosol by the stepwise-extraction thermal–optical-transmittance (SE-TOT) method. Atmos. Environ. 59, 551-558.

Chiappini, L., Verlhac, S., Aujay, R., Maenhaut, W., Putaud, J.P., Sciare, J., Jaffrezo, J.L., Liousse, C., Galy-Lacaux, C., Alleman, L.Y., Panteliadis, P., Leoz, E., Favez, O., 2014. Clues for a standardised thermal-optical protocol for the assessment of organic and elemental carbon within ambient air particulate matter. Atmos. Meas. Tech. 7, 1649-1661.

Choi, J.-K., Heo, J.-B., Ban, S.-J., Yi, S.-M., Zoh, K.-D., 2012. Chemical characteristics of PM2.5 aerosol in Incheon, Korea. Atmos. Environ. 60, 583-592.

Chou, C.-K., Lee, C., Cheng, M., Yuan, C., Chen, S., Wu, Y., Hsu, W., Lung, S., Hsu, S., Lin, C., 2010. Seasonal variation and spatial distribution of carbonaceous aerosols in Taiwan. Atmos. Chem. Phys. 10, 9563-9578.

Chow, J.C., Watson, J.G., Chen, L.W.A., Chang, M.C.O., Robinson, N.F., Trimble, D., Kohl, S., 2007. The IMPROVE A Temperature Protocol for Thermal/Optical Carbon Analysis: Maintaining Consistency with a Long-Term Database. J. Air Waste Manage. Assoc. 57, 1014-1023.

Chow, J.C., Watson, J.G., Pritchett, L.C., Pierson, W.R., Frazier, C.A., Purcell, R.G., 1993. The dri thermal/optical reflectance carbon analysis system: description, evaluation and applications in U.S. Air quality studies. Atmos. Environ., Part A 27, 1185-1201.

Chu, S.-H., 2005. Stable estimate of primary OC/EC ratios in the EC tracer method. Atmos. Environ. 39, 1383-1392.

Ciarelli, G., Aksoyoglu, S., Crippa, M., Jimenez, J.-L., Nemitz, E., Sellegri, K., Äijälä, M., Carbone, S., Mohr, C., O'Dowd, C., 2016a. Evaluation of European air quality modelled by CAMx including the volatility basis set scheme. Atmos. Chem. Phys. 16, 10313-10332.

Ciarelli, G., Aksoyoglu, S., Crippa, M., Jimenez, J.L., Nemitz, E., Sellegri, K., Äijälä, M., Carbone, S., Mohr, C., O'Dowd, C., Poulain, L., Baltensperger, U., Prévôt, A.S.H., 2016b. Evaluation of European air quality modelled by CAMx including the volatility basis set scheme. Atmos. Chem. Phys. 16, 10313-10332.

Ciarelli, G., Aksoyoglu, S., El Haddad, I., Bruns, E.A., Crippa, M., Poulain, L., Äijälä, M., Carbone, S., Freney, E., O'Dowd, C., Baltensperger, U., Prévôt, A.S.H., 2017. Modelling winter organic aerosol at the European scale with CAMx: evaluation and source apportionment with a VBS parameterization based on novel wood burning smog chamber experiments. Atmos. Chem. Phys. 17, 7653-7669.

Crenn, V., Sciare, J., Croteau, P.L., Verlhac, S., Fröhlich, R., Belis, C.A., Aas, W., Äijälä, M., Alastuey, A., Artiñano, B., Baisnée, D., Bonnaire, N., Bressi, M., Canagaratna, M., Canonaco, F., Carbone, C., Cavalli, F., Coz, E., Cubison, M.J., Esser-Gietl, J.K., Green, D.C., Gros, V., Heikkinen, L., Herrmann, H., Lunder, C., Minguillón, M.C., Močnik, G., O'Dowd, C.D., Ovadnevaite, J., Petit, J.E., Petralia, E., Poulain, L., Priestman, M., Riffault, V., Ripoll, A., Sarda-Estève, R., Slowik, J.G., Setyan, A., Wiedensohler, A., Baltensperger, U., Prévôt, A.S.H., Jayne, J.T., Favez, O., 2015. ACTRIS ACSM intercomparison – Part 1: Reproducibility of concentration and fragment results from 13 individual Quadrupole Aerosol Chemical Speciation Monitors (Q-ACSM) and consistency with co-located instruments. Atmos. Meas. Tech. 8, 5063-5087.

Crippa, M., Canonaco, F., Lanz, V.A., Äijälä, M., Allan, J.D., Carbone, S., Capes, G., Ceburnis, D., Dall'Osto, M., Day, D.A., DeCarlo, P.F., Ehn, M., Eriksson, A., Freney, E., Hildebrandt Ruiz, L., Hillamo, R., Jimenez, J.L., Junninen, H., Kiendler-Scharr, A., Kortelainen, A.M., Kulmala, M., Laaksonen, A., Mensah, A.A., Mohr, C., Nemitz, E., O'Dowd, C., Ovadnevaite, J., Pandis, S.N., Petäjä, T., Poulain, L., Saarikoski, S., Sellegri, K., Swietlicki, E., Tiitta, P., Worsnop, D.R., Baltensperger, U., Prévôt, A.S.H., 2014. Organic aerosol components derived from 25 AMS data sets across Europe using a consistent ME-2 based source apportionment approach. Atmos. Chem. Phys. 14, 6159-6176.

Crippa, M., Canonaco, F., Slowik, J.G., El Haddad, I., DeCarlo, P.F., Mohr, C., Heringa, M.F., Chirico, R., Marchand, N., Temime-Roussel, B., Abidi, E., Poulain, L., Wiedensohler, A., Baltensperger, U., Prévôt, A.S.H., 2013a. Primary and secondary organic aerosol origin by combined gas-particle phase source apportionment. Atmos. Chem. Phys. 13, 8411-8426.

Crippa, M., El Haddad, I., Slowik, J.G., DeCarlo, P.F., Mohr, C., Heringa, M.F., Chirico, R., Marchand, N., Sciare, J., Baltensperger, U., Prévôt, A.S.H., 2013b. Identification of marine and continental aerosol sources in Paris using high resolution aerosol mass spectrometry. J. Geophys. Res.-Atmos. 118, 1950-1963.

Daellenbach, K.R., Bozzetti, C., Křepelová, A., Canonaco, F., Wolf, R., Zotter, P., Fermo, P., Crippa, M., Slowik, J.G., Sosedova, Y., Zhang, Y., Huang, R.J., Poulain, L., Szidat, S., Baltensperger, U., El Haddad, I., Prévôt, A.S.H., 2016. Characterization and source apportionment of organic aerosol using offline aerosol mass spectrometry. Atmos. Meas. Tech. 9, 23-39.

Daellenbach, K.R., Stefenelli, G., Bozzetti, C., Vlachou, A., Fermo, P., Gonzalez, R., Piazzalunga, A., Colombi, C., Canonaco, F., Hueglin, C., Kasper-Giebl, A., Jaffrezo, J.L., Bianchi, F., Slowik, J.G., Baltensperger, U., El-Haddad, I., Prévôt, A.S.H., 2017. Long-term chemical analysis and organic aerosol source apportionment at nine sites in central Europe: source identification and uncertainty assessment. Atmos. Chem. Phys. 17, 13265-13282.

Daher, N., Ruprecht, A., Invernizzi, G., De Marco, C., Miller-Schulze, J., Heo, J.B., Shafer, M.M., Shelton, B.R., Schauer, J.J., Sioutas, C., 2012. Characterization, sources and redox activity of fine and coarse particulate matter in Milan, Italy. Atmos. Environ. 49, 130-141.

Day, M.C., Zhang, M., Pandis, S.N., 2015. Evaluation of the ability of the EC tracer method to estimate secondary organic carbon. Atmos. Environ. 112, 317-325.

DeCarlo, P.F., Kimmel, J.R., Trimborn, A., Northway, M.J., Jayne, J.T., Aiken, A.C., Gonin, M., Fuhrer, K., Horvath, T., Docherty, K.S., 2006. Field-deployable, high-resolution, time-of-flight aerosol mass spectrometer. Anal. Chem. 78, 8281-8289.

Denier van der Gon, H.A.C., Bergström, R., Fountoukis, C., Johansson, C., Pandis, S.N., Simpson, D., Visschedijk, A.J.H., 2015. Particulate emissions from residential wood combustion in Europe – revised estimates and an evaluation. Atmos. Chem. Phys. 15, 6503-6519.

Després, V., Nowoisky, J., Klose, M., Conrad, R., Andreae, M., Pöschl, U., 2007. Characterization of primary biogenic aerosol particles in urban, rural, and high-alpine air by DNA sequence and restriction fragment analysis of ribosomal RNA genes. Biogeosciences 4, 1127-1141.

Ding, X., He, Q.-F., Shen, R.-Q., Yu, Q.-Q., Zhang, Y.-Q., Xin, J.-Y., Wen, T.-X., Wang, X.-M., 2016. Spatial and seasonal variations of isoprene secondary organic aerosol in China: Significant impact of biomass burning during winter. Sci. Rep. 6, 20411.

Ding, X., He, Q.F., Shen, R.Q., Yu, Q.Q., Wang, X.M., 2014. Spatial distributions of secondary organic aerosols from isoprene, monoterpenes, β-caryophyllene, and aromatics over China during summer. J. Geophys. Res.-Atmos. 119.

Ding, X., Wang, X.-M., Gao, B., Fu, X.-X., He, Q.-F., Zhao, X.-Y., Yu, J.-Z., Zheng, M., 2012. Tracer-based estimation of secondary organic carbon in the Pearl River Delta, south China. J. Geophys. Res. 117.

Ding, X., Zheng, M., Edgerton, E.S., Jansen, J.J., Wang, X., 2008a. Contemporary or Fossil Origin: Split of Estimated Secondary Organic Carbon in the Southeastern United States. Environ. Sci. Technol. 42, 9122-9128.

Ding, X., Zheng, M., Yu, L., Zhang, X., Weber, R.J., Yan, B., Russell, A.G., Edgerton, E.S., Wang, X., 2008b. Spatial and Seasonal Trends in Biogenic Secondary Organic Aerosol Tracers and Water-Soluble Organic Carbon in the Southeastern United States. Environ. Sci. Technol. 42, 5171-5176.

Ding, Y., Pang, Y., Eatough, D.J., 2002. High-volume diffusion denuder sampler for the routine monitoring of fine particulate matter: I. Design and optimization of the PC-BOSS. Aerosol Sci. Technol. 36, 369-382.

Docherty, K.S., Aiken, A.C., Huffman, J.A., Ulbrich, I.M., DeCarlo, P.F., Sueper, D., Worsnop, D.R., Snyder, D.C., Peltier, R.E., Weber, R.J., Grover, B.D., Eatough, D.J., Williams, B.J., Goldstein, A.H., Ziemann, P.J., Jimenez, J.L., 2011. The 2005 Study of Organic Aerosols at Riverside (SOAR-1): instrumental intercomparisons and fine particle composition. Atmos. Chem. Phys. 11, 12387-12420.

Docherty, K.S., Stone, E.A., Ulbrich, I.M., DeCarlo, P.F., Snyder, D.C., Schauer, J.J., Peltier, R.E., Weber, R.J., Murphy, S.M., Seinfeld, J.H., 2008. Apportionment of primary and secondary organic aerosols in Southern California during the 2005 Study of Organic Aerosols in Riverside (SOAR-1). Environ. Sci. Technol. 42, 7655-7662.

Doezema, L.A., Longin, T., Cody, W., Perraud, V., Dawson, M.L., Ezell, M.J., Greaves, J., Johnson, K.R., Finlayson-Pitts, B.J., 2012. Analysis of secondary organic aerosols in air using extractive electrospray ionization mass spectrometry (EESI-MS). RSC Advances 2, 2930-2938.

Donahue, N.M., Robinson, A.L., Pandis, S.N., 2009. Atmospheric organic particulate matter: From smoke to secondary organic aerosol. Atmos. Environ. 43, 94-106.

Dreyfus, M.A., Adou, K., Zucker, S.M., Johnston, M.V., 2009. Organic aerosol source apportionment from highly time-resolved molecular composition measurements. Atmos. Environ. 43, 2901-2910.

Du, H., Kong, L., Cheng, T., Chen, J., Du, J., Li, L., Xia, X., Leng, C., Huang, G., 2011. Insights into summertime haze pollution events over Shanghai based on online water-soluble ionic composition of aerosols. Atmos. Environ. 45, 5131-5137.

Duan, J., Tan, J., Cheng, D., Bi, X., Deng, W., Sheng, G., Fu, J., Wong, M., 2007. Sources and characteristics of carbonaceous aerosol in two largest cities in Pearl River Delta Region, China. Atmos. Environ. 41, 2895-2903.

Eichler, P., Müller, M., D'Anna, B., Wisthaler, A., 2015. A novel inlet system for online chemical analysis of semi-volatile submicron particulate matter. Atmos. Meas. Tech. 8, 1353-1360.

El Haddad, I., D'Anna, B., Temime-Roussel, B., Nicolas, M., Boreave, A., Favez, O., Voisin, D., Sciare, J., George, C., Jaffrezo, J.L., Wortham, H., Marchand, N., 2013. Towards a better understanding of the origins, chemical composition and aging of oxygenated organic aerosols: case study of a Mediterranean industrialized environment, Marseille. Atmos. Chem. Phys. 13, 7875-7894.

El Haddad, I., Marchand, N., Dron, J., Temime-Roussel, B., Quivet, E., Wortham, H., Jaffrezo, J.L., Baduel, C., Voisin, D., Besombes, J.L., Gille, G., 2009. Comprehensive primary particulate organic characterization of vehicular exhaust emissions in France. Atmos. Environ. 43, 6190-6198.

El Haddad, I., Marchand, N., Temime-Roussel, B., Wortham, H., Piot, C., Besombes, J.L., Baduel, C., Voisin, D., Armengaud, A., Jaffrezo, J.L., 2011. Insights into the secondary fraction of the organic aerosol in a Mediterranean urban area: Marseille. Atmos. Chem. Phys. 11, 2059-2079.

Facchini, M.C., Decesari, S., Rinaldi, M., Carbone, C., Finessi, E., Mircea, M., Fuzzi, S., Moretti, F., Tagliavini, E., Ceburnis, D., O'Dowd, C.D., 2008. Important Source of Marine Secondary Organic Aerosol from Biogenic Amines. Environ. Sci. Technol. 42, 9116-9121.

Fan, X., Song, J., Peng, P.a., 2016. Temporal variations of the abundance and optical properties of water soluble Humic-Like Substances (HULIS) in PM2.5 at Guangzhou, China. Atmos. Res. 172–173, 8-15.

Favez, O., Cachier, H., Sciare, J., Alfaro, S.C., El-Araby, T.M., Harhash, M.A., Abdelwahab, M.M., 2008. Seasonality of major aerosol species and their transformations in Cairo megacity. Atmos. Environ. 42, 1503-1516.

Favez, O., Cachier, H., Sciare, J., Le Moullec, Y., 2007. Characterization and contribution to PM2.5 of semi-volatile aerosols in Paris (France). Atmos. Environ. 41, 7969-7976.

Favez, O., El Haddad, I., Piot, C., Boréave, A., Abidi, E., Marchand, N., Jaffrezo, J.L., Besombes, J.L., Personnaz, M.B., Sciare, J., Wortham, H., George, C., D'Anna, B., 2010. Inter-comparison of source apportionment models for the estimation of wood burning aerosols during wintertime in an Alpine city (Grenoble, France). Atmos. Chem. Phys. 10, 5295-5314.

Feng, J., Li, M., Zhang, P., Gong, S., Zhong, M., Wu, M., Zheng, M., Chen, C., Wang, H., Lou, S., 2013. Investigation of the sources and seasonal variations of secondary organic aerosols in PM2.5 in Shanghai with organic tracers. Atmos. Environ. 79, 614-622.

Feng, Y., Chen, Y., Guo, H., Zhi, G., Xiong, S., Li, J., Sheng, G., Fu, J., 2009. Characteristics of organic and elemental carbon in PM2.5 samples in Shanghai, China. Atmos. Res. 92, 434-442.

Foster, T.L., Caradonna, J.P., 2003. Fe2+-Catalyzed Heterolytic RO−OH Bond Cleavage and Substrate Oxidation: A Functional Synthetic Non-Heme Iron Monooxygenase System. J. Am. Chem. Soc. 125, 3678-3679.

Fountoukis, C., Butler, T., Lawrence, M.G., Denier van der Gon, H.A.C., Visschedijk, A.J.H., Charalampidis, P., Pilinis, C., Pandis, S.N., 2014. Impacts of controlling biomass burning emissions on wintertime carbonaceous aerosol in Europe. Atmos. Environ. 87, 175-182.

Fröhlich, R., Crenn, V., Setyan, A., Belis, C.A., Canonaco, F., Favez, O., Riffault, V., Slowik, J.G., Aas, W., Aijälä, M., Alastuey, A., Artiñano, B., Bonnaire, N., Bozzetti, C., Bressi, M., Carbone, C., Coz, E., Croteau, P.L., Cubison, M.J., Esser-Gietl, J.K., Green, D.C., Gros, V., Heikkinen, L., Herrmann, H., Jayne, J.T., Lunder, C.R., Minguillón, M.C., Močnik, G., O'Dowd, C.D., Ovadnevaite, J., Petralia, E., Poulain, L., Priestman, M., Ripoll, A., Sarda-Estève, R., Wiedensohler, A., Baltensperger, U., Sciare, J., Prévôt, A.S.H., 2015a. ACTRIS ACSM intercomparison – Part 2: Intercomparison of ME-2 organic source apportionment results from 15 individual, co-located aerosol mass spectrometers. Atmos. Meas. Tech. 8, 2555-2576.

Fröhlich, R., Cubison, M.J., Slowik, J.G., Bukowiecki, N., Canonaco, F., Croteau, P.L., Gysel, M., Henne, S., Herrmann, E., Jayne, J.T., Steinbacher, M., Worsnop, D.R., Baltensperger, U.,

Prévôt, A.S.H., 2015b. Fourteen months of on-line measurements of the non-refractory submicron aerosol at the Jungfraujoch (3580 m a.s.l.) – chemical composition, origins and organic aerosol sources. Atmos. Chem. Phys. 15, 11373-11398.

Fröhlich, R., Cubison, M.J., Slowik, J.G., Bukowiecki, N., Prévôt, A.S.H., Baltensperger, U., Schneider, J., Kimmel, J.R., Gonin, M., Rohner, U., Worsnop, D.R., Jayne, J.T., 2013. The ToF-ACSM: a portable aerosol chemical speciation monitor with TOFMS detection. Atmos. Meas. Tech. 6, 3225-3241.

Fu, P., Aggarwal, S.G., Chen, J., Li, J., Sun, Y., Wang, Z., Chen, H., Liao, H., Ding, A., Umarji, G.S., Patil, R.S., Chen, Q., Kawamura, K., 2016. Molecular Markers of Secondary Organic Aerosol in Mumbai, India. Environ. Sci. Technol. 50, 4659-4667.

Fu, P., Kawamura, K., 2011. Diurnal variations of polar organic tracers in summer forest aerosols: A case study of a Quercus and Picea mixed forest in Hokkaido, Japan. Geochem. J. 45, 297-308.

Fu, P., Kawamura, K., Chen, J., Barrie, L.A., 2009a. Isoprene, monoterpene, and sesquiterpene oxidation products in the high Arctic aerosols during late winter to early summer. Environ. Sci. Technol. 43, 4022-4028.

Fu, P., Kawamura, K., Chen, J., Charrière, B., Sempéré, R., 2013. Organic molecular composition of marine aerosols over the Arctic Ocean in summer: contributions of primary emission and secondary aerosol formation. Biogeosciences 10, 653-667.

Fu, P., Kawamura, K., Kanaya, Y., Wang, Z., 2010. Contributions of biogenic volatile organic compounds to the formation of secondary organic aerosols over Mt. Tai, Central East China. Atmos. Environ. 44, 4817-4826.

Fu, P.Q., Kawamura, K., Chen, J., Li, J., Sun, Y.L., Liu, Y., Tachibana, E., Aggarwal, S.G., Okuzawa, K., Tanimoto, H., Kanaya, Y., Wang, Z.F., 2012. Diurnal variations of organic molecular tracers and stable carbon isotopic composition in atmospheric aerosols over Mt. Tai in the North China Plain: an influence of biomass burning. Atmos. Chem. Phys. 12, 8359-8375.

Fu, P.Q., Kawamura, K., Pochanart, P., Tanimoto, H., Kanaya, Y., Wang, Z.F., 2009b. Summertime contributions of isoprene, monoterpenes, and sesquiterpene oxidation to the formation of secondary organic aerosol in the troposphere over Mt. Tai, Central East China during MTX2006. Atmos. Chem. Phys. Discuss. 9, 16941-16972.

Gallimore, P.J., Giorio, C., Mahon, B.M., Kalberer, M., 2017. Online molecular characterisation of organic aerosols in an atmospheric chamber using extractive electrospray ionisation mass spectrometry. Atmos. Chem. Phys. 17, 14485-14500.

Gallimore, P.J., Kalberer, M., 2013. Characterizing an Extractive Electrospray Ionization (EESI) Source for the Online Mass Spectrometry Analysis of Organic Aerosols. Environ. Sci. Technol. 47, 7324-7331.

Gelencsér, A., May, B., Simpson, D., Sánchez-Ochoa, A., Kasper-Giebl, A., Puxbaum, H., Caseiro, A., Pio, C., Legrand, M., 2007. Source apportionment of PM2.5 organic aerosol over Europe: Primary/secondary, natural/anthropogenic, and fossil/biogenic origin. J. Geophys. Res. 112.

Gianini, M.F.D., Fischer, A., Gehrig, R., Ulrich, A., Wichser, A., Piot, C., Besombes, J.L., Hueglin, C., 2012. Comparative source apportionment of PM10 in Switzerland for 2008/2009 and 1998/1999 by Positive Matrix Factorisation. Atmos. Environ. 54, 149-158.

Gilardoni, S., Vignati, E., Cavalli, F., Putaud, J., Larsen, B., Karl, M., Stenström, K., Genberg, J., Henne, S., Dentener, F., 2011. Better constraints on sources of carbonaceous aerosols using a combined 14 C–macro tracer analysis in a European rural background site. Atmos. Chem. Phys. 11, 5685-5700.

Gkatzelis, G.I., Tillmann, R., Hohaus, T., Müller, M., Eichler, P., Xu, K.M., Schlag, P., Schmitt, S.H., Wegener, R., Kaminski, M., Holzinger, R., Wisthaler, A., Kiendler-Scharr, A., 2017. Comparison of three aerosol chemical characterization techniques utilizing PTR-ToF-MS: A study on freshly formed and aged biogenic SOA. Atmos. Meas. Tech. Discuss. 2017, 1-31.

Goldstein, A.H., Galbally, I.E., 2007. Known and unexplored organic constituents in the earth's atmosphere. ACS Publications.

Goriaux, M., Jourdain, B., Temime, B., Besombes, J.L., Marchand, N., Albinet, A., Leoz-Garziandia, E., Wortham, H., 2006. Field comparison of particulate PAH measurements using a low-flow denuder device and conventional sampling systems. Environ. Sci. Technol. 40, 6398-6404.

Gray, H.A., Cass, G.R., Huntzicker, J.J., Heyerdahl, E.K., Rau, J.A., 1986. Characteristics of atmospheric organic and elemental carbon particle concentrations in Los Angeles. Environ. Sci. Technol. 20, 580-589.

Griffin, R.J., Cocker, D.R., Flagan, R.C., Seinfeld, J.H., 1999. Organic aerosol formation from the oxidation of biogenic hydrocarbons. J. Geophys. Res. 104, 3555.

Grivas, G., Cheristanidis, S., Chaloulakou, A., 2012. Elemental and organic carbon in the urban environment of Athens. Seasonal and diurnal variations and estimates of secondary organic carbon. Sci. Total Environ. 414, 535-545.

Grosjean, D., 1984. Particulate carbon in Los Angeles air. Sci. Total Environ. 32, 133-145.

Gu, J., Bai, Z., Liu, A., Wu, L., Xie, Y., Li, W., Dong, H., Zhang, X., 2010. Characterization of atmospheric organic carbon and element carbon of PM2.5 and PM10 at Tianjin, China. Aerosol Air Qual. Res 10, 167-176.

Guenther, A., Karl, T., Harley, P., Wiedinmyer, C., Palmer, P.I., Geron, C., 2006. Estimates of global terrestrial isoprene emissions using MEGAN (Model of Emissions of Gases and Aerosols from Nature). Atmos. Chem. Phys. 6, 3181-3210.

Guo, S., Hu, M., Guo, Q., Zhang, X., Zheng, M., Zheng, J., Chang, C.C., Schauer, J.J., Zhang, R., 2012. Primary Sources and Secondary Formation of Organic Aerosols in Beijing, China. Environ. Sci. Technol. 46, 9846-9853.

Guo, S., Hu, M., Zamora, M.L., Peng, J., Shang, D., Zheng, J., Du, Z., Wu, Z., Shao, M., Zeng, L., Molina, M.J., Zhang, R., 2014. Elucidating severe urban haze formation in China. Proc. Natl. Acad. Sci. U. S. A. 111, 17373-17378.

Hallquist, M., Wenger, J., Baltensperger, U., Rudich, Y., Simpson, D., Claeys, M., Dommen, J., Donahue, N., George, C., Goldstein, A., 2009. The formation, properties and impact of secondary organic aerosol: current and emerging issues. Atmos. Chem. Phys. 9, 5155-5236.

Hamad, S.H., Schauer, J.J., Heo, J., Kadhim, A.K.H., 2015. Source apportionment of PM2.5 carbonaceous aerosol in Baghdad, Iraq. Atmos. Res. 156, 80-90.

Han, T., Liu, X., Zhang, Y., Qu, Y., Zeng, L., Hu, M., Zhu, T., 2015. Role of secondary aerosols in haze formation in summer in the Megacity Beijing. J Environ Sci (China) 31, 51-60.

Hantson, S., Knorr, W., Schurgers, G., Pugh, T.A., Arneth, A., 2017. Global isoprene and monoterpene emissions under changing climate, vegetation, CO2 and land use. Atmos. Environ. 155, 35-45.

Harrison, R.M., Yin, J., 2008. Sources and processes affecting carbonaceous aerosol in central England. Atmos. Environ. 42, 1413-1423.

Hasheminassab, S., Daher, N., Schauer, J.J., Sioutas, C., 2013. Source apportionment and organic compound characterization of ambient ultrafine particulate matter (PM) in the Los Angeles Basin. Atmos. Environ. 79, 529-539.

Heald, C.L., Henze, D.K., Horowitz, L.W., Feddema, J., Lamarque, J.F., Guenther, A., Hess, P.G., Vitt, F., Seinfeld, J.H., Goldstein, A.H., Fung, I., 2008. Predicted change in global secondary organic aerosol concentrations in response to future climate, emissions, and land use change. J. Geophys. Res.-Atmos. 113.

Hennigan, C.J., Sullivan, A.P., Collett, J.L., Robinson, A.L., 2010. Levoglucosan stability in biomass burning particles exposed to hydroxyl radicals. Geophys. Res. Lett. 37.

Henze, D., Seinfeld, J., Ng, N., Kroll, J., Fu, T.-M., Jacob, D.J., Heald, C., 2008. Global modeling of secondary organic aerosol formation from aromatic hydrocarbons: high-vs. low-yield pathways. Atmos. Chem. Phys. 8, 2405-2420.

Heo, J., Dulger, M., Olson, M.R., McGinnis, J.E., Shelton, B.R., Matsunaga, A., Sioutas, C., Schauer, J.J., 2013. Source apportionments of PM2.5 organic carbon using molecular marker Positive Matrix Factorization and comparison of results from different receptor models. Atmos. Environ. 73, 51-61.

Hildemann, L.M., Klinedinst, D.B., Klouda, G.A., Currie, L.A., Cass, G.R., 1994. Sources of urban contemporary carbon aerosol. Environ. Sci. Technol. 28, 1565-1576.

Hodzic, A., Kasibhatla, P.S., Jo, D.S., Cappa, C.D., Jimenez, J.L., Madronich, S., Park, R.J., 2016. Rethinking the global secondary organic aerosol (SOA) budget: stronger production, faster removal, shorter lifetime. Atmos. Chem. Phys. 16, 7917-7941.

Holzinger, R., Williams, J., Herrmann, F., Lelieveld, J., Donahue, N.M., Röckmann, T., 2010. Aerosol analysis using a Thermal-Desorption Proton-Transfer-Reaction Mass Spectrometer (TD-PTR-MS): a new approach to study processing of organic aerosols. Atmos. Chem. Phys. 10, 2257-2267.

Hooda, R.K., Hyvärinen, A.P., Vestenius, M., Gilardoni, S., Sharma, V.P., Vignati, E., Kulmala, M., Lihavainen, H., 2016. Atmospheric aerosols local–regional discrimination for a semi-urban area in India. Atmos. Res. 168, 13-23.

Hu, D., Bian, Q., Lau, A.K.H., Yu, J.Z., 2010. Source apportioning of primary and secondary organic carbon in summer PM2.5 in Hong Kong using positive matrix factorization of secondary and primary organic tracer data. J. Geophys. Res.-Atmos. 115.

Hu, D., Bian, Q., Li, T.W.Y., Lau, A.K.H., Yu, J.Z., 2008. Contributions of isoprene, monoterpenes, β-caryophyllene, and toluene to secondary organic aerosols in Hong Kong during the summer of 2006. J. Geophys. Res.-Atmos. 113, D22206.

Hu, Q.-H., Xie, Z.-Q., Wang, X.-M., Kang, H., He, Q.-F., Zhang, P., 2013. Secondary organic aerosols over oceans via oxidation of isoprene and monoterpenes from Arctic to Antarctic. Sci. Rep. 3, 2280.

Hu, W., Hu, M., Deng, Z., Xiao, R., Kondo, Y., Takegawa, N., Zhao, Y., Guo, S., Zhang, Y., 2012. The characteristics and origins of carbonaceous aerosol at a rural site of PRD in summer of 2006. Atmos. Chem. Phys. 12, 1811-1822.

Hu, W.W., Campuzano-Jost, P., Palm, B.B., Day, D.A., Ortega, A.M., Hayes, P.L., Krechmer, J.E., Chen, Q., Kuwata, M., Liu, Y.J., de Sá, S.S., McKinney, K., Martin, S.T., Hu, M., Budisulistiorini, S.H., Riva, M., Surratt, J.D., St. Clair, J.M., Isaacman-Van Wertz, G., Yee, L.D., Goldstein, A.H., Carbone, S., Brito, J., Artaxo, P., de Gouw, J.A., Koss, A., Wisthaler, A., Mikoviny, T., Karl, T., Kaser, L., Jud, W., Hansel, A., Docherty, K.S., Alexander, M.L., Robinson, N.H., Coe, H., Allan, J.D., Canagaratna, M.R., Paulot, F., Jimenez, J.L., 2015. Characterization of a real-time tracer for isoprene epoxydiols-derived secondary organic aerosol (IEPOX-SOA) from aerosol mass spectrometer measurements. Atmos. Chem. Phys. 15, 11807-11833.

Huang, H., Ho, K.F., Lee, S.C., Tsang, P.K., Ho, S.S.H., Zou, C.W., Zou, S.C., Cao, J.J., Xu, H.M., 2012. Characteristics of carbonaceous aerosol in PM2.5: Pearl Delta River Region, China. Atmos. Res. 104–105, 227-236.

Huang, L., Wang, G., 2014. Chemical characteristics and source apportionment of atmospheric particles during heating period in Harbin, China. J. Environ. Sci. 26, 2475-2483.

Huang, R.-J., Zhang, Y., Bozzetti, C., Ho, K.-F., Cao, J.-J., Han, Y., Daellenbach, K.R., Slowik, J.G., Platt, S.M., Canonaco, F., Zotter, P., Wolf, R., Pieber, S.M., Bruns, E.A., Crippa, M., Ciarelli, G., Piazzalunga, A., Schwikowski, M., Abbaszade, G., Schnelle-Kreis, J., Zimmermann, R., An, Z., Szidat, S., Baltensperger, U., Haddad, I.E., Prevot, A.S.H., 2014. High secondary aerosol contribution to particulate pollution during haze events in China. Nature 514, 218-222.

Huang, X.-F., Xue, L., Tian, X.-D., Shao, W.-W., Sun, T.-L., Gong, Z.-H., Ju, W.-W., Jiang, B., Hu, M., He, L.-Y., 2013. Highly time-resolved carbonaceous aerosol characterization in Yangtze River Delta of China: Composition, mixing state and secondary formation. Atmos. Environ. 64, 200-207.

Huang, X.F., He, L.Y., Hu, M., Canagaratna, M.R., Sun, Y., Zhang, Q., Zhu, T., Xue, L., Zeng, L.W., Liu, X.G., Zhang, Y.H., Jayne, J.T., Ng, N.L., Worsnop, D.R., 2010. Highly time-resolved chemical characterization of atmospheric submicron particles during 2008 Beijing Olympic Games using an Aerodyne High-Resolution Aerosol Mass Spectrometer. Atmos. Chem. Phys. 10, 8933-8945.

Ichikawa, Y., Naito, S., Oohashi, H., 2015. Seasonal Variation of PM 2.5 Components Observed in an Industrial Area of Chiba Prefecture, Japan. Asian J. Atmos. Environ. 9, 66-77.

Iinuma, Y., Boge, O., Grafe, R., Herrmann, H., 2010. Methyl-nitrocatechols: atmospheric tracer compounds for biomass burning secondary organic aerosols. Environ. Sci. Technol. 44, 8453-8459.

Iinuma, Y., Müller, C., Berndt, T., Böge, O., Claeys, M., Herrmann, H., 2007. Evidence for the existence of organosulfates from β-pinene ozonolysis in ambient secondary organic aerosol. Environ. Sci. Technol. 41, 6678-6683.

Jaeckels, J.M., Bae, M.-S., Schauer, J.J., 2007. Positive matrix factorization (PMF) analysis of molecular marker measurements to quantify the sources of organic aerosols. Environ. Sci. Technol. 41, 5763-5769.

Jaenicke, R., 2005. Abundance of cellular material and proteins in the atmosphere. Science 308, 73.

Jaoui, M., Kleindienst, T.E., Lewandowski, M., Offenberg, J.H., Edney, E.O., 2005. Identification and Quantification of Aerosol Polar Oxygenated Compounds Bearing Carboxylic or Hydroxyl Groups. 2. Organic Tracer Compounds from Monoterpenes. Environ. Sci. Technol. 39, 5661-5673.

Jaoui, M., Lewandowski, M., Kleindienst, T.E., Offenberg, J.H., Edney, E.O., 2007. β-caryophyllinic acid: An atmospheric tracer for β-caryophyllene secondary organic aerosol. Geophys. Res. Lett. 34, L05816.

Jayarathne, T., Rathnayake, C.M., Stone, E.A., 2016. Local source impacts on primary and secondary aerosols in the Midwestern United States. Atmos. Environ. 130, 74-83.

Jayne, J.T., Leard, D.C., Zhang, X., Davidovits, P., Smith, K.A., Kolb, C.E., Worsnop, D.R., 2000. Development of an Aerosol Mass Spectrometer for Size and Composition Analysis of Submicron Particles. Aerosol Sci. Technol. 33, 49-70.

Ji, D., Zhang, J., He, J., Wang, X., Pang, B., Liu, Z., Wang, L., Wang, Y., 2016. Characteristics of atmospheric organic and elemental carbon aerosols in urban Beijing, China. Atmos. Environ. 125, Part A, 293-306.

Jimenez, J., Canagaratna, M., Donahue, N., Prevot, A., Zhang, Q., Kroll, J.H., DeCarlo, P.F., Allan, J.D., Coe, H., Ng, N., 2009. Evolution of organic aerosols in the atmosphere. Science 326, 1525-1529.

Jimenez, J.L., Jayne, J.T., Shi, Q., Kolb, C.E., Worsnop, D.R., Yourshaw, I., Seinfeld, J.H., Flagan, R.C., Zhang, X., Smith, K.A., 2003. Ambient aerosol sampling using the aerodyne aerosol mass spectrometer. J. Geophys. Res.-Atmos. 108.

Johnson, D., Utembe, S., Jenkin, M., Derwent, R., Hayman, G., Alfarra, M., Coe, H., McFiggans, G., 2006. Simulating regional scale secondary organic aerosol formation during the TORCH 2003 campaign in the southern UK. Atmos. Chem. Phys. 6, 403-418.

Joseph, A.E., Unnikrishnan, S., Kumar, R., 2012. Chemical characterization and mass closure of fine aerosol for different land use patterns in Mumbai city. Aerosol. Air Qual. Res. 12, 61-72.

Kanakidou, M., Seinfeld, J., Pandis, S., Barnes, I., Dentener, F., Facchini, M., Dingenen, R.V., Ervens, B., Nenes, A., Nielsen, C., 2005. Organic aerosol and global climate modelling: a review. Atmos. Chem. Phys. 5, 1053-1123.

Karanasiou, A., Minguillón, M., Viana, M., Alastuey, A., Putaud, J.-P., Maenhaut, W., Panteliadis, P., Močnik, G., Favez, O., Kuhlbusch, T., 2015. Thermal-optical analysis for the

measurement of elemental carbon (EC) and organic carbon (OC) in ambient air a literature review. Atmos. Meas. Tech. Discuss. 8.

Kaulfus, A.S., Nair, U., Jaffe, D., Christopher, S.A., Goodrick, S., 2017. Biomass Burning Smoke Climatology of the United States: Implications for Particulate Matter Air Quality. Environ. Sci. Technol. 51, 11731-11741.

Kawamura, K., Sakaguchi, F., 1999. Molecular distributions of water soluble dicarboxylic acids in marine aerosols over the Pacific Ocean including tropics. J. Geophys. Res.-Atmos. 104, 3501-3509.

Ke, L., Ding, X., Tanner, R.L., Schauer, J.J., Zheng, M., 2007. Source contributions to carbonaceous aerosols in the Tennessee Valley Region. Atmos. Environ. 41, 8898-8923.

Ke, L., Liu, W., Wang, Y., Russell, A.G., Edgerton, E.S., Zheng, M., 2008. Comparison of PM2.5 source apportionment using positive matrix factorization and molecular marker-based chemical mass balance. Sci. Total Environ. 394, 290-302.

Kessler, S.H., Smith, J.D., Che, D.L., Worsnop, D.R., Wilson, K.R., Kroll, J.H., 2010. Chemical Sinks of Organic Aerosol: Kinetics and Products of the Heterogeneous Oxidation of Erythritol and Levoglucosan. Environ. Sci. Technol. 44, 7005-7010.

Kettle, A.J., Andreae, M.O., 2000. Flux of dimethylsulfide from the oceans: A comparison of updated data sets and flux models. J. Geophys. Res.-Atmos. 105, 26793-26808.

Khan, M.B., Masiol, M., Formenton, G., Di Gilio, A., de Gennaro, G., Agostinelli, C., Pavoni, B., 2016. Carbonaceous PM2.5 and secondary organic aerosol across the Veneto region (NE Italy). Sci. Total Environ. 542, Part A, 172-181.

Khan, M.F., Shirasuna, Y., Hirano, K., Masunaga, S., 2010. Characterization of PM2.5, PM2.5–10 and PM>10 in ambient air, Yokohama, Japan. Atmos. Res. 96, 159-172.

Kiendler-Scharr, A., Mensah, A.A., Friese, E., Topping, D., Nemitz, E., Prevot, A.S.H., Äijälä, M., Allan, J., Canonaco, F., Canagaratna, M., Carbone, S., Crippa, M., Dall Osto, M., Day, D.A., De Carlo, P., Di Marco, C.F., Elbern, H., Eriksson, A., Freney, E., Hao, L., Herrmann, H., Hildebrandt, L., Hillamo, R., Jimenez, J.L., Laaksonen, A., McFiggans, G., Mohr, C., O'Dowd, C., Otjes, R., Ovadnevaite, J., Pandis, S.N., Poulain, L., Schlag, P., Sellegri, K., Swietlicki, E., Tiitta, P., Vermeulen, A., Wahner, A., Worsnop, D., Wu, H.C., 2016. Ubiquity of organic nitrates from nighttime chemistry in the European submicron aerosol. Geophys. Res. Lett. 43, 7735-7744.

Kim, W., Lee, H., Kim, J., Jeong, U., Kweon, J., 2012. Estimation of seasonal diurnal variations in primary and secondary organic carbon concentrations in the urban atmosphere: EC tracer and multiple regression approaches. Atmos. Environ. 56, 101-108.

Kleeman, M.J., Ying, Q., Lu, J., Mysliwiec, M.J., Griffin, R.J., Chen, J., Clegg, S., 2007. Source apportionment of secondary organic aerosol during a severe photochemical smog episode. Atmos. Environ. 41, 576-591.

Kleindienst, T.E., Jaoui, M., Lewandowski, M., Offenberg, J.H., Docherty, K.S., 2012. The formation of SOA and chemical tracer compounds from the photooxidation of naphthalene and its methyl analogs in the presence and absence of nitrogen oxides. Atmos. Chem. Phys. 12, 8711-8726.

Kleindienst, T.E., Jaoui, M., Lewandowski, M., Offenberg, J.H., Lewis, C.W., Bhave, P.V., Edney, E.O., 2007. Estimates of the contributions of biogenic and anthropogenic hydrocarbons to secondary organic aerosol at a southeastern US location. Atmos. Environ. 41, 8288-8300.

Kleindienst, T.E., Lewandowski, M., Offenberg, J.H., Edney, E.O., Jaoui, M., Zheng, M., Ding, X., Edgerton, E.S., 2010. Contribution of Primary and Secondary Sources to Organic Aerosol and PM2.5at SEARCH Network Sites. J. Air Waste Manage. Assoc. 60, 1388-1399.

Kong, S., Han, B., Bai, Z., Chen, L., Shi, J., Xu, Z., 2010. Receptor modeling of PM2.5, PM10 and TSP in different seasons and long-range transport analysis at a coastal site of Tianjin, China. Sci. Total Environ. 408, 4681-4694.

Kostenidou, E., Karnezi, E., Kolodziejczyk, A., Szmigielski, R., Pandis, S., 2017. Physical and chemical properties of 3-methyl-1,2,3-butanetricarboxylic acid (MBTCA) aerosol. Environ. Sci. Technol.

Kourtchev, I., Copolovici, L., Claeys, M., Maenhaut, W., 2009. Characterization of atmospheric aerosols at a forested site in Central Europe. Environ. Sci. Technol. 43, 4665-4671.

Kourtchev, I., Hellebust, S., Bell, J.M., O'Connor, I.P., Healy, R.M., Allanic, A., Healy, D., Wenger, J.C., Sodeau, J.R., 2011. The use of polar organic compounds to estimate the contribution of domestic solid fuel combustion and biogenic sources to ambient levels of organic carbon and PM2.5 in Cork Harbour, Ireland. Sci. Total Environ. 409, 2143-2155.

Kourtchev, I., Warnke, J., Maenhaut, W., Hoffmann, T., Claeys, M., 2008. Polar organic marker compounds in PM2.5 aerosol from a mixed forest site in western Germany. Chemosphere 73, 1308-1314.

Kumar, A., Ram, K., Ojha, N., 2016. Variations in carbonaceous species at a high-altitude site in western India: Role of synoptic scale transport. Atmos. Environ. 125, Part B, 371-382.

Lai, C., Liu, Y., Ma, J., Ma, Q., Chu, B., He, H., 2015. Heterogeneous Kinetics of cis-Pinonic Acid with Hydroxyl Radical under Different Environmental Conditions. J. Phys. Chem. A 119, 6583-6593.

Lai, S., Zhao, Y., Ding, A., Zhang, Y., Song, T., Zheng, J., Ho, K.F., Lee, S.-c., Zhong, L., 2016. Characterization of PM2.5 and the major chemical components during a 1-year campaign in rural Guangzhou, Southern China. Atmos. Res. 167, 208-215.

Lamkaddam, H., Gratien, A., Pangui, E., Cazaunau, M., Picquet-Varrault, B., Doussin, J.-F., 2017. High-NOx Photooxidation of n-Dodecane: Temperature Dependence of SOA Formation. Environ. Sci. Technol. 51, 192-201.

Lanz, V.A., Alfarra, M.R., Baltensperger, U., Buchmann, B., Hueglin, C., Prévôt, A.S.H., 2007. Source apportionment of submicron organic aerosols at an urban site by factor analytical modelling of aerosol mass spectra. Atmos. Chem. Phys. 7, 1503-1522.

Laongsri, B., Harrison, R.M., 2013. Atmospheric behaviour of particulate oxalate at UK urban background and rural sites. Atmos. Environ. 71, 319-326.

Lathiere, J., Hauglustaine, D., Friend, A., Noblet-Ducoudré, N.D., Viovy, N., Folberth, G., 2006. Impact of climate variability and land use changes on global biogenic volatile organic compound emissions. Atmos. Chem. Phys. 6, 2129-2146.

Lee, A.K., 2015. Haze formation in China: Importance of secondary aerosol. J Environ Sci (China) 33, 261-262.

Lee, H., Park, S.S., Kim, K.W., Kim, Y.J., 2008a. Source identification of PM2.5 particles measured in Gwangju, Korea. Atmos. Res. 88, 199-211.

Lee, S., Liu, W., Wang, Y., Russell, A.G., Edgerton, E.S., 2008b. Source apportionment of PM 2.5: Comparing PMF and CMB results for four ambient monitoring sites in the southeastern United States. Atmos. Environ. 42, 4126-4137.

Lewandowski, M., Jaoui, M., Offenberg, J.H., Kleindienst, T.E., Edney, E.O., Sheesley, R.J., Schauer, J.J., 2008. Primary and secondary contributions to ambient PM in the midwestern United States. Environ. Sci. Technol. 42, 3303-3309.

Lewandowski, M., Piletic, I.R., Kleindienst, T.E., Offenberg, J.H., Beaver, M.R., Jaoui, M., Docherty, K.S., Edney, E.O., 2013. Secondary organic aerosol characterisation at field sites across the United States during the spring–summer period. Int. J. Environ. Anal. Chem. 93, 1084-1103.

Li, A., Jang, J.-K., Scheff, P.A., 2003. Application of EPA CMB8. 2 model for source apportionment of sediment PAHs in Lake Calumet, Chicago. Environ. Sci. Technol. 37, 2958-2965.

Li, B., Zhang, J., Zhao, Y., Yuan, S., Zhao, Q., Shen, G., Wu, H., 2015a. Seasonal variation of urban carbonaceous aerosols in a typical city Nanjing in Yangtze River Delta, China. Atmos. Environ. 106, 223-231.

Li, W., Bai, Z., 2009. Characteristics of organic and elemental carbon in atmospheric fine particles in Tianjin, China. Particuology 7, 432-437.

Li, Y.-C., Yu, J.Z., Ho, S.S.H., Schauer, J.J., Yuan, Z., Lau, A.K.H., Louie, P.K.K., 2013. Chemical characteristics and source apportionment of fine particulate organic carbon in Hong Kong during high particulate matter episodes in winter 2003. Atmos. Res. 120–121, 88-98.

Li, Y.-C., Yu, J.Z., Ho, S.S.H., Yuan, Z., Lau, A.K.H., Huang, X.-F., 2012. Chemical characteristics of PM2.5 and organic aerosol source analysis during cold front episodes in Hong Kong, China. Atmos. Res. 118, 41-51.

Li, Y.J., Lee, B.P., Su, L., Fung, J.C.H., Chan, C.K., 2015b. Seasonal characteristics of fine particulate matter (PM) based on high-resolution time-of-flight aerosol mass spectrometric (HR-ToF-AMS) measurements at the HKUST Supersite in Hong Kong. Atmos. Chem. Phys. 15, 37-53.

Lim, H.-J., Turpin, B.J., 2002. Origins of Primary and Secondary Organic Aerosol in Atlanta: Results of Time-Resolved Measurements during the Atlanta Supersite Experiment. Environ. Sci. Technol. 36, 4489-4496.

Lim, Y.B., Ziemann, P.J., 2005. Products and mechanism of secondary organic aerosol formation from reactions of n-alkanes with OH radicals in the presence of NO x. Environ. Sci. Technol. 39, 9229-9236.

Lim, Y.B., Ziemann, P.J., 2009. Effects of Molecular Structure on Aerosol Yields from OH Radical-Initiated Reactions of Linear, Branched, and Cyclic Alkanes in the Presence of NOx. Environ. Sci. Technol. 43, 2328-2334.

Lin, P., Hu, M., Deng, Z., Slanina, J., Han, S., Kondo, Y., Takegawa, N., Miyazaki, Y., Zhao, Y., Sugimoto, N., 2009. Seasonal and diurnal variations of organic carbon in PM2.5 in Beijing and the estimation of secondary organic carbon. J. Geophys. Res.-Atmos. 114.

Liu, J., Li, J., Liu, D., Ding, P., Shen, C., Mo, Y., Wang, X., Luo, C., Cheng, Z., Szidat, S., Zhang, Y., Chen, Y., Zhang, G., 2016. Source apportionment and dynamic changes of carbonaceous aerosols during the haze bloom-decay process in China based on radiocarbon and organic molecular tracers. Atmos. Chem. Phys. 16, 2985-2996.

Liu, J., Li, J., Zhang, Y., Liu, D., Ding, P., Shen, C., Shen, K., He, Q., Ding, X., Wang, X., 2014. Source Apportionment Using Radiocarbon and Organic Tracers for PM2. 5 Carbonaceous Aerosols in Guangzhou, South China: Contrasting Local-and Regional-Scale Haze Events. Environ. Sci. Technol. 48, 12002-12011.

Lonati, G., Ozgen, S., Giugliano, M., 2007. Primary and secondary carbonaceous species in PM2.5 samples in Milan (Italy). Atmos. Environ. 41, 4599-4610.

Lopez-Hilfiker, F.D., Mohr, C., Ehn, M., Rubach, F., Kleist, E., Wildt, J., Mentel, T.F., Lutz, A., Hallquist, M., Worsnop, D., Thornton, J.A., 2014. A novel method for online analysis of gas and particle composition: description and evaluation of a Filter Inlet for Gases and AEROsols (FIGAERO). Atmos. Meas. Tech. 7, 983-1001.

Lv, B., Zhang, B., Bai, Y., 2016. A systematic analysis of PM2.5 in Beijing and its sources from 2000 to 2012. Atmos. Environ. 124, Part B, 98-108.

Mader, B.T., Pankow, J.F., 2001. Gas/solid partitioning of semivolatile organic compounds (SOCs) to air filters. 3. An analysis of gas adsorption artifacts in measurements of atmospheric SOCs and organic carbon (OC) when using Teflon membrane filters and quartz fiber filters. Environ. Sci. Technol. 35, 3422-3432.

Mancilla, Y., Herckes, P., Fraser, M.P., Mendoza, A., 2015. Secondary organic aerosol contributions to PM2.5 in Monterrey, Mexico: Temporal and seasonal variation. Atmos. Res. 153, 348-359.

Marta, G.V., Manuel, S., 2010. Secondary Organic Aerosol Formation from the Oxidation of a Mixture of Organic Gases in a Chamber.

Martín-Reviejo, M., Wirtz, K., 2005. Is benzene a precursor for secondary organic aerosol? Environ. Sci. Technol. 39, 1045-1054.

Martinez, M.A., Caballero, P., Carrillo, O., Mendoza, A., Mejia, G.M., 2012. Chemical characterization and factor analysis of PM2. 5 in two sites of Monterrey, Mexico. J. Air Waste Manage. Assoc. 62, 817-827.

McDow, S.R., Huntzicker, J.J., 1990. Vapor adsorption artifact in the sampling of organic aerosol: face velocity effects. Atmos. Environ., Part A 24, 2563-2571.

McGuire, M., Chang, R.-W., Slowik, J., Jeong, C.-H., Healy, R., Lu, G., Mihele, C., Abbatt, J., Brook, J., Evans, G., 2014. Enhancing non-refractory aerosol apportionment from an urban industrial site through receptor modeling of complete high time-resolution aerosol mass spectra. Atmos. Chem. Phys. 14, 8017-8042.

Mihele, C.M., Wiebe, H.A., Lane, D.A., 2002. Particle formation and gas/particle partition measurements of the products of the naphthalene-OH radical reaction in a smog chamber. Polycyclic Aromat. Compd. 22, 729-736.

Miller-Schulze, J.P., Shafer, M.M., Schauer, J.J., Solomon, P.A., Lantz, J., Artamonova, M., Chen, B., Imashev, S., Sverdlik, L., Carmichael, G.R., Deminter, J.T., 2011. Characteristics of fine particle carbonaceous aerosol at two remote sites in Central Asia. Atmos. Environ. 45, 6955-6964.

Minguillón, M.C., Arhami, M., Schauer, J.J., Sioutas, C., 2008. Seasonal and spatial variations of sources of fine and quasi-ultrafine particulate matter in neighborhoods near the Los Angeles–Long Beach harbor. Atmos. Environ. 42, 7317-7328.

Mirante, F., Salvador, P., Pio, C., Alves, C., Artiñano, B., Caseiro, A., Revuelta, M.A., 2014. Size fractionated aerosol composition at roadside and background environments in the Madrid urban atmosphere. Atmos. Res. 138, 278-292.

Miyazaki, Y., Fu, P.Q., Kawamura, K., Mizoguchi, Y., Yamanoi, K., 2012a. Seasonal variations of stable carbon isotopic composition and biogenic tracer compounds of water-soluble organic aerosols in a deciduous forest. Atmos. Chem. Phys. 12, 1367-1376.

Miyazaki, Y., Fu, P.Q., Kawamura, K., Mizoguchi, Y., Yamanoi, K., 2012b. Seasonal variations of stable carbon isotopic composition and biogenic tracer compounds of water-soluble organic aerosols in a deciduous forest. Atmos. Chem. Phys. 12, 1367-1376.

Mochida, M., Kawamura, K., Fu, P., Takemura, T., 2010. Seasonal variation of levoglucosan in aerosols over the western North Pacific and its assessment as a biomass-burning tracer. Atmos. Environ. 44, 3511-3518.

Morino, Y., Ohara, T., Xu, J., Hasegawa, S., Zhao, B., Fushimi, A., Tanabe, K., Kondo, M., Uchida, M., Yamaji, K., 2015. Diurnal variations of fossil and nonfossil carbonaceous aerosols in Beijing. Atmos. Environ. 122, 349-356.

Murillo, J.H., Marin, J.F.R., Roman, S.R., Guerrero, V.H.B., Arias, D.S., Ramos, A.C., Gonzalez, B.C., Baumgardner, D.G., 2013. Temporal and spatial variations in organic and elemental carbon concentrations in PM10/PM2.5 in the metropolitan area of Costa Rica, Central America. Atmos. Pollut. Res. 4, 53-63.

Na, K., Sawant, A.A., Song, C., Cocker Iii, D.R., 2004. Primary and secondary carbonaceous species in the atmosphere of Western Riverside County, California. Atmos. Environ. 38, 1345-1355.

Ng, N.L., Canagaratna, M.R., Zhang, Q., Jimenez, J.L., Tian, J., Ulbrich, I.M., Kroll, J.H., Docherty, K.S., Chhabra, P.S., Bahreini, R., Murphy, S.M., Seinfeld, J.H., Hildebrandt, L., Donahue, N.M., DeCarlo, P.F., Lanz, V.A., Prévôt, A.S.H., Dinar, E., Rudich, Y., Worsnop, D.R., 2010. Organic aerosol components observed in Northern Hemispheric datasets from Aerosol Mass Spectrometry. Atmos. Chem. Phys. 10, 4625-4641.

Ng, N.L., Herndon, S.C., Trimborn, A., Canagaratna, M.R., Croteau, P.L., Onasch, T.B., Sueper, D., Worsnop, D.R., Zhang, Q., Sun, Y.L., Jayne, J.T., 2011. An Aerosol Chemical Speciation Monitor (ACSM) for Routine Monitoring of the Composition and Mass Concentrations of Ambient Aerosol. Aerosol Sci. Technol. 45, 780-794.

Niu, Z., Zhang, F., Chen, J., Yin, L., Wang, S., Xu, L., 2013. Carbonaceous species in PM2.5 in the coastal urban agglomeration in the Western Taiwan Strait Region, China. Atmos. Res. 122, 102-110.

Nozière, B., Kalberer, M., Claeys, M., Allan, J., D'Anna, B., Decesari, S., Finessi, E., Glasius, M., Grgić, I., Hamilton, J.F., Hoffmann, T., Iinuma, Y., Jaoui, M., Kahnt, A., Kampf, C.J., Kourtchev, I., Maenhaut, W., Marsden, N., Saarikoski, S., Schnelle-Kreis, J., Surratt, J.D., Szidat, S., Szmigielski, R., Wisthaler, A., 2015. The Molecular Identification of Organic Compounds in the Atmosphere: State of the Art and Challenges. Chem. Rev.

Odum, J.R., Hoffmann, T., Bowman, F., Collins, D., Flagan, R.C., Seinfeld, J.H., 1996. Gas/Particle Partitioning and Secondary Organic Aerosol Yields. Environ. Sci. Technol. 30, 2580-2585.

Odum, J.R., Jungkamp, T.P.W., Griffin, R.J., Flagan, R.C., Seinfeld, J.H., 1997. The Atmospheric Aerosol-Forming Potential of Whole Gasoline Vapor. Science 276, 96-99.

Offenberg, J.H., 2011. Contributions of Biogenic and Anthropogenic Hydrocarbons to Secondary Organic Aerosol during 2006 in Research Triangle Park, NC. Aerosol. Air Qual. Res.

Offenberg, J.H., Lewandowski, M., Jaoui, M., Kleindienst, T.E., 2011. Contributions of biogenic and anthropogenic hydrocarbons to secondary organic aerosol during 2006 in Research Triangle Park, NC. Aerosol. Air Qual. Res. 11, 99-108.

Offenberg, J.H., Lewis, C.W., Lewandowski, M., Jaoui, M., Kleindienst, T.E., Edney, E.O., 2007. Contributions of toluene and α-pinene to SOA formed in an irradiated toluene/α-pinene/NOx/air mixture: Comparison of results using 14C content and SOA organic tracer methods. Environ. Sci. Technol. 41, 3972-3976.

Paatero, P., 1997. Least squares formulation of robust non-negative factor analysis. Chemom. Intell. Lab. Syst. 37, 23-35.

Paatero, P., Tapper, U., 1994. Positive matrix factorization: A non-negative factor model with optimal utilization of error estimates of data values. Environmetrics 5, 111-126.

Pachon, J.E., Balachandran, S., Hu, Y., Weber, R.J., Mulholland, J.A., Russell, A.G., 2010. Comparison of SOC estimates and uncertainties from aerosol chemical composition and gas phase data in Atlanta. Atmos. Environ. 44, 3907-3914.

Pandis, S.N., Harley, R.A., Cass, G.R., Seinfeld, J.H., 1992. Secondary organic aerosol formation and transport. Atmos. Environ., Part A 26, 2269-2282.

Pant, P., Shukla, A., Kohl, S.D., Chow, J.C., Watson, J.G., Harrison, R.M., 2015. Characterization of ambient PM2.5 at a pollution hotspot in New Delhi, India and inference of sources. Atmos. Environ. 109, 178-189.

Pant, P., Yin, J., Harrison, R.M., 2014. Sensitivity of a Chemical Mass Balance model to different molecular marker traffic source profiles. Atmos. Environ. 82, 238-249.

Paraskevopoulou, D., Liakakou, E., Gerasopoulos, E., Theodosi, C., Mihalopoulos, N., 2014. Long-term characterization of organic and elemental carbon in the PM2.5 fraction: the case of Athens, Greece. Atmos. Chem. Phys. 14, 13313-13325.

Park, S.S., Cho, S.Y., 2011. Tracking sources and behaviors of water-soluble organic carbon in fine particulate matter measured at an urban site in Korea. Atmos. Environ. 45, 60-72.

Pernigotti, D., Belis, C.A., Spanò, L., 2016. SPECIEUROPE: The European data base for PM source profiles. Atmos. Pollut. Res. 7, 307-314.

Perrone, M.G., Larsen, B.R., Ferrero, L., Sangiorgi, G., De Gennaro, G., Udisti, R., Zangrando, R., Gambaro, A., Bolzacchini, E., 2012. Sources of high PM2.5 concentrations in Milan, Northern Italy: Molecular marker data and CMB modelling. Sci. Total Environ. 414, 343-355.

Petit, J.-E., Amodeo, T., Meleux, F., Bessagnet, B., Menut, L., Grenier, D., Pellan, Y., Ockler, A., Rocq, B., Gros, V., 2017. Characterising an intense PM pollution episode in March 2015 in France from multi-site approach and near real time data: Climatology, variabilities, geographical origins and model evaluation. Atmos. Environ. 155, 68-84.

Petit, J.E., Favez, O., Sciare, J., Canonaco, F., Croteau, P., Močnik, G., Jayne, J., Worsnop, D., Leoz-Garziandia, E., 2014. Submicron aerosol source apportionment of wintertime pollution in Paris, France by double positive matrix factorization (PMF2) using an aerosol chemical speciation monitor (ACSM) and a multi-wavelength Aethalometer. Atmos. Chem. Phys. 14, 13773-13787.

Petit, J.E., Favez, O., Sciare, J., Crenn, V., Sarda-Estève, R., Bonnaire, N., Močnik, G., Dupont, J.C., Haeffelin, M., Leoz-Garziandia, E., 2015. Two years of near real-time chemical composition of submicron aerosols in the region of Paris using an Aerosol Chemical Speciation Monitor (ACSM) and a multi-wavelength Aethalometer. Atmos. Chem. Phys. 15, 2985-3005.

Pietrogrande, M.C., Bacco, D., Ferrari, S., Ricciardelli, I., Scotto, F., Trentini, A., Visentin, M., 2016. Characteristics and major sources of carbonaceous aerosols in PM2.5 in Emilia Romagna Region (Northern Italy) from four-year observations. Sci. Total Environ. 553, 172-183.

Pipal, A.S., Gursumeeran Satsangi, P., 2015. Study of carbonaceous species, morphology and sources of fine (PM2.5) and coarse (PM10) particles along with their climatic nature in India. Atmos. Res. 154, 103-115.

Pirovano, G., Colombi, C., Balzarini, A., Riva, G., Gianelle, V., Lonati, G., 2015. PM2. 5 source apportionment in Lombardy (Italy): comparison of receptor and chemistry-transport modelling results. Atmos. Environ. 106, 56-70.

Plaza, J., Gómez-Moreno, F.J., Núñez, L., Pujadas, M., Artíñano, B., 2006. Estimation of secondary organic aerosol formation from semi-continuous OC–EC measurements in a Madrid suburban area. Atmos. Environ. 40, 1134-1147.

Polidori, A., Turpin, B.J., Lim, H.J., Cabada, J.C., Subramanian, R., Pandis, S.N., Robinson, A.L., 2006. Local and regional secondary organic aerosol: Insights from a year of semi-continuous carbon measurements at Pittsburgh. Aerosol Sci. Technol. 40, 861-872.

Polissar, A.V., Hopke, P.K., Paatero, P., Malm, W.C., Sisler, J.F., 1998. Atmospheric aerosol over Alaska: 2. Elemental composition and sources. J. Geophys. Res.-Atmos. 103, 19045-19057.

Qiao, T., Zhao, M., Xiu, G., Yu, J., 2016. Simultaneous monitoring and compositions analysis of PM1 and PM2.5 in Shanghai: Implications for characterization of haze pollution and source apportionment. Sci. Total Environ. 557–558, 386-394.

Querol, X., Viana, M., Alastuey, A., Amato, F., Moreno, T., Castillo, S., Pey, J., de la Rosa, J., Sánchez de la Campa, A., Artíñano, B., Salvador, P., García Dos Santos, S., Fernández-Patier, R., Moreno-Grau, S., Negral, L., Minguillón, M.C., Monfort, E., Gil, J.I., Inza, A., Ortega, L.A., Santamaría, J.M., Zabalza, J., 2007. Source origin of trace elements in PM from regional background, urban and industrial sites of Spain. Atmos. Environ. 41, 7219-7231.

Rengarajan, R., Sudheer, A., Sarin, M., 2011. Aerosol acidity and secondary organic aerosol formation during wintertime over urban environment in western India. Atmos. Environ. 45, 1940-1945.

Riva, M., Tomaz, S., Cui, T., Lin, Y.H., Perraudin, E., Gold, A., Stone, E.A., Villenave, E., Surratt, J.D., 2015. Evidence for an unrecognized secondary anthropogenic source of organosulfates and sulfonates: gas-phase oxidation of polycyclic aromatic hydrocarbons in the presence of sulfate aerosol. Environ. Sci. Technol. 49, 6654-6664.

Robinson, A.L., Donahue, N.M., Shrivastava, M.K., Weitkamp, E.A., Sage, A.M., Grieshop, A.P., Lane, T.E., Pierce, J.R., Pandis, S.N., 2007. Rethinking Organic Aerosols: Semivolatile Emissions and Photochemical Aging. Science 315, 1259-1262.

Roy, A., Choi, Y., Souri, A.H., Jeon, W., Diao, L., Pan, S., Westenbarger, D., 2018. Effects of Biomass Burning Emissions on Air Quality Over the Continental USA: A Three-Year Comprehensive Evaluation Accounting for Sensitivities Due to Boundary Conditions and Plume Rise Height, in: Gupta, T., Agarwal, A.K., Agarwal, R.A., Labhsetwar, N.K. (Eds.), Environmental Contaminants: Measurement, Modelling and Control. Springer Singapore, Singapore, pp. 245-278.

Rutter, A.P., Snyder, D.C., Stone, E.A., Shelton, B., DeMinter, J., Schauer, J.J., 2014. Preliminary assessment of the anthropogenic and biogenic contributions to secondary organic aerosols at two industrial cities in the upper Midwest. Atmos. Environ. 84, 307-313.

Safai, P.D., Raju, M.P., Rao, P.S.P., Pandithurai, G., 2014. Characterization of carbonaceous aerosols over the urban tropical location and a new approach to evaluate their climatic importance. Atmos. Environ. 92, 493-500.

Saffari, A., Hasheminassab, S., Shafer, M.M., Schauer, J.J., Chatila, T.A., Sioutas, C., 2016. Nighttime aqueous-phase secondary organic aerosols in Los Angeles and its implication for fine particulate matter composition and oxidative potential. Atmos. Environ. 133, 112-122.

Salcedo, D., Onasch, T.B., Dzepina, K., Canagaratna, M., Zhang, Q., Huffman, J., DeCarlo, P., Jayne, J., Mortimer, P., Worsnop, D.R., 2006. Characterization of ambient aerosols in Mexico City during the MCMA-2003 campaign with Aerosol Mass Spectrometry: results from the CENICA Supersite. Atmos. Chem. Phys. 6, 925-946.

Salvador, C.M., Ho, T.T., Chou, C.C.K., Chen, M.J., Huang, W.R., Huang, S.H., 2016. Characterization of the organic matter in submicron urban aerosols using a Thermo-Desorption Proton-Transfer-Reaction Time-of-Flight Mass Spectrometer (TD-PTR-TOF-MS). Atmos. Environ. 140, 565-575.

Samara, C., Voutsa, D., Kouras, A., Eleftheriadis, K., Maggos, T., Saraga, D., Petrakakis, M., 2014. Organic and elemental carbon associated to PM10 and PM2. 5 at urban sites of northern Greece. Environ. Sci. Pollut. Res. 21, 1769-1785.

Sara, C., Luisa, C., Bernd, G., 2009. Positive Matrix Factorisation (PMF) - An Introduction to the Chemometric Evaluation of Environmental Monitoring Data Using PMF.

Sareen, N., Waxman, E.M., Turpin, B.J., Volkamer, R., Carlton, A.G., 2017. Potential of Aerosol Liquid Water to Facilitate Organic Aerosol Formation: Assessing Knowledge Gaps about Precursors and Partitioning. Environ. Sci. Technol. 51, 3327-3335.

Sasaki, J., Aschmann, S.M., Kwok, E.S.C., Atkinson, R., Arey, J., 1997. Products of the Gas-Phase OH and NO3 Radical-Initiated Reactions of Naphthalene. Environ. Sci. Technol. 31, 3173-3179.

Saylor, R.D., Edgerton, E.S., Hartsell, B.E., 2006. Linear regression techniques for use in the EC tracer method of secondary organic aerosol estimation. Atmos. Environ. 40, 7546-7556.

Schauer, J.J., Kleeman, M.J., Cass, G.R., Simoneit, B.R.T., 1999. Measurement of Emissions from Air Pollution Sources. 2. C1 through C30 Organic Compounds from Medium Duty Diesel Trucks. Environ. Sci. Technol. 33, 1578-1587.

Schauer, J.J., Kleeman, M.J., Cass, G.R., Simoneit, B.R.T., 2001. Measurement of Emissions from Air Pollution Sources. 4. C1−C27 Organic Compounds from Cooking with Seed Oils. Environ. Sci. Technol. 36, 567-575.

Schauer, J.J., Rogge, W.F., Hildemann, L.M., Mazurek, M.A., Cass, G.R., Simoneit, B.R., 1996. Source apportionment of airborne particulate matter using organic compounds as tracers. Atmos. Environ. 30, 3837-3855.

Schichtel, B.A., Malm, W.C., Bench, G., Fallon, S., McDade, C.E., Chow, J.C., Watson, J.G., 2008. Fossil and contemporary fine particulate carbon fractions at 12 rural and urban sites in the United States. J. Geophys. Res.-Atmos. 113.

Schilling Fahnestock, K.A., Yee, L.D., Loza, C.L., Coggon, M.M., Schwantes, R., Zhang, X., Dalleska, N.F., Seinfeld, J.H., 2015. Secondary Organic Aerosol Composition from C12 Alkanes. J. Phys. Chem. A 119, 4281-4297.

Seguel A, R., Morales S, R.G.E., Leiva G, M.A., 2009. Estimations of primary and secondary organic carbon formation in PM2.5 aerosols of Santiago City, Chile. Atmos. Environ. 43, 2125-2131.

Seinfeld, J., Pandis, S., 2006. Atmospheric chemistry and physics. Hoboken. NJ: Wiley.

Seinfeld, J.H., Pandis, S.N., 1998. Atmospheric Chemistry and Physics, 1326 pp. John Wiley, Hoboken, NJ.

Shakya, K.M., Griffin, R.J., 2010. Secondary Organic Aerosol from Photooxidation of Polycyclic Aromatic Hydrocarbons. Environ. Sci. Technol. 44, 8134-8139.

Sheesley, R.J., Schauer, J.J., Zheng, M., Wang, B., 2007. Sensitivity of molecular marker-based CMB models to biomass burning source profiles. Atmos. Environ. 41, 9050-9063.

Shen, R.Q., Ding, X., He, Q.F., Cong, Z.Y., Yu, Q.Q., Wang, X.M., 2015. Seasonal variation of secondary organic aerosol tracers in Central Tibetan Plateau. Atmos. Chem. Phys. 15, 8781-8793.

Shi, G.-L., Tian, Y.-Z., Zhang, Y.-F., Ye, W.-Y., Li, X., Tie, X.-X., Feng, Y.-C., Zhu, T., 2011. Estimation of the concentrations of primary and secondary organic carbon in ambient particulate matter: Application of the CMB-Iteration method. Atmos. Environ. 45, 5692-5698.

Shirmohammadi, F., Hasheminassab, S., Saffari, A., Schauer, J.J., Delfino, R.J., Sioutas, C., 2016. Fine and ultrafine particulate organic carbon in the Los Angeles basin: Trends in sources and composition. Sci. Total Environ. 541, 1083-1096.

Shrivastava, M.K., Subramanian, R., Rogge, W.F., Robinson, A.L., 2007. Sources of organic aerosol: Positive matrix factorization of molecular marker data and comparison of results from different source apportionment models. Atmos. Environ. 41, 9353-9369.

Simon, H., Beck, L., Bhave, P.V., Divita, F., Hsu, Y., Luecken, D., Mobley, J.D., Pouliot, G.A., Reff, A., Sarwar, G., Strum, M., 2010. The development and uses of EPA's SPECIATE database. Atmos. Pollut. Res. 1, 196-206.

Simoneit, B.R., Mazurek, M.A., 1982. Organic matter of the troposphere—II.For Part I, see Simoneit et al.(1977). Natural background of biogenic lipid matter in aerosols over the rural western united states. Atmos. Environ. 16, 2139-2159.

Simoneit, B.R., Schauer, J.J., Nolte, C., Oros, D.R., Elias, V.O., Fraser, M., Rogge, W., Cass, G.R., 1999. Levoglucosan, a tracer for cellulose in biomass burning and atmospheric particles. Atmos. Environ. 33, 173-182.

Slowik, J.G., Lopez-Hilfiker, F., Pospisilova, V., Qi, L., Stefenelli, G., Tong, Y., Vogel, A.L., Wang, L., Yuan, B., Xiao, M., Huang, W., Mohr, C., Dommen, J., El Haddad, I., Baltensperger, U., Prévôt, A.S.H., 2017. Towards Quantitative Organic Aerosol Sampling with an Extractive Electrospray Ionization Time-of-Flight Mass Spectrometer (EESI-TOF). AAAR, Raleigh (USA).

Slowik, J.G., Vlasenko, A., McGuire, M., Evans, G.J., Abbatt, J.P.D., 2010. Simultaneous factor analysis of organic particle and gas mass spectra: AMS and PTR-MS measurements at an urban site. Atmos. Chem. Phys. 10, 1969-1988.

Sofowote, U.M., Healy, R.M., Su, Y., Debosz, J., Noble, M., Munoz, A., Jeong, C.H., Wang, J.M., Hilker, N., Evans, G.J., Hopke, P.K., 2018. Understanding the PM2.5 imbalance between a far and near-road location: Results of high temporal frequency source apportionment and parameterization of black carbon. Atmos. Environ. 173, 277-288.

Srivastava, D., Favez, O., Bonnaire, N., Lucarelli, F., Perraudin, E., Gros, V., Villenave, E., Albinet, A., 2018a. Speciation of organic fractions does matter for aerosol source apportionment. Part 2: intensive campaign in the Paris area (France). Sci. Total Environ.

Srivastava, D., Tomaz, S., Favez, O., Lanzafame, G.M., Golly, B., Besombes, J.-L., Alleman, L.Y., Jaffrezo, J.-L., Jacob, V., Perraudin, E., Villenave, E., Albinet, A., 2018b. Speciation of organic fraction does matter for source apportionment. Part 1: A one-year campaign in Grenoble (France). Sci. Total Environ., In press.

Stefenelli, G., Lopez-Hilfiker, F., Pospisilova, V., Vogel, A.L., Hueglin, C., Rigler, M., Baltensperger, U., Prévôt, A.S.H., Slowik, J.G., 2017. Investigation of Biogenic Influences and Day/Night Chemistry on Secondary Organic Aerosol by Extractive Electrospray Ionization Time-Of-Flight Mass Spectrometry (EESI-TOF). AAAR, Raleigh (USA).

Steinbrecher, R., Smiatek, G., Köble, R., Seufert, G., Theloke, J., Hauff, K., Ciccioli, P., Vautard, R., Curci, G., 2009. Intra- and inter-annual variability of VOC emissions from natural and semi-natural vegetation in Europe and neighbouring countries. Atmos. Environ. 43, 1380-1391.

Stone, E., Schauer, J., Quraishi, T.A., Mahmood, A., 2010a. Chemical characterization and source apportionment of fine and coarse particulate matter in Lahore, Pakistan. Atmos. Environ. 44, 1062-1070.

Stone, E.A., Hedman, C.J., Zhou, J., Mieritz, M., Schauer, J.J., 2010b. Insights into the nature of secondary organic aerosol in Mexico City during the MILAGRO experiment 2006. Atmos. Environ. 44, 312-319.

Stone, E.A., Snyder, D.C., Sheesley, R.J., Sullivan, A., Weber, R., Schauer, J., 2008. Source apportionment of fine organic aerosol in Mexico City during the MILAGRO experiment 2006. Atmos. Chem. Phys. 8, 1249-1259.

Stone, E.A., Zhou, J., Snyder, D.C., Rutter, A.P., Mieritz, M., Schauer, J.J., 2009. A Comparison of Summertime Secondary Organic Aerosol Source Contributions at Contrasting Urban Locations. Environ. Sci. Technol. 43, 3448-3454.

Strader, R., Lurmann, F., Pandis, S.N., 1999. Evaluation of secondary organic aerosol formation in winter. Atmos. Environ. 33, 4849-4863.

Stuiver, M., Polach, H.A., 1977. Discussion reporting of 14 C data. Radiocarbon 19, 355-363.

Subramanian, R., Donahue, N.M., Bernardo-Bricker, A., Rogge, W.F., Robinson, A.L., 2007. Insights into the primary–secondary and regional–local contributions to organic aerosol and PM2.5 mass in Pittsburgh, Pennsylvania. Atmos. Environ. 41, 7414-7433.

Subramanian, R., Khlystov, A.Y., Cabada, J.C., Robinson, A.L., 2004. Positive and negative artifacts in particulate organic carbon measurements with denuded and undenuded sampler configurations special issue of aerosol science and technology on findings from the fine particulate matter supersites program. Aerosol Sci. Technol. 38, 27-48.

Subramoney, P., Karnae, S., Farooqui, Z., John, K., Gupta, A.K., 2013. Identification of PM2. 5 sources affecting a semi-arid coastal region using a chemical mass balance model. Aerosol Air Qual Res 13, 60-71.

Sudheer, A.K., Rengarajan, R., Sheel, V., 2015. Secondary organic aerosol over an urban environment in a semi–arid region of western India. Atmos. Pollut. Res. 6, 11-20.

Sui, X., Yang, L.-X., Yi, H., Yuan, Q., Yan, C., Dong, C., Meng, C.-P., Yao, L., Yang, F., Wang, W.-X., 2015. Influence of Seasonal Variation and Long-Range Transport of Carbonaceous Aerosols on Haze Formation at a Seaside Background Site, China. Aerosol. Air Qual. Res. 15, 1251-1260.

Sun, Y., Zhang, Q., Schwab, J., Yang, T., Ng, N., Demerjian, K., 2012. Factor analysis of combined organic and inorganic aerosol mass spectra from high resolution aerosol mass spectrometer measurements. Atmos. Chem. Phys. 12, 8537-8551.

Sun, Y.L., Zhang, Q., Schwab, J.J., Demerjian, K.L., Chen, W.N., Bae, M.S., Hung, H.M., Hogrefe, O., Frank, B., Rattigan, O.V., Lin, Y.C., 2011. Characterization of the sources and

processes of organic and inorganic aerosols in New York city with a high-resolution time-of-flight aerosol mass apectrometer. Atmos. Chem. Phys. 11, 1581-1602.

Sunder Raman, R., Hopke, P.K., Holsen, T.M., 2008. Carbonaceous aerosol at two rural locations in New York State: Characterization and behavior. J. Geophys. Res.-Atmos. 113.

Surratt, J.D., Lewandowski, M., Offenberg, J.H., Jaoui, M., Kleindienst, T.E., Edney, E.O., Seinfeld, J.H., 2007. Effect of acidity on secondary organic aerosol formation from isoprene. Environ. Sci. Technol. 41, 5363-5369.

Szidat, S., Ruff, M., Perron, N., Wacker, L., Synal, H.-A., Hallquist, M., Shannigrahi, A.S., Yttri, K.E., Dye, C., Simpson, D., 2009. Fossil and non-fossil sources of organic carbon (OC) and elemental carbon (EC) in Göteborg, Sweden. Atmos. Chem. Phys. 9, 1521-1535.

Tao, J., Ho, K.-F., Chen, L., Zhu, L., Han, J., Xu, Z., 2009. Effect of chemical composition of PM 2.5 on visibility in Guangzhou, China, 2007 spring. Particuology 7, 68-75.

Tian, M., Wang, H., Chen, Y., Yang, F., Zhang, X., Zou, Q., Zhang, R., Ma, Y., He, K., 2016. Characteristics of aerosol pollution during heavy haze events in Suzhou, China. Atmos. Chem. Phys. 16, 7357-7371.

Tie, X., Li, G., Ying, Z., Guenther, A., Madronich, S., 2006. Biogenic emissions of isoprenoids and NO in China and comparison to anthropogenic emissions. Sci. Total Environ. 371, 238-251.

Tkacik, D.S., Presto, A.A., Donahue, N.M., Robinson, A.L., 2012. Secondary Organic Aerosol Formation from Intermediate-Volatility Organic Compounds: Cyclic, Linear, and Branched Alkanes. Environ. Sci. Technol. 46, 8773-8781.

Toro Araya, R., Flocchini, R., Morales Segura, R.G., Leiva Guzman, M.A., 2014. Carbonaceous aerosols in fine particulate matter of Santiago Metropolitan Area, Chile. Sci. World J. 2014, 794590.

Tsapakis, M., Stephanou, E.G., 2003. Collection of gas and particle semi-volatile organic compounds: use of an oxidant denuder to minimize polycyclic aromatic hydrocarbons degradation during high-volume air sampling. Atmos. Environ. 37, 4935-4944.

Tsigaridis, K., Daskalakis, N., Kanakidou, M., Adams, P., Artaxo, P., Bahadur, R., Balkanski, Y., Bauer, S., Bellouin, N., Benedetti, A., 2014. The AeroCom evaluation and intercomparison of organic aerosol in global models. Atmos. Chem. Phys. 14, 10845-10895.

Tsigaridis, K., Kanakidou, M., 2007. Secondary organic aerosol importance in the future atmosphere. Atmos. Environ. 41, 4682-4692.

Turpin, B.J., Huntzicker, J.J., 1995. Identification of secondary organic aerosol episodes and quantitation of primary and secondary organic aerosol concentrations during SCAQS. Atmos. Environ. 29, 3527-3544.

Turpin, B.J., Huntzicker, J.J., Hering, S.V., 1994. Investigation of organic aerosol sampling artifacts in the los angeles basin. Atmos. Environ. 28, 3061-3071.

Turpin, B.J., Huntzicker, J.J., Larson, S.M., Cass, G.R., 1991. Los Angeles summer midday particulate carbon: primary and secondary aerosol. Environ. Sci. Technol. 25, 1788-1793.

Turpin, B.J., Saxena, P., Andrews, E., 2000. Measuring and simulating particulate organics in the atmosphere: problems and prospects. Atmos. Environ. 34, 2983-3013.

Vega, E., Eidels, S., Ruiz, H., López-Veneroni, D., Sosa, G., Gonzalez, E., Gasca, J., Mora, V., Reyes, E., Sánchez-Reyna, G., 2010. Particulate air pollution in Mexico City: a detailed view. Aerosol. Air Qual. Res. 10, 193-211.

Viana, M., Alastuey, A., Querol, X., Guerreiro, C., Vogt, M., Colette, A., Collet, S., Albinet, A., Fraboulet, I., Lacome, J.-M., 2015. Contribution of residential combustion to ambient air pollution and greenhouse gas emissions. ETC/ACM Technical Paper 1.

Villalobos, A.M., Amonov, M.O., Shafer, M.M., Devi, J.J., Gupta, T., Tripathi, S.N., Rana, K.S., McKenzie, M., Bergin, M.H., Schauer, J.J., 2015. Source apportionment of carbonaceous fine particulate matter (PM2.5) in two contrasting cities across the Indo–Gangetic Plain. Atmos. Pollut. Res. 6, 398-405.

Vlachou, A., Daellenbach, K.R., Bozzetti, C., Chazeau, B., Salazar, G.A., Szidat, S., Jaffrezo, J.L., Hueglin, C., Baltensperger, U., El Haddad, I., Prévôt, A.S.H., 2017. Advanced source apportionment of carbonaceous aerosols by coupling offline AMS and radiocarbon size segregated measurements over a nearly two-year period. Atmos. Chem. Phys. Discuss. 2017, 1-25.

Volkamer, R., Jimenez, J.L., San Martini, F., Dzepina, K., Zhang, Q., Salcedo, D., Molina, L.T., Worsnop, D.R., Molina, M.J., 2006. Secondary organic aerosol formation from anthropogenic air pollution: Rapid and higher than expected. Geophys. Res. Lett. 33.

von Schneidemesser, E., Schauer, J.J., Hagler, G.S.W., Bergin, M.H., 2009. Concentrations and sources of carbonaceous aerosol in the atmosphere of Summit, Greenland. Atmos. Environ. 43, 4155-4162.

von Schneidemesser, E., Zhou, I., Stone, E.A., Schauer, J.I., Shpund, J., Brenner, S., Qasrawi, R., Abdeen, Z., Sarnat, J.A., 2010a. Spatial variability of carbonaceous aerosol concentrations in East and West Jerusalem. Environ. Sci. Technol. 44, 1911-1917.

von Schneidemesser, E., Zhou, J., Stone, E.A., Schauer, J.J., Qasrawi, R., Abdeen, Z., Shpund, J., Vanger, A., Sharf, G., Moise, T., Brenner, S., Nassar, K., Saleh, R., Al-Mahasneh, Q.M., Sarnat, J.A., 2010b. Seasonal and spatial trends in the sources of fine particle organic carbon in Israel, Jordan, and Palestine. Atmos. Environ. 44, 3669-3678.

Wagener, S., Langner, M., Hansen, U., Moriske, H.-J., Endlicher, W., 2014. Assessing the Influence of Seasonal and Spatial Variations on the Estimation of Secondary Organic Carbon in Urban Particulate Matter by Applying the EC-Tracer Method. Atmosphere 5, 252-272.

Wang, F., Guo, Z., Lin, T., Rose, N.L., 2016a. Seasonal variation of carbonaceous pollutants in PM2.5 at an urban 'supersite' in Shanghai, China. Chemosphere 146, 238-244.

Wang, J., Ho, S.S.H., Ma, S., Cao, J., Dai, W., Liu, S., Shen, Z., Huang, R., Wang, G., Han, Y., 2016b. Characterization of PM2.5 in Guangzhou, China: uses of organic markers for supporting source apportionment. Sci. Total Environ. 550, 961-971.

Wang, L., Atkinson, R., Arey, J., 2007. Dicarbonyl Products of the OH Radical-Initiated Reactions of Naphthalene and the C1- and C2-Alkylnaphthalenes. Environ. Sci. Technol. 41, 2803-2810.

Wang, Y., Hopke, P.K., Xia, X., Rattigan, O.V., Chalupa, D.C., Utell, M.J., 2012a. Source apportionment of airborne particulate matter using inorganic and organic species as tracers. Atmos. Environ. 55, 525-532.

Wang, Z., Wang, T., Guo, J., Gao, R., Xue, L., Zhang, J., Zhou, Y., Zhou, X., Zhang, Q., Wang, W., 2012b. Formation of secondary organic carbon and cloud impact on carbonaceous aerosols at Mount Tai, North China. Atmos. Environ. 46, 516-527.

Watson, J.G., Chow, J.C., Fujita, E.M., 2001. Review of volatile organic compound source apportionment by chemical mass balance. Atmos. Environ. 35, 1567-1584.

Watson, J.G., Cooper, J.A., Huntzicker, J.J., 1984. The effective variance weighting for least squares calculations applied to the mass balance receptor model. Atmos. Environ. 18, 1347-1355.

Watson, J.G., Robinson, N.F., Chow, J.C., Henry, R.C., Kim, B., Pace, T., Meyer, E.L., Nguyen, Q., 1990. The USEPA/DRI chemical mass balance receptor model, CMB 7.0. Environmental Software 5, 38-49.

Watson, J.G., Zhu, T., Chow, J.C., Engelbrecht, J., Fujita, E.M., Wilson, W.E., 2002. Receptor modeling application framework for particle source apportionment. Chemosphere 49, 1093-1136.

Weber, R.J., Sullivan, A.P., Peltier, R.E., Russell, A., Yan, B., Zheng, M., de Gouw, J., Warneke, C., Brock, C., Holloway, J.S., Atlas, E.L., Edgerton, E., 2007. A study of secondary organic aerosol formation in the anthropogenic-influenced southeastern United States. J. Geophys. Res.-Atmos. 112, D13302.

Williams, B.J., Goldstein, A.H., Kreisberg, N.M., Hering, S.V., Worsnop, D.R., Ulbrich, I.M., Docherty, K.S., Jimenez, J.L., 2010. Major components of atmospheric organic aerosol in southern California as determined by hourly measurements of source marker compounds. Atmos. Chem. Phys. 10, 11577-11603.

Williams, B.J., Jayne, J.T., Lambe, A.T., Hohaus, T., Kimmel, J.R., Sueper, D., Brooks, W., Williams, L.R., Trimborn, A.M., Martinez, R.E., Hayes, P.L., Jimenez, J.L., Kreisberg, N.M., Hering, S.V., Worton, D.R., Goldstein, A.H., Worsnop, D.R., 2014. The First Combined Thermal Desorption Aerosol Gas Chromatograph—Aerosol Mass Spectrometer (TAG-AMS). Aerosol Sci. Technol. 48, 358-370.

Wu, C., Huang, X.H.H., Ng, W.M., Griffith, S.M., Yu, J.Z., 2016. Inter-comparison of NIOSH and IMPROVE protocols for OC and EC determination: implications for inter-protocol data conversion. Atmos. Meas. Tech. 9, 4547-4560.

Wu, C., Yu, J.Z., 2016. Determination of primary combustion source organic carbon-to-elemental carbon (OC/EC) ratio using ambient OC and EC measurements: secondary OC-EC correlation minimization method. Atmos. Chem. Phys. 16, 5453-5465.

Wu, H., Zhang, Y.-f., Han, S.-q., Wu, J.-h., Bi, X.-h., Shi, G.-l., Wang, J., Yao, Q., Cai, Z.-y., Liu, J.-l., Feng, Y.-c., 2015. Vertical characteristics of PM2.5 during the heating season in Tianjin, China. Sci. Total Environ. 523, 152-160.

Xu, J., Zhang, Q., Chen, M., Ge, X., Ren, J., Qin, D., 2014. Chemical composition, sources, and processes of urban aerosols during summertime in northwest China: insights from high-resolution aerosol mass spectrometry. Atmos. Chem. Phys. 14, 12593-12611.

Xu, L., Pye, H.O.T., He, J., Chen, Y., Murphy, B.N., Ng, N.L., 2018. Large Contributions from Biogenic Monoterpenes and Sesquiterpenes to Organic Aerosol in the Southeastern United States. Atmos. Chem. Phys. Discuss. 2018, 1-47.

Xu, Z., Wen, T., Li, X., Wang, J., Wang, Y., 2015. Characteristics of carbonaceous aerosols in Beijing based on two–year observation. Atmos. Pollut. Res. 6, 202-208.

Yang, F., Kawamura, K., Chen, J., Ho, K., Lee, S., Gao, Y., Cui, L., Wang, T., Fu, P., 2016. Anthropogenic and biogenic organic compounds in summertime fine aerosols (PM2.5) in Beijing, China. Atmos. Environ. 124, Part B, 166-175.

Yang, H., Yu, J.Z., Ho, S.S.H., Xu, J., Wu, W.-S., Wan, C.H., Wang, X., Wang, X., Wang, L., 2005. The chemical composition of inorganic and carbonaceous materials in PM2.5 in Nanjing, China. Atmos. Environ. 39, 3735-3749.

Yao, L., Yang, L., Chen, J., Wang, X., Xue, L., Li, W., Sui, X., Wen, L., Chi, J., Zhu, Y., Zhang, J., Xu, C., Zhu, T., Wang, W., 2016. Characteristics of carbonaceous aerosols: Impact of biomass burning and secondary formation in summertime in a rural area of the North China Plain. Sci. Total Environ. 557–558, 520-530.

Ye, P., Zhao, Y., Chuang, W.K., Robinson, A.L., Donahue, N.M., 2017. Secondary organic aerosol production from pinanediol, a semi-volatile surrogate for first-generation oxidation products of monoterpenes. Atmos. Chem. Phys. Discuss. 2017, 1-46.

Yee, L., Kautzman, K., Loza, C., Schilling, K., Coggon, M., Chhabra, P., Chan, M., Chan, A., Hersey, S., Crounse, J., 2013. Secondary organic aerosol formation from biomass burning intermediates: phenol and methoxyphenols. Atmos. Chem. Phys. 13, 8019-8043.

Yin, J., Harrison, R.M., Chen, Q., Rutter, A., Schauer, J.J., 2010. Source apportionment of fine particles at urban background and rural sites in the UK atmosphere. Atmos. Environ. 44, 841-851.

Yu, J., Chen, T., Benjamin, G., Helene, C., Yu, T., Liu, W., Wang, X., 2006. Characteristics of carbonaceous particles in Beijing during winter and summer 2003. Adv. Atmospheric Sci. 23, 468-473.

Yu, S., Bhave, P.V., Dennis, R.L., Mathur, R., 2007. Seasonal and Regional Variations of Primary and Secondary Organic Aerosols over the Continental United States: Semi-Empirical Estimates and Model Evaluation. Environ. Sci. Technol. 41, 4690-4697.

Yu, S., Dennis, R.L., Bhave, P.V., Eder, B.K., 2004. Primary and secondary organic aerosols over the United States: estimates on the basis of observed organic carbon (OC) and elemental carbon (EC), and air quality modeled primary OC/EC ratios. Atmos. Environ. 38, 5257-5268.

Yuan, Z., Lau, A.K.H., Zhang, H., Yu, J.Z., Louie, P.K., Fung, J.C., 2006a. Identification and spatiotemporal variations of dominant PM10 sources over Hong Kong. Atmos. Environ. 40, 1803-1815.

Yuan, Z., Yu, J., Lau, A., Louie, P., Fung, J.C.H., 2006b. Application of positive matrix factorization in estimating aerosol secondary organic carbon in Hong Kong and its relationship with secondary sulfate. Atmos. Chem. Phys. 6, 25-34.

Yubero, E., Galindo, N., Nicolás, J., Crespo, J., Calzolai, G., Lucarelli, F., 2015. Temporal variations of PM1 major components in an urban street canyon. Environ. Sci. Pollut. Res. 22, 13328-13335.

Zhang, F., Xu, L., Chen, J., Chen, X., Niu, Z., Lei, T., Li, C., Zhao, J., 2013. Chemical characteristics of PM 2.5 during haze episodes in the urban of Fuzhou, China. Particuology 11, 264-272.

Zhang, F., Zhao, J., Chen, J., Xu, Y., Xu, L., 2011a. Pollution characteristics of organic and elemental carbon in PM2.5 in Xiamen, China. J. Environ. Sci. 23, 1342-1349.

Zhang, H., 2012. Secondary organic aerosol from polycyclic aromatic hydrocarbons in Southeast Texas. Atmos. Environ. v. 55, pp. 279-287-2012 v.2055.

Zhang, H., Yee, L.D., Lee, B.H., Curtis, M.P., Worton, D.R., Isaacman-VanWertz, G., Offenberg, J.H., Lewandowski, M., Kleindienst, T.E., Beaver, M.R., Holder, A.L., Lonneman, W.A., Docherty, K.S., Jaoui, M., Pye, H.O.T., Hu, W., Day, D.A., Campuzano-Jost, P., Jimenez, J.L., Guo, H., Weber, R.J., de Gouw, J., Koss, A.R., Edgerton, E.S., Brune, W., Mohr, C., Lopez-Hilfiker, F.D., Lutz, A., Kreisberg, N.M., Spielman, S.R., Hering, S.V., Wilson, K.R., Thornton, J.A., Goldstein, A.H., 2018. Monoterpenes are the largest source of summertime organic aerosol in the southeastern United States. Proc. Natl. Acad. Sci. 115, 2038-2043.

Zhang, Q., Jimenez, J.L., Canagaratna, M.R., Allan, J.D., Coe, H., Ulbrich, I., Alfarra, M.R., Takami, A., Middlebrook, A.M., Sun, Y.L., Dzepina, K., Dunlea, E., Docherty, K., DeCarlo, P.F., Salcedo, D., Onasch, T., Jayne, J.T., Miyoshi, T., Shimono, A., Hatakeyama, S., Takegawa, N., Kondo, Y., Schneider, J., Drewnick, F., Borrmann, S., Weimer, S., Demerjian, K., Williams, P., Bower, K., Bahreini, R., Cottrell, L., Griffin, R.J., Rautiainen, J., Sun, J.Y., Zhang, Y.M., Worsnop, D.R., 2007. Ubiquity and dominance of oxygenated species in organic aerosols in anthropogenically-influenced Northern Hemisphere midlatitudes. Geophys. Res. Lett. 34.

Zhang, Q., Jimenez, J.L., Canagaratna, M.R., Ulbrich, I.M., Ng, N.L., Worsnop, D.R., Sun, Y., 2011b. Understanding atmospheric organic aerosols via factor analysis of aerosol mass spectrometry: a review. Anal. Bioanal. Chem. 401, 3045-3067.

Zhang, Q., Worsnop, D., Canagaratna, M., Jimenez, J., 2005. Hydrocarbon-like and oxygenated organic aerosols in Pittsburgh: insights into sources and processes of organic aerosols. Atmos. Chem. Phys. 5, 3289-3311.

Zhang, R., Tao, J., Ho, K., Shen, Z., Wang, G., Cao, J., Liu, S., Zhang, L., Lee, S., 2012. Characterization of atmospheric organic and elemental carbon of PM2. 5 in a typical semi-arid area of Northeastern China. Aerosol. Air Qual. Res. 12, 792.

Zhang, Y., Sheesley, R.J., Bae, M.-S., Schauer, J.J., 2009a. Sensitivity of a molecular marker based positive matrix factorization model to the number of receptor observations. Atmos. Environ. 43, 4951-4958.

Zhang, Y., Sheesley, R.J., Schauer, J.J., Lewandowski, M., Jaoui, M., Offenberg, J.H., Kleindienst, T.E., Edney, E.O., 2009b. Source apportionment of primary and secondary organic aerosols using positive matrix factorization (PMF) of molecular markers. Atmos. Environ. 43, 5567-5574.

Zhang, Y., Tang, L., Sun, Y., Favez, O., Canonaco, F., Albinet, A., Couvidat, F., Liu, D., Jayne, J.T., Wang, Z., Croteau, P.L., Canagaratna, M.R., Zhou, H.-c., Prévôt, A.S.H., Worsnop, D.R., 2017. Limited formation of isoprene epoxydiols-derived secondary organic aerosol under NOx-rich environments in Eastern China. Geophys. Res. Lett. 44.

Zhang, Y., Williams, B.J., Goldstein, A.H., Docherty, K.S., Jimenez, J.L., 2016. A technique for rapid source apportionment applied to ambient organic aerosol measurements from a thermal desorption aerosol gas chromatograph (TAG). Atmos. Meas. Tech. 9, 5637-5653.

Zhao, R., Mungall, E.L., Lee, A.K.Y., Aljawhary, D., Abbatt, J.P.D., 2014a. Aqueous-phase photooxidation of levoglucosan – a mechanistic study using aerosol time-of-flight chemical ionization mass spectrometry (Aerosol ToF-CIMS). Atmos. Chem. Phys. 14, 9695-9706.

Zhao, Y., Hennigan, C.J., May, A.A., Tkacik, D.S., de Gouw, J.A., Gilman, J.B., Kuster, W.C., Borbon, A., Robinson, A.L., 2014b. Intermediate-volatility organic compounds: a large source of secondary organic aerosol. Environ. Sci. Technol. 48, 13743-13750.

Zhao, Y., Kreisberg, N.M., Worton, D.R., Isaacman, G., Gentner, D.R., Chan, A.W.H., Weber, R.J., Liu, S., Day, D.A., Russell, L.M., Hering, S.V., Goldstein, A.H., 2013. Sources of organic aerosol investigated using organic compounds as tracers measured during CalNex in Bakersfield. J. Geophys. Res.-Atmos. 118, 2012JD019248.

Zheng, G.J., Duan, F.K., Su, H., Ma, Y.L., Cheng, Y., Zheng, B., Zhang, Q., Huang, T., Kimoto, T., Chang, D., Pöschl, U., Cheng, Y.F., He, K.B., 2015. Exploring the severe winter haze in Beijing: the impact of synoptic weather, regional transport and heterogeneous reactions. Atmos. Chem. Phys. 15, 2969-2983.

Zheng, M., Cass, G.R., Ke, L., Wang, F., Schauer, J.J., Edgerton, E.S., Russell, A.G., 2007. Source apportionment of daily fine particulate matter at Jefferson Street, Atlanta, GA, during summer and winter. J Air Waste Manag Assoc 57, 228-242.

Zheng, M., Hagler, G.S., Ke, L., Bergin, M.H., Wang, F., Louie, P.K., Salmon, L., Sin, D.W., Yu, J.Z., Schauer, J.J., 2006a. Composition and sources of carbonaceous aerosols at three contrasting sites in Hong Kong. J. Geophys. Res.-Atmos. 111.

Zheng, M., Ke, L., Edgerton, E.S., Schauer, J.J., Dong, M., Russell, A.G., 2006b. Spatial distribution of carbonaceous aerosol in the southeastern United States using molecular markers and carbon isotope data. J. Geophys. Res.-Atmos. 111.

Zheng, M., Wang, F., Hagler, G.S.W., Hou, X., Bergin, M., Cheng, Y., Salmon, L.G., Schauer, J.J., Louie, P.K.K., Zeng, L., Zhang, Y., 2011. Sources of excess urban carbonaceous aerosol in the Pearl River Delta Region, China. Atmos. Environ. 45, 1175-1182.

Zheng, M., Zhao, X., Cheng, Y., Yan, C., Shi, W., Zhang, X., Weber, R.J., Schauer, J.J., Wang, X., Edgerton, E.S., 2014. Sources of primary and secondary organic aerosol and their diurnal variations. J. Hazard. Mater. 264, 536-544.

Zhou, J., Xing, Z., Deng, J., Du, K., 2016. Characterizing and sourcing ambient PM2.5 over key emission regions in China I: Water-soluble ions and carbonaceous fractions. Atmos. Environ. 135, 20-30.

Zhou, S., Wang, T., Wang, Z., Li, W., Xu, Z., Wang, X., Yuan, C., Poon, C.N., Louie, P.K.K., Luk, C.W.Y., Wang, W., 2014. Photochemical evolution of organic aerosols observed in urban plumes from Hong Kong and the Pearl River Delta of China. Atmos. Environ. 88, 219-229.

Zhou, S., Wang, Z., Gao, R., Xue, L., Yuan, C., Wang, T., Gao, X., Wang, X., Nie, W., Xu, Z., Zhang, Q., Wang, W., 2012. Formation of secondary organic carbon and long-range transport of carbonaceous aerosols at Mount Heng in South China. Atmos. Environ. 63, 203-212.

Ziemann, P.J., Atkinson, R., 2012. Kinetics, products, and mechanisms of secondary organic aerosol formation. Chem. Soc. Rev. 41, 6582-6605.

Supplementary Material

Comparison of methodologies based on measurement data to apportion secondary organic carbon (SOC) in $PM_{2.5}$: a review of recent studies

D. Srivastava[1, 2,3], O. Favez[1, *], E. Perraudin[2,3], E. Villenave[2,3], A. Albinet[1, *]

[1]INERIS, Parc Technologique Alata, BP 2, 60550 Verneuil-en-Halatte, France

[2]CNRS, EPOC, UMR 5805 CNRS, 33405 Talence, France

[3]Université de Bordeaux, EPOC, UMR 5805 CNRS, 33405 Talence, France

[*] Correspondence to: alexandre.albinet@gmail.com; alexandre.albinet@ineris.fr; olivier.favez@ineris.fr

Annex A: Use of EC tracer method

Calculation of [OC]/[EC] ratio and $[OC]_{non\text{-}comb.}$

The application of the EC tracer method requires the measurements of [OC] and [EC] concentrations together with the determination of the $[OC/EC]_p$ ratio (ratio of OC to EC for the primary sources affecting the site of interest), as well as the non-combustion contribution to the primary OC ($[OC]_{non\text{-}comb)}$ (Cabada et al., 2004; Strader et al., 1999; Turpin and Huntzicker, 1995). $[OC/EC]_p$ and $[OC]_{non\text{-}comb.}$ depend on the dataset used and on the averaging period. The estimation of these parameters is based on linear regressions between [OC] and [EC]. Considering that no OC from secondary processes is formed, $[OC/EC]_p$ can be estimated as the slope of the best straight fit line through the data and $[OC]_{non\text{-}comb.}$ as the y-intercept.

As observed by Turpin and Huntzicker (1995), the linear least-squares is probably not an appropriate method. This linear regression model assumes that the x-values are controlled variables with an exact precision and that all the measurement errors are included in the y variables. However, in the EC tracer method, errors exist for both, [OC] (y variable) and [EC] (x variable). Errors on the x variable result in a significant underestimation of the slope and in a large fictitious positive intercept. Thus, the use of the ordinary least squares is not recommended for the estimation of $[OC/EC]_p$ in the EC tracer method. Deming and York regressions sound more accurate. Both regression models have been formulated to explicitly account for the errors in both coordinates. York regression is the most general while the Deming model is a specific case of the York one (York et al., 2004). By comparison to the Deming regression, the power of the York regression lies in its ability to use information about measurement uncertainties in the regressed variables to improve the linear fit. Saylor et al. (2006) have made corrections on the work done by Chu (2005) using the York regression and showed that if data on the measurement uncertainties are available as a function of the measured concentrations, the use of this regression is preferred for the estimation of the parameters of the

EC tracer method. If only limited data are available, then the Deming regression should be used. This regression should be also preferred when $[OC]_{non\text{-}comb.}$ is non-null but this tends to overcorrect the problem by slightly overestimating the slope and underestimating the intercept (Chu, 2005).

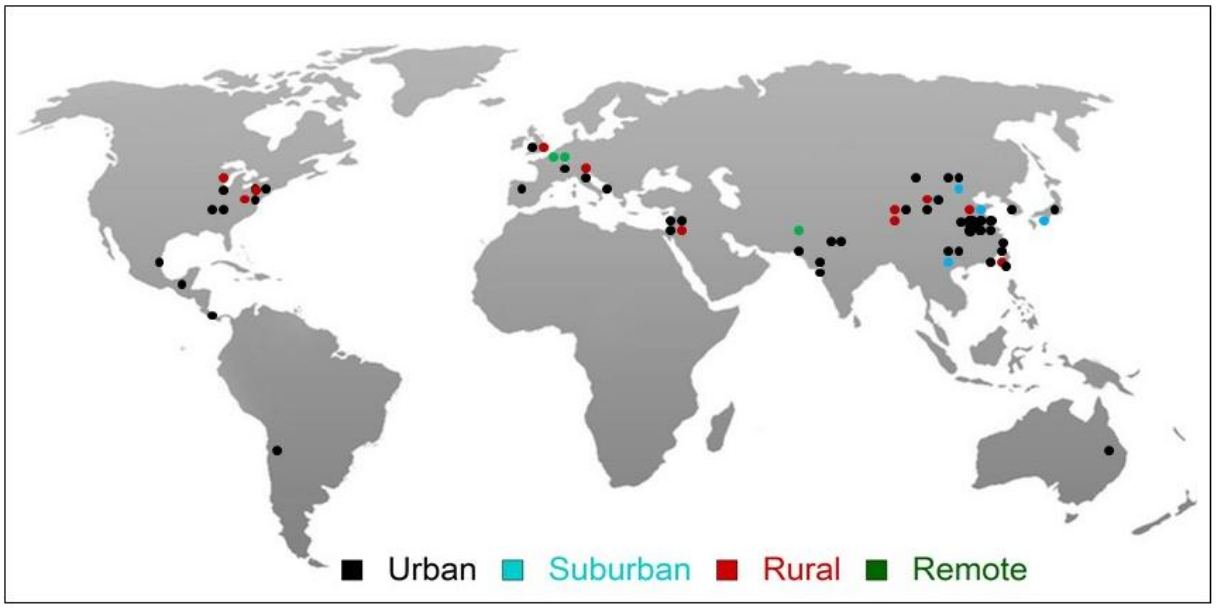

Figure A1. Location of the monitored sites of the studies considered in this review reporting the use of the EC tracer method for the evaluation of SOC $PM_{2.5}$. In black, urban sites; in blue, suburban sites; in red, rural sites and in green, remote sites.

Table A1. Reported [OC/EC] ratios in $PM_{2.5}$ for some locations worldwide.

Locations	Sampling period	[OC/EC]	References
Toronto (Canada)	July 2001	10.5	(Fan et al., 2003)
Vancouver (Canada)	August 2001	11.2	(Fan et al., 2004)
Seattle (USA)	April - May 1999	6.1	(Lewtas et al., 2001)
Pittsburgh (USA)	July 2001	4.4	(Day et al., 2015)
Atlanta (USA)	July 2001	5.2	(Day et al., 2015)
Chicago (USA)	July 2001	3.3	(Day et al., 2015)
New York (USA)	July 2001	1.5	(Day et al., 2015)
Monterrey (Mexico)	May - June 2011	6.1	(Mancilla et al., 2015)
Monterrey (Mexico)	October - November 2011	3.6	(Mancilla et al., 2015)
Helsinki (Finland)	July 2000 - July 2001	2.5	(Viidanoja et al., 2002)
Barcelona (Spain)	July - December 2004	2.6	(Viana et al., 2007)
Ghent (Belgium)	June 2005 - February 2005	4.1	(Viana et al., 2007)
Amsterdam (Netherlands)	July 2005 - February 2006	2.9	(Viana et al., 2007)
Milan (Italy)	August 2002 - December 2003	6.6	(Lonati et al., 2007)
Budapest (Hungary)	April - May 2002	2.1	(Salma et al., 2004)
Sonnblick (Austria)	May - June 2003	7.9	(Pio et al., 2007)
Jungfraujoch (Switzerland)	July - August 1998	3.6	(Krivacsy et al., 2001)
Xiamen (China)	April 2009	6.2	(Zhang et al., 2011)
Xiamen (China)	July 2009	4.4	(Zhang et al., 2011)
Xiamen (China)	October 2009	6.6	(Zhang et al., 2011)
Xiamen (China)	January 2009	6.1	(Zhang et al., 2011)
Beijing (China)	January 2002 - July 2003	2.9	(Feng et al., 2006)
Beijing (China)	July, November 2002	4.6	(Feng et al., 2006)
Shanghai (China)	October 2005 - August 2006	5	(Feng et al., 2009)
Shanghai (China)	October 2005 - August 2006	5.6	(Feng et al., 2009)
Shanghai (China)	November 2002, August 2003	3.8	(Feng et al., 2009)
Guangzhou (China)	July - November 2002	3.8	(Feng et al., 2009)
Guangzhou (China)	December 2002, July 2003	3.5	(Feng et al., 2006)
Nanjing (China)	February - September 2001	3.6	(Yang et al., 2005)
Nanjing (China)	February 2001	4.9	(Yang et al., 2005)
Tianjin (China)	Spring 2008	3	(Gu et al., 2010)
Tianjin (China)	Summer 2008	1.8	(Gu et al., 2010)
Tianjin (China)	Fall 2008	2.8	(Gu et al., 2010)
Tianjin (China)	Winter 2008	3.8	(Gu et al., 2010)
Taiyuan (China)	December 2005 - February 2006	7	(Meng et al., 2007)
Hong Kong (China)	August 2004 - March 2005	3.5	(Duan et al., 2007)
Hong Kong (China)	February 2005 - March 2005	2.6	(Duan et al., 2007)
Hong Kong (China)	August - September 2004, February - March 2005	5.2	(Duan et al., 2007)
Mount Heng (China)	March - May 2009	5.2	(Zhou et al., 2012)
Mount Tai (China)	March - April 2007	5	(Zhou et al., 2012)
Mt Abu (India)	March - June 2007	3.3	(Kumar et al., 2016)
Mt Abu (India)	October 2007 - February 2008	2.8	(Kumar et al., 2016)
Pune (India)	April 2012 - March 2013	2.4	(Safai et al., 2014)
Gwangju (Korea)	June - August 2008	3.1	(Park and Cho, 2011)
Gwangju (Korea)	December 2008 - February 2009	3.0	(Park and Cho, 2011)

Black: urban; Blue: suburban; Green: Remote; Red: rural.

Table A2. List of the studies considered for the annual SOC contribution to $PM_{2.5}$ OC estimated using the EC tracer method for all the monitored sites from 2006 to 2016.

Black: urban; Blue: suburban; Green: Remote; Red: rural.

Locations	SOC (µgC m^{-3})	POC (µgC m^{-3})	References
Atlanta (USA)	1.5	3.3	(Day et al., 2015; Kleindienst et al., 2010; Pachon et al., 2010; Saylor et al., 2006)
Yorkville (USA)	1.1	2.3	(Saylor et al., 2006)
Birmingham (USA)	2.7	3.1	(Day et al., 2015; Kleindienst et al., 2010; Saylor et al., 2006)
Centreville (USA)	1.1	2.9	(Kleindienst et al., 2010; Saylor et al., 2006)
Pittsburgh (USA)	1.4	1.5	(Day et al., 2015; Polidori et al., 2006)
Chicago (USA)	2.3	3.3	(Day et al., 2015)
New York City (USA)	1.1	2.4	(Day et al., 2015)
Potsdam (USA)	1.5	0.7	(Sunder Raman et al., 2008)
Stockton (USA)	1.6	1.2	(Sunder Raman et al., 2008)
Monterrey (Mexico)	4.2	3.2	(Mancilla et al., 2015)
Costa Rica	3.9	3.5	(Murillo et al., 2013)
Santiago (Chile)	3.2	7.1	(Toro Araya et al., 2014)
Madrid (Spain)	2.7	1.0	(Mirante et al., 2014; Plaza et al., 2006)
Veneto region (Italy)	3.8	1.7	(Khan et al., 2016)
San Pietro Capofiume (Italy)	2.2	2.1	(Pietrogrande et al., 2016)
Bologna (Italy)	2.1	2.3	(Pietrogrande et al., 2016)
Thessaloniki (Greece)	3.7	4.4	(Samara et al., 2014)
Zloty Potok (Poland)	3.2	5.3	(Błaszczak et al., 2016)
Raciborz (Poland)	4.9	8.7	(Błaszczak et al., 2016)
Birmingham (UK)	1.6	0.6	(Harrison and Yin, 2008; Laongsri and Harrison, 2013)
Birmingham (UK)	1.8	0.7	(Harrison and Yin, 2008; Laongsri and Harrison, 2013)
Hebron (Palestine)	2.8	2.7	(Abdeen et al., 2014)
Zarqa (Jordan)	4.9	4.2	(Abdeen et al., 2014)
Rachma (Jordan)	1.4	0.8	(Abdeen et al., 2014)
Aqaba (Jordan)	2.3	1.4	(Abdeen et al., 2014)
Amman (Jordan)	3.4	3.3	(Abdeen et al., 2014)
West Jerusalem (Israel)	2.6	1.9	(Abdeen et al., 2014)
Tel Aviv (Israel)	3.0	1.8	(Abdeen et al., 2014)
Haifa (Israel)	1.8	1.7	(Abdeen et al., 2014)
Eilat (Israel)	2.7	0.6	(Abdeen et al., 2014)
Mumbai (India)	11.4	15.9	(Joseph et al., 2012)
Ahmedabad (India)	6.1	7.3	(Rengarajan et al., 2011; Sudheer et al., 2015)
Mt Abu (India)	1.2	1.4	(Kumar et al., 2016)
New Delhi (India)	26.4	34.6	(Pant et al., 2015)
Pune (India)	12.8	9.5	(Pipal and Gursumeeran Satsangi, 2015; Safai et al., 2014)
Gurgoan (India)	13.1	15.3	(Hooda et al., 2016)
Beijing (China)	5.3	8.7	(Cao et al., 2007; Ji et al., 2016; Lin et al., 2009; Lv et al., 2016; Yu et al., 2006)
Shanghai (China)	4.7	6.2	(Feng et al., 2013; Feng et al., 2009; Qiao et al., 2016; Wang et al., 2016a; Zhou et al., 2016)
Shanghai (China)	5.4	9.0	(Feng et al., 2013; Feng et al., 2009)
Wangqingsha (China)	5.4	9.8	(Ding et al., 2012)
Yellow river delta (China)	3.6	4.0	(Sui et al., 2015)
Nancun (China)	2.8	4.0	(Wu and Yu, 2016)

Changchun (China)	9.6	16.4	(Cao et al., 2007)
Jinchang (China)	5.8	9.9	(Cao et al., 2007)
Qingdao (China)	5.8	10.0	(Cao et al., 2007)
Tianjin (China)	11.7	11.9	(Cao et al., 2007; Gu et al., 2010; Li and Bai, 2009; Zhou et al., 2016)
Xi'an (China)	23.9	40.9	(Cao et al., 2007)
Yulin (China)	8.5	14.6	(Cao et al., 2007)
Chongqing (China)	11.4	21.8	(Cao et al., 2007; Chen et al., 2014)
Guangzhao (China)	5.6	8.9	(Cao et al., 2007; Duan et al., 2007; Fan et al., 2016; Huang et al., 2012; Lai et al., 2016)
HongKong (China)	3.1	3.0	(Cao et al., 2007)
Hangzhou (China)	10.3	13.6	(Cao et al., 2007)
Wuhan (China)	9.0	11.9	(Cao et al., 2007)
Xiamen (China)	7.3	7.2	(Cao et al., 2007; Zhang et al., 2011)
Nanjing (China)	4.9	8.9	(Li et al., 2015a)
Fozhou (China)	2.5	6.4	(Niu et al., 2013; Zhang et al., 2013)
Xinhua (China)	5.9	8.2	(Zhang et al., 2012)
Zhaoqing (China)	3.5	4.7	(Huang et al., 2012)
Chengdu (China)	5.1	13.9	(Chen et al., 2014)
Neijing (China)	4.5	13.8	(Chen et al., 2014)
Haining (China)	5.6	3.4	(Zhou et al., 2016)
Zhongshan (China)	4.4	2.6	(Zhou et al., 2016)
Deyang (China)	8.6	5.2	(Zhou et al., 2016)
Cape Fuguei (Taiwan)	2.2	1.6	(Chou et al., 2010)
Taipei (Taiwan)	4.5	2.1	(Chou et al., 2010)
Taichung (Taiwan)	6.1	3.4	(Chou et al., 2010)
Tainan (Taiwan)	5.7	2.3	(Chou et al., 2010)
Pingtung (Taiwan)	7.8	2.8	(Chou et al., 2010)
Penghu (Taiwan)	1.2	1.0	(Chou et al., 2010)
Hualien (Taiwan)	2.6	1.5	(Chou et al., 2010)
Ichikara (Japan)	1.2	2.0	(Ichikawa et al., 2015)
Yokohama (Japan)	1.9	1.9	(Khan et al., 2010)
Seoul (Korea)	1.1	6.2	(Kim et al., 2012)
Gwangju (Korea)	1.9	4.8	(Park and Cho, 2011)
Incheon (Korea)	4.6	3.3	(Choi et al., 2012)
Brisbane (Australia)	1.6	0.9	(Crilley et al., 2016)

Table A3. List of the studies considered for the spring-summer SOC contribution to $PM_{2.5}$ OC estimated using the EC tracer method for all the monitored sites from 2006 to 2016.

Locations	SOC (µgC m^{-3})	POC (µgC m^{-3})	References
Atlanta (USA)	1.4	2.6	(Kleindienst et al., 2010; Pachon et al., 2010)
Birmingham (USA)	1.8	2.5	(Kleindienst et al., 2010)
Centreville (USA)	1.2	2.8	(Kleindienst et al., 2010)
Pittsburgh (USA)	1.0	2.3	(Polidori et al., 2006)
Santiago (Chile)	4.7	10.1	(Toro Araya et al., 2014)
Monterrey (Mexico)	5.3	2.7	(Mancilla et al., 2015)
Milan (Italy)	4.4	0.9	(Lonati et al., 2007)
Veneto region (Italy)	0.9	1.3	(Khan et al., 2016)
Birmingham (UK)	1.6	0.7	(Harrison and Yin, 2008)
Birmingham (UK)	1.6	1.0	(Harrison and Yin, 2008)
Madrid (Spain)	2.8	0.7	(Mirante et al., 2014; Plaza et al., 2006)
Raciborz (Poland)	1.5	1.7	(Błaszczak et al., 2016)
Zloty Potok (Poland)	1.7	1.2	(Błaszczak et al., 2016)
Thessaloniki (Greece)	2.2	3.1	(Samara et al., 2014)
Penteli, Athens (Greece)	1.6	0.5	(Paraskevopoulou et al., 2014)
Bologna (Italy)	1.7	1.4	(Pietrogrande et al., 2016)
San Pietro Capofiume (Italy)	1.1	2.0	(Pietrogrande et al., 2016)
Cape Fuguei (Taiwan)	1.6	2.3	(Chou et al., 2010)
Taipei (Taiwan)	2.2	5.0	(Chou et al., 2010)
Taichung (Taiwan)	3.7	4.8	(Chou et al., 2010)
Tainan (Taiwan)	1.7	5.0	(Chou et al., 2010)
Pingtung (Taiwan)	2.9	6.9	(Chou et al., 2010)
Penghu (Taiwan)	1.0	1.1	(Chou et al., 2010)
Hualien (Taiwan)	1.4	2.5	(Chou et al., 2010)
Chiba Prefecture (Japan)	1.4	1.8	(Ichikawa et al., 2015)
Yokohama (Japan)	2.1	2.1	(Khan et al., 2010)
Gwangiu (Korea)	5.7	4.6	(Park and Cho, 2011)
Gosan (Korea)	1.9	2.2	(Batmunkh et al., 2011)
Seoul (Korea)	1.1	5.2	(Kim et al., 2012)
Incheon (Korea)	3.6	2.9	(Choi et al., 2012)
Guangzhou (China)	4.0	7.3	(Cao et al., 2007; Duan et al., 2007; Hu et al., 2012; Huang et al., 2012; Lai et al., 2016; Tao et al., 2009)
Beijing (China)	4.3	7.6	(Cao et al., 2007; Cheng et al., 2012; Han et al., 2015; Hu et al., 2012; Ji et al., 2016; Lin et al., 2009; Lv et al., 2016; Yu et al., 2006)
Back Garden (China)	2.0	3.7	(Hu et al., 2012)
Shanghai (China)	2.9	6.1	(Feng et al., 2013; Feng et al., 2009; Qiao et al., 2016; Wang et al., 2016a; Zhou et al., 2016)
Shanghai (China)	3.6	8.4	(Feng et al., 2013; Feng et al., 2009)
Mr Tai (China)	11.2	5.3	(Wang et al., 2012b)
Wangqingsha (China)	3.2	4.6	(Ding et al., 2012)
Yellow river delta (China)	4.3	3.0	(Sui et al., 2015)
Changchun (China)	5.6	6.9	(Cao et al., 2007)
Jinchang (China)	3.6	4.5	(Cao et al., 2007)
Qingdao (China)	2.2	2.8	(Cao et al., 2007)
Tianjin (China)	6.8	7.5	(Cao et al., 2007; Gu et al., 2010; Li and Bai, 2009; Li et al., 2015b)
Xi'an (China)	12.2	15.1	(Cao et al., 2007)
Yulin (China)	6.1	7.6	(Cao et al., 2007)

Chongqing (China)	5.8	10.1	(Cao et al., 2007; Chen et al., 2014)
Hong Kong (China)	2.4	1.8	(Cao et al., 2007; Zhou et al., 2014)
Hangzhou (China)	9.1	8.0	(Cao et al., 2007)
Wuhan (China)	7.5	6.7	(Cao et al., 2007)
Xiamen (China)	5.0	4.3	(Cao et al., 2007; Zhang et al., 2011)
Nanjing (China)	2.9	5.2	(Li et al., 2015b)
Fozhou (China)	2.5	6.7	(Niu et al., 2013; Zhang et al., 2013)
Mount Heng (China)	1.9	1.2	(Zhou et al., 2012)
Zhaoqing (China)	2.1	3.0	(Huang et al., 2012)
Chengdu (China)	4.3	12.9	Chen et al 2014
Neijing (China)	3.2	11.8	Chen et al 2014
Putian City (China)	3.1	9.9	(Niu et al., 2013)
Quanzhou City(China)	2.3	7.1	(Niu et al., 2013)
Shandong (China)	4.7	4.8	(Duan et al., 2007)
Taishan (China)	4.7	7.9	(Han et al., 2015)
Ahmedabad (India)	4.3	4.5	(Rengarajan et al., 2011; Sudheer et al., 2015)
New Delhi (India)	10.4	7.2	(Pant et al., 2015)
Pune (India)	19.4	6.4	(Pipal and Gursumeeran Satsangi, 2015; Safai et al., 2014)
Mt Abu (India)	0.8	0.7	(Kumar et al., 2016)
Brisbane (Australia)	1.3	1.1	(Crilley et al., 2016)

Black: urban; Blue: suburban; Green: Remote; Red: rural.

Annex B. Use of CMB.

Table B1. List of the molecular markers commonly used to apportion primary aerosol sources using CMB.

Primary Markers	Primary Sources	References
Levoglucosan, resin acids, syringaldehyde, acetosyringone, PAHs	Biomass burning	(Robinson et al., 2006; Sheesley et al., 2007; Stone et al., 2010b; Stone et al., 2009)
Hopanes, PAHs	Gasoline motor vehicles	(Lough et al., 2007; Stone et al., 2010b; Stone et al., 2009)
Elemental carbon, hopanes, PAHs	Diesel engines	(Lough et al., 2007; Stone et al., 2009)
C29-C33 n-alkanes with odd carbon preferences	Vegetative detritus	(Rogge et al., 1993; Stone et al., 2009)
n-Hexadecanoic acid, n-octadecanoic acid, 9-hexadecanoic acid, 9-octadecanoic acid, cholesterol	Cooking emissions	(Rogge et al., 1991; Schauer and Cass, 2000; Schauer et al., 1996)
Syringaldehyde, acetosyringone, syringic acid	Hard wood combustion	(Rogge et al., 1998; Simoneit, 2002)
Resin acids (predominantly dehydroabietic acid, and 7-oxodehydroabietic acid)	Soft wood combustion	(Robinson et al., 2006; Rogge et al., 1998; Simoneit, 2002)
Picene	Coal combustion	(Schauer et al., 1996; Yin et al., 2015)
n-Hentriacontane (C31), n-Dotriacontane (C32), n-Tritriacontane (C33)	Cigarette smoke	(Schauer et al., 1996)

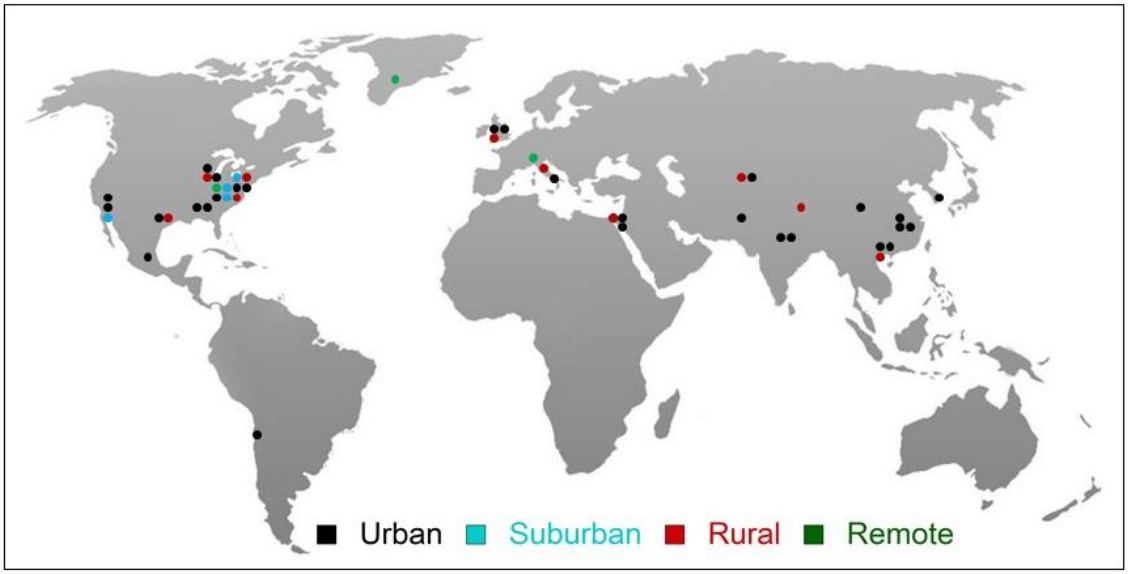

Figure B1. Location of the monitored sites of the studies considered in this review reporting the use of the CMB approach for the evaluation of SOC in $PM_{2.5}$. In black, urban sites; in blue, suburban sites; in red, rural sites and in green, remote sites.

Table B2. List of the studies considered for the annual SOC contribution to $PM_{2.5}$ OC estimated using CMB for all the monitored sites from 2006 to 2016.

Locations	SOC (µgC m^{-3})	POC (µgC m^{-3})	References
Santiago (Chile)	2.7	6.4	(Villalobos et al., 2015b)
Central LA (USA)	1.2	2.1	(Heo et al., 2013; Minguillón et al., 2008; Shirmohammadi et al., 2016)
Anaheim (USA)	0.2	2.6	(Shirmohammadi et al., 2016)
Riverside (USA)	2.2	1.1	(Heo et al., 2013)
Texas (USA)	1.6	0.9	(Subramoney et al., 2013)
Texas (USA)	1.1	0.7	(Subramoney et al., 2013)
Pensacola (USA)	4.1	2.9	(Zheng et al., 2006b)
Atlanta (USA)	2.7	2.4	(Pachon et al., 2010; Zheng et al., 2007; Zheng et al., 2006b)
Birmingham (USA)	4.6	5.2	(Zheng et al., 2006b)
Charlotte (USA)	1.6	2.2	(Sheesley et al., 2007)
Winston- Salem (USA)	1.3	2.3	(Sheesley et al., 2007)
Hickory (USA)	1.1	3.0	(Sheesley et al., 2007)
Lexington (USA)	1.3	2.5	(Sheesley et al., 2007)
Centreville (USA)	4.1	2.2	(Zheng et al., 2006b)
Northern Minnesota (USA)	0.0	0.8	(Chen et al., 2010)
Southern Minnesota (USA)	0.0	1.1	(Chen et al., 2010)
Mille Lacs Lake (USA)	0.5	1.2	(Chen et al., 2010)
Minneapolis (USA)	0.1	2.9	(Chen et al., 2010)
St. Paul-NC (USA)	0.1	2.7	(Chen et al., 2010)
Rochester (USA)	0.3	1.8	(Chen et al., 2010)
London (UK)	1.2	2.2	(Pant et al., 2014)
Birmingham (UK)	1.2	1.6	(Pant et al., 2014; Yin et al., 2010)
Birmingham (UK)	0.9	1.6	(Pant et al., 2014; Yin et al., 2010)
Milan (Italy)	0.7	6.0	(Daher et al., 2012)
Nablus (Palestine)	3.8	4.8	(von Schneidemesser et al., 2010b)
Hebron (Palestine)	3.0	2.8	(von Schneidemesser et al., 2010b)
East Jerusalem (Palestine)	1.9	3.5	(von Schneidemesser et al., 2010b)
Zarqa (Jordan)	4.9	4.2	(von Schneidemesser et al., 2010b)
Rachma (Jordan)	1.4	0.8	(von Schneidemesser et al., 2010b)
Aqaba (Jordan)	2.3	1.4	(von Schneidemesser et al., 2010b)
Amman (Jordan)	3.4	3.3	(von Schneidemesser et al., 2010b)
West Jerusalem (Israel)	2.0	2.7	(von Schneidemesser et al., 2010b)
Tel Aviv (Israel)	3.0	1.8	(von Schneidemesser et al., 2010b)
Haifa (Israel)	1.8	1.7	(von Schneidemesser et al., 2010b)
Eilat (Israel)	2.2	1.1	(von Schneidemesser et al., 2010b)
Bagdad (Iraq)	5.5	7.5	(Hamad et al., 2015)
Bishkek (Kyrgyzstan)	0.7	0.8	(Miller-Schulze et al., 2011)
Teploklyuchenka (Kyrgyzstan)	1.0	0.5	(Miller-Schulze et al., 2011)
Lahore (Pakistan)	7.7	53.6	(Stone et al., 2010a)
Kanpur (India)	4.8	4.5	(Villalobos et al., 2015a)
Agra (India)	3.3	6.9	(Villalobos et al., 2015a)
Godavari (Nepal)	3.4	1.7	(Stone et al., 2008)
Harbin (China)	2.1	6.3	(Huang and Wang, 2014)
Tianjin (China)	1.2	7.2	(Wu et al., 2015)
Hong Kong (China)	1.6	1.7	(Zheng et al., 2006a)
Hong Kong (China)	2.3	3.6	(Zheng et al., 2006a; Zheng et al., 2011)
Guangzhou (China)	3.1	10.9	(Wang et al., 2016b)
Chonghua (China)	3.3	6.1	(Zheng et al., 2011)
Zhongshan (China)	2.1	8.5	(Zheng et al., 2011)

Shenzhen (China)	2.8	8.0	(Zheng et al., 2011)
Gwangju (Korea)	1.9	4.6	(Lee et al., 2008a)

Black: urban; Blue: suburban; Green: Remote; Red: rural.

Table B3. List of the studies considered for the spring-summer SOC contribution to $PM_{2.5}$ OC estimated using CMB for all the monitored sites from 2006 to 2016.

Locations	SOC (µgC m^{-3})	POC (µgC m^{-3})	References
Central LA (USA)	0.7	2.3	(Minguillón et al., 2008; Shirmohammadi et al., 2016)
Anaheim (USA)	0.2	1.9	(Shirmohammadi et al., 2016)
Atlanta (USA)	3.2	0.8	(Zheng et al., 2007; Zheng et al., 2014)
Tennessee Valley (USA)	2.8	1.1	(Ke et al., 2007)
Yorkville (USA)	2.4	0.4	(Zheng et al., 2014)
Pittsburgh (USA)	2.7	0.9	(Subramanian et al., 2007)
Mexico	3.3	5.3	(Stone et al., 2008)
Santiago (Chile)	2.5	8.0	(Villalobos et al., 2015b)
Summit (Greenland)	0.1	0.0	(von Schneidemesser et al., 2009)
Birmingham (UK)	1.5	1.6	(Pant et al., 2014)
Birmingham (UK)	1.2	1.7	(Pant et al., 2014)
Marseille (France)	3.7	1.0	(El Haddad et al., 2011)
Milan (Italy)	1.4	2.7	(Daher et al., 2012; Perrone et al., 2012)
Oasi Le Bine, Cremona (Italy)	1.1	1.4	(Perrone et al., 2012)
Alps (Italy)	1.2	2.8	(Perrone et al., 2012)
West Jerusalem (Israel)	1.9	2.9	(von Schneidemesser et al., 2010a)
East Jerusalem (Israel)	2.5	2.7	(von Schneidemesser et al., 2010a)
Bishkek (Kyrgyzstan)	1.5	0.4	(Miller-Schulze et al., 2011)
Teploklyuchenka (Kyrgyzstan)	0.8	0.3	(Miller-Schulze et al., 2011)
Lahore (Pakistan)	3.7	29.1	(Stone et al., 2010a)
Kanpur (India)	5.4	8.1	(Villalobos et al., 2015a)
Agra (India)	4.3	5.9	(Villalobos et al., 2015a)
Godavari (Nepal)	3.1	1.6	(Stone et al., 2008)
Harbin (China)	1.1	2.8	(Huang and Wang, 2014)
Hong Kong (China)	1.2	1.1	(Zheng et al., 2006a; Zheng et al., 2011)
Hong Kong (China)	2.9	2.4	(Zheng et al., 2006a; Zheng et al., 2011)
Guangzhou (China)	4.6	10.8	(Zheng et al., 2011)
Chonghua (China)	4.8	5.6	(Zheng et al., 2011)
Zhongshan (China)	3.7	4.1	(Zheng et al., 2011)
Shenzhen (China)	3.8	5.6	(Zheng et al., 2011)

Black: urban; Blue: suburban; Green: Remote; Red: rural.

Annex C. Use of the SOA tracer method

Table C1. Details of the SOA tracers considered in the SOA tracer method and laboratory generated aerosol mass fractions (Kleindienst et al., 2007).

Organic markers	Precursors	MW (g mol^{-1})	f_{SOA}	f_{SOC}	SOA/SOC
2-Methylglyceric acid	Isoprene	134	0.063±0.016	0.155±0.039	1.37±0.15
2-Methylthreitol		136			
2-Methylerythritol		136			
3-Isopropylpentanedioic acid	α-Pinene	174	0.168±0.081	0.231±0.111	1.98±0.14
3-Acetylpentanedioic acid		174			
2-Hydroxy-4-isopropyladipic acid		204			
3-Acetylhexanedioic acid		188			
3-Hydroxyglutaric acid		148			
2-Hydroxy-4,4-dimethylglutaric acid		176			
3-(2-Hydroxy-ethyl)-2,2-dimethylcyclobutane-carboxylic acid		172			
Pinic acid		186			
Pinonic acid		184			
2,3-Dihydroxy-4-oxopentanoic acid (DHOPA)	Toluene	148	0.040±0.0013	0.079±0.0026	2.47±0.55
β-Caryophyllinic acid	β-Caryophyllene	254	0.0109±0.0022	0.0230±0.0046	2.11±0.65

Table C2. List of the studies considered for the annual SOC contribution to $PM_{2.5}$ OC estimated using the SOA tracer method for all the monitored sites from 2006 to 2016. SOC and POC concentrations in µgC m^{-3}.

Locations	$SOC_{isoprene}$	$SOC_{\alpha\text{-pinene}}$	$SOC_{toluene}$	$SOC_{\beta\text{-caryophyllene}}$	POC	References
Research Triangle Park (USA)	0.5	0.3	0.2	0.2	2.5	(Kleindienst et al., 2007; Offenberg et al., 2011)
Cincinnati (USA)	0.6	0.1	0.2	0.2	1.7	(Lewandowski et al., 2008a)
Detroit (USA)	0.3	0.3	0.3	0.2	2.8	(Lewandowski et al., 2008a)
Bondville (USA)	0.3	0.1	0.2	0.2	0.7	(Lewandowski et al., 2008a)
East St. Louis (USA)	0.9	0.1	0.2	0.2	2.9	(Lewandowski et al., 2008a)
Northbrook (USA)	0.2	0.2	0.2	0.1	1.7	(Lewandowski et al., 2008a)
Nam Co Lake (Tibet)	0.1	0.02	0.1	0.01	1.5	(Shen et al., 2015)
Shanghai (China)	0.1	0.02	0.2	0.03	10.2	(Feng et al., 2013)
Shanghai (China)	0.1	0.02	0.2	0.1	11.1	(Feng et al., 2013)

Black: urban; Blue: suburban; Green: Remote; Red: rural.

Table C3. List of the studies considered for the spring-summer SOC contribution to $PM_{2.5}$ OC estimated using the SOA tracer method for all the monitored sites from 2006 to 2016. SOC and POC concentrations in µgC m^{-3}.

Locations	$SOC_{isoprene}$	$SOC_{\alpha\text{-pinene}}$	$SOC_{toluene}$	$SOC_{\beta\text{-caryophyllene}}$	POC	References
Research Triangle park (USA)	0.9	0.7	0.4	0.9	1.6	(Kleindienst et al., 2007; Lewandowski et al., 2013)
Cincinnati (USA)	1.1	0.2	0.3	0.2	1.5	(Lewandowski et al., 2008b; Lewandowski et al., 2013)
Detroit (USA)	0.5	0.3	0.6	0.2	2.0	(Lewandowski et al., 2008b; Lewandowski et al., 2013; Stone et al., 2009)
Cleveland (USA)	0.5	0.2	0.6	0.1	1.4	(Lewandowski et al., 2008b; Lewandowski et al., 2013; Stone et al., 2009)
Medina (USA)	0.8	0.3	0.3	0.1	0.01	(Lewandowski et al., 2013)
Bondville (USA)	0.7	0.2	0.3	0.2	0.4	(Lewandowski et al., 2008b; Lewandowski et al., 2013)
East St. Louis (USA)	0.8	0.2	0.2	0.1	2.6	(Lewandowski et al., 2008b; Lewandowski et al., 2013)
Northbrook (USA)	0.4	0.2	0.3	0.2	1.0	(Lewandowski et al., 2008b; Lewandowski et al., 2013)
Bakersfield (USA)	0.1	0.1	0.1	-	5.0	(Lewandowski et al., 2013)
Pasedena (USA)	0.04	0.1	0.1	-	3.2	(Lewandowski et al., 2013)
Riverside (USA)	0.1	0.2	0.9	0.1	4.2	(Kleindienst et al., 2010; Stone et al., 2009)
Mexico city (Mexico)	0.2	0.2	1.9	0.2	3.5	(Stone et al., 2010b)
Pensacola (USA)	0.7	0.5	0.3	0.04	4.3	(Kleindienst et al., 2010; Lewandowski et al., 2013)
Centerville (USA)	1.6	0.7	0.1	0.02	4.0	(Kleindienst et al., 2010; Lewandowski et al., 2013)
Birmingham (USA)	1.7	0.5	0.2	0.1	10.9	(Kleindienst et al., 2010; Lewandowski et al., 2013)
Atlanta (USA)	0.8	0.3	0.2	0.01	6.2	(Kleindienst et al., 2010; Lewandowski et al., 2013)
K-puszta (Hungary)	0.3	0.2	-	-	3.5	(Kourtchev et al., 2009)
Mumbai (India)	0.01	0.04	0.01	0.03	4.4	(Fu et al., 2016)
Nam Co Lake (Tibet)	0.4	0.04	0.1	0.04	1.2	(Shen et al., 2015)
Hong Kong (China)	0.3	1.4	0.3	0.1	5.1	(Hu et al., 2008)
Hong Kong (China)	0.3	1.2	0.2	0.7	2.4	(Hu et al., 2008)
Dinghu (China)	0.2	-	-	-	4.9	(Wang et al., 2008)
PRD (China)	0.6	0.1	2.3	0.1	4.7	(Ding et al., 2012)
Shanghai (China)	0.3	0.03	0.2	0.03	5.7	(Feng et al., 2013)

Shanghai (China)	0.4	0.04	0.3	0.1	5.7	(Feng et al., 2013)
Chongming (China)	0.03	-	-	-	9.9	(Wang et al., 2008)
Mt Tai (China)	1.0	0.2	-	0.5	15.9	(Fu et al., 2010; Fu et al., 2012; Fu et al., 2009)
Changbai (China)	0.3	-	-	-	4.5	(Wang et al., 2008)
Beijing (China)	0.9	0.5	1.7	0.2	7.1	(Guo et al., 2012)
Beijing (China)	1.3	0.5	1.5	0.2	5.8	(Guo et al., 2012)
Hokkaido (Japan)	0.5	0.1	-	0.03	3.6	(Fu and Kawamura, 2011)
Julich (Germany)	0.1	0.1	-	-	4.4	(Kourtchev et al., 2008)
Marseille (France)	0.02	0.1	-	0.01	4.1	(El Haddad et al., 2011)
Cork Harbor (Ireland)	0.02	-	-	-	1.1	(Kourtchev et al., 2011)

Black: urban; Blue: suburban; Green: Remote; Red: rural.

Annex D. PMF approach.

Table D1. List of the studies considered for the annual SOC contribution to $PM_{2.5}$ OC estimated using the PMF approach (filer based) for all the monitored sites from 2006 to 2016. SOC and OC concentrations in µgC m^{-3}.

Locations	SOC	OC	SOC contribution (%)	Molecular markers used for SOC estimation	References
Yorkville (USA)[1]	1.0	2.9	34	-	(Lee et al., 2008b)
Rochester (USA)[2]	0.04	0.4	12	√	(Wang et al., 2012a)
Pittsburgh (USA)[3]	1.0	2.9	34	√	(Shrivastava et al., 2007)
Cincinnati (USA)[4]	1.2	2.8	43	√	(Zhang et al., 2009b)
Detroit (USA)[4]	1.6	3.2	51	√	(Zhang et al., 2009b)
East St. Louis (USA)[4]	1.01	3.5	30	√	(Zhang et al., 2009b)
East St. Louis (USA)[5]	0.8	3.8	21	√	(Zhang et al., 2009a)
East St. Louis (USA)[5]	0.8	4.0	20	√	(Jaeckels et al., 2007)
Bondville (USA)[4]	0.9	1.6	57	√	(Zhang et al., 2009b)
Northbrook (USA)[4]	1.0	2.4	43	√	(Zhang et al., 2009b)
Riverside (USA)[6]	1.3	3.3	39	√	(Heo et al., 2013)
Central LA (USA)[6]	1.5	3.9	39	√	(Heo et al., 2013)
Centreville (USA)[1]	0.7	2.8	26	-	(Lee et al., 2008b)
Birmingham (USA)[1]	0.9	4.3	21	-	(Lee et al., 2008b)
Atlanta (USA)[1]	1.0	4.2	23	-	(Lee et al., 2008b; Pachon et al., 2010)
Shanghai (China)[6,7]	2.5	6.8[7]	37	√	(Feng et al., 2013)
Hong Kong (China)[6*]	6.8	10.4	66	√	(Hu et al., 2010)
Hong Kong (China)[6**]	0.7	2.9	24	√	(Hu et al., 2010)

Black: urban; Blue: suburban; Green: Remote; Red: rural;
[1]SOC based on sulfate and nitrate factors;
[2]SOC based on isoprene + other SOA factors;
[3]SOC based on biogenic SOA factor;
[4]SOC based on isoprene + pinene + caryophyllene SOA factors;
[5]SOC based on anthropogenic SOA factor;
[6]SOC based on biogenic + anthropogenic SOA + sulfate and nitrate factors;
[7] both urban and suburban sites considered;
[*] Regional days;
[**] Clean days.

Table D2. List of the studies considered for the spring-summer SOC contribution estimated using the PMF approach (AMS/ACSM based). SOC and OC concentrations in µgC m^{-3}.

Locations	SOC	OC	SOC contribution (%)	References
Vancouver (Canada)	1.3	3.4	37	(Jimenez et al., 2009)
Chebogue Pt. (Canada)[1]	0.8	0.9	81	(Jimenez et al., 2009)
Boulder (USA)	1.28	1.7	74	(Jimenez et al., 2009)
New York City (USA)	2.3	4.2	64	(Jimenez et al., 2009; Sun et al., 2011; Zhang et al., 2007)
Riverside (USA)	3.2	5.5	58	(Jimenez et al., 2009; Zhang et al., 2007)
Houston (USA)	1.4	4.2	33	(Jimenez et al., 2009)
Storm Peak (USA)[1]	0.4	0.5	67	(Jimenez et al., 2009)
Thompson Farm (USA)[1]	2.2	3.1	68	(Jimenez et al., 2009)
Pinnacle Park (USA)[1]	2.8	3.0	91	(Jimenez et al., 2009)
Mexico City (Mexico)	1.5	13.3	33	(Jimenez et al., 2009; Zhang et al., 2007)
Mace Head (Ireland)	2.8	5.3	52	(Crippa et al., 2014)
Essex (UK)	1.4	2.2	64	(Zhang et al., 2007)
Essex (UK)	0.8	1.3	60	(Zhang et al., 2007)
Chelmsford (UK)	0.9	1.6	56	(Jimenez et al., 2009)
Manchester (UK)	1.5	4.6	33	(Jimenez et al., 2009; Zhang et al., 2007)
Edinburgh (UK)	0.6	2.3	27	(Jimenez et al., 2009)
Hyytiälä (Finland)	3.9	4.5	87	(Crippa et al., 2014)
Helsinki (Finland)	3.0	5.2	57	(Crippa et al., 2014)
Chilbolton (UK)	2.5	5.5	46	(Crippa et al., 2014)
Vavihill (Sweden)	2.9	5.2	56	(Crippa et al., 2014)
Cabauw (Netherlands)	3.1	5.0	61	(Crippa et al., 2014)
Payerne (Switzerland)	3.5	4.7	75	(Crippa et al., 2014)
Zurich (Switzerland)	2.2	2.7	83	(Jimenez et al., 2009)
Jungfraujoch (Switzerland)	3.5	4.7	74	(Crippa et al., 2014)
Taunus (Germany)	4.1	5.5	74	(Jimenez et al., 2009)
Melpitz (Germany)	3.7	4.6	80	(Crippa et al., 2014)
Paris (France)	0.6	0.9	61	(Crippa et al., 2013)
Puy de Dome (France)	3.2	5.0	64	(Crippa et al., 2014)
Barcelona (Spain)	2.1	4.4	47	(Crippa et al., 2014)
Montseny (Spain)	3.5	4.7	75	(Crippa et al., 2014)
San Pietro Capofiume (Italy)	3.3	4.9	67	(Crippa et al., 2014)
Finokalia (Greece)	4.0	4.3	93	(Crippa et al., 2014)
Beijing (China)	7.7	15.2	51	(Huang et al., 2010; Jimenez et al., 2009; Li et al., 2015b; Xu et al., 2014; Zhang et al., 2007)
Shanghai (China)	5.1	7.3	71	(Li et al., 2015b; Xu et al., 2014)
Lanzhou (China)	3.5	7.7	45	(Xu et al., 2014)
Shenzhen (China)	8.6	15.9	54	(Li et al., 2015b)
Jiaxing (China)	3.7	6.7	55	(Huang et al., 2013)
Back Garden (China)	3.8	7.3	52	(Xu et al., 2014)
Jiaxing (China)	5.3	8.4	62	(Li et al., 2015b; Xu et al., 2014)
Changdao (China)	4.1	7.3	56	(Xu et al., 2014)
Hong Kong (China)	3.7	5.3	73	(Li et al., 2015b; Xu et al., 2014)
Tokyo (Japan)	2.21	4.2	52	(Jimenez et al., 2009; Zhang et al., 2007)
Fukue (Japan)[1]	2.4	2.7	88	(Jimenez et al., 2009; Zhang et al., 2007)
Okinawa Island (Japan)[1]	2.2	2.2	100	(Zhang et al., 2007)
Cheju (Korea)[1]	0.2	0.5	43	(Jimenez et al., 2009)

Black: urban; Blue: suburban; Green: Remote; Red: rural; Italic: High altitude; Bold: Urban Downwind
[1] mentioned as Remote/ Rural, not clearly specified.

Annex E. Radiocarbon (^{14}C) measurements.

Table E1. List of the studies considered for the spring-summer SOC contribution to $PM_{2.5}$ OC estimated ^{14}C measurements in combination with another methodology.

Locations	$SOC_{contemporary}$ ($\mu gC\ m^{-3}$)	SOC_{fossil} ($\mu gC\ m^{-3}$)	POC ($\mu gC\ m^{-3}$)	Methodology used to estimate SOC	References
Great Smoky Mt. (USA)	0.7	0.1	1.1	EC tracer method	(Schichtel et al., 2008)
Brigantine (USA)	0.6	0.1	1.0	EC tracer method	(Schichtel et al., 2008)
Proctor Maple (USA)	0.6	0.02	0.9	EC tracer method	(Schichtel et al., 2008)
Sula (USA)	0.4	0.0	0.6	EC tracer method	(Schichtel et al., 2008)
Puget Sound (USA)	0.4	0.3	1.0	EC tracer method	(Schichtel et al., 2008)
Mount Rainier (USA)	0.6	0.1	1.0	EC tracer method	(Schichtel et al., 2008)
Yosemite (USA)	1.3	0.04	2.1	EC tracer method	(Schichtel et al., 2008)
Grand Canyon (USA)	0.3	0.01	0.4	EC tracer method	(Schichtel et al., 2008)
Tonto (USA)	0.3	0.04	0.5	EC tracer method	(Schichtel et al., 2008)
Phoenix (USA)	0.5	0.2	1.0	EC tracer method	(Schichtel et al., 2008)
Rocky Mountain (USA)	0.4	0.04	0.7	EC tracer method	(Schichtel et al., 2008)
Pensacola (USA)	1.9	1.0	1.4	CMB approach	(Ding et al., 2008)
Centreville (USA)	3.0	0.7	0.9	CMB approach	(Ding et al., 2008)
Birmingham (USA)	2.3	2.6	2.3	CMB approach	(Ding et al., 2008)
Atlanta (USA)	3.7	1.6	1.6	CMB approach	(Ding et al., 2008)
Aveiro (Portugal)	1.3	0.2	2.0	Using empirical equations	(Gelencsér et al., 2007)
Marseille (France)	2.0	0.6	0.8	PMF-AMS & CMB approaches	(El Haddad et al., 2013; El Haddad et al., 2011)
Puy de Dome (France)	2.0	0.3	2.4	Empirical equations	(Gelencsér et al., 2007)
Po Valley (Italy)	3.4	1.3	1.2	Empirical equations	(Gilardoni et al., 2011)
K-puszta (Hungary)	1.8	0.1	2.6	Empirical equations	(Gelencsér et al., 2007)
Sonnblick (Austrian Alps)	0.6	0.1	0.8	Empirical equations	(Gelencsér et al., 2007)
Schauinsland (Germany)	1.5	0.3	2.0	Empirical equations	(Gelencsér et al., 2007)
Goteborg (Sweden)	-	0.5	1.8	WSOC based method	(Szidat et al., 2009)
Beijing (China)	3.7	3.9	7.7	Simulations and empirical equations	(Liu et al., 2016; Morino et al., 2015)
Guangzhou (China)	4.1	2.0	4.2	Empirical equations	(Liu et al., 2016)

Black: urban; Blue: suburban; Green: Remote; Red: rural;

References

Abdeen, Z., Qasrawi, R., Heo, J., Wu, B., Shpund, J., Vanger, A., Sharf, G., Moise, T., Brenner, S., Nassar, K., Saleh, R., Al-Mahasneh, Q.M., Sarnat, J.A., Schauer, J.J., 2014. Spatial and Temporal Variation in Fine Particulate Matter Mass and Chemical Composition: The Middle East Consortium for Aerosol Research Study. Sci. World J. 2014, 878704.

Batmunkh, T., Kim, Y.J., Lee, K.Y., Cayetano, M.G., Jung, J.S., Kim, S.Y., Kim, K.C., Lee, S.J., Kim, J.S., Chang, L.S., An, J.Y., 2011. Time-Resolved Measurements of PM2.5 Carbonaceous Aerosols at Gosan, Korea. J. Air Waste Manage. Assoc. 61, 1174-1182.

Błaszczak, B., Rogula-Kozłowska, W., Mathews, B., Juda-Rezler, K., Klejnowski, K., Rogula-Kopiec, P., 2016. Chemical Compositions of PM2.5 at Two Non-Urban Sites from the Polluted Region in Europe. Aerosol. Air Qual. Res. 16, 2333-2348.

Cabada, J.C., Pandis, S.N., Subramanian, R., Robinson, A.L., Polidori, A., Turpin, B., 2004. Estimating the Secondary Organic Aerosol Contribution to PM2.5 Using the EC Tracer Method Special Issue of Aerosol Science and Technology on Findings from the Fine Particulate Matter Supersites Program. Aerosol Sci. Technol. 38, 140-155.

Cao, J., Lee, S., Chow, J.C., Watson, J.G., Ho, K., Zhang, R., Jin, Z., Shen, Z., Chen, G., Kang, Y., 2007. Spatial and seasonal distributions of carbonaceous aerosols over China. J. Geophys. Res.-Atmos. 112.

Chen, L.-W.A., Watson, J.G., Chow, J.C., DuBois, D.W., Herschberger, L., 2010. Chemical mass balance source apportionment for combined PM2.5 measurements from US non-urban and urban long-term networks. Atmos. Environ. 44, 4908-4918.

Chen, Y., Xie, S., Luo, B., Zhai, C., 2014. Characteristics and origins of carbonaceous aerosol in the Sichuan Basin, China. Atmos. Environ. 94, 215-223.

Cheng, Y., He, K.-b., Duan, F.-k., Du, Z.-y., Zheng, M., Ma, Y.-l., 2012. Characterization of carbonaceous aerosol by the stepwise-extraction thermal–optical-transmittance (SE-TOT) method. Atmos. Environ. 59, 551-558.

Choi, J.-K., Heo, J.-B., Ban, S.-J., Yi, S.-M., Zoh, K.-D., 2012. Chemical characteristics of PM2.5 aerosol in Incheon, Korea. Atmos. Environ. 60, 583-592.

Chou, C.-K., Lee, C., Cheng, M., Yuan, C., Chen, S., Wu, Y., Hsu, W., Lung, S., Hsu, S., Lin, C., 2010. Seasonal variation and spatial distribution of carbonaceous aerosols in Taiwan. Atmos. Chem. Phys. 10, 9563-9578.

Chu, S.-H., 2005. Stable estimate of primary OC/EC ratios in the EC tracer method. Atmos. Environ. 39, 1383-1392.

Crilley, L.R., Ayoko, G.A., Mazaheri, M., Morawska, L., 2016. Factors influencing the outdoor concentration of carbonaceous aerosols at urban schools in Brisbane, Australia: Implications for children's exposure. Environ. Pollut. 208, Part A, 249-255.

Crippa, M., Canonaco, F., Lanz, V.A., Äijälä, M., Allan, J.D., Carbone, S., Capes, G., Ceburnis, D., Dall'Osto, M., Day, D.A., DeCarlo, P.F., Ehn, M., Eriksson, A., Freney, E., Hildebrandt Ruiz, L., Hillamo, R., Jimenez, J.L., Junninen, H., Kiendler-Scharr, A., Kortelainen, A.M., Kulmala, M., Laaksonen, A., Mensah, A.A., Mohr, C., Nemitz, E., O'Dowd, C., Ovadnevaite,

J., Pandis, S.N., Petäjä, T., Poulain, L., Saarikoski, S., Sellegri, K., Swietlicki, E., Tiitta, P., Worsnop, D.R., Baltensperger, U., Prévôt, A.S.H., 2014. Organic aerosol components derived from 25 AMS data sets across Europe using a consistent ME-2 based source apportionment approach. Atmos. Chem. Phys. 14, 6159-6176.

Crippa, M., Canonaco, F., Slowik, J.G., El Haddad, I., DeCarlo, P.F., Mohr, C., Heringa, M.F., Chirico, R., Marchand, N., Temime-Roussel, B., Abidi, E., Poulain, L., Wiedensohler, A., Baltensperger, U., Prévôt, A.S.H., 2013. Primary and secondary organic aerosol origin by combined gas-particle phase source apportionment. Atmos. Chem. Phys. 13, 8411-8426.

Daher, N., Ruprecht, A., Invernizzi, G., De Marco, C., Miller-Schulze, J., Heo, J.B., Shafer, M.M., Shelton, B.R., Schauer, J.J., Sioutas, C., 2012. Characterization, sources and redox activity of fine and coarse particulate matter in Milan, Italy. Atmos. Environ. 49, 130-141.

Day, M.C., Zhang, M., Pandis, S.N., 2015. Evaluation of the ability of the EC tracer method to estimate secondary organic carbon. Atmos. Environ. 112, 317-325.

Ding, X., Wang, X.-M., Gao, B., Fu, X.-X., He, Q.-F., Zhao, X.-Y., Yu, J.-Z., Zheng, M., 2012. Tracer-based estimation of secondary organic carbon in the Pearl River Delta, south China. J. Geophys. Res. 117.

Ding, X., Zheng, M., Edgerton, E.S., Jansen, J.J., Wang, X., 2008. Contemporary or Fossil Origin: Split of Estimated Secondary Organic Carbon in the Southeastern United States. Environ. Sci. Technol. 42, 9122-9128.

Duan, J., Tan, J., Cheng, D., Bi, X., Deng, W., Sheng, G., Fu, J., Wong, M., 2007. Sources and characteristics of carbonaceous aerosol in two largest cities in Pearl River Delta Region, China. Atmos. Environ. 41, 2895-2903.

El Haddad, I., D'Anna, B., Temime-Roussel, B., Nicolas, M., Boreave, A., Favez, O., Voisin, D., Sciare, J., George, C., Jaffrezo, J.L., Wortham, H., Marchand, N., 2013. Towards a better understanding of the origins, chemical composition and aging of oxygenated organic aerosols: case study of a Mediterranean industrialized environment, Marseille. Atmos. Chem. Phys. 13, 7875-7894.

El Haddad, I., Marchand, N., Temime-Roussel, B., Wortham, H., Piot, C., Besombes, J.L., Baduel, C., Voisin, D., Armengaud, A., Jaffrezo, J.L., 2011. Insights into the secondary fraction of the organic aerosol in a Mediterranean urban area: Marseille. Atmos. Chem. Phys. 11, 2059-2079.

Fan, X., Brook, J.R., Mabury, S.A., 2003. Sampling Atmospheric Carbonaceous Aerosols Using an Integrated Organic Gas and Particle Sampler. Environ. Sci. Technol. 37, 3145-3151.

Fan, X., Brook, J.R., Mabury, S.A., 2004. Measurement of organic and elemental carbon associated with PM2.5 during Pacific 2001 study using an integrated organic gas and particle sampler. Atmos. Environ. 38, 5801-5810.

Fan, X., Song, J., Peng, P.a., 2016. Temporal variations of the abundance and optical properties of water soluble Humic-Like Substances (HULIS) in PM2.5 at Guangzhou, China. Atmos. Res. 172–173, 8-15.

Feng, J., Hu, M., Chan, C.K., Lau, P.S., Fang, M., He, L., Tang, X., 2006. A comparative study of the organic matter in PM2.5 from three Chinese megacities in three different climatic zones. Atmos. Environ. 40, 3983-3994.

Feng, J., Li, M., Zhang, P., Gong, S., Zhong, M., Wu, M., Zheng, M., Chen, C., Wang, H., Lou, S., 2013. Investigation of the sources and seasonal variations of secondary organic aerosols in PM2.5 in Shanghai with organic tracers. Atmos. Environ. 79, 614-622.

Feng, Y., Chen, Y., Guo, H., Zhi, G., Xiong, S., Li, J., Sheng, G., Fu, J., 2009. Characteristics of organic and elemental carbon in PM2.5 samples in Shanghai, China. Atmos. Res. 92, 434-442.

Fu, P., Aggarwal, S.G., Chen, J., Li, J., Sun, Y., Wang, Z., Chen, H., Liao, H., Ding, A., Umarji, G.S., Patil, R.S., Chen, Q., Kawamura, K., 2016. Molecular Markers of Secondary Organic Aerosol in Mumbai, India. Environ. Sci. Technol.

Fu, P., Kawamura, K., 2011. Diurnal variations of polar organic tracers in summer forest aerosols: A case study of a Quercus and Picea mixed forest in Hokkaido, Japan. Geochem. J. 45, 297-308.

Fu, P., Kawamura, K., Kanaya, Y., Wang, Z., 2010. Contributions of biogenic volatile organic compounds to the formation of secondary organic aerosols over Mt. Tai, Central East China. Atmos. Environ. 44, 4817-4826.

Fu, P.Q., Kawamura, K., Chen, J., Li, J., Sun, Y.L., Liu, Y., Tachibana, E., Aggarwal, S.G., Okuzawa, K., Tanimoto, H., Kanaya, Y., Wang, Z.F., 2012. Diurnal variations of organic molecular tracers and stable carbon isotopic composition in atmospheric aerosols over Mt. Tai in the North China Plain: an influence of biomass burning. Atmos. Chem. Phys. 12, 8359-8375.

Fu, P.Q., Kawamura, K., Pochanart, P., Tanimoto, H., Kanaya, Y., Wang, Z.F., 2009. Summertime contributions of isoprene, monoterpenes, and sesquiterpene oxidation to the formation of secondary organic aerosol in the troposphere over Mt. Tai, Central East China during MTX2006. Atmos. Chem. Phys. Discuss. 9, 16941-16972.

Gelencsér, A., May, B., Simpson, D., Sánchez-Ochoa, A., Kasper-Giebl, A., Puxbaum, H., Caseiro, A., Pio, C., Legrand, M., 2007. Source apportionment of PM2.5 organic aerosol over Europe: Primary/secondary, natural/anthropogenic, and fossil/biogenic origin. J. Geophys. Res. 112.

Gilardoni, S., Vignati, E., Cavalli, F., Putaud, J., Larsen, B., Karl, M., Stenström, K., Genberg, J., Henne, S., Dentener, F., 2011. Better constraints on sources of carbonaceous aerosols using a combined 14 C–macro tracer analysis in a European rural background site. Atmos. Chem. Phys. 11, 5685-5700.

Gu, J., Bai, Z., Liu, A., Wu, L., Xie, Y., Li, W., Dong, H., Zhang, X., 2010. Characterization of atmospheric organic carbon and element carbon of PM2.5 and PM10 at Tianjin, China. Aerosol Air Qual. Res 10, 167-176.

Guo, S., Hu, M., Guo, Q., Zhang, X., Zheng, M., Zheng, J., Chang, C.C., Schauer, J.J., Zhang, R., 2012. Primary sources and secondary formation of organic aerosols in Beijing, China. Environ. Sci. Technol. 46, 9846-9853.

Hamad, S.H., Schauer, J.J., Heo, J., Kadhim, A.K.H., 2015. Source apportionment of PM2.5 carbonaceous aerosol in Baghdad, Iraq. Atmos. Res. 156, 80-90.

Han, T., Liu, X., Zhang, Y., Qu, Y., Zeng, L., Hu, M., Zhu, T., 2015. Role of secondary aerosols in haze formation in summer in the Megacity Beijing. J Environ Sci (China) 31, 51-60.

Harrison, R.M., Yin, J., 2008. Sources and processes affecting carbonaceous aerosol in central England. Atmos. Environ. 42, 1413-1423.

Heo, J., Dulger, M., Olson, M.R., McGinnis, J.E., Shelton, B.R., Matsunaga, A., Sioutas, C., Schauer, J.J., 2013. Source apportionments of PM2.5 organic carbon using molecular marker Positive Matrix Factorization and comparison of results from different receptor models. Atmos. Environ. 73, 51-61.

Hooda, R.K., Hyvärinen, A.P., Vestenius, M., Gilardoni, S., Sharma, V.P., Vignati, E., Kulmala, M., Lihavainen, H., 2016. Atmospheric aerosols local–regional discrimination for a semi-urban area in India. Atmos. Res. 168, 13-23.

Hu, D., Bian, Q., Lau, A.K.H., Yu, J.Z., 2010. Source apportioning of primary and secondary organic carbon in summer PM2.5 in Hong Kong using positive matrix factorization of secondary and primary organic tracer data. J. Geophys. Res.-Atmos. 115.

Hu, D., Bian, Q., Li, T.W.Y., Lau, A.K.H., Yu, J.Z., 2008. Contributions of isoprene, monoterpenes, β-caryophyllene, and toluene to secondary organic aerosols in Hong Kong during the summer of 2006. J. Geophys. Res.-Atmos. 113, D22206.

Hu, W., Hu, M., Deng, Z., Xiao, R., Kondo, Y., Takegawa, N., Zhao, Y., Guo, S., Zhang, Y., 2012. The characteristics and origins of carbonaceous aerosol at a rural site of PRD in summer of 2006. Atmos. Chem. Phys. 12, 1811-1822.

Huang, H., Ho, K.F., Lee, S.C., Tsang, P.K., Ho, S.S.H., Zou, C.W., Zou, S.C., Cao, J.J., Xu, H.M., 2012. Characteristics of carbonaceous aerosol in PM2.5: Pearl Delta River Region, China. Atmos. Res. 104–105, 227-236.

Huang, L., Wang, G., 2014. Chemical characteristics and source apportionment of atmospheric particles during heating period in Harbin, China. J. Environ. Sci. 26, 2475-2483.

Huang, X.-F., Xue, L., Tian, X.-D., Shao, W.-W., Sun, T.-L., Gong, Z.-H., Ju, W.-W., Jiang, B., Hu, M., He, L.-Y., 2013. Highly time-resolved carbonaceous aerosol characterization in Yangtze River Delta of China: Composition, mixing state and secondary formation. Atmos. Environ. 64, 200-207.

Huang, X.F., He, L.Y., Hu, M., Canagaratna, M.R., Sun, Y., Zhang, Q., Zhu, T., Xue, L., Zeng, L.W., Liu, X.G., Zhang, Y.H., Jayne, J.T., Ng, N.L., Worsnop, D.R., 2010. Highly time-resolved chemical characterization of atmospheric submicron particles during 2008 Beijing Olympic Games using an Aerodyne High-Resolution Aerosol Mass Spectrometer. Atmos. Chem. Phys. 10, 8933-8945.

Ichikawa, Y., Naito, S., Oohashi, H., 2015. Seasonal Variation of PM 2.5 Components Observed in an Industrial Area of Chiba Prefecture, Japan. Asian J. Atmos. Environ. 9, 66-77.

Jaeckels, J.M., Bae, M.-S., Schauer, J.J., 2007. Positive Matrix Factorization (PMF) Analysis of Molecular Marker Measurements to Quantify the Sources of Organic Aerosols. Environ. Sci. Technol. 41, 5763-5769.

Ji, D., Zhang, J., He, J., Wang, X., Pang, B., Liu, Z., Wang, L., Wang, Y., 2016. Characteristics of atmospheric organic and elemental carbon aerosols in urban Beijing, China. Atmos. Environ. 125, Part A, 293-306.

Jimenez, J., Canagaratna, M., Donahue, N., Prevot, A., Zhang, Q., Kroll, J.H., DeCarlo, P.F., Allan, J.D., Coe, H., Ng, N., 2009. Evolution of organic aerosols in the atmosphere. Science 326, 1525-1529.

Joseph, A.E., Unnikrishnan, S., Kumar, R., 2012. Chemical characterization and mass closure of fine aerosol for different land use patterns in Mumbai city. Aerosol. Air Qual. Res. 12, 61-72.

Ke, L., Ding, X., Tanner, R.L., Schauer, J.J., Zheng, M., 2007. Source contributions to carbonaceous aerosols in the Tennessee Valley Region. Atmos. Environ. 41, 8898-8923.

Khan, M.B., Masiol, M., Formenton, G., Di Gilio, A., de Gennaro, G., Agostinelli, C., Pavoni, B., 2016. Carbonaceous PM 2.5 and secondary organic aerosol across the Veneto region (NE Italy). Sci. Total Environ. 542, 172-181.

Khan, M.F., Shirasuna, Y., Hirano, K., Masunaga, S., 2010. Characterization of PM2.5, PM2.5–10 and PM>10 in ambient air, Yokohama, Japan. Atmos. Res. 96, 159-172.

Kim, W., Lee, H., Kim, J., Jeong, U., Kweon, J., 2012. Estimation of seasonal diurnal variations in primary and secondary organic carbon concentrations in the urban atmosphere: EC tracer and multiple regression approaches. Atmos. Environ. 56, 101-108.

Kleindienst, T.E., Jaoui, M., Lewandowski, M., Offenberg, J.H., Lewis, C.W., Bhave, P.V., Edney, E.O., 2007. Estimates of the contributions of biogenic and anthropogenic hydrocarbons to secondary organic aerosol at a southeastern US location. Atmos. Environ. 41, 8288-8300.

Kleindienst, T.E., Lewandowski, M., Offenberg, J.H., Edney, E.O., Jaoui, M., Zheng, M., Ding, X., Edgerton, E.S., 2010. Contribution of Primary and Secondary Sources to Organic Aerosol and PM2.5at SEARCH Network Sites. J. Air Waste Manage. Assoc. 60, 1388-1399.

Kourtchev, I., Copolovici, L., Claeys, M., Maenhaut, W., 2009. Characterization of atmospheric aerosols at a forested site in central Europe. Environ. Sci. Technol. 43, 4665-4671.

Kourtchev, I., Hellebust, S., Bell, J.M., O'Connor, I.P., Healy, R.M., Allanic, A., Healy, D., Wenger, J.C., Sodeau, J.R., 2011. The use of polar organic compounds to estimate the contribution of domestic solid fuel combustion and biogenic sources to ambient levels of organic carbon and PM2.5 in Cork Harbour, Ireland. Sci. Total Environ. 409, 2143-2155.

Kourtchev, I., Warnke, J., Maenhaut, W., Hoffmann, T., Claeys, M., 2008. Polar organic marker compounds in PM2.5 aerosol from a mixed forest site in western Germany. Chemosphere 73, 1308-1314.

Krivacsy, Z., Hoffer, A., Sarvari, Z., Temesi, D., Baltensperger, U., Nyeki, S., Weingartner, E., Kleefeld, S., Jennings, S., 2001. Role of organic and black carbon in the chemical composition of atmospheric aerosol at European background sites. Atmos. Environ. 35, 6231-6244.

Kumar, A., Ram, K., Ojha, N., 2016. Variations in carbonaceous species at a high-altitude site in western India: Role of synoptic scale transport. Atmos. Environ. 125, Part B, 371-382.

Lai, S., Zhao, Y., Ding, A., Zhang, Y., Song, T., Zheng, J., Ho, K.F., Lee, S.-c., Zhong, L., 2016. Characterization of PM2.5 and the major chemical components during a 1-year campaign in rural Guangzhou, Southern China. Atmos. Res. 167, 208-215.

Laongsri, B., Harrison, R.M., 2013. Atmospheric behaviour of particulate oxalate at UK urban background and rural sites. Atmos. Environ. 71, 319-326.

Lee, H., Park, S.S., Kim, K.W., Kim, Y.J., 2008a. Source identification of PM2.5 particles measured in Gwangju, Korea. Atmos. Res. 88, 199-211.

Lee, S., Liu, W., Wang, Y., Russell, A.G., Edgerton, E.S., 2008b. Source apportionment of PM 2.5: Comparing PMF and CMB results for four ambient monitoring sites in the southeastern United States. Atmos. Environ. 42, 4126-4137.

Lewandowski, M., Jaoui, M., Offenberg, J.H., Kleindienst, T.E., Edney, E.O., Sheesley, R.J., Schauer, J.J., 2008a. Primary and secondary contributions to ambient PM in the midwestern United States. Environ. Sci. Technol. 42, 3303-3309.

Lewandowski, M., Jaoui, M., Offenberg, J.H., Kleindienst, T.E., Edney, E.O., Sheesley, R.J., Schauer, J.J., 2008b. Primary and secondary contributions to ambient PM in the midwestern United States. Environ. Sci. Technol. 42, 3303-3309.

Lewandowski, M., Piletic, I.R., Kleindienst, T.E., Offenberg, J.H., Beaver, M.R., Jaoui, M., Docherty, K.S., Edney, E.O., 2013. Secondary organic aerosol characterisation at field sites across the United States during the spring–summer period. Int. J. Environ. Anal. Chem. 93, 1084-1103.

Lewtas, J., Pang, Y., Booth, D., Reimer, S., Eatough, D.J., Gundel, L.A., 2001. Comparison of sampling methods for semi-volatile organic carbon associated with PM2.5. Aerosol Sci. Technol. 34, 9-22.

Li, B., Zhang, J., Zhao, Y., Yuan, S., Zhao, Q., Shen, G., Wu, H., 2015a. Seasonal variation of urban carbonaceous aerosols in a typical city Nanjing in Yangtze River Delta, China. Atmos. Environ. 106, 223-231.

Li, W., Bai, Z., 2009. Characteristics of organic and elemental carbon in atmospheric fine particles in Tianjin, China. Particuology 7, 432-437.

Li, Y.J., Lee, B.P., Su, L., Fung, J.C.H., Chan, C.K., 2015b. Seasonal characteristics of fine particulate matter (PM) based on high-resolution time-of-flight aerosol mass spectrometric (HR-ToF-AMS) measurements at the HKUST Supersite in Hong Kong. Atmos. Chem. Phys. 15, 37-53.

Lin, P., Hu, M., Deng, Z., Slanina, J., Han, S., Kondo, Y., Takegawa, N., Miyazaki, Y., Zhao, Y., Sugimoto, N., 2009. Seasonal and diurnal variations of organic carbon in PM2.5 in Beijing and the estimation of secondary organic carbon. J. Geophys. Res.-Atmos. 114.

Liu, J., Li, J., Liu, D., Ding, P., Shen, C., Mo, Y., Wang, X., Luo, C., Cheng, Z., Szidat, S., Zhang, Y., Chen, Y., Zhang, G., 2016. Source apportionment and dynamic changes of carbonaceous aerosols during the haze bloom-decay process in China based on radiocarbon and organic molecular tracers. Atmos. Chem. Phys. 16, 2985-2996.

Lonati, G., Ozgen, S., Giugliano, M., 2007. Primary and secondary carbonaceous species in PM2.5 samples in Milan (Italy). Atmos. Environ. 41, 4599-4610.

Lough, G.C., Christensen, C.G., Schauer, J.J., Tortorelli, J., Mani, E., Lawson, D.R., Clark, N.N., Gabele, P.A., 2007. Development of molecular marker source profiles for emissions from on-road gasoline and diesel vehicle fleets. J Air Waste Manag Assoc 57, 1190-1199.

Lv, B., Zhang, B., Bai, Y., 2016. A systematic analysis of PM2.5 in Beijing and its sources from 2000 to 2012. Atmos. Environ. 124, Part B, 98-108.

Mancilla, Y., Herckes, P., Fraser, M.P., Mendoza, A., 2015. Secondary organic aerosol contributions to PM2.5 in Monterrey, Mexico: Temporal and seasonal variation. Atmos. Res. 153, 348-359.

Meng, Z.Y., Jiang, X.M., Yan, P., Lin, W.L., Zhang, H.D., Wang, Y., 2007. Characteristics and sources of PM2.5 and carbonaceous species during winter in Taiyuan, China. Atmos. Environ. 41, 6901-6908.

Miller-Schulze, J.P., Shafer, M.M., Schauer, J.J., Solomon, P.A., Lantz, J., Artamonova, M., Chen, B., Imashev, S., Sverdlik, L., Carmichael, G.R., 2011a. Characteristics of fine particle carbonaceous aerosol at two remote sites in Central Asia. Atmos. Environ. 45, 6955-6964.

Minguillón, M.C., Arhami, M., Schauer, J.J., Sioutas, C., 2008. Seasonal and spatial variations of sources of fine and quasi-ultrafine particulate matter in neighborhoods near the Los Angeles–Long Beach harbor. Atmos. Environ. 42, 7317-7328.

Mirante, F., Salvador, P., Pio, C., Alves, C., Artiñano, B., Caseiro, A., Revuelta, M.A., 2014. Size fractionated aerosol composition at roadside and background environments in the Madrid urban atmosphere. Atmos. Res. 138, 278-292.

Morino, Y., Ohara, T., Xu, J., Hasegawa, S., Zhao, B., Fushimi, A., Tanabe, K., Kondo, M., Uchida, M., Yamaji, K., 2015. Diurnal variations of fossil and nonfossil carbonaceous aerosols in Beijing. Atmos. Environ. 122, 349-356.

Murillo, J.H., Marin, J.F.R., Roman, S.R., Guerrero, V.H.B., Arias, D.S., Ramos, A.C., Gonzalez, B.C., Baumgardner, D.G., 2013. Temporal and spatial variations in organic and elemental carbon concentrations in PM10/PM2.5 in the metropolitan area of Costa Rica, Central America. Atmos. Pollut. Res. 4, 53-63.

Niu, Z., Zhang, F., Chen, J., Yin, L., Wang, S., Xu, L., 2013. Carbonaceous species in PM2.5 in the coastal urban agglomeration in the Western Taiwan Strait Region, China. Atmos. Res. 122, 102-110.

Offenberg, J.H., Lewandowski, M., Jaoui, M., Kleindienst, T.E., 2011. Contributions of biogenic and anthropogenic hydrocarbons to secondary organic aerosol during 2006 in Research Triangle Park, NC. Aerosol. Air Qual. Res. 11, 99-108.

Pachon, J.E., Balachandran, S., Hu, Y., Weber, R.J., Mulholland, J.A., Russell, A.G., 2010. Comparison of SOC estimates and uncertainties from aerosol chemical composition and gas phase data in Atlanta. Atmos. Environ. 44, 3907-3914.

Pant, P., Shukla, A., Kohl, S.D., Chow, J.C., Watson, J.G., Harrison, R.M., 2015. Characterization of ambient PM2.5 at a pollution hotspot in New Delhi, India and inference of sources. Atmos. Environ. 109, 178-189.

Pant, P., Yin, J., Harrison, R.M., 2014. Sensitivity of a Chemical Mass Balance model to different molecular marker traffic source profiles. Atmos. Environ. 82, 238-249.

Paraskevopoulou, D., Liakakou, E., Gerasopoulos, E., Theodosi, C., Mihalopoulos, N., 2014. Long-term characterization of organic and elemental carbon in the PM2.5 fraction: the case of Athens, Greece. Atmos. Chem. Phys. 14, 13313-13325.

Park, S.S., Cho, S.Y., 2011. Tracking sources and behaviors of water-soluble organic carbon in fine particulate matter measured at an urban site in Korea. Atmos. Environ. 45, 60-72.

Perrone, M.G., Larsen, B.R., Ferrero, L., Sangiorgi, G., De Gennaro, G., Udisti, R., Zangrando, R., Gambaro, A., Bolzacchini, E., 2012. Sources of high PM2.5 concentrations in Milan, Northern Italy: Molecular marker data and CMB modelling. Sci. Total Environ. 414, 343-355.

Pietrogrande, M.C., Bacco, D., Ferrari, S., Ricciardelli, I., Scotto, F., Trentini, A., Visentin, M., 2016. Characteristics and major sources of carbonaceous aerosols in PM2.5 in Emilia Romagna Region (Northern Italy) from four-year observations. Sci. Total Environ. 553, 172-183.

Pio, C., Legrand, M., Oliveira, T., Afonso, J., Santos, C., Caseiro, A., Fialho, P., Barata, F., Puxbaum, H., Sanchez-Ochoa, A., 2007. Climatology of aerosol composition (organic versus inorganic) at nonurban sites on a west-east transect across Europe. J. Geophys. Res.-Atmos. 112.

Pipal, A.S., Gursumeeran Satsangi, P., 2015. Study of carbonaceous species, morphology and sources of fine (PM2.5) and coarse (PM10) particles along with their climatic nature in India. Atmos. Res. 154, 103-115.

Plaza, J., Gómez-Moreno, F.J., Núñez, L., Pujadas, M., Artíñano, B., 2006. Estimation of secondary organic aerosol formation from semi-continuous OC–EC measurements in a Madrid suburban area. Atmos. Environ. 40, 1134-1147.

Polidori, A., Turpin, B.J., Lim, H.J., Cabada, J.C., Subramanian, R., Pandis, S.N., Robinson, A.L., 2006. Local and regional secondary organic aerosol: Insights from a year of semi-continuous carbon measurements at Pittsburgh. Aerosol Sci. Technol. 40, 861-872.

Qiao, T., Zhao, M., Xiu, G., Yu, J., 2016. Simultaneous monitoring and compositions analysis of PM1 and PM2.5 in Shanghai: Implications for characterization of haze pollution and source apportionment. Sci. Total Environ. 557–558, 386-394.

Rengarajan, R., Sudheer, A., Sarin, M., 2011. Aerosol acidity and secondary organic aerosol formation during wintertime over urban environment in western India. Atmos. Environ. 45, 1940-1945.

Robinson, A.L., Subramanian, R., Donahue, N.M., Bernardo-Bricker, A., Rogge, W.F., 2006. Source apportionment of molecular markers and organic aerosol. 2. Biomass smoke. Environ. Sci. Technol. 40, 7811-7819.

Rogge, W.F., Hildemann, L.M., Mazurek, M.A., Cass, G.R., Simoneit, B.R., 1991. Sources of fine organic aerosol. 1. Charbroilers and meat cooking operations. Environ. Sci. Technol. 25, 1112-1125.

Rogge, W.F., Hildemann, L.M., Mazurek, M.A., Cass, G.R., Simoneit, B.R., 1998. Sources of fine organic aerosol. 9. Pine, oak, and synthetic log combustion in residential fireplaces. Environ. Sci. Technol. 32, 13-22.

Rogge, W.F., Hildemann, L.M., Mazurek, M.A., Cass, G.R., Simoneit, B.R.T., 1993. Sources of fine organic aerosol. 4. Particulate abrasion products from leaf surfaces of urban plants. Environ. Sci. Technol. 27, 2700-2711.

Safai, P.D., Raju, M.P., Rao, P.S.P., Pandithurai, G., 2014. Characterization of carbonaceous aerosols over the urban tropical location and a new approach to evaluate their climatic importance. Atmos. Environ. 92, 493-500.

Salma, I., Chi, X., Maenhaut, W., 2004. Elemental and organic carbon in urban canyon and background environments in Budapest, Hungary. Atmos. Environ. 38, 27-36.

Samara, C., Voutsa, D., Kouras, A., Eleftheriadis, K., Maggos, T., Saraga, D., Petrakakis, M., 2014. Organic and elemental carbon associated to PM10 and PM2. 5 at urban sites of northern Greece. Environ. Sci. Pollut. Res. 21, 1769-1785.

Saylor, R.D., Edgerton, E.S., Hartsell, B.E., 2006. Linear regression techniques for use in the EC tracer method of secondary organic aerosol estimation. Atmos. Environ. 40, 7546-7556.

Schauer, J.J., Cass, G.R., 2000. Source apportionment of wintertime gas-phase and particle-phase air pollutants using organic compounds as tracers. Environ. Sci. Technol. 34, 1821-1832.

Schauer, J.J., Rogge, W.F., Hildemann, L.M., Mazurek, M.A., Cass, G.R., Simoneit, B.R.T., 1996. Source apportionment of airborne particulate matter using organic compounds as tracers. Atmos. Environ. 30, 3837-3855.

Schichtel, B.A., Malm, W.C., Bench, G., Fallon, S., McDade, C.E., Chow, J.C., Watson, J.G., 2008. Fossil and contemporary fine particulate carbon fractions at 12 rural and urban sites in the United States. J. Geophys. Res.-Atmos. 113.

Sheesley, R.J., Schauer, J.J., Zheng, M., Wang, B., 2007. Sensitivity of molecular marker-based CMB models to biomass burning source profiles. Atmos. Environ. 41, 9050-9063.

Shen, R.Q., Ding, X., He, Q.F., Cong, Z.Y., Yu, Q.Q., Wang, X.M., 2015. Seasonal variation of secondary organic aerosol tracers in Central Tibetan Plateau. Atmos. Chem. Phys. 15, 8781-8793.

Shirmohammadi, F., Hasheminassab, S., Saffari, A., Schauer, J.J., Delfino, R.J., Sioutas, C., 2016. Fine and ultrafine particulate organic carbon in the Los Angeles basin: Trends in sources and composition. Sci. Total Environ. 541, 1083-1096.

Shrivastava, M.K., Subramanian, R., Rogge, W.F., Robinson, A.L., 2007. Sources of organic aerosol: Positive matrix factorization of molecular marker data and comparison of results from different source apportionment models. Atmos. Environ. 41, 9353-9369.

Simoneit, B.R., 2002. Biomass burning—a review of organic tracers for smoke from incomplete combustion. Appl. Geochem. 17, 129-162.

Stone, E., Schauer, J., Quraishi, T.A., Mahmood, A., 2010a. Chemical characterization and source apportionment of fine and coarse particulate matter in Lahore, Pakistan. Atmos. Environ. 44, 1062-1070.

Stone, E.A., Hedman, C.J., Zhou, J., Mieritz, M., Schauer, J.J., 2010b. Insights into the nature of secondary organic aerosol in Mexico City during the MILAGRO experiment 2006. Atmos. Environ. 44, 312-319.

Stone, E.A., Snyder, D.C., Sheesley, R.J., Sullivan, A., Weber, R., Schauer, J., 2008. Source apportionment of fine organic aerosol in Mexico City during the MILAGRO experiment 2006. Atmos. Chem. Phys. 8, 1249-1259.

Stone, E.A., Zhou, J., Snyder, D.C., Rutter, A.P., Mieritz, M., Schauer, J.J., 2009. A Comparison of Summertime Secondary Organic Aerosol Source Contributions at Contrasting Urban Locations. Environ. Sci. Technol. 43, 3448-3454.

Strader, R., Lurmann, F., Pandis, S.N., 1999. Evaluation of secondary organic aerosol formation in winter. Atmos. Environ. 33, 4849-4863.

Subramanian, R., Donahue, N.M., Bernardo-Bricker, A., Rogge, W.F., Robinson, A.L., 2007. Insights into the primary–secondary and regional–local contributions to organic aerosol and PM2.5 mass in Pittsburgh, Pennsylvania. Atmos. Environ. 41, 7414-7433.

Subramoney, P., Karnae, S., Farooqui, Z., John, K., Gupta, A.K., 2013. Identification of PM2. 5 sources affecting a semi-arid coastal region using a chemical mass balance model. Aerosol Air Qual Res 13, 60-71.

Sudheer, A.K., Rengarajan, R., Sheel, V., 2015. Secondary organic aerosol over an urban environment in a semi–arid region of western India. Atmos. Pollut. Res. 6, 11-20.

Sui, X., Yang, L.-X., Yi, H., Yuan, Q., Yan, C., Dong, C., Meng, C.-P., Yao, L., Yang, F., Wang, W.-X., 2015. Influence of Seasonal Variation and Long-Range Transport of Carbonaceous Aerosols on Haze Formation at a Seaside Background Site, China. Aerosol. Air Qual. Res. 15, 1251-1260.

Sun, Y.L., Zhang, Q., Schwab, J.J., Demerjian, K.L., Chen, W.N., Bae, M.S., Hung, H.M., Hogrefe, O., Frank, B., Rattigan, O.V., Lin, Y.C., 2011. Characterization of the sources and processes of organic and inorganic aerosols in New York city with a high-resolution time-of-flight aerosol mass apectrometer. Atmos. Chem. Phys. 11, 1581-1602.

Sunder Raman, R., Hopke, P.K., Holsen, T.M., 2008. Carbonaceous aerosol at two rural locations in New York State: Characterization and behavior. J. Geophys. Res.-Atmos. 113.

Szidat, S., Ruff, M., Perron, N., Wacker, L., Synal, H.-A., Hallquist, M., Shannigrahi, A.S., Yttri, K.E., Dye, C., Simpson, D., 2009. Fossil and non-fossil sources of organic carbon (OC) and elemental carbon (EC) in Göteborg, Sweden. Atmos. Chem. Phys. 9, 1521-1535.

Tao, J., Ho, K.-F., Chen, L., Zhu, L., Han, J., Xu, Z., 2009. Effect of chemical composition of PM 2.5 on visibility in Guangzhou, China, 2007 spring. Particuology 7, 68-75.

Toro Araya, R., Flocchini, R., Morales Segura, R.G., Leiva Guzman, M.A., 2014. Carbonaceous aerosols in fine particulate matter of Santiago Metropolitan Area, Chile. Sci. World J. 2014, 794590.

Turpin, B.J., Huntzicker, J.J., 1995. Identification of secondary organic aerosol episodes and quantitation of primary and secondary organic aerosol concentrations during SCAQS. Atmos. Environ. 29, 3527-3544.

Viana, M., Maenhaut, W., Ten Brink, H., Chi, X., Weijers, E., Querol, X., Alastuey, A., Mikuška, P., Večeřa, Z., 2007. Comparative analysis of organic and elemental carbon concentrations in carbonaceous aerosols in three European cities. Atmos. Environ. 41, 5972-5983.

Viidanoja, J., Sillanpää, M., Laakia, J., Kerminen, V.-M., Hillamo, R., Aarnio, P., Koskentalo, T., 2002. Organic and black carbon in PM 2.5 and PM 10: 1 year of data from an urban site in Helsinki, Finland. Atmos. Environ. 36, 3183-3193.

Villalobos, A.M., Amonov, M.O., Shafer, M.M., Devi, J.J., Gupta, T., Tripathi, S.N., Rana, K.S., McKenzie, M., Bergin, M.H., Schauer, J.J., 2015a. Source apportionment of carbonaceous fine particulate matter (PM2.5) in two contrasting cities across the Indo–Gangetic Plain. Atmos. Pollut. Res. 6, 398-405.

Villalobos, A.M., Barraza, F., Jorquera, H., Schauer, J.J., 2015b. Chemical speciation and source apportionment of fine particulate matter in Santiago, Chile, 2013. Sci. Total Environ. 512–513, 133-142.

von Schneidemesser, E., Schauer, J.J., Hagler, G.S.W., Bergin, M.H., 2009. Concentrations and sources of carbonaceous aerosol in the atmosphere of Summit, Greenland. Atmos. Environ. 43, 4155-4162.

von Schneidemesser, E., Zhou, I., Stone, E.A., Schauer, J.I., Shpund, J., Brenner, S., Qasrawi, R., Abdeen, Z., Sarnat, J.A., 2010a. Spatial variability of carbonaceous aerosol concentrations in East and West Jerusalem. Environ. Sci. Technol. 44, 1911-1917.

von Schneidemesser, E., Zhou, J., Stone, E.A., Schauer, J.J., Qasrawi, R., Abdeen, Z., Shpund, J., Vanger, A., Sharf, G., Moise, T., Brenner, S., Nassar, K., Saleh, R., Al-Mahasneh, Q.M., Sarnat, J.A., 2010b. Seasonal and spatial trends in the sources of fine particle organic carbon in Israel, Jordan, and Palestine. Atmos. Environ. 44, 3669-3678.

Wang, F., Guo, Z., Lin, T., Rose, N.L., 2016a. Seasonal variation of carbonaceous pollutants in PM2.5 at an urban 'supersite' in Shanghai, China. Chemosphere 146, 238-244.

Wang, J., Ho, S.S.H., Ma, S., Cao, J., Dai, W., Liu, S., Shen, Z., Huang, R., Wang, G., Han, Y., 2016b. Characterization of PM2.5 in Guangzhou, China: uses of organic markers for supporting source apportionment. Sci. Total Environ. 550, 961-971.

Wang, W., Wu, M., Li, L., Zhang, T., Liu, X., Feng, J., Li, H., Wang, Y., Sheng, G., Claeys, M., 2008. Polar organic tracers in PM 2.5 aerosols from forests in eastern China. Atmos. Chem. Phys. 8, 7507-7518.

Wang, Y., Hopke, P.K., Xia, X., Rattigan, O.V., Chalupa, D.C., Utell, M.J., 2012a. Source apportionment of airborne particulate matter using inorganic and organic species as tracers. Atmos. Environ. 55, 525-532.

Wang, Z., Wang, T., Guo, J., Gao, R., Xue, L., Zhang, J., Zhou, Y., Zhou, X., Zhang, Q., Wang, W., 2012b. Formation of secondary organic carbon and cloud impact on carbonaceous aerosols at Mount Tai, North China. Atmos. Environ. 46, 516-527.

Wu, C., Yu, J.Z., 2016. Determination of primary combustion source organic carbon-to-elemental carbon (OC/EC) ratio using ambient OC and EC measurements: secondary OC-EC correlation minimization method. Atmos. Chem. Phys. 16, 5453-5465.

Wu, H., Zhang, Y.-f., Han, S.-q., Wu, J.-h., Bi, X.-h., Shi, G.-l., Wang, J., Yao, Q., Cai, Z.-y., Liu, J.-l., Feng, Y.-c., 2015. Vertical characteristics of PM2.5 during the heating season in Tianjin, China. Sci. Total Environ. 523, 152-160.

Xu, J., Zhang, Q., Chen, M., Ge, X., Ren, J., Qin, D., 2014. Chemical composition, sources, and processes of urban aerosols during summertime in northwest China: insights from high-resolution aerosol mass spectrometry. Atmos. Chem. Phys. 14, 12593-12611.

Yang, H., Yu, J.Z., Ho, S.S.H., Xu, J., Wu, W.-S., Wan, C.H., Wang, X., Wang, X., Wang, L., 2005. The chemical composition of inorganic and carbonaceous materials in PM2.5 in Nanjing, China. Atmos. Environ. 39, 3735-3749.

Yin, J., Cumberland, S.A., Harrison, R.M., Allan, J., Young, D.E., Williams, P.I., Coe, H., 2015. Receptor modelling of fine particles in southern England using CMB including comparison with AMS-PMF factors. Atmos. Chem. Phys. 15, 2139-2158.

Yin, J., Harrison, R.M., Chen, Q., Rutter, A., Schauer, J.J., 2010. Source apportionment of fine particles at urban background and rural sites in the UK atmosphere. Atmos. Environ. 44, 841-851.

York, D., Evensen, N.M., Martínez, M.L., De Basabe Delgado, J., 2004. Unified equations for the slope, intercept, and standard errors of the best straight line. American Journal of Physics 72, 367-375.

Yu, J., Chen, T., Benjamin, G., Helene, C., Yu, T., Liu, W., Wang, X., 2006. Characteristics of carbonaceous particles in Beijing during winter and summer 2003. Adv. Atmospheric Sci. 23, 468-473.

Zhang, F., Xu, L., Chen, J., Chen, X., Niu, Z., Lei, T., Li, C., Zhao, J., 2013. Chemical characteristics of PM 2.5 during haze episodes in the urban of Fuzhou, China. Particuology 11, 264-272.

Zhang, F., Zhao, J., Chen, J., Xu, Y., Xu, L., 2011. Pollution characteristics of organic and elemental carbon in PM2.5 in Xiamen, China. J. Environ. Sci. 23, 1342-1349.

Zhang, Q., Jimenez, J.L., Canagaratna, M.R., Allan, J.D., Coe, H., Ulbrich, I., Alfarra, M.R., Takami, A., Middlebrook, A.M., Sun, Y.L., Dzepina, K., Dunlea, E., Docherty, K., DeCarlo, P.F., Salcedo, D., Onasch, T., Jayne, J.T., Miyoshi, T., Shimono, A., Hatakeyama, S., Takegawa, N., Kondo, Y., Schneider, J., Drewnick, F., Borrmann, S., Weimer, S., Demerjian, K., Williams, P., Bower, K., Bahreini, R., Cottrell, L., Griffin, R.J., Rautiainen, J., Sun, J.Y., Zhang, Y.M., Worsnop, D.R., 2007. Ubiquity and dominance of oxygenated species in organic aerosols in anthropogenically-influenced Northern Hemisphere midlatitudes. Geophys. Res. Lett. 34.

Zhang, R., Tao, J., Ho, K., Shen, Z., Wang, G., Cao, J., Liu, S., Zhang, L., Lee, S., 2012. Characterization of atmospheric organic and elemental carbon of PM2. 5 in a typical semi-arid area of Northeastern China. Aerosol. Air Qual. Res. 12, 792.

Zhang, Y., Sheesley, R.J., Bae, M.-S., Schauer, J.J., 2009a. Sensitivity of a molecular marker based positive matrix factorization model to the number of receptor observations. Atmos. Environ. 43, 4951-4958.

Zhang, Y., Sheesley, R.J., Schauer, J.J., Lewandowski, M., Jaoui, M., Offenberg, J.H., Kleindienst, T.E., Edney, E.O., 2009b. Source apportionment of primary and secondary organic aerosols using positive matrix factorization (PMF) of molecular markers. Atmos. Environ. 43, 5567-5574.

Zheng, M., Cass, G.R., Ke, L., Wang, F., Schauer, J.J., Edgerton, E.S., Russell, A.G., 2007. Source apportionment of daily fine particulate matter at Jefferson Street, Atlanta, GA, during summer and winter. J Air Waste Manag Assoc 57, 228-242.

Zheng, M., Hagler, G.S., Ke, L., Bergin, M.H., Wang, F., Louie, P.K., Salmon, L., Sin, D.W., Yu, J.Z., Schauer, J.J., 2006a. Composition and sources of carbonaceous aerosols at three contrasting sites in Hong Kong. J. Geophys. Res.-Atmos. 111.

Zheng, M., Ke, L., Edgerton, E.S., Schauer, J.J., Dong, M., Russell, A.G., 2006b. Spatial distribution of carbonaceous aerosol in the southeastern United States using molecular markers and carbon isotope data. J. Geophys. Res.-Atmos. 111.

Zheng, M., Wang, F., Hagler, G.S.W., Hou, X., Bergin, M., Cheng, Y., Salmon, L.G., Schauer, J.J., Louie, P.K.K., Zeng, L., Zhang, Y., 2011. Sources of excess urban carbonaceous aerosol in the Pearl River Delta Region, China. Atmos. Environ. 45, 1175-1182.

Zheng, M., Zhao, X., Cheng, Y., Yan, C., Shi, W., Zhang, X., Weber, R.J., Schauer, J.J., Wang, X., Edgerton, E.S., 2014. Sources of primary and secondary organic aerosol and their diurnal variations. J. Hazard. Mater. 264, 536-544.

Zhou, J., Xing, Z., Deng, J., Du, K., 2016. Characterizing and sourcing ambient PM2.5 over key emission regions in China I: Water-soluble ions and carbonaceous fractions. Atmos. Environ. 135, 20-30.

Zhou, S., Wang, T., Wang, Z., Li, W., Xu, Z., Wang, X., Yuan, C., Poon, C.N., Louie, P.K.K., Luk, C.W.Y., Wang, W., 2014. Photochemical evolution of organic aerosols observed in urban plumes from Hong Kong and the Pearl River Delta of China. Atmos. Environ. 88, 219-229.

Zhou, S., Wang, Z., Gao, R., Xue, L., Yuan, C., Wang, T., Gao, X., Wang, X., Nie, W., Xu, Z., Zhang, Q., Wang, W., 2012. Formation of secondary organic carbon and long-range transport of carbonaceous aerosols at Mount Heng in South China. Atmos. Environ. 63, 203-212.

Chapter III

Experimental section

Under the framework of this PhD, two different urban environments have been investigated. This section presents the sampling sites, instruments and strategies used for this work. Details related to the chemical analyses performed on the collected samples including additional information on the analytical procedures that have been especially improved/developed, are also given in this chapter.

3.1. Sampling sites

One year study in Grenoble, France (2013)

Figure III.1. *Location of the sampling site "Les Frênes" in Grenoble and relief of the valley.*

The sampling site was located at the urban background sampling station of "Les Frênes" (45° 09' 41" N, 5° 44' 07" E) in Grenoble (France). The city, surrounded by three mountainous ranges, is considered as the most densely populated area (160,000 inhabitants) of the French Alps (Figure III.1).

The city has been experiencing frequent severe PM pollution events (PM_{10} >50 µg m^{-3} for at least 3 consecutive days) in winter due to the formation of thermal inversion layers (due to the geomorphology of the site), resulting in a stagnation of the air masses and ultimately a stagnation of pollutants over the city. In addition to the urbanized area, forests, including both deciduous and coniferous species, and agricultural areas (pastures) dominate the land cover around Grenoble (Figure III.2). Residential heating, mainly biomass combustion, accounts for the major fraction of the total $PM_{2.5}$ during winter in the Alpine valleys (Bonvalot et al., 2016; Favez et al., 2010; Jaffrezo et al., 2005a; Marchand et al., 2004). In addition, traffic and industrial activities also contribute significantly to the observed PM levels in Grenoble (Polo-Rehn et al., 2014).

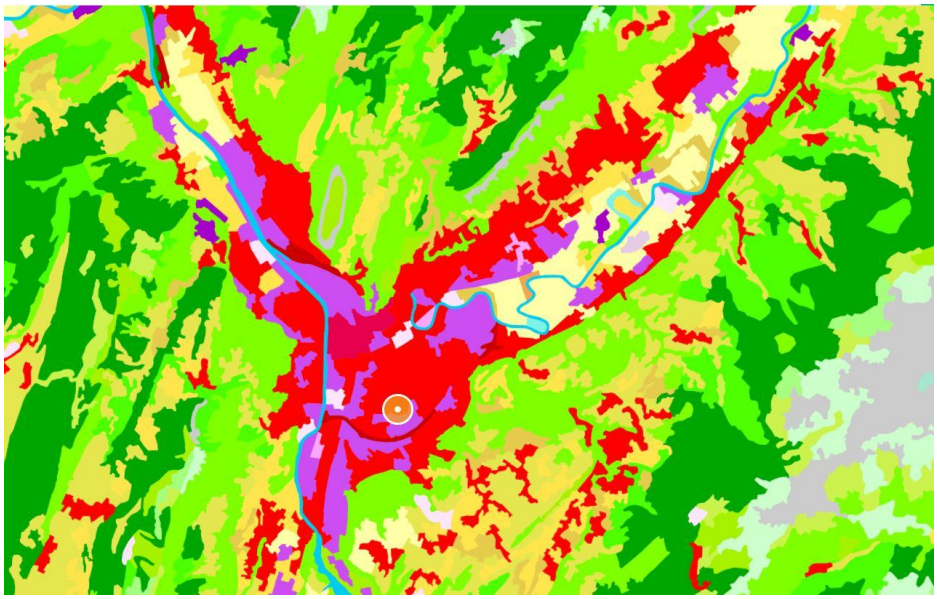

Figure III.2. *Map of the land cover around Grenoble. Urbanized area: red/purple/pink, forest area: green, agriculture/pasture area: yellow, sparsely vegetated area: grey (https://www.geoportail.gouv.fr).*

Intensive sampling campaign in the Paris region, France (March 2015)

Measurements were conducted at SIRTA (Site Instrumental de Recherche par Télédétection Atmosphérique, 2.15° E; 48.71° N; 150 ma.s.l; http://sirta.ipsl.fr) (Haeffelin et al., 2005), a well arranged monitoring station at the edge of the Paris megacity (Figure III.3). The SIRTA facility is part of the ACTRIS (Aerosols, Clouds, and Trace gases Research InfraStructure) research network. It gathers a wide variety of instruments for in situ and remote sensing measurements of meteorological as well as physical and chemical atmospheric parameters. This site is considered as representative of the suburban background conditions of the Ile-de-France region (Crippa et al., 2013; Petit et al., 2017; Petit et al., 2014; Sciare et al., 2011).

Figure III.3. *Location and pictures of the SIRTA sampling station.*

3.2. Sampling periods and sample collection

PM_{10} samples (Tissu-quartz fibre filter, Pallflex, Ø=150 mm) were collected using high volume sampler (Digitel DA-80; flow rate: 30 m^3 h^{-1}) for particulate phase at both sites. Prior to sampling, quartz fibre filters were pre-heated at 500 °C for 12 h to avoid any trace of organic contamination. After collection, samples were wrapped in aluminum foils, sealed in

polyethylene bags, and stored at −20 °C until analysis. Shipping of the samples to the different laboratories for analyses have been done by express post using cool boxes (<5 °C).

At Grenoble, samples were collected every third day (24 h sampling) for one year from 01/01/2013 to 01/01/2014 using high volume sampler and was conducted by the regional air quality network Atmo Rhône-Alpes-Auvergne (Atmo AuRa). A total of 123 samples and 9 field blanks were analysed for an extended chemical characterization following the protocols described in section 3.4.

At SIRTA, an intensive campaign was performed from 6-21, March 2015, and samples were collected every 4 h. The late winter-early spring period was chosen on purpose as intense PM pollution events are usually observed in Northern France (and more generally in North-Western Europe) during this period of the year (Figure III.4). These pollution events are occurring under anticyclonic conditions favouring the accumulation of pollutants and photochemical processes (Bressi et al., 2013; Crippa et al., 2013; Dupont et al., 2016; Favez et al., 2012; Fröhlich et al., 2015; Petit et al., 2017; Petit et al., 2014; Sciare et al., 2011; Waked et al., 2014). Such atmospheric conditions are notably enhancing the formation of secondary aerosols from gaseous precursors emitted by road transport, agricultural activities (including manure spreading) and residential heating (Bressi et al., 2013; Crippa et al., 2013; Dupont et al., 2016; Favez et al., 2012; Fröhlich et al., 2015; Petit et al., 2017; Petit et al., 2014; Sciare et al., 2011; Waked et al., 2014).

A total of 92 samples and 5 field blanks were collected and analysed for an extended chemical characterization following the protocols described in section 3.4.

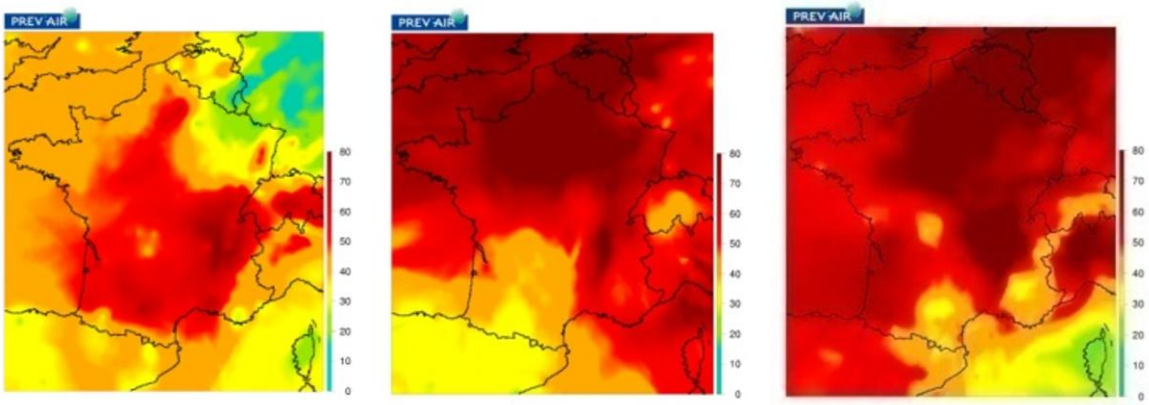

Figure III.4. *Examples of typical days showing high PM (PM_{10}, µg m^{-3}) pollution events in the end of winter-beginning of spring period (Prevair forecast model) (a) 27 February 2013 (b) 14 March 2014 (c) 20 March 2015 (http://www.prevair.org/en/index.php).*

3.3. On line measurements

Atmospheric pollutants related to mandatory monitoring in the frame of the air quality Directives were measured at both sites. These measurements notably included PM_{10}, $PM_{2.5}$, NO_x, and O_3, using instrumentation presented in Table III.1. $PM_{2.5}$ and PM_{10} TEOM-FDMS (Tapered Element Oscillating Microbalance equipped with a Filter Dynamic Measurement System) measurements were conducted at both sites following the European standard procedures (CEN, 2017). At the Grenoble site, NO_x and O_3 measurements were also achieved following European standard procedures (CEN, 2012a; CEN, 2012b). As part of a research network, these measurements were performed following ACTRIS guidelines (www.actris.eu) at SIRTA.

Black carbon and main submicron non-refractory chemical species were also continuously measured by means of a multi-wavelength aethalometer (AE33) and aerosol chemical speciation monitor (ACSM), respectively, at SIRTA. The ACSM offers the measurement of the major chemical species of non-refractory submicron aerosols. Concentrations of organic matter (OM), nitrate (NO_3^-), sulphate (SO_4^{2-}), ammonium (NH_4^+) and chloride (Cl^-) are determined with a time resolution around 30 min. The particles are sampled at 3 L min^{-1}, and sub-sampled

at 0.1 L min^{-1} through a focusing lens allowing a submicron aerosol beam to be focused on a 600 °C heated vaporizer. Particles are flash-vaporized, and instantaneously ionized and fragmented by electron impact at 70 eV. The produced mass fragments are separated by a quadrupole analyser before their detection; a fragmentation panel (Allan et al., 2004) eventually allows the calculation of chemical species following their fragmentation patterns.

Ammonium nitrate is used as the calibration aerosol. Since the ACSM does not have the fast detection electronics to time-resolve single particle pulses, the measured NO^+ and NO_2^+ nitrate signals are averaged over many calibration particles and compared with the input mass of NO_3^- estimated using a Condensation Particle Counter (CPC). Mono-disperse ammonium nitrate particles (300 nm), generated with an atomizer and passed through a diffusion dryer and size selected with a DMA (Differential Mobility Analyser), are injected into both the ACSM and the CPC. Knowing the particle size and number concentrations, the mass of the particles can be calculated (Jayne et al., 2000; Jimenez et al., 2003). A response factor of 2.44×10^{-11} A/µg/m^3 and relative ion efficiencies (RIE) of 5.25 for NH_4^+ were used in the present study. Default values of 1.2 and 1.4 were used for sulfate and OA RIE, respectively. Collection efficiencies (CE) have been corrected following the ammonium nitrate mass fraction by the algorithm proposed by Middlebrook et al. (2012).

BC concentrations obtained at SIRTA were deconvolved into BC from wood burning (BC_{wb}) and fossil fuel (BC_{ff}) emissions using the so-called "aethalometer model" (Drinovec et al., 2015; Sandradewi et al., 2008), assuming that biomass burning and fossil fuel combustion were the two predominant combustion sources. This methodology has already been used successfully in the Ile-de-France region (Favez et al., 2009; Sciare et al., 2011) and Grenoble (Favez et al., 2010). One of the major uncertainties in this approach is the choice of the Ångström absorption exponents of fossil fuel and biomass burning (α_{ff} and α_{wb}, respectively) that may vary from site to site. These two parameters were determined from the investigation of the diurnal distribution

of the Ångström exponent. A sensitivity test was also performed by documenting the impact of small changes in Ångström exponents for wood burning (α_{wb}) and fossil fuel (α_{ff}) by varying the initial values by ± 0.05 with a step of 0.01. Eventually, due to high inorganic species loading during the studied period, manual corrections have been applied to improve the separation between BC_{wb} and BC_{ff} (Petit et al., 2017).

Table III.1. *Instrumentation details for both sites.*

Instrument	Instrumentation		Measured species	Time-resolution	
	Les Frênes-Grenoble	SIRTA-Paris		Les Frênes-Grenoble	SIRTA-Paris
ACSM	-	Quadrupole-ACSM, Aerodyne Research Inc.	Organics, Cl^-, SO_4^{2-}, NO_3^-, NH_4^+	-	30 min
Aethalometer	-	AE33, Magee Scientific	BC	-	1 min
TEOM-FDMS	1405F model, Thermo	1405F model, Thermo	$PM_{2.5}$ and PM_{10}	15 min	15 min
NOx analyser	TEI 42I, Thermo	T200UP, Teledyne API	NO, NO_2	15 min	1 min
O_3 analyser	TEI 49I, Thermo	T400 Teledyne API	O_3	15 min	1 min

3.4. Chemical Characterization

3.4.1. Analytical procedures

A large chemical characterization was performed at both sites. Overall, approximately 194 and 71 species were quantified in each sample collected in the Grenoble valley and the Paris region, respectively. The collected filters were cut into pieces (punches) and each punch was dedicated to specific analyses. The size of filter punches depends on the analytical procedure used for the quantification of a species. A typical example of punches made on the collected filter sample for Grenoble and SIRTA is presented in Figure III.5.

Figure III.5. *Example of punches made on the collected filter sample at Grenoble – Les Frênes (Left) and SIRTA (right).*

EC/OC, major ions (Cl^-, NO_3^-, SO_4^{2-}, NH_4^+, Ca^{2+}, Na^+, Mg^{2+}, K^+), methanesulfonic acid (MSA) and oxalate ($C_2O_4^{2-}$), metal elements (Grenoble, by ICP/MS: n=34; SIRTA, by PIXE: n=7), cellulose combustion markers (biomass burning) (levoglucosan, mannosan and galactosan), polyols (arabitol, sorbitol and mannitol), glucose, polycyclic aromatic hydrocarbons (PAHs) (Grenoble: n=21; SIRTA: n=9), oxy-PAHs (Grenoble: n=27; SIRTA: n=14), nitro-PAHs (Grenoble: n=32; SIRTA: n=8) and 13 SOA markers (notably including α-methylglyceric acid, pinic acid, and methyl-nitrocatechols) (Nozière et al., 2015) were analysed using the protocols reported in Table III.2 at both sites (Albinet et al., 2006; Albinet et al., 2014; Albinet et al., 2013; Alleman et al., 2010; Guinot et al., 2007b; Jaffrezo et al., 2005b; Lucarelli et al., 2017; Lucarelli et al., 2011; Piot et al., 2012; Srivastava et al., 2018; Tomaz et al., 2016; Verlhac et al., 2013; Yttri et al., 2015). In addition, 27 higher alkanes (C13-C39), 10 hopanes, pristane, phytane, 5 sulfur-containing PAHs, and 5 lignin combustion markers (vanillin, coniferaldehyde..) and HuLiS (humic like substances) were also quantified on the Grenoble samples (Baduel et al., 2010; Golly et al., 2015). All the quantified PM_{10} species at Grenoble and SIRTA are given in the **Articles II & III** (Supplementary information (SI), Articles 2 and 3). Offline aerosol mass spectrometer (AMS) analysis was also performed on PM_{10} filter samples collected at SIRTA following the protocols described in Daellenbach et al. (2016) and discussed briefly in **Article IV** (SI, Article IV).

Table III.2. *Detailed information on the off-line chemical characterization of the samples collected at Grenoble and SIRTA.*

Species	Analytical method	References	
		Les Frênes- Grenoble	**SIRTA-Paris**
EC/OC	EUSAAR[1]-2 thermal protocol	(Cavalli et al., 2010)	(Cavalli et al., 2010)
Anions/Cations, MSA, Oxalate	Ion chromatography	(Jaffrezo et al., 2005b)	(Guinot et al., 2007b)
Levoglucosan, Polyols	HPLC-PAD[2]	(Piot et al., 2012)	(Verlhac et al., 2013; Yttri et al., 2015)
PAHS (P&G)	UPLC/UV-Fluorescence[3], QuEChERS[4]	(Albinet et al., 2014; Albinet et al., 2013; Tomaz et al., 2016)	(Albinet et al., 2014; Albinet et al., 2013; Tomaz et al., 2016)
OPAHs and NPAHs (P&G)*	GC-NICI/MS[5], QuEChERS[4]	(Albinet et al., 2006; Albinet et al., 2014; Albinet et al., 2013; Tomaz et al., 2016)	(Albinet et al., 2006; Albinet et al., 2014; Albinet et al., 2013; Tomaz et al., 2016)
Metals	ICP-MS[6]/PIXE[7]	(Alleman et al., 2010)**	(Lucarelli et al., 2017; Lucarelli et al., 2011)[#]
Alkanes (C13-C39), hopanes, pristane, phytane, sulfur containing PAHs and lignin combustion markers	GC/MS[8]	(Baduel et al., 2010; Golly et al., 2015)	-
HuLiS	TOC[9] analyser/ UV-Visible spectroscopy	(Baduel et al., 2010)	-
SOA markers	GC-EI/MS[10], QuEChERS[4]	(Srivastava et al., 2018)[¥]	(Srivastava et al., 2018)[¥]
Offline AMS	AMS[11]	-	(Daellenbach et al., 2016)

[1]EUSAAR: European Supersites for Atmospheric Aerosol Research
[2]HPLC-PAD: High-Performance Liquid Chromatography with Pulsed Amperometric Detector
[3]UPLC/UV- fluorescence: Ultra High-Performance Liquid Chromatography (UPLC) coupled with UV and fluorescence detection
[4]QuEChERS: Quick Easy Cheap Effective Rugged and Safe
[5]GC-NICI/MS: Gas Chromatography-Negative Ion Chemical Ionization/Mass spectrometry
[6]ICP-MS: Inductively Coupled Plasma Mass Spectrometry
[7]PIXE: Particle-Induced X-ray Emission
[8]GC/MS: Gas Chromatography/Mass Spectrometry
[9]TOC: Total Organic Carbon
[10]GC-EI/MS: Gas Chromatography-Electron Ionization/mass spectrometry
[11]AMS: Aerosol Mass Spectrometry
*P-particulate phase; G-gas phase
** ICP-MS: used for metal analysis at Grenoble
[#]PIXE: used for metal analysis at SIRTA
[¥]Authentic standards were used for the quantification

3.4.2. PAHs and their derivatives

In this PhD work, slight modifications have been made in the protocol used for the analyses of nitro-and oxy-PAHs of the SIRTA samples. The purification step has been improved to make it more automated and a change in the GC column used for the analysis has been made to improve the separation of key compounds such has 2- and 3-nitrofluoranthenes (Albinet et al., 2008). The initial analytical procedure applied for the samples collected at Grenoble has already been presented elsewhere (Albinet et al., 2006; Albinet et al., 2014; Tomaz et al., 2016) and the modifications made are detailed below. Details can be found in the **Article III** (SI, Article III), only essential information has been discussed here.

3.4.2.1. Sample extraction and purification

Separate filter punches (∅=47 mm) dedicated to the analysis of PAHs and PAH derivatives, were extracted using a QuEChERS-like procedure (Albinet et al., 2014; Albinet et al., 2013) with acetonitrile (ACN, 7 mL) using a multi-tube vortexer (DVX-2500, VWR) for 1.5 min.

For nitro- and oxy-PAHs, a mixture of surrogate standards containing 2 deuterated oxy-PAHs and 7 deuterated nitro-PAHs were added to the filter samples prior to extraction (1 ng μL^{-1} for nitro-PAHs and 5 ng μL^{-1} for oxy-PAHs; 5 µL of a solution at 1 ng μL^{-1}) and used for the quantification of oxy- and nitro-PAHs (Tables III.3 and III.4). For PAHs, a known amount of 6-methylchrysene was added to the samples prior to extraction (10 µL of a solution at 1 ng μL^{-1}) and used as surrogate standard to check the PAH extraction efficiency according to the EN 15549 and TS 16645 standard procedures (Albinet et al., 2014; Albinet et al., 2013; CEN, 2008; CEN, 2014; Tomaz et al., 2016).

After QuEChERS extraction, extracts dedicated to the PAH analyses were reduced under a gentle nitrogen stream to near dryness and dissolved in 1 ml of ACN.

As explained above, an improvement has been made in the purification step for the analysis of nitro- and oxy-PAHs. A SPE GILSON (ASPEC GX-274) device was used to perform the clean-up of the extracts automatically over the manual procedure used before (Figure III.6). Alumina and silica SPE cartridges (ALOX Chromabond, SiOH, Chromabond, Macherey Nagel, 3 mL, 500 mg) were used for the cleaning in two steps. Alumina SPE cartridges were conditioned with 3 mL of methanol (MeOH), ACN, and dichloromethane (DCM), respectively. Extracts were loaded and rinsed with 1 mL of ACN and MeOH. The collection of the eluted extracts was done in two steps with the elution of a first fraction with 4 mL of ACN, and a second fraction with 5.5 mL of DCM. Both fractions were then mixed. Extracts were then reduced under a gentle stream of nitrogen to a volume of about 100 µL. Extracts were further cleaned using silica SPE cartridges. Silica cartridges were conditioned with 1 mL of DCM, followed by 3 mL of pentane. Extracts were loaded, and rinsed with 1 mL of pentane (discarded), followed by an elution with 6 mL of a pentane/ DCM mixture (65:35; v/v). Extracts were then concentrated to near dryness under a gentle stream of nitrogen and dissolved with about 100 µL of ACN. Before analysis, purified samples were spiked with a known amounts of labelled internal standards (9-fluorenone-d8 and 1-nitropyrene-d9; 5 µL of a solution at 1 ng μL^{-1}) to evaluate the surrogate recoveries.

Extraction efficiencies were checked using NIST standard SRM1649b (urban dust). Results obtained were in good agreement with NIST reference and indicative concentration values and with the ones previously reported in the literature, and notably using QuEChERS extraction procedure (Albinet et al., 2014 and references therein).

3.4.2.2. Nitro-PAH and oxy-PAH analyses

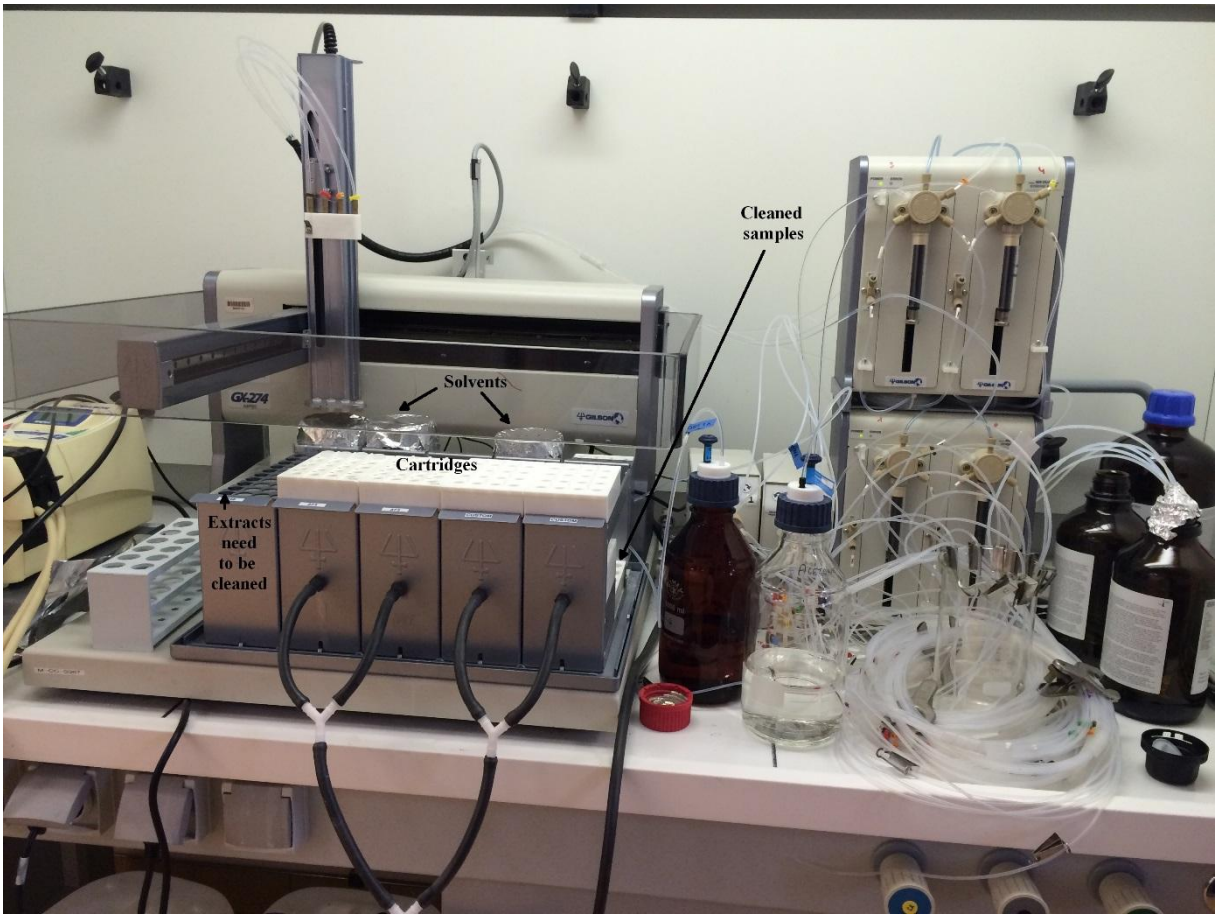

Figure III.6. *Clean-up of the sample extracts performed using SPE GILSON device (ASPEC GX-274) for the analysis of oxy- and -nitro PAHs.*

The quantification of nitro- and oxy-PAHs has been performed following the same protocol described previously (Albinet et al., 2006; Albinet et al., 2014; Tomaz et al., 2016) by using GC/NICI-MS (Agilent 7890A GC coupled to 5975C MS) and Rxi-PAH Restek column (30 m × 250 µm × 0.10 µm). 2 µl of the purified extracts have been injected into the pulsed splitless mode for analysis. Note that the column phase used here allowed the separation of 2- and 3-nitrofluoranthene isomers. Particularly, 2-nitrofluoranthene, known to be secondarily formed from the oxidation of PAH (fluoranthene) (Arey et al., 1986; Atkinson et al., 1987), can be used as a marker to estimate SOA PAHs contribution. The use of 2-nitrofluoranthene in the source receptor models may provide meaningful results, and was demonstrated by the source

apportionment study conducted at SIRTA (**Article III**). Therefore, the separation of 2- and 3-nitrofluoranthene isomers are very important and have been achieved here by using a new GC column.

3.4.2.3. Blank values and detection/quantification limit

The background contamination related to sample collection was also evaluated by using filter field blanks (n=5). The final results only considers the compounds with following characteristics: concentration values above the detection limit, field blank values less than 30% of the mean concentrations, and mainly associated with the particulate phase (Albinet et al., 2007; Albinet et al., 2008; Albinet et al., 2010; Isaacman-VanWertz et al., 2016; Lai et al., 2015; Tomaz et al., 2016). The LQ (limit of quantification) was defined as the lowest concentrations of the compound that can be quantified with a signal to noise ratio of 10. The lowest point of the calibration range has been used to make these calculations. Samples with concentrations below LQ were replaced by LQ/2.

Table III.3. *List of oxy-PAHs and oxygenated compounds quantified, selected monitored ions and instrumental LQ by GC/NICI/MS.*

Compounds	***Abbreviation***	***Retention time (min)***	***Monitored ions (m/z)***	***Dwell time (s)***	***Deuterated surrogate standards***	***Retention time (min)***	***Monitored ions (m/z)***	***Instrumental LOQs (pg injected)***
Phthaldialdehyde	Pht	7.59	134	0.06	1,4-Naphthoquinone-d_6	8.32	164	0.23
1,4-Naphthoquinone	1,4-NQ	8.33	158	0.06				0.05
1-Naphthaldehyde	1-Nay	8.66	156	0.10				0.22
Phthalic anhydride	PhtA	7.96	148	0.06				0.12
2-Formyl-trans-cinnamaldehyde	2-FCin	8.91	160	0.10				0.11
1,2-Naphthoquinone	1,2-NQ	9.39	158	0.05				9.65
Benzophenone	Bzophe	9.14	182	0.06				0.24
1-Acenaphthenone	1-Aceone	9.56	168	0.05				0.39
9-Fluorenone	9-Fluo	9.98	180	0.05				0.11
Naphthalic-1,2-anhydride	1,2-NA	11.10	198	0.06				0.12
Biphenyl-2,2'-dicarboxaldehyde	Biph 2,2'	11.07	210	0.06	9,10-Anthraquinone-d_8	12.29	216	0.04
Xanthone	Xanth	10.99	196	0.06				0.58
Acenaphthenequinone	AceQ	11.76	182	0.06				0.14
2,3-Naphthalene dicarboxylic anhydride	2,3-NA	11.75	198	0.03				15.77
Anthrone	Anthro	12.05	194	0.03				4.77
6H-Dibenzo[b,d]pyrene-6-one	6H-DPone	12.22	196	0.03				16.34
9,10-Anthraquinone	9,10-ANQ	12.36	208	0.03				0.19
Naphthalic-1,8-anhydride	1,8-NA	13.82	198	0.03				0.04
1,4-Anthraquinone	1,4-ANQ	13.49	208	0.03				1.47
Biphenyl-4,4'-dicarboxaldehyde	Biph 4,4'	13.63	210	0.03				0.08
2-Methylanthraquinone	2-MANQ	13.80	222	0.04				0.07
9-Phenanthrenecarboxaldehyde	9-PheCar	14.22	206	0.04				0.05
9,10-Phenanthrenequinone	9,10-PQ	15.54	208	0.06				38.97
2-Nitro-9-fluorenone	2N9fluo	15.58	225	0.06				0.07
Benzo[a]fluorenone	BaFone	17.18	230	0.15				0.06
Benzo[b]fluorenone	BbFone	18.19	230	0.15				0.12
Benzanthrone	Bzone	19.81	230	0.15				0.04
1-Pyrenecarboxaldehyde	1-PyrCar	19.94	230	0.15				0.07
Aceanthrenequinone	AceanQ	20.95	232	0.01				0.08
Benz[a]anthracene-7,12-dione	B-7,12-D	20.96	258	0.01				0.07
1,4-Chrysenequinone	1,4-CHRQ	22.33	258	0.01				0.09
5,6-Chrysenequinone	5,6-CHRQ	25.12	258	0.01				22.55

Table III.4. *List of nitro-PAHs quantified, selected monitored ions and instrumental LQ by GC/NICI/MS.*

Compounds	***Abbreviation***	***Retention time (min)***	***Monitored ions (m/z)***	***Dwell time (s)***	***Deuterated surrogate standards***	***Retention time (min)***	***Monitored ions (m/z)***	***Instrumental LOQs (pg injected)***
1-Nitronaphthalene	1-NN	9.16	173	0.06	1-Nitronaphthalene-d_7	9.14	180	0.16
2-Methyl-1-nitronaphthalene + 1-Methyl-5-nitronaphthalene [a]	2-M1NN + 1-M5NN	9.18	187	0.06				0.32
2-Nitronaphthalene	2-NN	9.40	173	0.06				0.06
2-Methyl-4-nitronaphthalene	2-M4NN	9.95	187	0.06				0.36
1-Methyl-4-nitronaphthalene	1-M4NN	10.11	187	0.06				0.35
1-Methyl-6-nitronaphthalene	1-M6NN	10.23	187	0.06				0.02
1,5-Dinitronaphthalene	1,5-DNN	12.48	218	0.03				0.03
2-Nitrobiphenyl	2-Nbi	9.59	199	0.03	2-Nitrobiphenyl-d_9	9.56	208	0.07
3-Nitrobiphenyl	3-Nbi	10.46	199	0.03				0.17
3-Nitrodibenzofuran	3-NDibf	12.22	213	0.03				0.20
5-Nitroacenaphthene	5-NAce	12.27	199	0.03				0.16
2-Nitrofluorene	2-NF	13.97	211	0.03	2-Nitrofluorene-d_9	13.87	220	0.38
9-Nitroanthracene	9-NA	14.22	223	0.09	9-Nitroanthracene-d_9	14.14	232	0.09
9-Nitrophenanthrene	9-NPhe	15.30	223	0.09				0.06
2-Nitrodibenzothiophene	2-NDithio	15.85	229	0.09				0.28
3-Nitrophenanthrene	3-NPhe	15.97	223	0.09				0.08
2-Nitroanthracene	2-NA	16.76	223	0.09				0.20
9-Methyl-10-nitroanthracene	9-M10NA	16.79	237	0.09				0.08
2-Nitrofluoranthene	2-NFlt	20.13	247	0.10	1-Nitropyrene-d_9	21.30	256	0.09
3-Nitrofluoranthene	3-NFlt	20.40	247	0.10				0.09
4-Nitropyrene	4-NP	20.67	247	0.10				0.07
1-Nitropyrene	1-NP	21.38	247	0.10				0.07
2-Nitropyrene	2-NP	21.70	247	0.10				0.20
7-Nitrobenz[a]anthracene	7-NBaA	23.72	273	0.06	6-Nitrochrysene-d_{11}	25.01	284	0.10
6-Nitrochrysene	6-NChry	25.13	273	0.06				0.03
1,3-Dinitropyrene	1,3-DNP	26.71	292	0.25				0.07
1,6-Dinitropyrene	1,6-DNP	28.17	292	0.25				0.13

1,8-Dinitropyrene	1,8-DNP	28.42	292	0.25				0.20
1-Nitrobenzo[e]pyrene	1-NBeP	29.75	297	0.12	6-Nitrobenzo[a]pyrene-d_{11}	29.63	308	0.14
6-Nitrobenzo[a]pyrene	6-NBaP	31.61	297	0.12				0.14
3-Nitrobenzo[e]pyrene	3-NBeP	31.17	297	0.12				0.85

[a] 2-M1NN and 1-M5NN are not separated with the column used.

3.4.3. Analysis of SOA markers

The analytical procedure for the analysis of the SOA markers has been developed during this PhD work. Details on the sample preparation, derivatization and analyses are discussed in **Article II** (SI, Article II). Only a succinct description is reported here. Note, that the quantification has been based on authentic standards for all the SOA markers compounds and this has never been reported before.

3.4.3.1. Sample extraction and derivatization

Filter punches (∅=47 mm) for SOA analysis were extracted with MeOH (7 mL) using a QuEChERS like procedure (Albinet et al., 2014; Albinet et al., 2013). Extracts were collected and reduced to dryness under a gentle nitrogen stream to avoid the presence of hydroxyl group prior to derivatization. Extracts were further dissolved into 50 µL of ACN and subjected to derivatization (silylation) for 30 minutes at 60°C after addition of 50 µL of N-Methyl-N-(trimethylsilyl) trifluoroacetamide (MSTFA) with 1% trimethyl-chlorosilane (TMS). Surrogate and internal standards were used for the quantification of SOA markers, and to evaluate the surrogate recoveries in the samples. The list of all SOA markers quantified, their precursors, retention time, quantification ions and limit of quantification are given in Table III.5.

Extraction efficiencies were checked using NIST standard SRM1649b (urban dust) and discussed in section 3.4.3.3.

3.4.3.2. Sample analysis

The quantification of SOA markers was achieved using GC/MS (Agilent 7890A GC coupled to 5975C MS) in electron ionisation mode (EI, 70 eV) on a DB-5MS-column (Agilent J&W, 60 m × 0.25 mm × 0.25 µm). 2 µL of the extracts were injected in the splitless mode.

Blank values and detection/quantification limits have been determined following the same procedures as for oxy- and nitro-PAHs (please cf. 3.4.2.3).

Table III.5. *List of SOA markers quantified, selected monitored ions and instrumental limit of quantification (LQ) by GC/MS.*

Compounds	***Precursor***	***Chemical formula***	***Retention time (min)***	***Monitored ions (m/z)***	***Dwell time (s)***	***Deuterated surrogate standards***	***Retention time (min)***	***Monitored ions (m/z)***	***Dwell time (s)***	***Instrumental LQs (pg injected)***
Succinic acid	Cyclic olefins and aliphatic diolefins	$C_4H_6O_4$	20.62	129, 247	0.035	Succinic-2,2,3,3-d4 acid	20.51	147, 251	0.035	1.3
α-Methylglyceric acid (α-MGA)	Isoprene	$C_4H_8O_4$	20.69	219, 306	0.035					1.0
2,3-Dihydroxy-4-oxopentanoic acid (DHOPA)	Toluene	$C_5H_8O_5$	25.71	218, 350	0.05					8.4
Pinonic acid	α-pinene	$C_{10}H_{16}O_3$	26.35	171, 125	0.05					2.2
3-Hydroxyglutaric acid (3-HGA)	α-pinene	$C_5H_8O_5$	27.24	349, 185	0.05					1.3
Pinic acid	α-pinene	$C_9H_{14}O_4$	29.53	129, 171	0.05					6.3
Phthalic acid	Naphthalene	$C_8H_6O_4$	30.09	295, 221	0.05					0.9
2-Methylerythritol (2-MT)	Isoprene	$C_5H_{12}O_4$	26.67	219, 117	0.05	Meso-erythritol-1,1,2,4,4-d6	25.43	208, 220	0.1	1.1
3-Methylbutane-1,2,3-tricarboxylic acid (MBTCA)	α-pinene	$C_8H_{12}O_6$	31.31	204, 245	0.05	1,9-Nonanedioic-d14	32.12	331, 213	0.035	0.6
β-Caryophyllinic acid	β-caryophyllene	$C_{14}H_{22}O_4$	37.06	117, 200	0.05					14.3
1,2,3,4-Cyclobutane tetracarboxylic acid	α-pinene	$C_8H_8O_8$	37.83	505, 387	0.05					0.3

3.4.3.3. Method validation

As mentioned in the literature (Nozière et al., 2015), the molecular characterization of sources or processes is often achieved by comparing specific tracers/ markers to well-identified reference compounds. In most cases, no authentic standards are available for these compounds (SOA markers), and proxy compounds are generally used for the quantification. No certified analytical protocols are defined even for the quantification and the identification of these compounds. In addition, no concentration values have been reported yet for SOA markers in any certified material. Inter-comparisons between different techniques or instruments can be considered as a good investigating tool to evaluate the analytical repeatability and reproducibility of the measurements and to highlight any bias or factor influencing the results. These are very important parameters for the quality control of the sampling and analysis method.

Thus, an inter-comparison on the SOA marker analysis has been conducted including three laboratories: INERIS, NIST (Gaithersburg, MD, USA) and LSCE. Notably the quantification has been based on authentic standards for all the SOA markers compounds. For the first time, SRM 1649b (urban dust) provided by NIST, was analysed to report concentration values for SOA marker in this kind of material and later, these results were used to compare and validate the accuracy and the precision of the developed analytical methods. Five samples of SRM 1649b of about 50 mg (balance precision = 0.01 mg) were extracted using both methods, sonication and QuEChERS, and analysed by GC-EI/MS and LC-MS/MS. Three injections were made for each individual sample to verify the reproducibility of the obtained results and the operating conditions of the instruments. The moisture content of each sample was determined using Karl Fischer method (2.94 % moisture analyser HR 73, Mettler Toledo; Viroflay, France). SOA marker concentrations were corrected and reported as dry-mass basis (Figure III.7).

At NIST, this work was performed in collaboration with *Federica Nalin*. Initially, MeOH, and a mixture of MeOH and ACN (1:1) were investigated to determine their suitability as extraction solvents for the sonication. The results revealed the recovery of the surrogates was substantially higher when SRM1649b was extracted using MeOH. Therefore, MeOH was selected as the extraction solvent for SOA marker analysis for this inter-comparison activity. Finally, SRM1649b (50 mg) for SOA analysis was extracted with MeOH (7 mL) using sonication for 15 min., and then subjected to dryness under a gentle nitrogen stream to avoid the presence of hydroxyl group prior to derivatization. Extracts were dissolved into 50 μL of ACN and followed by the addition of N, O-Bistrifluoroacetamide (BSTFA) with 1% trimethyl-chlorosilane (TMS) for derivatization (silylation). Details on the operation parameters used for SOA markers analysis by GC-EI/MS, were the same as described in section 3.4.3.2.

The quantification of SOA markers analysis at INERIS was made using both extraction methods, sonication and QuEChERS, with 7 ml of MeOH as explained above (section 3.4.3.1). Note that, MSTFA with TMS was used in this case as the derivatization reagent.

At LSCE, this work was performed in collaboration with *Nicolas Bonnaire*. The quantification of SOA markers was achieved by LC-MS/MS (Triple quadrupole mass, AB Sciex brand, model 3200QTRAP) using both sonication and QuEChERS, procedures for sample extraction. Two columns were used for the analyses: Hypercarb column (2.1 mm × 150 mm × 3 μm) and UPLC® HSST3 Acquity column (2.1 mm × 100 mm × 1.8 μm). MiliQ water and MeOH were used as the solvent phase depending on the solubility of each compound. 10 μL of the extracts were injected for sample analysis. More details on the analytical protocols can be found elsewhere (Ayachi, 2015).

To the best of our knowledge, this inter-comparison study is probably the first one to report concentration values of SOA markers in SRM1649b (urban dust). The results showed good consistency for most of the compounds except for succinic acid and 2-C-methyl-D-erythritol (Figure III.7). The observed concentration values for these two compounds have shown large variation, making it difficult to provide any common range. Interestingly, the efficacy of both extraction procedures, sonication and QuEChERS, was similar for all the analysed SOA markers supporting the choice rather QuEchERS extraction was then applied routinely for the analysis of all the samples. The analysis of the NIST SRM 1649b (urban dust) was then used as quality control for the SOA marker analyses performed in this PhD work.

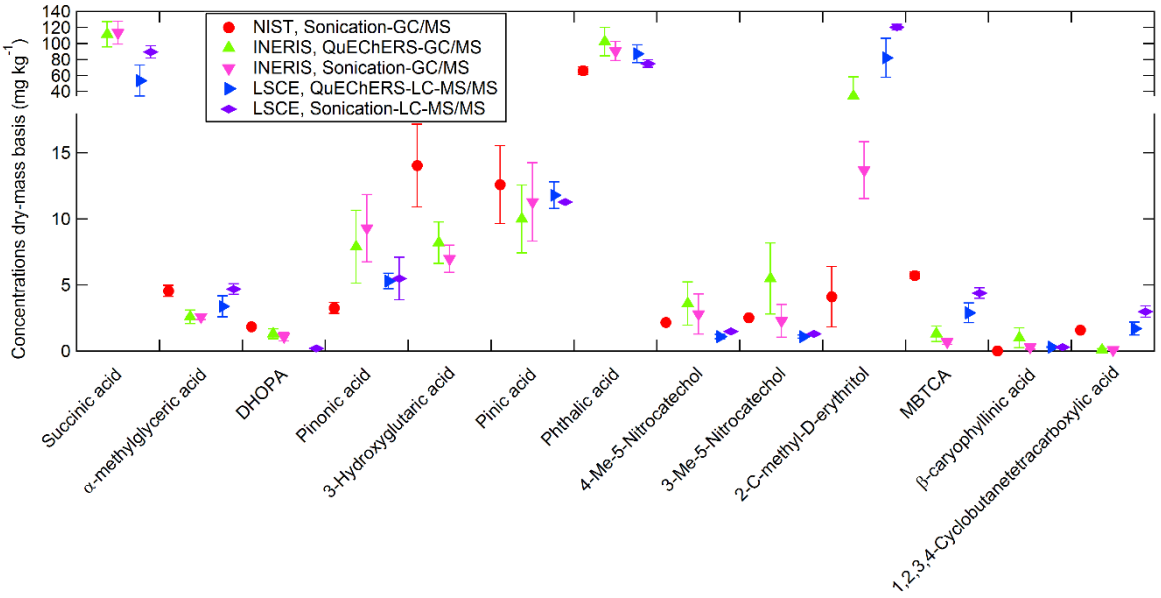

Figure III.7. *Comparison of the results obtained using different extraction and analytical techniques for the quantification of SOA markers in the NIST SRM 1649b (urban dust). Error bars show the standard deviations from 5 full experiments (extraction and analysis) and triplicate injections (n=15).*

3.5. Chemical Mass Closures

PM_{10} Filter datasets

As shown, a large chemical characterization was carried out during the PhD work, and a general way to check the data validation is by performing the chemical mass balance which allows to assess the extent to which the PM_{10} concentration measured can be explained by the measured chemical species. In this work, the chemical mass balance was achieved according to the procedure explained in Bressi et al. (2013).

$PM_{modeled}$= [Sea salt] + [Dust] + [Secondary inorganic aerosols] + [Carbonaceous aerosols]

Sea salt (ss) concentrations are calculated from the six major ions accounting for more than 99% of the mass of salts dissolved in seawater:

$[Sea\ salt] = [Na^+] + [Cl^-] + [Mg^{2+}] + [ssK^+] + [ssCa^{2+}] + [ssSO_4^{2-}]$

with $[ssK^+] = 0.036 \cdot [Na^+]$; $[ssCa^{2+}] = 0.038 \cdot [Na^+]$ and $[ssSO_4^{2-}] = 0.252 \cdot [Na^+]$

Dust can be calculated by assuming the 15% contribution of non-sea salt calcium is in mineral dust (Guinot et al., 2007a):

$[Dust] = [nssCa^{2+}]/0.15$

Secondary inorganic aerosols are calculated as:

$[Secondary\ Inorganic\ Aerosols] = [nssSO_4^{2-}] + [NO_3^-] + [NH_4^+]$

where $[nssSO_4^{2-}] = [SO_4^{2-}] - [ssSO_4^{2}]$

Finally, carbonaceous aerosols can be expressed as:

[Carbonaceous aerosols] = [EC] + [OA]

Assuming a OC-to-OA conversion factor around 1.8 (Sciare et al., 2011), the amount of carbonaceous matter was estimated and final calculations were made according to the above mentioned equations to model PM_{10} mass. The reconstructed PM mass was compared with online

PM_{10} measurements (TEOM-FDMS) and showed a very good correlation for both sites (r^2 = 0.87-0.96; n = 92 (Figure III.8)). The observed results highlighted the consistency of chemical analyses, and confirmed that all the major aerosol chemical species were considered.

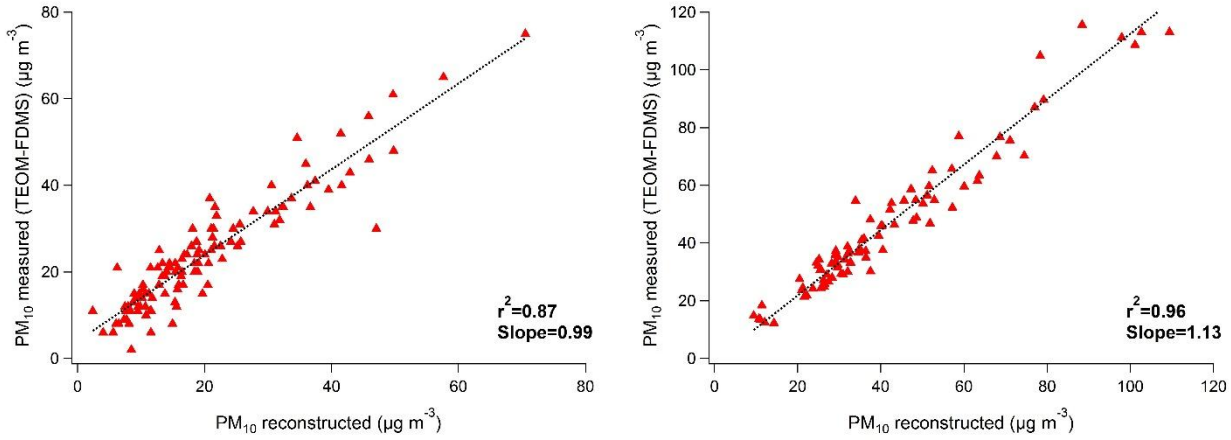

Figure III.8. *Comparison between PM_{10} measured (TEOM-FDMS) and PM_{10} reconstructed from filter chemical speciation, at Grenoble (Left) and at SIRTA (Right).*

Online measurements

The reconstructed NR-PM_1 mass from ACSM (sum of organic aerosol (OA), nitrate (NO_3^-), sulphate (SO_4^{2-}), ammonium (NH_4^+) and chloride (Cl^-)) was compared with online PM_1 measurements (TEOM-FDMS), and showed good correlation (r^2 = 0.87; slope=0.99; n = 92) (Figure III.9).

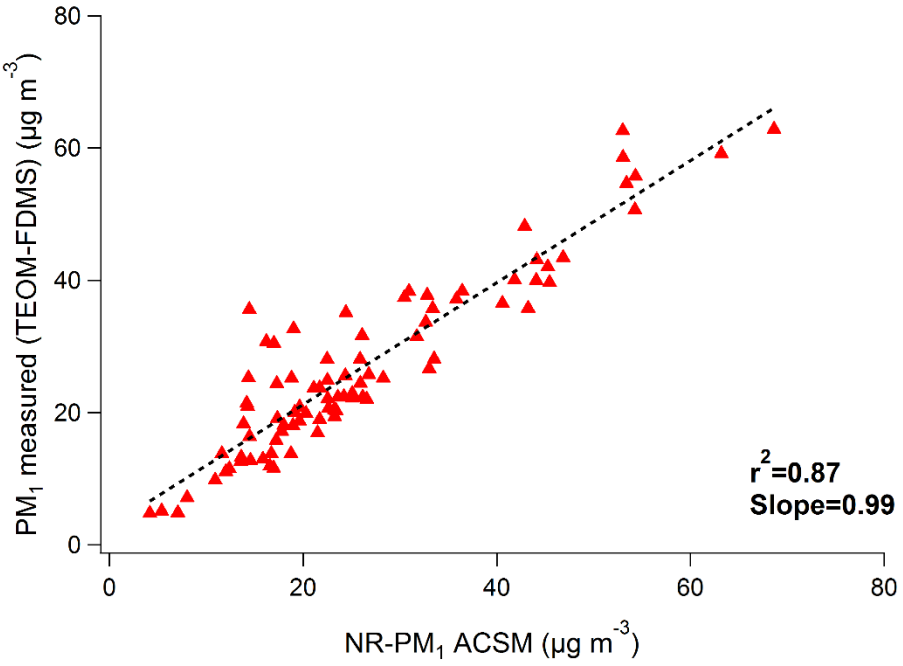

Figure III.9. *Comparison between measured PM_1 (TEOM-FDMS) and reconstructed NR-PM_1 (ACSM).*

References

Albinet, A., Leoz-Garziandia, E., Budzinski, H., Villenave, E., 2006. Simultaneous analysis of oxygenated and nitrated polycyclic aromatic hydrocarbons on standard reference material 1649a (urban dust) and on natural ambient air samples by gas chromatography–mass spectrometry with negative ion chemical ionisation. J. Chromatogr. A. 1121, 106-113.

Albinet, A., Leoz-Garziandia, E., Budzinski, H., Villenave, E., 2007. Polycyclic aromatic hydrocarbons (PAHs), nitrated PAHs and oxygenated PAHs in ambient air of the Marseilles area (South of France): Concentrations and sources. Sci. Total Environ. 384, 280-292.

Albinet, A., Leoz-Garziandia, E., Budzinski, H., Villenave, E., Jaffrezo, J. L., 2008. Nitrated and oxygenated derivatives of polycyclic aromatic hydrocarbons in the ambient air of two French alpine valleys Part 2: Particle size distribution. Atmos. Environ. 42, 55-64.

Albinet, A., Minero, C., Vione, D., 2010. Phototransformation processes of 2,4-dinitrophenol, relevant to atmospheric water droplets. Chemosphere. 80, 753-758.

Albinet, A., Nalin, F., Tomaz, S., Beaumont, J., Lestremau, F., 2014. A simple QuEChERS-like extraction approach for molecular chemical characterization of organic aerosols: application to nitrated and oxygenated PAH derivatives (NPAH and OPAH) quantified by GC–NICIMS. Anal. Bioanal. Chem. 406, 3131-3148.

Albinet, A., Tomaz, S., Lestremau, F., 2013. A really quick easy cheap effective rugged and safe (QuEChERS) extraction procedure for the analysis of particle-bound PAHs in ambient air and emission samples. Sci. Total Environ. 450-451, 31-8.

Allan, J. D., Delia, A. E., Coe, H., Bower, K. N., Alfarra, M. R., Jimenez, J. L., Middlebrook, A. M., Drewnick, F., Onasch, T. B., Canagaratna, M. R., 2004. A generalised method for the extraction of chemically resolved mass spectra from Aerodyne aerosol mass spectrometer data. J. Aerosol Sci. 35, 909-922.

Alleman, L. Y., Lamaison, L., Perdrix, E., Robache, A., Galloo, J.-C., 2010. PM10 metal concentrations and source identification using positive matrix factorization and wind sectoring in a French industrial zone. Atmos. Res. 96, 612-625.

Arey, J., Zielinska, B., Atkinson, R., Winer, A. M., Ramdahl, T., Pitts, J. N., 1986. The formation of nitro-PAH from the gas-phase reactions of fluoranthene and pyrene with the OH radical in the presence of NOx. Atmos. Environ. 20, 2339-2345.

Atkinson, R., Arey, J., Zielinska, B., Pitts, J. N., Winer, A. M., 1987. Evidence for the transformation of polycyclic organic matter in the atmosphere. Atmos. Environ. 21, 2261-2262.

Ayachi, S., 2015. Mise au point d'une méthode d'analyse des aérosols secondaires organiques provenant de la combustion de la biomasse. LSCE.

Baduel, C., Voisin, D., Jaffrezo, J. L., 2010. Seasonal variations of concentrations and optical properties of water soluble HULIS collected in urban environments. Atmos. Chem. Phys. 10, 4085-4095.

Bonvalot, L., Tuna, T., Fagault, Y., Jaffrezo, J. L., Jacob, V., Chevrier, F., Bard, E., 2016. Estimating contributions from biomass burning, fossil fuel combustion, and biogenic carbon to carbonaceous aerosols in the Valley of Chamonix: a dual approach based on radiocarbon and levoglucosan. Atmos. Chem. Phys. 16, 13753-13772.

Bressi, M., Sciare, J., Ghersi, V., Bonnaire, N., Nicolas, J. B., Petit, J. E., Moukhtar, S., Rosso, A., Mihalopoulos, N., Féron, A., 2013. A one-year comprehensive chemical characterisation of fine aerosol (PM2.5) at urban, suburban and rural background sites in the region of Paris (France). Atmos. Chem. Phys. 13, 7825-7844.

Cavalli, F., Viana, M., Yttri, K., Genberg, J., Putaud, J.-P., 2010. Toward a standardised thermal-optical protocol for measuring atmospheric organic and elemental carbon: the EUSAAR protocol. Atmos. Meas. Tech. 3, 79-89.

CEN, 2008. European Committee for Standardization, EN 15549: 2008 - Air Quality - Standard Method for the Measurement of the Concentration of Benzo[a]pyrene in Air. CEN, Brussels (Belgium).

CEN, 2012a. European Committee for Standardization, EN-14625: 2012 - Ambient Air - Standard Method For The Measurement Of The Concentration Of Ozone By Ultraviolet Photometry. CEN, Brussels (Belgium). .

CEN, 2012b. European Committee for Standardization, EN 14211: 2012-Ambient air. Standard method for the measurement of the concentration of nitrogen dioxide and nitrogen monoxide by chemiluminescence. CEN, Brussels (Belgium). .

CEN, 2014. European Committee for Standardization, TS-16645: 2014- Ambient Air –Method for the Measurement of Benz[a]anthracene, Benzo[b]fluoranthene, Benzo[j]fluoranthene, Benzo[k]fluoranthene, Dibenz[a,h]anthracene, Indeno[1,2,3-cd]pyrene et Benzo[ghi]perylene. CEN, Brussels (Belgium).

CEN, 2017. European Committee for Standardization, EN-16450: 2017 - Ambient Air – automated measuring systems for the measurement of the concentration of particulate matter (PM10, PM2.5). CEN, Brussels (Belgium). .

Crippa, M., Canonaco, F., Slowik, J. G., El Haddad, I., DeCarlo, P. F., Mohr, C., Heringa, M. F., Chirico, R., Marchand, N., Temime-Roussel, B., Abidi, E., Poulain, L., Wiedensohler, A., Baltensperger, U., Prévôt, A. S. H., 2013. Primary and secondary organic aerosol origin by combined gas-particle phase source apportionment. Atmos. Chem. Phys. 13, 8411-8426.

Daellenbach, K. R., Bozzetti, C., Křepelová, A., Canonaco, F., Wolf, R., Zotter, P., Fermo, P., Crippa, M., Slowik, J. G., Sosedova, Y., Zhang, Y., Huang, R. J., Poulain, L., Szidat, S., Baltensperger, U., El Haddad, I., Prévôt, A. S. H., 2016. Characterization and source apportionment of organic aerosol using offline aerosol mass spectrometry. Atmos. Meas. Tech. 9, 23-39.

Drinovec, L., Močnik, G., Zotter, P., Prévôt, A. S. H., Ruckstuhl, C., Coz, E., Rupakheti, M., Sciare, J., Müller, T., Wiedensohler, A., Hansen, A. D. A., 2015. The "dual-spot" Aethalometer: an improved measurement of aerosol black carbon with real-time loading compensation. Atmos. Meas. Tech. 8, 1965-1979.

Dupont, J., Haeffelin, M., Badosa, J., Elias, T., Favez, O., Petit, J., Meleux, F., Sciare, J., Crenn, V., Bonne, J. L., 2016. Role of the boundary layer dynamics effects on an extreme air pollution event in Paris. Atmos. Environ. 141, 571 - 579.

Favez, O., Cachier, H., Sciare, J., Sarda-Estève, R., Martinon, L., 2009. Evidence for a significant contribution of wood burning aerosols to PM2.5 during the winter season in Paris, France. Atmos. Environ. 43, 3640-3644.

Favez, O., El Haddad, I., Piot, C., Boréave, A., Abidi, E., Marchand, N., Jaffrezo, J. L., Besombes, J. L., Personnaz, M. B., Sciare, J., Wortham, H., George, C., D'Anna, B., 2010. Inter-comparison of source apportionment models for the estimation of wood burning aerosols during wintertime in an Alpine city (Grenoble, France). Atmos. Chem. Phys. 10, 5295-5314.

Favez, O., Petit, J.-E., Bessagnet, B., Meleux, F., Chiappini, L., Lemeur, S., Labartette, C., Chappaz, C., Guergnion, P.-Y., Saison, J.-Y., 2012. Caractéristiques et origines principales des épisodes de pollution hivernaux aux PM10 en France. Pollution Atmosphérique: climat, santé, société. 163-181.

Fröhlich, R., Crenn, V., Setyan, A., Belis, C. A., Canonaco, F., Favez, O., Riffault, V., Slowik, J. G., Aas, W., Aijälä, M., Alastuey, A., Artiñano, B., Bonnaire, N., Bozzetti, C., Bressi, M., Carbone, C., Coz, E., Croteau, P. L., Cubison, M. J., Esser-Gietl, J. K., Green, D. C., Gros, V., Heikkinen, L., Herrmann, H., Jayne, J. T., Lunder, C. R., Minguillón, M. C., Močnik, G., O'Dowd, C. D., Ovadnevaite, J., Petralia, E., Poulain, L., Priestman, M., Ripoll, A., Sarda-Estève, R., Wiedensohler, A., Baltensperger, U., Sciare, J., Prévôt, A. S. H., 2015. ACTRIS ACSM intercomparison – Part 2: Intercomparison of ME-2 organic source apportionment results from 15 individual, co-located aerosol mass spectrometers. Atmos. Meas. Tech. 8, 2555-2576.

Golly, B., Brulfert, G., Berlioux, G., Jaffrezo, J. L., Besombes, J. L., 2015. Large chemical characterisation of PM10 emitted from graphite material production: Application in source apportionment. Sci. Total Environ. 538, 634-43.

Guinot, B., Cachier, H., Oikonomou, K., 2007a. Geochemical perspectives from a new aerosol chemical mass closure. Atmos. Chem. Phys. 7, 1657-1670.

Guinot, B., Cachier, H., Sciare, J., Tong, Y., Xin, W., Jianhua, Y., 2007b. Beijing aerosol: Atmospheric interactions and new trends. J. Geophys. Res.-Atmos. 112, n/a-n/a.

Haeffelin, M., Barthès, L., Bock, O., Boitel, C., Bony, S., Bouniol, D., Chepfer, H., Chiriaco, M., Cuesta, J., Delanoë, J., Drobinski, P., Dufresne, J. L., Flamant, C., Grall, M., Hodzic, A., Hourdin, F., Lapouge, F., Lemaître, Y., Mathieu, A., Morille, Y., Naud, C., Noël, V., O'Hirok, W., Pelon, J., Pietras, C., Protat, A., Romand, B., Scialom, G., Vautard, R., 2005.

SIRTA, a ground-based atmospheric observatory for cloud and aerosol research. Ann. Geophys. 23, 253-275.

Isaacman-VanWertz, G., Yee, L. D., Kreisberg, N. M., Wernis, R., Moss, J. A., Hering, S. V., De Sá, S. S., Martin, S. T., Alexander, M. L., Palm, B. B., 2016. Ambient gas-particle partitioning of tracers for biogenic oxidation. Environ. Sci. Technol. 50, 9952-9962.

Jaffrezo, J.-L., Aymoz, G., Delaval, C., Cozic, J., 2005a. Seasonal variations of the water soluble organic carbon mass fraction of aerosol in two valleys of the French Alps. Atmos. Chem. Phys. 5, 2809-2821.

Jaffrezo, J. L., Aymoz, G., Delaval, C., Cozic, J., 2005b. Seasonal variations of the water soluble organic carbon mass fraction of aerosol in two valleys of the French Alps. Atmos. Chem. Phys. 5, 2809-2821.

Jayne, J. T., Leard, D. C., Zhang, X., Davidovits, P., Smith, K. A., Kolb, C. E., Worsnop, D. R., 2000. Development of an Aerosol Mass Spectrometer for Size and Composition Analysis of Submicron Particles. Aerosol Sci. Technol. 33, 49-70.

Jimenez, J. L., Jayne, J. T., Shi, Q., Kolb, C. E., Worsnop, D. R., Yourshaw, I., Seinfeld, J. H., Flagan, R. C., Zhang, X., Smith, K. A., 2003. Ambient aerosol sampling using the aerodyne aerosol mass spectrometer. J. Geophys. Res.-Atmos. 108,

Lai, C., Liu, Y., Ma, J., Ma, Q., Chu, B., He, H., 2015. Heterogeneous Kinetics of cis-Pinonic Acid with Hydroxyl Radical under Different Environmental Conditions. The Journal of Physical Chemistry A. 119, 6583-6593.

Lucarelli, F., Calzolai, G., Chiari, M., Nava, S., Carraresi, L., 2017. Study of atmospheric aerosols by IBA techniques: The LABEC experience. Nucl. Instrum. Methods Phys. Res., Sect. B.

Lucarelli, F., Nava, S., Calzolai, G., Chiari, M., Udisti, R., Marino, F., 2011. Is PIXE still a useful technique for the analysis of atmospheric aerosols? The LABEC experience. X-Ray Spectrom. 40, 162-167.

Marchand, N., Besombes, J. L., Chevron, N., Masclet, P., Aymoz, G., Jaffrezo, J. L., 2004. Polycyclic aromatic hydrocarbons (PAHs) in the atmospheres of two French alpine valleys: sources and temporal patterns. Atmos. Chem. Phys. 4, 1167-1181.

Middlebrook, A. M., Bahreini, R., Jimenez, J. L., Canagaratna, M. R., 2012. Evaluation of Composition-Dependent Collection Efficiencies for the Aerodyne Aerosol Mass Spectrometer using Field Data. Aerosol Sci. Technol. 46, 258-271.

Nozière, B., Kalberer, M., Claeys, M., Allan, J., D'Anna, B., Decesari, S., Finessi, E., Glasius, M., Grgić, I., Hamilton, J. F., Hoffmann, T., Iinuma, Y., Jaoui, M., Kahnt, A., Kampf, C. J., Kourtchev, I., Maenhaut, W., Marsden, N., Saarikoski, S., Schnelle-Kreis, J., Surratt, J. D., Szidat, S., Szmigielski, R., Wisthaler, A., 2015. The Molecular Identification of Organic Compounds in the Atmosphere: State of the Art and Challenges. Chem. Rev.

Petit, J.-E., Amodeo, T., Meleux, F., Bessagnet, B., Menut, L., Grenier, D., Pellan, Y., Ockler, A., Rocq, B., Gros, V., 2017. Characterising an intense PM pollution episode in March 2015

in France from multi-site approach and near real time data: Climatology, variabilities, geographical origins and model evaluation. Atmos. Environ. 155, 68-84.

Petit, J.-E., Favez, O., Sciare, J., Canonaco, F., Croteau, P., Močnik, G., Jayne, J., Worsnop, D., Leoz-Garziandia, E., 2014. Submicron aerosol source apportionment of wintertime pollution in Paris, France by double positive matrix factorization (PMF 2) using an aerosol chemical speciation monitor (ACSM) and a multi-wavelength Aethalometer. Atmos. Chem. Phys. 14, 13773-13787.

Piot, C., Jaffrezo, J.-L., Cozic, J., Pissot, N., El Haddad, I., Marchand, N., Besombes, J.-L., 2012. Quantification of levoglucosan and its isomers by High Performance Liquid Chromatography-Electrospray Ionization tandem Mass Spectrometry and its application to atmospheric and soil samples. Atmos. Meas. Tech. 5, 141-148.

Polo-Rehn, L., Waked, A., Charron, A., Piot, C., Besombes, J.-L., Marchand, N., Guillaud, G., Favez, O., Jaffrezo, J.-L., 2014. Estimation de la contribution des émissions véhiculaires à l'échappement et hors échappement aux teneurs atmosphériques en PM10 par Positive Matrix Factorization (PMF). Pollution atmosphérique. 221,

Sandradewi, J., Prévôt, A. S. H., Szidat, S., Perron, N., Alfarra, M. R., Lanz, V. A., Weingartner, E., Baltensperger, U., 2008. Using Aerosol Light Absorption Measurements for the Quantitative Determination of Wood Burning and Traffic Emission Contributions to Particulate Matter. Environ. Sci. Technol. 42, 3316-3323.

Sciare, J., D'Argouges, O., Sarda-Esteve, R., Gaimoz, C., Dolgorouky, C., Bonnaire, N., Favez, O., Bonsang, B., Gros, V., 2011. Large contribution of water-insoluble secondary organic aerosols in the region of Paris (France) during wintertime. J. Geophys. Res.-Atmos. 116, D22203.

Srivastava, D., Tomaz, S., Favez, O., Lanzafame, G. M., Golly, B., Besombes, J.-L., Alleman, L. Y., Jaffrezo, J.-L., Jacob, V., Perraudin, E., Villenave, E., Albinet, A., 2018. Speciation of organic fraction does matter for source apportionment. Part 1: A one-year campaign in Grenoble (France). Sci. Total Environ. In press.

Tomaz, S., Shahpoury, P., Jaffrezo, J. L., Lammel, G., Perraudin, E., Villenave, E., Albinet, A., 2016. One-year study of polycyclic aromatic compounds at an urban site in Grenoble (France): Seasonal variations, gas/particle partitioning and cancer risk estimation. Sci. Total Environ. 565, 1071-1083.

Verlhac. S, Favez.O, Albinet. A, 2013. Comparaison inter laboratoires organisée pour les laboratoires européens impliqués dans l'analyse du lévoglucosan et de ses isomères LCSQA / INERIS http://www.lcsqa.org/rapport/2013/ineris/comparaison-inter-laboratoires-organisee-laboratoires-europeens-impliques-analys,

Waked, A., Favez, O., Alleman, L. Y., Piot, C., Petit, J. E., Delaunay, T., Verlinden, E., Golly, B., Besombes, J. L., Jaffrezo, J. L., Leoz-Garziandia, E., 2014. Source apportionment of PM10 in a north-western Europe regional urban background site (Lens, France) using positive matrix factorization and including primary biogenic emissions. Atmos. Chem. Phys. 14, 3325-3346.

Yttri, K. E., Schnelle-Kreis, J., Maenhaut, W., Abbaszade, G., Alves, C., Bjerke, A., Bonnier, N., Bossi, R., Claeys, M., Dye, C., Evtyugina, M., García-Gacio, D., Hillamo, R., Hoffer, A., Hyder, M., Iinuma, Y., Jaffrezo, J. L., Kasper-Giebl, A., Kiss, G., López-Mahia, P. L., Pio, C., Piot, C., Ramirez-Santa-Cruz, C., Sciare, J., Teinilä, K., Vermeylen, R., Vicente, A., Zimmermann, R., 2015. An intercomparison study of analytical methods used for quantification of levoglucosan in ambient aerosol filter samples. Atmos. Meas. Tech. 8, 125-147.

Chapter IV

Speciation of organic fraction does matter for source apportionment

Article II

Speciation of organic fraction does matter for source apportionment. Part 1: a one-year campaign in Grenoble (France)

Published in Science of The Total Environment

Science of the Total Environment 624 (2018) 1598–1611

Contents lists available at ScienceDirect

Science of the Total Environment

journal homepage: www.elsevier.com/locate/scitotenv

Speciation of organic fraction does matter for source apportionment. Part 1: A one-year campaign in Grenoble (France)

Deepchandra Srivastava [a,b,c], Sophie Tomaz [a,b,c], Olivier Favez [a,*], Grazia Maria Lanzafame [a], Benjamin Golly [d,f], Jean-Luc Besombes [d], Laurent Y. Alleman [e], Jean-Luc Jaffrezo [f], Véronique Jacob [f], Emilie Perraudin [b,c], Eric Villenave [b,c], Alexandre Albinet [a,*]

[a] INERIS, Parc Technologique Alata, BP 2, 60550 Verneuil-en-Halatte, France
[b] CNRS, EPOC, UMR 5805 CNRS, 33405 Talence, France
[c] Université de Bordeaux, EPOC, UMR 5805 CNRS, 33405 Talence, France
[d] Univ. Savoie Mont Blanc, LCME, 73000 Chambéry, France
[e] IMT Lille Douai, SAGE, 59000 Lille, France
[f] Univ. Grenoble Alpes, CNRS, IRD, IGE, F-38000 Grenoble, France

HIGHLIGHTS

- Source apportionment using key primary and secondary organic molecular markers
- Uncommon resolved sources: plant debris, fungal spores, biogenic & anthropogenic SOA
- High contribution of anthropogenic SOA (PAH SOA) noticed in winter PM pollution event
- Investigation of HuLiS origins: both, primary and secondary contributions highlighted

GRAPHICAL ABSTRACT

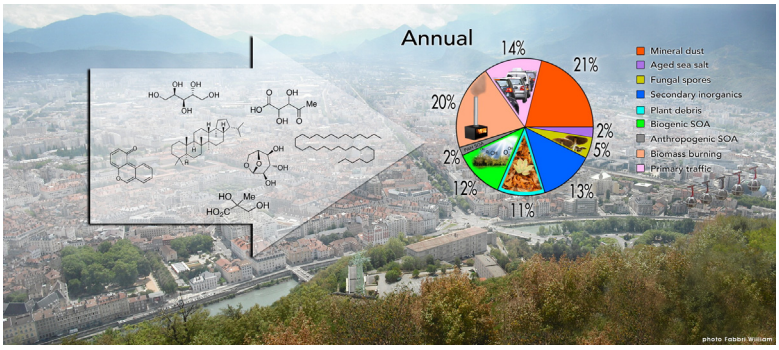

ARTICLE INFO

Article history:
Received 3 October 2017
Received in revised form 11 December 2017
Accepted 12 December 2017
Available online 21 December 2017

Editor: D. Barcelo

Keywords:
Aerosol
Source apportionment
Primary biogenic organics
SOA
Molecular markers
HuLiS

ABSTRACT

PM_{10} source apportionment was performed by positive matrix factorization (PMF) using specific primary and secondary organic molecular markers on samples collected over a one year period (2013) at an urban station in Grenoble (France). The results provided a 9-factor optimum solution, including sources rarely apportioned in the literature, such as two types of primary biogenic organic aerosols (fungal spores and plant debris), as well as specific biogenic and anthropogenic secondary organic aerosols (SOA). These sources were identified thanks to the use of key organic markers, namely, polyols, odd number higher alkanes, and several SOA markers related to the oxidation of isoprene, α-pinene, toluene and polycyclic aromatic hydrocarbons (PAHs). Primary and secondary biogenic contributions together accounted for at least 68% of the total organic carbon (OC) in the summer, while anthropogenic primary and secondary sources represented at least 71% of OC during wintertime. A very significant contribution of anthropogenic SOA was estimated in the winter during an intense PM pollution event ($PM_{10} > 50\ \mu g\ m^{-3}$ for several days; 18% of PM_{10} and 42% of OC). Specific meteorological conditions with a stagnation of pollutants over 10 days and possibly Fenton-like chemistry and self-amplification cycle of SOA formation could explain such high anthropogenic SOA concentrations during this period. Finally, PMF outputs were also used to investigate the origins of humic-like substances (HuLiS), which represented 16% of OC on an annual average basis. The results indicated that HuLiS were mainly associated with biomass burning

* Corresponding authors.
E-mail addresses: olivier.favez@ineris.fr (O. Favez), alexandre.albinet@ineris.fr, alexandre.albinet@gmail.com (A. Albinet).

https://doi.org/10.1016/j.scitotenv.2017.12.135

(22%), secondary inorganic (22%), mineral dust (15%) and biogenic SOA (14%) factors. This study is probably the first to state that HuLiS are significantly associated with mineral dust.

1. Introduction

Airborne particles (particulate matter, PM) are a major concern of current research in atmospheric science due to their impact on both climate (Boucher et al., 2013) and air quality (Heal et al., 2012). Elucidating their emission sources and transformation processes constitutes a crucial step for the elaboration of efficient and cost-effective abatement strategies.

Organic matter (OM) is a major PM component. Organic aerosols (OA) are categorized into either primary organic aerosol (POA), directly emitted from anthropogenic and natural sources, or secondary organic aerosol (SOA), formed in the atmosphere notably via gas-particle conversion processes such as nucleation, condensation and heterogeneous multiphase chemical reactions involving (semi-) volatile compounds (VOCs or SVOCs) (Carlton et al., 2009; Ziemann and Atkinson, 2012). Due to the multiplicity of sources and of transformation mechanisms, the apportionment of the relative contribution of each of the different primary and secondary OA fractions is still fairly uncertain.

Specific organic compounds can provide insight into OA sources (Schauer et al., 1996). They are commonly referred to as molecular markers (tracers), such as levoglucosan for biomass burning (Simoneit et al., 1999a) or α-methylglyceric acid for SOA from isoprene oxidation (Carlton et al., 2009). Source-receptor models, such as positive matrix factorization (PMF), have been widely implemented using traditional aerosol chemical speciation, such as elemental carbon (EC), organic carbon (OC), major ions, and metals. The inclusion of a comprehensive set of organic molecular markers potentially offers a closer link between factors and sources, but it has been rarely applied in PMF studies because it requires large datasets and intensive lab-work (Jaeckels et al., 2007; Laing et al., 2015; Schembari et al., 2014; Shrivastava et al., 2007; Srimuruganandam and Shiva Nagendra, 2012; Waked et al., 2014; Wang et al., 2012; Zhang et al., 2009).

Source apportionment studies based on the use of source-receptor models assume that organic molecular markers are chemically stable in the atmosphere (defined as tracer compounds) (Schauer et al., 1996). However, these compounds can react in the atmosphere by photochemical processes involving sunlight and atmospheric oxidants such as O_3, NO_x, radicals OH, NO_3... For instance, levoglucosan is usually assumed to be very stable (Simoneit et al., 1999b) but recent studied have shown its significant atmospheric chemical degradation (Hennigan et al., 2010; Kessler et al., 2010; Mochida et al., 2010; Zhao et al., 2014). For most of these compounds, experimental data about their stability or atmospheric lifetimes are very scarce or not available. They are usually based on empirical calculations like for SOA markers (Nozière et al., 2015). If some markers have tendency to undergo a rapid decay in the atmosphere, so short lifetime, their use may cause a bias in the source apportionment results.

The main objective of this work is to apportion specific primary and secondary OA fractions using various and distinctive molecular markers in a PMF model. The present paper is based on results obtained from a year-long campaign conducted in an Alpine city, while a following paper will be dedicated to the use of a similar approach in the Paris region during a 3-week intensive sampling campaign, with a higher time resolution for filter samplings (every 4 h) through an intense PM pollution event (Srivastava et al., in preparation). A focus has been put here on usually unresolved PM sources, such as primary biogenic sources and secondary sources such as biogenic SOA formed from pinene or isoprene oxidation, and anthropogenic SOA formed from the oxidation of polycyclic aromatic hydrocarbons (PAHs), toluene and phenol. In addition, this work provides insight into the sources of total OC and of humic-like substances (HuLiS), a significant fraction of OM which plays an important role in the atmosphere (Graber and Rudich, 2006) and has not been extensively explored.

2. Methodology

2.1. Sampling site

The sampling site was located at the urban background sampling station of "Les Frênes" (45°09′41″ N, 5°44′07″ E) in Grenoble (France). The city, surrounded by three mountain ranges, is considered the most densely populated area (160,000 inhabitants) of the French Alps (Fig. S1). In addition to the urbanized area, forests, including both deciduous and coniferous species, and agriculture areas (pastures) dominate the land cover around Grenoble (Fig. S2). This region experiences frequent severe PM pollution events ($PM_{10} > 50\ \mu g\ m^{-3}$ for at least 3 consecutive days) in the winter due to the formation of thermal inversion layers that may promote pollutant accumulation. Previous studies have shown that residential heating, mainly biomass burning, accounts for a major fraction of $PM_{2.5}$ in the winter (Favez et al., 2010). In addition, traffic and industrial activities contribute significantly to the observed PM concentration levels in Grenoble (Polo-Rehn et al., 2014).

2.2. Sample collection

PM_{10} samples (Tissu-quartz, Pallflex, Ø = 150 mm) were collected every third day for one year from 01/01/2013 to 01/01/2014 using two parallel high volume samplers (DA-80, Digitel; sampling duration of 24 h at 30 $m^3\ h^{-1}$). Details on the preparation and conservation of these filter samples have already been presented elsewhere (Tomaz et al., 2017; Tomaz et al., 2016) and are reported in the Supplementary material. A total of 123 samples and 9 field blanks were collected and analysed for an extended chemical characterization following the protocols described in Section 2.3.

Atmospheric concentrations of PM_{10} and $PM_{2.5}$ (1405F TEOM-FDMS, Thermo), NO_x (TEI 42I, Thermo) and O_3 (TEI 49I, Thermo) were monitored by the local air quality network in Grenoble (Atmo Rhône-Alpes-Auvergne) at a 15-min resolution. Together with the ROMMA network (Meteorological network of the Alpine massif), they also measured and provided meteorological parameters (temperature, wind direction, wind speed and relative humidity) (Figs. 1 and S3). Temperature and pressure data from several locations at different altitudes were used to evaluate the duration of thermal inversion layers in the valley. Details of the calculation of thermal inversion layers have been described previously (Tomaz et al., 2017).

2.3. Analytical procedures

Overall, approximately 194 species were quantified in each sample. EC/OC was measured using a Sunset lab analyzer using the EUSAAR-2 thermal protocol (Cavalli et al., 2010). HuLiS were analysed following the protocol described by Baduel et al. (2010). Anions (Cl^-, NO_3^-, SO_4^{2-}), cations (NH_4^+, Ca^{2+}, Na^+, Mg^{2+}, K^+), methanesulfonic acid (MSA) and oxalate ($C_2O_4^{2-}$) were analysed by ionic chromatography (Jaffrezo et al., 2005). Thirty-four metals and trace elements were quantified by ICP-MS (Alleman et al., 2010). Cellulose combustion markers (biomass burning) (levoglucosan, mannosan and galactosan), 3 polyols (arabitol, sorbitol and mannitol) and glucose were quantified using HPLC-PAD (Piot et al., 2012). Twenty-one PAHs, 27 oxy-PAHs, and 32 nitro-PAHs were quantified using UPLC/UV-Fluorescence and GC/NICI-

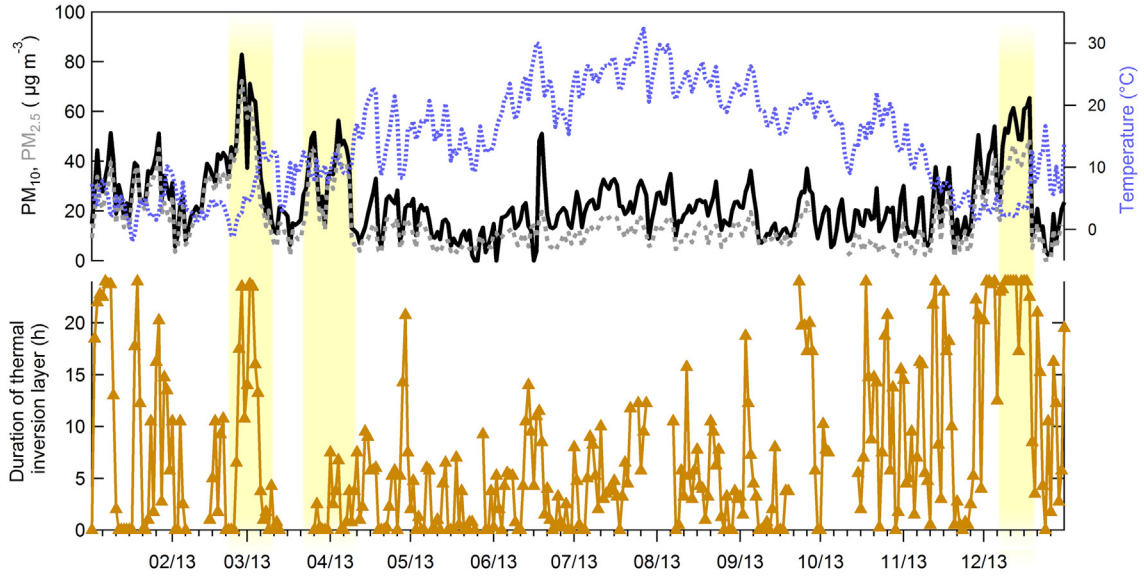

Fig. 1. Temporal variation of PM_{10} and $PM_{2.5}$ concentrations along with the temperature and duration of thermal inversion layers at Grenoble, Les Frênes (2013).

MS (Albinet et al., 2006; Albinet et al., 2014; Albinet et al., 2013; Tomaz et al., 2016). Twenty-seven higher alkanes (C13–C39), 10 hopanes, pristane, phytane, 5 sulfur containing PAHs, 5 lignin combustion markers (vanillin, coniferaldehyde …) (Golly et al., 2015) and 11 compounds usually recognized as SOA markers (α-methylglyceric acid, pinic acid, methyl-nitrocatechols…) (Nozière et al., 2015) were analysed by GC/EI-MS. Note that the quantification of all SOA markers was performed using authentic standards. Details of the analytical procedures and sample preparation for the analysis of the SOA markers are provided in the Supplementary material (Tables S1 and S2).

2.4. Source apportionment methodology

2.4.1. Receptor modelling

The goal of receptor models is to solve the chemical mass balance equation between the measured species concentrations and source profiles as a linear combination of factors p, species profile *f* of each source, and the amount of mass *g* contributed to each individual sample (Eq. (1)):

$$X_i j = \sum_{k=1}^{p} g_{ik} f_{kj} + e_i j \quad (1)$$

where X_{ij} represents the measured data for species *j* in sample *i*, and e_{ij} represents the residual of each sample/species not fitted by the model.

PMF is a multivariate factor analysis tool that decomposes a matrix of the observed chemistry of the samples into two matrices (factor contributions (G) and factor profiles (F)) that need to be ascribed to a specific source. The best model solution is obtained by minimizing the function Q (Eq. (2)):

$$Q = \sum_i \sum_j \left(\frac{e_{ij}}{\sigma_{ij}}\right)^2 \quad (2)$$

where σ_{ij} represents the measurement uncertainty of each data point.

In this work, we used the U.S. Environmental Protection Agency (US-EPA) PMF 5.0 software to perform the source apportionment.

2.4.2. Uncertainty calculations

The estimation of uncertainties for the filter-based measurements was calculated using Eq. (3) (Polissar et al., 1998):

$$\sigma_{ij} = \begin{cases} \frac{5}{6} LD_j & \text{if } X_{ij} < LD_j \\ \sqrt{(LD_j)^2 + (CV_j X_{ij})^2 + (aX_{ij})^2} & \text{if } X_{ij} \geq LD_j \end{cases} \quad (3)$$

where LD_j is the detection limit for compound *j* (defined as the lowest concentrations of the compound that can be measured with a signal to noise ratio of 3), CV_j is the coefficient of variation for compound *j* (calculated as the standard deviation of repeated analyses divided by the mean value of the repeated analyses), and *a* is a factor (0.03) applied to account for additional sources of uncertainty (Gianini et al., 2012). Missing concentration values were replaced by the geometric mean of the concentrations of compound *j*, and their accompanying uncertainties were set at 4 times this value.

2.4.3. Criteria for the selection of species

Inclusion or exclusion of a chemical species in the PMF matrix is usually based on the signal to noise ratio (S/N) (Paatero and Hopke, 2003). S/N ratios for all the quantified species in this study are given in Table S3. Species with an S/N ratio below 0.2 were automatically excluded. Additional criteria for the final selection of the input species in the PMF have been applied; compounds that are analytically difficult to quantify, i.e., with a large number of data points below the detection limit (>60% of total data points), those mainly associated with the gas phase (e.g., pinonic acid, low molecular weight PAHs, oxy and nitro-PAHs) (Albinet et al., 2007; Albinet et al., 2008; Isaacman-VanWertz et al., 2016; Tomaz et al., 2016), and those that are not specific markers of a given source or those with no observed temporal trends (single events or spikes, e.g., pinic acid) were excluded.

In addition, to limit the input data matrix according to the total number of samples (n = 123), some species were also not included if they belonged to a single source and were well correlated with another marker of this source (e.g., cellulose combustion: levoglucosan, mannosan, galactosan ($r = 0.97–0.99$, $n = 123$, $p < 0.05$); fungal spores: arabitol, sorbitol, glucose, mannitol ($r = 0.85–0.92$, $n = 123$, $p < 0.05$)). In this case, only one or two representative species were kept for the input matrix. Some other specific organic compounds, such as oxalate, MSA and methyl-nitrocatechols, were also discarded due to poor

predictions by the preliminary model runs. Finally, a total of 47 species were used in the model (Table S4). Details about the species in the final input and the exclusion of the former ones are reported in the Supplementary material and Table S4. PM_{10} concentrations were included as the total variable in the model to directly determine the source contributions to the daily mass concentrations. The total variable was defined as weak (low weight) in the model to not have influence on the solution obtained.

2.4.4. Applied constraints

Several constraints were applied to the base run to obtain clearer chemical source profiles in the final solution. To limit the change in the Q-value, only "soft pulling" constraints were applied. Change in the Q-robust was finally approximately 7%. Details related to the constraints applied to each factor profile are given in Table S5.

2.4.5. Optimization of the final solution

The selection of the final solution was made based on three criteria, including the bootstrap results to evaluate its stability, the comparison between observed and predicted concentrations, and the evaluation of the sensitivity to the applied constraints. A mapping of over 80% of the factors for the bootstrap was taken as the threshold to indicate that the chosen solution may be appropriate. Species showing poor correlations ($r < 0.5$) between observed and modelled concentrations were evaluated carefully to determine whether they should be down-weighted or excluded. A few species were finally kept despite their low correlation coefficients due to their significant role in the interpretation of selected factors (Table S6). Student's *t*-test was used to evaluate the effectiveness of applied constraints on the base model run and to verify whether the differences were statistically insignificant for all source profiles (two-tailed paired *t*-test significance test at $p < 0.05$ probability).

3. Results and discussions

3.1. Overview of the PM_{10} concentrations and pollution events

The daily PM_{10} mass concentrations ranged from 2 to 83 μg m^{-3}, with an annual average of approximately 24 μg m^{-3} (Fig. 1). Two severe PM pollution events, which also affected the rest of France (Favez, 2013), were observed in early spring (02/25–04/08/2013) and winter (12/09–12/19/2013). A large contribution of OM and the presence of thermal inversion layers were observed during the first part of the spring PM pollution events, while the second part was influenced by long range transport and characterized by a large contribution of inorganic species, such as ammonium nitrate and sulfate. The winter pollution episode was associated with the occurrence of thermal inversion layers over a period of 10 consecutive days (Tomaz et al., 2017), where OM was the major contributor to the total PM_{10} loadings (Fig. 1). During this winter pollution event, air quality was expected to be mainly influenced by local combustion sources, such as residential heating, notably wood combustion, and traffic, as shown by the high concentrations of primary species such as levoglucosan, NO, and PAHs (Tomaz et al., 2017; Tomaz et al., 2016).

3.2. PM_{10} source apportionment

A nine-factor output provides the most reasonable solution for this PM_{10} source apportionment in the Grenoble valley (Fig. 2). It includes traditional aerosol sources, such as primary traffic, biomass burning, mineral dust, secondary inorganics and aged sea salt, and uncommonly resolved ones, such as primary biogenic organic aerosols (fungal spores and plant debris), as well as specific biogenic and anthropogenic SOA, all identified by the chosen molecular organic markers analysed in the PM_{10} fraction. The selection of factors was based on the variability explained by the Q/Q_{exp} ratio, the chemical interpretation of the obtained factors and the total reconstructed mass. Forcing PMF to explain the variability with a less number of factors (<8) resulted in high Q value (Fig. S4), thus only solutions with eight factors and more were checked. The solutions with eight sources were less explanatory, and some factors were merged (Figs. S5 and S6). Conversely, an increase in the number of sources led to the split of meaningful source profiles into two unrealistic ones (Figs. S7 and S8). In the final solution, the comparison of the reconstructed PM_{10} contributions from all sources with measured PM_{10} concentrations showed very good mass closure ($r = 0.93$, $n = 123$, $p < 0.05$) (Fig. 2 and Table S6). Note that results from the chemical characterization of the last 2 days of the year were not validated and were excluded from the PMF matrix. In addition, most of the species showed good agreement with the measured concentrations. Few of them were poorly reconstructed by the PMF (e.g., Sb, hopanes, DHOPA (2,3-Dihydroxy-4-oxopentanoic acid) and phthalic acid ($r < 0.34$)). Low correlation coefficients were due to some single events that occurred during the year and were not well reproduced by the model. Bootstrapping on the final solution showed stable results with ≥84 out of 100 bootstrap mapped factors (Table S7). Finally, no significant difference ($p > 0.05$) was observed in the source chemical profiles between the base and the constrained runs (Table S8, Figs. S9 and S10).

Overall, mineral dust (21%) and biomass burning (20%) sources were the main contributors to the total PM_{10} mass on an annual scale. Primary traffic emissions, secondary inorganic aerosols, plant debris and biogenic SOA also presented significant contributions (11 to 14%). Aged sea salt, fungal spores and anthropogenic SOA contributed to approximately 2 to 5% of total PM_{10} (Fig. 2). Identified aerosol sources, chemical profiles and temporal evolutions are shown in Figs. 3 and 4 and discussed individually below.

3.2.1. Secondary inorganics

The secondary inorganics source factor (nitrate-rich) was characterized by high contributions of NO_3^- and NH_4^+ (69% and 63% of these species being attributed to this factor, respectively), with an annual average concentration of 2.9 μg m^{-3} and accounted for approximately 13% of PM_{10} mass on an annual scale (Figs. 2 and 3). Cl^- and SO_4^{2-} also

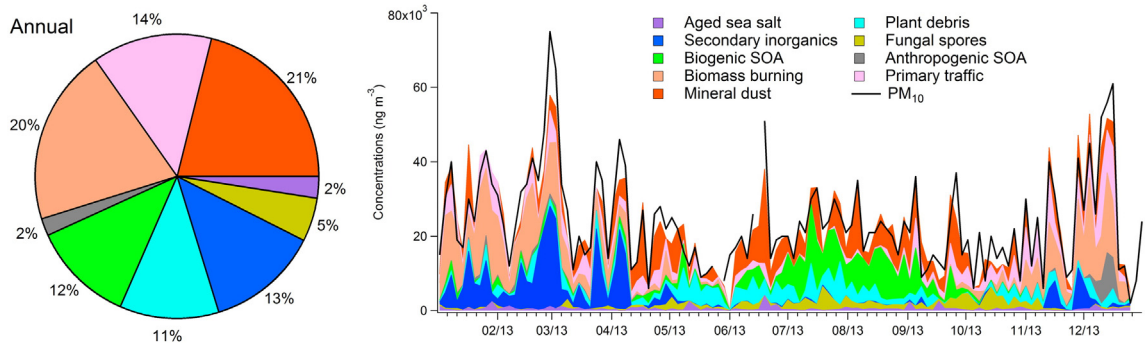

Fig. 2. Annual average contributions (left) and temporal evolution (right) of the identified sources to PM_{10} mass concentrations in Grenoble, Les Frênes (2013).

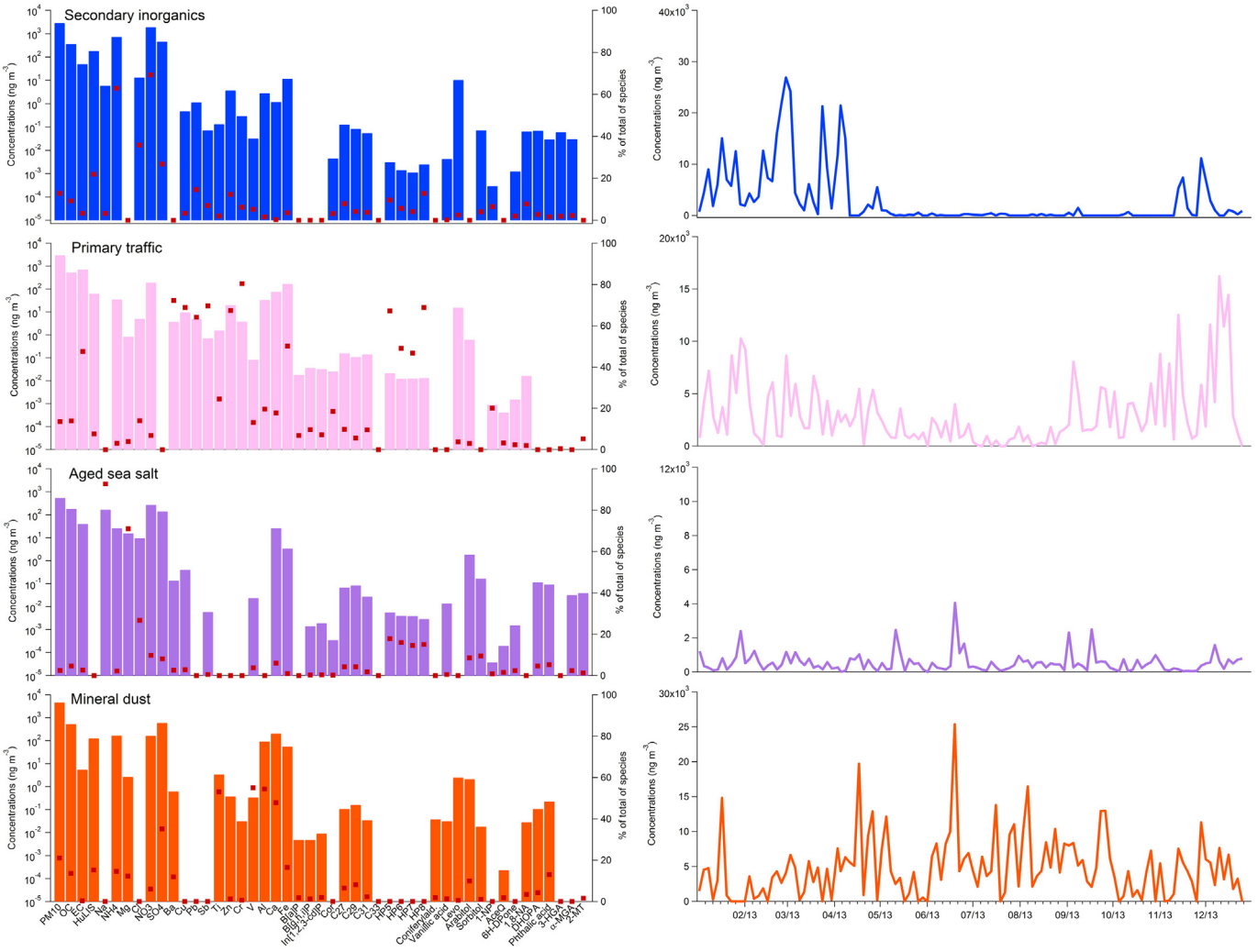

Fig. 3. Source profiles and temporal evolution of secondary inorganic, primary traffic, aged sea salt and mineral dust factors identified at Grenoble, Les Frênes (2013).

contributed to this source factor by approximately 30–35%. The source showed large seasonal variations with very high concentrations and PM contributions during both severe PM pollution events in the early spring and, to a lesser extent, in the winter (Fig. 3). In the early spring, the high PM_{10} concentration levels, concomitant to the high contributions of ammonium nitrate, were related to secondary formation processes, long range transport of aged air masses and direct emissions from biomass burning (Tomaz et al., 2017). On average, the sources of secondary inorganics accounted for approximately 47% of the PM_{10} mass during this spring pollution event. Conversely, during the December PM pollution event, this factor accounted for only approximately 1% of the total PM_{10} mass.

3.2.2. Primary traffic (exhaust and non-exhaust)

The PMF model always grouped the four hopanes (HP5 to HP8, 46% to 69% of the total mass of each compound) together with a significant amount of EC (48% of its total mass) into one factor (Fig. 3). These species are typical of traffic exhaust emissions and this factor was significantly correlated with NO_x ($r = 0.6$, $n = 123$, $p < 0.05$). As expected and following the applied constraints, this factor showed high contributions of several metals, such as Ba (72%), Cu (69%), Sb (70%), Pb (64%) and Fe (50%), known as additional good indicators of road traffic emissions (Pant and Harrison, 2012; Srivastava et al., 2016; Sternbeck et al., 2002). In particular, Ba and Sb are known as specific markers of vehicular brake abrasion (Johansson et al., 2009), showing that this factor accounted for both exhaust and non-exhaust traffic emissions. Regarding OC/EC (0.9) and PM_{10}/EC (4.3) ratios in the factor profile, their values obtained here are in good agreement with the literature data reported for primary traffic emissions (El Haddad et al., 2009; Fine et al., 2002). Interestingly, only 20% of 1-nitropyrene (1-NP), expected to be a marker of diesel emissions (Keyte et al., 2016), was associated with this factor. Despite several efforts, PMF was unable to increase the 1-NP contribution into this factor and it remained distributed in the biomass burning factor due its strong correlation with levoglucosan. The mixing of sources on 24 h filter samples, together with the specific geomorphology of Grenoble as well the atmospheric dynamic could explain such observed correlations.

Primary traffic sources accounted for 14% of the PM_{10} mass on a yearly average (Fig. 2), corresponding to an annual mean concentration of 3.0 μg m^{-3}. These values are in the range of those commonly observed at other urban background locations in Europe (5–25%) (Belis et al., 2013; Waked et al., 2014) and with a previous study conducted at an heavy traffic site in Grenoble (traffic exhaust = 17%, traffic non-exhaust = 13%, contribution to PM_{10}) (Polo-Rehn et al., 2014). This source showed seasonal variations with higher concentrations in a cold period, notably due to the typical atmospheric dynamic in the valley of Grenoble. However, its contribution to PM_{10} was rather constant through the year, except in July–August (summer vacations) when it

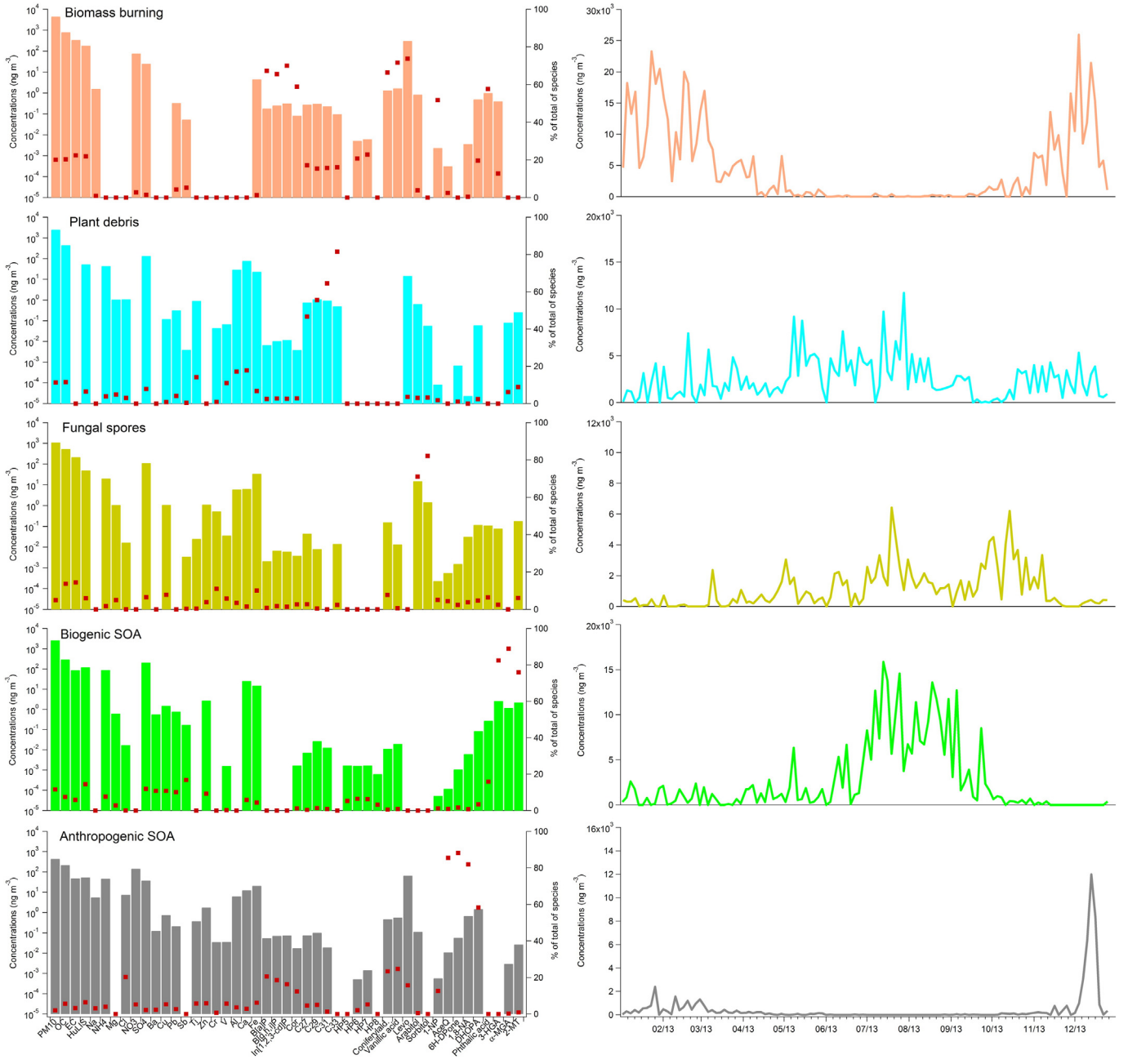

Fig. 4. Source profiles and temporal evolution of plant debris, fungal spores, biogenic SOA and anthropogenic SOA identified at Grenoble, Les Frênes (2013).

was slightly lower (Fig. 3). The highest concentrations of this source were observed during the December PM pollution event, but no drastic change of its relative contribution to PM_{10} was noticed even during this episode.

3.2.3. Aged sea salt

Given the constraints applied, this factor showed major contributions of Na^+ (92% in this factor) and Mg^{2+} (71% in this factor), highlighting that this source was chiefly from sea salt particles (Fig. 3). The Mg^{2+}/Na^+ ratio (0.10) was comparable to the expected ratio found for sea water (i.e., 0.11) (Curran et al., 1998; Seinfeld and Pandis, 2012) and similar to the values found at the same site in a previous study (Polo-Rehn et al., 2014). The low Cl^- content (27%) resulted in ageing processes, including well-known heterogeneous reactions between airborne sea-salt| particles and acidic pollutants (e.g., nitric and sulfuric acid) leading to the volatilization of HCl (Seinfeld and Pandis, 2012). This source was rather constant throughout the year, with a very low annual contribution (2%) to the PM_{10} mass (Fig. 2) and a yearly average concentration of 0.5 μg m^{-3}, which was in agreement with the sampling site location relatively far from the Atlantic and Mediterranean coasts (~200–500 km).

3.2.4. Mineral dust

This factor showed a relatively high content of mineral elements such as Ti (53% in this factor), Ca (49% in this factor), and Al (54% in this factor), commonly originating from soils and road dust (Andersen et al., 2007; Mossetti et al., 2005; Querol et al., 2004a; Yin et al., 2005) (Fig. 3). This was one of the major PM sources, corresponding to an average of 4.7 μg m^{-3} and accounting for 21% of the PM_{10} mass on an annual average (Fig. 2). It showed a typical seasonal evolution with high concentrations and contributions in the summer (dry season). Significant amounts of OM (including HuLiS) and sulfate were also observed in the chemical profile of this source, in agreement with the presence of these species in soils, within resuspended particles, and/or as

condensation products onto crustal material (Falkovich et al., 2004; Kögel-Knabner, 2000).

3.2.5. Biomass burning

The source of the biomass burning factor was characterized by very high loadings of levoglucosan (levo), coniferaldehyde (conyferald.), and vanillic acid. This factor also showed significant contributions of PAHs (B[*a*]P, B[*ghi*]P, In[1,2,3-*cd*]P and Cor). It followed typical seasonal variations, with a largely higher contribution in winter (Fig. 4). This source accounted for 20% of the PM_{10} mass on a yearly average (4.5 μg m^{-3}) (Fig. 2), with maximum contributions in winter of approximately 39%. These results were in very good agreement with previous observations reported in Europe (Herich et al., 2014; Viana et al., 2015) and at the same site in the winter by Favez et al. (2010). Approximately 22–25% of OC and HuLiS were associated with this factor on an annual average. Both species showed strong correlations with levoglucosan, especially during the cold period ($r = 0.85$ and 0.71, $n = 91$, $p < 0.05$, i.e., late autumn and winter months). These results highlighted that biomass burning is a significant source of HuLiS, as already shown in previous field studies (Baduel et al., 2010; El Haddad et al., 2011; Lin et al., 2010). Finally, OC/levoglucosan and OC/EC ratios (=4.2 and 3.8, respectively) were in good agreement with those generally reported for aerosols from biomass burning (El Haddad et al., 2009; Favez et al., 2010; Fine et al., 2002; Gianini et al., 2013).

The biomass burning factor also included significant contributions from phthalic acid (58%) and, to a lesser extent, from DHOPA (20%). Both compounds are known as markers of SOA formation from the photooxidation of naphthalene and toluene, respectively (Al-Naiema and Stone, 2017; Kleindienst et al., 2004; Kleindienst et al., 2012; Kleindienst et al., 2007). In addition to vehicle exhaust, both these latter species are largely emitted by biomass burning (Baudic et al., 2016; Nalin et al., 2016; Shen et al., 2012), and previous chamber experiments have shown that SOA formation from biomass burning mainly involved the photooxidation of phenolic compounds, naphthalene, and benzene, which could together contribute up to 80% of the total observed SOA (Bruns et al., 2016). It is then expected that the factor obtained here includes both fresh and processed aerosols from biomass burning.

3.2.6. Primary biogenics 1: plant debris

This factor was characterized by a typical chemical fingerprint from plant waxes with significant amounts (47–82%) of odd number higher alkanes (C27 to C31) (Rogge et al., 1993) (Fig. 4). This source accounted for 11% of the PM_{10} mass on an annual average (2.5 μg m^{-3}) (Fig. 2) and exhibited a clear seasonal pattern, with relatively higher concentrations in the warm period (May–August), in agreement with plant metabolic activity. However, concentrations were also significant for the rest of the year. PM source apportionment from plant emissions is usually not achieved in the literature. To the best of our knowledge, this is the first report of the identification of a plant debris source factor using higher alkanes in a PMF model (at least in Europe). A similar source has been identified in similar studies using other source apportionment models (van Drooge and Grimalt, 2015). However, as shown by the presence of elements such as Ti, V, Al, and Ca, the influence of other sources, such as resuspension from road dust and soil particles, cannot be ruled out.

3.2.7. Primary biogenics 2: fungal spores

This source factor was characterized by the large proportions of polyols (arabitol and sorbitol, 75–85% of the total mass of each compound in this factor) (Fig. 2). These compounds have been identified in the literature as markers of primary biogenic emissions originating from primary biological aerosol particles, notably fungal spores and microbes (Bauer et al., 2008; Caseiro et al., 2009; Rogge et al., 2007; Yttri et al., 2011), and previously used to apportion primary biogenic aerosols via a PMF analysis in France (Lens) (Waked et al., 2014). This factor contributed approximately 5% of the PM_{10} mass on an annual average, with a concentration of 1.1 μg m^{-3}, which was significantly lower than the contribution estimated by Waked et al. (2014) (9% on a yearly average). This lower contribution might be explained by the fact that the present study allowed for better separation between two types of primary biogenic aerosols, as well as between primary and secondary organic aerosols.

Temporal evolution showed a clear seasonality, with maximum concentrations observed in the summer and fall seasons (from June to early November), in agreement with the higher biological activity due to higher temperatures and humidity inducing an increase in the emissions of fungal spores, fern spores and pollen grains (Graham et al., 2003; Verma et al., 2017). Maximum concentrations of arabitol and sorbitol have already been observed during the warm period in several previous studies (Bauer et al., 2008; Verma et al., 2017; Waked et al., 2014; Yttri et al., 2011).

3.2.8. Biogenic SOA

The sources of the biogenic SOA factor was resolved by the use of oxidation products of isoprene (α-methylglyceric acid (α-MGA and 2-methylerythritol (2-MT)) and of α-pinene (hydroxyglutaric acid (3-HGA)) (Carlton et al., 2009; Jaoui et al., 2008). The source factor showed very high contributions of these three SOA markers (78–90% of the total mass of each compound). The apportionment of biogenic SOA is not commonly achieved in PMF or other models based studies (Heo et al., 2013; Hu et al., 2010; Shrivastava et al., 2007; van Drooge and Grimalt, 2015; Zhang et al., 2009). Here, the evaluation of both biogenic SOA precursors to the total biogenic SOA contribution was not possible due to the strong correlation observed between isoprene and α-pinene SOA markers (e.g., (α-MGA and 2-MT vs 3-HGA, $r = 0.84$ and 0.86, respectively; $n = 123$, $p < 0.05$)). The source of biogenic SOA showed a significant contribution to the PM_{10} mass of 12% on an annual average, corresponding to a concentration of 2.6 μg m^{-3} (Fig. 2). A clear seasonal variation with larger contributions and concentrations in the summer was observed (up to 20% of PM and 16 μg m^{-3}), in agreement with the higher biogenic SOC contributions already noticed during the warmer months in related studies (Kleindienst et al., 2007; Shrivastava et al., 2007; Zhang et al., 2009) (Fig. 4).

3.2.9. Anthropogenic SOA

The last factor was characterized by high loadings of acenaphthenequinone (86%), 6H–dibenzo[*b*,*d*]pyran-6-one (88%), 1,8-naphthalic anhydride (83%) and DHOPA (58%). As mentioned previously, DHOPA is considered a marker of SOA formation from toluene photooxidation (Al-Naiema and Stone, 2017; Kleindienst et al., 2004; Kleindienst et al., 2007), while the three other compounds are typically by-products of PAH oxidation (phenanthrene, acenaphthene and acenaphthylene) resulting in SOA formation (Lee and Lane, 2010; Lee et al., 2012; Perraudin et al., 2007; Tomaz et al., 2017; Zhou and Wenger, 2013a; Zhou and Wenger, 2013b). Thus, this factor seemed characteristic of SOA from anthropogenic sources, including combustion processes such as biomass burning and traffic. Note that the primary emission of PAH oxidation products, notably by biomass burning, cannot be ignored. However, poor correlations with levoglucosan have been observed ($r < 0.39$, $n = 123$, $p < 0.05$) and confirmed that these compounds were mainly originated from secondary processes in the Grenoble valley.

Anthropogenic SOA accounted for approximately 2% of the total PM_{10} mass, with a concentration of 0.5 μg m^{-3} on an annual average (Fig. 2).

The source showed higher concentrations during the winter season and especially in December during the severe PM pollution event, with a contribution to PM_{10} of up to 18% (Fig. 4).

To the best of our knowledge, this study is probably the first report of the use of PAH derivatives (here oxy-PAHs) for the apportionment of an anthropogenic SOA (PAH SOA) source. Additional tests have been performed to investigate the validity of this factor. To do this, we excluded

the December data points from the complete dataset and ran the PMF model again (Table S9). The new PMF results showed that the nine factors solution was also found to be optimum and quite stable (with bootstrap >98%) (Table S10). The chemical and temporal profiles for all the factors were totally similar to those obtained with the entire dataset, even including this factor (Figs. S11 and S12, Table S11). These results confirmed the robustness of PMF outputs, which are not perturbated by the severe winter pollution event.

The large concentration peak of the source of anthropogenic SOA observed during the December PM pollution event was also noticed for all primary pollutants, including EC, levoglucosan, hopanes, several alkanes, PAHs, 1-nitropyrene and NO, underlining the large impact of primary combustion sources during this period (Tomaz et al., 2017; Tomaz et al., 2016). In addition, several secondary compounds from anthropogenic precursors, such as DHOPA, methyl-nitrocatechols (markers for biomass burning SOA) (Iinuma et al., 2010), succinic and phthalic acids (Kawamura and Ikushima, 1993; Kleindienst et al., 2012) and nitro- and oxy-PAHs, exhibited very high concentrations during this period (Fig. 5).

Such an event and anthropogenic SOA concentrations could be explained by a combination of several factors. First, the meteorological conditions and the geomorphology around Grenoble promoted the formation and the occurrence of thermal inversion layers for >10 consecutive days (Fig. 1) (Tomaz et al., 2017). Together with the low wind speed (<2 m s^{-1}) (Fig. S3), this led to the stagnation of polluted air masses over a long period, allowing favourable conditions for chemical reactions and intense secondary formation processes. Second and interestingly, most of the metallic species and notably the transition metals (Fe, Cu, Cr, V…) showed a concentration peak during the December PM pollution event (Fig. 6). Such an increase of concentrations is still not fully understood, but these redox-active metals, and especially Fe and Cu, are known to be involved in the catalysis of Fenton-like reactions in which they may react with hydrogen peroxide (H_2O_2) to generate OH radicals (Walling, 1975). In addition, recent studies have stated the role of a Fenton reagent (Fe, Cu/H_2O_2) in both SOA formation and PAH oxidation (Singh and Gupta, 2016; Singh and Gupta, 2017; Singh et al., 2017). Thus, transition metals could have played a significant role in the enhancement of the chemical processes and the anthropogenic SOA formation during this period. Last, Tong et al. (2016) have recently shown that SOA decomposition may also lead to the formation of OH radicals. The OH production rate by SOA decomposition depends on Fe^{2+}, SOA precursors and concentrations. Such a process seems quantitatively comparable to the Fenton reaction in most conditions and may be the main source of OH radicals at low concentrations of H_2O_2 and Fe^{2+}. Then, the OH radicals generated would promote SOA chemical ageing, especially in the presence of iron, increasing auto-oxidation in the condensed phase and further resulting in a self-amplification cycle of SOA formation (Tong et al., 2016). All these conditions were present during the December PM pollution event to promote these processes and enhance SOA formation.

3.3. Sources of coarse and fine aerosol fractions

Overall, the coarse aerosol fraction (PM_{10}-$PM_{2.5}$) accounted for one-third of the PM_{10} mass. Such a proportion is in agreement with those previously reported in many different urban environments (Masri et al., 2015; Querol et al., 2004b). Fig. 7 shows the tentative reconstruction of both aerosol fractions using apportioned PM sources. Interestingly, the sum of the three source factors, namely plant debris, aged sea salt, and mineral dust, showed a significant correlation with the PM mass concentration of the coarse particle mode ($r = 0.71$; $n = 123$, $p < 0.05$). Note that to date, no consensus has emerged to precisely decide whether the source of fungal spores belongs to the fine or the coarse aerosol fraction (Liang et al., 2013; Waked et al., 2014; Wang et al., 2011). The sum of the 5 or 6 other source factors identified ($PM_{2.5}$ vs. $\Sigma_5$factors, $r = 0.91$; $n = 123$, $p < 0.05$) ($PM_{2.5}$ vs. $\Sigma_6$factors, $r = 0.92$; $n = 123$, $p < 0.05$) was in very good agreement with the fine aerosol mass fraction. These results highlighted that fine particles were associated mostly with primary carbonaceous emissions together with secondary processes, while coarse particles consisted mostly of mineral dust and organic matter.

3.4. Organic aerosol source apportionment

3.4.1. Organic carbon (OC)

OC source contributions apportioned from the present PMF analysis are presented in Fig. 8. On an annual average, the major contributors to OC were biomass burning (25%), primary traffic (12%), mineral dust (13%), fungal spores (12%), secondary inorganics (11%) and plant debris (10%), followed by both SOA fractions (14% in total) and aged sea salt (3%).

These results highlighted the large contributions of primary OA sources, namely, biomass burning, traffic and biogenic source (59% in total on an annual average). The significant impact of biomass burning within OC was in good agreement with previous findings at Grenoble (Favez et al., 2010). As expected, elevated contributions of this source

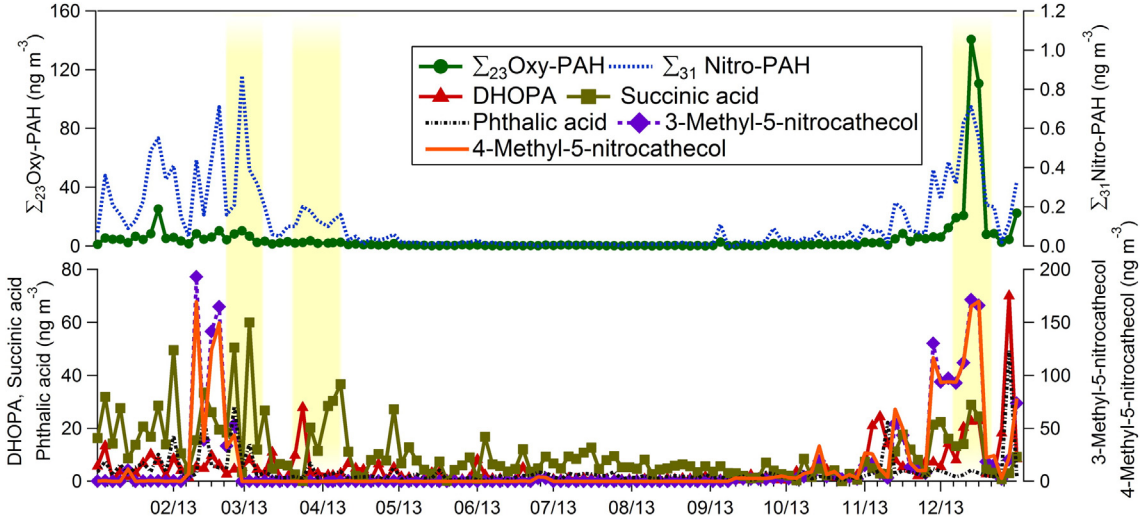

Fig. 5. Temporal variation of the concentrations of Σ_{23}Oxy-PAHs, Σ_{31}Nitro-PAHs, DHOPA, methyl-nitrocatechols, succinic and phthalic acids observed at Grenoble, Les Frênes (2013).

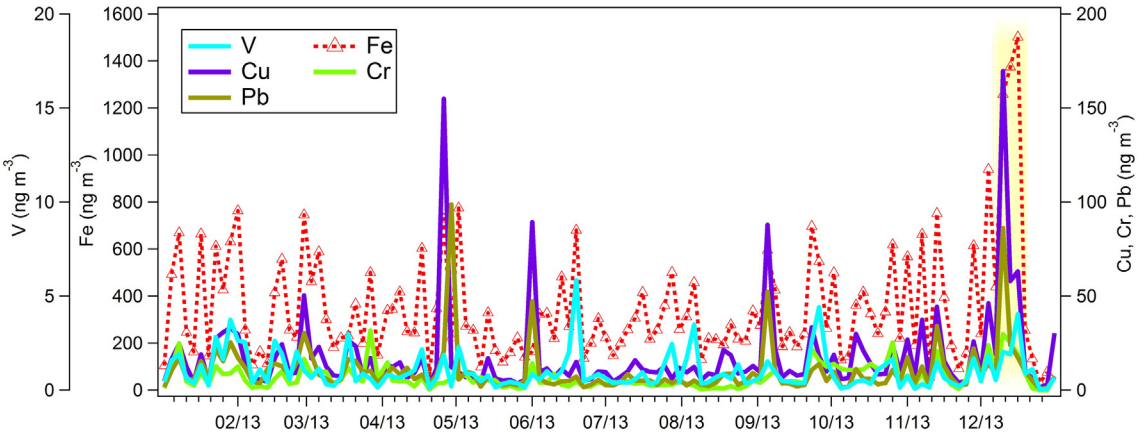

Fig. 6. Temporal variation of selected metal concentrations (Fe, Cu, Cr, Pb, and V) observed at Grenoble, Les Frênes (2013).

to OC were obtained during the long residential heating periods in this region (20%, 20% and 43% for the spring, fall and winter seasons, respectively). In addition, the traffic contribution was in the same range as that previously reported (Favez et al., 2010). The primary biogenic fraction, consisting of fungal spores and plant debris, accounted for a considerable fraction of OC (22%), with a typical seasonal variation along with maximum concentrations and contributions up to 40% in the summer, which was related to the increase in biological activity.

Other sources, secondary inorganics, mineral dust and aged sea salt accounted together for 27% of the total OC load on a yearly basis. The primary or secondary origins of OC for these sources are discussed hereafter. The source of secondary inorganics showed a conspicuous seasonal time trend. High contributions during the spring and winter seasons were likely associated with the PM pollution events. This source factor showed a good correlation with oxalate only in the winter ($r = 0.84$, $n = 31$, $p < 0.05$) and fall ($r = 0.70$, $n = 30$, $p < 0.05$), indicating the influence of secondary origins for this OA source. The source of mineral dust showed a higher contribution in the summer (22%), similar to the time trend, followed by secondary processes. The presence of HuLiS, phthalic acid, and sulfate in this source factor suggested that a part of OC was likely to be secondary. The condensation of secondary organic species on mineral dust could occur during long range transport. In addition, mineral dust may facilitate very active redox chemistry on its surface under certain conditions (i.e., in the presence of metal oxides such as TiO_2, ZnO, iron oxides and their exposure to sunlight) and lead to the formation of a number of different oxidized products (Aymoz et al., 2004; George et al., 2015). Similarly, the OC fraction in the aged sea-salt factor may be produced via a primary or bubble-mediated production mechanism at the ocean surface (Ceburnis et al., 2008), but their ageing could be explained by exposure to secondary organic aerosols precursors during the transport of air masses (Song and Carmichael, 1999).

SOA fractions from clearly identified biogenic and anthropogenic precursor origins together accounted for 14% of OC on an annual basis and ranged from 7% to 27% depending on the season. This rather low contribution could be explained by the presence of SOA in other source factors, as discussed above. The maximum contribution was observed in the summer and is of biogenic origin. Conversely, anthropogenic SOA accounted for 15% of OC in the winter and up to 42% during the December PM pollution event.

Clear-cut anthropogenic sources (i.e., primary traffic, biomass burning and anthropogenic SOA) and biogenic sources (primary and secondary) accounted for 43% and 30% of total OC on an annual average, respectively. The remaining 27% (distributed between mineral dust, secondary inorganics and aged sea salt factors) could not be unambiguously ascribed to either anthropogenic or biogenic origins. The maximum anthropogenic OC contribution was obtained during the winter season (>71%), notably due to the impact of residential heating and

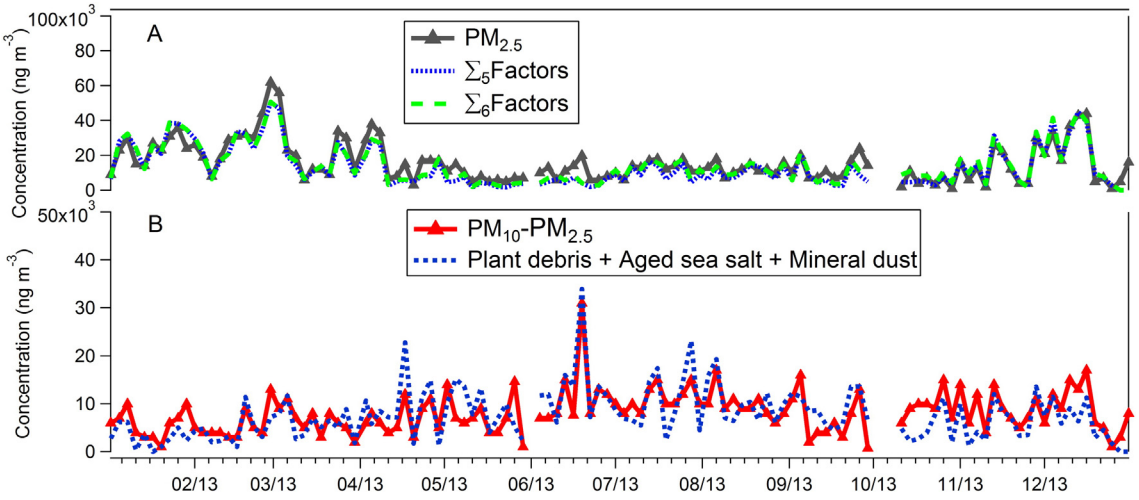

Fig. 7. Tentative reconstruction of fine ($PM_{2.5}$) (A) and coarse (PM_{10}-$PM_{2.5}$) (B) aerosol fractions observed at Grenoble, Les Frênes (2013) using identified PM sources by PMF model. Σ_5Factors = Primary traffic + Secondary inorganic + Biomass burning + Anthropogenic SOA + Biogenic SOA.; Σ_6Factors = Primary traffic + Secondary inorganic + Biomass burning + Anthropogenic SOA + Biogenic SOA + Fungal spores.

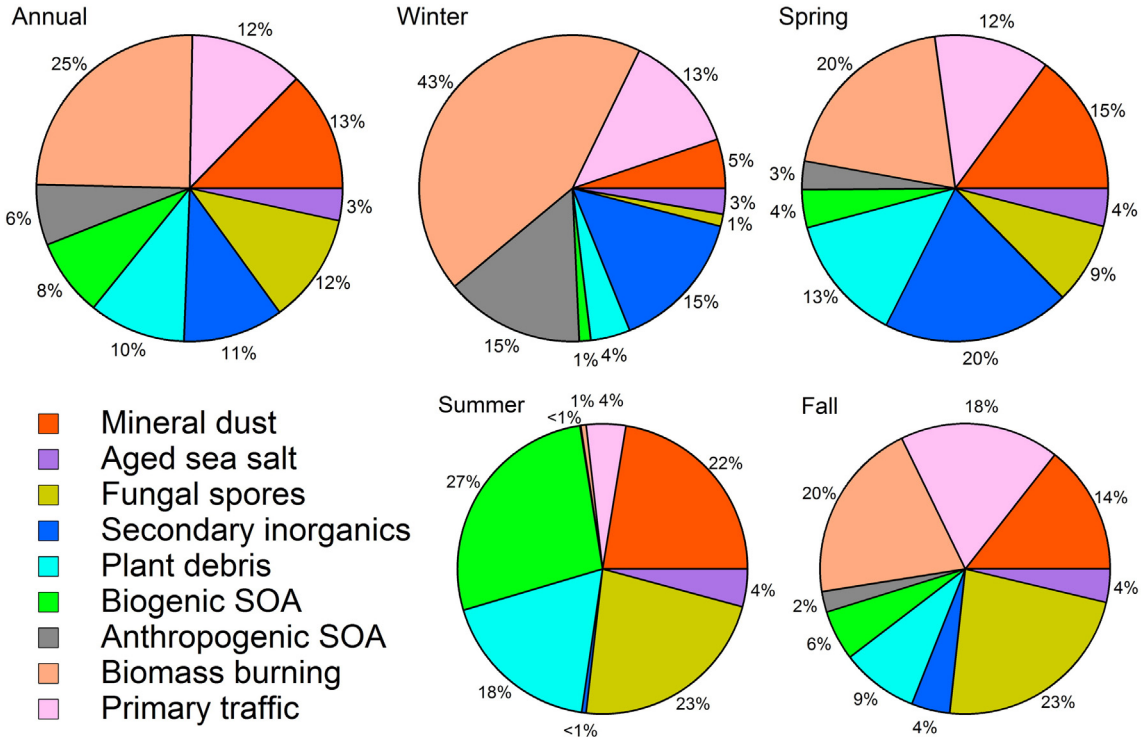

Fig. 8. Annual and seasonal contributions of the identified sources to OC concentrations at Grenoble, Les Frênes (2013).

the accumulation of pollutants in the valley of Grenoble, whereas the biogenic OC contribution was greatest in the summer (>68%).

3.4.2. Humic like substances (HuLiS)

HuLiS play an important role in the atmosphere by affecting the growth of particles (Gysel et al., 2004), cloud condensation and ice nuclei formation (Facchini et al., 1999; Wang and Knopf, 2011) due to their hygroscopic and surface-active properties. They account for a significant fraction of OM (approximately 10 to 30%) (Feczko et al., 2007). They are probably poorly photoactive (Albinet et al., 2010) but may directly react with oxidants (Baduel et al., 2011). They have been found to catalytically enhance the generation of reactive oxygen species (ROS) under simulated physiological conditions and may contribute to PM health impacts (Lin and Yu, 2011). The current knowledge and understanding

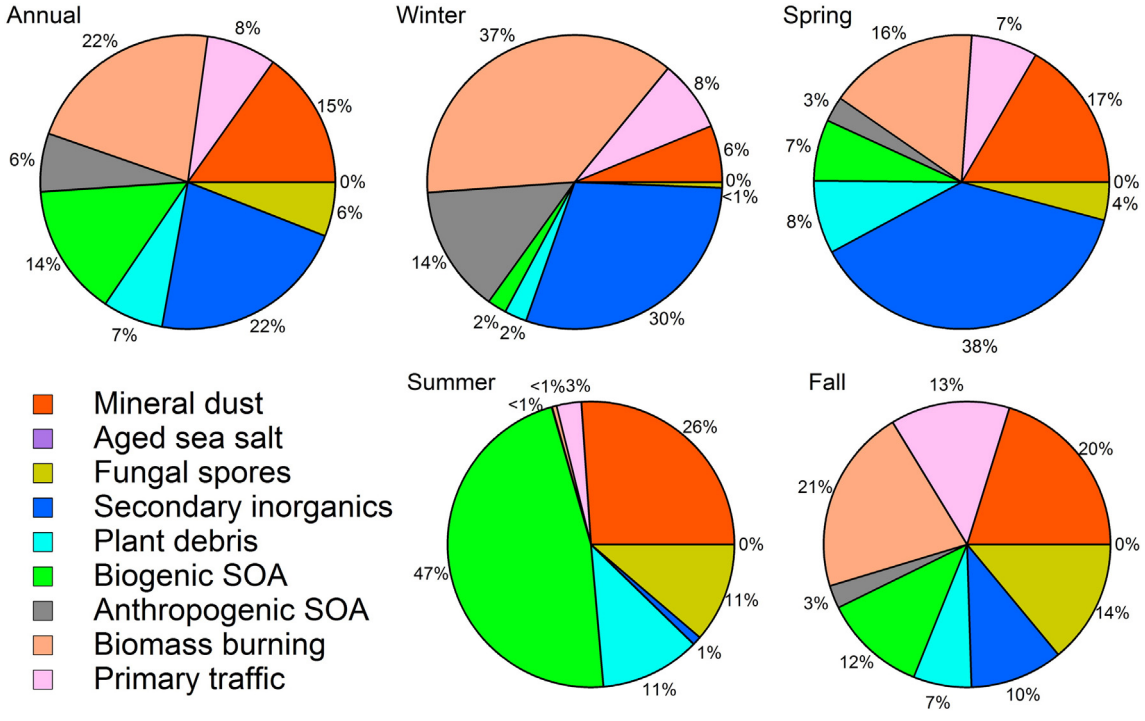

Fig. 9. Annual and seasonal contributions of the identified sources to HuLiS concentrations at Grenoble, Les Frênes (2013).

of the sources and formation mechanisms of HuLiS are still rather poor due to the lack of source apportionment studies of this OA component (Baduel et al., 2010).

On an annual average, HuLiS accounted for approximately 8% of OM in Grenoble (from 2 to 20%) and among the nine sources resolved by PMF, only aged sea salt did not contribute to HuLiS mass (Fig. 9). Overall, 22%, 22%, 15%, and 14% of HuLiS mass were respectively associated with biomass burning, secondary inorganics, mineral dust and biogenic SOA on an annual average. PMF outputs also indicated that a non-negligible amount of HuLiS mass was attributed to plant debris, primary biogenic and primary traffic. Each of these latter sources contributed to approximately 6–8% on annual average of total HuLiS, with higher contributions in the summer for plant debris (11%) and in the summer and fall for fungal spores (11–14%). While traffic emission origins have already been assigned to HuLiS (Kuang et al., 2015), no previous study explicitly reported the contribution of primary biogenics (fungal spores + plant debris) OA to these compounds.

The contribution of biomass burning to HuLiS showed a strong seasonal trend (Fig. 9). It is well known that biomass combustion processes release large quantities of aromatic species into the atmosphere (Graham et al., 2002) and represent the most likely contributor to HuLiS mass in urban areas during the cold season (Baduel et al., 2010). This was confirmed by the strong correlation observed between HuLiS and levoglucosan ($r = 0.81$) and the major contribution of this source to HuLiS in the winter (37%).

Secondary inorganics showed high contributions to HuLiS in the spring and winter (30–38%) and negligible input in the summer. Significant correlations were observed between HuLiS and secondary inorganic species in the spring (HuLiS vs. NH_4^+, SO_4^{2-}, NO_3^-, $r = 0.82$–0.84, $n = 30$, $p < 0.05$) and winter (HuLiS vs. NH_4^+, SO_4^{2-}, NO_3^-, $r = 0.68$–0.76, $n = 31$, $p < 0.05$). Both chamber and field studies reported up to now have shown that heterogeneous reactions of organic compounds with sulfate aerosols lead to the formation of organosulfates (Riva et al., 2015; Surratt et al., 2008), which are a major class of compounds of the HuLiS fraction (Lin et al., 2012). Sulfate aerosols, VOCs and SVOCs (including PAHs) were abundant in the Grenoble valley during the PM pollution events and could cause enhanced HuLiS formation. In addition to organosulfates, nitrated organic compounds (organonitrates) have been reported to be constituents of HuLiS (Lin et al., 2012). Organonitrates may contribute substantially to OM, especially in Europe (Kiendler-Scharr et al., 2009), and notably could have been formed during the spring PM pollution events, as has been shown for nitro-PAHs (Tomaz et al., 2017).

The large contribution of the biogenic SOA factor to HuLiS observed in the summer (47%) can also be explained by secondary formation processes. Indeed, aqueous-phase oxidation and heterogeneous reactions involving oxidation products of biogenic VOCs (i.e., isoprene, α-pinene, limonene, etc.) are known to produce HuLiS (Surratt et al., 2008). In addition, anthropogenic SOA showed a low contribution to HuLiS on an annual average (6%) but was remarkably higher in winter (14%), especially during the December PM pollution event, as described previously. Organosulfate formation from the gas phase oxidation of PAHs (Riva et al., 2015) and the formation of HuLiS from secondary processes in liquid phase from aromatic acid precursors during biomass burning events (Altieri et al., 2008; Baduel et al., 2010; El Haddad et al., 2011) may explain such observations.

Finally, mineral dust also contributed significantly to HuLiS, especially in the warm period (17%–26%), with the highest contribution in the summer, which could be explained by both primary and secondary origins. HuLiS are known to be partly emitted as a primary source from soils (Graber and Rudich, 2006). High correlations were noticed between HuLiS and oxalate and O_3 ($r = 0.60$–0.70, $n = 31$, $p < 0.05$) in the summer (Fig. S13). As discussed before, mineral dust could also play a major role in secondary redox processes under favourable atmospheric conditions (George et al., 2015), and the link between HuLiS and mineral dust could be partly related to such processes.

4. Conclusion

Source apportionment performed using specific primary and secondary molecular markers indicated nine major PM_{10} sources in Grenoble (France), including sources rarely apportioned, such as primary biogenics (fungal spores + plant debris) as well as explicit SOA factors. Major contributors to PM_{10} mass on an annual average were biomass burning and mineral dust (~20% of PM_{10} for each of them), followed by primary traffic (14%). A high contribution of anthropogenic SOA was also observed during an intense wintertime PM pollution event. This could be explained by the accumulation of pollutants due to specific meteorological conditions and the enhancement of SOA formation via probable Fenton-like reactions and self-amplification cycles.

PMF outputs also allowed the clear identification of the overwhelming biogenic origins of organic aerosols during the summer season (>68% of total OC), contrasting with the predominance of anthropogenic OC during wintertime. Moreover, a peculiar emphasis was put on the sources of HuLiS, a class of compounds that constitutes a significant fraction of organic matter and is commonly considered a proxy of low volatile oxygenated organic aerosols. The results obtained here enlightened the diversity of the primary and secondary origins of these compounds, being mainly associated with biomass burning (22%), secondary inorganics (22%), mineral dust (15%), and biogenic SOA (14%) on an annual scale in Grenoble.

The findings presented in this paper demonstrate that the speciation of the organic aerosol fraction and the input of specific molecular markers into source-receptor model are powerful tools to evaluate the contributions of discriminated OA sources and to get a better understanding of PM origins. Future works could try to incorporate even more markers (e.g., organosulfates and organonitrates) to further discriminate the nature (e.g., biogenic vs. anthropogenic) of organic aerosols that are associated with secondary inorganics, as well as mineral dusts. The use of higher time-resolution datasets (e.g., filter sampling every 6 h or less) could also allow the better apportionment of the influence of various secondary formation mechanisms that present different diurnal cycles.

Acknowledgements

The authors wish to thank the French Ministry of the Environment (MTEL) and the French Ministry of Research for their financial support. This work was done as part of the LCSQA activities (French reference laboratory for air quality monitoring). The authors thank Atmo Rhône-Alpes-Auvergne for filter samplings, air quality and meteorological data, Nadine Guillaumet and Noémie Nuttens for PAH analyses, Coralie Connes and Vincent Lucaire for the EC/OC, IC, sugars, organic acids and HuLis measurements, Nathalie Bocquet and Robin Aujay-Plouzeau for sample preparation and Patrick Bodu for the graphical abstract design. The Labex OSUG@2020 (ANR-10-LABX-56) is gratefully acknowledged for the analytical equipment at IGE.

Appendix A. Supplementary data

Supplementary data to this article can be found online at https://doi.org/10.1016/j.scitotenv.2017.12.135.

References

Albinet, A., Leoz-Garziandia, E., Budzinski, H., Villenave, E., 2006. Simultaneous analysis of oxygenated and nitrated polycyclic aromatic hydrocarbons on standard reference material 1649a (urban dust) and on natural ambient air samples by gas chromatography–mass spectrometry with negative ion chemical ionisation. J. Chromatogr. A 1121, 106–113.

Albinet, A., Leoz-Garziandia, E., Budzinski, H., Villenave, E., 2007. Polycyclic aromatic hydrocarbons (PAHs), nitrated PAHs and oxygenated PAHs in ambient air of the Marseilles area (south of France): concentrations and sources. Sci. Total Environ. 384, 280–292.

Albinet, A., Leoz-Garziandia, E., Budzinski, H., Villenave, E., Jaffrezo, J.-L., 2008. Nitrated and oxygenated derivatives of polycyclic aromatic hydrocarbons in the ambient air of two French alpine valleys: part 1: concentrations, sources and gas/particle partitioning. Atmos. Environ. 42, 43–54.
Albinet, A., Minero, C., Vione, D., 2010. Photochemical generation of reactive species upon irradiation of rainwater: negligible photoactivity of dissolved organic matter. Sci. Total Environ. 408, 3367–3373.
Albinet, A., Tomaz, S., Lestremau, F., 2013. A really quick easy cheap effective rugged and safe (QuEChERS) extraction procedure for the analysis of particle-bound PAHs in ambient air and emission samples. Sci. Total Environ. 450-451, 31–38.
Albinet, A., Nalin, F., Tomaz, S., Beaumont, J., Lestremau, F., 2014. A simple QuEChERS-like extraction approach for molecular chemical characterization of organic aerosols: application to nitrated and oxygenated PAH derivatives (NPAH and OPAH) quantified by GC–NICIMS. Anal. Bioanal. Chem. 406, 3131–3148.
Alleman, L.Y., Lamaison, L., Perdrix, E., Robache, A., Galloo, J.-C., 2010. PM10 metal concentrations and source identification using positive matrix factorization and wind sectoring in a French industrial zone. Atmos. Res. 96, 612–625.
Al-Naiema, I.M., Stone, E.A., 2017. Evaluation of anthropogenic secondary organic aerosol tracers from aromatic hydrocarbons. Atmos. Chem. Phys. 17, 2053–2065.
Altieri, K., Seitzinger, S., Carlton, A., Turpin, B., Klein, G., Marshall, A., 2008. Oligomers formed through in-cloud methylglyoxal reactions: chemical composition, properties, and mechanisms investigated by ultra-high resolution FT-ICR mass spectrometry. Atmos. Environ. 42, 1476–1490.
Andersen, Z.J., Wahlin, P., Raaschou-Nielsen, O., Scheike, T., Loft, S., 2007. Ambient particle source apportionment and daily hospital admissions among children and elderly in Copenhagen. J. Expo. Sci. Environ. Epidemiol. 17, 625.
Aymoz, G., Jaffrezo, J.-L., Jacob, V., Colomb, A., George, C., 2004. Evolution of organic and inorganic components of aerosol during a Saharan dust episode observed in the French Alps. Atmos. Chem. Phys. 4, 2499–2512.
Baduel, C., Voisin, D., Jaffrezo, J.L., 2010. Seasonal variations of concentrations and optical properties of water soluble HULIS collected in urban environments. Atmos. Chem. Phys. 10, 4085–4095.
Baduel, C., Monge, M.E., Voisin, D., Jaffrezo, J.-L., George, C., Haddad, I.E., Marchand, N., D'anna, B., 2011. Oxidation of atmospheric humic like substances by ozone: a kinetic and structural analysis approach. Environ. Sci. Technol. 45, 5238–5244.
Baudic, A., Gros, V., Sauvage, S., Locoge, N., Sanchez, O., Sarda-Estève, R., Kalogridis, C., Petit, J.-E., Bonnaire, N., Baisnée, D., 2016. Seasonal variability and source apportionment of volatile organic compounds (VOCs) in the Paris megacity (France). Atmos. Chem. Phys. 16, 11961–11989.
Bauer, H., Claeys, M., Vermeylen, R., Schueller, E., Weinke, G., Berger, A., Puxbaum, H., 2008. Arabitol and mannitol as tracers for the quantification of airborne fungal spores. Atmos. Environ. 42, 588–593.
Belis, C.A., Karagulian, F., Larsen, B.R., Hopke, P.K., 2013. Critical review and meta-analysis of ambient particulate matter source apportionment using receptor models in Europe. Atmos. Environ. 69, 94–108.
Boucher, O., Randall, D., Artaxo, P., Bretherton, C., Feingold, G., Forster, P., Kerminen, V.-M., Kondo, Y., Liao, H., Lohmann, U., 2013. Clouds and Aerosols. Climate Change 2013: The Physical Science Basis. Contribution of Working Group I to the Fifth Assessment Report of the Intergovernmental Panel on Climate Change. Cambridge University Press, pp. 571–657.
Bruns, E.A., El Haddad, I., Slowik, J.G., Kilic, D., Klein, F., Baltensperger, U., Prévôt, A.S.H., 2016. Identification of significant precursor gases of secondary organic aerosols from residential wood combustion. Sci. Rep. 6, 27881.
Carlton, A.G., Wiedinmyer, C., Kroll, J.H., 2009. A review of secondary organic aerosol (SOA) formation from isoprene. Atmos. Chem. Phys. 9, 4987–5005.
Caseiro, A., Bauer, H., Schmidl, C., Pio, C.A., Puxbaum, H., 2009. Wood burning impact on PM10 in three Austrian regions. Atmos. Environ. 43, 2186–2195.
Cavalli, F., Viana, M., Yttri, K., Genberg, J., Putaud, J.-P., 2010. Toward a standardised thermal-optical protocol for measuring atmospheric organic and elemental carbon: the EUSAAR protocol. Atmos. Meas. Tech. 3, 79–89.
Ceburnis, D., O'Dowd, C.D., Jennings, G.S., Facchini, M.C., Emblico, L., Decesari, S., Fuzzi, S., Sakalys, J., 2008. Marine aerosol chemistry gradients: elucidating primary and secondary processes and fluxes. Geophys. Res. Lett. 35.
Curran, M.A., Van Ommen, T.D., Morgan, V., 1998. Seasonal characteristics of the major ions in the high-accumulation Dome Summit South ice core, Law Dome, Antarctica. Ann. Glaciol. 27, 385–390.
van Drooge, B.L., Grimalt, J.O., 2015. Particle size-resolved source apportionment of primary and secondary organic tracer compounds at urban and rural locations in Spain. Atmos. Chem. Phys. 15, 7735–7752.
El Haddad, I., Marchand, N., Dron, J., Temime-Roussel, B., Quivet, E., Wortham, H., Jaffrezo, J.L., Baduel, C., Voisin, D., Besombes, J.L., Gille, G., 2009. Comprehensive primary particulate organic characterization of vehicular exhaust emissions in France. Atmos. Environ. 43, 6190–6198.
El Haddad, I., Marchand, N., Temime-Roussel, B., Wortham, H., Piot, C., Besombes, J.L., Baduel, C., Voisin, D., Armengaud, A., Jaffrezo, J.L., 2011. Insights into the secondary fraction of the organic aerosol in a Mediterranean urban area: Marseille. Atmos. Chem. Phys. 11, 2059–2079.
Facchini, M.C., Fuzzi, S., Zappoli, S., Andracchio, A., Gelencsér, A., Kiss, G., Krivácsy, Z., Mészáros, E., Hansson, H.C., Alsberg, T., 1999. Partitioning of the organic aerosol component between fog droplets and interstitial air. J. Geophys. Res.-Atmos. 104, 26821–26832.
Falkovich, A.H., Schkolnik, G., Ganor, E., Rudich, Y., 2004. Adsorption of organic compounds pertinent to urban environments onto mineral dust particles. J. Geophys. Res.-Atmos. 109.
Favez, O., 2013. Synthèse des travaux 2013 du programme CARA. LCSQA (French language). DRC-13-136071-14096A. https://www.lcsqa.org/rapport/2013/ineris/synthese-travaux-2013-programme-cara.
Favez, O., El Haddad, I., Piot, C., Boréave, A., Abidi, E., Marchand, N., Jaffrezo, J.L., Besombes, J.L., Personnaz, M.B., Sciare, J., Wortham, H., George, C., D'Anna, B., 2010. Inter-comparison of source apportionment models for the estimation of wood burning aerosols during wintertime in an alpine city (Grenoble, France). Atmos. Chem. Phys. 10, 5295–5314.
Feczko, T., Puxbaum, H., Kasper-Giebl, A., Handler, M., Limbeck, A., Gelencsér, A., Pio, C., Preunkert, S., Legrand, M., 2007. Determination of water and alkaline extractable atmospheric humic-like substances with the TU Vienna HULIS analyzer in samples from six background sites in Europe. J. Geophys. Res.-Atmos. 112, D23S10.
Fine, P.M., Cass, G.R., Simoneit, B.R.T., 2002. Chemical characterization of fine particle emissions from the fireplace combustion of woods grown in the southern United States. Environ. Sci. Technol. 36, 1442–1451.
George, C., Ammann, M., D'Anna, B., Donaldson, D.J., Nizkorodov, S.A., 2015. Heterogeneous photochemistry in the atmosphere. Chem. Rev. 115, 4218–4258.
Gianini, M.F.D., Fischer, A., Gehrig, R., Ulrich, A., Wichser, A., Piot, C., Besombes, J.L., Hueglin, C., 2012. Comparative source apportionment of PM10 in Switzerland for 2008/2009 and 1998/1999 by positive matrix factorisation. Atmos. Environ. 54, 149–158.
Gianini, M., Piot, C., Herich, H., Besombes, J.-L., Jaffrezo, J.-L., Hueglin, C., 2013. Source apportionment of PM10, organic carbon and elemental carbon at Swiss sites: an intercomparison of different approaches. Sci. Total Environ. 454, 99–108.
Golly, B., Brulfert, G., Berlioux, G., Jaffrezo, J.L., Besombes, J.L., 2015. Large chemical characterisation of PM10 emitted from graphite material production: application in source apportionment. Sci. Total Environ. 538, 634–643.
Graber, E.R., Rudich, Y., 2006. Atmospheric HULIS: how humic-like are they? A comprehensive and critical review. Atmos. Chem. Phys. 6, 729–753.
Graham, B., Mayol-Bracero, O.L., Guyon, P., Roberts, G.C., Decesari, S., Facchini, M.C., Artaxo, P., Maenhaut, W., Koll, P., Andreae, M.O., 2002. Water-soluble organic compounds in biomass burning aerosols over Amazonia - 1. Characterization by NMR and GC-MS. J. Geophys. Res.-Atmos. 107.
Graham, B., Guyon, P., Maenhaut, W., Taylor, P.E., Ebert, M., Matthias-Maser, S., Mayol-Bracero, O.L., Godoi, R.H., Artaxo, P., Meixner, F.X., 2003. Composition and diurnal variability of the natural Amazonian aerosol. J. Geophys. Res.-Atmos. 108.
Gysel, M., Weingartner, E., Nyeki, S., Paulsen, D., Baltensperger, U., Galambos, I., et al., 2004. Hygroscopic properties of water-soluble matter and humic-like organics in atmospheric fine aerosol. Atmos. Chem. Phys. 4, 35–50.
Heal, M.R., Kumar, P., Harrison, R.M., 2012. Particles, air quality, policy and health. Chem. Soc. Rev. 41, 6606–6630.
Hennigan, C.J., Sullivan, A.P., Collett, J.L., Robinson, A.L., 2010. Levoglucosan stability in biomass burning particles exposed to hydroxyl radicals. Geophys. Res. Lett. 37, L09806.
Heo, J., Dulger, M., Olson, M.R., McGinnis, J.E., Shelton, B.R., Matsunaga, A., Sioutas, C., Schauer, J.J., 2013. Source apportionments of PM2.5 organic carbon using molecular marker positive matrix factorization and comparison of results from different receptor models. Atmos. Environ. 73, 51–61.
Herich, H., Gianini, M., Piot, C., Močnik, G., Jaffrezo, J.-L., Besombes, J.-L., Prévôt, A., Hueglin, C., 2014. Overview of the impact of wood burning emissions on carbonaceous aerosols and PM in large parts of the Alpine region. Atmos. Environ. 89, 64–75.
Hu, D., Bian, Q., Lau, A.K.H., Yu, J.Z., 2010. Source apportioning of primary and secondary organic carbon in summer PM2.5 in Hong Kong using positive matrix factorization of secondary and primary organic tracer data. J. Geophys. Res.-Atmos. 115.
Iinuma, Y., Boge, O., Grafe, R., Herrmann, H., 2010. Methyl-nitrocatechols: atmospheric tracer compounds for biomass burning secondary organic aerosols. Environ. Sci. Technol. 44, 8453–8459.
Isaacman-VanWertz, G., Yee, L.D., Kreisberg, N.M., Wernis, R., Moss, J.A., Hering, S.V., De Sá, S.S., Martin, S.T., Alexander, M.L., Palm, B.B., 2016. Ambient gas-particle partitioning of tracers for biogenic oxidation. Environ. Sci. Technol. 50, 9952–9962.
Jaeckels, J.M., Bae, M.-S., Schauer, J.J., 2007. Positive matrix factorization (PMF) analysis of molecular marker measurements to quantify the sources of organic aerosols. Environ. Sci. Technol. 41, 5763–5769.
Jaffrezo, J.L., Aymoz, G., Delaval, C., Cozic, J., 2005. Seasonal variations of the water soluble organic carbon mass fraction of aerosol in two valleys of the French Alps. Atmos. Chem. Phys. 5, 2809–2821.
Jaoui, M., Edney, E.O., Kleindienst, T.E., Lewandowski, M., Offenberg, J.H., Surratt, J.D., Seinfeld, J.H., 2008. Formation of secondary organic aerosol from irradiated α-pinene/toluene/NOx mixtures and the effect of isoprene and sulfur dioxide. J. Geophys. Res.-Atmos. 113, D09303.
Johansson, C., Norman, M., Burman, L., 2009. Road traffic emission factors for heavy metals. Atmos. Environ. 43, 4681–4688.
Kawamura, K., Ikushima, K., 1993. Seasonal changes in the distribution of dicarboxylic acids in the urban atmosphere. Environ. Sci. Technol. 27, 2227–2235.
Kessler, S.H., Smith, J.D., Che, D.L., Worsnop, D.R., Wilson, K.R., Kroll, J.H., 2010. Chemical sinks of organic aerosol: kinetics and products of the heterogeneous oxidation of erythritol and levoglucosan. Environ. Sci. Technol. 44, 7005–7010.
Keyte, I.J., Albinet, A., Harrison, R.M., 2016. On-road traffic emissions of polycyclic aromatic hydrocarbons and their oxy- and nitro- derivative compounds measured in road tunnel environments. Sci. Total Environ. 566–567, 1131–1142.
Kiendler-Scharr, A., Zhang, Q., Hohaus, T., Kleist, E., Mensah, A., Mentel, T.F., Spindler, C., Uerlings, R., Tillmann, R., Wildt, J., 2009. Aerosol mass spectrometric features of biogenic SOA: observations from a plant chamber and in rural atmospheric environments. Environ. Sci. Technol. 43, 8166–8172.
Kleindienst, T., Conver, T., McIver, C., Edney, E., 2004. Determination of secondary organic aerosol products from the photooxidation of toluene and their implications in ambient PM2. 5. J. Atmos. Chem. 47, 79–100.
Kleindienst, T.E., Jaoui, M., Lewandowski, M., Offenberg, J.H., Lewis, C.W., Bhave, P.V., Edney, E.O., 2007. Estimates of the contributions of biogenic and anthropogenic

hydrocarbons to secondary organic aerosol at a southeastern US location. Atmos. Environ. 41, 8288–8300.
Kleindienst, T.E., Jaoui, M., Lewandowski, M., Offenberg, J.H., Docherty, K.S., 2012. The formation of SOA and chemical tracer compounds from the photooxidation of naphthalene and its methyl analogs in the presence and absence of nitrogen oxides. Atmos. Chem. Phys. 12, 8711–8726.
Kögel-Knabner, I., 2000. Analytical approaches for characterizing soil organic matter. Org. Geochem. 31, 609–625.
Kuang, B., Lin, P., Huang, X.H.H., Yu, J., 2015. Sources of humic-like substances in the Pearl River Delta, China: positive matrix factorization analysis of PM 2.5 major components and source markers. Atmos. Chem. Phys. 15, 1995–2008.
Laing, J.R., Hopke, P.K., Hopke, E.F., Husain, L., Dutkiewicz, V.A., Paatero, J., Viisanen, Y., 2015. Positive matrix factorization of 47 years of particle measurements in Finnish Arctic. Aerosol Air Qual. Res. 15, 188–207.
Lee, J., Lane, D.A., 2010. Formation of oxidized products from the reaction of gaseous phenanthrene with the OH radical in a reaction chamber. Atmos. Environ. 44, 2469–2477.
Lee, J.Y., Lane, D.A., Heo, J.B., Yi, S.-M., Kim, Y.P., 2012. Quantification and seasonal pattern of atmospheric reaction products of gas phase PAHs in PM2. 5. Atmos. Environ. 55, 17–25.
Liang, L., Engling, G., He, K., Du, Z., Cheng, Y., Duan, F., 2013. Evaluation of fungal spore characteristics in Beijing, China, based on molecular tracer measurements. Environ. Res. Lett. 8, 014005.
Lin, P., Yu, J.Z., 2011. Generation of reactive oxygen species mediated by humic-like substances in atmospheric aerosols. Environ. Sci. Technol. 45, 10362–10368.
Lin, P., Huang, X.-F., He, L.-Y., Zhen Yu, J., 2010. Abundance and size distribution of HULIS in ambient aerosols at a rural site in South China. J. Aerosol Sci. 41, 74–87.
Lin, P., Yu, J.Z., Engling, G., Kalberer, M., 2012. Organosulfates in humic-like substance fraction isolated from aerosols at seven locations in East Asia: a study by ultra-high-resolution mass spectrometry. Environ. Sci. Technol. 46, 13118–13127.
Masri, S., Kang, C.M., Koutrakis, P., 2015. Composition and sources of fine and coarse particles collected during 2002–2010 in Boston, MA. J. Air Waste Manage. Assoc. 65, 287–297.
Mochida, M., Kawamura, K., Fu, P., Takemura, T., 2010. Seasonal variation of levoglucosan in aerosols over the western North Pacific and its assessment as a biomass-burning tracer. Atmos. Environ. 44, 3511–3518.
Mossetti, S., Angius, S.P., Angelino, E., 2005. Assessing the impact of particulate matter sources in the Milan urban area. Int. J. Environ. Pollut. 24, 247–259.
Nalin, F., Golly, B., Besombes, J.-L., Pelletier, C., Aujay-Plouzeau, R., Verlhac, S., Dermigny, A., Fievet, A., Karoski, N., Dubois, P., 2016. Fast oxidation processes from emission to ambient air introduction of aerosol emitted by residential log wood stoves. Atmos. Environ. 143, 15–26.
Nozière, B., Kalberer, M., Claeys, M., Allan, J., D'Anna, B., Decesari, S., Finessi, E., Glasius, M., Grgić, I., Hamilton, J.F., Hoffmann, T., Iinuma, Y., Jaoui, M., Kahnt, A., Kampf, C.J., Kourtchev, I., Maenhaut, W., Marsden, N., Saarikoski, S., Schnelle-Kreis, J., Surratt, J.D., Szidat, S., Szmigielski, R., Wisthaler, A., 2015. The molecular identification of organic compounds in the atmosphere: state of the art and challenges. Chem. Rev. 115, 3919–3983.
Paatero, P., Hopke, P.K., 2003. Discarding or downweighting high-noise variables in factor analytic models. Anal. Chim. Acta 490, 277–289.
Pant, P., Harrison, R.M., 2012. Critical review of receptor modelling for particulate matter: a case study of India. Atmos. Environ. 49, 1–12.
Perraudin, E., Budzinski, H., Villenave, E., 2007. Identification and quantification of ozonation products of anthracene and phenanthrene adsorbed on silica particles. Atmos. Environ. 41, 6005–6017.
Piot, C., Jaffrezo, J.-L., Cozic, J., Pissot, N., El Haddad, I., Marchand, N., Besombes, J.-L., 2012. Quantification of levoglucosan and its isomers by high performance liquid chromatography-electrospray ionization tandem mass spectrometry and its application to atmospheric and soil samples. Atmos. Meas. Tech. 5, 141–148.
Polissar, A.V., Hopke, P.K., Paatero, P., Malm, W.C., Sisler, J.F., 1998. Atmospheric aerosol over Alaska: 2. Elemental composition and sources. J. Geophys. Res.-Atmos. 103, 19045–19057.
Polo-Rehn, L., Waked, A., Charron, A., Piot, C., Besombes, J.-L., Marchand, N., Guillaud, G., Favez, O., Jaffrezo, J.-L., 2014. Estimation de la contribution des émissions véhiculaires à l'échappement et hors échappement aux teneurs atmosphériques en PM10 par Positive Matrix Factorization (PMF). Pollut. Atmos. 221.
Querol, X., Alastuey, A., Viana, M., Rodriguez, S., Artíñano, B., Salvador, P., Do Santos, S.G., Patier, R.F., Ruiz, C., De la Rosa, J., 2004a. Speciation and origin of PM10 and PM2. 5 in Spain. J. Aerosol Sci. 35, 1151–1172.
Querol, X., Alastuey, A., Viana, M.M., Rodriguez, S., Artiñano, B., Salvador, P., Garcia do Santos, S., Fernandez Patier, R., Ruiz, C.R., de la Rosa, J., Sanchez de la Campa, A., Menendez, M., Gil, J.I., 2004b. Speciation and origin of PM10 and PM2.5 in Spain. J. Aerosol Sci. 35, 1151–1172.
Riva, M., Tomaz, S., Cui, T., Lin, Y.H., Perraudin, E., Gold, A., Stone, E.A., Villenave, E., Surratt, J.D., 2015. Evidence for an unrecognized secondary anthropogenic source of organosulfates and sulfonates: gas-phase oxidation of polycyclic aromatic hydrocarbons in the presence of sulfate aerosol. Environ. Sci. Technol. 49, 6654–6664.
Rogge, W.F., Hildemann, L.M., Mazurek, M.A., Cass, G.R., Simoneit, B.R.T., 1993. Sources of fine organic aerosol. 4. Particulate abrasion products from leaf surfaces of urban plants. Environ. Sci. Technol. 27, 2700–2711.
Rogge, W.F., Medeiros, P.M., Simoneit, B.R., 2007. Organic marker compounds in surface soils of crop fields from the San Joaquin Valley fugitive dust characterization study. Atmos. Environ. 41, 8183–8204.
Schauer, J.J., Rogge, W.F., Hildemann, L.M., Mazurek, M.A., Cass, G.R., Simoneit, B.R., 1996. Source apportionment of airborne particulate matter using organic compounds as tracers. Atmos. Environ. 30, 3837–3855.
Schembari, C., Bove, M.C., Cuccia, E., Cavalli, F., Hjorth, J., Massabò, D., Nava, S., Udisti, R., Prati, P., 2014. Source apportionment of PM10 in the western Mediterranean based on observations from a cruise ship. Atmos. Environ. 98, 510–518.
Seinfeld, J.H., Pandis, S.N., 2012. Atmospheric Chemistry and Physics: From Air Pollution to Climate Change. John Wiley & Sons.
Shen, G., Tao, S., Wei, S., Zhang, Y., Wang, R., Wang, B., Li, W., Shen, H., Huang, Y., Chen, Y., 2012. Emissions of parent, nitro, and oxygenated polycyclic aromatic hydrocarbons from residential wood combustion in rural China. Environ. Sci. Technol. 46, 8123–8130.
Shrivastava, M.K., Subramanian, R., Rogge, W.F., Robinson, A.L., 2007. Sources of organic aerosol: positive matrix factorization of molecular marker data and comparison of results from different source apportionment models. Atmos. Environ. 41, 9353–9369.
Simoneit, B.R., Schauer, J.J., Nolte, C., Oros, D.R., Elias, V.O., Fraser, M., Rogge, W., Cass, G.R., 1999a. Levoglucosan, a tracer for cellulose in biomass burning and atmospheric particles. Atmos. Environ. 33, 173–182.
Simoneit, B.R.T., Schauer, J.J., Nolte, C.G., Oros, D.R., Elias, V.O., Fraser, M.P., Rogge, W.F., Cass, G.R., 1999b. Levoglucosan, a tracer for cellulose in biomass burning and atmospheric particles. Atmos. Environ. 33, 173–182.
Singh, D.K., Gupta, T., 2016. Role of transition metals with water soluble organic carbon in the formation of secondary organic aerosol and metallo-organics in PM 1 sampled during post monsoon and pre-winter time. J. Aerosol Sci. 94, 56–69.
Singh, D.K., Gupta, T., 2017. Role of ammonium ion and transition metals in the formation of secondary organic aerosol and metallo-organic complex within fog processed ambient deliquescent submicron particles collected in central part of Indo-Gangetic Plain. Chemosphere 181, 725–737.
Singh, D.K., Kawamura, K., Yanase, A., Barrie, L.A., 2017. Distributions of polycyclic aromatic hydrocarbons, aromatic ketones, carboxylic acids, and trace metals in Arctic aerosols: long-range atmospheric transport, photochemical degradation/production at polar sunrise. Environ. Sci. Technol. 51, 8992–9004.
Song, C.H., Carmichael, G.R., 1999. The aging process of naturally emitted aerosol (sea-salt and mineral aerosol) during long range transport. Atmos. Environ. 33, 2203–2218.
Srimuruganandam, B., Shiva Nagendra, S.M., 2012. Application of positive matrix factorization in characterization of PM10 and PM2.5 emission sources at urban roadside. Chemosphere 88, 120–130.
Srivastava, D., Goel, A., Agrawal, M., 2016. Particle bound metals at major intersections in an urban location and source identification through use of metal markers. Proc. Natl. Acad. Sci., India, Sect. A 86, 209–220.
Srivastava, D., Favez, O., Bonnaire, N., Lucarelli, F., Perraudin, E., Gros, V., Villenave, E., Albinet, A. (in preparation). Speciation of organic fractions does matter for aerosol source apportionment. Part 2: intensive campaign in the Paris area (France). Sci. Total Environ.
Sternbeck, J., Sjödin, Å., Andréasson, K., 2002. Metal emissions from road traffic and the influence of resuspension—results from two tunnel studies. Atmos. Environ. 36, 4735–4744.
Surratt, J.D., Gómez-González, Y., Chan, A.W.H., Vermeylen, R., Shahgholi, M., Kleindienst, T.E., Edney, E.O., Offenberg, J.H., Lewandowski, M., Jaoui, M., Maenhaut, W., Claeys, M., Flagan, R.C., Seinfeld, J.H., 2008. Organosulfate formation in biogenic secondary organic aerosol. J. Phys. Chem. A 112, 8345–8378.
Tomaz, S., Shahpoury, P., Jaffrezo, J.-L., Lammel, G., Perraudin, E., Villenave, E., Albinet, A., 2016. One-year study of polycyclic aromatic compounds at an urban site in Grenoble (France): seasonal variations, gas/particle partitioning and cancer risk estimation. Sci. Total Environ. 565, 1071–1083.
Tomaz, S., Jaffrezo, J.-L., Favez, O., Perraudin, E., Villenave, E., Albinet, A., 2017. Sources and atmospheric chemistry of oxy- and nitro-PAHs in the ambient air of Grenoble (France). Atmos. Environ. 161, 144–154.
Tong, H., Arangio, A.M., Lakey, P.S.J., Berkemeier, T., Liu, F., Kampf, C.J., Brune, W.H., Pöschl, U., Shiraiwa, M., 2016. Hydroxyl radicals from secondary organic aerosol decomposition in water. Atmos. Chem. Phys. 16, 1761–1771.
Verma, S.K., Kawamura, K., Chen, J., Fu, P., 2017. Thirteen-years of observations on primary sugars and sugar alcohols over remote Chichijima Island in the western North Pacific. Atmos. Chem. Phys. 2017, 1–50.
Viana, M., Alastuey, A., Querol, X., Guerreiro, C., Vogt, M., Colette, A., Collet, S., Albinet, A., Fraboulet, I., Lacome, J.-M., 2015. Contribution of Residential Combustion to Ambient Air Pollution and Greenhouse Gas Emissions. ETC/ACM Technical Paper. 1.
Waked, A., Favez, O., Alleman, L.Y., Piot, C., Petit, J.E., Delaunay, T., Verlinden, E., Golly, B., Besombes, J.L., Jaffrezo, J.L., Leoz-Garziandia, E., 2014. Source apportionment of PM10 in a north-western Europe regional urban background site (Lens, France) using positive matrix factorization and including primary biogenic emissions. Atmos. Chem. Phys. 14, 3325–3346.
Walling, C., 1975. Fenton's reagent revisited. Acc. Chem. Res. 8, 125–131.
Wang, B., Knopf, D.A., 2011. Heterogeneous ice nucleation on particles composed of humic-like substances impacted by O_3. J. Geophys. Res.-Atmos. 116.
Wang, G., Chen, C., Li, J., Zhou, B., Xie, M., Hu, S., Kawamura, K., Chen, Y., 2011. Molecular composition and size distribution of sugars, sugar-alcohols and carboxylic acids in airborne particles during a severe urban haze event caused by wheat straw burning. Atmos. Environ. 45, 2473–2479.
Wang, Y., Hopke, P.K., Xia, X., Rattigan, O.V., Chalupa, D.C., Utell, M.J., 2012. Source apportionment of airborne particulate matter using inorganic and organic species as tracers. Atmos. Environ. 55, 525–532.
Yin, J., Allen, A., Harrison, R., Jennings, S., Wright, E., Fitzpatrick, M., Healy, T., Barry, E., Ceburnis, D., McCusker, D., 2005. Major component composition of urban PM 10 and PM 2.5 in Ireland. Atmos. Res. 78, 149–165.
Yttri, K.E., Simpson, D., Stenström, K., Puxbaum, H., Svendby, T., 2011. Source apportionment of the carbonaceous aerosol in Norway — quantitative estimates based on 14 C, thermal-optical and organic tracer analysis. Atmos. Chem. Phys. 11, 9375–9394.

Zhang, Y., Sheesley, R.J., Schauer, J.J., Lewandowski, M., Jaoui, M., Offenberg, J.H., Kleindienst, T.E., Edney, E.O., 2009. Source apportionment of primary and secondary organic aerosols using positive matrix factorization (PMF) of molecular markers. Atmos. Environ. 43, 5567–5574.

Zhao, R., Mungall, E.L., Lee, A.K.Y., Aljawhary, D., Abbatt, J.P.D., 2014. Aqueous-phase photooxidation of levoglucosan – a mechanistic study using aerosol time-of-flight chemical ionization mass spectrometry (aerosol ToF-CIMS). Atmos. Chem. Phys. 14, 9695–9706.

Zhou, S., Wenger, J.C., 2013a. Kinetics and products of the gas-phase reactions of acenaphthene with hydroxyl radicals, nitrate radicals and ozone. Atmos. Environ. 72, 97–104.

Zhou, S., Wenger, J.C., 2013b. Kinetics and products of the gas-phase reactions of acenaphthylene with hydroxyl radicals, nitrate radicals and ozone. Atmos. Environ. 75, 103–112.

Ziemann, P.J., Atkinson, R., 2012. Kinetics, products, and mechanisms of secondary organic aerosol formation. Chem. Soc. Rev. 41, 6582–6605.

SUPPLEMENTARY MATERIAL (SM)

Speciation of organic fraction does matter for source apportionment. Part 1: a one-year campaign in Grenoble (France).

D. Srivastava[1, 2, 3], S. Tomaz[1,2,3], O. Favez[1,*], G. M. Lanzafame[1], B. Golly [4,6], J.-L. Besombes[4], L. Y. Alleman[5], J.-L. Jaffrezo[6], V. Jacob[6], E. Perraudin[2, 3], E. Villenave[2, 3], A. Albinet[1,*]

[1]INERIS, Parc Technologique Alata, BP 2, 60550 Verneuil-en-Halatte, France

[2]CNRS, EPOC, UMR 5805 CNRS, 33405 Talence, France

[3]Université de Bordeaux, EPOC, UMR 5805 CNRS, 33405 Talence, France

[4]Univ. Savoie Mont Blanc, LCME, 73000 Chambéry, France

[5]IMT Lille Douai, SAGE, 59000 Lille, France

[6]Univ. Grenoble Alpes, CNRS, IRD, IGE, F-38000 Grenoble, France

[*] Correspondence to: alexandre.albinet@ineris.fr; olivier.favez@ineris.fr

Phone – +33 3 4455 6485; 6949

Submitted for publication to Science of the Total Environment

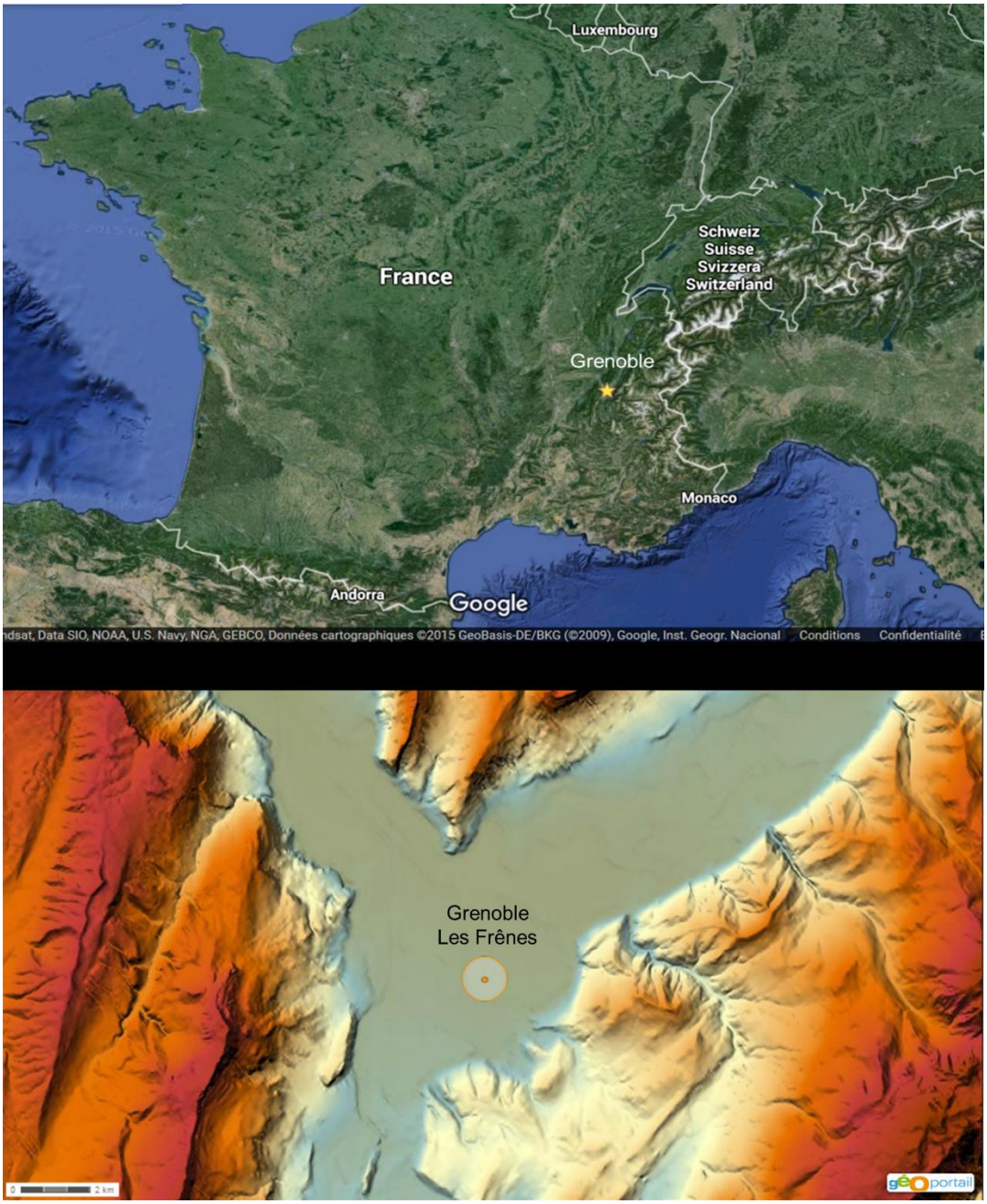

Figure S1. Map of France with the location of Grenoble and its relief.

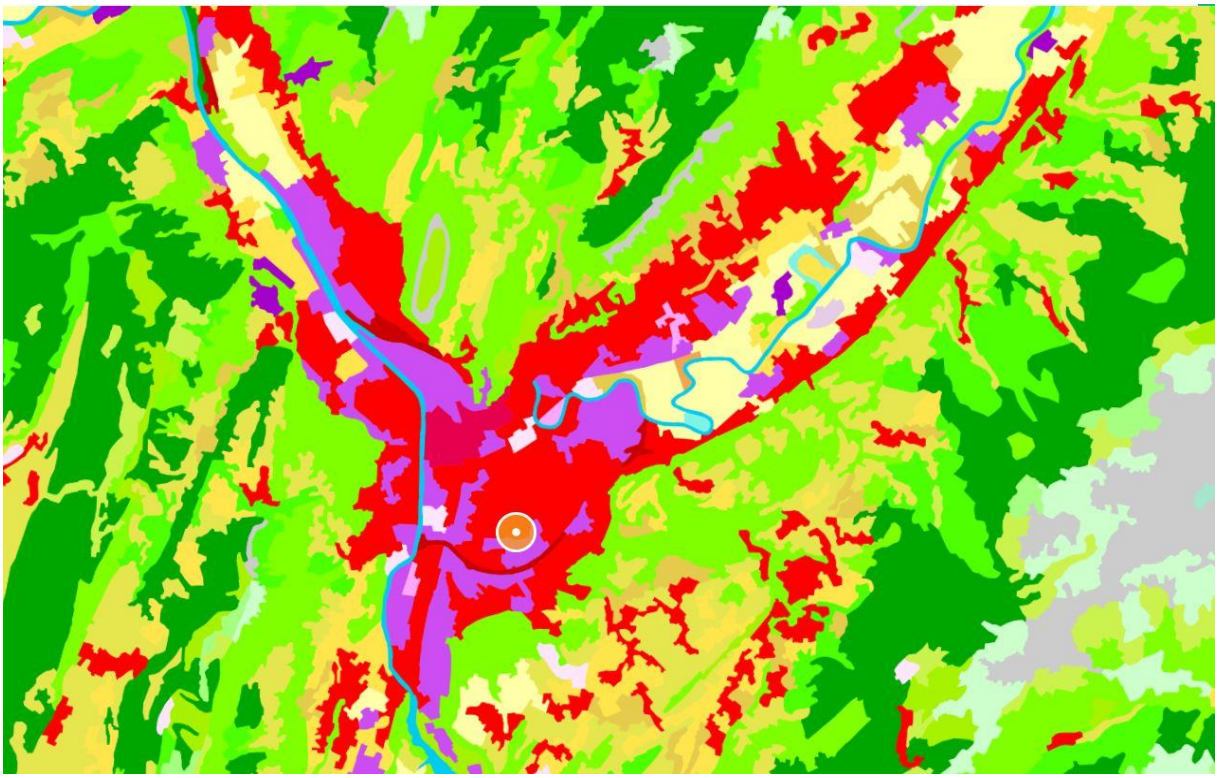

Figure S2. Map of the land cover around Grenoble. Urbanized area: red/purple/pink, forest area: green, agriculture/pasture area: yellow, sparsely vegetated area: grey (https://www.geoportail.gouv.fr).

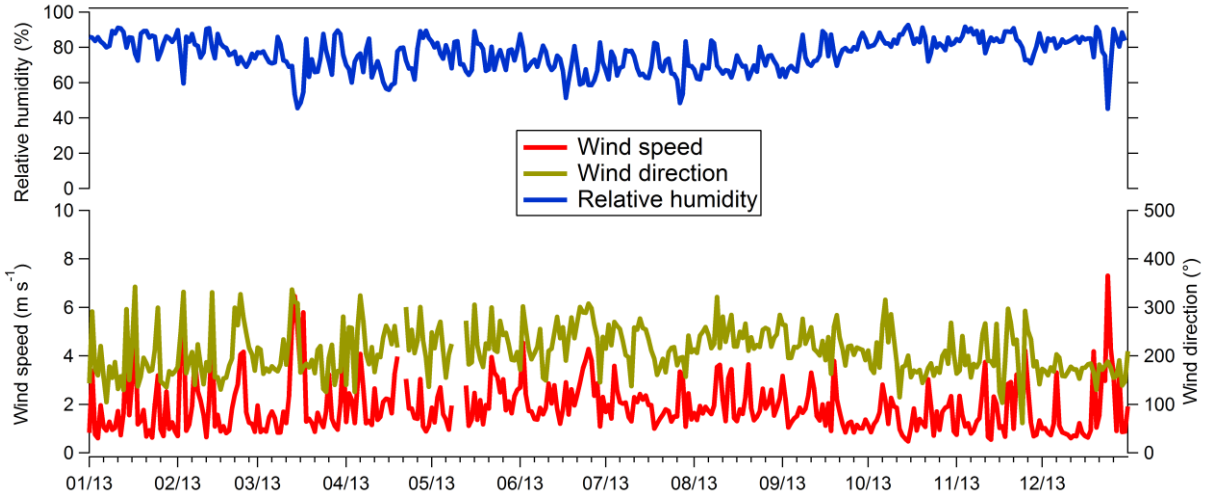

Figure S3. Temporal evolution of the meteorological parameters (wind direction, wind speed and relative humidity) at Grenoble, Les Frênes (2013).

Table S1. List of the chemicals, solvents and gases used and their characteristics.

Compounds	Supplier	Purity
3-Methyl-5-Nitrocatechol	Chiron	97 %
4-Methyl-5-Nitrocatechol	TRC	98 %
3-Methylbutane-1,2,3-tricarboxylic acid (MBTCA)	TRC	98 %
2,3-Dihydroxy-4-oxopentanoic acid (DHOPA)	TRC	98 %
2R, 3S-Dihydroxy-4-oxo-butanoic acid (DHOBA)	TRC	80 %
1,2,3,4-Cyclobutane tetracarboxylic acid	Sigma-Aldrich	98 %
Phthalic acid	Sigma-Aldrich	> 99.5 %
Pinonic acid	Sigma-Aldrich	98 %
Pinic acid	Santai labs	95 %
Succinic acid	Sigma-Aldrich	99 %
α-Methylglyceric acid (α-MGA)	Tractus	95 %
2-Methylerythritol (2-MT)	Sigma-Aldrich	90 %
β-Caryophyllinic acid	TRC	97 %
3-Hydroxyglutaric acid (3-HGA)	Santa Cruz Biotechnology	95%
Deuterated compounds		
Succinic-2,2,3,3-d4 acid	C/D/N isotopes	99 %
Meso-erythritol-1,1,2,4,4-d6	C/D/N isotopes	99.1 %
1,9-Nonanedioic-d14	C/D/N isotopes	99 %
Solvents		
Methanol	Sigma-Aldrich	> 99.9 %
Acetonitrile	VWR	> 99.9 %
Gases		
Helium	Air liquide	99.9 %
Nitrogen	Air liquide	99.9 %

Table S2. List of SOA markers quantified, selected monitored ions and instrumental limit of quantification (LQ) by GC/MS.

Compounds	***Retention time (min)***	***Monitored ions (m/z)***	***Dwell time (s)***	***Deuterated surrogate standards***	***Retention time (min)***	***Monitored ions (m/z)***	***Dwell time (s)***	***Instrumental LQs (pg injected)***
Succinic acid	20.62	129, 247	0.035	Succinic-2,2,3,3-d4 acid	20.51	147, 251	0.035	1.3
α-Methylglyceric acid (α-MGA)	20.69	219, 306	0.035					1.0
2,3-Dihydroxy-4-oxopentanoic acid (DHOPA)	25.71	218, 350	0.05					8.4
Pinonic acid	26.35	171, 125	0.05					2.2
3-Hydroxyglutaric acid (3-HGA)	27.24	349, 185	0.05					1.3
Pinic acid	29.53	129, 171	0.05					6.3
Phthalic acid	30.09	295, 221	0.05					0.9
2-Methylerythritol (2-MT)	26.67	219, 117	0.05	Meso-erythritol-1,1,2,4,4-d6	25.43	208, 220	0.1	1.1
3-Methylbutane-1,2,3-tricarboxylic acid (MBTCA)	31.31	204, 245	0.05	1,9-Nonanedioic-d14	32.12	331, 213	0.035	0.6
β-Caryophyllinic acid	37.06	117, 200	0.05					14.3
1,2,3,4-Cyclobutane tetracarboxylic acid	37.83	505, 387	0.05					0.3

Analysis of SOA markers

Sample extraction and derivatization.

Prior to extraction, a known amount of a mixture of surrogate standards containing 3 deuterated compounds (Table S1) were added to the filter samples (20 µL of a solution at 1 ng μL^{-1} in acetonitrile) and were used for the quantification of SOA markers (Table S2). Filter punches (∅=47 mm) for SOA analysis were extracted using a QuEChERS (Quick Easy Cheap Effective Rugged and Safe) like procedure developed previously for the analysis of particulate bound PAH and PAH derivatives (Albinet et al., 2014; Albinet et al., 2013). Punches were placed in centrifuge glass tubes, spiked with known amounts of surrogate standards and extracted with methanol (MeOH, 7 mL) using a multi-tube vortexer (DVX-2500, VWR) for 1.5 min. After extraction, samples were centrifuged for 5 min at 4500 rpm (Sigma 3-16 PK centrifuge). Supernatant extracts were collected and reduced to dryness under a gentle nitrogen stream to avoid the presence of hydroxyl group prior to derivatization. Extracts were dissolved into 50 µL of acetonitrile and subjected to derivatization (silylation) for 30 minutes at 60°C after addition of 50 µL of *N*-Methyl-*N*-(trimethylsilyl) trifluoroacetamide (MSTFA) with 10% trimethyl-chlorosilane (TMS). Before injection into the GC/MS for analysis, pentadecane-d32 was added to the extracts (5 µL of a solution at 10 ng μL^{-1} in acetonitrile) and used as internal standard to evaluate the surrogate recoveries in the samples.

Sample analysis.

The quantification of 11 SOA markers was achieved using GC/MS (Agilent 7890A GC coupled to 5975C MS) in electron ionisation mode (EI, 70 eV). 2 µL of the extracts were injected in the splitless mode. Compounds were separated on a DB-5MS-column (Agilent

J&W, 60 m × 0.25 mm × 0.25 μm) using the following temperature program: held at 70 °C for 1 min, then ramped to 260 °C at 5 °C min^{-1}, followed by a ramp to 290 °C at 20 °C min^{-1}, further followed by a ramp to 300 °C at 5 °C min^{-1}, then ramped to 320°C at 10 °C min^{-1} and subsequently held for 10 min. The carrier gas (He) flow was set to 1.5 mL min^{-1} throughout the analysis and transfer line heated at 320 °C. The ion source, ion trap, and interface temperatures were 200, 200, and 300 °C, respectively. Analyses were performed in selected ion monitoring mode (SIM). SOA markers were quantified using ten points' internal standard calibration curves. All SOA marker compounds were quantified using authentic standards. LQ is defined as the lowest concentrations of the compound that can be quantified with a signal to noise ratio of 10. The lowest point of the calibration range has been used to make these calculations (Table S2).

Table S3. Annual mean, min-max, concentrations (ng m^{-3}) and signal/noise ratios (S/N) of all individual species quantified in this study (n=123 for PM_{10} filter samples).

Species	Annual concentrations	Min	Max	S/N
O_3	$3.41\times10^{+04}$	$3.00\times10^{+02}$	$8.30\times10^{+04}$	$1.00\times10^{+01}$
NO	$9.94\times10^{+03}$	$0.00\times10^{+00}$	$1.08\times10^{+05}$	$8.70\times10^{+00}$
NO_2	$2.21\times10^{+04}$	$5.00\times10^{+03}$	$5.80\times10^{+04}$	$1.00\times10^{+01}$
PM_{10}	$2.39\times10^{+04}$	$2.00\times10^{+03}$	$7.50\times10^{+04}$	$1.00\times10^{+01}$
$PM_{2.5}$	$1.60\times10^{+04}$	$1.00\times10^{+03}$	$6.20\times10^{+04}$	$1.00\times10^{+01}$
OC	$5.57\times10^{+03}$	$9.20\times10^{+02}$	$1.75\times10^{+04}$	$1.00\times10^{+01}$
EC	$1.56\times10^{+03}$	$1.77\times10^{+02}$	$7.80\times10^{+03}$	$1.00\times10^{+01}$
HuLiS	$8.60\times10^{+02}$	$8.91\times10^{+01}$	$3.55\times10^{+03}$	$4.60\times10^{+00}$
Na^+	$1.79\times10^{+02}$	$1.55\times10^{+01}$	$1.20\times10^{+03}$	$1.00\times10^{+01}$
NH_4^+	$1.23\times10^{+03}$	$3.91\times10^{+01}$	$7.17\times10^{+03}$	$5.30\times10^{+00}$
K^+	$2.12\times10^{+02}$	$8.26\times10^{+00}$	$7.35\times10^{+03}$	$1.00\times10^{+01}$
Mg^{2+}	$2.73\times10^{+01}$	$2.50\times10^{+00}$	$4.10\times10^{+02}$	$7.80\times10^{+00}$
Ca^{2+}	$4.18\times10^{+02}$	$4.07\times10^{+01}$	$1.65\times10^{+03}$	$3.00\times10^{+00}$
Methanesulfonic acid (MSA)	$2.36\times10^{+01}$	8.05×10^{-02}	$2.32\times10^{+02}$	$2.80\times10^{+00}$
Cl^-	$1.36\times10^{+02}$	$3.59\times10^{+00}$	$1.10\times10^{+03}$	$9.60\times10^{+00}$
NO_3^-	$2.78\times10^{+03}$	$2.44\times10^{+01}$	$1.89\times10^{+04}$	$1.00\times10^{+01}$
SO_4^{2-}	$1.96\times10^{+03}$	$1.33\times10^{+02}$	$9.92\times10^{+03}$	$7.70\times10^{+00}$
Oxalate	$9.91\times10^{+01}$	$1.03\times10^{+00}$	$4.03\times10^{+02}$	$3.90\times10^{+00}$
Levoglucosan (Levo)	$4.47\times10^{+02}$	$8.77\times10^{+00}$	$2.96\times10^{+03}$	$9.90\times10^{+00}$
Mannosan	$3.85\times10^{+01}$	5.11×10^{-01}	$3.23\times10^{+02}$	$9.30\times10^{+00}$
Galactosan	$1.52\times10^{+01}$	1.67×10^{-04}	$1.10\times10^{+02}$	$8.50\times10^{+00}$
Arabitol	$2.23\times10^{+01}$	$1.95\times10^{+00}$	$9.66\times10^{+01}$	$8.30\times10^{+00}$
Sorbitol	$1.82\times10^{+00}$	1.96×10^{-02}	$1.01\times10^{+01}$	$2.50\times10^{+00}$
Mannitol	$2.24\times10^{+01}$	3.35×10^{-01}	$1.29\times10^{+02}$	$7.50\times10^{+00}$
Glucose	$2.99\times10^{+01}$	$3.20\times10^{+00}$	$9.95\times10^{+01}$	$1.00\times10^{+01}$
1-Methylnaphthalene	9.17×10^{-02}	5.62×10^{-03}	$3.58\times10^{+00}$	$2.70\times10^{+00}$
2-Methylnaphthalene	2.43×10^{-02}	$0.00\times10^{+00}$	6.23×10^{-01}	9.00×10^{-01}
Acenaphthene	1.32×10^{-02}	$0.00\times10^{+00}$	2.08×10^{-01}	$1.30\times10^{+00}$
Fluorene	1.90×10^{-02}	5.62×10^{-03}	5.72×10^{-01}	$1.40\times10^{+00}$
Phenanthrene	1.90×10^{-01}	3.25×10^{-02}	$5.56\times10^{+00}$	$3.80\times10^{+00}$
Anthracene	1.84×10^{-02}	5.62×10^{-03}	4.77×10^{-01}	$1.40\times10^{+00}$
Fluoranthene	3.01×10^{-01}	2.51×10^{-02}	$2.60\times10^{+00}$	$4.60\times10^{+00}$
2-Methylfluoranthene	3.03×10^{-02}	5.62×10^{-03}	1.65×10^{-01}	$2.30\times10^{+00}$
Pyrene	3.00×10^{-01}	2.69×10^{-02}	$2.10\times10^{+00}$	$3.70\times10^{+00}$
Chrysene	2.29×10^{-01}	6.35×10^{-03}	$2.38\times10^{+00}$	$6.00\times10^{+00}$
Benzo[a]anthracene	4.60×10^{-01}	2.78×10^{-02}	$4.55\times10^{+00}$	$8.20\times10^{+00}$
Retene	1.23×10^{-01}	5.62×10^{-03}	$1.21\times10^{+00}$	$2.70\times10^{+00}$
Benzo[e]pyrene	4.34×10^{-01}	6.49×10^{-03}	$3.99\times10^{+00}$	$4.70\times10^{+00}$
Benzo[j]fluoranthene	3.16×10^{-01}	5.62×10^{-03}	$2.15\times10^{+00}$	$5.10\times10^{+00}$
Benzo[b]fluoranthene	5.81×10^{-01}	2.12×10^{-02}	$4.98\times10^{+00}$	$6.00\times10^{+00}$
Benzo[k]fluoranthene	2.19×10^{-01}	6.35×10^{-03}	$1.75\times10^{+00}$	$4.00\times10^{+00}$
Benzo[a]pyrene (B[a]P)	4.16×10^{-01}	6.37×10^{-03}	$3.54\times10^{+00}$	$4.00\times10^{+00}$
Dibenzo[a,h]anthracene	9.08×10^{-02}	5.62×10^{-03}	8.02×10^{-01}	$2.20\times10^{+00}$
Benzo[g,h,i]perylene (B[g,h,i])P)	4.44×10^{-01}	1.86×10^{-02}	$3.12\times10^{+00}$	$4.40\times10^{+00}$
Indeno[1,2,3-cd]pyrene (In[1,2,3-cd]P)	5.22×10^{-01}	1.70×10^{-02}	$3.41\times10^{+00}$	$3.90\times10^{+00}$
Coronene (Cor)	1.51×10^{-01}	6.49×10^{-03}	8.58×10^{-01}	$7.70\times10^{+00}$
Phthaldialdehyde	4.25×10^{-03}	4.60×10^{-04}	2.73×10^{-02}	$1.00\times10^{+01}$
Phthalic anhydride	$1.31\times10^{+00}$	1.01×10^{-05}	$4.24\times10^{+01}$	$2.20\times10^{+00}$
1,4-Naphthoquinone	5.81×10^{-03}	7.47×10^{-06}	4.07×10^{-02}	$2.60\times10^{+00}$
1-Naphthaldehyde	2.17×10^{-02}	4.23×10^{-05}	1.75×10^{-01}	$9.00\times10^{+00}$

2-Formyl trans cinnamaldehyde	1.68×10^{-03}	2.61×10^{-05}	1.82×10^{-02}	$2.10\times10^{+00}$
1-Acenaphthenone	2.59×10^{-02}	8.22×10^{-05}	4.72×10^{-01}	$1.50\times10^{+00}$
9-Fluorenone	3.32×10^{-02}	2.37×10^{-05}	6.87×10^{-01}	$5.90\times10^{+00}$
1,2-Naphthalic anhydride	5.52×10^{-01}	1.63×10^{-05}	$2.35\times10^{+01}$	$2.50\times10^{+00}$
Xanthone	1.50×10^{-02}	1.33×10^{-04}	3.53×10^{-01}	$2.60\times10^{+00}$
Acenaphthenequinone	1.37×10^{-02}	2.53×10^{-04}	2.68×10^{-01}	$2.50\times10^{+00}$
6H-Dibenzo [b,d] pyran-6-one (6H-DPone)	9.47×10^{-02}	3.36×10^{-04}	$2.27\times10^{+00}$	$2.20\times10^{+00}$
9,10-Anthraquinone	2.46×10^{-01}	2.49×10^{-06}	$4.18\times10^{+00}$	$8.80\times10^{+00}$
1,8-Naphthalic anhydride	$1.09\times10^{+00}$	1.05×10^{-05}	$3.41\times10^{+01}$	$3.10\times10^{+00}$
1,4-Anthraquinone	1.14×10^{-02}	2.78×10^{-05}	4.15×10^{-01}	$6.10\times10^{+00}$
2-Methylanthraquinone	1.05×10^{-01}	7.92×10^{-04}	$2.39\times10^{+00}$	$1.00\times10^{+01}$
9-Phenanthrenecarboxaldehyde	1.72×10^{-02}	2.74×10^{-05}	6.69×10^{-01}	$9.80\times10^{+00}$
9,10-Phenanthrenequinone	2.02×10^{-02}	2.86×10^{-05}	3.79×10^{-01}	8.00×10^{-01}
Benzo[a]fluorenone	1.66×10^{-01}	1.16×10^{-03}	$4.67\times10^{+00}$	$6.10\times10^{+00}$
Benzo[b]fluorenone	2.79×10^{-01}	3.81×10^{-03}	$5.71\times10^{+00}$	$4.50\times10^{+00}$
Benzanthrone	7.61×10^{-01}	4.32×10^{-03}	$1.42\times10^{+01}$	$3.10\times10^{+00}$
1-Pyrenecarboxaldehyde	4.53×10^{-02}	2.29×10^{-04}	$1.26\times10^{+00}$	$4.60\times10^{+00}$
Aceanthrenequinone	2.38×10^{-02}	9.54×10^{-05}	5.58×10^{-01}	$2.30\times10^{+00}$
Benz[a]anthracene-7,12-dione	1.40×10^{-01}	2.85×10^{-03}	$2.51\times10^{+00}$	$5.20\times10^{+00}$
1-Nitronaphthalene	4.59×10^{-04}	6.23×10^{-06}	2.87×10^{-03}	$5.70\times10^{+00}$
2-Methyl-1-nitronaphthalene+ 1-Methyl-5-nitronaphthalene	1.29×10^{-04}	1.25×10^{-06}	9.62×10^{-04}	$8.40\times10^{+00}$
2-Nitronaphthalene	3.72×10^{-04}	1.25×10^{-05}	1.72×10^{-03}	$9.20\times10^{+00}$
2-Methyl-4-nitronaphthalene	1.43×10^{-04}	4.98×10^{-06}	6.21×10^{-04}	$1.80\times10^{+00}$
1-Methyl-4-nitronaphthalene	2.96×10^{-04}	1.39×10^{-05}	1.68×10^{-03}	$2.40\times10^{+00}$
1-Methyl-6-nitronaphthalene	1.64×10^{-04}	1.67×10^{-05}	8.72×10^{-04}	$2.00\times10^{+00}$
1,5-Dinitronaphthalene	4.38×10^{-04}	7.64×10^{-06}	4.91×10^{-03}	$5.10\times10^{+00}$
2-Nitrobiphenyl	1.94×10^{-05}	1.87×10^{-05}	2.08×10^{-05}	$3.40\times10^{+00}$
3-Nitrobiphenyl	3.88×10^{-05}	3.73×10^{-05}	4.16×10^{-05}	$3.60\times10^{+00}$
3-Nitrodibenzofuran	1.18×10^{-03}	5.11×10^{-05}	1.94×10^{-02}	$1.30\times10^{+00}$
5-Nitroacenaphthene	3.59×10^{-03}	1.30×10^{-05}	3.80×10^{-02}	$3.80\times10^{+00}$
2-Nitro-9-fluorenone	2.10×10^{-03}	1.91×10^{-05}	6.98×10^{-02}	$2.60\times10^{+00}$
2-Nitrofluorene	7.76×10^{-05}	7.47×10^{-05}	8.33×10^{-05}	$3.10\times10^{+00}$
9-Nitroanthracene	3.84×10^{-02}	4.29×10^{-05}	4.30×10^{-01}	$3.10\times10^{+00}$
9-Nitrophenanthrene	3.08×10^{-04}	9.13×10^{-06}	2.77×10^{-03}	$4.40\times10^{+00}$
2-Nitrodibenzothiophene	3.36×10^{-04}	1.14×10^{-05}	1.87×10^{-02}	$1.30\times10^{+00}$
3-Nitrophenanthrene	1.36×10^{-03}	1.03×10^{-05}	6.07×10^{-03}	$5.80\times10^{+00}$
2-Nitroanthracene	7.18×10^{-04}	3.15×10^{-05}	9.62×10^{-03}	2.00×10^{-01}
9-Methyl-10-nitroanthracene	2.75×10^{-03}	1.01×10^{-05}	5.45×10^{-02}	5.00×10^{-01}
2+3-Nitrofluoranthene	4.16×10^{-02}	1.16×10^{-03}	2.60×10^{-01}	$1.00\times10^{+01}$
4-Nitropyrene	1.77×10^{-04}	1.12×10^{-05}	2.09×10^{-03}	$1.00\times10^{+00}$
1-Nitropyrene (1-NP)	6.78×10^{-03}	3.57×10^{-04}	4.56×10^{-02}	$3.50\times10^{+00}$
2-Nitropyrene	4.25×10^{-03}	1.14×10^{-04}	3.13×10^{-02}	$3.40\times10^{+00}$
7-Nitrobenz[a]anthracene	1.45×10^{-02}	1.57×10^{-05}	8.07×10^{-02}	$3.30\times10^{+00}$
6-Nitrochrysene	1.77×10^{-04}	9.86×10^{-06}	1.44×10^{-03}	$1.30\times10^{+00}$
1,3-Dinitropyrene	1.10×10^{-04}	6.07×10^{-05}	1.05×10^{-03}	1.00×10^{-01}
1,6-Dinitropyrene	1.56×10^{-04}	3.56×10^{-05}	6.03×10^{-03}	7.00×10^{-01}
1,8-Dinitropyrene	9.62×10^{-05}	3.51×10^{-05}	1.35×10^{-03}	1.00×10^{-01}
1-Nitrobenzo[e]pyrene	2.94×10^{-04}	1.38×10^{-05}	3.14×10^{-03}	$2.00\times10^{+00}$
6-Nitrobenzo[a]pyrene	3.80×10^{-04}	1.27×10^{-05}	2.10×10^{-03}	$5.00\times10^{+00}$
3-Nitrobenzo[e]pyrene	9.62×10^{-04}	4.41×10^{-05}	8.96×10^{-03}	$2.70\times10^{+00}$
As	6.26×10^{-01}	1.16×10^{-03}	$2.87\times10^{+00}$	$9.00\times10^{+00}$
Ba	$9.04\times10^{+00}$	1.58×10^{-03}	$1.95\times10^{+02}$	$9.90\times10^{+00}$
Cd	1.94×10^{-01}	1.40×10^{-02}	$1.12\times10^{+00}$	$1.00\times10^{+01}$
Ce	3.57×10^{-01}	3.85×10^{-02}	$1.84\times10^{+00}$	$1.00\times10^{+01}$
Co	1.72×10^{-01}	4.62×10^{-05}	6.87×10^{-01}	$9.90\times10^{+00}$
Cs	7.20×10^{-02}	1.00×10^{-02}	2.58×10^{-01}	$1.00\times10^{+01}$

Cu	$1.78\times10^{+01}$	$1.51\times10^{+00}$	$1.70\times10^{+02}$	$1.00\times10^{+01}$
Hg	3.30×10^{-02}	1.03×10^{-03}	1.04×10^{-01}	$5.50\times10^{+00}$
La	1.43×10^{-01}	1.80×10^{-02}	5.92×10^{-01}	$1.00\times10^{+01}$
Li	1.65×10^{-01}	1.65×10^{-02}	6.83×10^{-01}	$5.60\times10^{+00}$
Mn	$9.02\times10^{+00}$	$1.06\times10^{+00}$	$4.19\times10^{+01}$	$1.00\times10^{+01}$
Mo	$1.07\times10^{+00}$	3.53×10^{-02}	$7.45\times10^{+00}$	$1.00\times10^{+01}$
Ni	$1.71\times10^{+00}$	7.43×10^{-02}	$1.46\times10^{+01}$	$1.00\times10^{+01}$
Pb	$1.02\times10^{+01}$	6.38×10^{-01}	$9.88\times10^{+01}$	$1.00\times10^{+01}$
Rb	$1.34\times10^{+00}$	2.58×10^{-01}	$5.00\times10^{+00}$	$1.00\times10^{+01}$
Sb	$1.28\times10^{+00}$	1.09×10^{-02}	$1.56\times10^{+01}$	$1.00\times10^{+01}$
Se	6.32×10^{-01}	8.39×10^{-03}	$2.59\times10^{+00}$	$1.00\times10^{+01}$
Sn	$2.65\times10^{+00}$	2.35×10^{-01}	$1.70\times10^{+01}$	$5.30\times10^{+00}$
Sr	$2.63\times10^{+00}$	2.66×10^{-01}	$7.73\times10^{+01}$	$1.00\times10^{+01}$
Th	2.49×10^{-02}	1.21×10^{-04}	1.60×10^{-01}	$1.00\times10^{+01}$
Ti	$7.52\times10^{+00}$	1.13×10^{-02}	$4.14\times10^{+01}$	$9.90\times10^{+00}$
Tl	8.39×10^{-02}	5.37×10^{-03}	5.84×10^{-01}	$5.80\times10^{+00}$
U	1.35×10^{-02}	1.32×10^{-05}	1.32×10^{-01}	$9.90\times10^{+00}$
Zn	$3.58\times10^{+01}$	$1.53\times10^{+00}$	$2.37\times10^{+02}$	$1.00\times10^{+01}$
Bi	3.80×10^{-01}	1.26×10^{-02}	$5.00\times10^{+00}$	$5.70\times10^{+00}$
Cr	$7.15\times10^{+00}$	5.03×10^{-03}	$3.18\times10^{+01}$	$5.70\times10^{+00}$
Sc	3.58×10^{-02}	6.24×10^{-05}	2.21×10^{-01}	$5.80\times10^{+00}$
V	$1.04\times10^{+00}$	5.39×10^{-02}	$5.83\times10^{+00}$	$1.00\times10^{+01}$
Al	$2.30\times10^{+02}$	$6.61\times10^{+00}$	$1.59\times10^{+03}$	$1.40\times10^{+00}$
Ca	$5.76\times10^{+02}$	$3.72\times10^{+01}$	$2.59\times10^{+03}$	$1.20\times10^{+00}$
Fe	$3.56\times10^{+02}$	$3.05\times10^{+01}$	$1.50\times10^{+03}$	$1.00\times10^{+01}$
K	$4.97\times10^{+02}$	$7.85\times10^{+01}$	$1.16\times10^{+04}$	$4.50\times10^{+00}$
Mg	$6.19\times10^{+01}$	$5.15\times10^{+00}$	$5.56\times10^{+02}$	$9.40\times10^{+00}$
Na	$3.38\times10^{+02}$	$3.90\times10^{+01}$	$2.00\times10^{+03}$	$7.70\times10^{+00}$
Tridecane (C13)	1.91×10^{-01}	6.69×10^{-04}	7.33×10^{-01}	$1.20\times10^{+00}$
Tetradecane (C14)	6.66×10^{-02}	5.09×10^{-03}	9.27×10^{-01}	$3.30\times10^{+00}$
Pentadecane (C15)	7.24×10^{-02}	1.50×10^{-02}	$1.06\times10^{+00}$	9.00×10^{-01}
Hexadecane (C16)	2.04×10^{-01}	4.69×10^{-03}	$2.53\times10^{+00}$	$2.20\times10^{+00}$
Heptadecane (C17)	1.06×10^{-01}	1.02×10^{-03}	6.23×10^{-01}	7.00×10^{-01}
n-Octadecane (C18)	6.54×10^{-02}	1.52×10^{-03}	3.56×10^{-01}	$1.80\times10^{+00}$
n-Nonadecane (C19)	8.11×10^{-02}	9.16×10^{-03}	3.59×10^{-01}	$2.20\times10^{+00}$
n-Eicosane (C20)	1.14×10^{-01}	6.89×10^{-04}	9.64×10^{-01}	$1.90\times10^{+00}$
n-Heneicosane (C21)	5.13×10^{-01}	1.46×10^{-01}	$1.83\times10^{+00}$	$4.00\times10^{+00}$
n-Docosane (C22)	6.90×10^{-01}	6.72×10^{-04}	$6.64\times10^{+00}$	$3.40\times10^{+00}$
n-Tricosane (C23)	$1.27\times10^{+00}$	7.96×10^{-02}	$8.58\times10^{+00}$	$4.50\times10^{+00}$
n-Tetracosane (C24)	$1.26\times10^{+00}$	7.99×10^{-02}	$1.02\times10^{+01}$	$4.70\times10^{+00}$
n-Pentacosane (C25)	$1.52\times10^{+00}$	2.52×10^{-01}	$6.78\times10^{+00}$	$5.80\times10^{+00}$
n-Hexacosane (C26)	8.39×10^{-01}	6.10×10^{-02}	$4.64\times10^{+00}$	$7.50\times10^{+00}$
n-Heptacosane (C27)	$1.65\times10^{+00}$	1.76×10^{-01}	$5.68\times10^{+00}$	$8.20\times10^{+00}$
n-Octacosane (C28)	5.34×10^{-01}	3.03×10^{-02}	$2.63\times10^{+00}$	$9.00\times10^{+00}$
n-Nonaconsane (C29)	$2.02\times10^{+00}$	1.48×10^{-01}	$7.14\times10^{+00}$	$9.10\times10^{+00}$
n-Triacontane (C30)	3.87×10^{-01}	6.19×10^{-04}	$2.06\times10^{+00}$	$9.30\times10^{+00}$
n-Hentriacontane (C31)	$1.50\times10^{+00}$	7.91×10^{-02}	$4.95\times10^{+00}$	$9.50\times10^{+00}$
n-Dotriacontane (C32)	2.74×10^{-01}	1.04×10^{-03}	$1.27\times10^{+00}$	$9.60\times10^{+00}$
n-tritriacontane (C33)	6.64×10^{-01}	1.51×10^{-02}	$2.39\times10^{+00}$	$7.80\times10^{+00}$
n-Tetratriacontane (C34)	1.42×10^{-01}	2.22×10^{-02}	9.68×10^{-01}	$1.20\times10^{+00}$
n-Pentatriacontane (C35)	1.86×10^{-01}	2.10×10^{-02}	6.11×10^{-01}	$1.70\times10^{+00}$
n-Hexatriacontane (C36)	1.64×10^{-01}	4.50×10^{-03}	$1.26\times10^{+01}$	3.00×10^{-01}
Heptatriacontane (C37)	6.29×10^{-02}	8.80×10^{-03}	4.16×10^{-01}	3.00×10^{-01}
Octatriacontane (C38)	4.79×10^{-02}	8.37×10^{-04}	4.66×10^{-01}	2.00×10^{-01}
Nonatriacontane (C39)	3.96×10^{-02}	3.61×10^{-04}	2.55×10^{-01}	1.00×10^{-01}
Pristane	4.61×10^{-02}	1.08×10^{-03}	3.09×10^{-01}	$1.70\times10^{+00}$
Phytane	2.45×10^{-02}	1.1710^{-03}	1.12×10^{-01}	$2.20\times10^{+00}$

Dibenzothiophene (DBT)	5.11×10^{-03}	4.49×10^{-04}	1.18×10^{-01}	2.00×10^{-01}
Phenanthro[4,5-bcd]thiophene (PheT (4,5))	7.92×10^{-03}	1.06×10^{-03}	1.61×10^{-01}	4.00×10^{-01}
Benzo[b]naphtho[2,1-d]thiophene (BNT (2,1))	1.59×10^{-02}	1.03×10^{-03}	1.55×10^{-01}	$1.40\times10^{+00}$
Benzo[b]naphtho[1,2-d]thiophene (BNT (1,2))	8.17×10^{-03}	8.15×10^{-04}	5.00×10^{-02}	6.00×10^{-01}
Benzo[b]naphtho[2,3-d]thiophene (BNT (2,3))	1.72×10^{-02}	6.02×10^{-04}	8.67×10^{-02}	2.00×10^{-01}
Trisnorneohopane (HP1)	2.38×10^{-02}	3.30×10^{-03}	1.92×10^{-01}	$2.00\times10^{+00}$
17α(H)-trisnorhopane (HP2)	2.88×10^{-02}	3.50×10^{-03}	2.33×10^{-01}	$2.30\times10^{+00}$
17α(H),21β(H)-norhopane (HP3)	1.12×10^{-01}	3.50×10^{-03}	7.40×10^{-01}	$6.80\times10^{+00}$
17α(H),21β(H)-hopane (HP4)	8.98×10^{-02}	3.50×10^{-03}	5.08×10^{-01}	$6.40\times10^{+00}$
22S,17α(H),21β(H)-homohopane (HP5)	4.12×10^{-02}	3.50×10^{-03}	2.16×10^{-01}	$3.70\times10^{+00}$
22R,17α(H),21β(H)-homohopane (HP6)	3.28×10^{-02}	2.34×10^{-03}	2.11×10^{-01}	$3.00\times10^{+00}$
22S,17α(H),21β(H)-bishomohopane (HP7)	3.43×10^{-02}	8.76×10^{-04}	1.84×10^{-01}	$3.10\times10^{+00}$
22R,17α(H),21β(H)-bishomohopane (HP8)	2.35×10^{-02}	8.76×10^{-04}	1.28×10^{-01}	$2.20\times10^{+00}$
22R,17α(H),21β(H)-bishomohopane (HP9)	1.95×10^{-02}	3.50×10^{-03}	1.02×10^{-01}	$1.80\times10^{+00}$
22R,17α(H),21β(H)-trishomohopane (HP10)	1.15×10^{-02}	3.50×10^{-03}	9.53×10^{-02}	7.00×10^{-01}
Vanillin	8.23×10^{-01}	5.85×10^{-02}	$5.71\times10^{+00}$	$2.90\times10^{+00}$
Coniferylaldehyde (Coniferald.)	$2.15\times10^{+00}$	2.74×10^{-01}	$2.36\times10^{+01}$	$2.20\times10^{+00}$
Vanillic acid	$2.59\times10^{+00}$	8.75×10^{-02}	$2.43\times10^{+01}$	$4.40\times10^{+00}$
Acetosyringone	$4.62\times10^{+00}$	1.38×10^{-01}	$6.99\times10^{+01}$	$3.40\times10^{+00}$
Syringic acid	$4.41\times10^{+00}$	3.97×10^{-02}	$5.46\times10^{+01}$	$4.60\times10^{+00}$
Succinic acid	$1.06\times10^{+01}$	6.62×10^{-06}	$6.00\times10^{+01}$	$5.40\times10^{+00}$
α-Methylglyceric acid (α-MGA)	$1.41\times10^{+00}$	1.10×10^{-05}	$9.14\times10^{+00}$	$9.20\times10^{+00}$
2,3-Dihydroxy-4-oxopentanoic acid (DHOPA)	$4.92\times10^{+00}$	3.22×10^{-01}	$7.01\times10^{+01}$	$1.00\times10^{+01}$
Pinonic acid	$1.35\times10^{+01}$	5.57×10^{-01}	$2.18\times10^{+02}$	$2.60\times10^{+00}$
3-Hydroxyglutaric acid (3-HGA)	$4.72\times10^{+00}$	2.31×10^{-01}	$2.32\times10^{+01}$	$6.50\times10^{+00}$
Pinic acid	$4.88\times10^{+00}$	5.24×10^{-01}	$5.91\times10^{+01}$	$4.90\times10^{+00}$
Phthalic acid	$3.58\times10^{+00}$	2.19×10^{-01}	$4.94\times10^{+01}$	$4.00\times10^{+00}$
4-Methyl-5-nitrocathecol	$1.57\times10^{+01}$	2.91×10^{-05}	$1.70\times10^{+02}$	$2.70\times10^{+00}$
3-Methyl-5-nitrocathecol	$1.55\times10^{+01}$	1.04×10^{-05}	$1.93\times10^{+02}$	$1.70\times10^{+00}$
2-Methylerythritol (2-MT)	$7.20\times10^{+00}$	2.00×10^{-01}	$4.89\times10^{+01}$	$5.70\times10^{+00}$
3-Methylbutane-1,2,3-tricarboxylic acid (MBTCA)	$4.78\times10^{+00}$	8.65×10^{-06}	$6.96\times10^{+01}$	$4.00\times10^{+00}$

Selection of the species in the input matrix

Oxalate is the most abundant dicarboxylic acid identified in aerosols (Kawamura and Ikushima, 1993). It can be primarily emitted from fossil fuel combustion, biomass burning, and biogenic activity. In addition, a large fraction of aerosol oxalate is probably produced from photochemical oxidation of VOCs such as ethene, toluene, isoprene, etc. (Carlton et al., 2007; Carlton et al., 2009; Jiang et al., 2011; Sullivan and Prather, 2007; Warneck, 1999). Thus, oxalate is considered as marker of secondary processes. In the present study, an initial PMF analysis showed that oxalate was poorly fitted by the model (large or nonnormally distributed scaled residuals, between +8 to -8, were obtained). Subsequent runs were performed down-weighting the species but results still showed large residual and a very poor correlation between measured and predicted concentrations of oxalate ($r<0.30$). Oxalate was then excluded of the final PMF input species.

MSA (methanesulfonic acid) has been successfully used in several source apportionment studies to account marine aerosol contribution (Laing et al., 2015; Schembari et al., 2014; Srimuruganandam and Shiva Nagendra, 2012) as dimethylsulfide (DMS), precursor of MSA, primarily originated from phytoplankton in the sea (Bates et al., 1992). Initial PMF runs showed the inclusion of MSA with other source factors. The increase in the number of factors did not resolve this issue. The additional factor obtained had no any geochemical and atmospheric chemistry significance. This issue could be very site-specific and vary according to the location. Grenoble is located far away from the sea (~200-500 km). and could explain that the apportionment of the marine contribution was not possible to achieve using MSA.

Methyl-nitrocatechols are potential markers of the formation of SOA from biomass burning especially from the oxidation of phenolic compounds (Iinuma et al., 2010). Results of

the inclusion of these species in PMF matrix showed large residuals and a poor fitting by the model. They were finally excluded of the PMF matrix.

Table S4. List of input species in the PMF model.

OC	Benzo[a]pyrene (B[a]P)	Sb	HP5
EC	Benzo[g,h,i]perylene (B[g,h,i])P)	Ti	HP6
HuLiS	Indeno[1,2,3-cd]pyrene (In[1,2,3-cd]P)	Zn	HP7
Na^+	Coronene	Cr	HP8
NH_4^+	Acenaphthenequinone	V	Coniferylaldehyde (Coniferald.)
Mg^{2+}	6H-Dibenzo [b,d] pyran-6-one (6H-DPone)	Al	Vanillic acid
Cl^-	1,8-Naphthalic anhydride	Ca	α-Methylglyceric acid (α-MGA)
NO_3^-	1-Nitropyrene (1-NP)	Fe	DHOPA
SO_4^{2-}	PM_{10}	C27	3-Hydroxyglutaric acid (3-HGA)
Levoglucosan (Levo)	Ba	C29	Phthalic acid
Arabitol	Cu	C31	2-Methylerythritol (2-MT)
Sorbitol	Pb	C33	

Table S5. List of the constraints applied on each factor profile in the PMF model to obtain the final solution.

Factors	Species	Constraint types
Mineral dust	2-Methylerythritol	Pull Down Maximally
Mineral dust	Phthalic acid	Pull Down Maximally
Biomass burning	1-Nitropyrene	Pull Down Maximally
Biomass burning	HP5	Pull Down Maximally
Biomass burning	HP6	Pull Down Maximally
Biomass burning	HP7	Pull Down Maximally
Biomass burning	HP8	Pull Down Maximally
Biomass burning	3-Hydroxyglutaric acid	Pull Down Maximally
Biomass burning	Levoglucosan	Pull Up Maximally
Biogenic SOA	Phthalic acid	Pull Down Maximally
Biogenic SOA	Arabitol	Pull Down Maximally
Biogenic SOA	Sorbitol	Pull Down Maximally
Plant debris	HP5	Pull Down Maximally
Plant debris	HP6	Pull Down Maximally
Plant debris	HP7	Pull Down Maximally
Plant debris	HP8	Pull Down Maximally
Secondary inorganics	Phthalic acid	Pull Down Maximally
Fungal spores	HP5	Pull Down Maximally
Fungal spores	HP6	Pull Down Maximally
Fungal spores	HP7	Pull Down Maximally
Fungal spores	HP8	Pull Down Maximally
Fungal spores	2-Methylerythritol	Pull Down Maximally
Fungal spores	Phthalic acid	Pull Down Maximally
Primary traffic	EC	Pull Up Maximally
Primary traffic	Ba	Pull Up Maximally
Primary traffic	Cu	Pull Up Maximally
Primary traffic	Pb	Pull Up Maximally
Primary traffic	Sb	Pull Up Maximally
Aged sea salt	Na^+	Pull Up Maximally
Aged sea salt	Mg^{2+}	Pull Up Maximally
Anthropogenic SOA	DHOPA	Pull Up Maximally
Anthropogenic SOA	1-Nitropyrene	Pull Down Maximally
Anthropogenic SOA	HP5	Pull Down Maximally
Anthropogenic SOA	HP6	Pull Down Maximally
Anthropogenic SOA	HP7	Pull Down Maximally
Anthropogenic SOA	HP8	Pull Down Maximally

Table S6. Values of the correlation coefficients (r) between observed and modelled concentrations.

Species	r	Species	r	Species	r	Species	r
OC	0.94	Benzo[a]pyrene	0.92	Sb	0.53	HP5	0.43
EC	0.97	Benzo[g,h,i]perylene	0.94	Ti	0.79	HP6	0.52
HuLiS	0.94	Indeno[1,2,3-cd]pyrene	0.94	Zn	0.89	HP7	0.57
Na^+	1.00	Coronene	0.96	Cr	0.77	HP8	0.45
NH_4^+	0.99	Acenaphthenequinone	0.96	V	0.65	Coniferylaldehyde	0.93
Mg^{2+}	0.94	6H-DPone	0.98	Al	0.68	Vanillic acid	0.96
Cl^-	0.73	1,8-Naphthalic anhydride	0.95	Ca	0.81	α -Methylglyceric acid	0.96
NO_3^-	0.99	1-Nitropyrene	0.94	Fe	0.96	DHOPA	0.58
SO_4^{2-}	0.84	PM_{10}	0.93	C27	0.97	3-Hydroxyglutaric acid	0.90
Levoglucosan	0.96	Ba	0.72	C29	0.97	Phthalic acid	0.34
Arabitol	0.96	Cu	0.74	C31	0.99	2-Methylerythritol	0.91
Sorbitol	0.85	Pb	0.62	C33	0.88		

Table S7. Results from bootstrap runs obtained for the final solution.

	Mineral dust	**Primary traffic**	**Biomass burning**	**Anthropogenic SOA**	**Biogenic SOA**	**Plant debris**	**Secondary inorganics**	**Fungal spores**	**Aged sea salt**
Mineral dust	94	0	2	0	3	0	0	0	0
Primary traffic	0	99	0	0	0	0	0	0	0
Biomass burning	0	0	98	1	0	0	0	0	0
Anthropogenic SOA	0	0	9	84	1	0	5	0	0
Biogenic SOA	0	0	0	0	99	0	0	0	0
Plant debris	0	0	0	0	0	99	0	0	0
Secondary inorganics	0	0	0	0	0	0	99	0	0
Fungal spores	0	0	3	0	0	0	0	96	0
Aged sea salt	0	0	0	0	0	0	0	0	99

Table S8. Comparison of source profiles before and after constraints. Results of observed P-value for each factor obtained using t-test.

	Mineral dust	**Primary traffic**	**Biomass burning**	**Anthropogenic SOA**	**Biogenic SOA**	**Plant debris**	**Secondary inorganics**	**Fungal spores**	**Aged sea salt**
P -value ($p<0.05$)	0.08	0.11	0.16	0.10	0.09	0.64	0.24	0.34	0.37

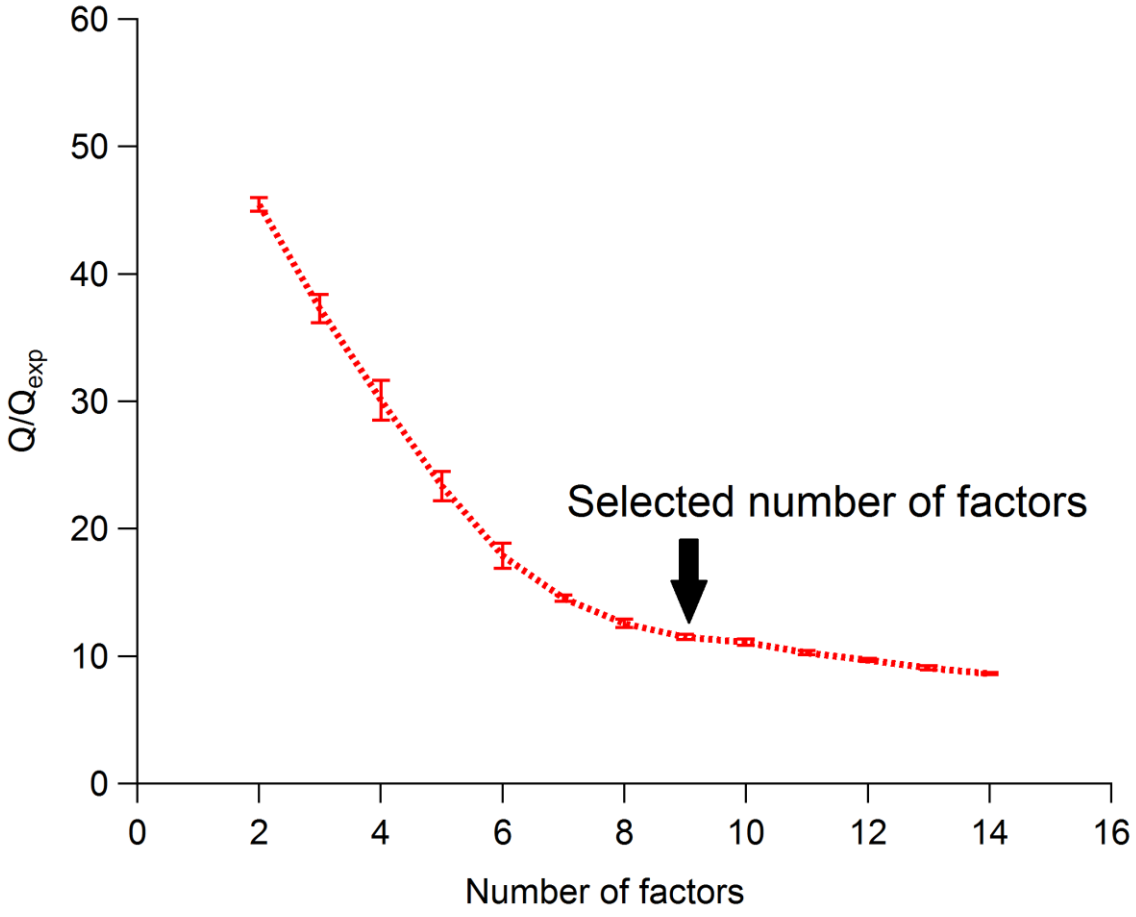

Figure S4. Q/Q_{exp} variation as a function of number of factors. 100 runs were performed in each case and error bars represent one standard deviation.

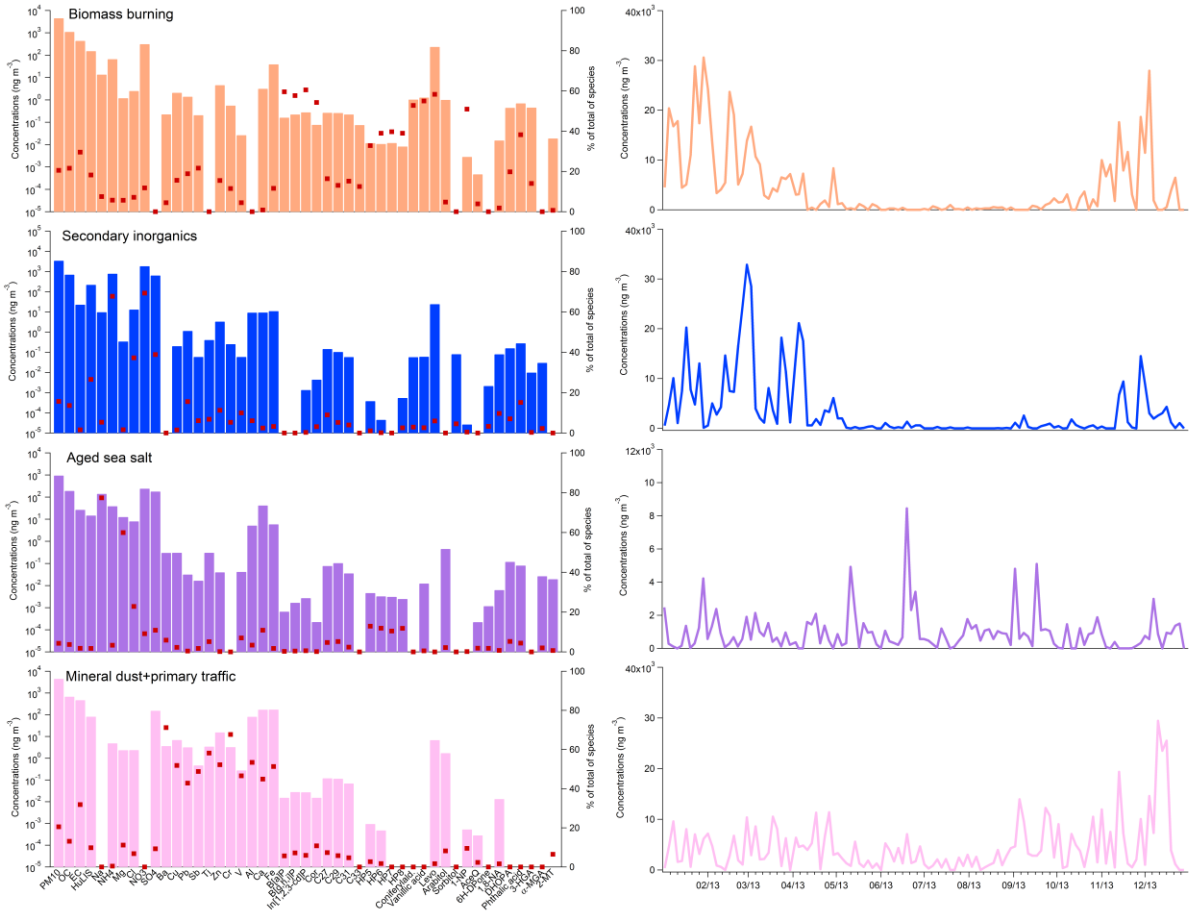

Figure S5. Source profiles and temporal evolution of biomass burning, secondary inorganics, aged sea salt and mineral dust + primary traffic factors for 8 factor solution (base run).

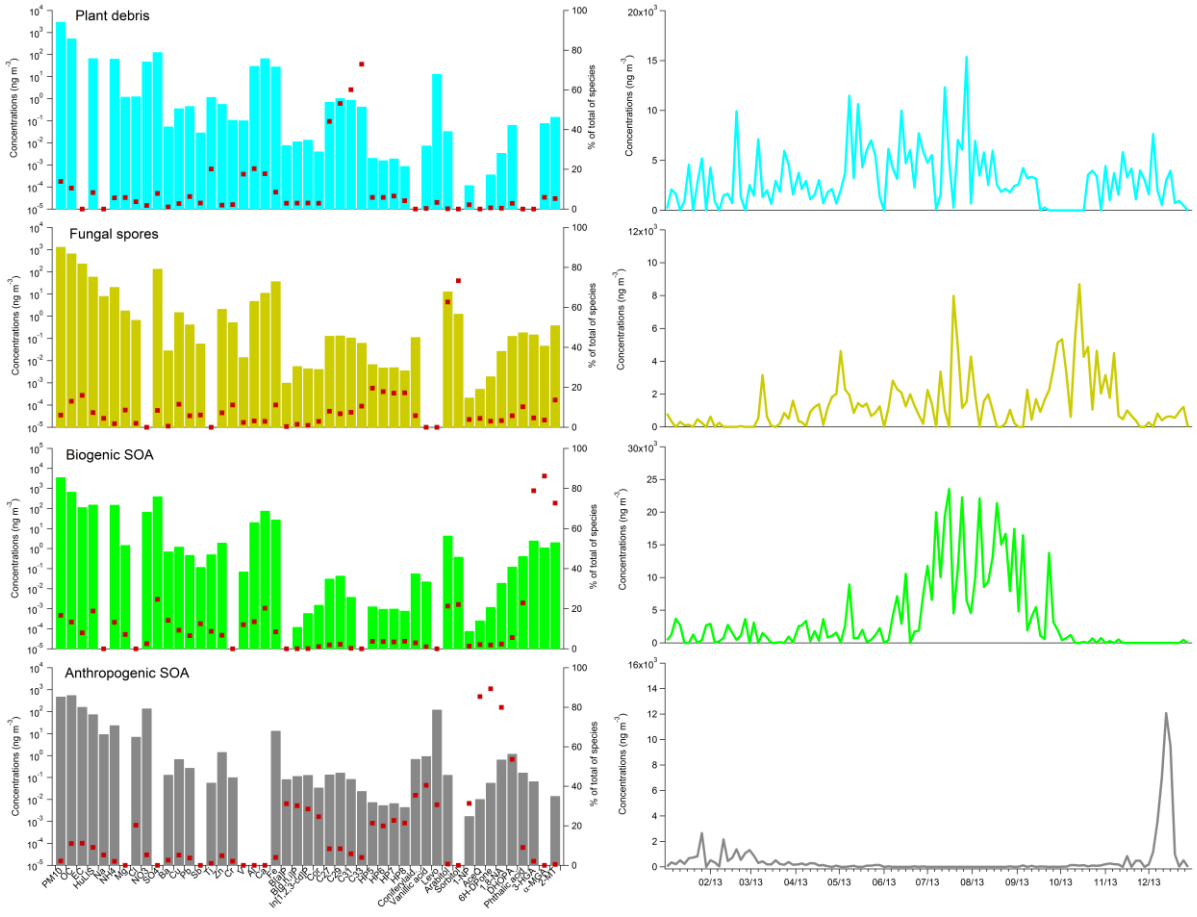

Figure S6. Source profiles and temporal evolution of plant debris, fungal spores, biogenic SOA and anthropogenic SOA factors for 8 factor solution (base run).

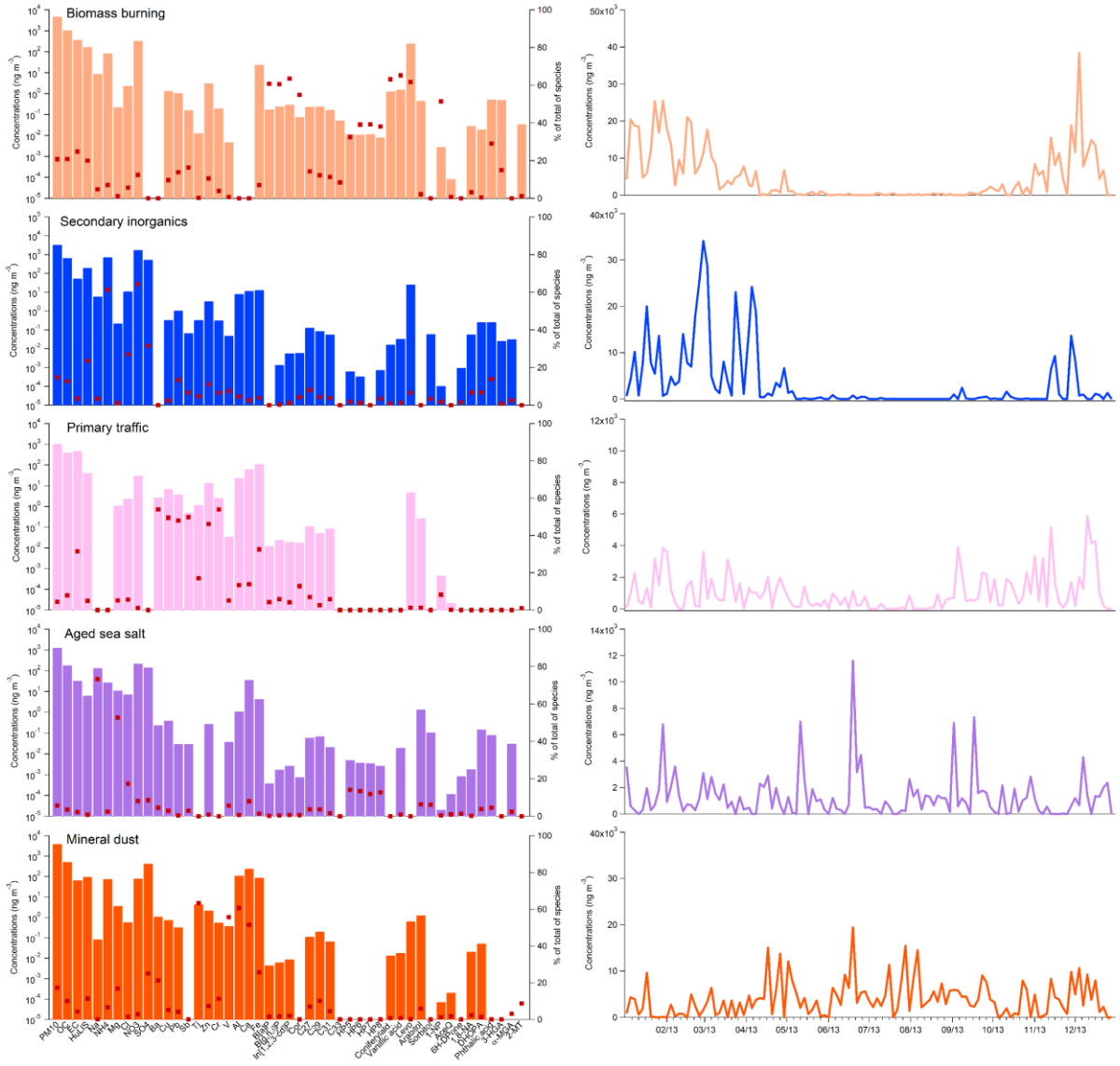

Figure S7. Source profiles and temporal evolution of biomass burning, secondary inorganics, primary traffic, aged sea salt, and mineral dust factors for 10 factor solution (base run).

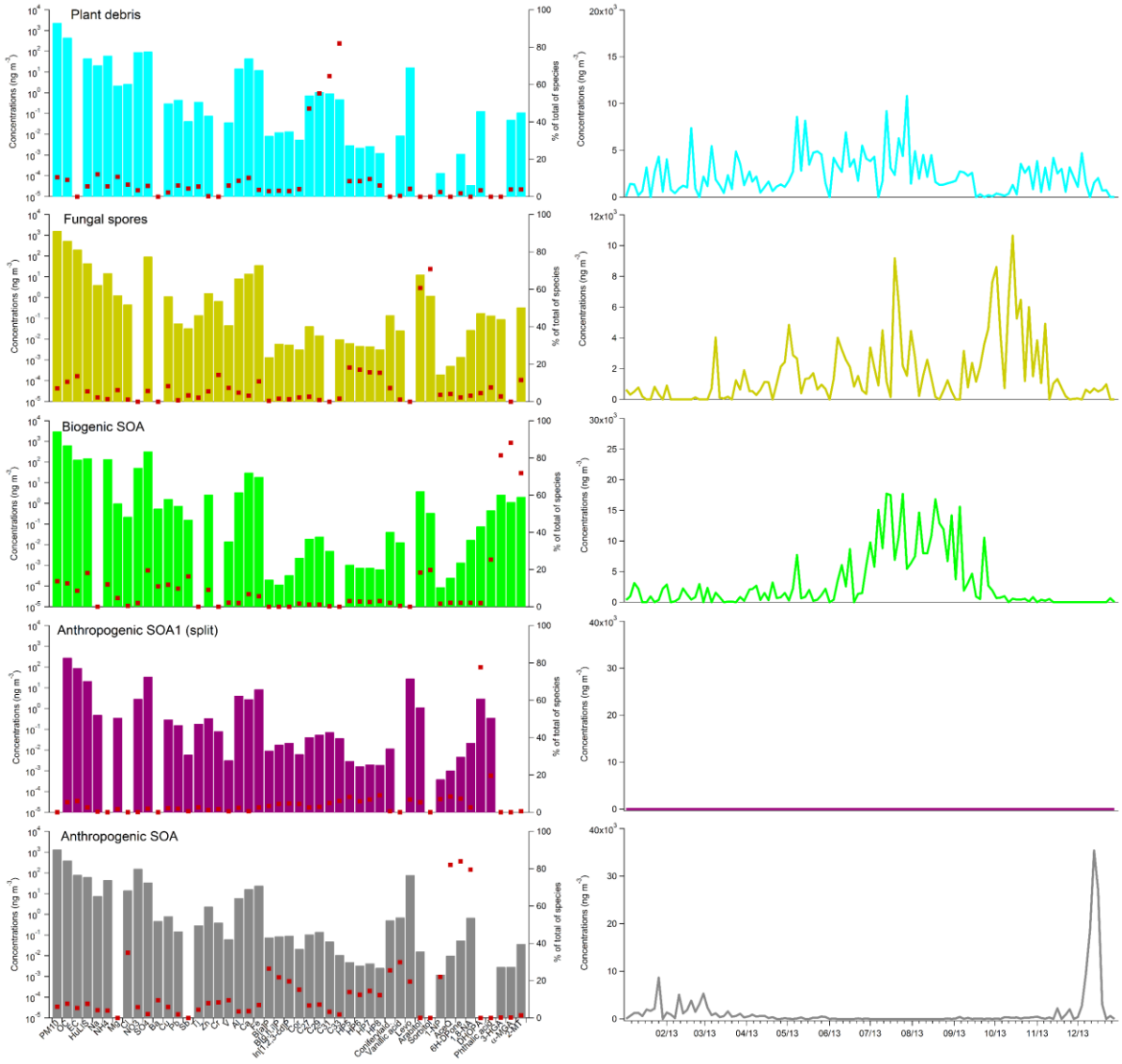

Figure S8. Source profiles and temporal evolution of plant debris, fungal spores, biogenic SOA, anthropogenic SOA1, and anthropogenic SOA factors for 10 factor solution (base run).

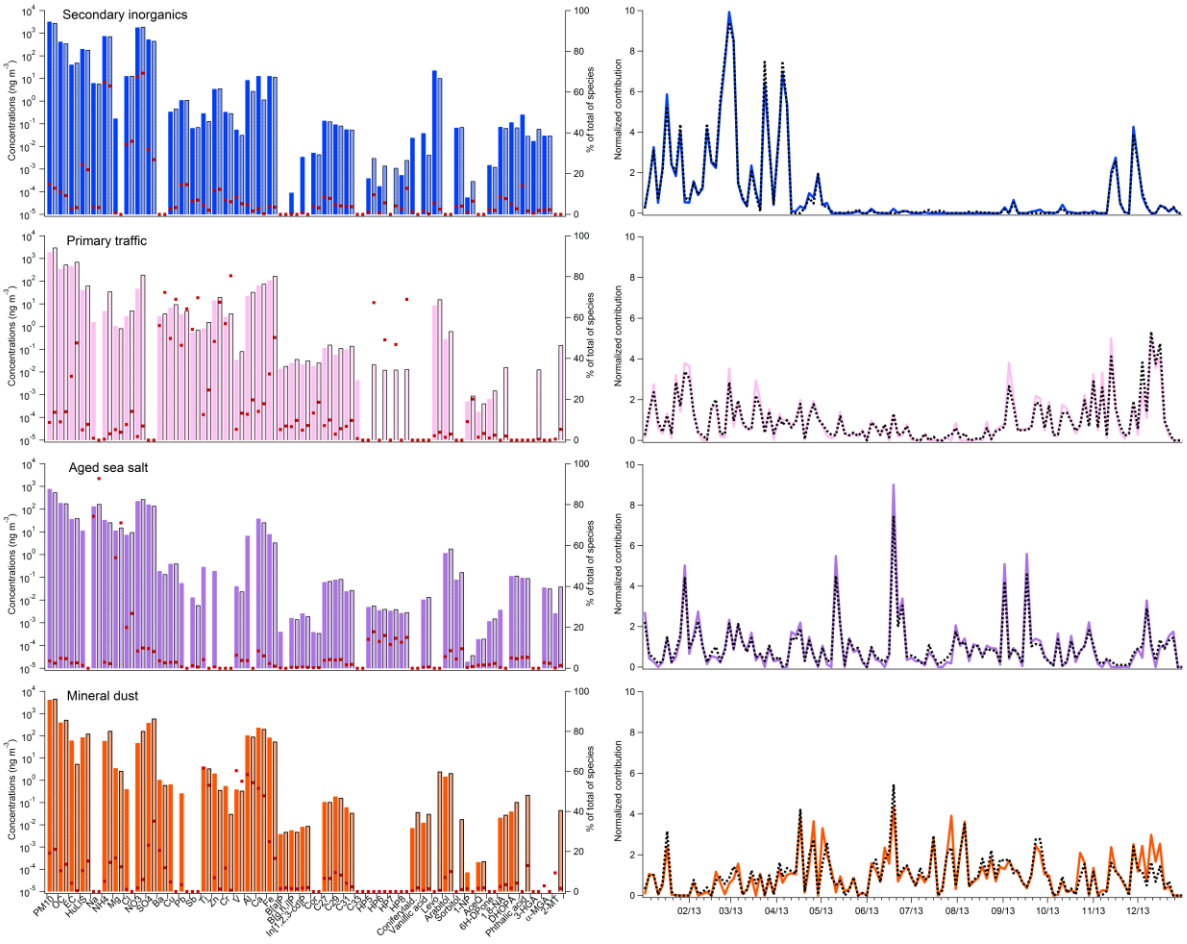

Figure S9. Source profiles and temporal evolution of secondary inorganics, primary traffic, aged sea salt and mineral dust factors for base and constrained runs. Coloured lines: base run, black/dashed lines: constrained run.

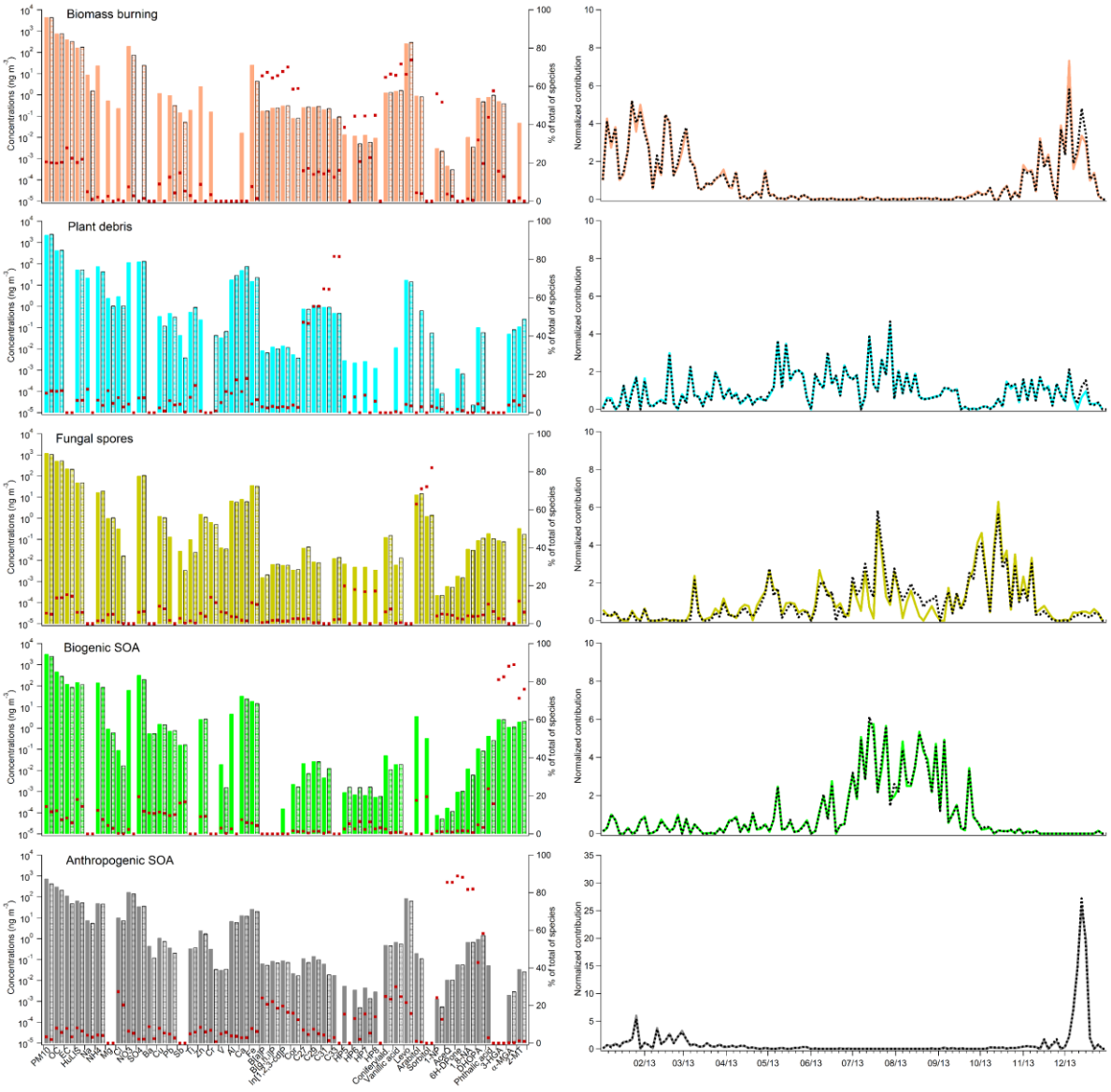

Figure S10. Source profiles and temporal evolution of biomass burning, plant debris, fungal spores, biogenic SOA and anthropogenic SOA factors for base and constrained runs. Coloured lines: base run, black/dashed lines: constrained run.

Table S9. List of the constraints applied on each factor profile in the PMF model excluding December data points.

Factors	Species	Constrain types
Biomass burning	3-Hydroxyglutaric acid	Pull Down Maximally
Biomass burning	HP5	Pull Down Maximally
Biomass burning	HP6	Pull Down Maximally
Biomass burning	HP7	Pull Down Maximally
Biomass burning	HP8	Pull Down Maximally
Biomass burning	1-Nitropyrene	Pull Down Maximally
Fungal spores	HP5	Pull Down Maximally
Fungal spores	HP6	Pull Down Maximally
Fungal spores	HP7	Pull Down Maximally
Fungal spores	HP8	Pull Down Maximally
Fungal spores	Phthalic acid	Pull Down Maximally
Biogenic SOA	Phthalic acid	Pull Down Maximally
Biogenic SOA	Arabitol	Pull Down Maximally
Biogenic SOA	Sorbitol	Pull Down Maximally
Biogenic SOA	HP5	Pull Down Maximally
Biogenic SOA	HP6	Pull Down Maximally
Biogenic SOA	HP7	Pull Down Maximally
Biogenic SOA	HP8	Pull Down Maximally
Secondary inorganics	1,8-Naphthalic anhydride	Pull Down Maximally
Anthropogenic SOA	HP5	Pull Down Maximally
Anthropogenic SOA	HP6	Pull Down Maximally
Anthropogenic SOA	HP7	Pull Down Maximally
Anthropogenic SOA	HP8	Pull Down Maximally
Anthropogenic SOA	1-Nitropyrene	Pull Down Maximally
Anthropogenic SOA	DHOPA	Pull Up Maximally
Primary traffic	EC	Pull Up Maximally
Primary traffic	Ba	Pull Up Maximally
Primary traffic	Cu	Pull Up Maximally
Primary traffic	Pb	Pull Up Maximally
Primary traffic	Sb	Pull Up Maximally

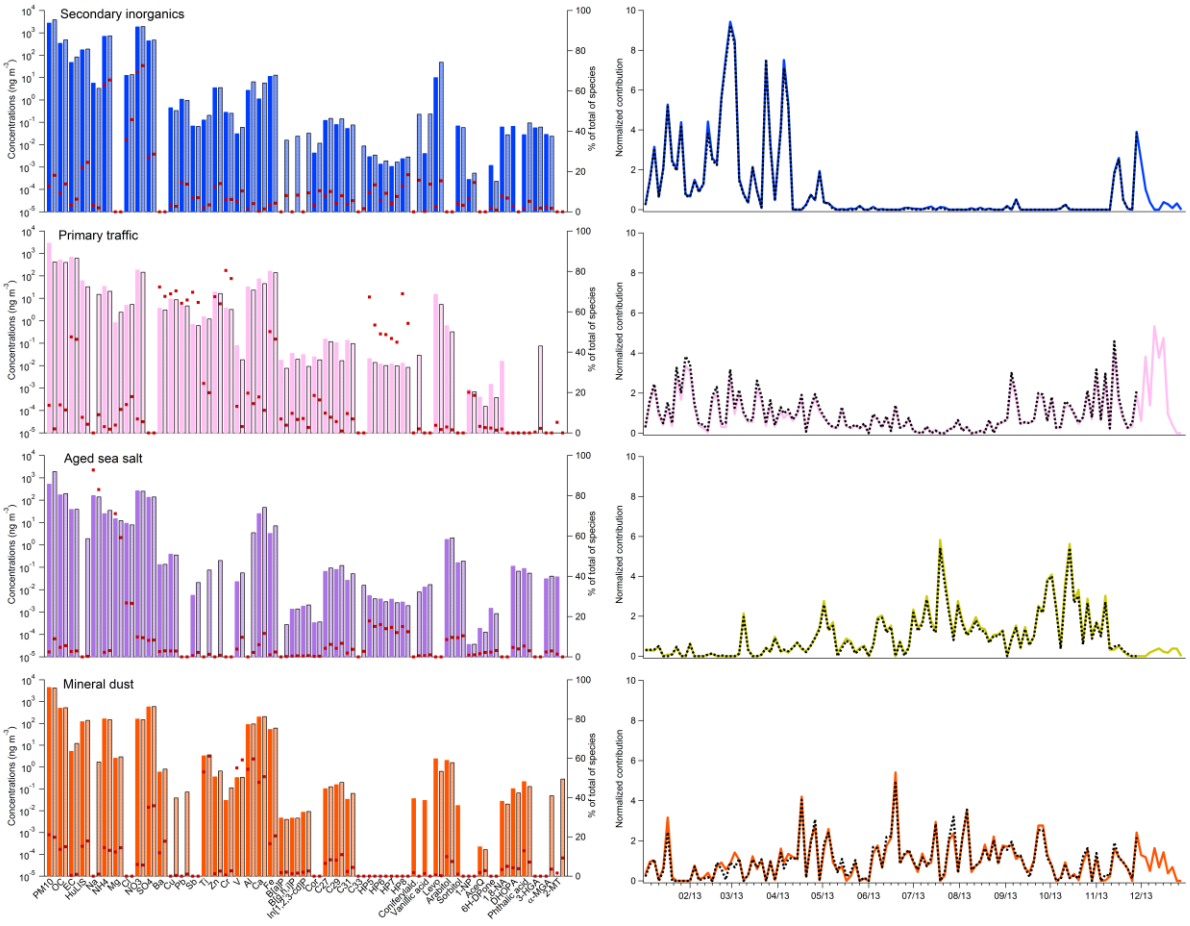

Figure S11. Source profiles and temporal evolution of secondary inorganics, primary traffic, aged sea salt and mineral dust factors for the full data set and excluding December data points. Coloured lines: full data set, black/dashed lines: data set without December.

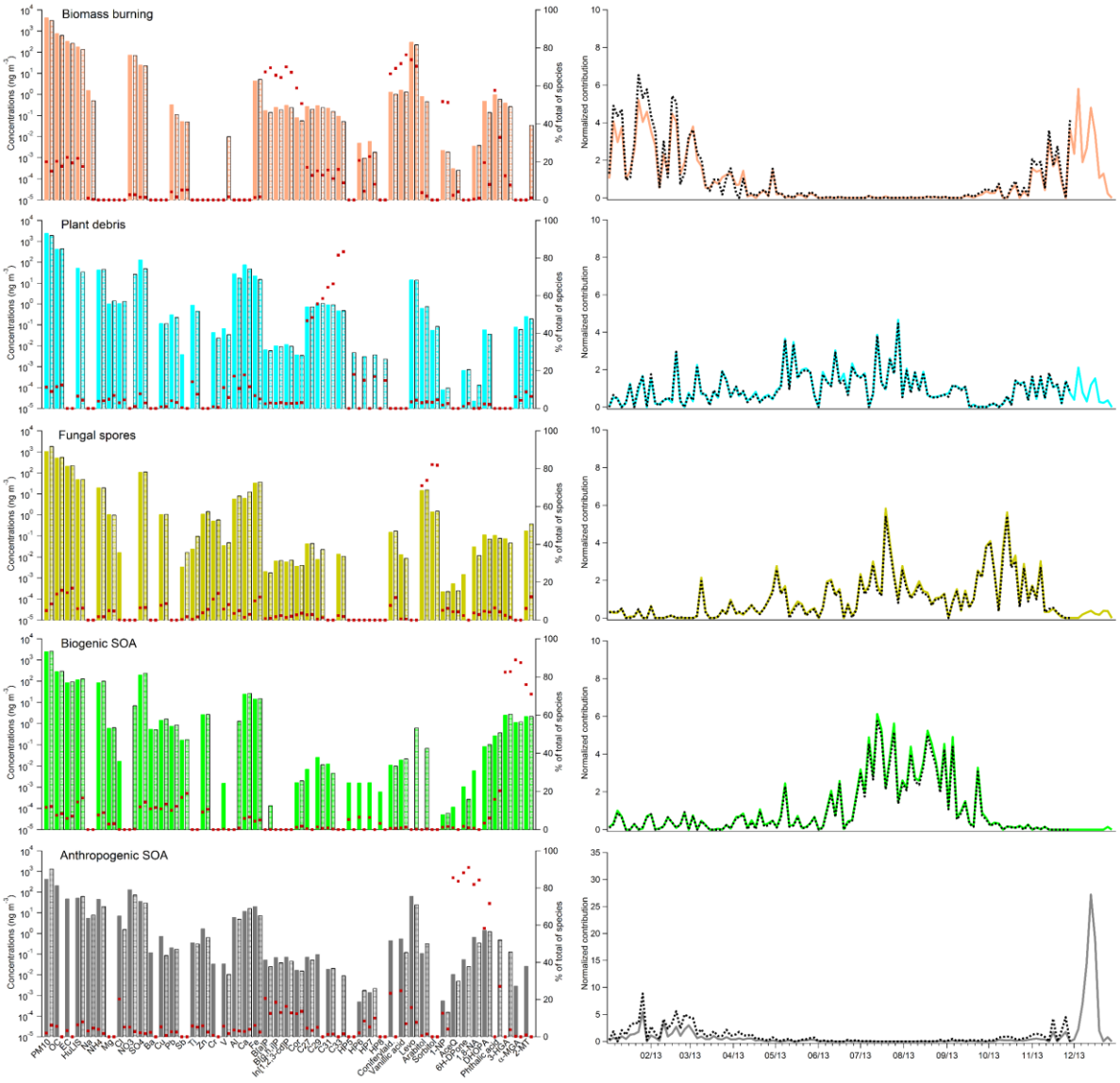

Figure S12. Source profiles and temporal evolution of biomass burning, plant debris, fungal spores, biogenic SOA and anthropogenic SOA factors for the full data set and excluding December data points. Coloured lines: full data set, black/dashed lines: data set without December.

Table S10. Results from bootstrap runs obtained excluding December data points.

	Aged sea salt	**Biomass burning**	**Fungal spores**	**Biogenic SOA**	**Plant debris**	**Primary traffic**	**Secondary inorganics**	**Mineral dust**	**Anthropogenic SOA**
Aged sea salt	100	0	0	0	0	0	0	0	0
Biomass burning	0	99	0	0	0	0	0	0	0
Fungal spores	0	1	98	1	0	0	0	0	0
Biogenic SOA	0	0	0	100	0	0	0	0	0
Plant debris	0	0	0	0	100	0	0	0	0
Primary traffic	0	0	0	0	0	100	0	0	0
Secondary inorganics	0	0	0	0	0	0	100	0	0
Mineral dust	0	0	0	0	0	0	0	100	0
Anthropogenic SOA	0	1	0	0	0	0	1	0	98

Table S11. Comparison of source profiles using full data set and excluding December data points. Results of observed P-value for each factor obtained using t-test.

	Mineral dust	**Primary traffic**	**Biomass burning**	**Anthropogenic SOA**	**Biogenic SOA**	**Plant debris**	**Secondary inorganics**	**Fungal spores**	**Aged sea salt**
P -value ($p<0.05$)	0.20	0.53	0.27	0.96	0.32	0.15	0.18	0.20	0.23

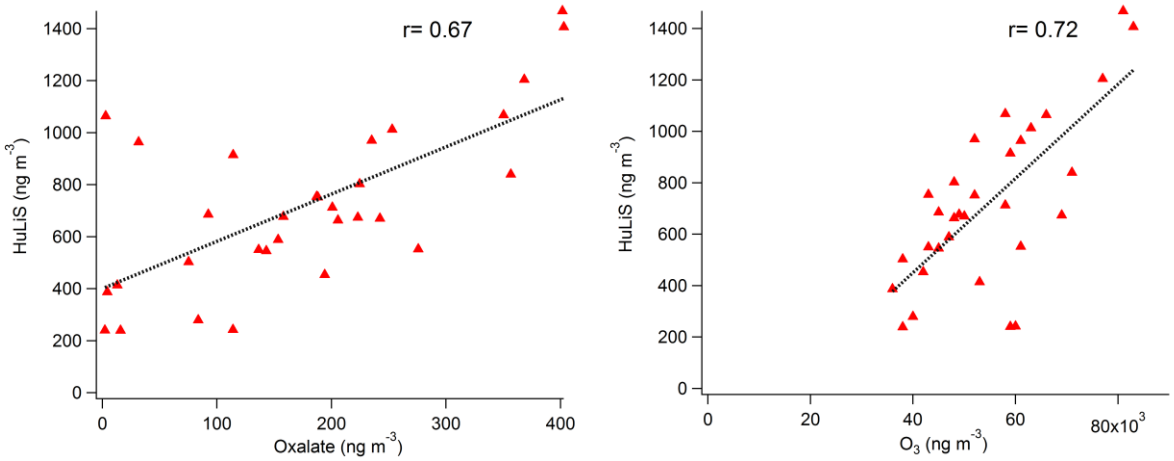

Figure S13. Correlations between oxalate and O_3 with HuLiS and in summer.

References

Albinet A, Nalin F, Tomaz S, Beaumont J, Lestremau F. A simple QuEChERS-like extraction approach for molecular chemical characterization of organic aerosols: application to nitrated and oxygenated PAH derivatives (NPAH and OPAH) quantified by GC-NICIMS. Anal Bioanal Chem 2014; 406: 3131-48.

Albinet A, Tomaz S, Lestremau F. A really quick easy cheap effective rugged and safe (QuEChERS) extraction procedure for the analysis of particle-bound PAHs in ambient air and emission samples. Sci Total Environ 2013; 450-451: 31-8.

Bates T, Lamb B, Guenther A, Dignon J, Stoiber R. Sulfur emissions to the atmosphere from natural sourees. Journal of Atmospheric Chemistry 1992; 14: 315-337.

Carlton AG, Turpin BJ, Altieri KE, Seitzinger S, Reff A, Lim H-J, et al. Atmospheric oxalic acid and SOA production from glyoxal: Results of aqueous photooxidation experiments. Atmospheric Environment 2007; 41: 7588-7602.

Carlton AG, Wiedinmyer C, Kroll JH. A review of Secondary Organic Aerosol (SOA) formation from isoprene. Atmos. Chem. Phys. 2009; 9: 4987-5005.

Iinuma Y, Boge O, Grafe R, Herrmann H. Methyl-nitrocatechols: atmospheric tracer compounds for biomass burning secondary organic aerosols. Environ Sci Technol 2010; 44: 8453-9.

Jiang Y, Zhuang G, Wang Q, Liu T, Huang K, Fu JS, et al. Characteristics, sources and formation of aerosol oxalate in an Eastern Asia megacity and its implication to haze pollution. Atmospheric Chemistry and Physics Discussions 2011; 11: 22075-22112.

Kawamura K, Ikushima K. Seasonal changes in the distribution of dicarboxylic acids in the urban atmosphere. Environmental Science & Technology 1993; 27: 2227-2235.

Laing JR, Hopke PK, Hopke EF, Husain L, Dutkiewicz VA, Paatero J, et al. Positive Matrix Factorization of 47 Years of Particle Measurements in Finnish Arctic. Aerosol and Air Quality Research 2015; 15: 188-207

Schembari C, Bove MC, Cuccia E, Cavalli F, Hjorth J, Massabò D, et al. Source apportionment of PM10 in the Western Mediterranean based on observations from a cruise ship. Atmospheric Environment 2014; 98: 510-518.

Srimuruganandam B, Shiva Nagendra SM. Application of positive matrix factorization in characterization of PM10 and PM2.5 emission sources at urban roadside. Chemosphere 2012; 88: 120-130.

Sullivan RC, Prather KA. Investigations of the Diurnal Cycle and Mixing State of Oxalic Acid in Individual Particles in Asian Aerosol Outflow. Environmental Science & Technology 2007; 41: 8062-8069.

Warneck P. The relative importance of various pathways for the oxidation of sulfur dioxide and nitrogen dioxide in sunlit continental fair weather clouds. Physical Chemistry Chemical Physics 1999; 1: 5471-5483.

Article III

Speciation of organic fractions does matter for aerosol source apportionment. Part 2: intensive short-term campaign in the Paris area (France)

Published in Science of The Total Environment

Science of the Total Environment 634 (2018) 267–278

Contents lists available at ScienceDirect

Science of the Total Environment

journal homepage: www.elsevier.com/locate/scitotenv

Speciation of organic fractions does matter for aerosol source apportionment. Part 2: Intensive short-term campaign in the Paris area (France)

D. Srivastava [a,b,c,*], O. Favez [a], N. Bonnaire [d], F. Lucarelli [e], M. Haeffelin [f], E. Perraudin [b,c], V. Gros [d], E. Villenave [b,c], A. Albinet [a,*]

[a] INERIS, Parc Technologique Alata, BP 2, 60550 Verneuil-en-Halatte, France
[b] CNRS, EPOC, UMR 5805 CNRS, 33405 Talence, France
[c] Université de Bordeaux, EPOC, UMR 5805 CNRS, 33405 Talence, France
[d] LSCE - UMR8212, CNRS-CEA-UVSQ, Gif-sur-Yvette, France
[e] University of Florence, Dipartimento di Fisica Astronomia, 50019 Sesto Fiorentino, Italy
[f] Institut Pierre Simon Laplace, CNRS, Ecole Polytechnique, 91128 Palaiseau, France

HIGHLIGHTS

- Source apportionment using key primary and secondary organic molecular markers
- High resolution filter data allowed the understanding of the atmospheric processes.
- 7 SOA factors identified including 2 specific biogenic SOA and 3 anthropogenic SOA
- Traffic and biomass burning SOA resolved using 1-nitropyrene and methylnitrocatechols
- Role of night-time chemistry for SOA related to nitro-PAHs and phenolic compounds

GRAPHICAL ABSTRACT

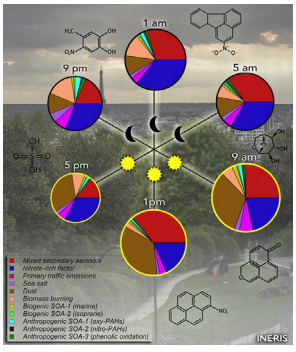

ARTICLE INFO

Article history:
Received 1 February 2018
Received in revised form 23 March 2018
Accepted 24 March 2018
Available online xxxx

Editor: D. Barcelo

Keywords:
Aerosol
Source apportionment
PMF
SOA
Molecular markers

ABSTRACT

The present study aimed at performing PM_{10} source apportionment, using positive matrix factorization (PMF), based on filter samples collected every 4 h at a sub-urban station in the Paris region (France) during a PM pollution event in March 2015 ($PM_{10} > 50\ \mu g\ m^{-3}$ for several consecutive days). The PMF model allowed to deconvolve 11 source factors. The use of specific primary and secondary organic molecular markers favoured the determination of common sources such as biomass burning and primary traffic emissions, as well as 2 specific biogenic SOA (marine + isoprene) and 3 anthropogenic SOA (nitro-PAHs + oxy-PAHs + phenolic compounds oxidation) factors. This study is probably the first one to report the use of methylnitrocatechol isomers as well as 1-nitropyrene to apportion secondary OA linked to biomass burning emissions and primary traffic emissions, respectively. Secondary organic carbon (SOC) fractions were found to account for 47% of the total OC. The use of organic molecular markers allowed the identification of 41% of the total SOC composed of anthropogenic SOA (namely, oxy-PAHs, nitro-PAHs and phenolic compounds oxidation, representing 15%, 9%, 11% of the total OC, respectively) and biogenic SOA (marine + isoprene) (6% in total). Results obtained also showed that 35% of the total SOC originated from anthropogenic sources and especially PAH SOA (oxy-PAHs + nitro-PAHs), accounting for 24% of the total SOC, highlighting its significant contribution in urban influenced environments. Anthropogenic SOA related to

* Corresponding authors at: INERIS, Parc Technologique Alata, BP 2, 60550 Verneuil-en-Halatte, France.
E-mail addresses: deepchandra.srivastava@gmail.com, (D. Srivastava), alexandre.albinet@gmail.com, alexandre.albinet@ineris.fr. (A. Albinet).

https://doi.org/10.1016/j.scitotenv.2018.03.296

nitro-PAHs and phenolic compounds exhibited a clear diurnal pattern with high concentrations during the night indicating the prominent role of night-time chemistry but with different chemical processes involved.

1. Introduction

Atmospheric particulate matter (PM) plays an important role on climate and air quality (Boucher et al., 2013; Heal et al., 2012). To design effective PM concentration reduction strategies, their sources and contributions from each source need to be known thoroughly. Thus, several source apportionment methods have been developed for this purpose. Receptor-oriented modelling is one of the approaches that have been extensively used for PM source apportionment studies in the past decades (Belis et al., 2015; Hopke, 2016). The most commonly used receptor models include chemical mass balance (CMB) (Chow and Watson, 2002; Watson et al., 2002), positive matrix factorization (PMF) (Paatero and Tapper, 1994), and UNMIX (Henry, 1997). PMF is a powerful multivariate method that can resolve the dominant positive factors without prior knowledge of sources (Hopke et al., 2006; Kim et al., 2003; Shrivastava et al., 2007; Zhang et al., 2009).

Typically, PMF uses trace elements, and organic and elemental carbon (OC/EC), as well as secondary ions and metals as the input data matrix to explore the "co-variances" between species (Kim and Hopke, 2004; Kim et al., 2003). The use of tracers with high source specificity in the PMF model can enhance the interpretation of the factors. For example, levoglucosan is often used to trace the biomass burning source (Simoneit, 2002). The use of organic molecular markers in the PMF has resulted in considerable progress in the understanding of the organic aerosol (OA) fraction (Jaeckels et al., 2007; Laing et al., 2015; Schembari et al., 2014; Shrivastava et al., 2007; Srimuruganandam and Shiva Nagendra, 2012; Waked et al., 2014; Wang et al., 2012; Zhang et al., 2009). However, these studies have often been based on 12 or 24 h sampling periods, making difficult to capture the information on "fast" chemical processes related to OA emissions and formation. The use of a higher time-resolution datasets (e.g. filter samplings every 6 h or less) may facilitate the understanding of the processes involved, for both primary and secondary sources, and the analysis of their diurnal cycles.

This paper is the second paper of a two-part series demonstrating that the speciation of the OA fraction is important for PM source apportionment. Note that, the use of organic molecular markers in source apportionment studies is based on the assumption that these compounds are chemically stable in the atmosphere (i.e. tracer compounds) (Schauer et al., 1996). Some molecules can undergo a decay in the atmosphere by photochemical processes involving sunlight and atmospheric oxidants and their use may cause a bias in the source apportionment. Nevertheless, the first paper (Srivastava et al., 2018) highlighted the advantage of using primary and secondary organic molecular markers to resolve sources rarely apportioned in the literature such as two types of primary biogenic organic aerosols (fungal spores and plant debris), as well as specific biogenic and anthropogenic secondary OA (SOA). This second paper focuses on the identification of sources during a major PM pollution event using high resolution filter data in order to apportion specific primary (POA) and secondary OA fractions using various and distinctive markers and to understand the atmospheric chemical processes involved.

2. Experimental

2.1. Monitoring site and sampling period

Measurements were conducted at the ACTRIS SIRTA atmospheric supersite (Site Instrumental de Recherche par Télédétection Atmosphérique, 2.15° E; 48.71° N; 150 m a.s.l; http://sirta.ipsl.fr; Haeffelin et al. (2005)). This site is located approximately 25 km southwest from Paris city centre (Fig. S1), surrounded by forests, agricultural fields and small villages, and is representative of suburban background conditions of the Paris region (Crippa et al., 2013a; Petit et al., 2017a; Petit et al., 2014; Sciare et al., 2011). An intensive campaign was performed from 6 to 21, March 2015. The late winter-early spring period was chosen on purpose as intense PM pollution events are usually observed in Northern France (and Europe) during this period of the year due to the combination of significant residential emissions, manure spreading, stagnant atmospheric conditions favouring the accumulation of pollutants and possible photochemical processes enhancing the formation of secondary aerosols (Bressi et al., 2013; Crippa et al., 2013a; Dupont et al., 2016; Favez et al., 2012; Fröhlich et al., 2015; Petit et al., 2017a; Petit et al., 2014; Sciare et al., 2011; Waked et al., 2014).

2.2. Sample collection and co-located measurements

PM_{10}samples (Tissu-quartz fibre filter, Pallflex, Ø = 150 mm) were collected every 4 h from 6 to 21, March 2015 using a high-volume sampler (DA-80, Digitel; 30 $m^3\ h^{-1}$). Prior to sampling, quartz fibre filters were pre-heated at 500 °C for 12 h. After collection, samples were wrapped in aluminium foils, sealed in polyethylene bags, and stored at −20 °C until analysis. Shipping of the samples to the different laboratories for analyses have been done by express post using cool boxes (<5 °C). A total of 92 samples and 5 field blanks were collected and analysed for an extended chemical characterization following the protocols described in Section 2.3.

PM_{10}, Black Carbon (BC), NO_x and O_3 concentrations were measured using co-located online analysers: TEOM-FDMS (1405F model, Thermo), multi-wavelength aethalometer (AE33 model, Magee Scientific), T200UP and T400 monitors (Teledyne API), respectively. Moreover, assuming that biomass burning and fossil fuel combustion were the two predominant combustion sources, BC from wood burning (BC_{wb}) and fossil fuel (BC_{ff}) emissions were estimated using the so-called "aethalometer model" (Drinovec et al., 2015; Sandradewi et al., 2008). The AE33 instrument uses a dual-spot technology which provides the automatic compensation (k) of the aerosol loading effect (Drinovec et al., 2015) over the 7 wavelengths of measurements of BC (from near UV to near IR). An inaccurate automatic compensation has been observed for several days due to high scattering during the pollution episode linked to high ammonium nitrate concentrations. The associated data were thus manually corrected with fixed k values as explained by Petit et al. (2017a) to improve the separation between BC_{wb} and BC_{ff}. Finally, meteorological parameters such as temperature, relative humidity (RH), wind direction, and wind speed were obtained from nearby weather station (about 5 km).

2.3. Analytical procedure

A total number of 71 different chemical species have been quantified on filter samples. Major ions (Cl^-, NO_3^-, SO_4^{2-}, NH_4^+, Ca^{2+}, Na^+, Mg^{2+}, K^+), methanesulfonic acid (MSA) and oxalate ($C_2O_4^{2-}$) were analysed using ion chromatography (Guinot et al., 2007). EC/OC was measured using a Sunset lab analyser and the EUSAAR-2 thermal protocol (Cavalli et al., 2010; CEN, 2017). Seven metal elements (namely Ca, Ti, Mn, Fe, Ni, Cu, and Pb) were quantified by PIXE (particle-induced X-ray emission) (Lucarelli et al., 2018; Lucarelli et al., 2011). Sugars, including known biomass burning markers (levoglucosan, mannosan

and galactosan) and 3 polyols (arabitol, sorbitol and mannitol), were quantified using LC-PAD (Verlhac et al., 2013; Yttri et al., 2015). Nine PAHs, 14 oxy-PAHs, and 8 nitro-PAHs were quantified by UPLC/UV-Fluorescence and GC/NICI-MS (Albinet et al., 2006; Albinet et al., 2014; Albinet et al., 2013; Tomaz et al., 2016) using QuEChERS-like (Quick Easy Cheap Effective Rugged and Safe) extraction procedure (Albinet et al., 2014; Albinet et al., 2013). Slight modifications have been made in the purification step and the GC column used for oxy- and nitro-PAHs analysis allowing notably the clear separation of 2- and 3-nitrofluoranthenes. Thirteen SOA markers (notably including α-methylglyceric acid, pinic acid, and methylnitrocatechols) (Nozière et al., 2015) were analysed by GC/EI-MS using authentic standards (Srivastava et al., 2018). Details of the analytical procedures and sample preparation for the analysis of PAHs and their derivatives, and SOA markers are provided in the Supplementary material (SM) (TablesS1to S4).

2.4. Source apportionment methodology

2.4.1. Receptor modelling: PMF

The U.S. Environmental Protection Agency (US-EPA) PMF 5.0 software has been used to perform PM_{10} source apportionment. PMF is based on a weighted least squares fit, where the weights are derived from the analytical uncertainty and provides the optimal solution by minimizing the residuals. Detailed information on this receptor modelling can be found elsewhere (Paatero, 1997; Paatero and Tapper, 1994) and in the SM, and also in the companion paper together with uncertainty calculation details (Srivastava et al., 2018). PM_{10} concentrations were included as the total variable with low weight (weak variable) in the model to determine the source contributions.

2.4.2. Criteria for the selection of species

The choice of the species used as input data for the PMF analysis is a crucial step, which can significantly influence the model results (Lim et al., 2010). Usually, the selection of the species is based on the signal-to-noise ratio (S/N) (Paatero and Hopke, 2003). Here, only species with a S/N ratio above 0.2 were considered (Table S5). In addition, the following set of criteria were used for the final selection of the input species: major PM chemical species, compounds with at least 40% of total data points above the detection limit, and those being considered as specific markers of a given source (e.g., α-methylglyceric (α-MGA) and 2-methylerythritol acid (2-MT) (SOA markers of isoprene oxidation), 2,3-dihydroxy-4-oxopentanoic acid (DHOPA) (SOA marker of toluene oxidation), methylnitrocatechol isomers (SOA from phenolic compound oxidation mainly emitted by biomass burning)) (Carlton et al., 2009; Iinuma et al., 2010; Kleindienst et al., 2004) (Table S6).

Furthermore, when several specific markers of a given source were available, criteria previously described by Srivastava et al. (2018), such as the selection of only one or two representative species per expected source and the selection of markers mainly present in the particulate phase, have been applied.

Finally, a total number of 34chemical species (listed in Table S6) were used in the present PM_{10} source apportionment study.

2.4.3. Optimization of the final solution

Optimization of the final solution was based on the application of constraints to obtained clear factor chemical profiles. The general framework for applying constraints to PMF solutions has already been discussed elsewhere (Amato and Hopke, 2012; Amato et al., 2009). A priori information is introduced into the model as auxiliary terms in the object function (Q) (see the SM for details) by the implementation of so-called "pulling" (Paatero and Hopke, 2009). "Soft pulling" (species pulled up maximally and/or pulled down maximally) and "hard pulling" (with defined limits) type of constraints were applied, where species in the factors were selectively pulled down or up. Details related to the constraints applied to each factor profile are given in Table S7.

The change in the Q values, were considered here as a diagnostic parameter to provide insight into the rotation of factors. All model runs were carefully monitored by examining the Q values obtained in the robust mode. The observed change in the Q-robust was approximately 5% (Norris et al., 2014).

Three criteria, including correlation coefficient (r) between the measured and modelled species, bootstrap, and *t*-test (two-tailed paired *t*-test) performed on the base and constraint runs, were used to select the optimal solution, as explained previously (Srivastava et al., 2018).

A threshold of 80% for the bootstrap was considered to indicate that the chosen solution may be appropriate. The species showing poor correlations ($r < 0.5$) between observed and modelled concentrations were carefully examined to determine whether the species should be down-weighted or excluded. Student's *t*-test was used to evaluate the effectiveness of the applied constraints and to verify if the differences were statistically insignificant for all source profiles (two-tailed paired t-test significance test at $p < 0.05$ probability).

The comparison between the reconstructed and measured input species showed very good agreement except for 2-methylerythritol ($r < 0.50$, $n = 92$, $p < 0.05$) (Table S8). Bootstrapping on the final solution showed stable results with ≥85 out of 100 bootstrap mapped factors (Table S9). No significant difference (p values in the range 0.07–0.40) was observed in the source chemical profiles between the base and the constrained runs (Table S10, Figs. S2 and S3).

2.5. Back trajectories and geographical origins

A study of the geographical origin of selected identified sources has been performed by concentration-weighted trajectory (CWT). Such approach combines concentration data measured at the receptor site (in this case for each PM source) with back trajectories and helps to localize the air parcel responsible for high observed concentrations. For this purpose, back trajectories were calculated every 3 h using the standalone version of HYSPLIT v4.1 (Draxler, 1999; Stein et al., 2015) and CWT calculations, and cluster analysis, were performed using the ZeFir Igor package (Petit et al., 2017b). Details about all these calculations have been reported previously (Petit et al., 2017a).

3. Results and discussion

3.1. Overview of the PM_{10} chemical composition

The daily PM_{10} mass concentrations ranged from 12 to 130 μg m^{-3}, with an average of 49 μg m^{-3} during the campaign. The PM chemical composition showed a large predominance of secondary inorganic species, especially ammonium nitrate, highlighting the significance of secondary processes throughout the studied period (Petit et al., 2017a). OM concentrations ranged from 2 to 25 μg m^{-3}, with an average value of about 12 μg m^{-3} (Fig. 1). Note that the slight differences observed between the measured and the reconstructed PM_{10} mass concentrations may be due to the PM water content and/or some sampling artefacts together with the measurement uncertainties (Schwab et al., 2006). The measurement period can be divided into 3 sub-periods according to the air mass origins. The SO_4/EC ratio was considered as a proxy to distinguish local from regional influences (Petit et al., 2015). This ratio showed a minimum value of about 2 during the period from 03/06 to 03/11, emphasizing the role of local emissions such as residential wood burning at the beginning of the studied period. This was notably supported by the high values of the levoglucosan/PM_{10} ratio observed during this period together with low wind speeds (recirculation) (Fig. S4). Nitrate concentrations started to slightly increase from 03/11 and then the increase was more pronounced from 03/13 together with the rise of the SO_4/EC ratio, and associated with higher wind speeds coming from the NE direction, suggesting an influence of medium range transport. A substantial change was noticed in the PM composition during the most intense part of the campaign (03/18–03/21).

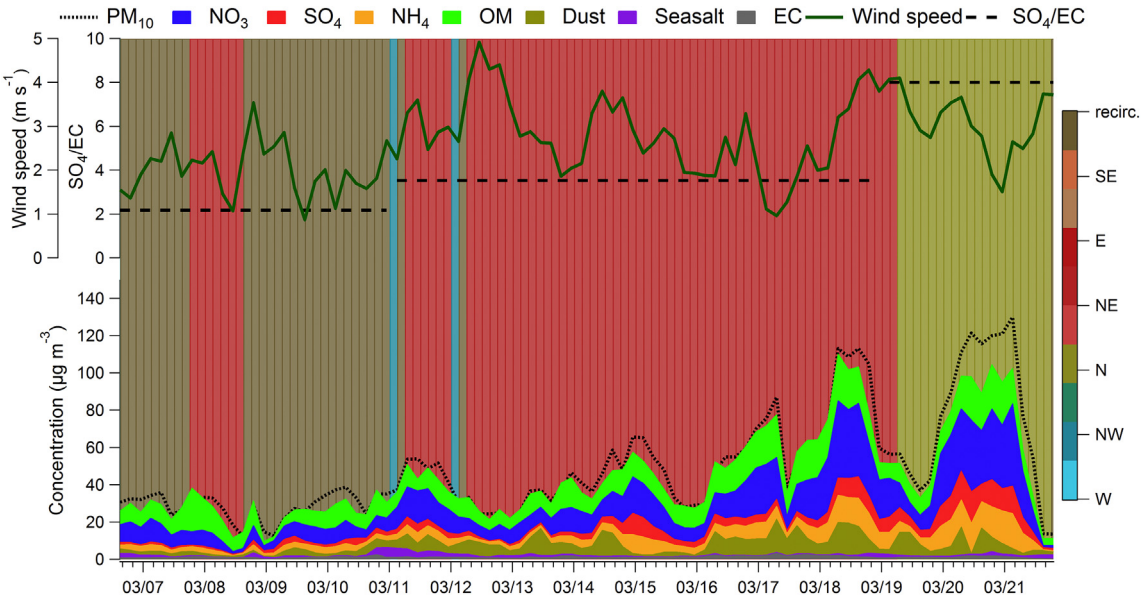

Fig. 1. Temporal variation of PM_{10} chemical composition, SO_4/EC ratio and wind speed observed at Paris-SIRTA, France (March 2015). Background colours refer to air mass clusters. Cluster analysis performed using ZeFir based on back trajectories calculated every 3 h with HYSPLIT model.

The air masses originated mostly from the NNE direction with relatively high wind speeds, and high SO_4/EC ratio (of about 8), indicating the advection of aged aerosols over the Paris region and highly impacted by long-range transport. In addition, the high concentration of oxalate (up to 0.5 µg m^{-3}) observed during this 3rd period (Fig. S5) suggests the significant role of photochemical processes enhancing the formation of more oxidized products.

3.2. Description of PMF factors

Based on the methodology described before (Section 2.4), a 11-factor solution provided the most reasonable PMF result. The use of specific molecular organic markers in the PMF model allowed to deconvolve common aerosol sources such as primary traffic emissions, biomass burning, dust, mixed secondary aerosols, nitrate-rich factor, and sea salt, as well as 2 specific biogenic- and 3 anthropogenic-SOA sources. The sum of all these apportioned PMF factors (reconstructed PM_{10}) showed a very good agreement with the measured PM_{10} concentrations ($r = 0.97$, $n = 92$, $p < 0.05$) (Fig. 2 and Table S8). Identified aerosol sources, their chemical profiles and temporal evolutions are shown on Figs. 3 and 4 and discussed individually hereafter.

3.2.1. Mixed secondary aerosols

This factor was obtained as the predominant one, with an average concentration of 18.2 µg m^{-3} and accounting for approximately 37% of the PM_{10} mass (Fig. 2). It was characterized by high contributions of NO_3^-, SO_4^{2-} and NH_4^+ (43%, 67% and 56% of the total mass, respectively) and showed a well-marked temporal variation, with very high concentrations during the second half of the campaign after 03/14 (Fig. 3). In addition, this factor showed significant contributions of oxalate (36% of the species within this factor), α-MGA (25%) and DHOPA (20%), known to be typical secondary organic species or to be markers of SOA formation from the oxidation of isoprene and toluene (Carlton et al., 2009; Kawamura and Ikushima, 1993; Kleindienst et al., 2012).

Such a high contribution of this secondary factor is expected to be related to the aging of air masses during long range transport. This was also confirmed by the high SO_4/EC ratio (=50) observed in the factor chemical profile. As detailed in Petit et al. (2017a), a dense cloud cover was observed over Northern France during this period, with a limited amount of sunshine, and relatively high wind speeds (Fig. 1) favouring the convective potential of lower atmospheric layer formation and advection of aged aerosol over the Paris region. This is furthermore supported by the CWT analysis showing low contribution of local/

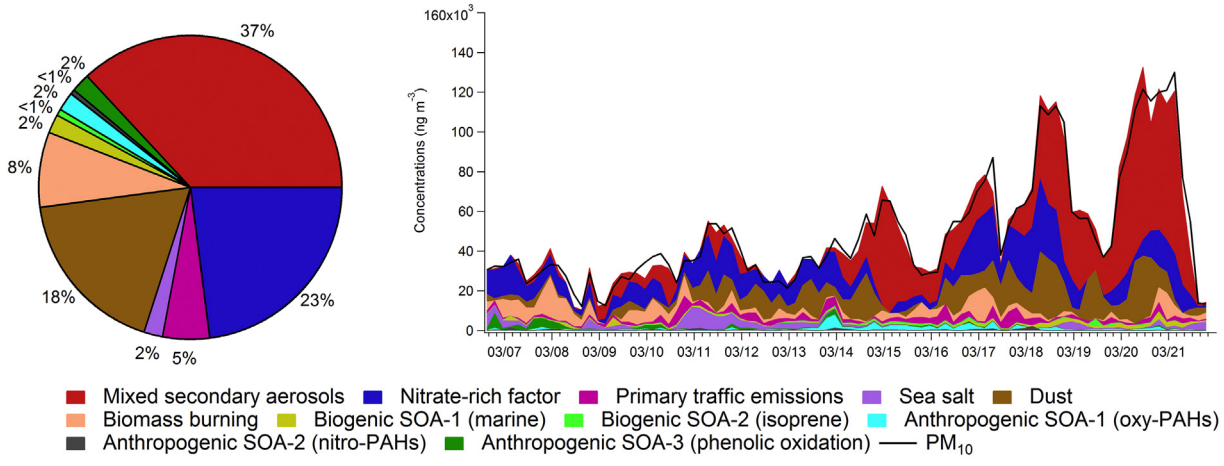

Fig. 2. Average contributions (left) and temporal evolution (right) of the identified sources to PM_{10} mass concentrations at Paris-SIRTA, France (March 2015).

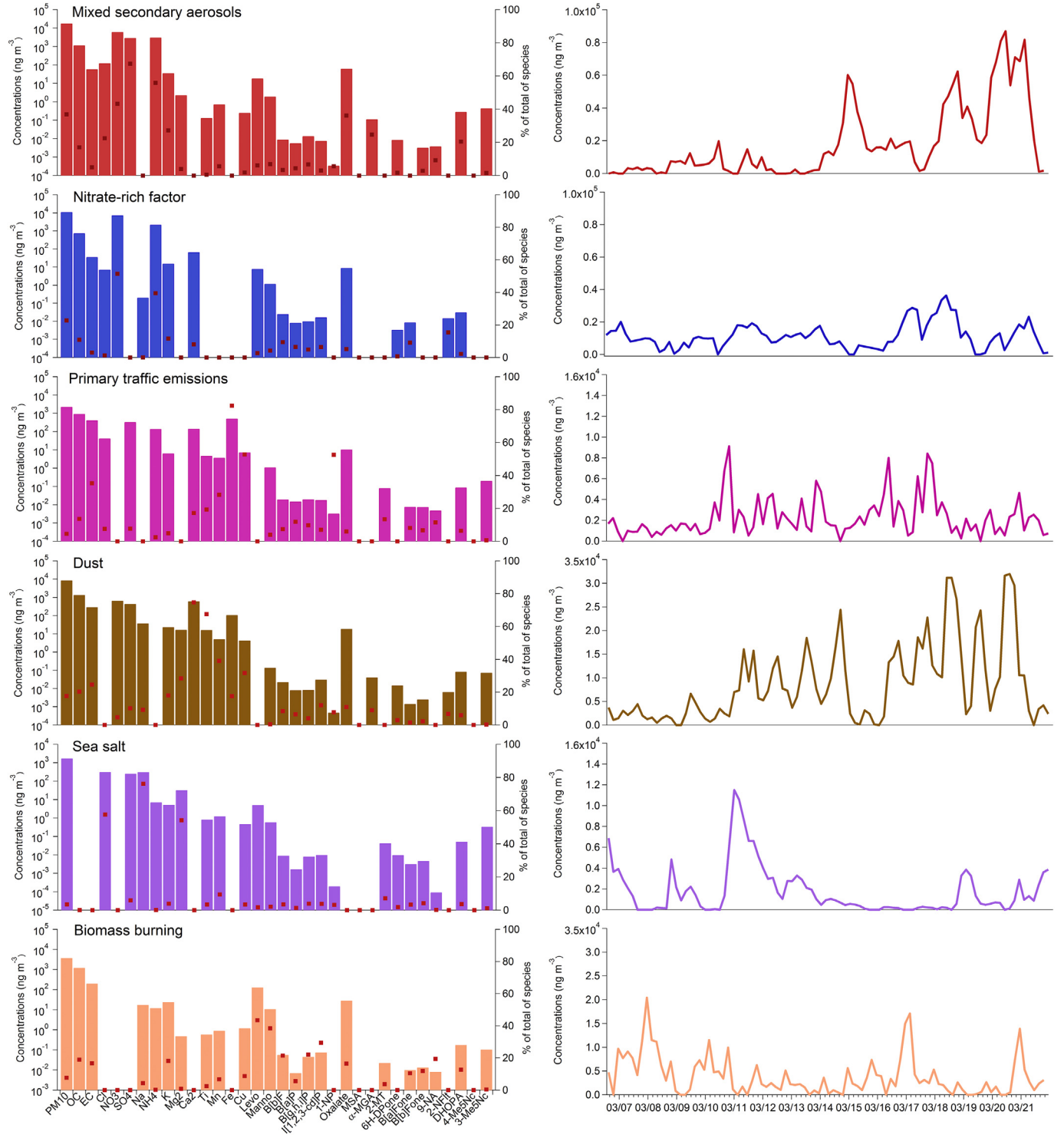

Fig. 3. Source profiles and temporal evolution of mixed secondary aerosols, nitrate-rich, primary traffic emissions, dust, sea salt and biomass burning factors identified at Paris-SIRTA, France (March 2015). Coloured bars and red dots represent the concentrations and the percentages of each species apportioned in the factor, respectively. (For interpretation of the references to colour in this figure legend, the reader is referred to the web version of this article.)

regional sources (Fig. S6), which is consistent with the advected pattern of sulfate in Western Europe. This is also seconded by the findings published previously for the same period using on-line instrumentation (aerosol chemical speciation monitor, ACSM) (Petit et al., 2017a).

3.2.2. Nitrate-rich factor

This factor was characterized by the large proportions of NO_3^- and NH_4^+ (51 and 40% of the total mass of each compound in this factor) (Fig. 3). This source represents nitrate-rich aerosols due to the dominant fraction of ammonium nitrate and accounted for 23% of the total PM_{10} mass (11.2 μg m^{-3}) (Fig. 2). This factor also included small contributions of species such as oxalate (5%) and 2-NF (15%), known to be secondarily formed from the oxidation of PAH (fluoranthene) (Arey et al., 1986; Atkinson et al., 1987), and also benzo[*a*]fluorenone (B[*a*]Fone) (9%), species probably of secondary origin during the studied period (see Section 3.2.9).

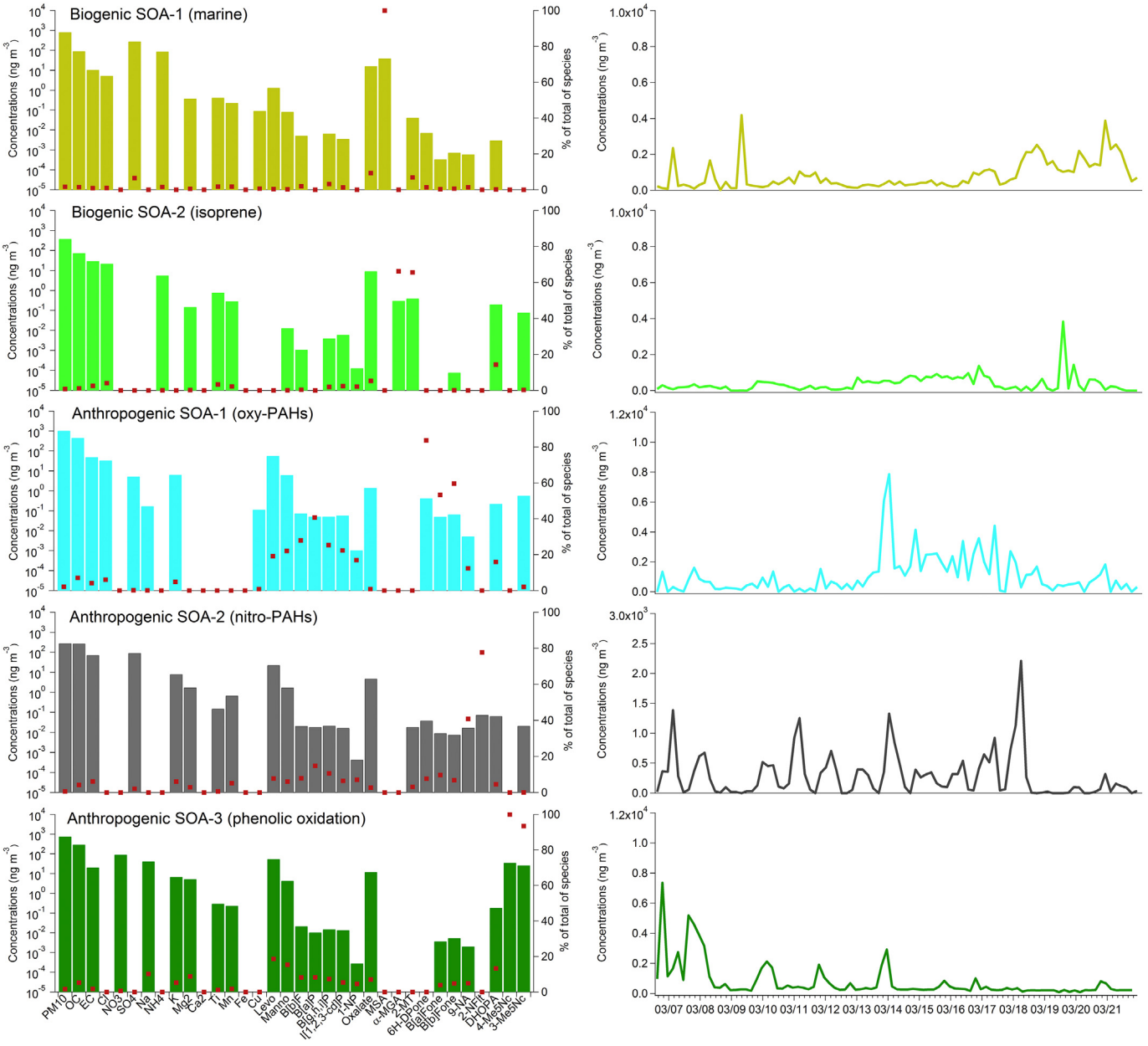

Fig. 4. Source profiles and temporal evolution of biogenic SOA-1, biogenic SOA-2, anthropogenic SOA-1, anthropogenic SOA-2 and anthropogenic SOA-3 identified at Paris-SIRTA, France (March 2015). Coloured bars and red dots represent the concentrations and the percentages of each species apportioned in the factor, respectively. (For interpretation of the references to colour in this figure legend, the reader is referred to the web version of this article.)

High contributions of this factor at low wind speeds were observed (Figs. 1 and 3), indicating the significant role of rather local formation of ammonium nitrate during this period. This was further supported by the CWT analysis (Fig. S6), and also confirmed by the previous observations at the same site for the same PM pollution event as specified above (Petit et al., 2017a).

3.2.3. Primary traffic emissions

Given the constraints applied, this factor showed a significant amount of EC (35% of species in this factor) along with relatively high content of metal elements such as Fe (82%), Cu (53%), and Mn (28%) (Fig. 3). These species are typically associated with road transport in (peri-) urban environments. Fe, Cu, and Mn may originate from brake and tire abrasion and/or road dust resuspension (Garg et al., 2000; Hildemann et al., 1991; Pant and Harrison, 2012; Srivastava et al., 2016; Sternbeck et al., 2002), notifying the influence of both, exhaust and non-exhaust traffic emissions in this factor. This source attribution is furthermore supported by significant correlations with BC_{ff} ($r = 0.5$, $n = 92$, $p < 0.05$) and NO_x ($r = 0.73$, $n = 70$, $p < 0.05$) (Fig. S7).

This factor accounted for 5% of the PM_{10} mass during the studied period, corresponding to an average concentration of 2.2 μg m^{-3} (Fig. 2). This value is in good agreement with the previous observations made in the Paris region (average concentrations of about 2.3 μg m^{-3} in spring season according to Bressi et al. (2014)).

Interestingly, the highest fraction of 1-nitropyrene (1-NP) (53%), likely to be a good marker of diesel emissions (Keyte et al., 2016; Schulte et al., 2015; Zielinska et al., 2004a; Zielinska et al., 2004b), was associated with this factor. Irrespective of the constraint applied on 1-NP, it always showed maximum attribution with this factor along with species mentioned above. In addition, 1-NP showed a good correlation with NO_x ($r = 0.71$, $n = 70$, $p < 0.05$) (Fig. S7). The traffic vehicle fleet in France was composed of about 61.5% of diesel engines in 2015 and up to 80%, taking into account all vehicle categories (including heavy trucks) (CCFA, 2016). These results showed that 1-NP can be used as a

good primary organic molecular marker to trace traffic (diesel) exhaust emissions. To the best of our knowledge, this is the first report of the use of 1-NP to resolve the sources of primary traffic emissions in PMF model.

3.2.4. Dust

This factor was found as one of the major PM_{10} contributor, with an average concentration of 8.7 μg m^{-3} and accounting for 18% of the PM_{10} mass (Fig. 2). It was notably composed of metals and cations, such as Ti, Ca^{2+}, Mg^{2+}, Cu, Mn and Fe (68%, 75%, 28%, 31%, 39% and 18% of species in this factor respectively), together with a significant amount of OC (20%) (Fig. 3). Therefore, this source was identified as dust, including the influence of construction work, soil abrasion and resuspension (Amato et al., 2016a; Amato et al., 2016b; Andersen et al., 2007; Mossetti et al., 2005; Querol et al., 2004; Yin et al., 2005). High concentrations observed during the entire campaign corresponded to the air masses originated from the NE to N directions (Fig. 1). Back trajectories analysis showed negligible impact from Sahara during this period (Fig. S8).

3.2.5. Sea salt

This factor was characterized by high contributions of Na^+ (76%), Mg^{2+} (54%) and Cl^- (58%) (Fig. 3). Cl^-/Na^+ and Mg^{2+}/Na^+ ratios of 1.0 and 0.1, respectively, were on the same order of magnitude as the standard sea water composition (1.2 and 0.1, respectively) (Tang et al., 1997), and also similar to the values reported for the Paris region in previous study ($Cl^-/Na^+ = 0.96$; $Mg^{2+}/Na^+ = 0.13$) (Bressi et al., 2014). The lower proportion of chloride can be explained by the occurrence of acid–base reactions between sea-salt particles and sulfuric and/or nitric acids, leading to the volatilization of HCl (Seinfeld and Pandis, 2012) during the transport of air masses from marine regions to the Paris area.

This source accounted for 2% of the total PM_{10} mass (1.8 μg m^{-3}) (Fig. 2) and showed its highest concentrations during the period from 03/10–03/12 when the origin of air masses changed from recirculation to the NE (Figs. 1 and 3). The results from the CWT analysis highlighted the geographical origin of this source from the Atlantic Ocean and to a lesser extent from the North Sea (Fig. S6).

3.2.6. Biomass burning

This factor was characterized by typical molecular markers from cellulose combustion with significant amounts of levoglucosan (levo, 44%) and mannosan (manno, 38%) (Simoneit, 2002; Simoneit, 1999) (Fig. 3). It also included significant contributions of PAHs (B[*a*]F, B[*ghi*]P, and In[1,2,3-*cd*]P) (21–29%) and K^+ (18%). Biomass burning concentrations were especially high at the beginning of the PM pollution event (Fig. 3). This source accounted for 8% of the PM_{10} mass, with an average concentration of 3.8 μg m^{-3} (Fig. 2). This factor also showed a good correlation with BC_{wb} ($r = 0.63$, $n = 92$, $p < 0.05$) (Fig. S9) even if the BC_{wb}/BC_{ff} separation was probably not optimal during the last period of the campaign due to high loading of inorganic aerosols (Petit et al., 2017a).

This factor also included small contributions of known secondary organic species such as oxalate (17%) and DHOPA (13%), and also of benzo[*a*]fluorenone (B[*a*]Fone) (11%), benzo[*b*]fluorenone (B[*b*]Fone) (12%) and 9-nitroanthracene (9-NA) (19%), species mainly of secondary origin during this specific event (see Sections 3.2.9 and 3.2.10). Thus, this factor may contain a part of oxidized primary organic aerosol (OPOA), arising from the oxidation of organic compounds between the emission point and their introduction in ambient air (Nalin et al., 2016), but not resolved by the model

3.2.7. Biogenic SOA-1 (marine)

This factor contained 100% of methanesulfonic acid (MSA), a known secondary oxidation product of dimethylsulfide (DMS), which is emitted by phytoplankton and several types of anaerobe bacteria and released from the ocean into the atmosphere (Charlson et al., 1987; Chasteen and Bentley, 2004; Crippa et al., 2013b).

The presence of DMS in seawater has been seen to covary with biological productivity and incident solar radiation at the Earth's surface (Andreae and Raemdonck, 1983; Bates et al., 1987). The CWT analysis showed a geographical origin of this factor from the North Sea (Fig. S6). The worldwide distribution of chlorophyll, used as a phytoplankton indicator, estimated using satellite-based measurements, showed a hot spot of phytoplankton bloom near the North Sea in March 2015 and further confirmed the identification and the geographical origin of this SOA source from marine emissions (Fig. S10).

The presence of SO_4^{2-} in this factor is also considered to be partly related to the oxidation of DMS, as the MSA/SO_4^{2-} ratio for this factor of 0.14 was similar to values previously reported in the literature for such source (e.g., about 0.08 in Bove et al. (2016)).

This factor accounted for 2% of the PM_{10} mass (0.8 μg m^{-3}) (Fig. 2) and followed a clear temporal variation with higher contributions during the period from 03/17 to 03/21 (Figs. 1 and 4). This was in agreement with long range transport and aging processes as highlighted by the high concentrations of NO_3^- and SO_4^{2-} during the last days of the PM pollution event (Petit et al., 2017a).

3.2.8. Biogenic SOA-2 (isoprene)

This factor was characterized by significant contributions of oxidation products of isoprene (α-MGA and 2-MT; 65 and 66%, respectively) (Carlton et al., 2009) (Fig. 4). As expected for the late winter and early spring seasons, biogenic SOA factor showed a very low contribution to the PM_{10} mass (<1%) corresponding to a concentration of 0.4 μg m^{-3} (Fig. 2).

3.2.9. Anthropogenic SOA-1 (oxy-PAHs)

The sources of anthropogenic SOA factor were resolved using oxy-PAHs (dibenzo[*b*,*d*]pyran-6-one (6H-DPone) (84%), benzo[*a*]fluorenone (53%) and benzo[*b*]fluorenone (60%)) (Fig. 4). Dibenzo[*b*,*d*]pyran-6-one, a product of phenanthrene photooxidation has been described as a good marker of PAH SOA formation (Lee and Lane, 2010; Perraudin et al., 2007; Tomaz et al., 2017) while benzo[*a*]fluorenone and benzo[*b*]fluorenone may originate from both primary and secondary processes (Albinet et al., 2007; Tomaz et al., 2017). Here, both compounds showed significant correlations ($r = 0.55–0.57$, $n = 92$, $p < 0.05$) with dibenzo[*b*,*d*]pyran-6-one, indicating the probable secondary origin of these compounds during the PM pollution event (Fig. S11). This factor also showed a relatively high amount (16% of species in this factor) of DHOPA, which is known as a SOA marker from toluene oxidation (Kleindienst et al., 2012). Finally, significant contributions of primary species such as PAHs (B[*a*]F, B[*a*]P, B[*ghi*]P, and In[1,2,3-*cd*]P) (23–41%), levoglucosan (19%), mannosan (22%) and 1-NP (17%) were also noticed. Thus, this factor seemed characteristic of PAH SOA from anthropogenic sources including combustion processes such as biomass burning and traffic. A similar factor was already resolved using oxy-PAHs in the companion paper (Srivastava et al., 2018).

Overall, anthropogenic SOA source (oxy-PAHs) accounted for approximately 2% of the total PM_{10} mass with a concentration of 1.1 μg m^{-3} on an average (Fig. 2). High concentrations (up to 8 μg m^{-3}) were especially observed during the 03/13–03/18 period, when air masses originated from the NE direction (Figs. 1 and 4).

3.2.10. Anthropogenic SOA-2 (nitro-PAHs)

This source was characterized by the high fraction of 2-nitrofluoranthene (2-NFlt) (78%) (Fig. 4). 2-NFlt is only secondarily formed from the gas phase reaction between fluoranthene and NO_2 initiated by OH (day-time)/NO_3(night-time) radicals (Arey et al., 1986; Atkinson et al., 1987). Therefore, this factor was identified as another PAH SOA source but with different chemical processes involved (see Section 3.3.2). In addition, this factor also included a significant contribution of 9-NA (41%) which may originated from both, primary and secondary sources (Albinet et al., 2007; Ringuet et al., 2012b), as both processes were dominant during the sampling campaign.

Overall, this source had a very low contribution to the PM_{10} mass (0.6%), corresponding to a concentration of 0.3 μg m^{-3} (Fig. 2). The discernible temporal pattern with higher concentrations during the night indicated the prominent role of night-time chemistry in the formation of nitro-PAHs during this period (Fig. 4) as previously observed at the same site (Ringuet et al., 2012a).

3.2.11. Anthropogenic SOA-3 (phenolic oxidation)

This factor was resolved using 4-methyl-5-nitrocatechol (4-Me5Nc) and 3-methyl-5-nitrocatechol (3-Me5Nc) with very high contributions of both compounds (94–100%) (Fig. 4). These species are typical by-products of SOA formation from the photooxidation of cresols mainly originating from biomass burning emissions (Bruns et al., 2016; Iinuma et al., 2010). In addition, this factor also showed significant contributions of levoglucosan (19%), mannosan (15%), and DHOPA (13%), mainly illustrating the characteristic of biomass burning SOA. To the best of our knowledge, this study is probably the first one reporting the use of methylnitrocatechol isomers for the apportionment, using PMF, of anthropogenic SOA linked to biomass burning.

The source showed a quite low contribution to the PM_{10} mass of 2% on an average corresponding to a concentration of 0.8 μg m^{-3} (Fig. 2). However, high concentrations and contributions were observed during the recirculation period (up to 1.4 μg m^{-3} corresponding to 5% of PM) in agreement with the dominant period of biomass burning emissions.

3.3. Focus on organic aerosols (OA)

3.3.1. OA sources and formation processes

Assuming a OC-to-OA conversion factor around 1.8 (Sciare et al., 2011), OA represented about 25% of the total PM_{10} mass during the studied period. Major contributors were dust (representing 20% of total OC on average for the campaign), biomass burning (19%), and mixed secondary aerosols (17%), followed by primary traffic emissions (14%) and nitrate-rich factor (11%). Only sea salt did not show any contribution to OC mass (Fig. S12). Primary OC (POC) was estimated as the sum of OC fractions associated with dust, biomass burning, and traffic, whereas OC present in the other factors (namely biogenic SOA-1 & 2, anthropogenic SOA-1, 2 & 3, mixed secondary aerosols and nitrate-rich factor) was considered as representing secondary OC (SOC). These calculations led to almost equivalent contributions of POC and SOC to the total OC (53% and 47% on average for the campaign, respectively).

As shown in Fig. 5, the use of specific organic molecular markers allowed the clear identification of 41% of the total SOC composed of anthropogenic SOA (oxy-PAHs, nitro-PAHs, phenolic oxidation, corresponding to average OC contributions of 15%, 9%, 11%, respectively) and biogenic SOA (marine + isoprene, 6% in total). The low contributions of these last two sources may be related to the low biogenic activity during the sampling period (end of winter, beginning of spring). Anthropogenic SOAs were thus considered as the dominant SOC contributors identified and in particular PAH SOA, accounting for 24% of the total SOC. This results highlights the significant contribution of anthropogenic SOA in urban influenced environments, in good agreement with the literature (Shakya and Griffin, 2010; Srivastava et al., 2018; Zhang and Ying, 2012).

Secondary processes leading to the presence of OA within the nitrate-rich factor and mixed secondary aerosols remained unknown. However, previous studies already suggested that OC fractions associated to nitrate- and/or sulfate-rich factors can be considered as secondary (Ke et al., 2008; Lee et al., 2008; Pekney et al., 2006). This was confirmed here by the presence of oxalate, α-MGA, 2-NFlt and DHOPA in both factors. Formation processes leading to OA directly associated with secondary inorganic aerosols may notably include condensation of semi-volatile organic compounds onto the surface of pre-existing particles (Amato et al., 2009; Favez et al., 2007; Surratt et al., 2007), and nucleation mechanisms from various gaseous precursors such as mono- and polyaromatic compounds, alkanes, alkenes… (Lim and Ziemann, 2005; Tkacik et al., 2012; Zhao et al., 2014), as well as the formation of organosulfates and/or organonitrates (Riva et al., 2015; Surratt et al., 2006). Further works are still needed to identify and quantify relevant and specific molecular markers that could help to evaluate the significance of these processes using source-receptor models such as PMF.

3.3.2. Diurnal profiles

Fig. 6 shows the diurnal profiles of significant and relevant OA factors obtained within the present study. The biomass burning factor showed a pronounced peak at night-time, which is consistent with human activities. As expected too, traffic exhibited two pronounced peaks corresponding to morning and evening commuting periods.

It is known that oxy-PAH secondary formation involves photochemical reactions of parent PAHs with ozone or OH radicals (Vione et al., 2004; Walgraeve et al., 2010). However, no specific trend was observed for anthropogenic SOA-1 during the studied period.

Both other anthropogenic SOA factors (nitro-PAHs and phenolic oxidation) exhibited a clear diurnal pattern with high concentrations at night with peaks at distinct times suggesting a significant role of night-time chemistry but with different chemical processes involved. For anthropogenic SOA-2 (nitro-PAHs), an increase of the concentrations from early night until early morning was observed. These diurnal profiles agreed with the ones usually reported for nitrate radical (Reisen and Arey, 2005), indicating the predominance of such processes in the secondary formation of nitro-PAHs. The peaks of concentrations for anthropogenic SOA-3 (phenolic oxidation) were observed in early

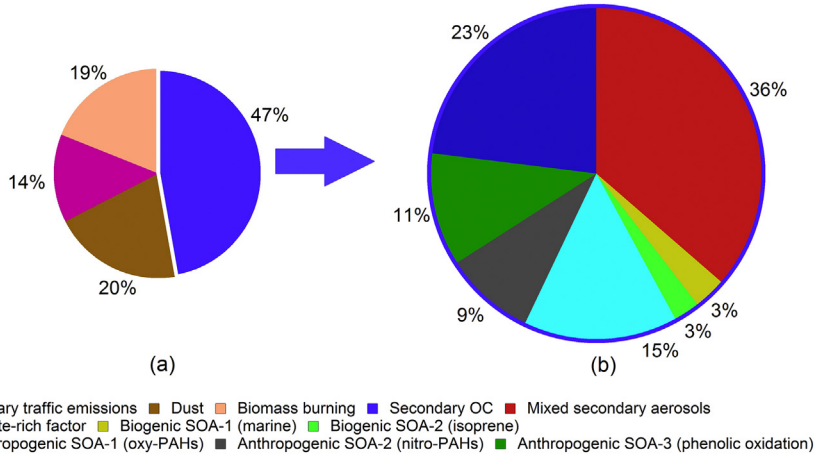

Fig. 5. Average contributions of the identified sources to the total OC (POC + SOC) (left) and SOC (right) mass concentrations at Paris-SIRTA, France (March 2015).

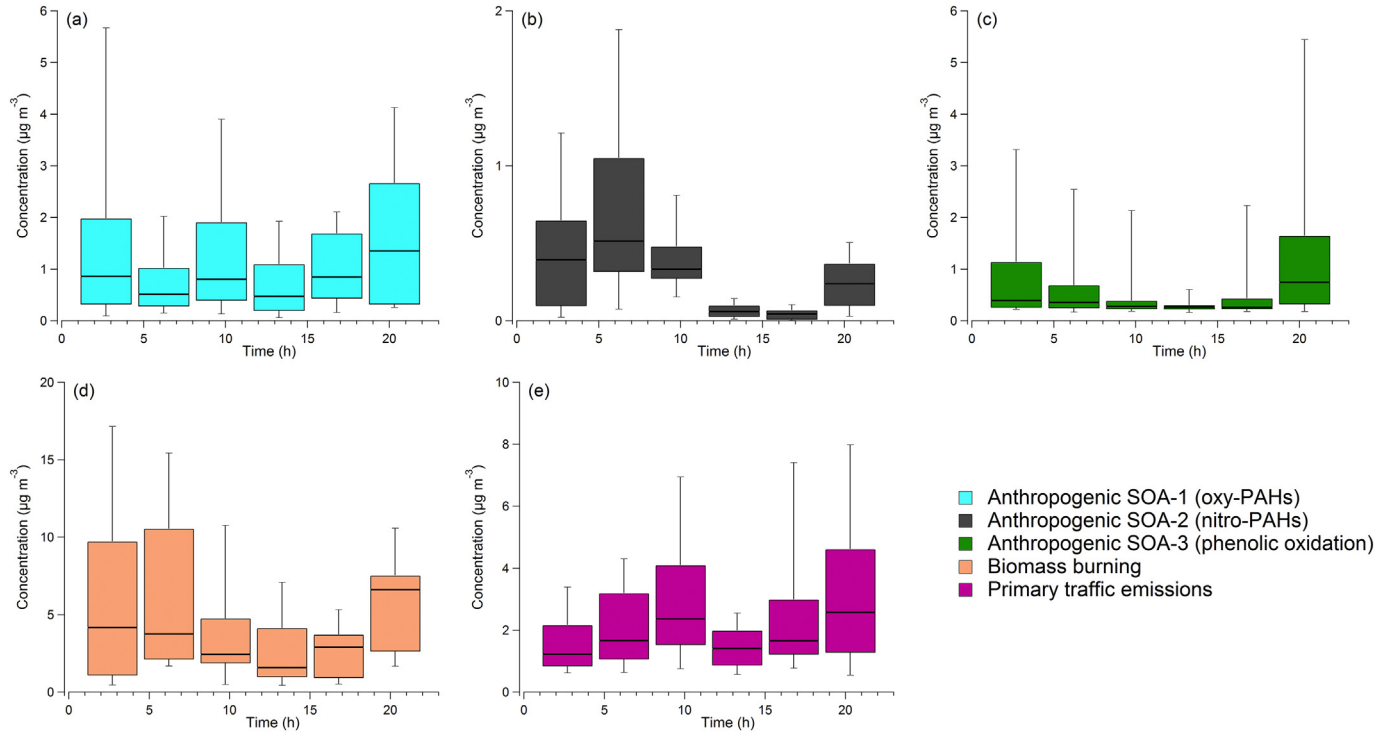

Fig. 6. Diurnal profiles of PMF resolved anthropogenic SOA factors (1, 2, and 3), biomass burning and traffic identified at Paris-SIRTA, France (March 2015).

night in coherence with the biomass burning emissions as the main source of phenolic SOA precursor compounds.

For both anthropogenic SOA-2 and-3, high RH conditions observed during the night (Fig. S13) could also favour secondary formation processes (Jia and Xu, 2014). However, the aerosol liquid water content, together with the higher solubility of the phenolic precursor compounds as well as methylnitrocatechols, could explain the low concentrations of anthropogenic SOA-3 observed during the second part of the night until the morning. Nitro-PAHs are less water soluble than methylnitrocatechols and consequently, they may tend to partition into the solid phase instead of the aqueous one, explaining the differences observed in the diurnal profiles between both factors. Finally, the degradation of both categories of compounds during the day-time under solar irradiation cannot be ruled out.

4. Conclusion

The use of specific primary and secondary molecular markers, with high time resolution data, in PMF model allowed to resolve 11 major PM_{10} sources during a PM pollution event observed in March 2015 in the Paris region. Besides common factors (biomass burning, traffic, dust, sea salt, secondary inorganic aerosols), 2 specific biogenic SOA (marine + isoprene) and 3 anthropogenic SOA (nitro-PAHs + oxy-PAHs + phenolic oxidation) factors have been identified. Results obtained showed that 1-NP can be used as a good primary organic molecular marker to trace traffic emissions and notably diesel exhaust ones.

A special attention was put on SOA, roughly accounting for half of the total OC loading. Molecular markers used in the present study allowed elucidating the probable precursor's origins of about 41% of the total SOC fraction. However, future studies are still needed to focus on the identification, and then the incorporation into PMF analysis, of molecular markers from other known SOA precursors (alkanes, alkenes, mono- and polyaromatic compounds) and of class of compounds which significantly contribute to the SOC fraction (i.e., organosulfates and organonitrates) to further discriminate the nature of OA associated with secondary inorganic sources.

The results obtained in this study highlighted that 35% of the total SOC originated from anthropogenic sources. In particular, PAH SOA (oxy-PAHs + nitro-PAHs) accounted for 24% of the total SOC, highlighting the significance of such SOA precursors in urban influenced environments.

Finally, high time-resolution filter dataset available for the present study allowed a better understanding of the chemical processes involved, notably based on the investigation of diurnal variations. Anthropogenic SOA related to nitro-PAHs and phenolic compounds exhibited a clear temporal pattern with high contributions during the night but with different chemical processes involved. The effects of relative humidity and liquid aerosol content in the formation of these secondary compounds are still not fully understood and should be investigated.

Acknowledgements

This work has notably been supported by the French Ministry of Environment (METL) and the national reference laboratory for air quality monitoring (LCSQA), as well as by the FP7 ACTRIS and H2020 ACTRIS projects. The authors gratefully acknowledge François Truong (LSCE) and Robin Aujay-Plouzeau (INERIS) for taking care of samples and instrumentation and other staff at the SIRTA observatory for providing weather-related data used in this study. They also thank François Kany and Serguei Stavrovski (INERIS) for sample preparation and PAH analyses and Patrick Bodu for the graphical abstract design.

Appendix A. Supplementary data

Supplementary data to this article can be found online at https://doi.org/10.1016/j.scitotenv.2018.03.296.

References

Albinet, A., Leoz-Garziandia, E., Budzinski, H., Villenave, E., 2006. Simultaneous analysis of oxygenated and nitrated polycyclic aromatic hydrocarbons on standard reference material 1649a (urban dust) and on natural ambient air samples by gas chromatography–mass spectrometry with negative ion chemical ionisation. J. Chromatogr. A 1121, 106–113.

Albinet, A., Leoz-Garziandia, E., Budzinski, H., Villenave, E., 2007. Polycyclic aromatic hydrocarbons (PAHs), nitrated PAHs and oxygenated PAHs in ambient air of the Marseilles area (south of France): concentrations and sources. Sci. Total Environ. 384, 280–292.
Albinet, A., Tomaz, S., Lestremau, F., 2013. A really quick easy cheap effective rugged and safe (QuEChERS) extraction procedure for the analysis of particle-bound PAHs in ambient air and emission samples. Sci. Total Environ. 450–451, 31–38.
Albinet, A., Nalin, F., Tomaz, S., Beaumont, J., Lestremau, F., 2014. A simple QuEChERS-like extraction approach for molecular chemical characterization of organic aerosols: application to nitrated and oxygenated PAH derivatives (NPAH and OPAH) quantified by GC–NICIMS. Anal. Bioanal. Chem. 406, 3131–3148.
Amato, F., Hopke, P.K., 2012. Source apportionment of the ambient PM2.5 across St. Louis using constrained positive matrix factorization. Atmos. Environ. 46, 329–337.
Amato, F., Pandolfi, M., Escrig, A., Querol, X., Alastuey, A., Pey, J., Perez, N., Hopke, P.K., 2009. Quantifying road dust resuspension in urban environment by multilinear engine: a comparison with PMF2. Atmos. Environ. 43, 2770–2780.
Amato, F., Alastuey, A., Karanasiou, A., Lucarelli, F., Nava, S., Calzolai, G., Severi, M., Becagli, S., Gianelle, V.L., Colombi, C., Alves, C., Custódio, D., Nunes, T., Cerqueira, M., Pio, C., Eleftheriadis, K., Diapouli, E., Reche, C., Minguillón, M.C., Manousakas, M.I., Maggos, T., Vratolis, S., Harrison, R.M., Querol, X., 2016a. AIRUSE-LIFE+: a harmonized PM speciation and source apportionment in five southern European cities. Atmos. Chem. Phys. 16, 3289–3309.
Amato, F., Favez, O., Pandolfi, M., Alastuey, A., Querol, X., Moukhtar, S., Bruge, B., Verlhac, S., Orza, J.A.G., Bonnaire, N., Le Priol, T., Petit, J.F., Sciare, J., 2016b. Traffic induced particle resuspension in Paris: emission factors and source contributions. Atmos. Environ. 129, 114–124.
Andersen, Z.J., Wahlin, P., Raaschou-Nielsen, O., Scheike, T., Loft, S., 2007. Ambient particle source apportionment and daily hospital admissions among children and elderly in Copenhagen. J. Expo. Sci. Environ. Epidemiol. 17, 625.
Andreae, M.O., Raemdonck, H., 1983. Dimethyl sulfide in the surface ocean and the marine atmosphere: a global view. Science 221, 744–747.
Arey, J., Zielinska, B., Atkinson, R., Winer, A.M., Ramdahl, T., Pitts, J.N., 1986. The formation of nitro-PAH from the gas-phase reactions of fluoranthene and pyrene with the OH radical in the presence of NOx. Atmos. Environ. 20, 2339–2345.
Atkinson, R., Arey, J., Zielinska, B., Pitts, J.N., Winer, A.M., 1987. Evidence for the transformation of polycyclic organic matter in the atmosphere. Atmos. Environ. 21, 2261–2262.
Bates, T.S., Charlson, R.J., Gammon, R.H., 1987. Evidence for the climatic role of marine biogenic sulphur. Nature 329, 319–321.
Belis, C.A., Karagulian, F., Amato, F., Almeida, M., Artaxo, P., Beddows, D.C.S., Bernardoni, V., Bove, M.C., Carbone, S., Cesari, D., Contini, D., Cuccia, E., Diapouli, E., Eleftheriadis, K., Favez, O., El Haddad, I., Harrison, R.M., Hellebust, S., Hovorka, J., Jang, E., Jorquera, H., Kammermeier, T., Karl, M., Lucarelli, F., Mooibroek, D., Nava, S., Nøjgaard, J.K., Paatero, P., Pandolfi, M., Perrone, M.G., Petit, J.E., Pietrodangelo, A., Pokorná, P., Prati, P., Prevot, A.S.H., Quass, U., Querol, X., Saraga, D., Sciare, J., Sfetsos, A., Valli, G., Vecchi, R., Vestenius, M., Yubero, E., Hopke, P.K., 2015. A new methodology to assess the performance and uncertainty of source apportionment models II: the results of two European intercomparison exercises. Atmos. Environ. 123, 240–250.
Boucher, O., Randall, D., Artaxo, P., Bretherton, C., Feingold, G., Forster, P., Kerminen, V.-M., Kondo, Y., Liao, H., Lohmann, U., 2013. Clouds and aerosols. Climate change 2013: the physical science basis. Contribution of Working Group I to the Fifth Assessment Report of the Intergovernmental Panel on Climate Change. Cambridge University Press, pp. 571–657.
Bove, M.C., Brotto, P., Calzolai, G., Cassola, F., Cavalli, F., Fermo, P., Hjorth, J., Massabò, D., Nava, S., Piazzalunga, A., Schembari, C., Prati, P., 2016. PM10 source apportionment applying PMF and chemical tracer analysis to ship-borne measurements in the Western Mediterranean. Atmos. Environ. 125, 140–151.
Bressi, M., Sciare, J., Ghersi, V., Bonnaire, N., Nicolas, J.B., Petit, J.E., Moukhtar, S., Rosso, A., Mihalopoulos, N., Féron, A., 2013. A one-year comprehensive chemical characterisation of fine aerosol (PM2.5) at urban, suburban and rural background sites in the region of Paris (France). Atmos. Chem. Phys. 13, 7825–7844.
Bressi, M., Sciare, J., Ghersi, V., Mihalopoulos, N., Petit, J.E., Nicolas, J.B., Moukhtar, S., Rosso, A., Féron, A., Bonnaire, N., Poulakis, E., Theodosi, C., 2014. Sources and geographical origins of fine aerosols in Paris (France). Atmos. Chem. Phys. 14, 8813–8839.
Bruns, E.A., El Haddad, I., Slowik, J.G., Kilic, D., Klein, F., Baltensperger, U., Prévôt, A.S.H., 2016. Identification of significant precursor gases of secondary organic aerosols from residential wood combustion. Sci. Rep. 6, 27881.
Carlton, A.G., Wiedinmyer, C., Kroll, J.H., 2009. A review of Secondary Organic Aerosol (SOA) formation from isoprene. Atmos. Chem. Phys. 9, 4987–5005.
Cavalli, F., Viana, M., Yttri, K., Genberg, J., Putaud, J.-P., 2010. Toward a standardised thermal-optical protocol for measuring atmospheric organic and elemental carbon: the EUSAAR protocol. Atmos. Meas. Tech. 3, 79–89.
CCFA, 2016. The French Automotive Industry. Analysis and Statistics 2016. CCFA (Comité des Constructeurs Français d'Automobiles). http://temis.documentation.developpement-durable.gouv.fr/document.html?id=Temis-0000921.
CEN, 2017. European Committee for Standardization, EN-16909: 2017 - Ambient Air – Measurements of Elemental Carbon (EC) and Organic Carbon (OC) Deposited on Filters. CEN, Brussels (Belgium).
Charlson, R.J., Lovelock, J.E., Andreae, M.O., Warren, S.G., 1987. Oceanic phytoplankton, atmospheric sulphur, cloud albedo and climate. Nature 326, 655–661.
Chasteen, T.G., Bentley, R., 2004. Volatile organic sulfur compounds of environmental interest: dimethyl sulfide and methanethiol. An introductory overview. J. Chem. Educ. 81, 1524.
Chow, J.C., Watson, J.G., 2002. Review of PM2.5 and PM10 apportionment for fossil fuel combustion and other sources by the chemical mass balance receptor model. Energy Fuel 16, 222–260.
Crippa, M., Canonaco, F., Slowik, J.G., El Haddad, I., DeCarlo, P.F., Mohr, C., Heringa, M.F., Chirico, R., Marchand, N., Temime-Roussel, B., Abidi, E., Poulain, L., Wiedensohler, A., Baltensperger, U., Prévôt, A.S.H., 2013a. Primary and secondary organic aerosol origin by combined gas-particle phase source apportionment. Atmos. Chem. Phys. 13, 8411–8426.
Crippa, M., El Haddad, I., Slowik, J.G., DeCarlo, P.F., Mohr, C., Heringa, M.F., Chirico, R., Marchand, N., Sciare, J., Baltensperger, U., Prévôt, A.S.H., 2013b. Identification of marine and continental aerosol sources in Paris using high resolution aerosol mass spectrometry. J. Geophys. Res.-Atmos. 118, 1950–1963.
Draxler, R., 1999. Hysplit4 user's guide. NOAA Tech. Memo. ERL ARL-230. (35 pp.). http://www.arl.noaa.gov/documents/reports/hysplit_user_guide.pdf.
Drinovec, L., Močnik, G., Zotter, P., Prévôt, A.S.H., Ruckstuhl, C., Coz, E., Rupakheti, M., Sciare, J., Müller, T., Wiedensohler, A., Hansen, A.D.A., 2015. The "dual-spot" Aethalometer: an improved measurement of aerosol black carbon with real-time loading compensation. Atmos. Meas. Tech. 8, 1965–1979.
Dupont, J., Haeffelin, M., Badosa, J., Elias, T., Favez, O., Petit, J., Meleux, F., Sciare, J., Crenn, V., Bonne, J.L., 2016. Role of the boundary layer dynamics effects on an extreme air pollution event in Paris. Atmos. Environ. 141, 571–579.
Favez, O., Cachier, H., Sciare, J., Le Moullec, Y., 2007. Characterization and contribution to PM2.5 of semi-volatile aerosols in Paris (France). Atmos. Environ. 41, 7969–7976.
Favez, O., Petit, J.-E., Bessagnet, B., Meleux, F., Chiappini, L., Lemeur, S., Labartette, C., Chappaz, C., Guergnion, P.-Y., Saison, J.-Y., 2012. Caractéristiques et origines principales des épisodes de pollution hivernaux aux PM10 en France. Pollut. Atmosph. Climat. Santé Soc. 163–181.
Fröhlich, R., Crenn, V., Setyan, A., Belis, C.A., Canonaco, F., Favez, O., Riffault, V., Slowik, J.G., Aas, W., Aijälä, M., Alastuey, A., Artiñano, B., Bonnaire, N., Bozzetti, C., Bressi, M., Carbone, C., Coz, E., Croteau, P.L., Cubison, M.J., Esser-Gietl, J.K., Green, D.C., Gros, V., Heikkinen, L., Herrmann, H., Jayne, J.T., Lunder, C.R., Minguillón, M.C., Močnik, G., O'Dowd, C.D., Ovadnevaite, J., Petralia, E., Poulain, L., Priestman, M., Ripoll, A., Sarda-Estève, R., Wiedensohler, A., Baltensperger, U., Sciare, J., Prévôt, A.S.H., 2015. ACTRIS ACSM intercomparison – part 2: Intercomparison of ME-2 organic source apportionment results from 15 individual, co-located aerosol mass spectrometers. Atmos. Meas. Tech. 8, 2555–2576.
Garg, B.D., Cadle, S.H., Mulawa, P.A., Groblicki, P.J., Laroo, C., Parr, G.A., 2000. Brake wear particulate matter emissions. Environ. Sci. Technol. 34, 4463–4469.
Guinot, B., Cachier, H., Sciare, J., Tong, Y., Xin, W., Jianhua, Y., 2007. Beijing aerosol: atmospheric interactions and new trends. J. Geophys. Res.-Atmos. 112.
Haeffelin, M., Barthès, L., Bock, O., Boitel, C., Bony, S., Bouniol, D., Chepfer, H., Chiriaco, M., Cuesta, J., Delanoë, J., Drobinski, P., Dufresne, J.L., Flamant, C., Grall, M., Hodzic, A., Hourdin, F., Lapouge, F., Lemaître, Y., Mathieu, A., Morille, Y., Naud, C., Noël, V., O'Hirok, W., Pelon, J., Pietras, C., Protat, A., Romand, B., Scialom, G., Vautard, R., 2005. SIRTA, a ground-based atmospheric observatory for cloud and aerosol research. Ann. Geophys. 23, 253–275.
Heal, M.R., Kumar, P., Harrison, R.M., 2012. Particles, air quality, policy and health. Chem. Soc. Rev. 41, 6606–6630.
Henry, R.C., 1997. History and fundamentals of multivariate air quality receptor models. Chemom. Intell. Lab. Syst. 37, 37–42.
Hildemann, L.M., Markowski, G.R., Cass, G.R., 1991. Chemical composition of emissions from urban sources of fine organic aerosol. Environ. Sci. Technol. 25, 744–759.
Hopke, P.K., 2016. Review of receptor modeling methods for source apportionment. J. Air Waste Manage. Assoc. 66, 237–259.
Hopke, P.K., Ito, K., Mar, T., Christensen, W.F., Eatough, D.J., Henry, R.C., Kim, E., Laden, F., Lall, R., Larson, T.V., Liu, H., Neas, L., Pinto, J., Stolzel, M., Suh, H., Paatero, P., Thurston, G.D., 2006. PM source apportionment and health effects: 1. Intercomparison of source apportionment results. J. Expo. Sci. Environ. Epidemiol. 16, 275–286.
Iinuma, Y., Boge, O., Grafe, R., Herrmann, H., 2010. Methyl-nitrocatechols: atmospheric tracer compounds for biomass burning secondary organic aerosols. Environ. Sci. Technol. 44, 8453–8459.
Jaeckels, J.M., Bae, M.-S., Schauer, J.J., 2007. Positive matrix factorization (PMF) analysis of molecular marker measurements to quantify the sources of organic aerosols. Environ. Sci. Technol. 41, 5763–5769.
Jia, L., Xu, Y., 2014. Effects of relative humidity on ozone and secondary organic aerosol formation from the photooxidation of benzene and ethylbenzene. Aerosol Sci. Technol. 48, 1–12.
Kawamura, K., Ikushima, K., 1993. Seasonal changes in the distribution of dicarboxylic acids in the urban atmosphere. Environ. Sci. Technol. 27, 2227–2235.
Ke, L., Liu, W., Wang, Y., Russell, A.G., Edgerton, E.S., Zheng, M., 2008. Comparison of PM2.5 source apportionment using positive matrix factorization and molecular marker-based chemical mass balance. Sci. Total Environ. 394, 290–302.
Keyte, I.J., Albinet, A., Harrison, R.M., 2016. On-road traffic emissions of polycyclic aromatic hydrocarbons and their oxy- and nitro- derivative compounds measured in road tunnel environments. Sci. Total Environ. 566–567, 1131–1142.
Kim, E., Hopke, P.K., 2004. Source apportionment of fine particles in Washington, DC, utilizing temperature-resolved carbon fractions. J. Air Waste Manage. Assoc. 54, 773–785.
Kim, E., Hopke, P.K., Edgerton, E.S., 2003. Source identification of Atlanta aerosol by positive matrix factorization. J. Air Waste Manage. Assoc. 53, 731–739.
Kleindienst, T., Conver, T., McIver, C., Edney, E., 2004. Determination of secondary organic aerosol products from the photooxidation of toluene and their implications in ambient PM2. 5. J. Atmos. Chem. 47, 79–100.
Kleindienst, T.E., Jaoui, M., Lewandowski, M., Offenberg, J.H., Docherty, K.S., 2012. The formation of SOA and chemical tracer compounds from the photooxidation of naphthalene and its methyl analogs in the presence and absence of nitrogen oxides. Atmos. Chem. Phys. 12, 8711–8726.
Laing, J.R., Hopke, P.K., Hopke, E.F., Husain, L., Dutkiewicz, V.A., Paatero, J., Viisanen, Y., 2015. Positive matrix factorization of 47 years of particle measurements in Finnish Arctic. Aerosol Air Qual. Res. 15, 188–207.

Lee, J., Lane, D.A., 2010. Formation of oxidized products from the reaction of gaseous phenanthrene with the OH radical in a reaction chamber. Atmos. Environ. 44, 2469–2477.
Lee, S., Liu, W., Wang, Y., Russell, A.G., Edgerton, E.S., 2008. Source apportionment of PM 2.5: comparing PMF and CMB results for four ambient monitoring sites in the southeastern United States. Atmos. Environ. 42, 4126–4137.
Lim, Y.B., Ziemann, P.J., 2005. Products and mechanism of secondary organic aerosol formation from reactions of n-alkanes with OH radicals in the presence of NOx. Environ. Sci. Technol. 39, 9229–9236.
Lim, J.-M., Lee, J.-H., Moon, J.-H., Chung, Y.-S., Kim, K.-H., 2010. Source apportionment of PM10 at a small industrial area using Positive Matrix Factorization. Atmos. Res. 95, 88–100.
Lucarelli, F., Nava, S., Calzolai, G., Chiari, M., Udisti, R., Marino, F., 2011. Is PIXE still a useful technique for the analysis of atmospheric aerosols? The LABEC experience. X-Ray Spectrom. 40, 162–167.
Lucarelli, F., Calzolai, G., Chiari, M., Nava, S., Carraresi, L., 2017. Study of atmospheric aerosols by IBA techniques: the LABEC experience. Nucl. Instrum. Methods Phys. Res., Sect. B 417, 121–127.
Mossetti, S., Angius, S.P., Angelino, E., 2005. Assessing the impact of particulate matter sources in the Milan urban area. Int. J. Environ. Pollut. 24, 247–259.
Nalin, F., Golly, B., Besombes, J.-L., Pelletier, C., Aujay-Plouzeau, R., Verlhac, S., Dermigny, A., Fievet, A., Karoski, N., Dubois, P., Collet, S., Favez, O., Albinet, A., 2016. Fast oxidation processes from emission to ambient air introduction of aerosol emitted by residential log wood stoves. Atmos. Environ. 143, 15–26.
Norris, G., Duvall, R., Brown, S., Bai, S., 2014. EPA Positive Matrix Factorization (PMF) 5.0 Fundamentals and User Guide Prepared for the US Environmental Protection Agency Office of Research and Development, Washington, DC. DC EPA/600/R-14/108.
Nozière, B., Kalberer, M., Claeys, M., Allan, J., D'Anna, B., Decesari, S., Finessi, E., Glasius, M., Grgić, I., Hamilton, J.F., Hoffmann, T., Iinuma, Y., Jaoui, M., Kahnt, A., Kampf, C.J., Kourtchev, I., Maenhaut, W., Marsden, N., Saarikoski, S., Schnelle-Kreis, J., Surratt, J.D., Szidat, S., Szmigielski, R., Wisthaler, A., 2015. The molecular identification of organic compounds in the atmosphere: state of the art and challenges. Chem. Rev. 115, 3919–3983.
Paatero, P., 1997. Least squares formulation of robust non-negative factor analysis. Chemom. Intell. Lab. Syst. 37, 23–35.
Paatero, P., Hopke, P.K., 2003. Discarding or downweighting high-noise variables in factor analytic models. Anal. Chim. Acta 490, 277–289.
Paatero, P., Hopke, P.K., 2009. Rotational tools for factor analytic models. J. Chemom. 23, 91–100.
Paatero, P., Tapper, U., 1994. Positive matrix factorization: a non-negative factor model with optimal utilization of error estimates of data values. Environmetrics 5, 111–126.
Pant, P., Harrison, R.M., 2012. Critical review of receptor modelling for particulate matter: a case study of India. Atmos. Environ. 49, 1–12.
Pekney, N.J., Davidson, C.I., Robinson, A., Zhou, L., Hopke, P., Eatough, D., Rogge, W.F., 2006. Major source categories for PM2.5 in Pittsburgh using PMF and UNMIX. Aerosol Sci. Technol. 40, 910–924.
Perraudin, E., Budzinski, H., Villenave, E., 2007. Identification and quantification of ozonation products of anthracene and phenanthrene adsorbed on silica particles. Atmos. Environ. 41, 6005–6017.
Petit, J.-E., Favez, O., Sciare, J., Canonaco, F., Croteau, P., Močnik, G., Jayne, J., Worsnop, D., Leoz-Garziandia, E., 2014. Submicron aerosol source apportionment of wintertime pollution in Paris, France by double positive matrix factorization (PMF 2) using an aerosol chemical speciation monitor (ACSM) and a multi-wavelength Aethalometer. Atmos. Chem. Phys. 14, 13773–13787.
Petit, J.E., Favez, O., Sciare, J., Crenn, V., Sarda-Estève, R., Bonnaire, N., Močnik, G., Dupont, J.C., Haeffelin, M., Leoz-Garziandia, E., 2015. Two years of near real-time chemical composition of submicron aerosols in the region of Paris using an Aerosol Chemical Speciation Monitor (ACSM) and a multi-wavelength Aethalometer. Atmos. Chem. Phys. 15, 2985–3005.
Petit, J.-E., Amodeo, T., Meleux, F., Bessagnet, B., Menut, L., Grenier, D., Pellan, Y., Ockler, A., Rocq, B., Gros, V., 2017a. Characterising an intense PM pollution episode in March 2015 in France from multi-site approach and near real time data: climatology, variabilities, geographical origins and model evaluation. Atmos. Environ. 155, 68–84.
Petit, J.E., Favez, O., Albinet, A., Canonaco, F., 2017b. A user-friendly tool for comprehensive evaluation of the geographical origins of atmospheric pollution: wind and trajectory analyses. Environ. Model. Softw. 88, 183–187.
Querol, X., Alastuey, A., Viana, M., Rodriguez, S., Artíñano, B., Salvador, P., Do Santos, S.G., Patier, R.F., Ruiz, C., De la Rosa, J., 2004. Speciation and origin of PM10 and PM2. 5 in Spain. J. Aerosol Sci. 35, 1151–1172.
Reisen, F., Arey, J., 2005. Atmospheric reactions influence seasonal PAH and nitro-PAH concentrations in the Los Angeles Basin. Environ. Sci. Technol. 39, 64–73.
Ringuet, J., Albinet, A., Leoz-Garziandia, E., Budzinski, H., Villenave, E., 2012a. Diurnal/nocturnal concentrations and sources of particulate-bound PAHs, OPAHs and NPAHs at traffic and suburban sites in the region of Paris (France). Sci. Total Environ. 437, 297–305.
Ringuet, J., Albinet, A., Leoz-Garziandia, E., Budzinski, H., Villenave, E., 2012b. Reactivity of polycyclic aromatic compounds (PAHs, NPAHs and OPAHs) adsorbed on natural aerosol particles exposed to atmospheric oxidants. Atmos. Environ. 61, 15–22.
Riva, M., Tomaz, S., Cui, T., Lin, Y.H., Perraudin, E., Gold, A., Stone, E.A., Villenave, E., Surratt, J.D., 2015. Evidence for an unrecognized secondary anthropogenic source of organosulfates and sulfonates: gas-phase oxidation of polycyclic aromatic hydrocarbons in the presence of sulfate aerosol. Environ. Sci. Technol. 49, 6654–6664.
Sandradewi, J., Prévôt, A.S.H., Szidat, S., Perron, N., Alfarra, M.R., Lanz, V.A., Weingartner, E., Baltensperger, U., 2008. Using aerosol light absorption measurements for the quantitative determination of wood burning and traffic emission contributions to particulate matter. Environ. Sci. Technol. 42, 3316–3323.
Schauer, J.J., Rogge, W.F., Hildemann, L.M., Mazurek, M.A., Cass, G.R., Simoneit, B.R., 1996. Source apportionment of airborne particulate matter using organic compounds as tracers. Atmos. Environ. 30, 3837–3855.
Schembari, C., Bove, M.C., Cuccia, E., Cavalli, F., Hjorth, J., Massabò, D., Nava, S., Udisti, R., Prati, P., 2014. Source apportionment of PM10 in the Western Mediterranean based on observations from a cruise ship. Atmos. Environ. 98, 510–518.
Schulte, J.K., Fox, J.R., Oron, A.P., Larson, T.V., Simpson, C.D., Paulsen, M., Beaudet, N., Kaufman, J.D., Magzamen, S., 2015. Neighborhood-scale spatial models of diesel exhaust concentration profile using 1-nitropyrene and other nitroarenes. Environ. Sci. Technol. 49, 13422–13430.
Schwab, J., Felton, D., Rattigan, O., L Demerjian, K., 2006. New York State Urban and Rural Measurements of Continuous PM2.5 Mass by FDMS, TEOM, and BAM. Vol. 56.
Sciare, J., D'Argouges, O., Sarda-Esteve, R., Gaimoz, C., Dolgorouky, C., Bonnaire, N., Favez, O., Bonsang, B., Gros, V., 2011. Large contribution of water-insoluble secondary organic aerosols in the region of Paris (France) during wintertime. J. Geophys. Res.-Atmos. 116, D22203.
Seinfeld, J.H., Pandis, S.N., 2012. Atmospheric Chemistry and Physics: From Air Pollution to Climate Change. John Wiley & Sons.
Shakya, K.M., Griffin, R.J., 2010. Secondary organic aerosol from photooxidation of polycyclic aromatic hydrocarbons. Environ. Sci. Technol. 44, 8134–8139.
Shrivastava, M.K., Subramanian, R., Rogge, W.F., Robinson, A.L., 2007. Sources of organic aerosol: positive matrix factorization of molecular marker data and comparison of results from different source apportionment models. Atmos. Environ. 41, 9353–9369.
Simoneit, B.T., 1999. A review of biomarker compounds as source indicators and tracers for air pollution. Environ. Sci. Pollut. Res. 6, 159–169.
Simoneit, B.R.T., 2002. Biomass burning — a review of organic tracers for smoke from incomplete combustion. Appl. Geochem. 17, 129–162.
Srimuruganandam, B., Shiva Nagendra, S.M., 2012. Application of positive matrix factorization in characterization of PM10 and PM2.5 emission sources at urban roadside. Chemosphere 88, 120–130.
Srivastava, D., Goel, A., Agrawal, M., 2016. Particle bound metals at major intersections in an urban location and source identification through use of metal markers. Proc. Natl. Acad. Sci. India Sect. A 86, 209–220.
Srivastava, D., Tomaz, S., Favez, O., Lanzafame, G.M., Golly, B., Besombes, J.-L., Alleman, L.Y., Jaffrezo, J.-L., Jacob, V., Perraudin, E., Villenave, E., Albinet, A., 2018. Speciation of organic fraction does matter for source apportionment. Part 1: a one-year campaign in Grenoble (France). Sci. Total Environ. 624, 1598–1611.
Stein, A.F., Draxler, R.R., Rolph, G.D., Stunder, B.J.B., Cohen, M.D., Ngan, F., 2015. NOAA's HYSPLIT atmospheric transport and dispersion modeling system. Bull. Am. Meteorol. Soc. 96, 2059–2077.
Sternbeck, J., Sjödin, Å., Andréasson, K., 2002. Metal emissions from road traffic and the influence of resuspension—results from two tunnel studies. Atmos. Environ. 36, 4735–4744.
Surratt, J.D., Kroll, J.H., Kleindienst, T.E., Edney, E.O., Claeys, M., Sorooshian, A., Ng, N.L., Offenberg, J.H., Lewandowski, M., Jaoui, M., Flagan, R.C., Seinfeld, J.H., 2006. Evidence for organosulfates in secondary organic aerosol. Environ. Sci. Technol. 41, 517–527.
Surratt, J.D., Lewandowski, M., Offenberg, J.H., Jaoui, M., Kleindienst, T.E., Edney, E.O., Seinfeld, J.H., 2007. Effect of acidity on secondary organic aerosol formation from isoprene. Environ. Sci. Technol. 41, 5363–5369.
Tang, I.N., Tridico, A.C., Fung, K.H., 1997. Thermodynamic and optical properties of sea salt aerosols. J. Geophys. Res.-Atmos. 102, 23269–23275.
Tkacik, D.S., Presto, A.A., Donahue, N.M., Robinson, A.L., 2012. Secondary organic aerosol formation from intermediate-volatility organic compounds: cyclic, linear, and branched alkanes. Environ. Sci. Technol. 46, 8773–8781.
Tomaz, S., Shahpoury, P., Jaffrezo, J.L., Lammel, G., Perraudin, E., Villenave, E., Albinet, A., 2016. One-year study of polycyclic aromatic compounds at an urban site in Grenoble (France): seasonal variations, gas/particle partitioning and cancer risk estimation. Sci. Total Environ. 565, 1071–1083.
Tomaz, S., Jaffrezo, J.-L., Favez, O., Perraudin, E., Villenave, E., Albinet, A., 2017. Sources and atmospheric chemistry of oxy- and nitro-PAHs in the ambient air of Grenoble (France). Atmos. Environ. 161, 144–154.
Verlhac, S., Favez, O., Albinet, A., 2013. Comparaison inter laboratoires organisée pour les laboratoires européens impliqués dans l'analyse du lévoglucosan et de ses isomères LCSQA/INERIS. http://www.lcsqa.org/rapport/2013/ineris/comparaison-inter-laboratoires-organisee-laboratoires-europeens-impliques-analys.
Vione, D., Barra, S., De Gennaro, G., De Rienzo, M., Gilardoni, S., Perrone, M.G., Pozzoli, L., 2004. Polycyclic aromatic hydrocarbons in the atmosphere: monitoring, sources, sinks and fate. II: sinks and fate. Ann. Chim. 94, 257–268.
Waked, A., Favez, O., Alleman, L.Y., Piot, C., Petit, J.E., Delaunay, T., Verlinden, E., Golly, B., Besombes, J.L., Jaffrezo, J.L., Leoz-Garziandia, E., 2014. Source apportionment of PM10 in a north-western Europe regional urban background site (Lens, France) using positive matrix factorization and including primary biogenic emissions. Atmos. Chem. Phys. 14, 3325–3346.
Walgraeve, C., Demeestere, K., Dewulf, J., Zimmermann, R., Van Langenhove, H., 2010. Oxygenated polycyclic aromatic hydrocarbons in atmospheric particulate matter: molecular characterization and occurrence. Atmos. Environ. 44, 1831–1846.
Wang, Y., Hopke, P.K., Xia, X., Rattigan, O.V., Chalupa, D.C., Utell, M.J., 2012. Source apportionment of airborne particulate matter using inorganic and organic species as tracers. Atmos. Environ. 55, 525–532.
Watson, J.G., Zhu, T., Chow, J.C., Engelbrecht, J., Fujita, E.M., Wilson, W.E., 2002. Receptor modeling application framework for particle source apportionment. Chemosphere 49, 1093–1136.
Yin, J., Allen, A., Harrison, R., Jennings, S., Wright, E., Fitzpatrick, M., Healy, T., Barry, E., Ceburnis, D., McCusker, D., 2005. Major component composition of urban PM 10 and PM 2.5 in Ireland. Atmos. Res. 78, 149–165.

Yttri, K.E., Schnelle-Kreis, J., Maenhaut, W., Abbaszade, G., Alves, C., Bjerke, A., Bonnier, N., Bossi, R., Claeys, M., Dye, C., Evtyugina, M., García-Gacio, D., Hillamo, R., Hoffer, A., Hyder, M., Iinuma, Y., Jaffrezo, J.L., Kasper-Giebl, A., Kiss, G., López-Mahia, P.L., Pio, C., Piot, C., Ramirez-Santa-Cruz, C., Sciare, J., Teinilä, K., Vermeylen, R., Vicente, A., Zimmermann, R., 2015. An intercomparison study of analytical methods used for quantification of levoglucosan in ambient aerosol filter samples. Atmos. Meas. Tech. 8, 125–147.

Zhang, H., Ying, Q., 2012. Secondary organic aerosol from polycyclic aromatic hydrocarbons in Southeast Texas. Atmos. Environ. 55, 279–287.

Zhang, Y., Sheesley, R.J., Schauer, J.J., Lewandowski, M., Jaoui, M., Offenberg, J.H., Kleindienst, T.E., Edney, E.O., 2009. Source apportionment of primary and secondary organic aerosols using positive matrix factorization (PMF) of molecular markers. Atmos. Environ. 43, 5567–5574.

Zhao, Y., Hennigan, C.J., May, A.A., Tkacik, D.S., de Gouw, J.A., Gilman, J.B., Kuster, W.C., Borbon, A., Robinson, A.L., 2014. Intermediate-volatility organic compounds: a large source of secondary organic aerosol. Environ. Sci. Technol. 48, 13743–13750.

Zielinska, B., Sagebiel, J., Arnott, W.P., Rogers, C.F., Kelly, K.E., Wagner, D.A., Lighty, J.S., Sarofim, A.F., Palmer, G., 2004a. Phase and size distribution of polycyclic aromatic hydrocarbons in diesel and gasoline vehicle emissions. Environ. Sci. Technol. 38, 2557–2567.

Zielinska, B., Sagebiel, J., McDonald, J.D., Whitney, K., Lawson, D.R., 2004b. Emission rates and comparative chemical composition from selected in-use diesel and gasoline-fueled vehicles. J. Air Waste Manage. Assoc. 54, 1138–1150.

SUPPLEMENTARY MATERIAL (SM)

Speciation of organic fractions does matter for aerosol source apportionment. Part 2: intensive short-term campaign in the Paris area (France)

D. Srivastava[1, 2, 3, *], O. Favez[1], N. Bonnaire[4], F. Lucarelli[5], M. Haeffelin[6], E. Perraudin[2, 3], V. Gros[4], E. Villenave[2, 3], A. Albinet[1*]

[1]INERIS, Parc Technologique Alata, BP 2, 60550 Verneuil-en-Halatte, France

[2]CNRS, EPOC, UMR 5805 CNRS, 33405 Talence, France

[3]Université de Bordeaux, EPOC, UMR 5805 CNRS, 33405 Talence, France

[4]LSCE - UMR8212, CNRS-CEA-UVSQ, Gif-sur-Yvette, France

[5]University of Florence, Dipartimento di Fisica Astronomia, 50019, Sesto Fiorentino, Italy

[6]Institut Pierre Simon Laplace, CNRS, Ecole Polytechnique, 91128 Palaiseau, France

Correspondence to: alexandre.albinet@gmail.com; alexandre.albinet@ineris.fr; deepchandra.srivastava@gmail.com

Phone – +33 3 4455 6485; 6949

Submitted for publication in Science of The Total Environment

Figure S1. Map of France with the location of SIRTA sampling station.

Table S1. List of the chemicals, solvents and gases used and their characteristics.

Compounds	Supplier	Purity
PAHs		
1-Methylnaphthalene	Dr. Ehrenstorfer	98.3%
2-Methylnaphthalene	Dr. Ehrenstorfer	99.5%
Acenaphthene	Dr. Ehrenstorfer	99.5%
Fluorene	Dr. Ehrenstorfer	99.5%
Phenanthrene	Dr. Ehrenstorfer	99.5%
Anthracene	Dr. Ehrenstorfer	99.5%
Fluoranthene	Dr. Ehrenstorfer	99.5%
2-Methylfluoranthene	Dr. Ehrenstorfer	96.5%
Pyrene	Dr. Ehrenstorfer	99.5%
Benz[a]anthracene	Dr. Ehrenstorfer	99.5%
Chrysene	Dr. Ehrenstorfer	99.5%
Retene	BCP Instruments	99.5%
Benzo[e]pyrene	Dr. Ehrenstorfer	98.7%
Benzo[j]fluoranthene	Dr. Ehrenstorfer	98.0%
Benzo[b]fluoranthene	Dr. Ehrenstorfer	99.5%
Benzo[k]fluoranthene	Dr. Ehrenstorfer	99.5%
Benzo[a]pyrene	Dr. Ehrenstorfer	99.5%
Dibenz[a,h]anthracene	Dr. Ehrenstorfer	99.5%
Benzo[g,h,i]perylene	Dr. Ehrenstorfer	99.5%
Indeno[1,2,3-cd]pyrene	Dr. Ehrenstorfer	99.5%
Coronene	Dr. Ehrenstorfer	99.5%
6-Methylchrysene	Supelco	99%
Oxy-PAHs		
1,2-Naphthalic anhydride	ABCR	98%
1,2-Naphthoquinone	Sigma-Aldrich	97%
1,4-Anthraquinone	Chiron	97.8%
1,4-Chrysenequinone	Chiron	99%
5,6-Chrysenequinone	BCP Instruments	99.8%
1,4-Naphthoquinone	Sigma-Aldrich	97%
1,8-Naphthalic anhydride	Sigma-Aldrich	98%
1-Acenaphthenone	ABCR	98%
1-Naphthaldehyde	Sigma-Aldrich	95%
1-Pyrenecarboxaldehyde	Sigma-Aldrich	99%
2,3-Naphthalene dicarboxylic anhydride	ABCR	95%
2-Formyl-trans-cinnamaldehyde	Santai Labs	99%
2-Methylanthraquinone	Sigma-Aldrich	> 95%
2-Nitro-9-fluorenone	Sigma-Aldrich	99%
Biphenyl-4,4'-dicarboxaldehyde	ABCR	97%
6H-Dibenzo[b,d]pyran-6-one	Syntheval	97%
9,10-Anthraquinone	Acros Organics	98%
9,10-Phenanthrenequinone	Sigma-Aldrich	> 99%
9-Fluorenone	Acros Organics	> 99%
9-Phenanthrenecarboxaldehyde	Sigma-Aldrich	97%
Aceanthrenequinone	Sigma-Aldrich	96%
Acenaphthenequinone	Sigma-Aldrich	> 90%
Anthrone	Acros Organics	98%
Benz[a]anthracene-7,12-dione	Acros Organics	99%
Benzanthrone	Acros Organics	99%
Benzo[a]fluorenone	Chiron	99.9%
Benzo[b]fluorenone	Chiron	99.8%
Benzophenone	Sigma-Aldrich	99%
Biphenyl-2-2'-dicarboxaldehyde	ABCR	97%

Phthaldialdehyde	Sigma-Aldrich	> 99%
Phthalic anhydride	Sigma-Aldrich	> 99%
Xanthone	Sigma-Aldrich	97%

Table S1(continued)

Compounds	**Supplier**	**Purity**
Nitro-PAHs		
1,3-Dinitropyrene	Chiron	95.6%
1,5-Dinitronaphthalene	Chiron	99.7%
1,6-Dinitropyrene	Chiron	96.3%
1,8-Dinitropyrene	Chiron	99.9%
1-Methyl-4-nitronaphthalene	Chiron	> 99%
1-Methyl-5-nitronaphthalene	Chiron	> 99.5%
1-Methyl-6-nitronaphthalene	Chiron	> 99%
1-Nitrobenzo[e]pyrene	Chiron	99.6%
1-Nitronaphthalene	Chiron	99.9%
1-Nitropyrene	Chiron	99%
2-Methyl-1-nitronaphthalene	Chiron	> 99.5%
2-Methyl-4-nitronaphthalene	Chiron	> 99%
2-Nitroanthracene	Chiron	99.8%
2-Nitrobiphenyl	Chiron	> 99%
2-Nitrodibenzothiophene	Sigma-Aldrich	99%
2-Nitrofluoranthene	Chiron	> 99%
2-Nitrofluorene	Acros Organics	99%
2-Nitronaphthalene	Chiron	99%
2-Nitropyrene	Chiron	99.9%
3-Nitrobenzo[e]pyrene	Chiron	95%
3-Nitrobiphenyl	Sigma-Aldrich	99%
3-Nitrodibenzofuran	Sigma-Aldrich	99%
3-Nitrofluoranthene	Acros Organics	99%
3-Nitrophenanthrene	Dr. Ehrenstorfer	99.7%
4-Nitropyrene	Chiron	99.8%
5-Nitroacenaphthene	Dr. Ehrenstorfer	90%
6-Nitrobenzo[a]pyrene	Chiron	95%
6-Nitrochrysene	Acros Organics	99%
7-Nitrobenz[a]anthracene	Accu Standard	99%
9-Methyl-10-nitroanthracene	Chiron	99%
9-Nitroanthracene (9-NA)	Chiron	97.0%
9-Nitrophenanthrene	Dr. Ehrenstorfer	99.5%
SOA markers		
3-Methyl-5-Nitrocatechol	Chiron	97%
4-Methyl-5-Nitrocatechol	TRC	98%
3-Methylbutane-1,2,3-tricarboxylic acid (MBTCA)	TRC	98%
2,3-Dihydroxy-4-oxopentanoic acid (DHOPA)	TRC	98%
2R, 3S-Dihydroxy-4-oxo-butanoic Acid (DHOBA)	TRC	80%
1,2,3,4-Cyclobutane tetracarboxylic acid	Sigma-Aldrich	98%
Phthalic acid	Sigma-Aldrich	> 99.5%
Pinonic acid	Sigma-Aldrich	98%
Pinic acid	Santai labs	95%
Succinic acid	Sigma-Aldrich	99%
α-Methylglyceric acid (α-MGA)	Tractus	95%
2-Methylerythritol (2-MT)	Sigma-Aldrich	90%
β-Caryophyllinic acid	TRC	97%
3-Hydroxyglutaric acid	Santa Cruz Biotechnology	95%

Table S1(continued)

Compounds	Supplier	Purity
Deuterated nitro-PAHs, oxy-PAHs and SOA markers		
1,4-Naphthoquinone-d_6	C/D/N isotopes	> 99%
Anthraquinone-d_8	C/D/N isotopes	> 99%
1-Nitronaphthalene-d_7	C/D/N isotopes	> 99%
1-Nitropyrene-d_9	C/D/N isotopes	> 99%
2-Nitrobiphenyl-d_9	C/D/N isotopes	> 99%
2-Nitrofluorene-d_9	C/D/N isotopes	> 99%
6-Nitrobenzo[a]pyrene-d_{11}	Chiron	98%
6-Nitrochrysene-d_{11}	C/D/N isotopes	> 99%
9-Fluorenone-d_8	C/D/N isotopes	> 99%
9-Nitroanthracene-d_9	C/D/N isotopes	> 99%
9-Nitrophenanthrene-d_9	Chiron	98%
Succinic-2,2,3,3-d4 acid	C/D/N isotopes	99%
Meso-erythritol-1,1,2,4,4-d6	C/D/N isotopes	99.1%
1,9-Nonanedioic-d14	C/D/N isotopes	99%
Solvents		
Acetone	Sigma-Aldrich	> 99.9%
Acetonitrile	VWR	> 99.9%
Dichloromethane	VWR	> 99.8%
Pentane	Sigma-Aldrich	> 99%
Methanol	Sigma-Aldrich	> 99.9%
Gases		
Helium	Air liquide	99.9%
Nitrogen	Air liquide	99.9%
Methane	Air liquide	99.9%

Analysis of oxy-PAHs, nitro-PAHs and PAHs

Sample extraction and purification

Filter punches (∅=47 mm), for PAHs and oxy-and nitro-PAHs, were extracted using a QuEChERS (Quick Easy Cheap Effective Rugged and Safe) like procedure (Albinet et al., 2014; Albinet et al., 2013). Briefly, punches were placed in centrifuge glass tubes, spiked with known amounts of surrogate standards and extracted with acetonitrile (ACN, 7 mL) using a multi-tube vortexer (DVX-2500, VWR) for 1.5 min. Supernatant extracts were collected and reduced to 100 µL under a gentle nitrogen stream.

For nitro- and oxy-PAHs, a mixture of surrogate standards containing 2 deuterated oxy-PAHs and 7 deuterated nitro-PAHs (Table S1) were added to the filter samples prior to extraction (1 ng μL^{-1} for nitro-PAHs and 5 ng μL^{-1} for oxy-PAHs; 5 µL of a solution at 1 ng μL^{-1}) and used for the quantification of oxy- and nitro-PAHs (Table S2, S3). For PAHs, a known amount of 6-methylchrysene was added to the samples prior to extraction (10 µL of a solution at 1 ng μL^{-1}) and used as surrogate standard to check the PAH extraction efficiency according to the EN 15549 and TS 16645 standard procedures (Albinet et al., 2014; Albinet et al., 2013; CEN, 2008; CEN, 2014; Tomaz et al., 2016).

After QuEChERS extraction, extracts dedicated to the PAH analyses were reduced under a gentle nitrogen stream to near dryness and dissolved in 1 ml of ACN.

An improvement has been made in the purification step for the analysis of nitro- and oxy-PAHs. The clean-up of the extracts was done automatically using a SPE GILSON (ASPEC GX-274) device using the following procedure. Alumina SPE cartridges (ALOX Chromabond, Macherey Nagel, 3 mL, 500 mg) were conditioned with 3 mL of methanol (MeOH), ACN, and dichloromethane (DCM), respectively. Extracts were loaded and rinsed with 1 mL of ACN and MeOH. The collection of the eluted extracts was done in two steps with the elution of a first fraction with 4 mL of ACN, and a second fraction with 5.5 mL of

DCM. Both fractions were then mixed. Extracts were then reduced under a gentle stream of nitrogen to a volume of about 100 µL. Extracts were further cleaned using silica SPE cartridges (SiOH Chromabond, Macherey Nagel, 3 mL, 500 mg). Silica cartridges were conditioned with 1 mL of DCM, followed by 3 mL of pentane. Extracts were loaded, and rinsed with 1 mL of pentane (discarded), followed by an elution with 6 mL of a pentane/ DCM mixture (65:35; v/v). Extracts were then concentrated to near dryness under a gentle stream of nitrogen and dissolved with about 100 µL of ACN. Before analysis, purified samples were spiked with known amount of labelled internal standards (9-fluorenone-d8 and 1-nitropyrene-d9; 5 µL of a solution at 1 ng μL^{-1}) to evaluate the surrogate recoveries.

PAH analyses

PAHs were analysed by UPLC/ UV-Fluorescence (Thermo Scientific, Dionex Ultimate 3000) using a C18 UPLC column (Zorbax Eclipse PAH, 2.1 mm × 150 mm × 1.8 µm). Details on analytical parameters have already been presented elsewhere (Albinet et al., 2013; Tomaz et al., 2016). 3µl of the extracts were injected into the system for the analyses.

Nitro-PAH and oxy-PAH analyses

The quantification of nitro- and oxy-PAHs have been performed using GC/NICI-MS (Agilent 7890A GC coupled to 5975C MS). Compounds were separated on a Rxi-PAH Restek column (30 m × 250 µm × 0.10 µm) following the same protocol described previously (Albinet et al., 2006; Albinet et al., 2014; Tomaz et al., 2016). The column phase used here allowed the separation of 2- and 3-nitrofluoranthene isomers. 2 µl of the purified extracts have been injected into the pulsed splitless mode for analysis.

Analysis of SOA markers

Sample extraction and derivatization

Sample preparation and derivatization of the extracts for analyses have been performed following the same procedure described previously (Srivastava et al., 2018). Prior to extraction, a known amount of a mixture of surrogate standards containing 3 deuterated compounds were added to the filter samples (20 µL of a solution at 1 ng μL^{-1} in ACN) and were used for the quantification of SOA markers (Table S4). Filter punches (∅=47 mm) for SOA analysis were extracted using a QuEChERS like procedure (Albinet et al., 2014; Albinet et al., 2013).

Extracts were collected and reduced to dryness under a gentle nitrogen stream to avoid the presence of hydroxyl group prior to derivatization. They were then dissolved into 50 µL of ACN and subjected to derivatization (silylation) for 30 minutes at 60°C after addition of 50 µL of N-Methyl-N-(trimethylsilyl) trifluoroacetamide (MSTFA) with 10% trimethyl-chlorosilane (TMS). Before injection into the GC/MS for analysis, pentadecane-d32 was added to the extracts (5 µL of a solution at 10 ng μL^{-1} in ACN) and used as internal standard to evaluate the surrogate recoveries in the samples.

Sample analysis

The quantification of SOA markers was achieved using GC/MS (Agilent 7890A GC coupled to 5975C MS) in electron ionisation mode (EI, 70 eV) on a DB-5MS-column (Agilent J&W, 60 m × 0.25 mm × 0.25 µm). 2 µL of the extracts were injected in the splitless mode. Details on GC-MS operating parameters have already been presented elsewhere (Srivastava et al., 2018).

Quality assurance

To evaluate the background contamination related to sample collection and analysis, filter field blanks (n=5) have been performed. Compounds showing mainly concentration values below the detection limit, those with field blank values higher than 30% of the mean concentrations, and those mainly associated with the gas phase (Albinet et al., 2007; Albinet et al., 2008; Albinet et al., 2010; Isaacman-VanWertz et al., 2016; Tomaz et al., 2016) were excluded from the final results. Samples with concentrations below limit of quantification (LQ) were replaced by LQ/2.

PAH and PAH derivative extraction efficiencies were checked using a NIST standard reference material (SRM1649b, urban dust). Results obtained for PAH and PAH derivatives were in good agreement with the NIST reference or indicative values and with the ones previously reported in the literature (Albinet et al., 2006; Albinet et al., 2014; Albinet et al., 2013). Finally, 9 PAHs, 14 oxy-PAHs, 9 nitro-PAHs and 13 SOA markers were quantified and included in the present study (Table S5).

Table S2. List of oxy-PAHs and oxygenated compounds quantified, selected monitored ions and instrumental LQ by GC/NICI/MS.

Compounds	***Abbreviation***	***Retention time (min)***	***Monitored ions (m/z)***	***Dwell time (s)***	***Deuterated surrogate standards***	***Retention time (min)***	***Monitored ions (m/z)***	***Instrumental LOQs (pg injected)***
Phthaldialdehyde	Pht	7.59	134	0.06	1,4-Naphthoquinone-d_6	8.32	164	0.23
1,4-Naphthoquinone	1,4-NQ	8.33	158	0.06				0.05
1-Naphthaldehyde	1-Nay	8.66	156	0.10				0.22
Phthalic anhydride	PhtA	7.96	148	0.06				0.12
2-Formyl-trans-cinnamaldehyde	2-FCin	8.91	160	0.10				0.11
1,2-Naphthoquinone	1,2-NQ	9.39	158	0.05				9.65
Benzophenone	Bzophe	9.14	182	0.06				0.24
1-Acenaphthenone	1-Aceone	9.56	168	0.05				0.39
9-Fluorenone	9-Fluo	9.98	180	0.05				0.11
Naphthalic-1,2-anhydride	1,2-NA	11.10	198	0.06				0.12
Biphenyl-2,2'-dicarboxaldehyde	Biph 2,2'	11.07	210	0.06	9,10-Anthraquinone-d_8	12.29	216	0.04
Xanthone	Xanth	10.99	196	0.06				0.58
Acenaphthenequinone	AceQ	11.76	182	0.06				0.14
2,3-Naphthalene dicarboxylique anhydride	2,3-NA	11.75	198	0.03				15.77
Anthrone	Anthro	12.05	194	0.03				4.77
6H-Dibenzo[b,d]pyrene-6-one	6H-DPone	12.22	196	0.03				16.34
9,10-Anthraquinone	9,10-ANQ	12.36	208	0.03				0.19
Naphthalic-1,8-anhydride	1,8-NA	13.82	198	0.03				0.04
1,4-Anthraquinone	1,4-ANQ	13.49	208	0.03				1.47
Biphenyl-4,4'-dicarboxaldehyde	Biph 4,4'	13.63	210	0.03				0.08
2-Methylanthraquinone	2-MANQ	13.80	222	0.04				0.07
9-Phenanthrenecarboxaldehyde	9-PheCar	14.22	206	0.04				0.05
9,10-Phenanthrenequinone	9,10-PQ	15.54	208	0.06				38.97
2-Nitro-9-fluorenone	2N9fluo	15.58	225	0.06				0.07
Benzo[a]fluorenone	BaFone	17.18	230	0.15				0.06
Benzo[b]fluorenone	BbFone	18.19	230	0.15				0.12
Benzanthrone	Bzone	19.81	230	0.15				0.04
1-Pyrenecarboxaldehyde	1-PyrCar	19.94	230	0.15				0.07
Aceanthrenequinone	AceanQ	20.95	232	0.01				0.08
Benz[a]anthracene-7,12-dione	B-7,12-D	20.96	258	0.01				0.07

1,4-Chrysenequinone	1,4-CHRQ	22.33	258	0.01				0.09
5,6-Chrysenequinone	5,6-CHRQ	25.12	258	0.01				22.55

Table S3. List of nitro-PAHs quantified, selected monitored ions and instrumental LQ by GC/NICI/MS.

Compounds	***Abbreviation***	***Retention time (min)***	***Monitored ions (m/z)***	***Dwell time (s)***	***Deuterated surrogate standards***	***Retention time (min)***	***Monitored ions (m/z)***	***Instrumental LOQs (pg injected)***
1-Nitronaphthalene	1-NN	9.16	173	0.06	1-Nitronaphthalene-d_7	9.14	180	0.16
2-Methyl-1-nitronaphthalene + 1-Methyl-5-nitronaphthalene [a]	2-M1NN + 1-M5NN	9.18	187	0.06				0.32
2-Nitronaphthalene	2-NN	9.40	173	0.06				0.06
2-Methyl-4-nitronaphthalene	2-M4NN	9.95	187	0.06				0.36
1-Methyl-4-nitronaphthalene	1-M4NN	10.11	187	0.06				0.35
1-Methyl-6-nitronaphthalene	1-M6NN	10.23	187	0.06				0.02
1,5-Dinitronaphthalene	1,5-DNN	12.48	218	0.03				0.03
2-Nitrobiphenyl	2-Nbi	9.59	199	0.03	2-Nitrobiphenyl-d_9	9.56	208	0.07
3-Nitrobiphenyl	3-Nbi	10.46	199	0.03				0.17
3-Nitrodibenzofuran	3-NDibf	12.22	213	0.03				0.20
5-Nitroacenaphthene	5-NAce	12.27	199	0.03				0.16
2-Nitrofluorene	2-NF	13.97	211	0.03	2-Nitrofluorene-d_9	13.87	220	0.38
9-Nitroanthracene	9-NA	14.22	223	0.09	9-Nitroanthracene-d_9	14.14	232	0.09
9-Nitrophenanthrene	9-NPhe	15.30	223	0.09				0.06
2-Nitrodibenzothiophene	2-NDithio	15.85	229	0.09				0.28
3-Nitrophenanthrene	3-NPhe	15.97	223	0.09				0.08
2-Nitroanthracene	2-NA	16.76	223	0.09				0.20
9-Methyl-10-nitroanthracene	9-M10NA	16.79	237	0.09				0.08
2-Nitrofluoranthene	2-NFlt	20.13	247	0.10	1-Nitropyrene-d_9	21.30	256	0.09
3-Nitrofluoranthene	3-NFlt	20.40	247	0.10				0.09
4-Nitropyrene	4-NP	20.67	247	0.10				0.07
1-Nitropyrene	1-NP	21.38	247	0.10				0.07
2-Nitropyrene	2-NP	21.70	247	0.10				0.20
7-Nitrobenz[a]anthracene	7-NBaA	23.72	273	0.06	6-Nitrochrysene-d_{11}	25.01	284	0.10
6-Nitrochrysene	6-NChry	25.13	273	0.06				0.03
1,3-Dinitropyrene	1,3-DNP	26.71	292	0.25				0.07
1,6-Dinitropyrene	1,6-DNP	28.17	292	0.25				0.13
1,8-Dinitropyrene	1,8-DNP	28.42	292	0.25				0.20
1-Nitrobenzo[e]pyrene	1-NBeP	29.75	297	0.12	6-	29.63	308	0.14

6-Nitrobenzo[a]pyrene	6-NBaP	31.61	297	0.12	Nitrobenzo[a]pyrene-d_{11}			0.14
3-Nitrobenzo[e]pyrene	3-NBeP	31.17	297	0.12				0.85

[a] 2-M1NN and 1-M5NN are not separated with the column used.

Table S4. List of SOA markers quantified and instrumental limits of quantification (LQ) by GC/EI-MS.

Compounds	***Instrumental LOQs (pg injected)***
Succinic acid	1.3
α-Methylglyceric acid (α-MGA)	1.0
2,3-Dihydroxy-4-oxopentanoic acid (DHOPA)	8.4
Pinonic acid	2.2
3-Hydroxyglutaric acid (3-HGA)	1.3
Pinic acid	6.3
Phthalic acid	0.9
2-Methylerythritol (2-MT)	1.1
3-Methylbutane-1,2,3-tricarboxylic acid (MBTCA)	0.6
β-Caryophyllinic acid	14.3
1,2,3,4-Cyclobutane tetracarboxylic acid	0.3
4-Methyl-5-Nitrocathecol (4-Me5Nc)	1.5
3-Methyl-5-Nitrocathecol (3-Me5Nc)	1.4

Positive matrix factorization (PMF)

PMF is a multivariate factor analysis tool that does not requires any prior information on the source profiles (Hopke, 2016; Paatero and Tapper, 1994). A chemical mass balance between the measured species concentrations and source profiles as a linear combination of factors *p*, species profile *f* of each source, the amount of mass *g* contributed to each individual sample is solved following Equation (1).

$$X_{ij} = \sum_{k=1}^{p} g_{ik} f_{kj} + e_{ij} \quad (1)$$

where X_{ij} represents measured data for species j in sample i and e_{ij} is the residual of each sample/species not fitted by the model. The best model solution is obtained by minimizing the function Q (Equation (2)).

$$Q = \sum_i \sum_j \left(\frac{e_{ij}}{\sigma_{ij}}\right)^2 \quad (2)$$

where σ_{ij} represents the measurement uncertainty of each data point.

Table S5. Mean, min-max, concentrations (ng m^{-3}) and signal/noise ratios (S/N) of all individual species quantified in this study (n=92 for PM_{10} filter samples).

Species	Mean concentrations	Min	Max	S/N
OC	$6.78\times10^{+03}$	$1.21\times10^{+03}$	$1.39\times10^{+04}$	$9.93\times10^{+00}$
EC	$1.20\times10^{+03}$	$1.30\times10^{+02}$	$3.19\times10^{+03}$	$6.19\times10^{+00}$
Methanesulfonic acid (MSA)	$3.94\times10^{+01}$	9.70×10^{-01}	$1.97\times10^{+02}$	$9.92\times10^{+00}$
Oxalate	$1.93\times10^{+02}$	$5.28\times10^{+01}$	$5.41\times10^{+02}$	$1.00\times10^{+01}$
Cl^-	$5.88\times10^{+02}$	$2.73\times10^{+01}$	$2.37\times10^{+03}$	$9.67\times10^{+00}$
NO_3^-	$1.44\times10^{+04}$	$1.19\times10^{+03}$	$4.42\times10^{+04}$	$1.00\times10^{+01}$
SO_4^{2-}	$4.30\times10^{+03}$	$3.45\times10^{+02}$	$1.71\times10^{+04}$	$1.00\times10^{+01}$
Na^+	$4.11\times10^{+02}$	$2.93\times10^{+01}$	$2.17\times10^{+03}$	$1.00\times10^{+01}$
NH_4^+	$5.66\times10^{+03}$	$4.61\times10^{+02}$	$1.87\times10^{+04}$	$1.00\times10^{+01}$
K^+	$1.40\times10^{+02}$	$1.67\times10^{+01}$	$3.63\times10^{+02}$	$1.00\times10^{+01}$
Mg^{2+}	$6.01\times10^{+01}$	$5.55\times10^{+00}$	$2.45\times10^{+02}$	$9.85\times10^{+00}$
Ca^{2+}	$8.65\times10^{+02}$	$5.21\times10^{+01}$	$2.65\times10^{+03}$	$1.00\times10^{+01}$
Levoglucosan (Levo)	$2.97\times10^{+02}$	$2.00\times10^{+01}$	$1.11\times10^{+03}$	$1.00\times10^{+01}$
Arabitol	$4.68\times10^{+00}$	5.12×10^{-01}	$1.79\times10^{+01}$	$8.48\times10^{+00}$
Mannosan (Manno)	$2.88\times10^{+01}$	7.66×10^{-02}	$9.67\times10^{+01}$	$9.89\times10^{+00}$
Mannitol	$2.08\times10^{+01}$	9.56×10^{-02}	$1.66\times10^{+02}$	$9.79\times10^{+00}$
Galactosan	$1.46\times10^{+01}$	7.66×10^{-02}	$7.74\times10^{+01}$	$8.81\times10^{+00}$
Glucose	$9.65\times10^{+00}$	7.66×10^{-02}	$5.83\times10^{+01}$	$6.78\times10^{+00}$
Xanthone	2.41×10^{-01}	2.67×10^{-02}	9.86×10^{-01}	$2.37\times10^{+00}$
Acenaphthenequinone	8.21×10^{-02}	1.71×10^{-06}	4.14×10^{-01}	$3.44\times10^{+00}$
2,3-Naphthalenedicarboxilicanhydride	4.42×10^{-01}	6.21×10^{-02}	$1.74\times10^{+00}$	$1.00\times10^{+01}$
Anthrone	5.43×10^{-01}	5.74×10^{-05}	$2.01\times10^{+00}$	$1.00\times10^{+01}$
6H-Dibenzo [b,d] pyran-6-one (6H-DPone)	6.82×10^{-01}	5.58×10^{-04}	$3.14\times10^{+00}$	$9.51\times10^{+00}$
9,10-Anthraquinone	3.38×10^{-01}	7.73×10^{-02}	$1.13\times10^{+00}$	$1.00\times10^{+01}$
2-Methylanthraquinone	1.17×10^{-01}	2.67×10^{-02}	6.11×10^{-01}	$9.74\times10^{+00}$
9-Phenanthrenecarboxaldehyde	2.47×10^{-02}	1.01×10^{-02}	1.16×10^{-01}	$1.00\times10^{+01}$
9,10-Phenanthrenequinone	4.31×10^{-01}	3.32×10^{-01}	$1.20\times10^{+00}$	$1.99\times10^{+00}$
Benzo[a]fluorenone (B[a]Fone)	1.06×10^{-01}	1.73×10^{-02}	5.47×10^{-01}	$1.00\times10^{+01}$
Benzo[b]fluorenone (B[b]Fone)	1.26×10^{-01}	2.10×10^{-02}	6.36×10^{-01}	$9.18\times10^{+00}$
Benzathrone	2.24×10^{-01}	2.10×10^{-02}	$1.26\times10^{+00}$	$7.30\times10^{+00}$
1-Pyrenecarboxaldehyde	2.24×10^{-02}	7.23×10^{-03}	1.05×10^{-01}	$8.36\times10^{+00}$
Benz[a]anthracene-7,12-dione	1.03×10^{-01}	1.73×10^{-02}	4.63×10^{-01}	$3.81\times10^{+00}$
9-Nitroanthracene (9-NA)	7.34×10^{-02}	3.61×10^{-03}	5.20×10^{-01}	$2.35\times10^{+00}$
2-Nitrodibenzothiophene	6.96×10^{-03}	3.39×10^{-06}	1.73×10^{-02}	$1.44\times10^{+00}$
9-Methyl-10-nitroanthracene	9.89×10^{-03}	9.15×10^{-07}	8.02×10^{-02}	$2.08\times10^{+00}$
2-Nitrofluoranthene (2-Nflt)	9.61×10^{-02}	4.34×10^{-03}	6.39×10^{-01}	$1.00\times10^{+01}$
1-Nitropyrene (1-NP)	6.36×10^{-03}	1.44×10^{-03}	2.74×10^{-02}	$1.00\times10^{+01}$
2-Nitropyrene	1.01×10^{-02}	2.39×10^{-06}	4.05×10^{-02}	$5.66\times10^{+00}$
7-Nitrobenzo[a]anthracene	1.43×10^{-02}	1.22×10^{-06}	1.44×10^{-01}	$1.94\times10^{+00}$
1-Nitrobenzo[a]pyrene	2.55×10^{-02}	3.57×10^{-06}	7.73×10^{-02}	$1.89\times10^{+00}$
Benzo[e]pyrene	1.61×10^{-01}	3.61×10^{-02}	4.52×10^{-01}	$5.19\times10^{+00}$
Benzo[j]fluoranthene	2.34×10^{-01}	3.61×10^{-02}	$1.20\times10^{+00}$	$6.07\times10^{+00}$
Benzo[b]fluoranthene	2.83×10^{-01}	3.61×10^{-02}	7.50×10^{-01}	$6.32\times10^{+00}$
Benzo[k]fluoranthene	7.64×10^{-02}	3.61×10^{-02}	2.50×10^{-01}	$4.45\times10^{+00}$
Benzo[a]pyrene (B[a]P)	1.61×10^{-01}	3.61×10^{-02}	5.55×10^{-01}	$4.51\times10^{+00}$
Dibenzo[a,h]anthracene	4.20×10^{-02}	3.61×10^{-02}	1.16×10^{-01}	$3.02\times10^{+00}$

Benzo[g,h,i]perylene(B[g,h,i])P)	2.22×10^{-01}	3.61×10^{-02}	6.20×10^{-01}	$4.61\times10^{+00}$
Indeno[1,2,3-cd]pyrene (In[1,2,3-cd]P)	2.92×10^{-01}	3.61×10^{-02}	6.99×10^{-01}	$4.06\times10^{+00}$
Coronene (Cor)	7.50×10^{-02}	3.70×10^{-02}	2.20×10^{-01}	$8.32\times10^{+00}$
Ca	$6.61\times10^{+02}$	$1.03\times10^{+02}$	$2.02\times10^{+03}$	$3.96\times10^{+00}$
Ti	$2.56\times10^{+01}$	$2.33\times10^{+00}$	$8.49\times10^{+01}$	$6.47\times10^{+00}$
Mn	$1.38\times10^{+01}$	6.20×10^{-01}	$2.82\times10^{+01}$	$9.02\times10^{+00}$
Fe	$5.25\times10^{+02}$	$1.05\times10^{+02}$	$1.32\times10^{+03}$	$1.11\times10^{+00}$
Ni	$4.73\times10^{+00}$	1.98×10^{-01}	$4.80\times10^{+01}$	$1.86\times10^{+00}$
Cu	$1.42\times10^{+01}$	$2.12\times10^{+00}$	$4.85\times10^{+01}$	$8.08\times10^{+00}$
Pb	$7.62\times10^{+00}$	9.65×10^{-01}	$2.20\times10^{+01}$	$7.39\times10^{+00}$
PM_{10}	$4.93\times10^{+04}$	$1.23\times10^{+04}$	$1.30\times10^{+05}$	$1.00\times10^{+01}$
PM_1	$2.79\times10^{+04}$	$4.76\times10^{+03}$	$6.29\times10^{+04}$	$1.00\times10^{+01}$
BC_{ff}	$9.59\times10^{+02}$	$1.77\times10^{+01}$	$2.90\times10^{+03}$	$3.59\times10^{+00}$
BC_{wb}	$2.69\times10^{+02}$	3.14×10^{-01}	$8.57\times10^{+02}$	$6.03\times10^{+00}$
Succinic Acid	$1.44\times10^{+01}$	5.50×10^{-06}	$8.70\times10^{+01}$	$5.41\times10^{+00}$
α-Methylglyceric acid (α-MGA)	5.10×10^{-01}	4.08×10^{-06}	$3.98\times10^{+00}$	$9.54\times10^{+00}$
2,3-Dihydroxy-4-oxopentanoic acid (DHOPA)	$1.49\times10^{+00}$	3.42×10^{-05}	$3.66\times10^{+00}$	$9.90\times10^{+00}$
Pinonic Acid	$4.00\times10^{+00}$	5.02×10^{-01}	$8.54\times10^{+01}$	$9.94\times10^{+00}$
3-Hydroxyglutaric acid (3-HGA)	$2.21\times10^{+00}$	5.04×10^{-02}	$8.88\times10^{+00}$	$6.56\times10^{+00}$
Pinic Acid	8.35×10^{-01}	2.56×10^{-05}	$2.09\times10^{+01}$	$9.00\times10^{+00}$
Phthalic Acid	$3.79\times10^{+00}$	3.63×10^{-06}	$2.65\times10^{+01}$	$1.00\times10^{+01}$
4-Methyl-5-Nitrocathecol (4-Me5Nc)	$4.12\times10^{+01}$	$4.26\times10^{+00}$	$5.72\times10^{+02}$	$1.00\times10^{+01}$
3-Methyl-5-Nitrocathecol (3-Me5Nc)	$3.03\times10^{+01}$	$4.77\times10^{+00}$	$3.92\times10^{+02}$	$7.64\times10^{+00}$
2-Methylerythritol (2-MT)	5.90×10^{-01}	4.43×10^{-06}	$1.32\times10^{+00}$	$9.67\times10^{+00}$
3-Methylbutane-1,2,3-tricarboxylic acid (MBTCA)	3.46×10^{-01}	2.58×10^{-06}	$6.83\times10^{+00}$	$1.68\times10^{+00}$

Table S6. List of input species in the PMF model.

PM_{10}	Mn	α-Methylglyceric acid (α-MGA)
OC	Fe	2-Methylerythritol (2-MT)
EC	Cu	6H-Dibenzo [b,d] pyran-6-one (6H-DPone)
Cl^-	Levoglucosan (Levo)	Benzo[a]fluorenone (B[a]Fone)
NO_3^-	Mannosan (Manno)	Benzo[b]fluorenone (B[b]Fone)
SO_4^{2-}	Benzo[b]fluoranthene (B[a]F)	9-Nitroanthracene (9-NA)
Na^+	Benzo[a]pyrene (B[a]P)	2-Nitrofluoranthene (2-NFlt)
NH_4^+	Benzo[g,h,i]perylene (B[g,h,i])P	DHOPA
K^+	Indeno[1,2,3-cd]pyrene (In[1,2,3-cd])P	4-Methyl-5-Nitrocathecol (4-Me5Nc)
Mg^{2+}	1-Nitropyrene (1-NP)	3-Methyl-5-Nitrocathecol (3-Me5Nc)
Ca^{2+}	Oxalate	
Ti	MSA	

Table S7. List of the constraints applied on each factor profile in the PMF model.

Factor	Element	Type
Mixed secondary aerosols	NH_4^+	Pull Up Maximally
Biogenic SOA-1 (marine)	MSA	Pull Up Maximally
Anthropogenic SOA-3 (phenolic oxidation)	4-Methyl-5-Nitrocathecol	Pull Up Maximally
Anthropogenic SOA-3 (phenolic oxidation)	3-Methyl-5-Nitrocathecol	Pull Up Maximally
Dust	Ca^{2+}	Pull Up Maximally
Dust	Ti	Pull Up Maximally
Anthropogenic SOA-2 (nitro- PAHs)	9-Nitroanthracene	Pull Up Maximally
Nitrate-rich factor	NO_3^-	Pull Up Maximally
Nitrate-rich factor	NH_4^+	Pull Up Maximally
Primary traffic emissions	Mn	Pull Up Maximally
Primary traffic emissions	Fe	Pull Up Maximally
Primary traffic emissions	Cu	Pull Up Maximally
Primary traffic emissions	2-Methylerythritol	Pull Down Maximally
Biogenic SOA-2 (isoprene)	α-Methylglyceric acid	Pull Up Maximally
Biogenic SOA-2 (isoprene)	2-Methylerythritol	Pull Up Maximally
Biogenic SOA-2 (isoprene)	DHOPA	Define Limits (0/0.2)
Biogenic SOA-2 (isoprene)	9-Nitroanthracene	Pull Down Maximally
Biomass burning	DHOPA	Pull Down Maximally
Anthropogenic SOA-1 (oxy- PAHs)	DHOPA	Pull Up Maximally

Table S8. Values of the Pearson coefficient (r) between observed and modelled concentrations.

Species	r	Species	r	Species	r
PM_{10}	0.99	Mn	0.86	α-Methylglyceric acid	0.91
OC	0.95	Fe	0.71	2-Methylerythritol	0.45
EC	0.94	Cu	0.94	6H-Dibenzo [b,d] pyran-6-one	0.62
Cl^-	0.95	Levoglucosan	1.00	Benzo[a]fluorenone	0.94
NO_3^-	1.00	Mannosan	0.98	Benzo[b]fluorenone	0.95
SO_4^{2-}	0.99	Benzo[b]fluoranthene	0.92	9-Nitroanthracene	0.67
Na^+	1.00	Benzo[a]pyrene	0.79	2-Nitrofluoranthene	1.00
NH_4^+	1.00	Benzo[g,h,i]perylene	0.91	DHOPA	0.76
K^+	0.91	Indeno[1,2,3-cd]pyrene	0.83	4-Methyl-5-Nitrocathecol	0.86
Mg^{2+}	0.99	1-Nitropyrene	0.97	3-Methyl-5-Nitrocathecol	0.85
Ca^{2+}	0.97	Oxalate	0.89		
Ti	0.92	MSA	1.00		

Table S9. Results from bootstrap runs

	Mixed secondary aerosols	Biogenic SOA-1 (marine)	Biogenic SOA-2 (isoprene)	Anthropogenic SOA-1 (oxy-PAHs)	Sea salt	Anthropogenic SOA-2 (nitro-PAHs)	Dust	Anthropogenic SOA-3 (phenolic oxidation)	Nitrate-rich factor	Primary traffic emissions	Biomass burning
Mixed secondary aerosols	98	0	0	0	0	0	0	0	0	0	0
Biogenic SOA-1 (marine)	0	98	0	0	0	0	0	0	0	0	0
Biogenic SOA-2 (isoprene)	0	0	98	0	0	0	0	0	0	0	0
Anthropogenic SOA-1 (oxy-PAHs)	0	0	1	97	0	0	0	0	0	0	0
Sea salt	0	0	0	0	98	0	0	0	0	0	0
Anthropogenic SOA-2 (nitro-PAHs)	0	0	0	0	0	96	0	0	0	0	0
Dust	0	0	0	0	0	0	98	0	0	0	0
Anthropogenic SOA-3 (phenolic oxidation)	0	0	0	1	0	0	0	98	0	0	1
Nitrate-rich factor	0	0	0	0	0	0	0	0	98	0	0
Primary traffic emissions	0	0	0	0	0	0	2	0	0	96	0
Biomass burning	0	0	0	0	0	0	0	0	0	0	98

Table S10. Observed P-value for each factor obtained using t-test.

	Mixed secondary aerosols	Biogenic SOA-1 (marine)	Biogenic SOA-2 (isoprene)	Anthropogenic SOA-1 (oxy-PAHs)	Sea salt	Anthropogenic SOA-2 (nitro-PAHs)	Dust	Anthropogenic SOA-3 (phenolic oxidation)	Nitrate-rich factor	Primary traffic emissions	Biomass burning
P -value ($p<0.05$)	0.14	0.14	0.20	0.11	0.22	0.40	0.20	0.13	0.15	0.07	0.10

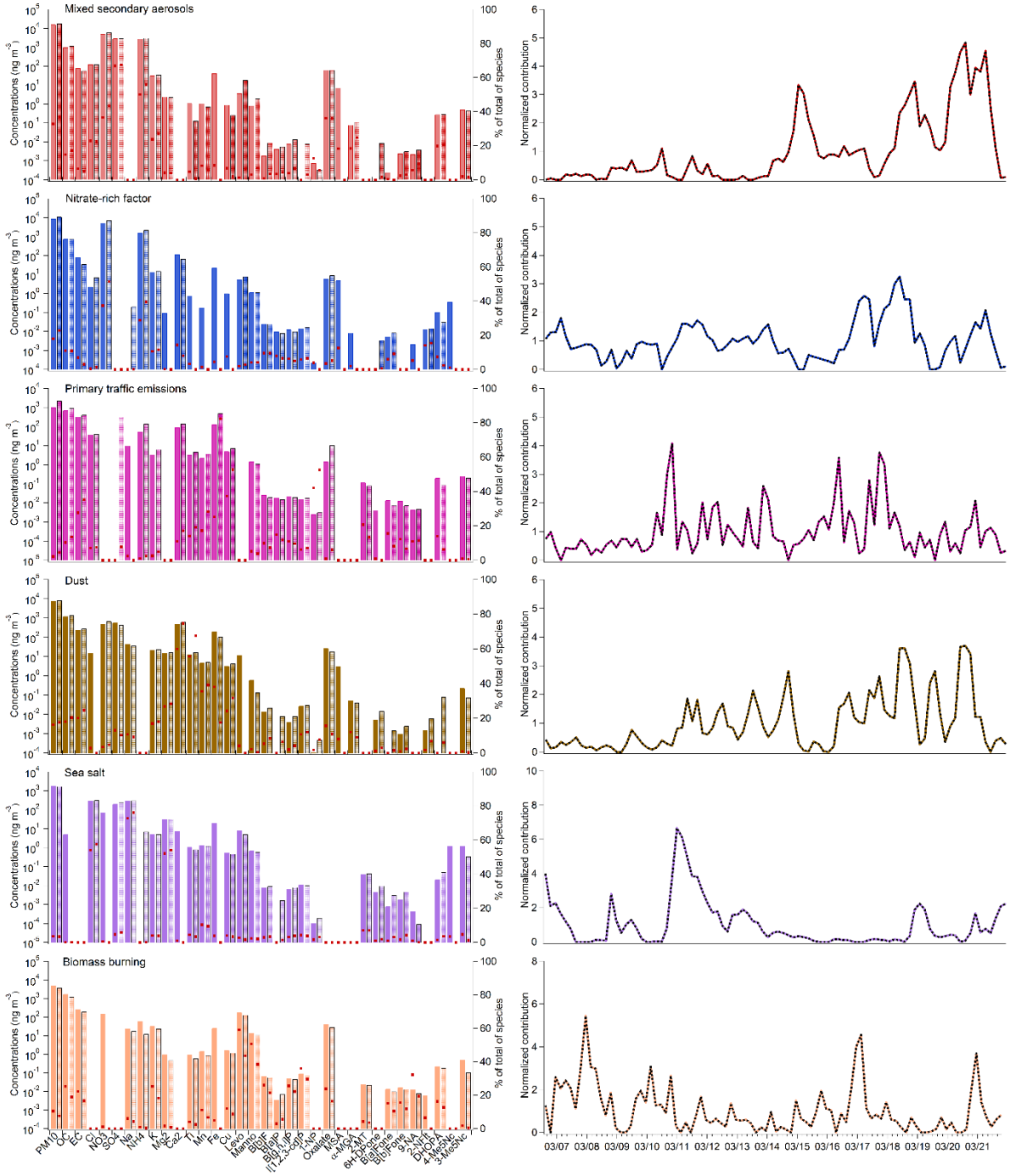

Figure S2. Source profiles and temporal evolution of mixed secondary aerosols, nitrate-rich, primary traffic emissions, dust, sea salt and biomass burning factors for base and constrained runs. Coloured bars and red dots represent the concentrations and the percentages of each species apportioned in the factor, respectively. Coloured lines: base run. Black/dashed lines: constrained run.

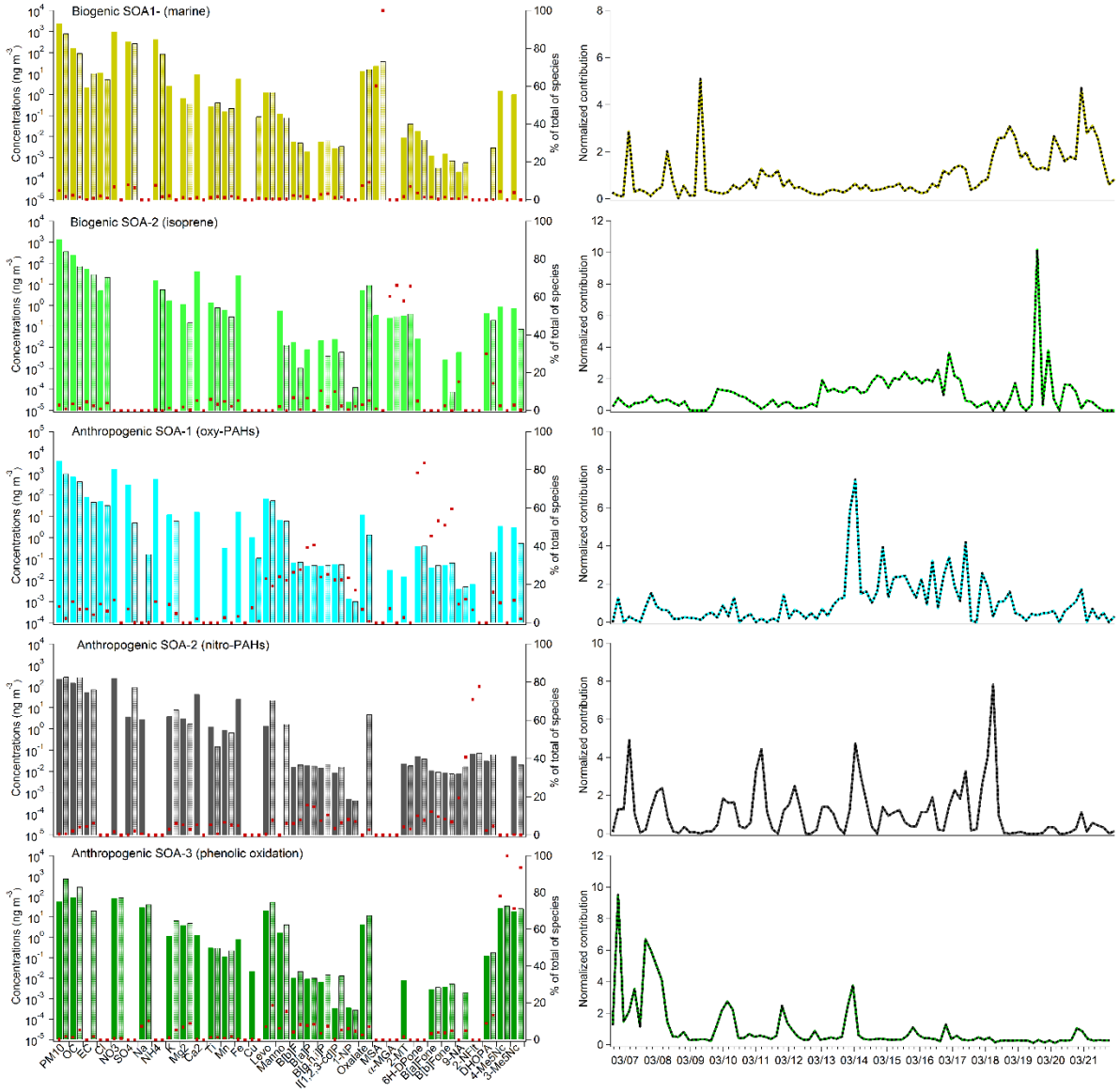

Figure S3. Source profiles and temporal evolution of biogenic SOA-1 (marine), biogenic SOA-2 (isoprene), anthropogenic SOA-1 (oxy-PAHs), anthropogenic SOA-2 (nitro-PAHs) and anthropogenic SOA-3 (phenolic oxidation) factors for base and constrained runs. Coloured bars and red dots represent the concentrations and the percentages of each species apportioned in the factor, respectively. Coloured lines: base run. Black/dashed lines: constrained run.

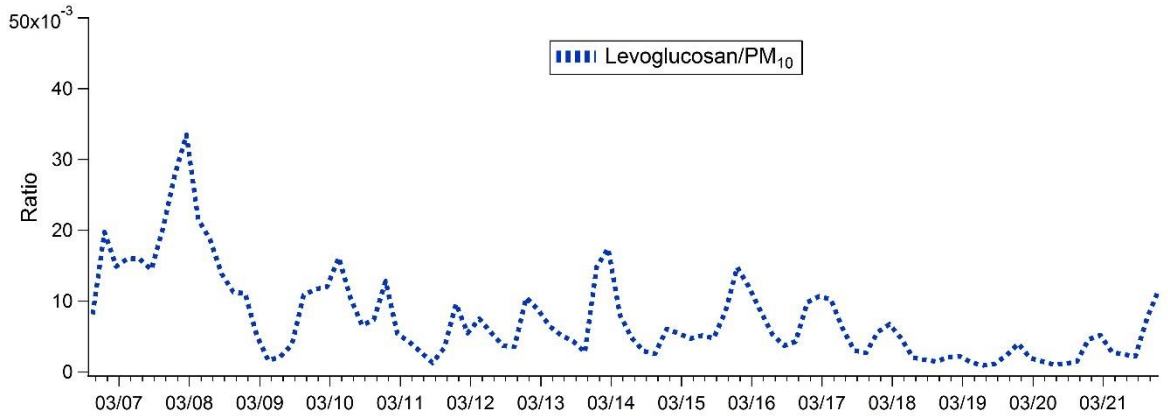

Figure S4. Temporal evolution of the levoglucosan/PM_{10} ratio observed at Paris-SIRTA, France (March 2015).

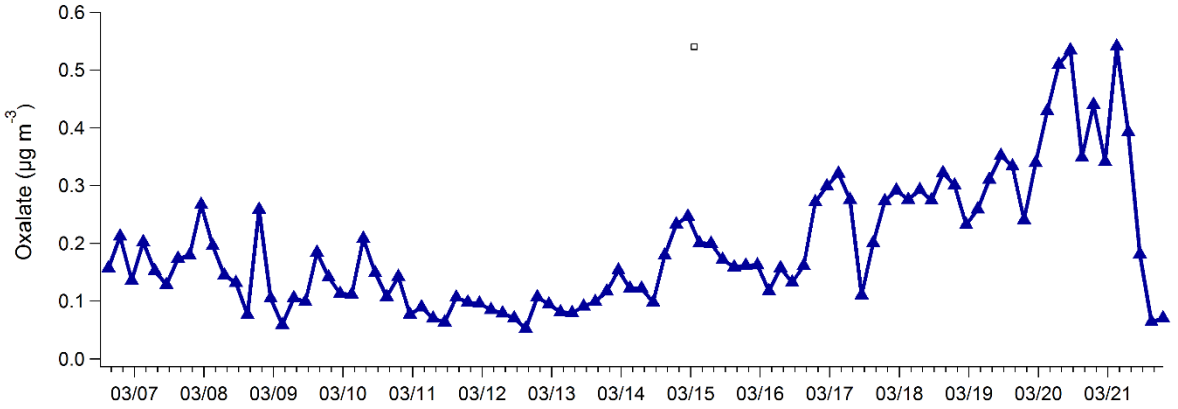

Figure S5. Temporal evolution of oxalate concentrations at Paris-SIRTA, France (March 2015).

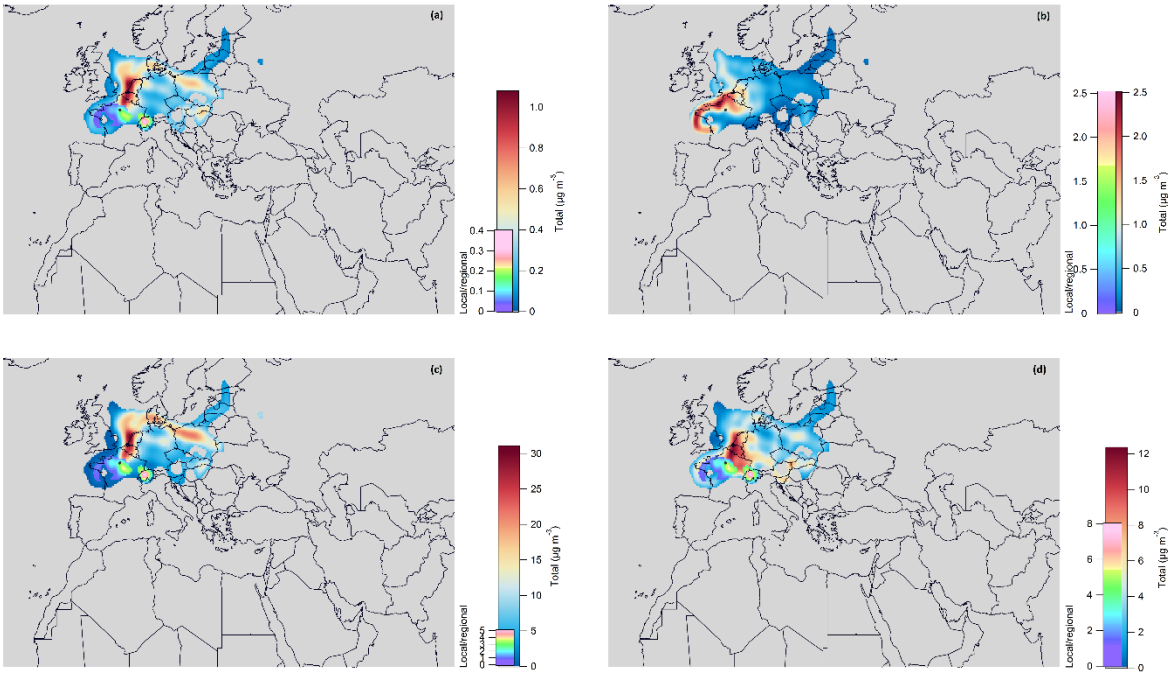

Figure S6. Concentration-Weighted Trajectory (CWT) results for (a) biogenic SOA-1 (marine), (b) sea salt, (c) mixed secondary aerosols and (d) nitrate-rich factors. "Total" represents the entire dataset, where "local/regional" is the subset when back trajectories were associated with low wind speeds. Low wind speeds have been defined as values below than the 10th percentile of the wind speeds observed during the campaign (<1.5 m/s). Scale sizes for "local/regional" are proportional.

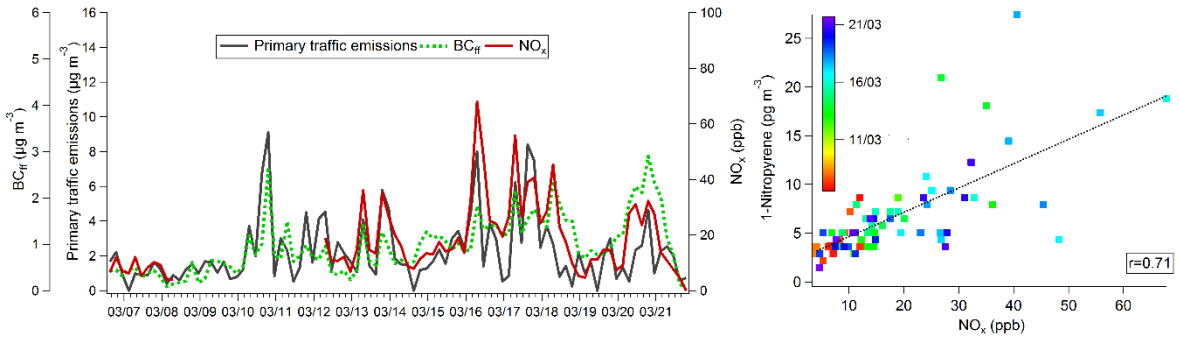

Figure S7. Temporal evolution of the primary traffic emissions factor, BC_{ff} and NO_x (left) and correlation between 1-nitropyrene and NO_x (right) at Paris-SIRTA, France (March 2015).

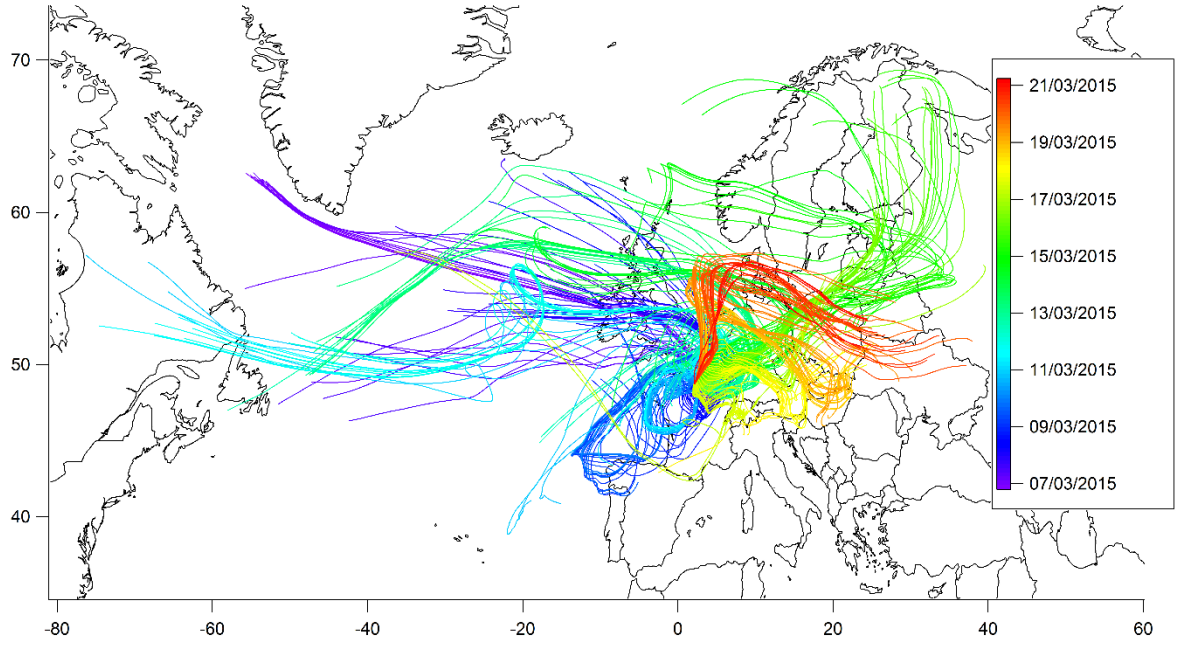

Figure S8. Compilation of the back trajectories from Paris-SIRTA in March 2015. Back trajectory calculations have been performed using HYSPIT model every 3 h for an altitude of 100 m above ground level and compiled using ZeFir (Petit et al., 2017).

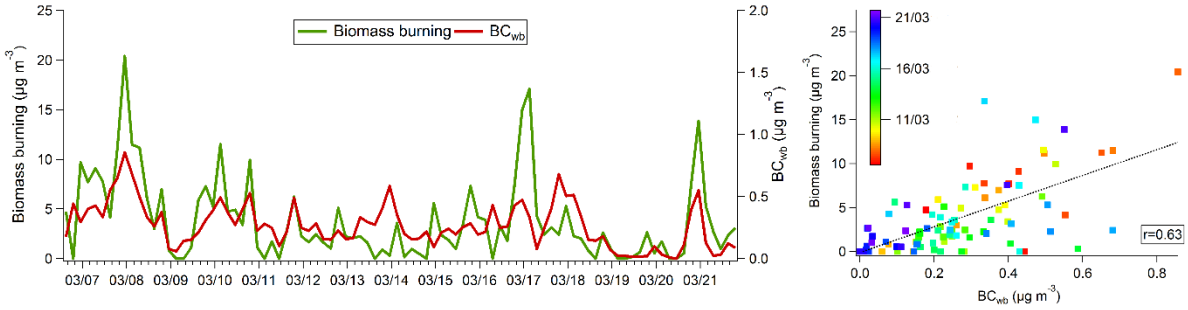

Figure S9. Temporal evolution of biomass burning and BC_{wb} (left) and correlation between biomass burning and BC_{wb} (right) at Paris-SIRTA, France (March 2015).

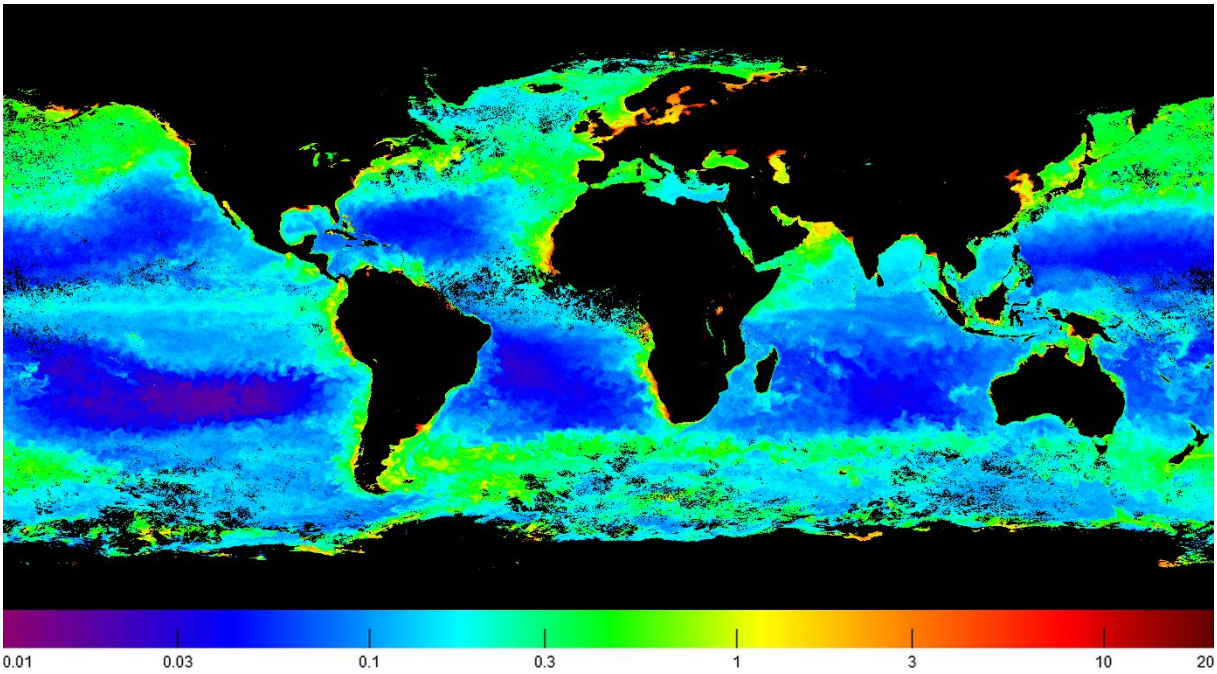

Figure S10. Worldwide distribution of chlorophyll in mg m^{-3} for March 2015 from satellite observations (https://www.oceancolour.org/).

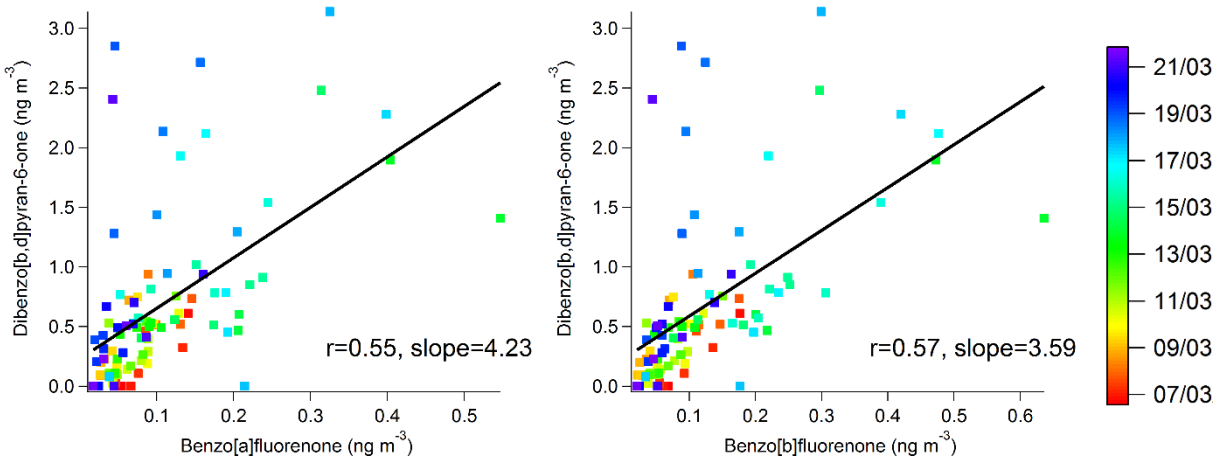

Figure S11. Correlations between benzo[a]fluorenone and benzo[b]fluorenone with dibenzo[b,d]pyran-6-one.

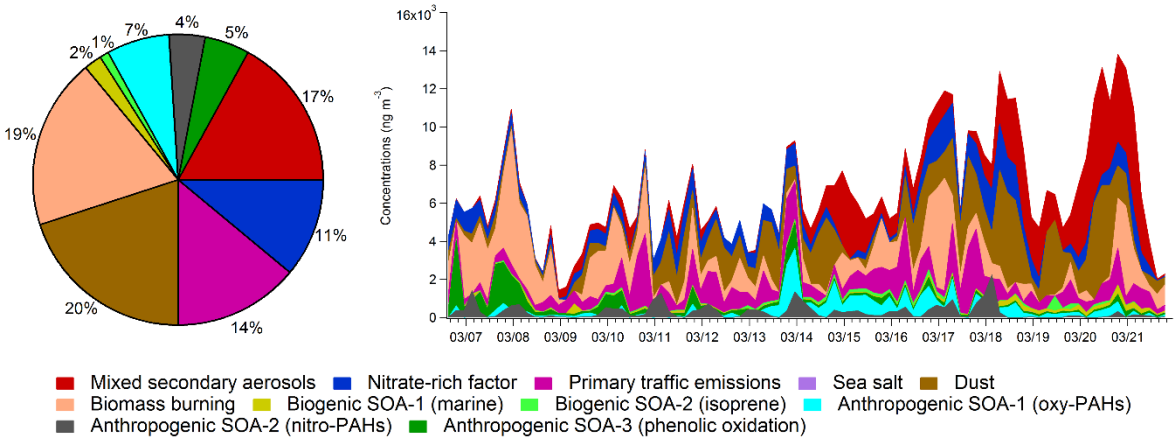

Figure S12. Average contributions (left) and temporal evolution (right) of the identified sources to OC mass concentrations at Paris-SIRTA, France (March 2015).

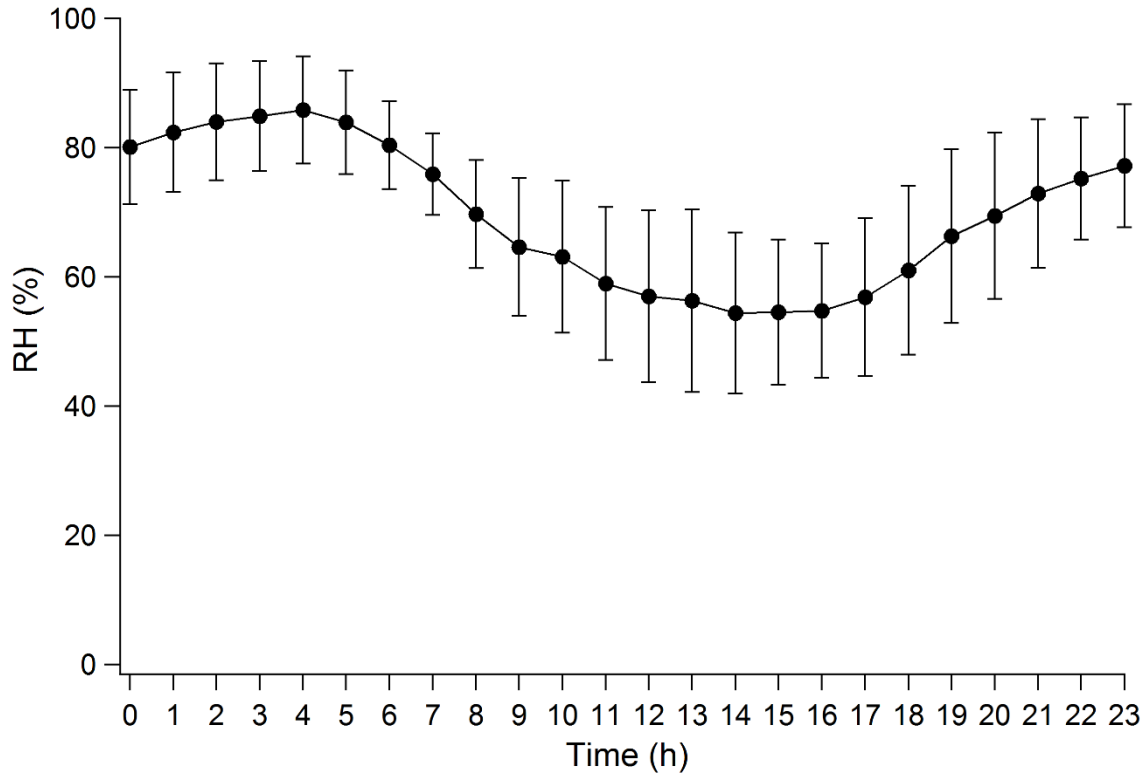

Figure S13. Diurnal profiles of relative humidity (RH, in %) measured at Paris-SIRTA, France (March 2015). Error bar represents two standard deviations (±1SD).

References

Albinet, A., Leoz-Garziandia, E., Budzinski, H., Villenave, E., 2006. Simultaneous analysis of oxygenated and nitrated polycyclic aromatic hydrocarbons on standard reference material 1649a (urban dust) and on natural ambient air samples by gas chromatography–mass spectrometry with negative ion chemical ionisation. J. Chromatogr. A. 1121, 106-113.

Albinet, A., Leoz-Garziandia, E., Budzinski, H., Villenave, E., 2007. Polycyclic aromatic hydrocarbons (PAHs), nitrated PAHs and oxygenated PAHs in ambient air of the Marseilles area (South of France): Concentrations and sources. Sci. Total Environ. 384, 280-292.

Albinet, A., Leoz-Garziandia, E., Budzinski, H., Villenave, E., Jaffrezo, J. L., 2008. Nitrated and oxygenated derivatives of polycyclic aromatic hydrocarbons in the ambient air of two French alpine valleys Part 2: Particle size distribution. Atmos. Environ. 42, 55-64.

Albinet, A., Minero, C., Vione, D., 2010. Phototransformation processes of 2,4-dinitrophenol, relevant to atmospheric water droplets. Chemosphere. 80, 753-758.

Albinet, A., Nalin, F., Tomaz, S., Beaumont, J., Lestremau, F., 2014. A simple QuEChERS-like extraction approach for molecular chemical characterization of organic aerosols: application to nitrated and oxygenated PAH derivatives (NPAH and OPAH) quantified by GC–NICIMS. Anal. Bioanal. Chem. 406, 3131-3148.

Albinet, A., Tomaz, S., Lestremau, F., 2013. A really quick easy cheap effective rugged and safe (QuEChERS) extraction procedure for the analysis of particle-bound PAHs in ambient air and emission samples. Sci. Total Environ. 450-451, 31-8.

CEN, 2008. European Committee for Standardization, EN 15549: 2008 - Air Quality - Standard Method for the Measurement of the Concentration of Benzo[a]pyrene in Air. CEN, Brussels (Belgium).

CEN, 2014. European Committee for Standardization, TS-16645: 2014- Ambient Air – Method for the Measurement of Benz[a]anthracene, Benzo[b]fluoranthene, Benzo[j]fluoranthene, Benzo[k]fluoranthene, Dibenz[a,h]anthracene, Indeno[1,2,3-cd]pyrene et Benzo[ghi]perylene. CEN, Brussels (Belgium).

Hopke, P. K., 2016. Review of receptor modeling methods for source apportionment. J Air Waste Manag Assoc. 66, 237-59.

Isaacman-VanWertz, G., Yee, L. D., Kreisberg, N. M., Wernis, R., Moss, J. A., Hering, S. V., De Sá, S. S., Martin, S. T., Alexander, M. L., Palm, B. B., 2016. Ambient gas-particle partitioning of tracers for biogenic oxidation. Environ. Sci. Technol. 50, 9952-9962.

Paatero, P., Tapper, U., 1994. Positive matrix factorization: A non-negative factor model with optimal utilization of error estimates of data values. Environmetrics. 5, 111-126.

Petit, J. E., Favez, O., Albinet, A., Canonaco, F., 2017. A user-friendly tool for comprehensive evaluation of the geographical origins of atmospheric pollution: Wind and trajectory analyses. Environ. Modell. Softw. 88, 183-187.

Srivastava, D., Tomaz, S., Favez, O., Lanzafame, G. M., Golly, B., Besombes, J.-L., Alleman, L. Y., Jaffrezo, J.-L., Jacob, V., Perraudin, E., Villenave, E., Albinet, A., 2018. Speciation of organic fraction does matter for source apportionment. Part 1: A one-year campaign in Grenoble (France). Sci. Total Environ. In press.

Tomaz, S., Shahpoury, P., Jaffrezo, J. L., Lammel, G., Perraudin, E., Villenave, E., Albinet, A., 2016. One-year study of polycyclic aromatic compounds at an urban site in Grenoble (France): Seasonal variations, gas/particle partitioning and cancer risk estimation. Sci. Total Environ. 565, 1071-1083.

Chapter V

Comparison of different POA and SOA estimation methodologies

Article IV

Comparison of different methodologies to discriminate between primary and secondary organic aerosols

In preparation, Environmental Science & Technology

Comparison of different methodologies to discriminate between primary and secondary organic aerosols

D. Srivastava[1,2,3], *K. R. Daellenbach*[4], *Y. Zhang*[1], *N. Bonnaire*[5], *E. Perraudin*[2,3], *V. Gros*[5], *E. Villenave*[2,3], *A. S. H. Prévôt*[4], *I. El Haddad*[4], *O. Favez*[1], *A. Albinet*[1,*]

[1]INERIS, Parc Technologique Alata, BP 2, 60550 Verneuil-en-Halatte, France

[2]CNRS, EPOC, UMR 5805 CNRS, 33405 Talence, France

[3]Université de Bordeaux, EPOC, UMR 5805 CNRS, 33405 Talence, France

[4]Paul Scherrer Institute, 5232 Villigen PSI, Switzerland

[5]LSCE - UMR8212, CNRS-CEA-UVSQ, Gif-sur-Yvette, France

Correspondence to: alexandre.albinet@ineris.fr; alexandre.albinet@gmail.com

Abstract

Atmospheric organic aerosols (OA) origins are still poorly known due to the multiplicity of their sources and/or formation processes. Here, we present results from commonly used source apportionment methodologies applied to different datasets (obtained from filter-based chemical speciation as well as online and offline mass spectrometry) to discriminate primary and secondary organic aerosols (POA and SOA). Filter sampling and online measurements were achieved during an intensive field campaign conducted in the Paris region (France) during a pollution event in March 2015. On average for this campaign, the so-called EC-tracer method and constrained positive matrix factorization (PMF) analyses - using the multi-linear engine (ME-2) solver and conducted on the chemical dataset as well as offline AMS (Aerosol Mass Spetrometer) measurements - consistently indicated a roughly equivalent distribution between primary and secondary organics within the PM_{10} aerosol fraction. Discarding coarse mode dust-related factors, the constrained PMF analysis applied to online ACSM (Aerosol Chemical Speciation Monitor) data also showed an overall good agreement with other PMF outputs. However, significant discrepancies were observed between individual POA and SOA factors that could be compared. The chemical speciation-based PMF was notably assessed to better apportion primary traffic-related OA. Finally, although implemented with biomass burning-related secondary species, the so-called SOA-tracer method was found to significantly underestimate total SOA loadings during long-range transport pollution episode, due to specific secondary species, possibly such as organonitrates and/or organosulfates, not taken into account.

Keywords: primary and secondary organic aerosols, EC-tracer method, SOA-tracer method, PMF, Offline AMS, ACSM

1. Introduction

Airborne organic aerosols are commonly classified as primary (POA), i.e., from direct emissions, or secondary (SOA), i.e., resulting from (trans-) formation processes occurring in the atmosphere.[1] A detailed understanding of their origins is crucial as they have major impacts on human health, biogeochemical cycles and Earth's climate.[2]

Several data treatment methodologies have been developed to apportion POA and/or SOA, including elemental carbon (EC) -tracer approach,[3-5] statistical receptor models (i.e., chemical mass balance (CMB) or positive matrix factorization (PMF)),[6-8] SOA-tracer method,[9] and radiocarbon (^{14}C) measurements.[10, 11] These methodologies are widely applied to filter-based datasets. In addition, recent advances in online measurements techniques, such as aerosol mass spectrometry, are now allowing for high time resolution OA measurement and source apportionment.[12, 13] However, the scientific community is still facing issues for the full comprehension of OA origins, mainly due to the complexity and variability of the processes involved.[14] The biggest challenge relies on the subjectivity in the choice of hypotheses and/or final solution within the used source apportionment method. The comparison of results obtained from different approaches applied to a single dataset, or to different datasets but for the same time period and location, should help reducing uncertainties. However, only few comprehensive studies have been focusing so far on the comparison of individual primary or secondary OA fractions retrieved from a wide range of source apportionment techniques.[15-19]

In the present work, primary and secondary OA fractions could be resolved using various source apportionment approaches applied to different offline/online datasets from a short-term intensive campaign in the Paris area. PMF analyses have been conducted using an extensive filter-based

chemical speciation data, as well as OA mass spectra obtained from online aerosol chemical speciation monitor (ACSM) and offline filter-based aerosol mass spectrometer (AMS) measurements. EC-tracer and SOA-tracer methods have also been performed on the filter-based dataset. This study aimed at evaluating the consistency of outputs retrieved from these various methodologies, notably allowing a better understanding of their potential limitations when applied independently to each other.

2. Experimental

Details about the monitoring site, online measurements, sample collection and chemical speciation analytical procedures can be found in a previous paper[20] and in supporting material (SM). Only the essential information is reported in this section.

2.1. Monitoring site

Measurements were conducted at the SIRTA facility (Site Instrumental de Recherche par Télédétection Atmosphérique, 2.15° E; 48.71° N; 150 m a.s.l; http://sirta.ipsl.fr), a well-established observatory for the long-term physical and chemical characterization of aerosols in the Paris region (France).[21] The site is located approximately 25 km southwest of Paris city centre, and is considered as representative of suburban background air quality in the Ile-de-France region. An intensive campaign was performed from 6 to 21 March 2015, to catch late winter–early spring conditions, a period of the year frequently witnessing exceedances of the European daily PM_{10} threshold (>50 µg m^{-3}).[22-24] During such pollution events, the combination of domestic heating, road transport and manure spreading with anticyclonic atmospheric conditions favors the transport and/or accumulation of pollutants as well as photochemical processes within the boundary layer in North-Western Europe.[24-26]

2.2. Online instrumentation

PM_{10} (TEOM 1405F, Thermo), NO_x (T200UP, Teledyne API), and O_3 (T400, Teledyne API) concentrations were measured at 15, 1 and 1-min time resolutions, respectively. In addition, meteorological parameters such as temperature, relative humidity (RH), wind direction, and wind speed were also measured at 1-min time resolution.

The aerosol chemical speciation monitor (ACSM, Aerodyne Research Inc.) allowed for the measurement of major submicron non-refractory chemical species at approx. 30-min time resolution [13, 26]

2.3. Filter sample collection and analysis

A high-volume sampler (DA-80, Digitel; flow rate: 30 m^3 h^{-1}) was used to collect particulate PM_{10} samples (Tissu-quartz fibre filter, Pallflex, Ø = 150 mm) every 4 hours. A total number of 92 filter samples were collected and analysed for an extended chemical speciation. Major ions (Cl^-, NO_3^-, SO_4^{2-}, NH_4^+, Ca^{2+}, Na^+, Mg^{2+}, K^+), EC and organic carbon (OC), 7 elemental species (Ca, Ti, Mn, Fe, Ni, Cu, Pb), methanesulfonic acid (MSA), oxalate ($C_2O_4^{2-}$), 3 anhydrosugars (levoglucosan, mannosan and galactosan), 3 sugar alcohols (arabitol, sorbitol and mannitol), 9 polycyclic aromatic hydrocarbons (PAHs), 14 oxy-PAHs, 8 nitro-PAHs and 13 other SOA markers (i.e., α-methylglyceric acid, pinic acid, and methylnitrocatechols) were analysed following the protocols detailed in Srivastava et al.[20]

Offline AMS analysis was also performed on PM_{10} filter samples following the procedure developed by Daellenbach et al.[27]

3. Source apportionment approaches

3.1. EC-tracer method

The EC-tracer method has been widely used to estimate the partitioning of measured particulate OC into primary and secondary fractions.[3-5, 28-30] Briefly, it takes the advantage of the fact that primary OC and EC are emitted by the same combustion sources to estimate secondary OC (SOC) from the magnitude of OC-to-EC ratios measured in ambient air. In the present study, a primary OC-to-EC ratio ($[OC/EC]_p$) of 2.9 was estimated from measurements during periods of lowest photochemical activity. This $[OC/EC]_p$ value was then used to calculate secondary organic carbon (SOC) concentration (Figure S1). Details on these calculations are provided in the SM.

3.2. SOA-tracer method

This method was developed to estimate the contribution of specific SOA fractions, associated with individual gaseous precursors. SOC mass fractions are determined using conversion factors (typically determined from chamber experiments) allowing to calculate SOC loadings from molecular marker concentrations.[9] A clear limitation of this methodology is related to the fact that only a limited number of organic markers can be quantified.

In the present study, SOC mass fractions corresponding to two biogenic SOA - i.e., isoprene and α-pinene byproducts - were estimated according to a subset of markers following the procedure proposed by Rutter et al.[31] and described in the SM.

Biomass burning SOA are not commonly estimated using the SOA-tracer method. Neglecting this SOA source might though lead to significant underestimates of the total wintertime SOC concentrations in Europe, due to high contributions of residential wood burning during this period of the year.[22, 32, 33] In the present study, this SOA fraction was evaluated using the measured concentrations of methylnitrocatechols, previously demonstrated as secondary photooxidation products of phenolic compounds (e.g., cresols, methoxy phenols), and based on conversion factors estimated from the literature (Table S1).[34, 35] To the best of our knowledge, this corresponds to the first attempt to include biomass burning SOA mass fractions in the SOA-tracer method.

3.3. PMF-based approaches

Detailed information on PMF principle can be found elsewhere.[7, 8] Briefly, this receptor model resolves factor profiles and contributions from a time series of observations using weighted least-squares fitting approach, where the weights are adjusted according to measurement uncertainties. The choice of the optimal solution is notably based on minimizing the residuals obtained between modeled and observed input species concentrations.

The U.S. Environmental Protection Agency (US-EPA) PMF 5.0 toolkit has been used to perform source apportionment on the PM_{10} filter chemical dataset (including water-soluble inorganics and metals, along with EC, OC and organic markers), as detailled in Srivastava et al.[20] OC concentrations obtained for each relevant factor were then used for the purpose of the present study. OA concentrations related to the different sources were further calculated applying OC-to-OA conversion factors specific to each source, i.e., 1.7 for biomass burning[32], 1.2 for vehicular emissions[36] and 2.0 for secondary organics.[37]

Detailed information on OA source apportionment using the ACSM and offline-AMS datasets is provided in the SM. For these analyses, OA mass spectra were treated using the Source Finder toolkit (SoFi)[38] implemented in Igor Pro software package (Wavemetrics, Inc., Portland, OR, USA).

Both US-EPA and SoFi toolkits make use of the multilinear engine (ME-2) algorithm, allowing for implementing constraints on the factor chemical profiles and/or timeseries.

4. Results & discussions

4.1. Number of factors

The complete information on the source apportionment results are provided in the SM (Figures S2 to S11). By definition, the EC-tracer method resulted in the estimation of 1 primary and 1 secondary factors. Due to the methodological strategy, the SOA-tracer method allowed for the quantification of 5 different SOA fractions. PMF analysis conducted on the chemical dataset (PMF-chemical data) led to 10 different factors, while analyses on the offline AMS and ACSM datasets (PMF-offline AMS and PMF-ACSM) comprised 6 and 4 factors, respectively.

The labelling chosen for each of these factors is summarized in Table 1. Combustion-related factors highly influenced by primary organic molecular markers (for PMF-chemical data) or by hydrogenated mass fragments (for PMF-offline AMS and PMF-ACSM) were attributed to the POA fraction. Conversely, every factor mainly influenced by secondary markers or oxygenated mass fragments was ascribed to the SOA fraction. Dust-related OA factors (retrieved from PMF-chemical data as well as PMF-offline AMS) could be linked to both primary and secondary aerosols, notably due to soil abrasion, resuspension and/or coagulation phenomena on the one hand, and condensation of gaseous organics onto mineral dust particles on the other hand. Here, it was

decided to primarily attribute them to the POA fraction. This choice relies on the fact that i) the corresponding PMF-chemical data factor was containing a significant content of EC (Figure S2), a species only originating from primary sources, and ii) PMF-offline AMS factor (SCOA, i.e., Sulfur-Containing OA) has been considered to mainly originate from primary emissions within previous studies.[33, 39]

Table 1. List of factors identified using each methodology.

	Primary factors		Secondary factors	
	Number	Labelling	Number	Labelling
EC-tracer method	1	POA	1	SOA
SOA-tracer method	Not applicable		4	isoprene SOA α-pinene SOA toluene SOA biomass burning SOA
PMF-chemical data	3	Primary traffic emissions Biomass burning Dust	7	biogenic SOA-1 biogenic SOA-2 anthropogenic SOA-1 anthropogenic SOA-2 anthropogenic SOA-3 mixed secondary aerosols nitrate-rich
PMF-ACSM	2	HOA BBOA	2	MO-OOA LO-OOA
PMF-offline AMS	4	HOA COA BBOA SCOA	2	OOA1 OOA2

Although expected, such a disparity in the factor number impeded a direct comparison of each individual factors retrieved from the various methodologies. However, the obtained results could be compared when discriminated and distributed into the primary and secondary organic aerosol fractions, as discussed hereafter.

4.2. Primary organic aerosols

Figure 1A presents timeseries of primary OC (POC) concentrations obtained from the various methodologies allowing for POA apportionment. We observed a relatively good agreement

between outputs from EC-tracer method, PMF-chemical data, and PMF-offline AMS. As shown in Figure 1B, averaged POC concentrations obtained from these three methodologies ranged between 3.2 and 3.7 µg m^{-3} representing ~50% of the total OC. The highest correlation coefficient (r^2=0.64, n=92, p<0.05) was observed between PMF-chemical data and EC-tracer method results (Table S3A).

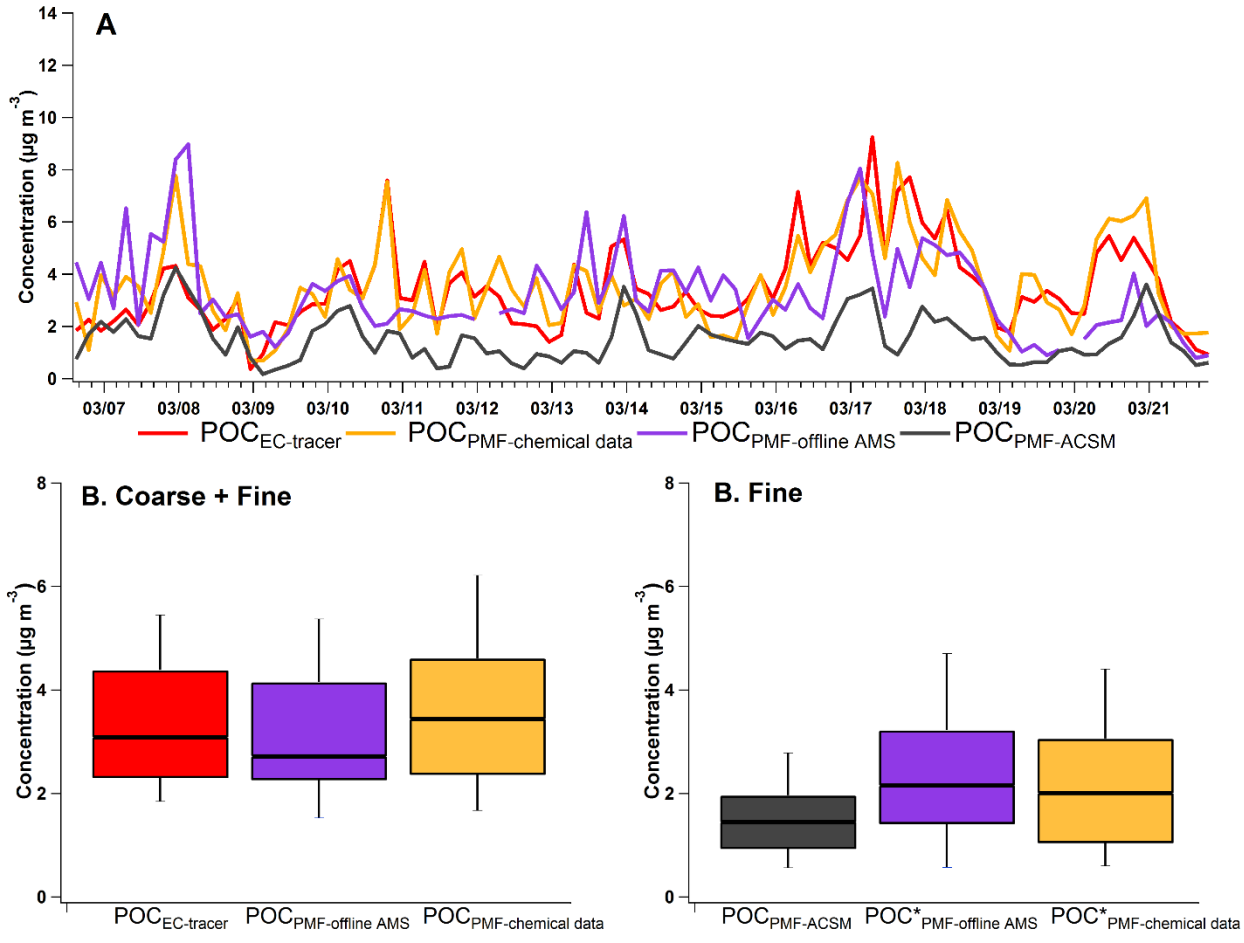

Figure 1. Comparison of total POC concentrations obtained from the different methodologies. 1A (upper panel): time series. 1B (bottom panel): Box plots indicate minimum, first quartile, median, third quartile and maximum values. POC*$_{PMF\text{-}chemical\ data}$: PMF-chemical data without dust; POC*$_{PMF\text{-}offline\ AMS}$: PMF-offline AMS without SCOA.

POC concentrations estimated from the PMF-analysis (ACSM) (averaged value of 2.0 µg m^{-3}) were significantly lower than the 3 other ones. This should be mainly related to the difference in sampling size cut-off (PM_1 for ACSM vs. PM_{10} for filter samples). As presented in Figure S13, the average contribution of the submicron fraction to total OA concentrations was estimated to be of about 77%. Interestingly, the remaining 23% that could be attributed to the coarse OA were in good agreement with the mean contribution to total OC (about 20%) that could be ascribed to the PMF-chemical data and PMF-offline AMS dust/SCOA factors. These results somehow validate the assumption of a predominant primary origin for the dust-related organic aerosols.

An attempt was then made to compare POC estimates in the fine aerosol mode between the three PMF approaches. To do so, SCOA and dust factors were removed from the total POC concentrations obtained respectively from PMF-offline AMS and PMF-chemical data. The results highlighted a slight increase in correlation between these two latter methologies (r^2=0.32 without dust and SCOA; r^2=0.21 with dust and SCOA) (Table S3B). Total POC concentrations from PMF-ACSM were then also in better agreement with the two other PMF approaches, as shown in Figure 1B and Table S3. On average for the whole period of study, total fine POC concentrations notably ranged from 2.0 µg m^{-3} (for PMF-ACSM) to 2.5 µg m^{-3} (for PMF-offline AMS).

Such a consistency allowed to further compare individual primary PMF factors related to the main combustion sources, i.e., biomass burning- and traffic-related aerosols.

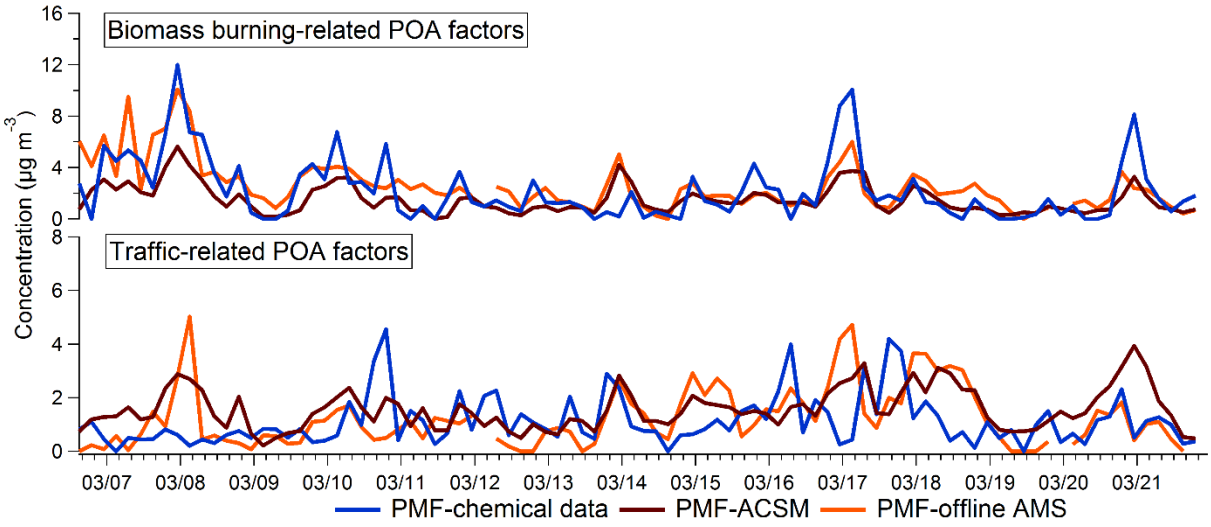

Figure 2. Time series of biomass burning- (top panel) and traffic-related (bottom panel) POA factors obtained from the three PMF approaches.

A very good agreement could be observed among all identified biomass burning-related factors, with correlation coefficients ranging from 0.48 to 0.61 (Table S4). Similar diurnal profiles were also obtained from the 3 PMF approaches, with a significant nighttime increase linked to domestic heating (Figure S14). As shown in Figure 2, PMF-chemical data and PMF-offline AMS concentration levels were roughly equivalent throughout the campaign except for a few data points. By contrast, PMF-ACSM showed slightly lowest BBOA concentration levels. A possible influence of submicrometer biomass burning-related aerosols cannot be totally ruledout. It may also be hypothesized that biomass burning OA may be partly accounted for other factors than BBOA, such as HOA as already shown by some previous ACSM-based studies.[22]

As a matter of fact, PMF-ACSM (and PMF-offline AMS) HOA timeserie(s) frequently showed higher concentrations levels than the PMF-chemical data traffic-related factor during BBOA concentration peaks (Figure 2). It should also be noted that the PMF-chemical data traffic factor displayed a more pronounced bimodal diurnal cycle (corresponding to morning and evening commuting time) than PMF-ACSM and -offline AMS HOA (Figure S14). This result suggested

that the PMF-chemical data analysis could more accurately describe primary traffic-related OA, which might be related to the use of key species, such as EC and 1-nitropyrene, in the input chemical data matrix.[20] However, relatively good agreement between averaged traffic-related POC concentrations (i.e., about 0.9 µg m^{-3} for both PMF-chemical data and PMF-offline AMS, 1.1 µg m^{-3} for PMF-ACSM) appeared to validate the assumption of the overall predominant vehicular exhaust origin for HOA factors, as already reported in many previous studies.[40-43]

Finally for the primary fraction, a relatively good agreement was observed between time series of the PMF-chemical data dust factor and the PMF-offline AMS SCOA factor (Figure 3). This result highlighted that SCOA may indeed be mainly related to primary dust aerosols, most probably in the coarse mode, in good agreement with previous assessments made in a few previous offline AMS-based studies .[33, 39]

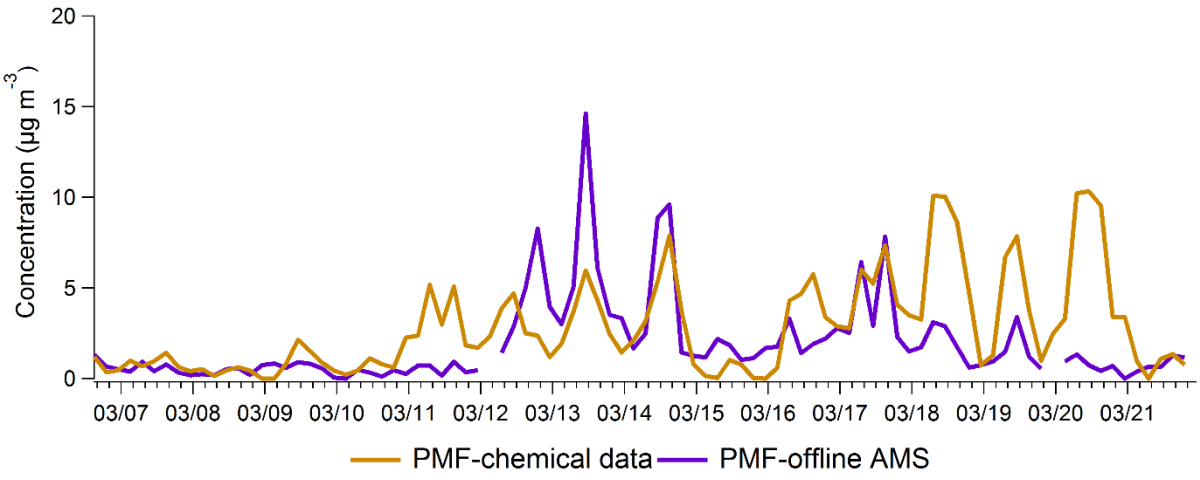

Figure 3. Time series of the dust and SCOA factors obtained respectively from the PMF-chemical data and PMF-offline AMS approaches.

4.3. Secondary organic aerosols

For total SOC concentrations, a relatively good agreement was observed between all source apportionment approaches, but the SOA-tracer method (Figure 4 and Table S6).

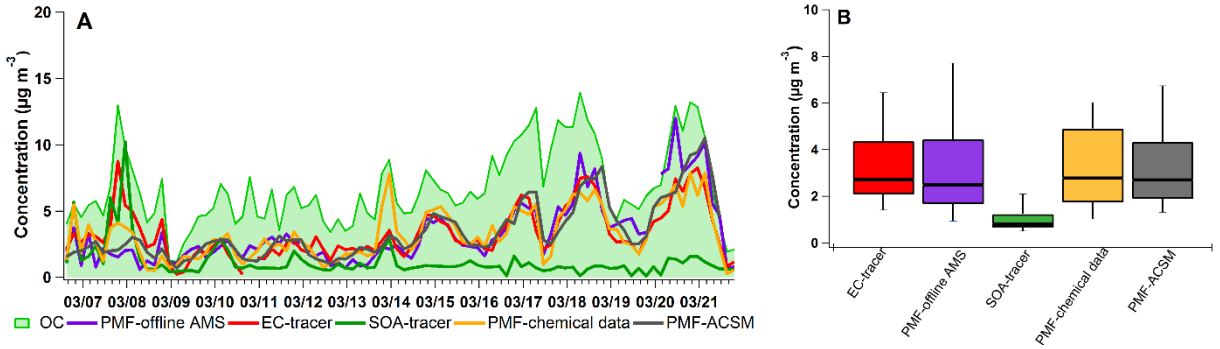

Figure 4. Comparison of total SOC concentrations obtained from the different methodologies. 4A: time series 4B: Box plots indicate minimum, first quartile, median, third quartile and maximum values.

Very similar campaign-mean values, of about 3.3 ± 0.1 µg m^{-3}, were obtained for EC-tracer method, PMF-Chemical data, PMF-offline AMS and PMF-ACSM (Figure 4B). Lowest concentrations derived from the SOA-tracer method (mean value of about 1.2 µg m^{-3}) were mainly noticeable for the second half of the campaign. In this study, $SOC_{SOA\text{-}tracer}$ concentrations only accounted for organics formed via the photooxidation of isoprene, α-pinene, naphthalene, toluene and phenolic compounds (section S2). Due to the lack of information on other possible SOA hydrocarbon precursors, such as mono- and poly-aromatic compounds, alkanes and/or alkenes,[44-46] the present SOA-tracer method analysis certainly missed significant additional SOA classes. In particular, relatively high organonitrate and/or organosulfate loadings[47, 48] could be expected between the 15th and the 21st of March, a period when PM_{10} concentrations were highly dominated by water-soluble inorganic species.[20]

Underestimations of the used mass fraction conversion factors (obtained from chamber studies results available in the literature) might also partly explain the lowest concentrations obtained from the SOA-tracer method. However, it should be noted that total SOC concentrations estimated by this methodology matched rather well outputs of other approaches during the first half of the campaign (Figure 4A), suggesting relatively fair estimates of SOA-tracer individual factors taken into account in the present study.

Regarding now the individual factors from the three PMF approaches, satisfactory correlation coefficients were only obtained between the two highly oxidised OA factors (namely OOA1 and MO-OOA, from PMF-offline AMS and PMF-ACSM analyses, respectively), marine biogenic SOA, and/or mixed secondary aerosols (both the latter ones being obtained by PMF-chemical data analysis) (Table S7). High concentrations of these factors were notably observed during the second half of the campaign (Figure 5). Along with the significance of inorganic loadings, a probable predominant long-range transport influence might be expected during this period.[20]

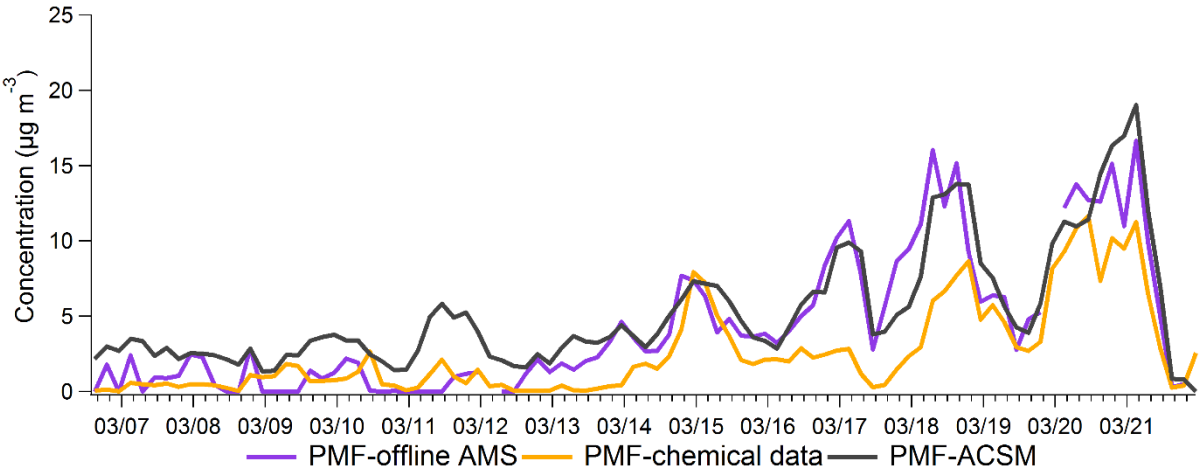

Figure 5. Comparison of highly oxidised OA factors obtained from PMF-offline AMS (OOA1) and PMF-ACSM (MO-OOA) with the sum of the mixed secondary aerosol and marine biogenic SOA factors obtained from PMF-chemical data.

Finally, no evident relation could be observed between any other individual SOA factor obtained from the different methodologies, highlighting the need for further and more comprehensive studies to fully describe the origins of the various SOA fractions regarding their oxidation states.

5. Conclusion

In the present study, three different source apportionment methodologies (namely, EC- and SOA-tracer method, as well as PMF) were applied on different measurements (filter-based chemical speciation datasets and offline AMS mass spectra, online ACSM mass spectra). Total POC and SOC concentrations obtained from the various approaches were globally consistent between each other, except for the SOA-tracer method. The identification of more molecular markers corresponding to SOA classes unaccounted so far, and their introduction in the latter approach, is deemed necessary to fix this discrepancy.

The primary biomass burning- and traffic-related factors were further supported by their respective diurnal profiles. They displayed a rather good consistency from one methodology to the other, with however some probable mixing issues in the cases of mass spectra PMF analyses.

It should also be noted that the dust and SCOA factors, obtained respectively from the PMF-chemical data and PMF-offline AMS analyses, displayed relatively similar temporal variations. This appeared to confirm that SCOA (already observed in a few European previous studies) may be mainly ascribed to primary coarse aerosols.

For individual SOA factors, mixed secondary aerosols obtained from PMF-chemical data were found to correlate well with highly oxidized OA factors retrieved from mass spectra analyses, suggesting similar origins for these factors. However, none of the used approach was able to fully identify the specific formation mechanisms and/or the gaseous precursors responsible for this SOA fraction (representing here about 25% of total OA in PM_{10}). Further studies are then still needed to

investigate the secondary processes associated with nitrate- and/or sulfate-rich aerosols during such pollution events.

Acknowledgements

This work has notably been supported by the French Ministry of Environment (MTES) and the national reference laboratory for air quality monitoring (LCSQA). Aerosol in situ measurements were part of the H2020 ACTRIS-2 project and partly funded by the ACTRIS-Fr/CLAP initiative at the national level. The authors gratefully acknowledge François Truong (LSCE) and Robin Aujay-Plouzeau (INERIS) for taking care of samples and instrumentation, as well as François Kany and Serguei Stavrovski (INERIS) for sample extraction and PAH analyses.

References

1. Hallquist, M.; Wenger, J.; Baltensperger, U.; Rudich, Y.; Simpson, D.; Claeys, M.; Dommen, J.; Donahue, N.; George, C.; Goldstein, A., The formation, properties and impact of secondary organic aerosol: current and emerging issues. *Atmos. Chem. Phys.* **2009,** *9*, (14), 5155-5236.

2. Kanakidou, M.; Seinfeld, J.; Pandis, S.; Barnes, I.; Dentener, F.; Facchini, M.; Dingenen, R. V.; Ervens, B.; Nenes, A.; Nielsen, C., Organic aerosol and global climate modelling: a review. *Atmos. Chem. Phys.* **2005,** *5*, (4), 1053-1123.

3. Grosjean, D., Particulate carbon in Los Angeles air. *Sci. Total Environ.* **1984,** *32*, (2), 133-45.

4. Turpin, B. J.; Huntzicker, J. J., Identification of secondary organic aerosol episodes and quantitation of primary and secondary organic aerosol concentrations during SCAQS. *Atmos. Environ.* **1995,** *29*, (23), 3527-3544.

5. Gray, H. A.; Cass, G. R.; Huntzicker, J. J.; Heyerdahl, E. K.; Rau, J. A., Characteristics of atmospheric organic and elemental carbon particle concentrations in Los Angeles. *Environ. Sci. Technol.* **1986,** *20*, (6), 580-589.

6. Watson, J. G.; Robinson, N. F.; Chow, J. C.; Henry, R. C.; Kim, B.; Pace, T.; Meyer, E. L.; Nguyen, Q., The USEPA/DRI chemical mass balance receptor model, CMB 7.0. *Environmental Software* **1990,** *5*, (1), 38-49.

7. Paatero, P., Least squares formulation of robust non-negative factor analysis. *Chemom. Intell. Lab. Syst.* **1997,** *37*, (1), 23-35.

8. Paatero, P.; Tapper, U., Positive matrix factorization: A non-negative factor model with optimal utilization of error estimates of data values. *Environmetrics* **1994,** *5*, (2), 111-126.

9. Kleindienst, T. E.; Jaoui, M.; Lewandowski, M.; Offenberg, J. H.; Lewis, C. W.; Bhave, P. V.; Edney, E. O., Estimates of the contributions of biogenic and anthropogenic hydrocarbons to secondary organic aerosol at a southeastern US location. *Atmos. Environ.* **2007,** *41*, (37), 8288-8300.

10. Szidat, S.; Ruff, M.; Perron, N.; Wacker, L.; Synal, H.-A.; Hallquist, M.; Shannigrahi, A. S.; Yttri, K. E.; Dye, C.; Simpson, D., Fossil and non-fossil sources of organic carbon (OC) and elemental carbon (EC) in Göteborg, Sweden. *Atmos. Chem. Phys.* **2009,** *9*, (5), 1521-1535.

11. Gelencsér, A.; May, B.; Simpson, D.; Sánchez-Ochoa, A.; Kasper-Giebl, A.; Puxbaum, H.; Caseiro, A.; Pio, C.; Legrand, M., Source apportionment of PM2.5 organic aerosol over Europe: Primary/secondary, natural/anthropogenic, and fossil/biogenic origin. *J. Geophys. Res.* **2007,** *112*, (D23).

12. Jayne, J. T.; Leard, D. C.; Zhang, X.; Davidovits, P.; Smith, K. A.; Kolb, C. E.; Worsnop, D. R., Development of an Aerosol Mass Spectrometer for Size and Composition Analysis of Submicron Particles. *Aerosol Sci. Technol.* **2000,** *33*, (1-2), 49-70.

13. Ng, N. L.; Herndon, S. C.; Trimborn, A.; Canagaratna, M. R.; Croteau, P. L.; Onasch, T. B.; Sueper, D.; Worsnop, D. R.; Zhang, Q.; Sun, Y. L.; Jayne, J. T., An Aerosol Chemical Speciation Monitor (ACSM) for Routine Monitoring of the Composition and Mass Concentrations of Ambient Aerosol. *Aerosol Sci. Technol.* **2011,** *45*, (7), 780-794.

14. Donahue, N. M.; Robinson, A. L.; Pandis, S. N., Atmospheric organic particulate matter: From smoke to secondary organic aerosol. *Atmos. Environ.* **2009,** *43*, (1), 94-106.

15. Song, Y.; Zhang, Y.; Xie, S.; Zeng, L.; Zheng, M.; Salmon, L. G.; Shao, M.; Slanina, S., Source apportionment of PM2.5 in Beijing by positive matrix factorization. *Atmos. Environ.* **2006,** *40*, (8), 1526-1537.

16. Pachon, J. E.; Balachandran, S.; Hu, Y.; Weber, R. J.; Mulholland, J. A.; Russell, A. G., Comparison of SOC estimates and uncertainties from aerosol chemical composition and gas phase data in Atlanta. *Atmos. Environ.* **2010,** *44*, (32), 3907-3914.

17. Kleindienst, T. E.; Lewandowski, M.; Offenberg, J. H.; Edney, E. O.; Jaoui, M.; Zheng, M.; Ding, X.; Edgerton, E. S., Contribution of Primary and Secondary Sources to Organic Aerosol and PM2.5at SEARCH Network Sites. *J. Air Waste Manage. Assoc.* **2010,** *60*, (11), 1388-1399.

18. Heo, J.; Dulger, M.; Olson, M. R.; McGinnis, J. E.; Shelton, B. R.; Matsunaga, A.; Sioutas, C.; Schauer, J. J., Source apportionments of PM2.5 organic carbon using molecular marker Positive Matrix Factorization and comparison of results from different receptor models. *Atmos. Environ.* **2013,** *73*, 51-61.

19. Kim, E.; Hopke, P. K.; Edgerton, E. S., Improving source identification of Atlanta aerosol using temperature resolved carbon fractions in positive matrix factorization. *Atmos. Environ.* **2004,** *38*, (20), 3349-3362.

20. Srivastava, D.; Favez, O.; Bonnaire, N.; Lucarelli, F.; Perraudin, E.; Gros, V.; Villenave, E.; Albinet, A., Speciation of organic fractions does matter for aerosol source apportionment. Part 2: intensive campaign in the Paris area (France). *Sci. Total Environ.* **2018**, Under review.

21. Haeffelin, M.; Barthès, L.; Bock, O.; Boitel, C.; Bony, S.; Bouniol, D.; Chepfer, H.; Chiriaco, M.; Cuesta, J.; Delanoë, J.; Drobinski, P.; Dufresne, J. L.; Flamant, C.; Grall, M.; Hodzic, A.; Hourdin, F.; Lapouge, F.; Lemaître, Y.; Mathieu, A.; Morille, Y.; Naud, C.; Noël, V.; O'Hirok, W.; Pelon, J.; Pietras, C.; Protat, A.; Romand, B.; Scialom, G.; Vautard, R., SIRTA, a ground-based atmospheric observatory for cloud and aerosol research. *Ann. Geophys.* **2005,** *23*, (2), 253-275.

22. Petit, J. E.; Favez, O.; Sciare, J.; Canonaco, F.; Croteau, P.; Močnik, G.; Jayne, J.; Worsnop, D.; Leoz-Garziandia, E., Submicron aerosol source apportionment of wintertime pollution in Paris, France by double positive matrix factorization (PMF2) using an aerosol chemical speciation monitor (ACSM) and a multi-wavelength Aethalometer. *Atmos. Chem. Phys.* **2014,** *14*, (24), 13773-13787.

23. Petit, J. E.; Favez, O.; Sciare, J.; Crenn, V.; Sarda-Estève, R.; Bonnaire, N.; Močnik, G.; Dupont, J. C.; Haeffelin, M.; Leoz-Garziandia, E., Two years of near real-time chemical composition of submicron aerosols in the region of Paris using an Aerosol Chemical Speciation

Monitor (ACSM) and a multi-wavelength Aethalometer. *Atmos. Chem. Phys.* **2015,** *15*, (6), 2985-3005.

24. Dupont, J.; Haeffelin, M.; Badosa, J.; Elias, T.; Favez, O.; Petit, J.; Meleux, F.; Sciare, J.; Crenn, V.; Bonne, J. L., Role of the boundary layer dynamics effects on an extreme air pollution event in Paris. *Atmos. Environ.* **2016,** *141*, (2), 571 - 579.

25. Waked, A.; Favez, O.; Alleman, L. Y.; Piot, C.; Petit, J. E.; Delaunay, T.; Verlinden, E.; Golly, B.; Besombes, J. L.; Jaffrezo, J. L.; Leoz-Garziandia, E., Source apportionment of PM10 in a north-western Europe regional urban background site (Lens, France) using positive matrix factorization and including primary biogenic emissions. *Atmos. Chem. Phys.* **2014,** *14*, (7), 3325-3346.

26. Petit, J.-E.; Amodeo, T.; Meleux, F.; Bessagnet, B.; Menut, L.; Grenier, D.; Pellan, Y.; Ockler, A.; Rocq, B.; Gros, V., Characterising an intense PM pollution episode in March 2015 in France from multi-site approach and near real time data: Climatology, variabilities, geographical origins and model evaluation. *Atmos. Environ.* **2017,** *155*, 68-84.

27. Daellenbach, K. R.; Bozzetti, C.; Křepelová, A.; Canonaco, F.; Wolf, R.; Zotter, P.; Fermo, P.; Crippa, M.; Slowik, J. G.; Sosedova, Y.; Zhang, Y.; Huang, R. J.; Poulain, L.; Szidat, S.; Baltensperger, U.; El Haddad, I.; Prévôt, A. S. H., Characterization and source apportionment of organic aerosol using offline aerosol mass spectrometry. *Atmos. Meas. Tech.* **2016,** *9*, (1), 23-39.

28. Castro, L. M.; Pio, C. A.; Harrison, R. M.; Smith, D. J. T., Carbonaceous aerosol in urban and rural European atmospheres: estimation of secondary organic carbon concentrations. *Atmos. Environ.* **1999,** *33*, (17), 2771-2781.

29. Chu, S.-H., Stable estimate of primary OC/EC ratios in the EC tracer method. *Atmos. Environ.* **2005,** *39*, (8), 1383-1392.

30. Saylor, R. D.; Edgerton, E. S.; Hartsell, B. E., Linear regression techniques for use in the EC tracer method of secondary organic aerosol estimation. *Atmos. Environ.* **2006,** *40*, (39), 7546-7556.

31. Rutter, A. P.; Snyder, D. C.; Stone, E. A.; Shelton, B.; DeMinter, J.; Schauer, J. J., Preliminary assessment of the anthropogenic and biogenic contributions to secondary organic aerosols at two industrial cities in the upper Midwest. *Atmos. Environ.* **2014,** *84*, 307-313.

32. Puxbaum, H.; Caseiro, A.; Sánchez-Ochoa, A.; Kasper-Giebl, A.; Claeys, M.; Gelencsér, A.; Legrand, M.; Preunkert, S.; Pio, C., Levoglucosan levels at background sites in Europe for assessing the impact of biomass combustion on the European aerosol background. *J. Geophys. Res.-Atmos.* **2007,** *112*, (D23).

33. Daellenbach, K. R.; Stefenelli, G.; Bozzetti, C.; Vlachou, A.; Fermo, P.; Gonzalez, R.; Piazzalunga, A.; Colombi, C.; Canonaco, F.; Hueglin, C.; Kasper-Giebl, A.; Jaffrezo, J. L.; Bianchi, F.; Slowik, J. G.; Baltensperger, U.; El-Haddad, I.; Prévôt, A. S. H., Long-term chemical analysis and organic aerosol source apportionment at nine sites in central Europe: source identification and uncertainty assessment. *Atmos. Chem. Phys.* **2017,** *17*, (21), 13265-13282.

34. Bruns, E. A.; El Haddad, I.; Slowik, J. G.; Kilic, D.; Klein, F.; Baltensperger, U.; Prévôt, A. S. H., Identification of significant precursor gases of secondary organic aerosols from residential wood combustion. *Sci. Rep.* **2016,** *6*, 27881.

35. Iinuma, Y.; Boge, O.; Grafe, R.; Herrmann, H., Methyl-nitrocatechols: atmospheric tracer compounds for biomass burning secondary organic aerosols. *Environ. Sci. Technol.* **2010,** *44*, (22), 8453-9.

36. van Drooge, B. L.; Grimalt, J. O., Particle sized-resolved source apportionment of primary and secondary organic tracer compounds at urban and rural locations in Spain. *Atmos. Chem. Phys. Discuss.* **2015,** *15*, (7), 9897-9939.

37. Mohr, C.; Huffman, J. A.; Cubison, M. J.; Aiken, A. C.; Docherty, K. S.; Kimmel, J. R.; Ulbrich, I. M.; Hannigan, M.; Jimenez, J. L., Characterization of Primary Organic Aerosol Emissions from Meat Cooking, Trash Burning, and Motor Vehicles with High-Resolution Aerosol Mass Spectrometry and Comparison with Ambient and Chamber Observations. *Environ. Sci. Technol.* **2009,** *43*, (7), 2443-2449.

38. Canonaco, F.; Crippa, M.; Slowik, J.; Baltensperger, U.; Prévôt, A., SoFi, an IGOR-based interface for the efficient use of the generalized multilinear engine (ME-2) for the source apportionment: ME-2 application to aerosol mass spectrometer data. *Atmos. Meas. Tech.* **2013,** *6*, (12), 3649-3661.

39. Vlachou, A.; Kaspar, R.; Bozzetti, C.; Chazeau, B.; Gary, A.; Salazar, S. S.; Jaffrezo, J.-L.; Hueglin, C.; Baltensperger, U.; El Haddad, I., Advanced source apportionment of carbonaceous aerosols by coupling offline AMS and radiocarbon size segregated measurements over a nearly two-year period. *Atmos. Chem. Phys. Discuss.* **2017,** *2017*, 1-25.

40. Lanz, V. A.; Alfarra, M. R.; Baltensperger, U.; Buchmann, B.; Hueglin, C.; Prévôt, A. S. H., Source apportionment of submicron organic aerosols at an urban site by factor analytical modelling of aerosol mass spectra. *Atmos. Chem. Phys.* **2007,** *7*, (6), 1503-1522.

41. Zhang, Q.; Jimenez, J. L.; Canagaratna, M. R.; Allan, J. D.; Coe, H.; Ulbrich, I.; Alfarra, M. R.; Takami, A.; Middlebrook, A. M.; Sun, Y. L.; Dzepina, K.; Dunlea, E.; Docherty, K.; DeCarlo, P. F.; Salcedo, D.; Onasch, T.; Jayne, J. T.; Miyoshi, T.; Shimono, A.; Hatakeyama, S.; Takegawa, N.; Kondo, Y.; Schneider, J.; Drewnick, F.; Borrmann, S.; Weimer, S.; Demerjian, K.; Williams, P.; Bower, K.; Bahreini, R.; Cottrell, L.; Griffin, R. J.; Rautiainen, J.; Sun, J. Y.; Zhang, Y. M.; Worsnop, D. R., Ubiquity and dominance of oxygenated species in organic aerosols in anthropogenically-influenced Northern Hemisphere midlatitudes. *Geophys. Res. Lett.* **2007,** *34*, (13).

42. Xu, J.; Zhang, Q.; Chen, M.; Ge, X.; Ren, J.; Qin, D., Chemical composition, sources, and processes of urban aerosols during summertime in northwest China: insights from high-resolution aerosol mass spectrometry. *Atmos. Chem. Phys.* **2014,** *14*, (23), 12593-12611.

43. Ulbrich, I. M.; Canagaratna, M. R.; Zhang, Q.; Worsnop, D. R.; Jimenez, J. L., Interpretation of organic components from Positive Matrix Factorization of aerosol mass spectrometric data. *Atmos. Chem. Phys.* **2009,** *9*, (9), 2891-2918.

44. Tkacik, D. S.; Presto, A. A.; Donahue, N. M.; Robinson, A. L., Secondary Organic Aerosol Formation from Intermediate-Volatility Organic Compounds: Cyclic, Linear, and Branched Alkanes. *Environ. Sci. Technol.* **2012,** *46*, (16), 8773-8781.

45. Lim, Y. B.; Ziemann, P. J., Products and mechanism of secondary organic aerosol formation from reactions of n-alkanes with OH radicals in the presence of NOx. *Environ. Sci. Technol.* **2005,** *39*, (23), 9229-36.

46. Zhao, Y.; Hennigan, C. J.; May, A. A.; Tkacik, D. S.; de Gouw, J. A.; Gilman, J. B.; Kuster, W. C.; Borbon, A.; Robinson, A. L., Intermediate-Volatility Organic Compounds: A Large Source of Secondary Organic Aerosol. *Environ. Sci. Technol.* **2014,** *48*, (23), 13743-13750.

47. Surratt, J. D.; Kroll, J. H.; Kleindienst, T. E.; Edney, E. O.; Claeys, M.; Sorooshian, A.; Ng, N. L.; Offenberg, J. H.; Lewandowski, M.; Jaoui, M.; Flagan, R. C.; Seinfeld, J. H., Evidence for Organosulfates in Secondary Organic Aerosol. *Environ. Sci. Technol.* **2006,** *41*, (2), 517-527.

48. Riva, M.; Tomaz, S.; Cui, T.; Lin, Y. H.; Perraudin, E.; Gold, A.; Stone, E. A.; Villenave, E.; Surratt, J. D., Evidence for an unrecognized secondary anthropogenic source of organosulfates and sulfonates: gas-phase oxidation of polycyclic aromatic hydrocarbons in the presence of sulfate aerosol. *Environ. Sci. Technol.* **2015,** *49*, (11), 6654-64.

Supporting material

Comparison of different methodologies to discriminate between primary and secondary organic aerosols

D. Srivastava[1,2,3], *K. R. Daellenbach*[4], *Y. Zhang*[1], *N. Bonnaire*[5], *E. Perraudin*[2,3], *V. Gros*[5], *E. Villenave*[2,3], *A. S. H. Prévôt*[4], *I. El Haddad*[4], *O. Favez*[1], *A. Albinet*[1,*]

[1]INERIS, Parc Technologique Alata, BP 2, 60550 Verneuil-en-Halatte, France

[2]CNRS, EPOC, UMR 5805 CNRS, 33405 Talence, France

[3]Université de Bordeaux, EPOC, UMR 5805 CNRS, 33405 Talence, France

[4]Paul Scherrer Institute, 5232 Villigen PSI, Switzerland

[5]LSCE - UMR8212, CNRS-CEA-UVSQ, Gif-sur-Yvette, France

Correspondence to: alexandre.albinet@ineris.fr; alexandre.albinet@gmail.com

To be submitted to Enviromental Science & Technology

S1. EC-tracer method

The EC-tracer method has been widely employed and takes the advantage of the primary OC and EC ratio ($[OC/EC]_p$) to estimate the SOC fraction.[1-6]

In this method, primary OC can be expressed as in Equation (1)

$$[OC]_p = \left[\frac{OC}{EC}\right]_p .[EC] + [OC]_{non-comb.} \quad (1)$$

The SOC fraction can be estimated using following Equation (2)

$$[OC]_S = [OC] - [OC]_P \quad (2)$$

where [OC] is the measured total OC concentration, $[OC]_p$ is the primary OC concentration, $[OC/EC]_p$ represents the ratio of OC to EC for the primary sources affecting the site of interest, and $[OC]_{non-comb.}$ is the non-combustion contribution to the primary OC, [EC] is the measured EC concentration, and $[OC]_S$ is the secondary OC.

Generally, $[OC/EC]_p$ in Equation (1) is determined from the linear regression between OC and EC[6] or can be estimated from days when primary or secondary activity is more pronounced.[7] For this study, $[OC/EC]_p$ ratio was estimated in three steps: (i) selected days during the campaign with low photochemical activity, low photochemical activity was defined as days with O_3 concentration below the 25th percentile, O_3<24 µg/m^3 (Figure S1), (ii) identified days when primary activity was more pronounced (using EC and OC/EC) (Figure S1), (iii) selected minimum OC/EC ratio (2.9) from those days as a representative of the ratio of OC to EC for the primary sources. In these conditions, the contribution of $[OC]_{non-comb.}$ to the primary OC is negligible,[8] and was considered zero in our calculations.

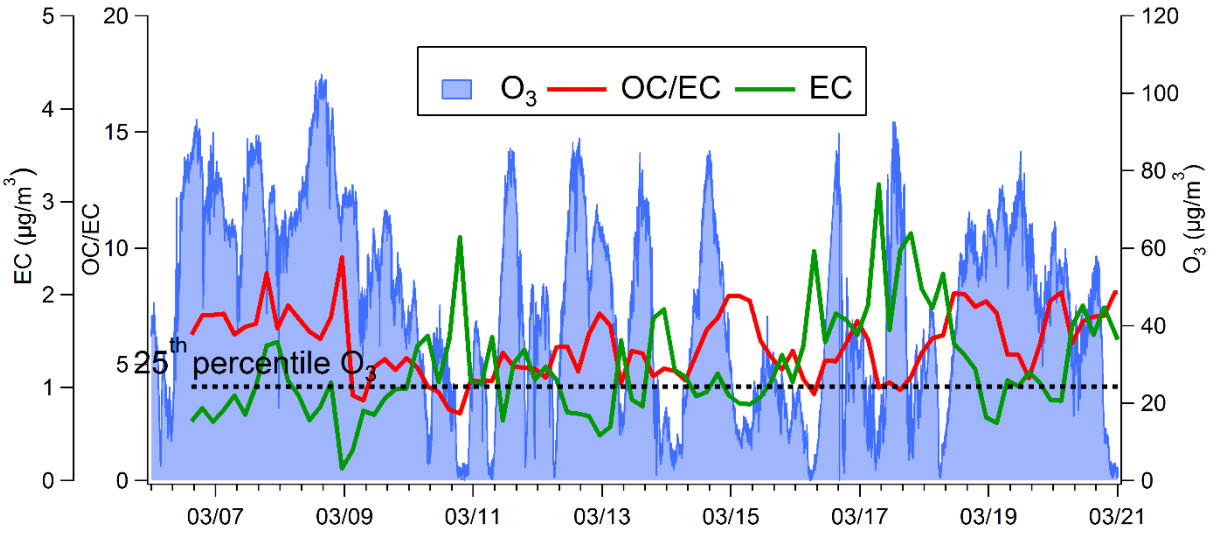

Figure S1. EC, OC/EC ratio and O_3 concentration identified at Paris-SIRTA, France (March 2015).

S2. SOA-tracer method

S2.1. Adjusted f_{SOC}

In the SOA-tracer method, the available (laboratory generated) SOA and SOC mass fractions are used to convert ambient SOC marker concentration to the total SOC mass for an individual precursor.

As mentioned previously in the SOA tracer method,[9] not the same number of markers were measured in this work. Therefore, the available mass fractions converting SOC marker concentrations to the total SOC mass published by Kleindienst et al.[9] were modified. The relative contributions of all of the individual markers to a given SOC class (i.e., SOC derived from α-pinene) were accounted for following the procedure proposed by Rutter et al.[10] This was done by using the following equations given below.

$$f_{SOA,I} = \frac{\sum_i tr_i}{[SOA]} \quad (3)$$

$$f_{SOA,I3} = f_{SOA,I} \frac{I3}{\sum_i tr_i} \quad (4)$$

$$SOA = \frac{I3}{f_{SOA,I3}} \quad (5)$$

where $f_{SOA,I}$ is a ratio of the sum of concentrations of all the measured markers, tr, to the total SOA formed from the individual class of precursor "I", and I3 is the measured marker of a precursor I. Individual marker concentrations were then used with the adjusted f_{SOA} values to determine total SOA concentrations for each precursor using Equation (5). The averages of the SOC concentrations derived from each of the individual markers were then calculated.

S2.2. f_{SOC} for biomass burning

Attempts were made to include the SOC mass fraction (f_{SOC}) for biomass burning (phenolic compounds, i.e., methylnitrocatechols) in the SOA tracer approach. The methylnitrocatechols, secondary photooxidation products of phenolic compounds (i.e., cresols),[11] known to account for a major fraction of SOA biomass burning,[12] were used to investigate f_{SOC} for biomass burning based on the information available from the literature.[11]

As explained previously, for each precursor, the aerosol mass fraction, $f_{SOA,}$, is defined by dividing the sum of the organic tracers by the total SOA concentration. The aerosol mass fraction is described following Equation (6).

$$f_{SOA,hc} = \frac{\sum_i [tr]_i}{[SOA]} \qquad (6)$$

In our calculation, $\Sigma[tr]$ = 412 ng m^{-3}; [SOA]= 8293 ng m^{-3}, values were taken from the literature[11] to calculate f_{SOA} from Equation (5). Further, the SOA mass fractions were converted into SOC mass fractions using SOA to SOC mass ratios. A ratio of 2 (secondary sources[13]) was used here to estimate the SOC mass fraction linked to biomass burning.

$$f_{SOC,hc} = f_{SOA,hc} \frac{[SOA]}{[SOC]} \qquad (7)$$

The estimated SOC mass fractions are given in Table S1.

Table S1. List of modified SOC mass fractions from individual precursors identified at Paris-SIRTA, France (March 2015).

SOA markers	**f_{SOC} adjusted values**
α-Methylglyceric acid	0.0775
2-Methylerythritol	0.0775
Pinonic acid	0.0987
3-Hydroxyglutaric acid	0.0663
Pinic acid	0.0378
3-Methylbutane-1,2,3-tricarboxylic acid	0.0282
2,3-Dihydroxy-4-oxopentanoic acid	0.0079
Pthalic acid	0.0400
4-Methyl-5-Nitrocatechol	0.0574
3-Methyl-5-Nitrocatechol	0.0420

Table S2. SOC mass from individual precursors identified at Paris-SIRTA, France (March 2015).

SOC	**Mass concentration (ng m^{-3})**
$SOC_{isoprene}$	15.13
SOC_{pinene}	47.39
$SOC_{toluene}$	320.66
$SOC_{naphthalene}$	117.29
$SOC_{biomass\ burning\ (phenolic)}$	716.03

S3. PMF analysis on the filter-based chemical dataset

PM_{10} source apportionment was performed on filter samples collected every 4 h at a sub-urban station in the Paris region (France) during a PM pollution event in March 2015. The use of specific primary and secondary molecular markers allowed to resolve 11 major PM_{10} sources including common factors (biomass burning, traffic, dust, sea salt, secondary inorganic aerosols), as well as 2 specific biogenic SOA (marine + isoprene) and 3 anthropogenic SOA (nitro-PAHs + oxy-PAHs + phenolic oxidation) factors (Figures S2 and S3).

All other details regarding this PMF solution, i.e, criteria for the selection of species, optimization of solution, stability and constrained runs, are already presented elsewhere.[14]

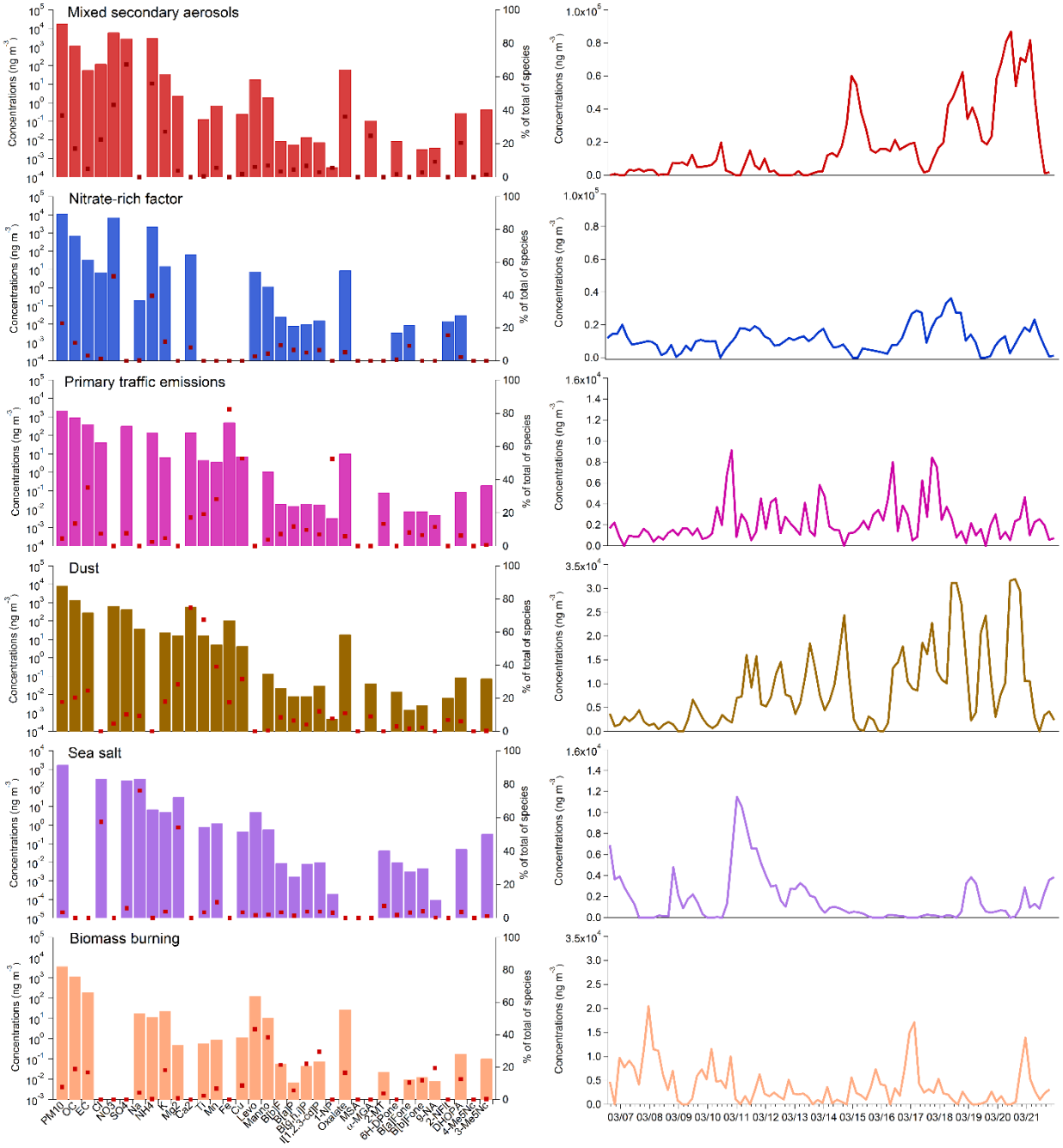

Figure S2. Source profiles and temporal evolution of mixed secondary aerosols, nitrate-rich factor, primary traffic emissions, dust, sea salt and biomass burning factors identified at Paris-SIRTA, France (March 2015).

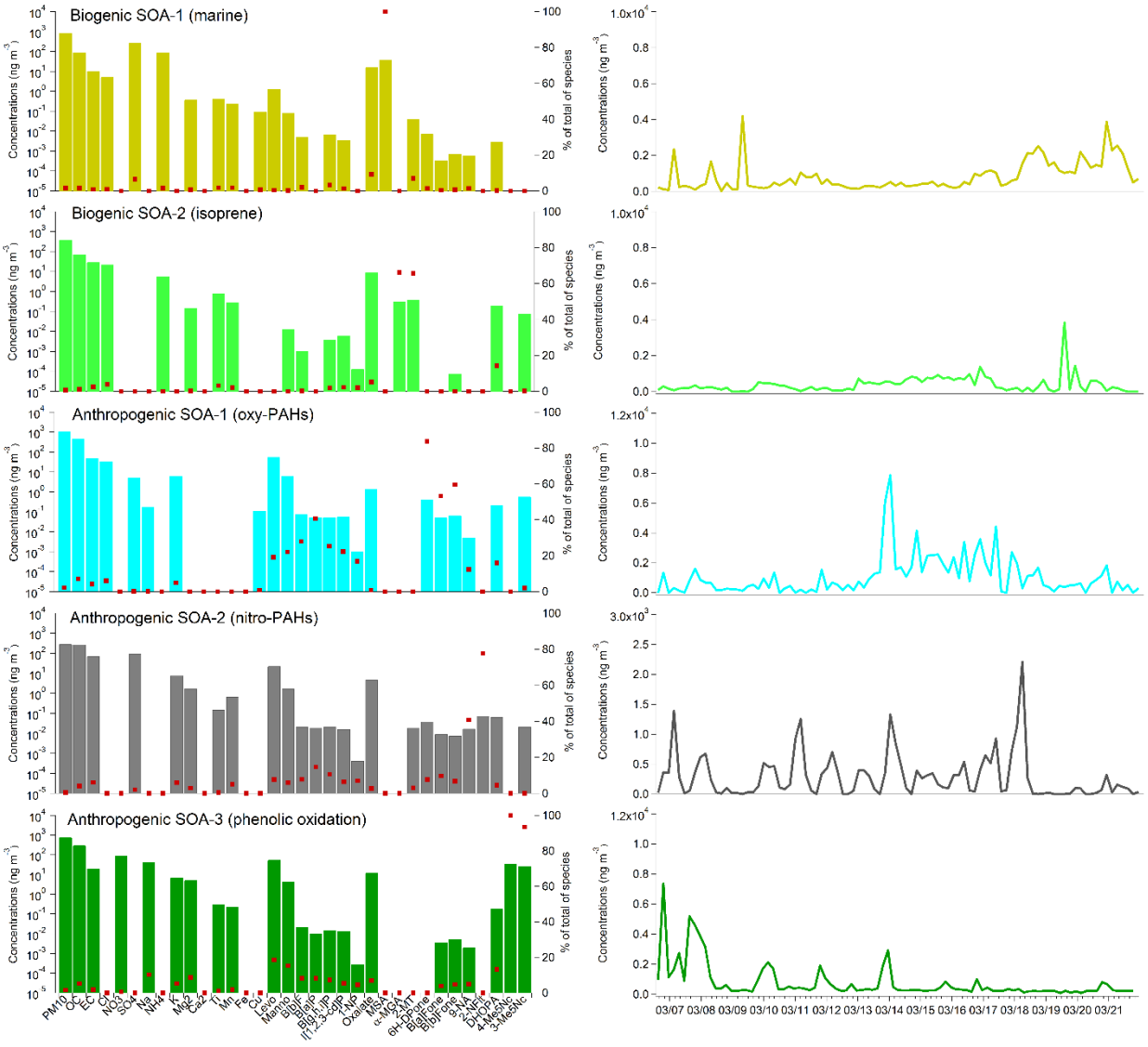

Figure S3. Source profiles and temporal evolution of biogenic SOA-1 (marine), biogenic SOA-2 (isoprene), anthropogenic SOA-1 (oxy-PAHs), anthropogenic SOA-2 (nitro-PAHs) and anthropogenic SOA-3 (phenolic oxidation) factors identified at Paris-SIRTA, France (March 2015).

S4. PMF analysis on ACSM OA mass spectra

In this study, PMF-ACSM was achieved using the multilinear engine-2 (ME-2) solver implemented in the Source Finder (SoFi) toolkit,[15] which enables an efficient exploration of the solution space by constraining the factor elements within a certain range defined by the scalar a ($0< a< 1$). Four OA factors, two primary OA (POA) factors, i.e., HOA (hydrocarbon like OA) and BBOA (biomass burning) and two secondary OA (SOA) factors including LO-OOA (low oxidized oxygenated OA) and MO-OOA (more oxidized oxygenated OA) were resolved by PMF (Figure S4).

The HOA and BBOA were constrained using reference mass spectra from Fröhlich et al.[16], and the other factors were unconstrained. The HOA spectrum was characterized by peaks characteristic of aliphatic hydrocarbons, including m/z 27 ($C_2H^+_3$), 41 ($C_3H^+_5$), 43 ($C_3H^+_7$), 55 ($C_4H^+_7$), 57 ($C_4H^+_9$), 69 ($C_5H^+_9$), and 71 ($C_5H^+_{11}$).[17] The mass spectrum of BBOA was characterized by the prominent signals of m/z 60 (mainly $C_2H_4O_2^+$) and 73 ($C_3H_5O_2^+$), two markers indicative of biomass burning emissions.[19, 20] The mass spectrum of MO-OOA is characterized by a dominant peak at *m/z* 44 (CO_2^+), similar to the more oxidized and low-volatility oxygenated OA (LV-OOA) factor determined at other urban/suburban sites.[20, 21] The mass spectrum of LO-OOA has lower f_{44}/f_{43} (fraction of *m/z* 43 and *m/z* 44 in the total OA signal) ratio and higher fraction of *m/z* 43 (mainly $C_2H_3O^+$) compared to MO-OOA, and represents the spectral pattern of previously reported semi-volatile OOA (SV-OOA).[21]

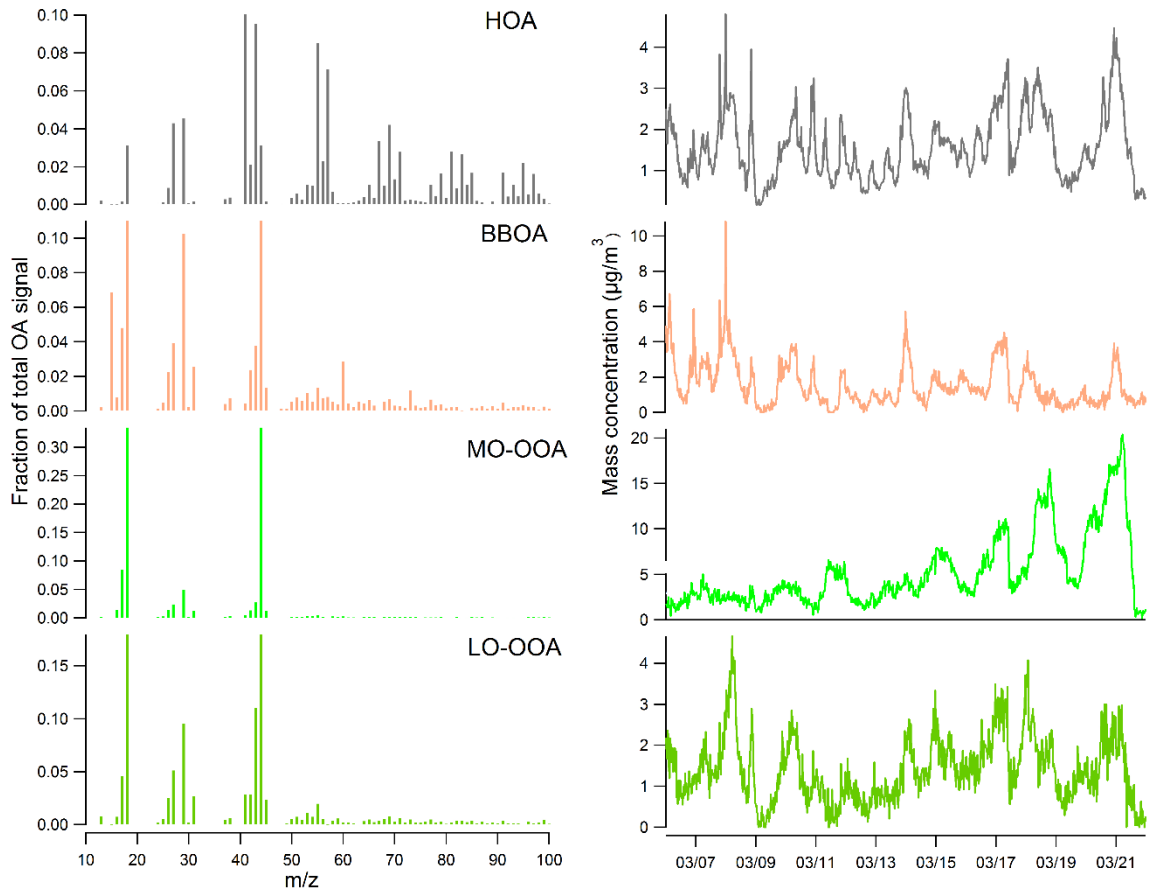

Figure S4. Chemical and temporal profiles of HOA, BBOA, MO-OA, and LO-OOA PMF factors identified at Paris-SIRTA, France (March 2015). HOA and BBOA are constrained.

S5. Offline AMS

S5.1. Analytical procedures

The offline AMS analysis was performed following the protocols developed by Daellenbach et al.[22] Briefly, for each analysed filter sample, three filter punches (1.5 cm^2 surface area) were extracted using ultra sonication in 10 mL of ultrapure water (18.2 MΩ cm, total organic carbon TOC< 5 ppb, 25°C) for 20 min at 30°C. Liquid extracts were filtered (0.45 μm), followed by nebulization in Argon (≥99.998 % Vol. abs., Carbagas, CH-3073 Gümligen, Switzerland) using a customized Apex Q nebulizer (Elemental Scientific Inc., Omaha, USA) operating at 60°C. The resulting aerosols were then subjected to drying, followed by analysis using the high-resolution time-of-flight AMS (Aerodyne HR-ToF-AMS). High-resolution mass spectral analysis was performed for each m/z (mass to charge) up to 115. The sample spectra were corrected for a procedural blank.

S5.2. Quantification of WSOM

In earlier studies,[23, 24] offline AMS fingerprints were scaled to the water-soluble organic matter (WSOC) using the WSOC measurements (TOC analyser) and OM/OC from the HR AMS analysis. Here, instead of using measured WSOC from external measurements, WSOC was empirically estimated using the offline AMS data. This was based on the assumption that nitrate (NO_3^-) was quantitatively extracted and measured by the AMS, and did not form any refractory salts. The ratio of WSOM to NO_3^- was measured by considering the different response of AMS to organics and nitrate using relative ionization efficiencies (RIE) as presented in Canagaratna et al.[25] ($RIENO_3$=1.1, RIEOrg=1.4). WSOM was quantified using the following equation (8).

$$WSOM_{i,j} = \left(\frac{\frac{WSOM_{i,j}}{RIE_{Org}}}{\frac{NO_3}{RIE_{NO_3}}} \right)_{oAMS} * NO_{3,IC}^{-} \quad (8)$$

Where WSOM is the modelled concentration and NO_3^- denotes nitrate concentration from ion chromatography. The modelled WSOC concentration ($WSOC=WSOM/(OM/OC)_{oAMS}$) was compared with the OC concentrations measured by the Sunset OC/ EC analyser. The comparison showed as expected lower WSOC than OC concentrations but a good correlation (Figure S5), highlighting the consistency of offline AMS analyses with the conventional methods. In addition, the modelled OC was also evaluated against the measured OC concentration and showed good agreement (Figure S6).

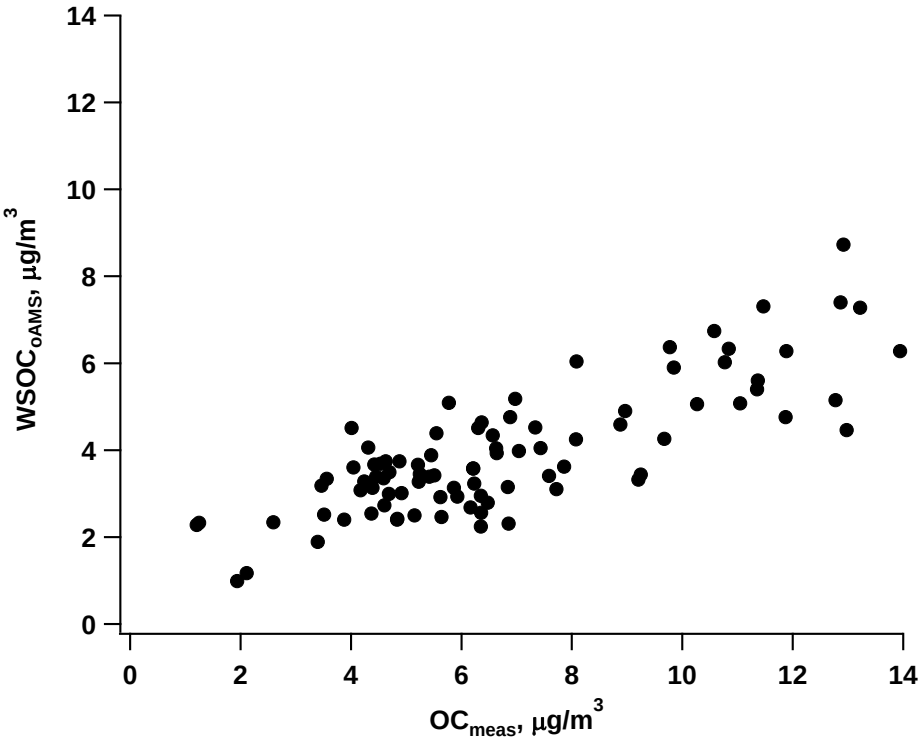

Figure S5: Correlation observed between the modelled WSOC concentration (by offline AMS) and the measured OC concentrations.

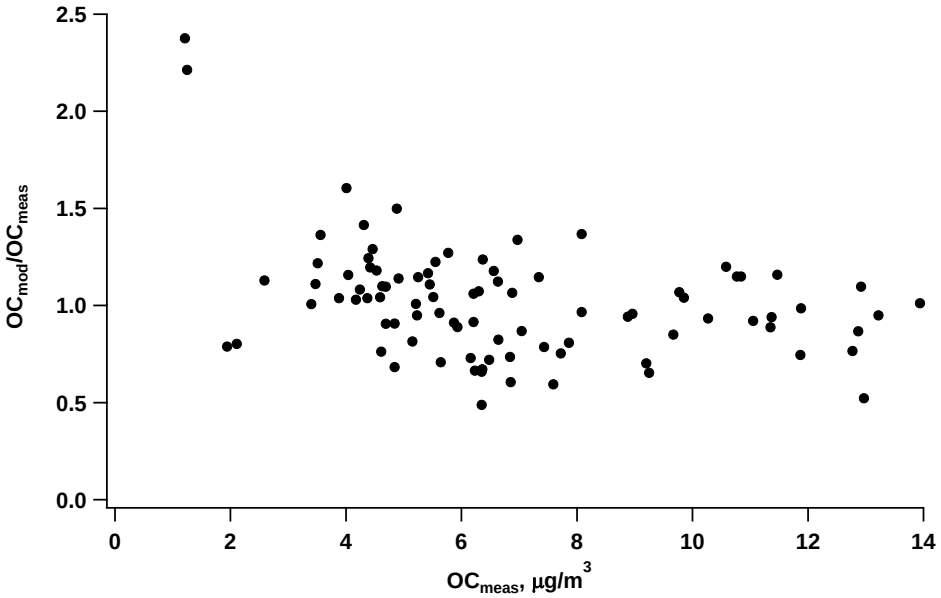

Figure S6: Ratio of modelled OC (OCmod) to measured OC (OCmeas, Sunset) as a function of the measured OC concentrations.

S5.3. Source apportionment

Source apportionment was performed by positive matrix factorization (PMF)[26, 27] using ME-2 algorithm in the Source Finder toolkit (SoFi)[15] as discussed above.

S5.3.1. a-value approach

Previous studies at this site have shown the influence of traffic (HOA), cooking (COA), biomass burning (BBOA), and secondary organic aerosol (OOA) in the submicron fraction.[16, 28-30] In the present study, HOA and COA factors were constrained using AMS reference mass spectra from earlier studies[28, 31] as described in Daellenbach et al.[23] Contrary to ACSM PMF analysis, BBOA was easily resolved without any constraint, showing the advantage of using high resolution instruments.

The constrained PMF solutions were explored, ranging from 1-10 factors (aHOA= 0-0.8, aCOA=0-0.8, 26 combinations in total). The impact of the number of factors on the residuals was assessed

(Figures S7 and S8). As expected, forcing PMF to explain the variability only with the 2 constrained factors resulted in very high Q/Q_{exp} (Figure S7). In order to explain the variability of OA during the PM pollution event, a minimum of 5 factors seemed necessary.

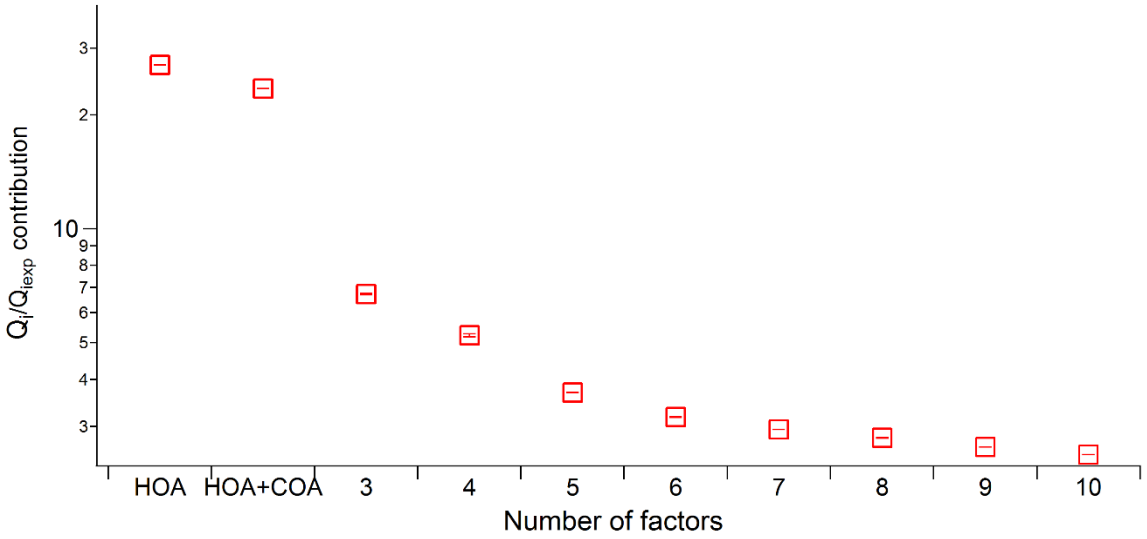

Figure S7. The $Q_i/Q_{i,exp}$ contribution as a function of the number of factors. $Q_i/Q_{i,exp}$ ratio was taken from the single seed with a-value combinations of 0.4 and 0.4.

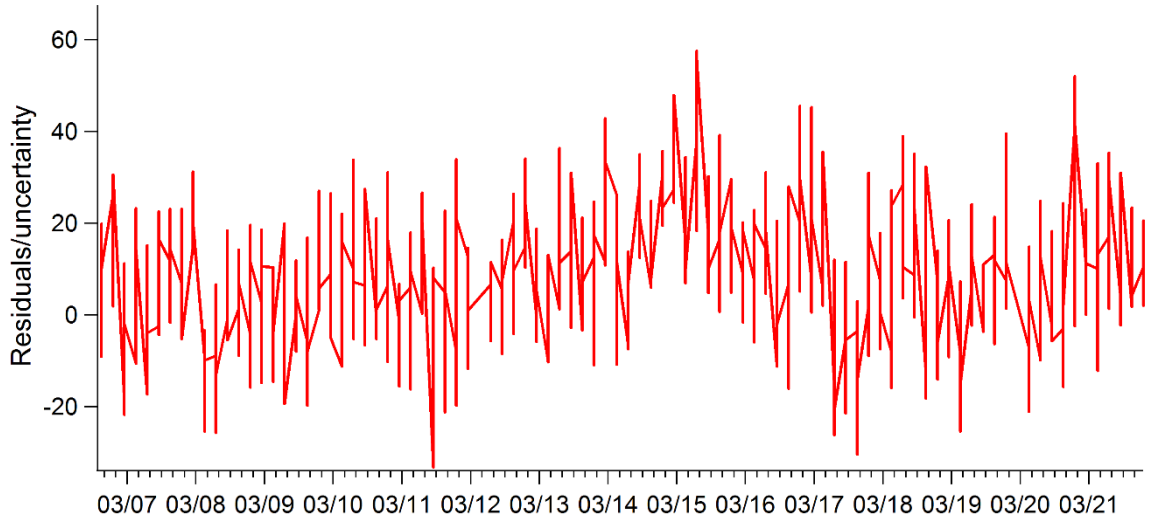

Figure S8. Residuals as a function of time. Residuals were taken from the single seed with a-value combinations of 0.4 and 0.4.

The introduction of 3 factors, BBOA and two OOA components, in addition to HOA and COA, resulted in a significant reduction in the residuals. BBOA exhibited a significant correlation with levoglucosan and contributed most to the explained variation of the fragment $C_2H_4O_2^+$ (m/z 60), normally originating from the decomposition of anhydrous sugars, and cellulose combustion. In addition, the two OOA components were identified based on their contribution from oxygenated fragments m/z 43 and 44. Introducing a 6^{th} factor allowed the explanation of the variability of sulfur containing fragments ($CH_3SO_2^+$), identified as SCOA and led to a subsequent decrease in the residuals. High order solutions (i.e., 7 or 8 factors) were also explored, but did not show any significant reduction in the residuals and aid in the interpretation of the resulting factors. The 6 factors solution provided the best possible PMF solution for this study, and did not reflect any variation in the residuals with time (Figure S9).

a-value sensitivity tests were performed by independently varying aHOA and aCOA (26 combinations). Only solutions fulfilling the following criteria were considered environmentally interpretable, all other solutions were discarded.

1. HOA correlates significantly with NO_x and BC_{ff} ($R_{wsHOA,BCff}>0$ & $R_{wsHOA,NOx}>0$; p-value<0.05).
2. HOA correlates significantly better with NO_x and BC_{ff} than COA ($R_{wsHOA,BCff}>R_{wsCOA,BCff}$ & $R_{wsHOA,NOx}>R_{wsCOA,NOx}$; p-value<0.05).
3. BBOA correlates significantly with levoglucosan ($R_{wsBBOA,levo}>0$; p-value<0.05).

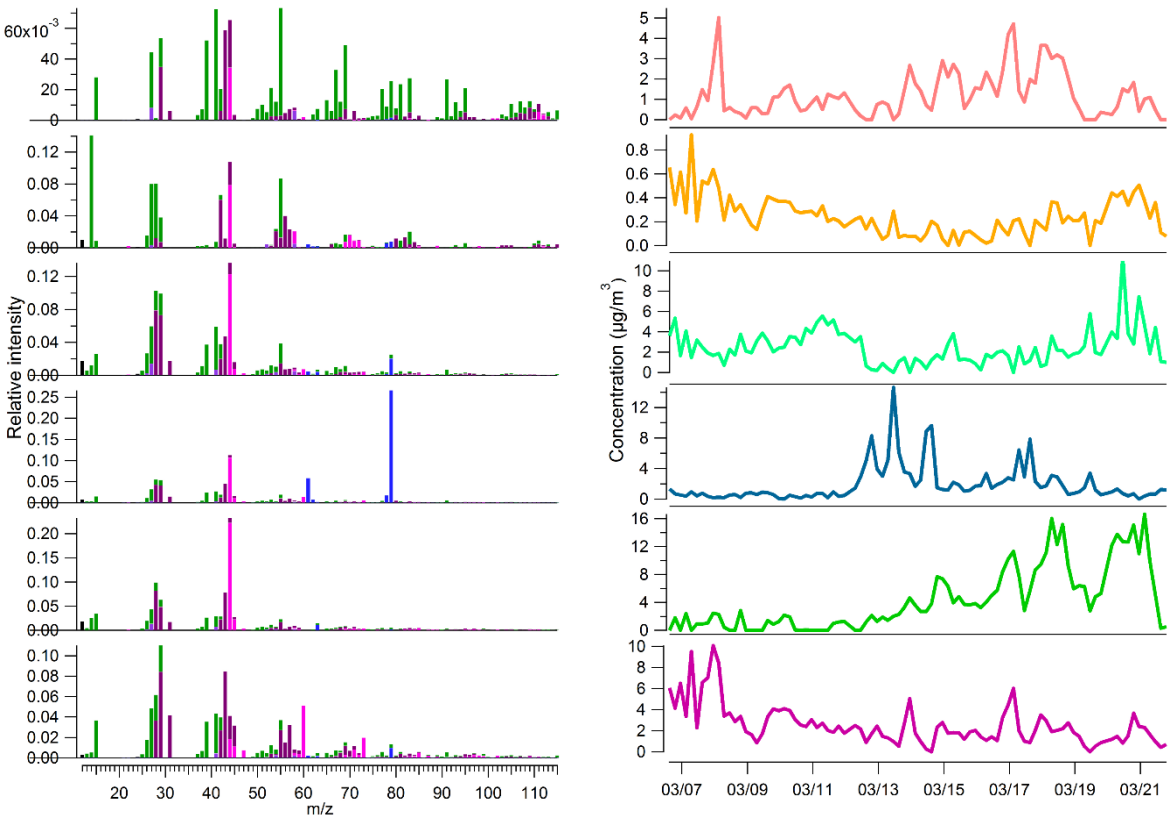

Figure S9. Chemical and temporal profiles of HOA, COA, OOA2, SCOA, OOA1, BBOA PMF factors identified at Paris-SIRTA, March 2015. Chemical profile is color-coded with ion family.

The evaluation of the correlation between factor and marker (e.g., BC_{ff}, NO_x, levoglucosan) time series was accomplished following the same statistical procedure as explained in Daellenbach et al.[23]. The aforementioned criteria were reviewed for each a-value combination, the selected a-values for the PMF solution are presented in Figure S10.

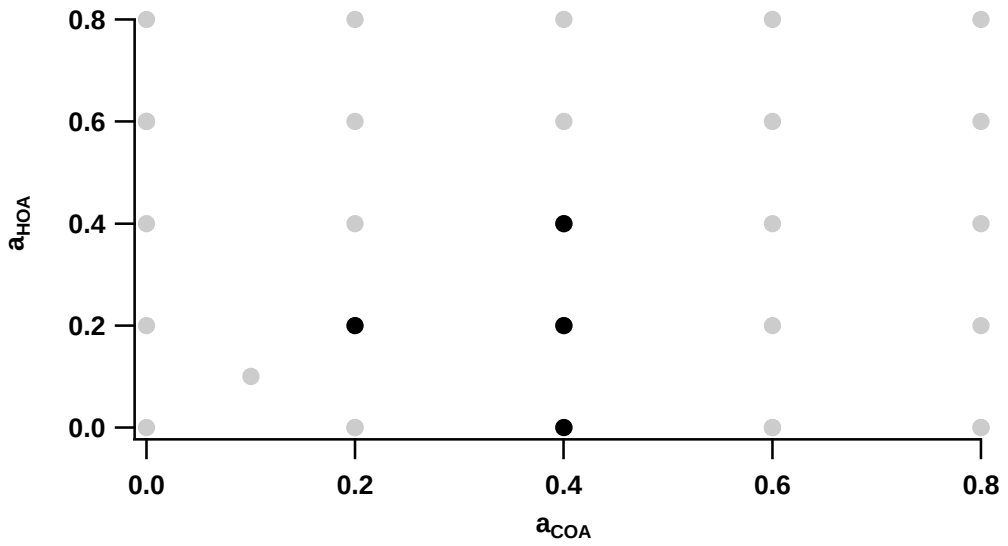

Figure S10. a-value combinations for HOA (a_{HOA}) and COA (a_{COA}) used for running PMF (grey) and the a-value combinations of the selected PMF solutions (black).

S5.3.2. Factor specific recovery

The water-soluble contributions from an identified aerosol source in a given sample were scaled to their total organic matter concentrations using factor-specific recoveries. Factor-specific recoveries, R_k, were computed by a multilinear fit according to the following equation:

$$OC = wsHOC * R_{HOC} + wsCOC * R_{COC} + wsBBOC * R_{BBOC} + wsSCOC * R_{SCOC} + wsOOC1 * R_{OOC1} + wsOOC2 * R_{OOC2} \quad (9)$$

where R_i represents the recoveries of the respective factor i. In the given equation, values of the recoveries for HOC and COC factors were constrained using the recoveries determined in Daellenbach et al.[22]. The probability distributions of R_k are displayed in Figure S11.

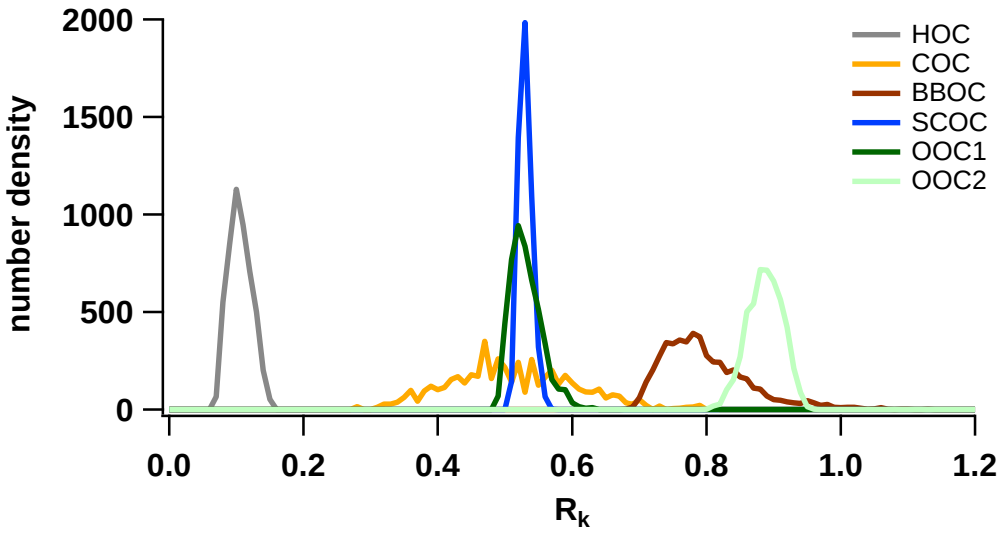

Figure S11. number density distributions of factor-specific recoveries for all 6 extracted PMF factors. While R_{HOC} and R_{COC} are constrained using Daellenbach et al.[22] since their temporal behavior does not influence the behavior of the bulk R (Rbulk), R_{BBOC}, R_{SCOC}, R_{OOC1} and R_{OOC2} are fitted.

To select the physically meaningful recoveries we applied a weighting factor f calculated by the following equation (10):

$$f = \begin{cases} 1 & ,for\ 0 < R_{i,k,max} \leq 1 \\ \dfrac{\frac{1}{\sigma\sqrt{2\pi}} exp * \left(-\frac{\left(R_{i,k,max} - \mu\right)^2}{2\sigma^2} \right)}{\frac{1}{\sigma\sqrt{2\pi}} exp * \left(-\frac{(1-\mu)^2}{2\sigma^2} \right)} & ,for\ R_{i,k,max} > 1 \end{cases} \quad (10)$$

Where σ = 0.05, μ = 1, i the number of iterations and k the factor.

A visualisation of the weighting factor is shown in Figure S12.

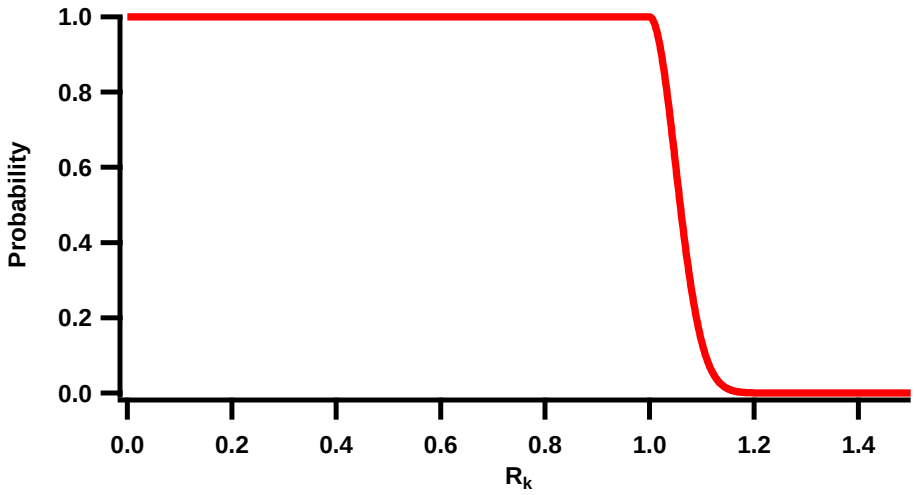

Figure S12. Probability of R_k occurrence.

S6. Comparison between PM_{10} filter-based OA estimation and OA ACSM data

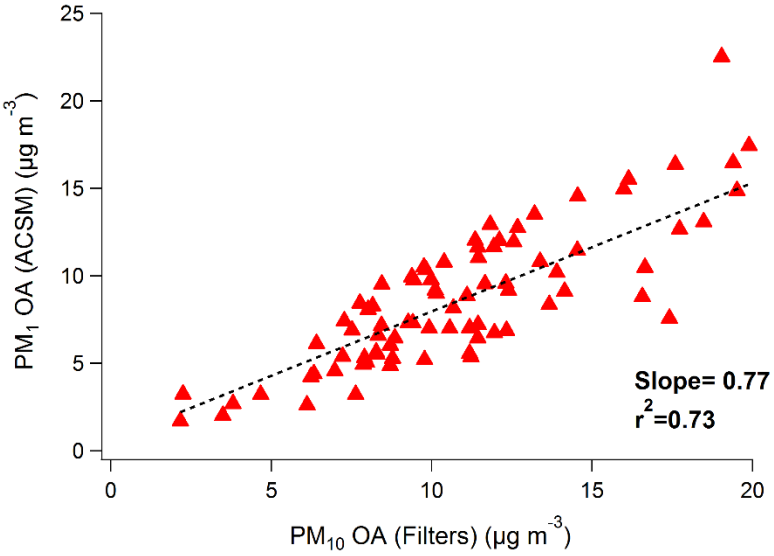

Figure S13. Comparison of total OA concentrations obtained from the PM_{10} filter-based and PM_1 ACSM measurements. OA mass linked to filter measurements was calculated applying an OC-to-OA conversion factor of 1.8.[32]

S7. POA factor correlations

Table S3A. Determination coefficient (r^2) matrix for total POC fraction estimated by each methodology.

	$POC_{PMF\text{-}chemical\ data}$	$POC_{PMF\text{-}offline\ AMS}$	$POC_{PMF\text{-}ACSM}$	$POC_{EC\text{-}tracer}$
$POC_{PMF\text{-}chemical\ data}$	1.00			
$POC_{PMF\text{-}offline\ AMS}$	0.21	1.00		
$POC_{PMF\text{-}ACSM}$	0.28	**0.42**	1.00	
$POC_{EC\text{-}tracer}$	**0.64**	0.11	0.25	1.00

Table S3B. Determination coefficient (r^2) matrix for total POC fraction except dust-related factor estimated by each methodologies.

	$POC_{PMF\text{-}chemical\ data}$ (without Dust)	$POC_{PMF\text{-}offline\ AMS}$ (without SCOA)	$POC_{PMF\text{-}ACSM}$	$POC_{EC\text{-}tracer}$
$POC_{PMF\text{-}Chemical\ data}$ (without Dust)	1.00			
$POC_{PMF\text{-}offline\ AMS}$ (without SCOA)	**0.32**	1.00		
$POC_{PMF\text{-}ACSM}$	**0.47**	**0.57**	1.00	
$POC_{EC\ tracer}$	0.26	0.07	0.25	1.00

Table S4. Determination coefficient (r^2) matrix for biomass burning-related primary OA factors.

	PMF-chemical data	PMF-ACSM	PMF-offline AMS
PMF-chemical data	1.00		
PMF-ACSM	**0.61**	1.00	
PMF-offline AMS	**0.48**	**0.56**	1.00

Table S5. Determination coefficient (r^2) matrix for traffic-related primary OA factors.

	PMF-chemical data	PMF-ACSM	PMF-offline AMS
PMF-chemical data	1.00		
PMF-ACSM	0.03	1.00	
PMF-offline AMS	0.01	**0.40**	1.00

S8. Diurnal variations of traffic- and biomass burning-related OA factors

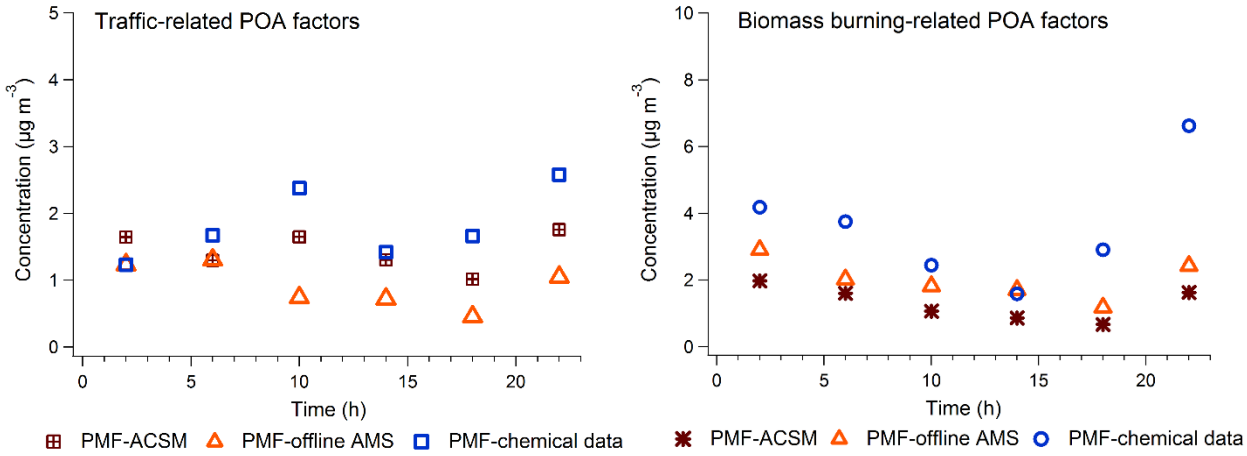

Figure S14. Diurnal profiles of traffic- and biomass burning-related OA factors.

S9. SOA factor correlations

Table S6. Determination coefficient (r^2) matrix for the total SOC fraction estimated by each methodology.

	$SOC_{PMF\text{-}chemical\ data}$	$SOC_{PMF\text{-}offline\ AMS}$	$SOC_{PMF\text{-}ACSM}$	$SOC_{SOA\text{-}tracer}$	$SOC_{EC\text{-}tracer}$
$SOC_{PMF\text{-}chemical\ data}$	1.00				
$SOC_{PMF\text{-}offline\ AMS}$	**0.64**	1.00			
$SOC_{PMF\text{-}ACSM}$	**0.66**	**0.77**	1.00		
$SOC_{SOA\text{-}tracer}$	0.04	0.01	0.00	1.00	
$SOC_{EC\text{-}tracer}$	**0.63**	**0.58**	**0.62**	0.06	1.00

Table S7. Determination coefficient (r^2) matrix within individual SOA factors resolved using the 3 PMF approaches.

	Biogenic SOA (marine)	Biogenic SOA (isoprene)	Anthropogenic SOA (oxy-PAHs)	Anthropogenic SOA (phenolic oxidation)	Anthropogenic SOA (nitro-PAHs)	Mixed secondary	Nitrate-rich	OOA1	OOA2	MO-OOA	LO-OOA
Biogenic SOA (marine)	1.00										
Biogenic SOA (isoprene)	0.01	1.00									
Anthropogenic SOA (oxy-PAHs)	0.01	0.06	1.00								
Anthropogenic SOA (phenolic oxidation)	0.05	0.01	0.02	1.00							
Anthropogenic SOA (nitro-PAHs)	0.00	0.01	0.11	0.04	1.00						
Mixed Secondary	**0.37**	0.01	0.00	0.08	0.04	1.00					
Nitrate-rich	0.15	0.04	0.03	0.03	0.23	0.01	1.00				
OOA1	**0.38**	0.01	0.05	0.05	0.01	**0.69**	0.26	1.00			
OOA2	0.08	0.00	0.06	0.00	0.02	0.13	0.00	0.02	1.00		
MO-OOA	**0.49**	0.00	0.01	0.05	0.01	**0.75**	0.20	**0.80**	0.07	1.00	
LO-OOA	0.03	0.01	0.10	0.03	0.19	0.09	0.15	0.26	0.01	0.16	1.00

References

1. Grosjean, D., Particulate carbon in Los Angeles air. *Sci. Total Environ.* **1984,** *32*, (2), 133-45.

2. Turpin, B. J.; Huntzicker, J. J., Identification of secondary organic aerosol episodes and quantitation of primary and secondary organic aerosol concentrations during SCAQS. *Atmos. Environ.* **1995,** *29*, (23), 3527-3544.

3. Gray, H. A.; Cass, G. R.; Huntzicker, J. J.; Heyerdahl, E. K.; Rau, J. A., Characteristics of atmospheric organic and elemental carbon particle concentrations in Los Angeles. *Environ. Sci. Technol.* **1986,** *20*, (6), 580-589.

4. Castro, L. M.; Pio, C. A.; Harrison, R. M.; Smith, D. J. T., Carbonaceous aerosol in urban and rural European atmospheres: estimation of secondary organic carbon concentrations. *Atmos. Environ.* **1999,** *33*, (17), 2771-2781.

5. Chu, S.-H., Stable estimate of primary OC/EC ratios in the EC tracer method. *Atmos. Environ.* **2005,** *39*, (8), 1383-1392.

6. Saylor, R. D.; Edgerton, E. S.; Hartsell, B. E., Linear regression techniques for use in the EC tracer method of secondary organic aerosol estimation. *Atmos. Environ.* **2006,** *40*, (39), 7546-7556.

7. Cabada, J. C.; Pandis, S. N.; Subramanian, R.; Robinson, A. L.; Polidori, A.; Turpin, B., Estimating the Secondary Organic Aerosol Contribution to PM2.5 Using the EC Tracer Method Special Issue of Aerosol Science and Technology on Findings from the Fine Particulate Matter Supersites Program. *Aerosol Sci. Technol.* **2004,** *38*, (sup1), 140-155.

8. Wu, C.; Yu, J. Z., Determination of primary combustion source organic carbon-to-elemental carbon (OC/EC) ratio using ambient OC and EC measurements: secondary OC-EC correlation minimization method. *Atmos. Chem. Phys.* **2016,** *16*, (8), 5453-5465.

9. Kleindienst, T. E.; Jaoui, M.; Lewandowski, M.; Offenberg, J. H.; Lewis, C. W.; Bhave, P. V.; Edney, E. O., Estimates of the contributions of biogenic and anthropogenic hydrocarbons to secondary organic aerosol at a southeastern US location. *Atmos. Environ.* **2007,** *41*, (37), 8288-8300.

10. Rutter, A. P.; Snyder, D. C.; Stone, E. A.; Shelton, B.; DeMinter, J.; Schauer, J. J., Preliminary assessment of the anthropogenic and biogenic contributions to secondary organic aerosols at two industrial cities in the upper Midwest. *Atmos. Environ.* **2014,** *84*, 307-313.

11. Iinuma, Y.; Boge, O.; Grafe, R.; Herrmann, H., Methyl-nitrocatechols: atmospheric tracer compounds for biomass burning secondary organic aerosols. *Environ. Sci. Technol.* **2010,** *44*, (22), 8453-9.

12. Bruns, E. A.; El Haddad, I.; Slowik, J. G.; Kilic, D.; Klein, F.; Baltensperger, U.; Prévôt, A. S. H., Identification of significant precursor gases of secondary organic aerosols from residential wood combustion. *Sci. Rep.* **2016,** *6*, 27881.

13. Aiken, A. C.; DeCarlo, P. F.; Kroll, J. H.; Worsnop, D. R.; Huffman, J. A.; Docherty, K. S.; Ulbrich, I. M.; Mohr, C.; Kimmel, J. R.; Sueper, D.; Sun, Y.; Zhang, Q.; Trimborn, A.;

Northway, M.; Ziemann, P. J.; Canagaratna, M. R.; Onasch, T. B.; Alfarra, M. R.; Prevot, A. S. H.; Dommen, J.; Duplissy, J.; Metzger, A.; Baltensperger, U.; Jimenez, J. L., O/C and OM/OC Ratios of Primary, Secondary, and Ambient Organic Aerosols with High-Resolution Time-of-Flight Aerosol Mass Spectrometry. *Environ. Sci. Technol.* **2008,** *42*, (12), 4478-4485.

14. Srivastava, D.; Favez, O.; Bonnaire, N.; Lucarelli, F.; Perraudin, E.; Gros, V.; Villenave, E.; Albinet, A., Speciation of organic fractions does matter for aerosol source apportionment. Part 2: intensive campaign in the Paris area (France). *Sci. Total Environ.* **2018**, Under review.

15. Canonaco, F.; Crippa, M.; Slowik, J.; Baltensperger, U.; Prévôt, A., SoFi, an IGOR-based interface for the efficient use of the generalized multilinear engine (ME-2) for the source apportionment: ME-2 application to aerosol mass spectrometer data. *Atmos. Meas. Tech.* **2013,** *6*, (12), 3649-3661.

16. Fröhlich, R.; Crenn, V.; Setyan, A.; Belis, C. A.; Canonaco, F.; Favez, O.; Riffault, V.; Slowik, J. G.; Aas, W.; Aijälä, M.; Alastuey, A.; Artiñano, B.; Bonnaire, N.; Bozzetti, C.; Bressi, M.; Carbone, C.; Coz, E.; Croteau, P. L.; Cubison, M. J.; Esser-Gietl, J. K.; Green, D. C.; Gros, V.; Heikkinen, L.; Herrmann, H.; Jayne, J. T.; Lunder, C. R.; Minguillón, M. C.; Močnik, G.; O'Dowd, C. D.; Ovadnevaite, J.; Petralia, E.; Poulain, L.; Priestman, M.; Ripoll, A.; Sarda-Estève, R.; Wiedensohler, A.; Baltensperger, U.; Sciare, J.; Prévôt, A. S. H., ACTRIS ACSM intercomparison – Part 2: Intercomparison of ME-2 organic source apportionment results from 15 individual, co-located aerosol mass spectrometers. *Atmos. Meas. Tech.* **2015,** *8*, (6), 2555-2576.

17. Aiken, A. C.; Salcedo, D.; Cubison, M. J.; Huffman, J. A.; DeCarlo, P. F.; Ulbrich, I. M.; Docherty, K. S.; Sueper, D.; Kimmel, J. R.; Worsnop, D. R.; Trimborn, A.; Northway, M.; Stone, E. A.; Schauer, J. J.; Volkamer, R. M.; Fortner, E.; de Foy, B.; Wang, J.; Laskin, A.; Shutthanandan, V.; Zheng, J.; Zhang, R.; Gaffney, J.; Marley, N. A.; Paredes-Miranda, G.; Arnott, W. P.; Molina, L. T.; Sosa, G.; Jimenez, J. L., Mexico City aerosol analysis during MILAGRO using high resolution aerosol mass spectrometry at the urban supersite (T0) – Part 1: Fine particle composition and organic source apportionment. *Atmos. Chem. Phys.* **2009,** *9*, (17), 6633-6653.

18. Lanz, V. A.; Alfarra, M. R.; Baltensperger, U.; Buchmann, B.; Hueglin, C.; Prévôt, A. S. H., Source apportionment of submicron organic aerosols at an urban site by factor analytical modelling of aerosol mass spectra. *Atmos. Chem. Phys.* **2007,** *7*, (6), 1503-1522.

19. Mohr, C.; Huffman, J. A.; Cubison, M. J.; Aiken, A. C.; Docherty, K. S.; Kimmel, J. R.; Ulbrich, I. M.; Hannigan, M.; Jimenez, J. L., Characterization of Primary Organic Aerosol Emissions from Meat Cooking, Trash Burning, and Motor Vehicles with High-Resolution Aerosol Mass Spectrometry and Comparison with Ambient and Chamber Observations. *Environ. Sci. Technol.* **2009,** *43*, (7), 2443-2449.

20. Ulbrich, I. M.; Canagaratna, M. R.; Zhang, Q.; Worsnop, D. R.; Jimenez, J. L., Interpretation of organic components from Positive Matrix Factorization of aerosol mass spectrometric data. *Atmos. Chem. Phys.* **2009,** *9*, (9), 2891-2918.

21. Ng, N. L.; Canagaratna, M. R.; Zhang, Q.; Jimenez, J. L.; Tian, J.; Ulbrich, I. M.; Kroll, J. H.; Docherty, K. S.; Chhabra, P. S.; Bahreini, R.; Murphy, S. M.; Seinfeld, J. H.; Hildebrandt, L.; Donahue, N. M.; DeCarlo, P. F.; Lanz, V. A.; Prévôt, A. S. H.; Dinar, E.; Rudich, Y.; Worsnop, D. R., Organic aerosol components observed in Northern Hemispheric datasets from Aerosol Mass Spectrometry. *Atmos. Chem. Phys.* **2010,** *10*, (10), 4625-4641.

22. Daellenbach, K. R.; Bozzetti, C.; Křepelová, A.; Canonaco, F.; Wolf, R.; Zotter, P.; Fermo, P.; Crippa, M.; Slowik, J. G.; Sosedova, Y.; Zhang, Y.; Huang, R. J.; Poulain, L.; Szidat, S.; Baltensperger, U.; El Haddad, I.; Prévôt, A. S. H., Characterization and source apportionment of organic aerosol using offline aerosol mass spectrometry. *Atmos. Meas. Tech.* **2016,** *9*, (1), 23-39.

23. Daellenbach, K. R.; Stefenelli, G.; Bozzetti, C.; Vlachou, A.; Fermo, P.; Gonzalez, R.; Piazzalunga, A.; Colombi, C.; Canonaco, F.; Hueglin, C.; Kasper-Giebl, A.; Jaffrezo, J. L.; Bianchi, F.; Slowik, J. G.; Baltensperger, U.; El-Haddad, I.; Prévôt, A. S. H., Long-term chemical analysis and organic aerosol source apportionment at nine sites in central Europe: source identification and uncertainty assessment. *Atmos. Chem. Phys.* **2017,** *17*, (21), 13265-13282.

24. Bozzetti, C.; Sosedova, Y.; Xiao, M.; Daellenbach, K. R.; Ulevicius, V.; Dudoitis, V.; Mordas, G.; Byčenkienė, S.; Plauškaitė, K.; Vlachou, A.; Golly, B.; Chazeau, B.; Besombes, J. L.; Baltensperger, U.; Jaffrezo, J. L.; Slowik, J. G.; El Haddad, I.; Prévôt, A. S. H., Argon offline-AMS source apportionment of organic aerosol over yearly cycles for an urban, rural and marine site in Northern Europe. *Atmos. Chem. Phys. Discuss.* **2016,** *2016*, 1-48.

25. Canagaratna, M. R.; Jayne, J. T.; Jimenez, J. L.; Allan, J. D.; Alfarra, M. R.; Zhang, Q.; Onasch, T. B.; Drewnick, F.; Coe, H.; Middlebrook, A.; Delia, A.; Williams, L. R.; Trimborn, A. M.; Northway, M. J.; DeCarlo, P. F.; Kolb, C. E.; Davidovits, P.; Worsnop, D. R., Chemical and microphysical characterization of ambient aerosols with the aerodyne aerosol mass spectrometer. *Mass Spectrom. Rev.* **2007,** *26*, (2), 185-222.

26. Paatero, P.; Tapper, U., Positive matrix factorization: A non-negative factor model with optimal utilization of error estimates of data values. *Environmetrics* **1994,** *5*, (2), 111-126.

27. Paatero, P.; Hopke, P. K.; Song, X.-H.; Ramadan, Z., Understanding and controlling rotations in factor analytic models. *Chemom. Intell. Lab. Syst.* **2002,** *60*, (1–2), 253-264.

28. Crippa, M.; El Haddad, I.; Slowik, J. G.; DeCarlo, P. F.; Mohr, C.; Heringa, M. F.; Chirico, R.; Marchand, N.; Sciare, J.; Baltensperger, U.; Prévôt, A. S. H., Identification of marine and continental aerosol sources in Paris using high resolution aerosol mass spectrometry. *J. Geophys. Res.-Atmos.* **2013,** *118*, (4), 1950-1963.

29. Crippa, M.; Canonaco, F.; Slowik, J. G.; El Haddad, I.; DeCarlo, P. F.; Mohr, C.; Heringa, M. F.; Chirico, R.; Marchand, N.; Temime-Roussel, B.; Abidi, E.; Poulain, L.; Wiedensohler, A.; Baltensperger, U.; Prévôt, A. S. H., Primary and secondary organic aerosol origin by combined gas-particle phase source apportionment. *Atmos. Chem. Phys.* **2013,** *13*, (16), 8411-8426.

30. Petit, J. E.; Favez, O.; Sciare, J.; Canonaco, F.; Croteau, P.; Močnik, G.; Jayne, J.; Worsnop, D.; Leoz-Garziandia, E., Submicron aerosol source apportionment of wintertime pollution in Paris, France by double positive matrix factorization (PMF2) using an aerosol chemical speciation monitor (ACSM) and a multi-wavelength Aethalometer. *Atmos. Chem. Phys.* **2014,** *14*, (24), 13773-13787.

31. Crippa, M.; DeCarlo, P. F.; Slowik, J. G.; Mohr, C.; Heringa, M. F.; Chirico, R.; Poulain, L.; Freutel, F.; Sciare, J.; Cozic, J.; Di Marco, C. F.; Elsasser, M.; Nicolas, J. B.; Marchand, N.; Abidi, E.; Wiedensohler, A.; Drewnick, F.; Schneider, J.; Borrmann, S.; Nemitz, E.; Zimmermann, R.; Jaffrezo, J. L.; Prevot, A. S. H.; Baltensperger, U., Wintertime aerosol

chemical composition and source apportionment of the organic fraction in the metropolitan area of Paris. *Atmos. Chem. Phys.* **2013,** *13*, (2), 961-981.

32. Sciare, J.; D'Argouges, O.; Sarda-Esteve, R.; Gaimoz, C.; Dolgorouky, C.; Bonnaire, N.; Favez, O.; Bonsang, B.; Gros, V., Large contribution of water-insoluble secondary organic aerosols in the region of Paris (France) during wintertime. *J. Geophys. Res.-Atmos.* **2011,** *116*, D22203.

Chapter VI

Development of a novel approach to resolve various OA sources

Article V

Combining off-line and on-line measurements does help differentiating between the different organic aerosols fractions

In preparation for publication in Atmospheric Chemistry & Physics

Combining off-line and on-line measurements does help differentiating between the different organic aerosols fractions

D. Srivastava[1,2,3], O. Favez[1*], J-E. Petit[4], Y. Zhang[1], U. M. Sofowote[5], P.K. Hopke[6,7], N. Bonnaire[4], E. Perraudin[2,3], V. Gros[4], E. Villenave[2,3], A. Albinet[1*]

[1]INERIS, Parc Technologique Alata, BP 2, 60550 Verneuil-en-Halatte, France

[2]CNRS, EPOC, UMR 5805 CNRS, 33405 Talence, France

[3]Université de Bordeaux, EPOC, UMR 5805 CNRS, 33405 Talence, France

[4]LSCE - UMR8212, CNRS-CEA-UVSQ, Gif-sur-Yvette, France

[5]Environmental Monitoring and Reporting Branch, Ontario Ministry of the Environment and Climate Change, Toronto, Canada

[6]Center for Air Resources Engineering and Science, Clarkson University, Potsdam, NY, USA

[7]Department of Public Health Sciences, University of Rochester School of Medicine and Dentistry, Rochester, NY USA

*Correspondence to: alexandre.albinet@ineris.fr; alexandre.albinet@gmail.com; olivier.favez@ineris.fr

Abstract

A novel methodology is proposed to refine the sources of organic aerosol (OA). The methodology has been applied on data from measurements performed in the Paris region (France) during a PM pollution event in March 2015. Positive matrix factorization (PMF) was performed using time synchronization multilinear engine (ME-2) algorithm on a combined dataset including OA ACSM (aerosol chemical speciation monitor) mass spectra and specific primary and secondary organic molecular markers from PM_{10} filters on their original time resolution (30 min for ACSM and 4 h for PM_{10} filters). The results allowed the deconvolution of 10 OA factors including 3 primary OA (POA) and 7 SOA (biogenic and anthropogenic SOA) factors. A very good agreement was observed between the PMF-combined analysis and the factors retrieved from the PMF-ACSM analysis. The new developed methodology allowed the clear identification of about half of the total SOA mass (75% of OA) observed during the sampling campaign. The identified secondary factors have been classified in terms of oxidation state, sources and/or precursors of SOA. The results obtained highlighted that 4 OA factors were linked to biomass burning emission with 2 primary sources (biomass burning OA (BBOA) and oxidized POA (OPOA)) and 2 secondary ones (from the oxidation of phenolic compounds and toluene). Interestingly, 80% of the total primary BBOA was related to OPOA. Anthropogenic SOA related to the oxidation of PAHs (characterized by nitro-PAHs), toluene, and phenolic compounds exhibited a clear diurnal pattern with high concentrations during the night indicating the prominent role of night-time chemistry.

Keywords: Source apportionment; ME-2; PMF; ACSM; Organic markers; SOA.

1. Introduction

Aerosols originate from a wide range of sources and atmospheric processes, and have significant impacts on air quality and climate change (Heal et al., 2012; Boucher et al., 2013). Particulate organic matter (POM) makes up a large, and often dominant, fraction of fine particulate mass in the atmosphere, typically 20–60% in the continental mid-latitudes (Kanakidou et al., 2005). Primary organic aerosols (POA) refer to the organic aerosols (OA) directly emitted from pollution sources. OA that formed in the atmosphere through the oxidation of gas-phase precursors, known as secondary organic aerosol (SOA) could also be a major contributor (20-80%) to the carbonaceous aerosol fraction (Carlton et al., 2009; Ziemann and Atkinson, 2012). If primary emissions could be controlled, secondary sources, influenced by biogenic emissions (and also anthropogenic) and by photochemistry, are difficult to regulate. Therefore, the discrimination of POA and SOA sources is a critical step towards developing efficient abatement strategies.

The positive matrix factorization (PMF), a bilinear model that constrains the factors to be non-negative (Paatero and Tapper, 1994; Paatero et al., 2002), has been widely applied using traditional speciation data (i.e. OC, elemental carbon (EC), major ions). However, many of these species are not source specific. Molecular markers have a high degree of source specificity which offers potential link between the factors and sources (Simoneit, 1999; Kleindienst et al., 2007). The use of molecular markers in PMF has opened new perspectives for aerosol source apportionment purposes (Shrivastava et al., 2007; Zhang et al., 2009; Jaeckels et al., 2007; Hu et al., 2010; Heo et al., 2013; Srivastava et al., 2018b; Srivastava et al., 2018a). Nevertheless, these techniques often rely on measurements linked to short-time resolution, showing the incapability associated with these methods to elucidate more information on the involved chemical processes. Recent advancements over the last decade, including the development of online instrumentation (e.g. AMS (aerosol mass spectrometer), ACSM (aerosol chemical

speciation monitor)) (Ng et al., 2011; Jayne et al., 2000; DeCarlo et al., 2006) have successfully improved the real-time measurements of the aerosol chemical composition. The PMF analysis of OA mass spectra from such measurements further permits the differentiation of primary and secondary OA sources (Lanz et al., 2007b; Ulbrich et al., 2009; Zhang et al., 2011). The secondary fractions from the PMF-AMS or -ACSM analyses typically distinguish SOA components based on their volatility and/or their oxidation state. These online approaches do not offer any potential link between the PMF factors and sources due to the non-specific nature of the mass fragments obtained.

Combining different datasets from several measurement systems to refine the source apportionment of OA, and notably SOA, is probably one of the best way to achieve this goal. Slowik et al. (2010) were the first ones to combine the AMS and PTR-MS (proton transfer reaction-mass spectrometer) data measurements, highlighting the capability of PMF to resolve more SOA (OOA) factors and improving the interpretations of their sources and photochemical processes (Crippa et al., 2013; Slowik et al., 2010). This kind of approach has been explored in other studies, with the combination of AMS or ACSM data with other measurements, such as ambient and thermally denuded OA spectra (TD-PMF-AMS) (Docherty et al., 2011), by merging high resolution mass spectra of organic and inorganic aerosols from AMS measurements (Sun et al., 2012; McGuire et al., 2014) or combining offline AMS data and organic markers or ^{14}C measurements (Huang et al., 2014; Vlachou et al., 2017). In addition, the combination of PMF-ACSM outputs with inorganic species and black carbon (BC) measurements (Petit et al., 2014) or ACSM mass spectra with metal concentrations (Sofowote et al., 2018), allowed the source apportionment of PM rather than only OA. However, the proper discrimination between primary and secondary OA sources using online instrumentation at the molecular level is still not achieved.

Here, a novel approach has been developed to refine OA sources, and to provide full comprehensive information on the involved atmospheric processes at the molecular level. This was accomplished by performing PMF analysis using time synchronization multilinear engine (ME-2) algorithm on the combined dataset. The combined dataset included ACSM OA matrix and specific primary and secondary organic molecular markers from PM_{10} filters on their original time resolution. The identified OA sources, their oxidation state and formation processes have been discussed. In addition, results from the PMF-combined analysis were also compared and validated using PMF-ACSM analysis.

4. Methodology

4.1. Monitoring site

Measurements were conducted at the ACTRIS SIRTA atmospheric supersite (Site Instrumental de Recherche par Télédétection Atmosphérique, 2.15° E; 48.71° N; 150 m asl (m above sea level); http://sirta.ipsl.fr). Located approximately 25 km southwest of Paris city centre, this site provides long-term in-situ observations of the chemical, optical and physical properties of the atmospheric aerosols and illustrates the suburban background conditions of the Paris region (France) (Crippa et al., 2013; Petit et al., 2014; Sciare et al., 2011; Petit et al., 2017; Srivastava et al., 2018a).

An intensive campaign was performed from 6-21, March 2015 during a severe PM pollution event (PM_{10} > 50 µg m^{-3} for several consecutive days). The late winter-early spring period was chosen on purpose as intense PM pollution events are usually observed in Northern France (and more generally in North-Western Europe) during this period of the year. These pollution events occur under anticyclonic conditions favouring the accumulation of pollutants with significant residential emissions, manure spreading, and possible photochemical processes enhancing the

formation of secondary aerosol (Waked et al., 2014; Bressi et al., 2013; Petit et al., 2017; Dupont et al., 2016).

4.2. Online instrumentation

PM_{10} and PM_1 concentrations were measured using co-located online analysers: TEOM-FDMS (1405F model, Thermo; 15 min time resolution). Meteorological parameters such as temperature, relative humidity (RH), wind direction, and wind speed were obtained from nearby (about 5 km) measurements at the main SIRTA facility.

The aerosol chemical speciation monitor (ACSM, Aerodyne Research Inc.) was also deployed at SIRTA to measure the major chemical composition of non-refractory submicron aerosols at 30-min resolution with a PM_1 cut-off (~800 nm). Details on the instrumental parameters used for the ACSM have been already described elsewhere (Petit et al., 2017).

4.3. Filter sample collection and analysis

PM_{10} samples (Tissu-quartz fibre filter, Pallflex, Ø=150 mm) were collected every 4 h from 6-21, March 2015 using a high-volume sampler (DA-80, Digitel; 30 m^3 h^{-1}). PM_{10} filter samples were analysed for a large set of chemical species (n=71) including EC/OC, methanesulfonic acid (MSA), oxalate ($C_2O_4^{2-}$), cellulose combustion markers (biomass burning) (levoglucosan, mannosan and galactosan), 3 polyols (arabitol, sorbitol and mannitol), 9 PAHs, 14 oxy-PAHs, 8 nitro-PAHs and 13 SOA markers (e.g. α-methylglyceric acid (MGA) and methylnitrocatechols), following the protocols described elsewhere (Guinot et al., 2007; Cavalli et al., 2010; Verlhac et al., 2013; Yttri et al., 2015; Albinet et al., 2006; Albinet et al., 2014; Albinet et al., 2013; Srivastava et al., 2018b; Srivastava et al., 2018a; Tomaz et al., 2016).

4.4. Source apportionment

4.4.1. Model description

In receptor modelling, including PMF, the principle of mass conservation is assumed and a mass balance analysis between the measured species concentrations and source profiles as a linear combination of factors *p*, species profile *f* of each source, the amount of mass *g* contributed to each individual sample is solved following Equation (1).

$$X_{ij} = \sum_{k=1}^{p} g_{ik} f_{kj} + e_{ij} \quad (1)$$

where X_{ij} represents measured data for species *j* in sample *i* and e_{ij} is the residual of each sample/species not fitted by the model. PMF, a multivariate method, requires no prior information of source profiles and iteratively calculates g_{ik} and f_{kj} by minimizing the residuals.

4.4.1.1. Multi-time/ time synchronization factor analysis

"Multi-time/ time synchronization" factor analysis using ME-2 (Norris et al., 2014) has been developed to use each measured concentration data point in its original time resolution (30 min for ACSM data and 4 h for the organic markers) (Sofowote et al., 2018; Crespi et al., 2016; Kuo et al., 2014; Liao et al., 2015; Liao et al., 2013; Ogulei et al., 2005; Zhou et al., 2004). To this aim, the main source-receptor model equation (Eq. (1)) has been modified as below (Zhou et al., 2004):

$$X_{sj} = \frac{1}{t_{s2} - t_{s1} + 1} \sum_{k=1}^{p} f_{kj} \sum_{ts1}^{ts2} \left(g_{sk} n_j \right) + e_{sj} \quad (2)$$

where *s* is the sample number, *j* represents the species, t_{s1} and t_{s2} are the starting and the ending times, respectively. The time unit corresponds to the shortest sampling interval of the available data (30 min in this work). As in Eq. (1), X_{sj} is the concentration of the j^{th} species in the s^{th} sample, f_{kj} is the mass fraction of the j^{th} species from the k^{th} source, g_{sk} is the contribution of source k during the sampling period of the s^{th} sample. η_j is an adjustment factor for replicated

species measured by more than one analytical method with different time resolutions. In this work, it has been set at η_j =1.

A source may contain only species measured at a relatively lower time resolution or both low and high time resolved species. Therefore, a smoothing Eq. (3) was used in order to eliminate unrealistic residuals (Ogulei et al., 2005). The values of 1.8 and 0.01 were used as the smoothing coefficients in the model.

$$g_{s+1,k} - g_{s,k} = \varepsilon_s \qquad (3)$$

where g_{sk} is the source contribution from the *k-th* source during the *s-th* time unit and ε denotes the residuals. The total residual sum of squares (Q) is composed of residuals from both Eqs. (2) and (3). When a source contains some high-resolution species, reducing the residual in Eq. (3) leads to an increase in the residuals of Eq. (2) and the high temporal variations tend to be conserved. The balance between both residuals can be controlled by multiplying the residual in Eq. (3) by a small coefficient.

These equations (Eqs. (2) and (3)) were solved using ME-2 algorithm (Paatero, 1999) which provides a weighted least-squares solution by minimizing the sum of squares, i.e. the so-called object function Q:

$$Q = Qmain + Qaux = \sum_{i=1}^{n}\sum_{j=1}^{m}\frac{e_{ij}}{\sigma_{ij}} + \sum_{i=1}^{n}\sum_{j=1}^{m}\frac{e'_{ij}}{\sigma'_{ij}} \qquad (4)$$

As shown in Eq. (4), both the main equation (Eq. (2)) and the auxiliary equations (e.g. smoothing equations, pulling equations and constraints) are taken into account in the object function Q; σ are the uncertainties of input data and σ′ are the uncertainties related to the auxiliary equations.

4.4.2. Error estimation/ Input matrix

The calculations of the uncertainties were made following the same procedure explained by Sofowote et al. (2018). The uncertainties (u_{sj}) have been solved using the ME-2 error model based on Eq. (5) (Paatero, 2000) (in this case, -14 error code was used).

$$u_{sj} = c_1 + c_3 max(|x_{sj}|, |y_{sj}|) \quad (5)$$

where, c_3 is a multiplier for adding extra uncertainty, x_{sj} and y_{sj} are the observed and modelled values, respectively, and c_1 is the measurement or estimated error.

Detection limits (DL) of the organic markers analysed using 4-hr PM_{10} filters were used as the basis for c_1. The optimization of errors included the investigation of histograms of the scaled residuals to determine the shape and symmetry of their distributions (Zhou et al., 2004). As the scaled residuals were not symmetrical, adjustments to the DL have been done to make the distribution more symmetrical.

In this study, adjustments have been made to satisfy both aspects of measurements, physical and mathematical. DL considered here for the markers is not the actual detection limit. The quantification of DL refers to instrumental detection limit based on the standard solutions. DL based on true samples may provide different values for these markers, and the difference could be a factor of 10 times or more. This was also supported by the observations found in the literature (Saadati et al., 2013). Therefore, according to this criteria DL of some of the molecular markers were adjusted by a factor ranging from 10-50. As described, a second adjustment was made by following normal iteration to further improve the scaled residuals with a step of 0.005. Note that both adjustments were made simultaneously. The original (instrumental) and optimized (adjusted) DLs of all molecular markers are given in the supplementary material (SM, Table S1). The scaled residuals (x) were near-normally distributed following the bell-like distribution (-4< x <4). The mid-points were very decently placed with centering around 0 and 1 (Figure S1). Note that, in the ideal scenario the scaled residual should be normally distributed and spread should lie between -1< x <1. However, wider residual distributions can be expected when using such kind of complex

models, and probably linked to model mis-specification of error. Thus, the points related to high residuals were also considered rather than excluding or further optimizing (c_1) to avoid any alteration in the physical meaning of the given dataset.

For the ACSM OA matrix (30 min), the errors have been calculated according to the developed standard procedure (Ng et al., 2011). It has been assumed that all measured ions follow the Poisson distribution.

For the ME-2 (PMF) analysis, the input data matrix included 774 discrete time units, 866 samples, 72 variables (57 m/z from the ACSM and 14 organic molecular markers + EC) and c_3 was set at 0.1. EC was included in the input matrix with the idea of being able to apportion the carbonaceous fraction rather than only OA mass. The selection of organic markers for this work was based on the PMF analysis performed only on filter measurements during the same PM pollution event at the same site (Srivastava et al., 2018a). A list of all organic species used in the ME-2 analysis is given in the SM (Table S1).

4.4.3. Optimization of the final solution

The selection of factors was based on the interpretation of obtained factors and their temporal variability. Forcing PMF to explain the variability with a lower number of factors (<8) always resulted in high *Q* value and less significant factor profiles. Only solutions with more than eight factors were checked. A ten-factor output provides the most reasonable solution for this combined ME-2 analysis.

ME-2 program also allows for the imposition of constraints based on a priori information about source profiles. The general framework for applying constraints to PMF solutions has already been discussed elsewhere (Amato et al., 2009; Amato and Hopke, 2012). Only one constraint has been applied in this study. 1-nitropyrene (1-NP) was pulled up maximally with allowed change of 100% in Q_{main} limit (dQ) and absolute expected change of pulled quantity of 0.4. No

notable change was observed between the base and the constrained runs factor profiles (Figures S2 and S3).

5. Results

5.1. Overview of the PM pollution event and chemical composition.

PM_{10} mass concentrations ranged from 12 to 130 µg m^{-3} during the sampling campaign. The PM_1 chemical composition showed a large predominance of secondary inorganic species, especially ammonium nitrate, highlighting the significance of secondary processes throughout the studied period (Petit et al., 2017). PM_1 OM concentrations ranged from 1.1 to 28.9 µg m^{-3} (Figure 1).

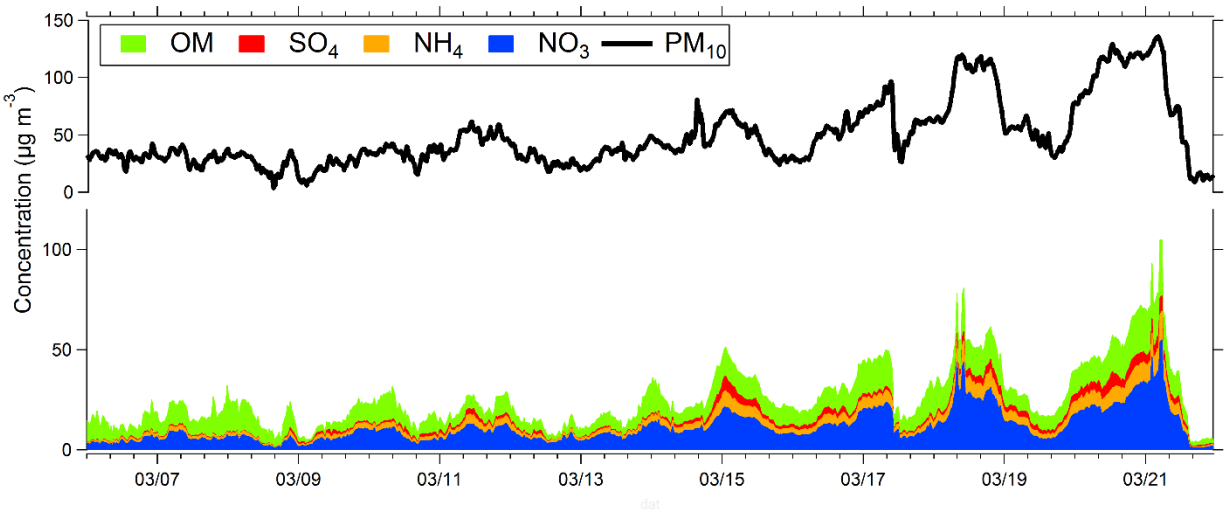

Figure 1. Temporal variations of PM_1 chemical composition using ACSM measurements and PM_{10} observed at Paris-SIRTA, France (March 2015).

To investigate air mass origins, the sampling period was divided into 3 sub-periods according to the value of the SO_4/EC ratio, considered here as a proxy to distinguish local to regional influence (Petit et al., 2015) (Figure S4). This ratio showed a minimum value of about 2 during the period from March 6-11, emphasizing the role of local emissions such as residential

wood burning at the beginning of the studied period. The period from March 11-18 with increased SO_4/EC ratio, and is associated with higher wind speeds coming from the NE direction, suggesting an influence of medium range transport. A substantial change was noticed in the PM composition during the most intense part of the campaign (March 18-21). The air masses originated mostly from the NNE direction with relatively high wind speeds, and high SO_4/EC ratio (of about 8), indicating the advection of aged aerosols over the Paris region and strong impact by long-range transport.

5.2. OA source apportionment using ACSM measurements

The results of the PMF analysis performed on the ASCM OA matrix are shown in Figure 2. All the details are given in the SM (Figure S5). Two POA factors, i.e., HOA (hydrocarbon-like OA) (16%) and BBOA (biomass burning OA) (14%) and two SOA factors including LO-OOA (low oxidized OOA) (15%) and MO-OOA (more oxidized OOA) (55%) have been resolved. About 75% of OA was accounted as SOA (OOAs). These results highlighted the significant role of secondary processes enhancing the formation of more oxidized products during the PM pollution event (Srivastava et al., 2018a; Petit et al., 2017).

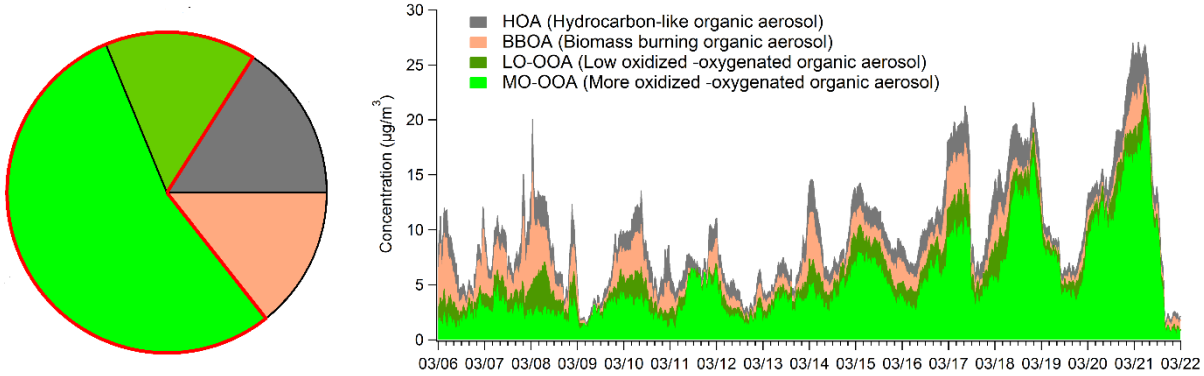

Figure 2. Average contributions (left) and temporal evolution (right) of the identified sources to OA mass concentrations at Paris-SIRTA (France) using ACSM measurements (March 2015).

5.3. OA source apportionment combining on-line and off-line measurements

By comparison to the PMF-ACSM based results, the PMF-combined analysis allowed the deconvolution of 10 OA factors including 3 POA factors and 7 SOA (biogenic and anthropogenic) factors (Figure 3). The use of specific molecular organic markers combined with ACSM mass spectra data in ME-2 allowed to deconvolve common OA sources such as primary traffic emissions (HOA), biomass burning (BBOA), as well as 2 specific biogenic- and 4 anthropogenic-SOA sources. Identified OA sources, their chemical profiles and temporal evolutions are shown on Figures 3 and 4, and discussed individually hereafter together with their diurnal variations (Figure 5).

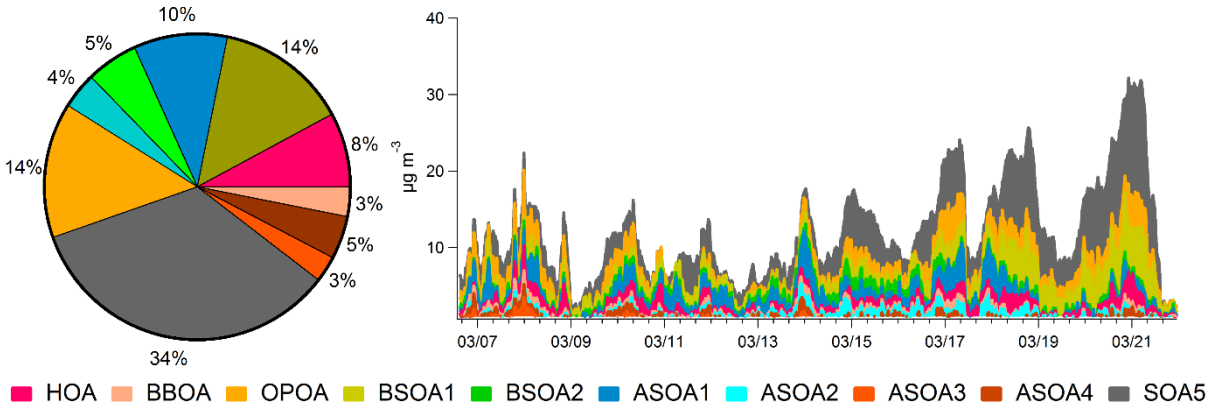

Figure 3. Average contributions (left) and temporal evolution (right) of the identified sources to OA fraction at Paris-SIRTA, France (March 2015). HOA: primary traffic emissions; BBOA: biomass burning OA; OPOA: oxidized primary OA; BSOA-1: biogenic SOA-1 (marine-rich); BSOA-2: biogenic SOA-2 (isoprene oxidation); ASOA-1: anthropogenic SOA-1 (oxy-PAHs); ASOA-2: anthropogenic SOA-2 (nitro-PAHs); ASOA-3: anthropogenic SOA-3 (phenolic compounds oxidation); ASOA-4: anthropogenic SOA-4 (toluene oxidation) and SOA-5.

5.3.1. Interpretation of resolved factors

5.3.1.1. Primary traffic emissions

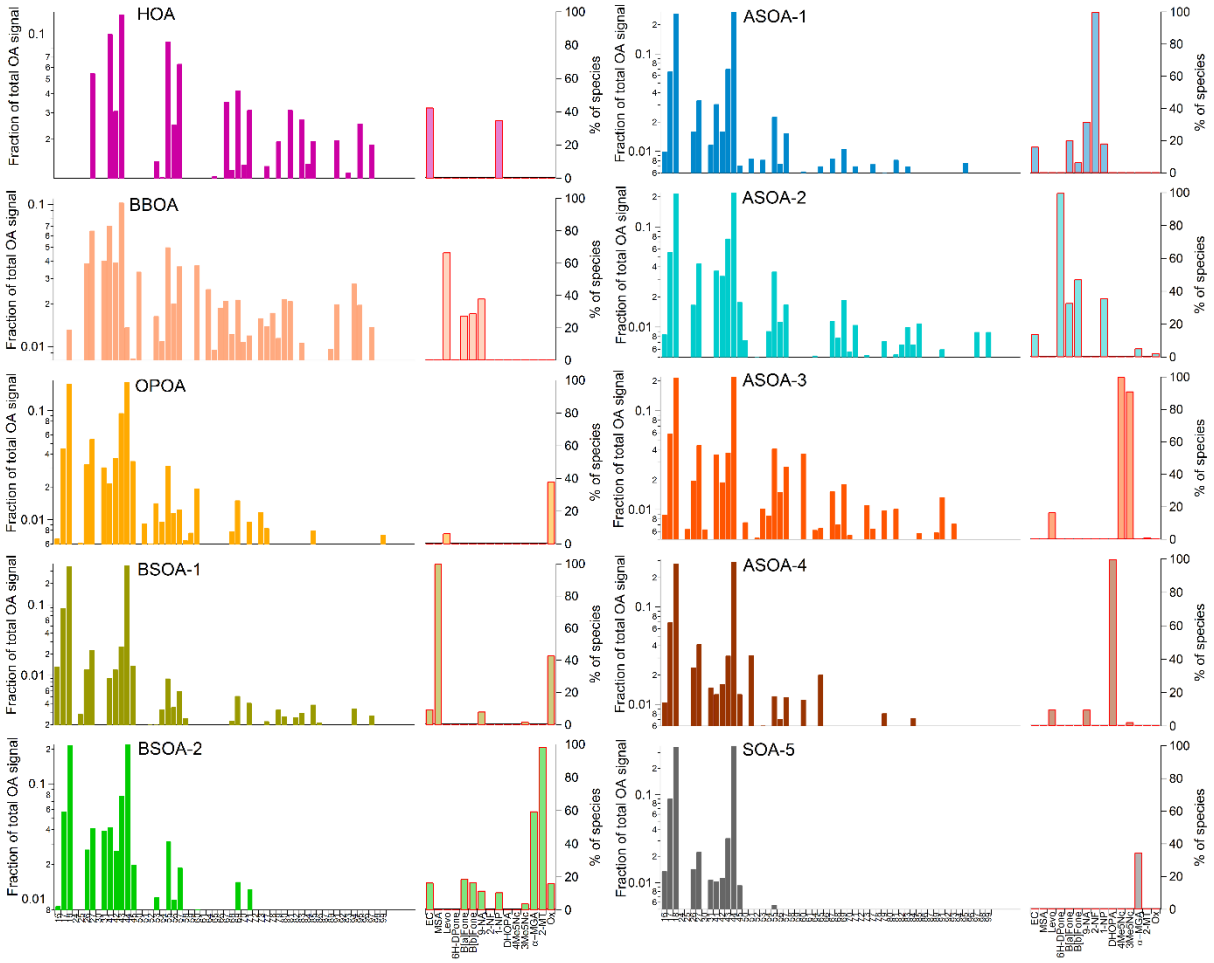

Figure 4. Chemical profiles of OA factors identified at Paris-SIRTA, France (March 2015). Left axis: ACSM mass fragments for each factor (log scale); Right axis: Contribution of organic markers in each factor. HOA: primary traffic emissions; BBOA: biomass burning OA; OPOA: oxidized primary OA; BSOA-1: biogenic SOA-1 (marine-rich); BSOA-2: biogenic SOA-2 (isoprene oxidation); ASOA-1: anthropogenic SOA-1 (oxy-PAHs); ASOA-2: anthropogenic SOA-2 (nitro-PAHs); ASOA-3: anthropogenic SOA-3 (phenolic compounds oxidation); ASOA-4: anthropogenic SOA-4 (toluene oxidation) and SOA-5.

Primary traffic emissions (HOA factor) were characterized by the presence of aliphatic hydrocarbons, especially m/z 27 ($C_2H^+_3$), 41 ($C_3H^+_5$), 55 ($C_4H^+_7$), 57 ($C_4H^+_9$), 69 ($C_5H^+_9$), and 71 ($C_5H^+_{11}$) (Aiken et al., 2009), including significant amount of EC (43%) and 1-nitropyrene (1-NP) (35%) (Figure 4). This factor accounted for 8% of the OA mass during the studied period

(Figure 3). These mass fragments are consistent with the mass spectral characteristics found for the primary combustion sources (i.e., fossil fuel combustion) and have been commonly used in urban environment to trace traffic emissions (Zhang et al., 2005; Mohr et al., 2009; Lanz et al., 2007a; Zhang et al., 2007; Ulbrich et al., 2009). Given the constraint applied (pulled up maximally), 1-NP, known to be a good marker of diesel emissions (Zielinska et al., 2004a; Zielinska et al., 2004b; Schulte et al., 2015; Keyte et al., 2016), was also found to be associated with this factor. The HOA factor also exhibited two pronounced peaks in agreement with the traffic rush hours in the morning and the evening (Figure 5).

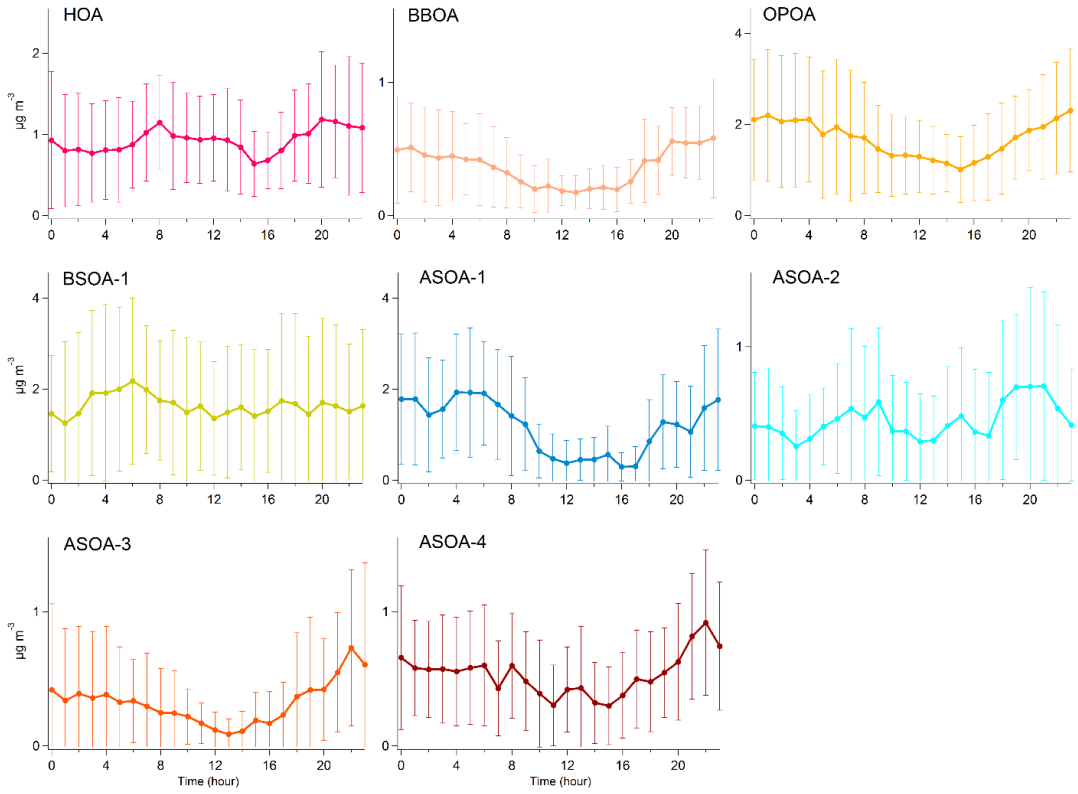

Figure 5. Diurnal profiles of OA factors resolved from the PMF-combined analysis at Paris-SIRTA, France (March 2015). Error bars represent ± 2SD (standard deviation). HOA: primary traffic emissions; BBOA: biomass burning OA; OPOA: oxidized primary OA; BSOA-1: biogenic SOA-1 (marine-rich); ASOA-1: anthropogenic SOA-1 (oxy-PAHs); ASOA-2: anthropogenic SOA-2 (nitro-PAHs); ASOA-3: anthropogenic SOA-3 (phenolic compounds oxidation); ASOA-4: anthropogenic SOA-4 (toluene oxidation).

5.3.1.2. Biomass burning

Biomass burning (BBOA factor) was identified based on high contributions from oxygenated fragments $C_2H_4O_2^+$ (m/z 60) and $C_3H_5O_2^+$ (m/z 73) (Figure 4). The ions are fragments of anhydrous sugars such as levoglucosan, which are produced during cellulose pyrolysis (Lanz et al., 2007b; Alfarra et al., 2007). This factor also showed high contribution of levoglucosan (67%), a known cellulose combustion marker (Simoneit et al., 1999). This factor also included significant contributions of species such as benzo[a]fluorenone (B[a]Fone) (26%), benzo[b]fluorenone (B[b]Fone) (29%) and 9-nitroanthracene (9-NA) (38%), which may originate from both primary and secondary processes (Tomaz et al., 2017; Albinet et al., 2007).

BBOA accounted for only 3% of the OA mass (Figure 3). The factor exhibited an expected temporal variation with slightly higher concentrations at the beginning of the PM pollution event, a period which was highly impacted by local emissions and notably residential heating (Srivastava et al., 2018a; Petit et al., 2017). The diurnal profile of BBOA showed a significant increase from the late afternoon until the night corresponding to the residential heating (Figure 5). In addition, the factor also showed a very good correlation with levoglucosan (r^2 = 0.93, n=92, $p < 0.05$) (Figure 6).

5.3.1.3. Oxidized primary OA (OPOA)

This factor was characterized by the presence of the oxygenated fragments $C_2H_4O_2^+$ (m/z 60), $C_3H_5O_2^+$ (m/z 73), $C_2H_3O^+$ (m/z 43) and CO_2^+ (m/z 44) and included contributions of levoglucosan (7%) and oxalate (38%) (Figure 4). The source showed a significant contribution to the OA mass about 14% on an average (Figure 3). Interestingly, this factor was found to be significantly correlated with levoglucosan (r^2=0.5, n=92, $p <0.05$), following a similar temporal evaluation (Figure S7). The observed diurnal profile of this factor also illustrated the same

behaviour as BBOA with high concentrations during the night corresponding to wood burning activities (Figure 5).

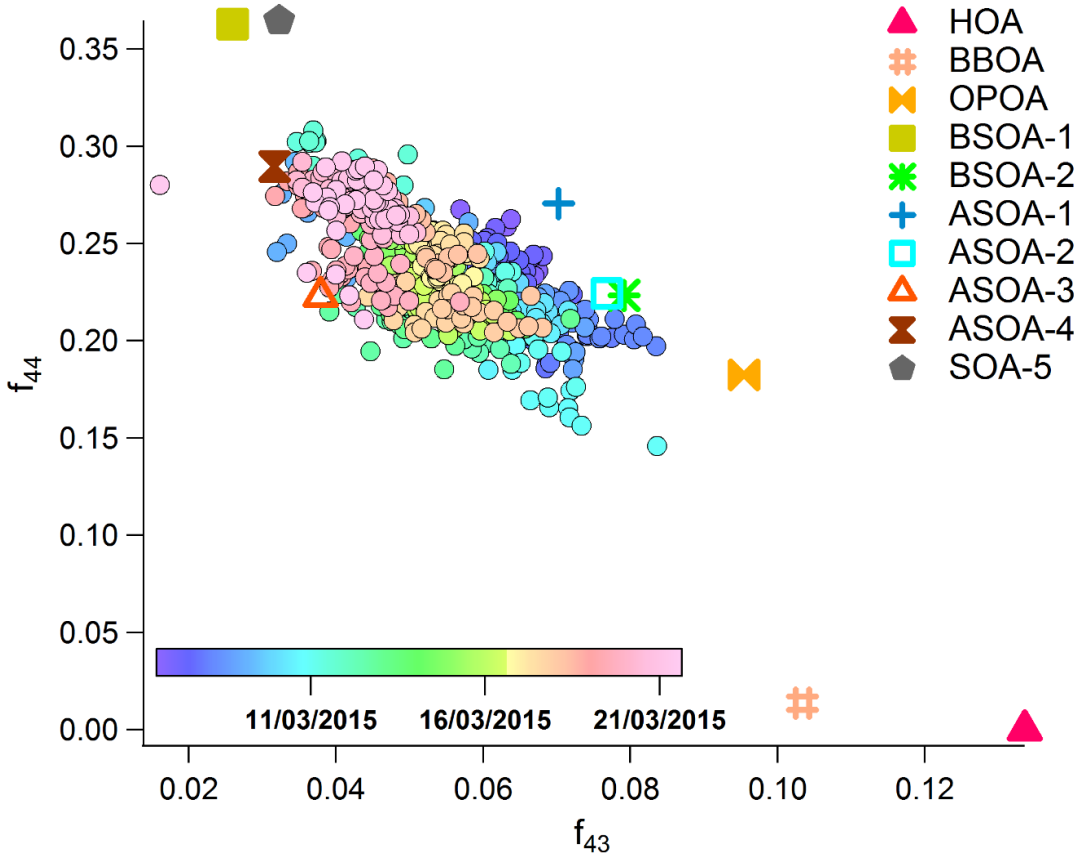

Figure 6. Triangle plot showing f_{44} vs. f_{43}. The dots are coloured according to the sampling dates. f_{44} and f_{43} represent the fraction of m/z 44 and m/z 43 in OA, respectively. HOA: primary traffic emissions; BBOA: biomass burning OA; OPOA: oxidized primary OA; BSOA-1: biogenic SOA-1 (marine-rich); BSOA-2: biogenic SOA-2 (isoprene); ASOA-1: anthropogenic SOA-1 (oxy-PAHs); ASOA-2: anthropogenic SOA-2 (nitro-PAHs); ASOA-3: anthropogenic SOA-3 (phenolic compounds oxidation); ASOA-4: anthropogenic SOA-4 (toluene oxidation) and SOA-5.

To further investigate the evolution of OA factors, the triangle plot f_{44} vs. f_{43} was studied; (fractions of m/z 44 and m/z 43 in OA, respectively) (Ng et al., 2010) (Figure 6). f_{44} can be considered as an indicator of atmospheric aging due to photochemical processes leading to the

increase of f_{44} in the atmosphere. Both, HOA and BBOA factors, identified above, showed low oxidative properties with varying f_{43}, which is located at the bottom right of the triangle plot and consistent with previously reported studies (Sun et al., 2012; Zhang et al., 2015). On the opposite, the present factor showed moderate oxidative properties with higher f_{44} values and still high values of f_{43} and f_{60} (Figures 6 and S8), showing a partial oxidation of this factor. Thus, this factor seemed to perceive the characteristics of OPOA linked to biomass burning, resulting from the rapid oxidation in the gas phase of low volatile and/or semi-volatile organics emitted by this source (Grieshop et al., 2009a).

5.3.1.4. SOA factors

As described previously, the f_{44} vs. f_{43} plot provides valuable information on the photochemical ageing of evolved SOA components (Ng et al., 2010; Zhang et al., 2011). All SOA components were noticed in the upper half of the triangle compared to the identified primary sources (Figure 6). The variability observed in f_{44} for these components suggested the role of various sources, precursors and different chemical pathways involved in their formation.

5.3.1.4.1. Biogenic SOA-1 (marine-rich) (BSOA-1)

This factor was characterized by high contributions of m/z 44 (CO_2^+), including 100% contribution of methanesulfonic acid (MSA) (Figure 2). MSA, a known secondary oxidation product of dimethylsulfide (DMS), is emitted by phytoplankton and several types of anaerobic bacteria in the oceanic environment (Charlson et al., 1987; Chasteen and Bentley, 2004; Zorn et al., 2008) (Figure 4). This factor accounted for 14% of the OA mass and showed higher contribution during the last days of the campaign (Figure 3). This factor was also associated with higher f_{44} (found on the top of the triangular plot, Figure 6), indicating highly oxidized aerosols (Ng et al., 2010). These results were in agreement with the impact of long range

transport and aging processes highlighted previously by high concentrations of NO_3^- and SO_4^{2-} together with high wind speed for the same pollution event during this period (Petit et al., 2017; Srivastava et al., 2018a) (Figure S4).

This factor also included a significant contribution of oxalate (43%), an ultimate end-product of photochemical oxidation processes. Secondary formation routes for oxalate are thought to be primarily driven by photochemical decomposition of gaseous anthropogenic (e.g., cycloalkanes) and biogenic (e.g., isoprene) organic compounds (Carlton et al., 2009; Carlton et al., 2007; Kawamura et al., 1996; Hatakeyama et al., 1987), photochemical formation followed by partitioning onto the condensed phase (Sullivan and Prather, 2007; Martinelango et al., 2007), and heterogeneous formation which includes in-cloud processing (Pun et al., 2000). Taken together, these observations suggest that BSOA-1 was principally linked to marine SOA but the impact of other sources (anthropogenic/ biogenic) should also be considered.

5.3.1.4.2. Biogenic SOA-2 (isoprene oxidation) (BSOA-2)

The identification of this factor was based on oxygenated fragments (m/z 44 and m/z 43) and significant contributions of oxidation products of isoprene (α-MGA and 2-MT (2-methylerythritol); 60 and 99%, respectively) (Carlton et al., 2009) (Figure 4). This factor accounted for 5% of the total OA mass (Figure 3).

This factor was found to be less oxidized similar to previous observation (Figure 6) (Xu et al., 2015). The formation of laboratory-generated isoprene SOA has been noticed via the reactive uptake of epoxydiols (IEPOX), an important oxidation product of isoprene when organic peroxyl radicals mainly react with hydroperoxyl radicals (Paulot et al., 2009). Good correlation was noticed previously between IEPOX SOA and filter-based 2-methylerythritol and 2-methylthreitol, which are known isoprene SOA tracers likely formed from IEPOX uptake

(Surratt et al., 2010). These previous findings suggest that the factor retrieved from the ME-2 analysis probably contains the characteristic of IEPOX SOA found in several studies (Xu et al., 2015; Budisulistiorini et al., 2013; Hu et al., 2015; Surratt et al., 2010; Zhang et al., 2017) as high correlation was noticed between this factor and 2-methylerythritol (r^2=0.95, n=92, p <0.05).

5.3.1.4.3. Anthropogenic SOA-1 (nitro-PAHs) (ASOA-1)

This factor was characterized by 100% contribution of 2-nitrofluoranthene (2-NFlt) and oxygenated mass fragments (m/z 44 and m/z 43) (Figure 4). 2-NFlt is a by-product of fluoranthene oxidation by gas phase reaction with NO_2 initiated by OH (day-time) or NO_3 (night-time) radicals (Arey et al., 1986; Atkinson et al., 1987). This factor seemed to be oxidized but also included a significant fraction of f_{43} (Figure 6). Therefore, this factor was found to be linked with PAH SOA from anthropogenic sources i.e., biomass burning and traffic. This factor showed significant contribution to the OA mass (10%) (Figure 3). The diurnal profile showed an increase of the concentrations from early night until early morning, indicating the predominance of night-time processes in the secondary formation of nitro-PAHs (Figure 5).

5.3.1.4.4. Anthropogenic SOA-2 (oxy-PAHs) (ASOA-2)

This factor was characterized by high proportions (~100%) of dibenzo[b,d]pyran-6-one (6H-DPone) and oxygenated mass fragments (m/z 44 and m/z 43). 6H-DPone, a secondary photooxidation product of phenanthrene, is often considered as a good marker of PAH SOA formation (Tomaz et al., 2017; Lee and Lane, 2010). This factor also included B[a]Fone (33%) and B[b]Fone (47%) which may originate from both primary and secondary processes (Tomaz et al., 2017; Albinet et al., 2007; Srivastava et al., 2018a) (Figure 4). Thus, this factor was identified as another PAH SOA and accounted for 4% of the OA mass (Figure 3).

This factor was less oxidized than the other PAH SOA (ASOA-1) mentioned before (Figure 6), emphasizing the fact that the formation of nitro- and oxy-PAHs were linked to different chemical processes. This was also supported by a completely different diurnal pattern observed for this factor with distinctive morning and evening peaks (Figure 5). High concentration observed during the day time suggests that the role of day time processes in the formation of oxy-PAHs, probably initiated by OH/ O_3 radical, still needs further investigations.

The characteristic mass fragments and species typically associated with traffic emissions such as m/z 27, 41, 43, 55, 57, 69, and 71, including significant amount of EC (14%) and 1-NP (36%) as mentioned before (Figure 4), have also been noticed in this factor chemical profile. These observations suggest that the given factor may contain a part of aged traffic aerosols but the impact of other combustion sources cannot be ignored.

5.3.1.4.5. Anthropogenic SOA-3 (phenolic compounds oxidation) (ASOA-3)

This factor was identified based on very high contribution of both compounds 4-methyl-5-nitrocatechol (4-Me5Nc) (100%) and 3-methyl-5-nitrocatechol (3-Me5Nc) (91%) as well as by m/z 44 and m/z 43 (oxidized fragments) (Figure 4). As mentioned in the literature, these species are the photooxidation products of phenolic compounds (i.e., cresols, methoxyphenols,..), and mostly associated with biomass burning emissions (Bruns et al., 2016; Iinuma et al., 2010). In addition, this factor also showed significant contributions of m/z 60, m/z 73 and levoglucosan (<17%), well-known tracer ions/compound of biomass burning emission as mentioned before. This factor was also found to be more oxidized than the previously identified anthropogenic SOA factors (ASOA-2 and ASOA-4) (Figure 6).

The source showed a quite low contribution to the OA mass of 3% on an average (Figure 3). The ASOA-3 factor followed a distinctive temporal evolution with higher concentrations at the beginning of the sampling campaign in agreement with the BBOA profile (Figure 3). The

diurnal profile presented peaks concentration during the early night concurrently with the biomass burning emissions (Figure 5). Therefore, this factor illustrated the characteristics of anthropogenic SOA linked to biomass burning. This was also supported by the f_{44} vs. f_{60} plot (Figure S8), which showed very high f_{60} values comparable to the BBOA factor.

5.3.1.4.6. Anthropogenic SOA-4 (toluene oxidation) (ASOA-4)

This factor was characterized by high contributions of m/z 44 (CO_2^+), including 100% contribution of 2,3-dihydroxy-4-oxopentanoic acid (DHOPA). DHOPA is a known secondary photooxidation product from toluene oxidation (Kleindienst et al., 2004). Therefore, this factor seemed to be another SOA from anthropogenic combustion sources, i.e. biomass burning and traffic. This factor exhibited low contribution to the OA mass (5%) (Figure 3).

This factor also included m/z 60 and levoglucosan (~10%) (Figure 4). A significant correlation was also noticed between this factor and levoglucosan (r^2=0.44, n=92, $p<0.05$) (Figure S10). The diurnal profile showed a pronounced peak at night, corresponding to biomass burning emissions. Therefore, these results suggest that the observed factor could be another anthropogenic SOA, probably linked to biomass burning emissions during this campaign. This was further confirmed by the low correlation obtained between the given factor and 1-NP (good marker of diesel emissions, section 3.3.1.1) (Figure S10). However, the impact of other sources cannot be neglected and was further confirmed by the observed low f_{60} fraction contrary to other biomass burning related factors (Figure S8). This factor was also found to be more oxidized than the other biomass burning SOA (ASOA-3) (Figure 6), showing the role of different chemical processes involved in the SOA formation.

5.3.1.4.7. SOA-5

This factor was characterized by high contributions of m/z 44 (CO_2^+) and a lower m/z 43 ($C_2H_3O^+$), similar to the more oxidized factor determined at other urban/suburban sites from online PMF characterization (Figure 4) (Ulbrich et al., 2009; Ng et al., 2010). It is interesting to note that no organic markers were found to be associated with this factor except a small contribution of isoprene oxidation product (α-MGA; ~30%). This factor was found as the predominant one, accounting for approximately 34% of the OA mass.

This factor showed a good correlation with secondary inorganic species ($r^2_{sulfate}$=0.67; $r^2_{nitrate}$=0.81; $r^2_{ammonium}$=0.83; n=774, $p<0.05$) (Figure S11). This factor exhibited a well-marked temporal variation, with very high concentrations during the end of the campaign (Figure 3). The impact of long range transport observed during this period (Figure S4) suggests that this factor may contain highly aged aerosol, and was also supported by previous findings during the same campaign at the same site (Srivastava et al., 2018a; Petit et al., 2017).

This was also confirmed by the very high oxidative properties shown by the triangle plot (Figure 6). Similar kind of OOA factor has also been observed at other European sites during winter following the same characteristics, i.e., high correlation with long-range transported secondary inorganic species (Lanz et al., 2007b; Daellenbach et al., 2017).

5.4. Comparison with PMF-ACSM source apportionment

5.4.1. Comparison of total OA

The results obtained from the PMF-combined analysis have been compared with the conventional PMF-ACSM results to investigate the consistency and the benefits of the developed OA source apportionment methodology.

The total reconstructed OA obtained from the PMF-combined analysis and OA from the ACSM measurements are shown on Figure 7. The results showed a very good correlation

between both methodologies (r^2=0.9, slope=1.28, n=774, p<0.05). These results highlighted that the total OA was well explained by the PMF-combined analysis including in terms of temporal evolution. However, the overestimation can be seen clearly at the end of the sampling campaign when the formation of SOA is more pronounced as discussed above. The observed overestimation could be linked to the uncertainty involved in the model.

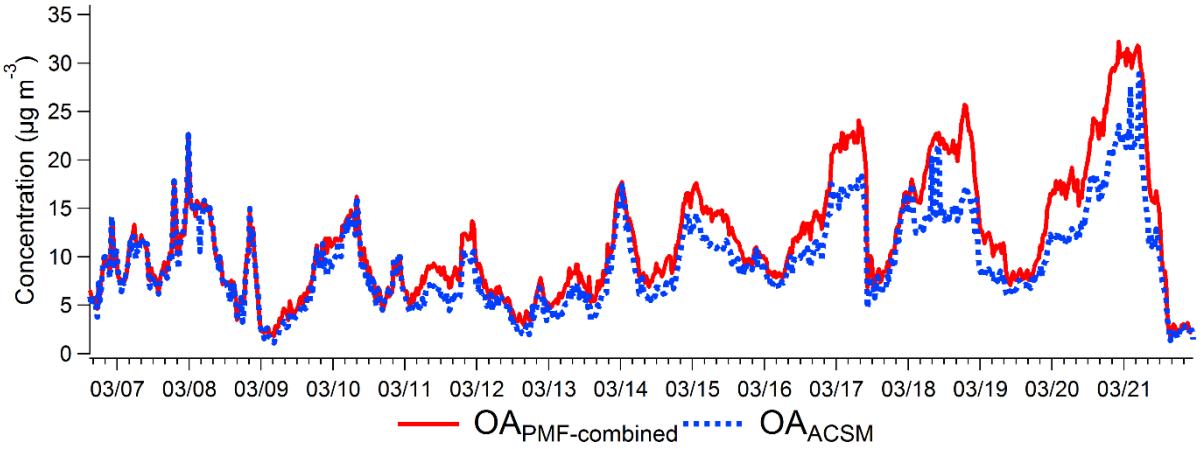

Figure 7. Temporal evolutions of the total reconstructed OA obtained from for the PMF-combined and OA from the ACSM measurements, observed at Paris-SIRTA, France (March 2015).

5.4.2. Comparison of POA factors

The comparison of POA factors (HOA and BBOA) from both PMF analyses are presented on Figure 8. A good agreement was noticed between HOA factors (r^2=0.8, slope=0.68, n=774, p< 0.05). In addition, the diurnal profile of the $HOA_{PMF\text{-}combined}$ exhibited sharper morning and evening peaks than $HOA_{ACSM\text{-}PMF}$ factor, indicating the improvement in the HOA apportionment by using the new methodology (Figure S12).

On the other hand, the primary BBOA factor from the PMF-combined analysis can be considered as the sum of two primary biomass burning factors (BBOA and OPOA) discussed previously (section 3.3.1). This was confirmed by a good correlation observed between primary

$BBOA_{PMF\text{-}combined}$ (BBOA + OPOA) and levoglucosan (r^2 = 0.61, n = 91, $p < 0.05$) (Figure S13), showing the influence of primary emissions on these factors. Later, the comparison of primary biomass burning factor from both approaches (primary $BBOA_{PMF\text{-}combined}$ and $BBOA_{PMF\text{-}ACSM}$) showed a good agreement (r^2 =0.6, slope=0.90, n=774, $p<0.05$) (Figure 8). This was also supported by the diurnal profiles observed for primary biomass burning factors from both approaches, showing high concentration during night-time (Figure S12).

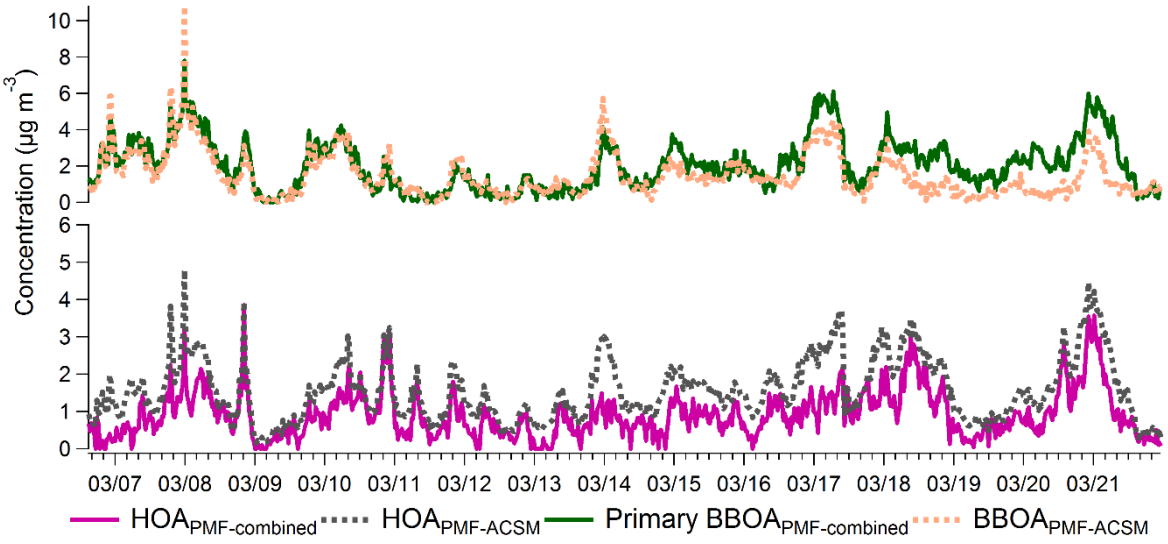

Figure 8. Temporal evolutions of POA factors identified using both PMF-ACSM and PMF-combined analyses identified at Paris-SIRTA, France (March 2015). Primary $BBOA_{PMF\text{-}combined}$ = $BBOA_{PMF\text{-}combined}$ + $OPOA_{PMF\text{-}combined}$. PMF-combined: plain lines; PMF-ACSM: dotted lines.

These results highlighted that the primary biomass burning source was well resolved by both approaches, however the PMF-combined analysis showed advantage over the PMF-ACSM analysis in terms of two primary BBOA factors rather than one.

Nalin et al. (2016) showed that the oxidation of organics between the emission point and their introduction in ambient air, leads to the formation of OPOA (Nalin et al., 2016). The chemical profiles observed for measurements performed directly at the emission and in close field (after dilution to simulate ambient air concentrations) have an impact on the emission

inventories. Therefore, this kind of chemical processes should be taken cautiously in air quality models. In general, the separation of such wood-smoke related OPOA is very difficult as it displays mass spectra like OOA factor (Grieshop et al., 2009b). By adding the molecular markers in the OA ACSM matrix, these processes were discriminated, yielding two primary biomass burning sources: actual primary BBOA (BBOA) and OPOA.

As observed in this study, more than 80% of the primary BBOA fraction was dominated by OPOA. This refers to the fact that the BBOA in the atmosphere is more like OPOA rather than the actual primary BBOA. Air quality models do not simulate the total primary BBOA (BBOA + OPOA). They only account for the actual primary BBOA (BBOA), which means 20 %. This is due to the use of emission inventories data, often taken from the measurement directly performed at the emission point. BBOA obtained from the online characterization (AMS/ACSM) includes OPOA (80% of the total primary BBOA), however models only simulate a small fraction (20%) of the total primary BBOA. This could explain the existing differences observed between measurements and models.

5.4.3. Comparison of total OOA (SOA)

The comparison of the total SOA estimates (OOA) from the PMF-combined and PMF-ACSM analyses are presented on Figure 9. Overall, both approaches showed a very good correlation (r^2=0.96, slope=1.10, n=774, $p < 0.05$). The total secondary estimates from the PMF-combined analysis was the sum of 7 OOA factors, while only 2 OOA factors (MO-OOA + LO-OOA) were obtained using the PMF-ACSM analysis. Thus, these results highlighted that the PMF-combined has given valuable insights into the secondary formation.

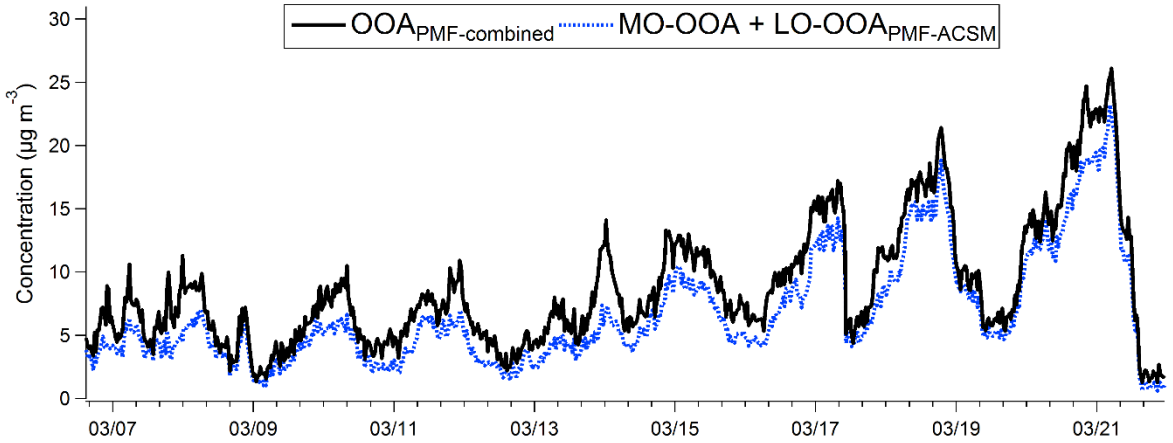

Figure 9. Temporal evolutions of total SOA estimates (total OOA) obtained from the PMF-combined and PMF-ACSM analyses at Paris-SIRTA, France (March 2015). Total $OOA_{PMF\text{-}combined}$ = BSOA-1 (marine-rich) + BSOA-2 (isoprene oxidation), ASOA-1 (nitro-PAHs) + A SOA-2 (oxy-PAHs) + ASOA-3 (phenolic compounds oxidation) + ASOA-4 (toluene oxidation) + SOA-5; Total $OOA_{PMF\text{-}ACSM}$ = $MO\text{-}OOA_{PMF\text{-}ACSM}$+ $LO\text{-}OOA_{PMF\text{-}ACSM}$.

5.4.4. Insights into SOA

In this section, individual SOA sources from both approaches have been compared to provide deeper insights into SOA formation. As explained, 7 SOA factors were resolved by the PMF-combined analysis instead of 2 SOA (OOA) factors from the PMF-ACMS analysis. Attempts have been made here to provide a link between SOA (OOA) components resolved from both approaches, explaining the sources of $MO\text{-}OOA_{PMF\text{-}ACSM}$ and $LO\text{-}OOA_{PMF\text{-}ACSM}$ factors by using SOA components resolved from the PMF-combined analysis.

No direct link was observed between the individual SOA factors obtained from both approaches, except between $MO\text{-}OOA_{PMF\text{-}ACSM}$ and BSOA-1 and SOA-5 (Table S3). $MO\text{-}OOA_{PMF\text{-}ACSM}$ was significantly correlated with BSOA-1 and SOA-5 (Table S3; r^2=0.76-0.89, n=774, $p < 0.05$). These results indicated that the $MO\text{-}OOA_{PMF\text{-}ACSM}$ was mainly composed of two factors from the combined PMF analysis, BSOA-1 and SOA-5. Both SOA factors were

found to be highly oxidized (Figure 6) and further confirmed their link with the MO-OOA$_{PMF-ACSM}$. Finally, the comparison made between MO-OOA$_{combined\ PMF}$, the sum of BSOA-1 and SOA-5, illustrated a very good agreement with MO-OOA$_{ACSM}$ (r^2=0.96, slope=1.13, n=774, p<0.05), following the similar temporal variability (Figure 10).

However, the development of a proper link between MO-OOA$_{PMF-ACSM}$ and the given sources are still difficult to achieve. As explained, SOA-5 retrieved from the PMF-combined analysis was not identified by any of the markers used during this work. This probably shows a clear identification of the more oxidized OOA is probably impossible to achieve as shown by its association only with quite ultimate oxidation end-products (MSA and oxalate).

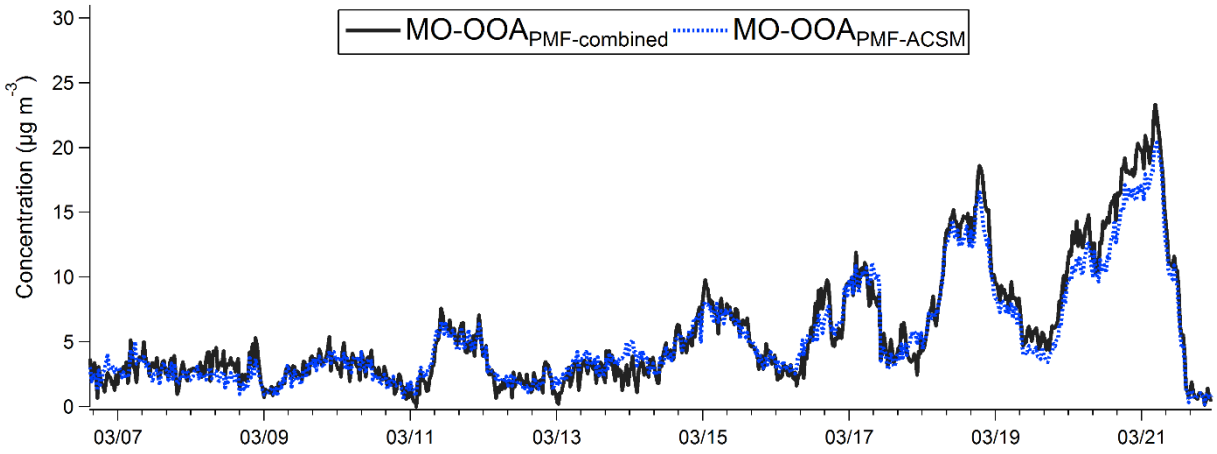

Figure 10 Temporal evolutions of MO-OOA$_{combined\ PMF}$ and MO-OOA$_{PMF-ACSM}$ factors identified at Paris-SIRTA, France (March 2015). MO-OOA$_{combined\ PMF}$ = biogenic SOA-1 (marine-rich) + SOA-5.

As shown, it is also not possible to establish a direct link for LO-OOA$_{PMF-ACSM}$ with any SOA sources. This highlights that LO-OOA$_{PMF-ACSM}$ does not stand for a single source, precursor or specific processes. However, the new methodology allowed the deconvolution of more SOA factors, illustrating more information on the processes involved in the SOA formation. This was

achieved by combining different measurements on their original time resolution to keep high time resolution characteristics.

5.5. Conclusions

Overall, compared to conventional approaches (PMF-AMS/ACSM analysis), this new methodology provided a more comprehensive description of various OA sources and their respective atmospheric processes. In this study, a novel approach has been proposed to investigate OA sources using ME-2 algorithm applied to the combined dataset including ACSM OA matrix and organic molecular markers from PM_{10} filters on their original time resolution. The use of combined data matrix allowed to resolve 10 OA factors. This included common OA sources such as primary traffic emissions (HOA), biomass burning (BBOA), as well as 2 specific biogenic- and 4 anthropogenic-SOA sources.

The consistency of this new methodology was also investigated by comparing the results with PMF-ACSM analysis. The results showed a very good agreement for both, primary and secondary fractions. However, particularly for the primary biomass burning, the PMF-combined analysis showed advantage over the PMF-ACSM analysis, showing two primary BBOA factors (BBOA and OPOA) rather than one. The results highlighted that more than 80% of the primary BBOA fraction was dominated by OPOA, emphasizing the fact that the BBOA in the atmosphere is more like OPOA. To bridge the gap between the measurements and models, air quality models should account for these processes (OPOA) carefully as it is not accounted in the current emission inventories.

The combination of OA mass spectra and specific SOA markers have allowed the deconvolution of 7 OOA factors instead of 2 OOA factors (MO-OOA, LO-OOA) resolved from the PMF-ACSM analysis. The use of combined matrix allowed the clear identification of 54% of the total SOC fraction. Of that, 28% of the total SOC fraction seemed to be related to

anthropogenic SOA (4 SOA factors) from combustion sources i.e., biomass burning and traffic emissions.

The development of a proper link between MO-OOA$_{PMF-ACSM}$/ LO-OOA$_{PMF-ACSM}$ and the given sources are still difficult to achieve. The results showed that the more oxidized OOA is probably associated with ultimate oxidation by-products while LO-OOA$_{PMF-ACSM}$ does not represent any single source or process. Finally, valuable insights into the formation and aging processes of secondary OA components compared to PMF-ACSM results were then obtained.

Acknowledgements

This work has notably been supported by the French Ministry of Environment (MTES) and the national reference laboratory for air quality monitoring (LCSQA), as well as by the FP7 ACTRIS and H2020 ACTRIS projects. The authors gratefully acknowledge François Truong (LSCE) and Robin Aujay-Plouzeau (INERIS) for taking care of samples and instrumentation and other staff at the SIRTA observatory for providing weather-related data used in this study. They also thank Patrick Bodu for the graphical abstract design.

References

Aiken, A. C., Salcedo, D., Cubison, M. J., Huffman, J. A., DeCarlo, P. F., Ulbrich, I. M., Docherty, K. S., Sueper, D., Kimmel, J. R., Worsnop, D. R., Trimborn, A., Northway, M., Stone, E. A., Schauer, J. J., Volkamer, R. M., Fortner, E., de Foy, B., Wang, J., Laskin, A., Shutthanandan, V., Zheng, J., Zhang, R., Gaffney, J., Marley, N. A., Paredes-Miranda, G., Arnott, W. P., Molina, L. T., Sosa, G., and Jimenez, J. L.: Mexico City aerosol analysis during MILAGRO using high resolution aerosol mass spectrometry at the urban supersite (T0) – Part 1: Fine particle composition and organic source apportionment, Atmos. Chem. Phys., 9, 6633-6653, 10.5194/acp-9-6633-2009, 2009.

Albinet, A., Leoz-Garziandia, E., Budzinski, H., and Villenave, E.: Simultaneous analysis of oxygenated and nitrated polycyclic aromatic hydrocarbons on standard reference material 1649a (urban dust) and on natural ambient air samples by gas chromatography–mass spectrometry with negative ion chemical ionisation, J. Chromatogr. A, 1121, 106-113, https://doi.org/10.1016/j.chroma.2006.04.043, 2006.

Albinet, A., Leoz-Garziandia, E., Budzinski, H., and Villenave, E.: Polycyclic aromatic hydrocarbons (PAHs), nitrated PAHs and oxygenated PAHs in ambient air of the Marseilles area (South of France): Concentrations and sources, Sci. Total Environ., 384, 280-292, http://dx.doi.org/10.1016/j.scitotenv.2007.04.028, 2007.

Albinet, A., Tomaz, S., and Lestremau, F.: A really quick easy cheap effective rugged and safe (QuEChERS) extraction procedure for the analysis of particle-bound PAHs in ambient air and emission samples, Sci. Total Environ., 450-451, 31-38, 10.1016/j.scitotenv.2013.01.068, 2013.

Albinet, A., Nalin, F., Tomaz, S., Beaumont, J., and Lestremau, F.: A simple QuEChERS-like extraction approach for molecular chemical characterization of organic aerosols: application to nitrated and oxygenated PAH derivatives (NPAH and OPAH) quantified by GC–NICIMS, Anal. Bioanal. Chem., 406, 3131-3148, 10.1007/s00216-014-7760-5, 2014.

Alfarra, M. R., Prevot, A. S. H., Szidat, S., Sandradewi, J., Weimer, S., Lanz, V. A., Schreiber, D., Mohr, M., and Baltensperger, U.: Identification of the Mass Spectral Signature of Organic Aerosols from Wood Burning Emissions, Environ. Sci. Technol., 41, 5770-5777, 10.1021/es062289b, 2007.

Amato, F., Pandolfi, M., Escrig, A., Querol, X., Alastuey, A., Pey, J., Perez, N., and Hopke, P. K.: Quantifying road dust resuspension in urban environment by Multilinear Engine: A comparison with PMF2, Atmos. Environ., 43, 2770-2780, https://doi.org/10.1016/j.atmosenv.2009.02.039, 2009.

Amato, F., and Hopke, P. K.: Source apportionment of the ambient PM2.5 across St. Louis using constrained positive matrix factorization, Atmos. Environ., 46, 329-337, https://doi.org/10.1016/j.atmosenv.2011.09.062, 2012.

Arey, J., Zielinska, B., Atkinson, R., Winer, A. M., Ramdahl, T., and Pitts, J. N.: The formation of nitro-PAH from the gas-phase reactions of fluoranthene and pyrene with the OH radical in the presence of NOx, Atmos. Environ., 20, 2339-2345, https://doi.org/10.1016/0004-6981(86)90064-8, 1986.

Atkinson, R., Arey, J., Zielinska, B., Pitts, J. N., and Winer, A. M.: Evidence for the transformation of polycyclic organic matter in the atmosphere, Atmos. Environ., 21, 2261-2262, https://doi.org/10.1016/0004-6981(87)90357-X, 1987.

Boucher, O., Randall, D., Artaxo, P., Bretherton, C., Feingold, G., Forster, P., Kerminen, V.-M., Kondo, Y., Liao, H., and Lohmann, U.: Clouds and aerosols, in: Climate change 2013: the physical science basis. Contribution of Working Group I to the Fifth Assessment Report of the Intergovernmental Panel on Climate Change, Cambridge University Press, 571-657, 2013.

Bressi, M., Sciare, J., Ghersi, V., Bonnaire, N., Nicolas, J. B., Petit, J. E., Moukhtar, S., Rosso, A., Mihalopoulos, N., and Féron, A.: A one-year comprehensive chemical characterisation of fine aerosol (PM2.5) at urban, suburban and rural background sites in the region of Paris (France), Atmos. Chem. Phys., 13, 7825-7844, 10.5194/acp-13-7825-2013, 2013.

Bruns, E. A., El Haddad, I., Slowik, J. G., Kilic, D., Klein, F., Baltensperger, U., and Prévôt, A. S. H.: Identification of significant precursor gases of secondary organic aerosols from residential wood combustion, Sci. Rep., 6, 27881, 10.1038/srep27881

http://www.nature.com/articles/srep27881#supplementary-information, 2016.

Budisulistiorini, S. H., Canagaratna, M. R., Croteau, P. L., Marth, W. J., Baumann, K., Edgerton, E. S., Shaw, S. L., Knipping, E. M., Worsnop, D. R., Jayne, J. T., Gold, A., and Surratt, J. D.: Real-Time Continuous Characterization of Secondary Organic Aerosol Derived from Isoprene Epoxydiols in Downtown Atlanta, Georgia, Using the Aerodyne Aerosol Chemical Speciation Monitor, Environ. Sci. Technol., 47, 5686-5694, 10.1021/es400023n, 2013.

Carlton, A. G., Turpin, B. J., Altieri, K. E., Seitzinger, S., Reff, A., Lim, H.-J., and Ervens, B.: Atmospheric oxalic acid and SOA production from glyoxal: Results of aqueous photooxidation experiments, Atmos. Environ., 41, 7588-7602, 2007.

Carlton, A. G., Wiedinmyer, C., and Kroll, J. H.: A review of Secondary Organic Aerosol (SOA) formation from isoprene, Atmos. Chem. Phys., 9, 4987-5005, 10.5194/acp-9-4987-2009, 2009.

Cavalli, F., Viana, M., Yttri, K., Genberg, J., and Putaud, J.-P.: Toward a standardised thermal-optical protocol for measuring atmospheric organic and elemental carbon: the EUSAAR protocol, Atmos. Meas. Tech., 3, 79-89, 2010.

Charlson, R. J., Lovelock, J. E., Andreae, M. O., and Warren, S. G.: Oceanic phytoplankton, atmospheric sulphur, cloud albedo and climate, Nature, 326, 655-661, 1987.

Chasteen, T. G., and Bentley, R.: Volatile Organic Sulfur Compounds of Environmental Interest: Dimethyl Sulfide and Methanethiol. An Introductory Overview, J. Chem. Educ., 81, 1524, 10.1021/ed081p1524, 2004.

Crespi, A., Bernardoni, V., Calzolai, G., Lucarelli, F., Nava, S., Valli, G., and Vecchi, R.: Implementing constrained multi-time approach with bootstrap analysis in ME-2: An application to PM2.5 data from Florence (Italy), Sci. Total Environ., 541, 502-511, 10.1016/j.scitotenv.2015.08.159, 2016.

Crippa, M., Canonaco, F., Slowik, J. G., El Haddad, I., DeCarlo, P. F., Mohr, C., Heringa, M. F., Chirico, R., Marchand, N., Temime-Roussel, B., Abidi, E., Poulain, L., Wiedensohler, A., Baltensperger, U., and Prévôt, A. S. H.: Primary and secondary organic aerosol origin by

combined gas-particle phase source apportionment, Atmos. Chem. Phys., 13, 8411-8426, 10.5194/acp-13-8411-2013, 2013.

Daellenbach, K. R., Stefenelli, G., Bozzetti, C., Vlachou, A., Fermo, P., Gonzalez, R., Piazzalunga, A., Colombi, C., Canonaco, F., Hueglin, C., Kasper-Giebl, A., Jaffrezo, J. L., Bianchi, F., Slowik, J. G., Baltensperger, U., El-Haddad, I., and Prévôt, A. S. H.: Long-term chemical analysis and organic aerosol source apportionment at nine sites in central Europe: source identification and uncertainty assessment, Atmos. Chem. Phys., 17, 13265-13282, 10.5194/acp-17-13265-2017, 2017.

DeCarlo, P. F., Kimmel, J. R., Trimborn, A., Northway, M. J., Jayne, J. T., Aiken, A. C., Gonin, M., Fuhrer, K., Horvath, T., and Docherty, K. S.: Field-deployable, high-resolution, time-of-flight aerosol mass spectrometer, Anal. Chem., 78, 8281-8289, 2006.

Docherty, K. S., Aiken, A. C., Huffman, J. A., Ulbrich, I. M., DeCarlo, P. F., Sueper, D., Worsnop, D. R., Snyder, D. C., Peltier, R. E., Weber, R. J., Grover, B. D., Eatough, D. J., Williams, B. J., Goldstein, A. H., Ziemann, P. J., and Jimenez, J. L.: The 2005 Study of Organic Aerosols at Riverside (SOAR-1): instrumental intercomparisons and fine particle composition, Atmos. Chem. Phys., 11, 12387-12420, 10.5194/acp-11-12387-2011, 2011.

Dupont, J., Haeffelin, M., Badosa, J., Elias, T., Favez, O., Petit, J., Meleux, F., Sciare, J., Crenn, V., and Bonne, J. L.: Role of the boundary layer dynamics effects on an extreme air pollution event in Paris, Atmos. Environ., 141, 571 - 579, 10.1016/j.atmosenv.2016.06.061, 2016.

Grieshop, A., Logue, J., Donahue, N., and Robinson, A.: Laboratory investigation of photochemical oxidation of organic aerosol from wood fires 1: measurement and simulation of organic aerosol evolution, Atmos. Chem. Phys., 9, 1263-1277, 2009a.

Grieshop, A. P., Donahue, N. M., and Robinson, A. L.: Laboratory investigation of photochemical oxidation of organic aerosol from wood fires 2: analysis of aerosol mass spectrometer data, Atmos. Chem. Phys., 9, 2227-2240, 10.5194/acp-9-2227-2009, 2009b.

Guinot, B., Cachier, H., Sciare, J., Tong, Y., Xin, W., and Jianhua, Y.: Beijing aerosol: Atmospheric interactions and new trends, J. Geophys. Res.-Atmos., 112, 10.1029/2006JD008195, 2007.

Hatakeyama, S., Ohno, M., Weng, J., Takagi, H., and Akimoto, H.: Mechanism for the formation of gaseous and particulate products from ozone-cycloalkene reactions in air, Environ. Sci. Technol., 21, 52-57, 1987.

Heal, M. R., Kumar, P., and Harrison, R. M.: Particles, air quality, policy and health, Chem. Soc. Rev., 41, 6606-6630, 2012.

Heo, J., Dulger, M., Olson, M. R., McGinnis, J. E., Shelton, B. R., Matsunaga, A., Sioutas, C., and Schauer, J. J.: Source apportionments of PM2.5 organic carbon using molecular marker Positive Matrix Factorization and comparison of results from different receptor models, Atmos. Environ., 73, 51-61, http://dx.doi.org/10.1016/j.atmosenv.2013.03.004, 2013.

Hu, D., Bian, Q., Lau, A. K. H., and Yu, J. Z.: Source apportioning of primary and secondary organic carbon in summer PM2.5 in Hong Kong using positive matrix factorization of secondary and primary organic tracer data, J. Geophys. Res.-Atmos., 115, 10.1029/2009JD012498, 2010.

Hu, W. W., Campuzano-Jost, P., Palm, B. B., Day, D. A., Ortega, A. M., Hayes, P. L., Krechmer, J. E., Chen, Q., Kuwata, M., Liu, Y. J., de Sá, S. S., McKinney, K., Martin, S. T., Hu, M., Budisulistiorini, S. H., Riva, M., Surratt, J. D., St. Clair, J. M., Isaacman-Van Wertz, G., Yee, L. D., Goldstein, A. H., Carbone, S., Brito, J., Artaxo, P., de Gouw, J. A., Koss, A., Wisthaler, A., Mikoviny, T., Karl, T., Kaser, L., Jud, W., Hansel, A., Docherty, K. S., Alexander, M. L., Robinson, N. H., Coe, H., Allan, J. D., Canagaratna, M. R., Paulot, F., and Jimenez, J. L.: Characterization of a real-time tracer for isoprene epoxydiols-derived secondary organic aerosol (IEPOX-SOA) from aerosol mass spectrometer measurements, Atmos. Chem. Phys., 15, 11807-11833, 10.5194/acp-15-11807-2015, 2015.

Huang, R.-J., Zhang, Y., Bozzetti, C., Ho, K.-F., Cao, J.-J., Han, Y., Daellenbach, K. R., Slowik, J. G., Platt, S. M., Canonaco, F., Zotter, P., Wolf, R., Pieber, S. M., Bruns, E. A., Crippa, M., Ciarelli, G., Piazzalunga, A., Schwikowski, M., Abbaszade, G., Schnelle-Kreis, J., Zimmermann, R., An, Z., Szidat, S., Baltensperger, U., Haddad, I. E., and Prevot, A. S. H.: High secondary aerosol contribution to particulate pollution during haze events in China, Nature, 514, 218-222, 10.1038/nature13774 http://www.nature.com/nature/journal/v514/n7521/abs/nature13774.html#supplementary-information, 2014.

Iinuma, Y., Boge, O., Grafe, R., and Herrmann, H.: Methyl-nitrocatechols: atmospheric tracer compounds for biomass burning secondary organic aerosols, Environ. Sci. Technol., 44, 8453-8459, 10.1021/es102938a, 2010.

Jaeckels, J. M., Bae, M.-S., and Schauer, J. J.: Positive matrix factorization (PMF) analysis of molecular marker measurements to quantify the sources of organic aerosols, Environ. Sci. Technol., 41, 5763-5769, 2007.

Jayne, J. T., Leard, D. C., Zhang, X., Davidovits, P., Smith, K. A., Kolb, C. E., and Worsnop, D. R.: Development of an Aerosol Mass Spectrometer for Size and Composition Analysis of Submicron Particles, Aerosol Sci. Technol., 33, 49-70, 10.1080/027868200410840, 2000.

Kanakidou, M., Seinfeld, J., Pandis, S., Barnes, I., Dentener, F., Facchini, M., Dingenen, R. V., Ervens, B., Nenes, A., and Nielsen, C.: Organic aerosol and global climate modelling: a review, Atmos. Chem. Phys., 5, 1053-1123, 2005.

Kawamura, K., Kasukabe, H., and Barrie, L. A.: Source and reaction pathways of dicarboxylic acids, ketoacids and dicarbonyls in arctic aerosols: One year of observations, Atmos. Environ., 30, 1709-1722, 1996.

Keyte, I. J., Albinet, A., and Harrison, R. M.: On-road traffic emissions of polycyclic aromatic hydrocarbons and their oxy- and nitro- derivative compounds measured in road tunnel environments, Sci. Total Environ., 566–567, 1131-1142, https://doi.org/10.1016/j.scitotenv.2016.05.152, 2016.

Kleindienst, T., Conver, T., McIver, C., and Edney, E.: Determination of secondary organic aerosol products from the photooxidation of toluene and their implications in ambient PM2. 5, J. Atmos. Chem., 47, 79-100, 2004.

Kleindienst, T. E., Jaoui, M., Lewandowski, M., Offenberg, J. H., Lewis, C. W., Bhave, P. V., and Edney, E. O.: Estimates of the contributions of biogenic and anthropogenic hydrocarbons to secondary organic aerosol at a southeastern US location, Atmos. Environ., 41, 8288-8300, http://dx.doi.org/10.1016/j.atmosenv.2007.06.045, 2007.

Kuo, C. P., Liao, H. T., Chou, C. C., and Wu, C. F.: Source apportionment of particulate matter and selected volatile organic compounds with multiple time resolution data, Sci. Total Environ., 472, 880-887, 10.1016/j.scitotenv.2013.11.114, 2014.

Lanz, V. A., Alfarra, M. R., Baltensperger, U., Buchmann, B., Hueglin, C., and Prévôt, A. S. H.: Source apportionment of submicron organic aerosols at an urban site by factor analytical modelling of aerosol mass spectra, Atmos. Chem. Phys., 7, 1503-1522, 10.5194/acp-7-1503-2007, 2007a.

Lanz, V. A., Alfarra, M. R., Baltensperger, U., Buchmann, B., Hueglin, C., Szidat, S., Wehrli, M. N., Wacker, L., Weimer, S., and Caseiro, A.: Source attribution of submicron organic aerosols during wintertime inversions by advanced factor analysis of aerosol mass spectra, Environ. Sci. Technol., 42, 214-220, 2007b.

Lee, J., and Lane, D. A.: Formation of oxidized products from the reaction of gaseous phenanthrene with the OH radical in a reaction chamber, Atmos. Environ., 44, 2469-2477, 10.1016/j.atmosenv.2010.03.008, 2010.

Liao, H.-T., Kuo, C.-P., Hopke, P. K., and Wu, C.-F.: Evaluation of a Modified Receptor Model for Solving Multiple Time Resolution Equations: A Simulation Study, Aerosol. Air Qual. Res., 13, 1253-1262, 10.4209/aaqr.2012.11.0322, 2013.

Liao, H.-T., Chou, C. C. K., Chow, J. C., Watson, J. G., Hopke, P. K., and Wu, C.-F.: Source and risk apportionment of selected VOCs and PM2.5 species using partially constrained receptor models with multiple time resolution data, Environ. Pollut., 205, 121-130, https://doi.org/10.1016/j.envpol.2015.05.035, 2015.

Martinelango, P. K., Dasgupta, P. K., and Al-Horr, R. S.: Atmospheric production of oxalic acid/oxalate and nitric acid/nitrate in the Tampa Bay airshed: Parallel pathways, Atmos. Environ., 41, 4258-4269, https://doi.org/10.1016/j.atmosenv.2006.05.085, 2007.

McGuire, M., Chang, R.-W., Slowik, J., Jeong, C.-H., Healy, R., Lu, G., Mihele, C., Abbatt, J., Brook, J., and Evans, G.: Enhancing non-refractory aerosol apportionment from an urban industrial site through receptor modeling of complete high time-resolution aerosol mass spectra, Atmos. Chem. Phys., 14, 8017-8042, 2014.

Mohr, C., Huffman, J. A., Cubison, M. J., Aiken, A. C., Docherty, K. S., Kimmel, J. R., Ulbrich, I. M., Hannigan, M., and Jimenez, J. L.: Characterization of Primary Organic Aerosol Emissions from Meat Cooking, Trash Burning, and Motor Vehicles with High-Resolution Aerosol Mass Spectrometry and Comparison with Ambient and Chamber Observations, Environ. Sci. Technol., 43, 2443-2449, 10.1021/es8011518, 2009.

Nalin, F., Golly, B., Besombes, J.-L., Pelletier, C., Aujay-Plouzeau, R., Verlhac, S., Dermigny, A., Fievet, A., Karoski, N., Dubois, P., Collet, S., Favez, O., and Albinet, A.: Fast oxidation processes from emission to ambient air introduction of aerosol emitted by residential log wood stoves, Atmos. Environ., 143, 15-26, https://doi.org/10.1016/j.atmosenv.2016.08.002, 2016.

Ng, N. L., Canagaratna, M. R., Zhang, Q., Jimenez, J. L., Tian, J., Ulbrich, I. M., Kroll, J. H., Docherty, K. S., Chhabra, P. S., Bahreini, R., Murphy, S. M., Seinfeld, J. H., Hildebrandt, L., Donahue, N. M., DeCarlo, P. F., Lanz, V. A., Prévôt, A. S. H., Dinar, E., Rudich, Y., and Worsnop, D. R.: Organic aerosol components observed in Northern Hemispheric datasets from Aerosol Mass Spectrometry, Atmos. Chem. Phys., 10, 4625-4641, 10.5194/acp-10-4625-2010, 2010.

Ng, N. L., Herndon, S. C., Trimborn, A., Canagaratna, M. R., Croteau, P. L., Onasch, T. B., Sueper, D., Worsnop, D. R., Zhang, Q., Sun, Y. L., and Jayne, J. T.: An Aerosol Chemical Speciation Monitor (ACSM) for Routine Monitoring of the Composition and Mass Concentrations of Ambient Aerosol, Aerosol Sci. Technol., 45, 780-794, 10.1080/02786826.2011.560211, 2011.

Norris, G., Duvall, R., Brown, S., and Bai, S.: EPA Positive Matrix Factorization (PMF) 5.0 fundamentals and User Guide Prepared for the US Environmental Protection Agency Office of Research and Development, Washington, DC, DC EPA/600/R-14/108, 2014.

Ogulei, D., Hopke, P. K., Zhou, L., Paatero, P., Park, S. S., and Ondov, J. M.: Receptor modeling for multiple time resolved species: The Baltimore supersite, Atmos. Environ., 39, 3751-3762, https://doi.org/10.1016/j.atmosenv.2005.03.012, 2005.

Paatero, P., and Tapper, U.: Positive matrix factorization: A non-negative factor model with optimal utilization of error estimates of data values, Environmetrics, 5, 111-126, 1994.

Paatero, P.: The Multilinear Engine—A Table-Driven, Least Squares Program for Solving Multilinear Problems, Including the n-Way Parallel Factor Analysis Model, J. Comput. Graph. Stat., 8, 854-888, 10.1080/10618600.1999.10474853, 1999.

Paatero, P.: User's guide for the multilinear engine program "ME2" for fitting multilinear and quasi-multilinear models, University of Helsinki, Finland, 2000.

Paatero, P., Hopke, P. K., Song, X.-H., and Ramadan, Z.: Understanding and controlling rotations in factor analytic models, Chemom. Intell. Lab. Syst., 60, 253-264, http://dx.doi.org/10.1016/S0169-7439(01)00200-3, 2002.

Paulot, F., Crounse, J. D., Kjaergaard, H. G., Kurten, A., St Clair, J. M., Seinfeld, J. H., and Wennberg, P. O.: Unexpected epoxide formation in the gas-phase photooxidation of isoprene, Science, 325, 730-733, 10.1126/science.1172910, 2009.

Petit, J.-E., Amodeo, T., Meleux, F., Bessagnet, B., Menut, L., Grenier, D., Pellan, Y., Ockler, A., Rocq, B., and Gros, V.: Characterising an intense PM pollution episode in March 2015 in France from multi-site approach and near real time data: Climatology, variabilities, geographical origins and model evaluation, Atmos. Environ., 155, 68-84, 2017.

Petit, J. E., Favez, O., Sciare, J., Canonaco, F., Croteau, P., Močnik, G., Jayne, J., Worsnop, D., and Leoz-Garziandia, E.: Submicron aerosol source apportionment of wintertime pollution in Paris, France by double positive matrix factorization (PMF2) using an aerosol chemical speciation monitor (ACSM) and a multi-wavelength Aethalometer, Atmos. Chem. Phys., 14, 13773-13787, 10.5194/acp-14-13773-2014, 2014.

Petit, J. E., Favez, O., Sciare, J., Crenn, V., Sarda-Estève, R., Bonnaire, N., Močnik, G., Dupont, J. C., Haeffelin, M., and Leoz-Garziandia, E.: Two years of near real-time chemical composition of submicron aerosols in the region of Paris using an Aerosol Chemical Speciation Monitor (ACSM) and a multi-wavelength Aethalometer, Atmos. Chem. Phys., 15, 2985-3005, 10.5194/acp-15-2985-2015, 2015.

Pun, B. K., Seigneur, C., Grosjean, D., and Saxena, P.: Gas-phase formation of water-soluble organic compounds in the atmosphere: A retrosynthetic analysis, J. Atmos. Chem., 35, 199-223, 2000.

Saadati, N., Abdullah, M. P., Zakaria, Z., Sany, S. B. T., Rezayi, M., and Hassonizadeh, H.: Limit of detection and limit of quantification development procedures for organochlorine pesticides analysis in water and sediment matrices, Chemistry Central Journal, 7, 63, 2013.

Schulte, J. K., Fox, J. R., Oron, A. P., Larson, T. V., Simpson, C. D., Paulsen, M., Beaudet, N., Kaufman, J. D., and Magzamen, S.: Neighborhood-Scale Spatial Models of Diesel Exhaust Concentration Profile Using 1-Nitropyrene and Other Nitroarenes, Environ. Sci. Technol., 49, 13422-13430, 10.1021/acs.est.5b03639, 2015.

Sciare, J., D'Argouges, O., Sarda-Esteve, R., Gaimoz, C., Dolgorouky, C., Bonnaire, N., Favez, O., Bonsang, B., and Gros, V.: Large contribution of water-insoluble secondary organic aerosols in the region of Paris (France) during wintertime, J. Geophys. Res.-Atmos., 116, D22203, 10.1029/2011jd015756, 2011.

Shrivastava, M. K., Subramanian, R., Rogge, W. F., and Robinson, A. L.: Sources of organic aerosol: Positive matrix factorization of molecular marker data and comparison of results from different source apportionment models, Atmos. Environ., 41, 9353-9369, 10.1016/j.atmosenv.2007.09.016, 2007.

Simoneit, B. R.: A review of biomarker compounds as source indicators and tracers for air pollution, Environ. Sci. Pollut. Res., 6, 159-169, 1999.

Simoneit, B. R., Schauer, J. J., Nolte, C., Oros, D. R., Elias, V. O., Fraser, M., Rogge, W., and Cass, G. R.: Levoglucosan, a tracer for cellulose in biomass burning and atmospheric particles, Atmos. Environ., 33, 173-182, 1999.

Slowik, J. G., Vlasenko, A., McGuire, M., Evans, G. J., and Abbatt, J. P. D.: Simultaneous factor analysis of organic particle and gas mass spectra: AMS and PTR-MS measurements at an urban site, Atmos. Chem. Phys., 10, 1969-1988, 10.5194/acp-10-1969-2010, 2010.

Sofowote, U. M., Healy, R. M., Su, Y., Debosz, J., Noble, M., Munoz, A., Jeong, C. H., Wang, J. M., Hilker, N., Evans, G. J., and Hopke, P. K.: Understanding the PM2.5 imbalance between a far and near-road location: Results of high temporal frequency source apportionment and parameterization of black carbon, Atmos. Environ., 173, 277-288, https://doi.org/10.1016/j.atmosenv.2017.10.063, 2018.

Srivastava, D., Favez, O., Bonnaire, N., Lucarelli, F., Perraudin, E., Gros, V., Villenave, E., and Albinet, A.: Speciation of organic fractions does matter for aerosol source apportionment. Part 2: intensive campaign in the Paris area (France), Sci. Total Environ., Under review, 2018a.

Srivastava, D., Tomaz, S., Favez, O., Lanzafame, G. M., Golly, B., Besombes, J.-L., Alleman, L. Y., Jaffrezo, J.-L., Jacob, V., Perraudin, E., Villenave, E., and Albinet, A.: Speciation of organic fraction does matter for source apportionment. Part 1: A one-year campaign in Grenoble (France), Sci. Total Environ., In press, https://doi.org/10.1016/j.scitotenv.2017.12.135, 2018b.

Sullivan, R. C., and Prather, K. A.: Investigations of the Diurnal Cycle and Mixing State of Oxalic Acid in Individual Particles in Asian Aerosol Outflow, Environ. Sci. Technol., 41, 8062-8069, 10.1021/es071134g, 2007.

Sun, Y., Zhang, Q., Schwab, J., Yang, T., Ng, N., and Demerjian, K.: Factor analysis of combined organic and inorganic aerosol mass spectra from high resolution aerosol mass spectrometer measurements, Atmos. Chem. Phys., 12, 8537-8551, 2012.

Surratt, J. D., Chan, A. W., Eddingsaas, N. C., Chan, M., Loza, C. L., Kwan, A. J., Hersey, S. P., Flagan, R. C., Wennberg, P. O., and Seinfeld, J. H.: Reactive intermediates revealed in secondary organic aerosol formation from isoprene, Proc. Natl. Acad. Sci., 107, 6640-6645, 2010.

Tomaz, S., Shahpoury, P., Jaffrezo, J. L., Lammel, G., Perraudin, E., Villenave, E., and Albinet, A.: One-year study of polycyclic aromatic compounds at an urban site in Grenoble (France): Seasonal variations, gas/particle partitioning and cancer risk estimation, Sci. Total Environ., 565, 1071-1083, 10.1016/j.scitotenv.2016.05.137, 2016.

Tomaz, S., Jaffrezo, J.-L., Favez, O., Perraudin, E., Villenave, E., and Albinet, A.: Sources and atmospheric chemistry of oxy- and nitro-PAHs in the ambient air of Grenoble (France), Atmos. Environ., 161, 144-154, https://doi.org/10.1016/j.atmosenv.2017.04.042, 2017.

Ulbrich, I. M., Canagaratna, M. R., Zhang, Q., Worsnop, D. R., and Jimenez, J. L.: Interpretation of organic components from Positive Matrix Factorization of aerosol mass spectrometric data, Atmos. Chem. Phys., 9, 2891-2918, 10.5194/acp-9-2891-2009, 2009.

Verlhac, S., Favez, O., and Albinet, A.: Comparaison inter laboratoires organisée pour les laboratoires européens impliqués dans l'analyse du lévoglucosan et de ses isomères LCSQA / INERIS http://www.lcsqa.org/rapport/2013/ineris/comparaison-inter-laboratoires-organisee-laboratoires-europeens-impliques-analys, 2013.

Vlachou, A., Daellenbach, K. R., Bozzetti, C., Chazeau, B., Salazar, G. A., Szidat, S., Jaffrezo, J. L., Hueglin, C., Baltensperger, U., El Haddad, I., and Prévôt, A. S. H.: Advanced source apportionment of carbonaceous aerosols by coupling offline AMS and radiocarbon size segregated measurements over a nearly two-year period, Atmos. Chem. Phys. Discuss., 2017, 1-25, 10.5194/acp-2017-1102, 2017.

Waked, A., Favez, O., Alleman, L. Y., Piot, C., Petit, J. E., Delaunay, T., Verlinden, E., Golly, B., Besombes, J. L., Jaffrezo, J. L., and Leoz-Garziandia, E.: Source apportionment of PM10 in a north-western Europe regional urban background site (Lens, France) using positive matrix factorization and including primary biogenic emissions, Atmos. Chem. Phys., 14, 3325-3346, 10.5194/acp-14-3325-2014, 2014.

Xu, L., Guo, H., Boyd, C. M., Klein, M., Bougiatioti, A., Cerully, K. M., Hite, J. R., Isaacman-VanWertz, G., Kreisberg, N. M., Knote, C., Olson, K., Koss, A., Goldstein, A. H., Hering, S. V., de Gouw, J., Baumann, K., Lee, S.-H., Nenes, A., Weber, R. J., and Ng, N. L.: Effects of anthropogenic emissions on aerosol formation from isoprene and monoterpenes in the southeastern United States, Proc. Natl. Acad. Sci., 112, 37-42, 10.1073/pnas.1417609112, 2015.

Yttri, K. E., Schnelle-Kreis, J., Maenhaut, W., Abbaszade, G., Alves, C., Bjerke, A., Bonnier, N., Bossi, R., Claeys, M., Dye, C., Evtyugina, M., García-Gacio, D., Hillamo, R., Hoffer, A., Hyder, M., Iinuma, Y., Jaffrezo, J. L., Kasper-Giebl, A., Kiss, G., López-Mahia, P. L., Pio, C., Piot, C., Ramirez-Santa-Cruz, C., Sciare, J., Teinilä, K., Vermeylen, R., Vicente, A., and Zimmermann, R.: An intercomparison study of analytical methods used for quantification of levoglucosan in ambient aerosol filter samples, Atmos. Meas. Tech., 8, 125-147, 10.5194/amt-8-125-2015, 2015.

Zhang, Q., Alfarra, M. R., Worsnop, D. R., Allan, J. D., Coe, H., Canagaratna, M. R., and Jimenez, J. L.: Deconvolution and quantification of hydrocarbon-like and oxygenated organic aerosols based on aerosol mass spectrometry, Environ. Sci. Technol., 39, 4938-4952, 2005.

Zhang, Q., Jimenez, J. L., Canagaratna, M. R., Allan, J. D., Coe, H., Ulbrich, I., Alfarra, M. R., Takami, A., Middlebrook, A. M., Sun, Y. L., Dzepina, K., Dunlea, E., Docherty, K., DeCarlo, P. F., Salcedo, D., Onasch, T., Jayne, J. T., Miyoshi, T., Shimono, A., Hatakeyama, S., Takegawa, N., Kondo, Y., Schneider, J., Drewnick, F., Borrmann, S., Weimer, S., Demerjian, K., Williams, P., Bower, K., Bahreini, R., Cottrell, L., Griffin, R. J., Rautiainen, J., Sun, J. Y., Zhang, Y. M., and Worsnop, D. R.: Ubiquity and dominance of oxygenated species in organic aerosols in anthropogenically-influenced Northern Hemisphere midlatitudes, Geophys. Res. Lett., 34, 10.1029/2007gl029979, 2007.

Zhang, Q., Jimenez, J. L., Canagaratna, M. R., Ulbrich, I. M., Ng, N. L., Worsnop, D. R., and Sun, Y.: Understanding atmospheric organic aerosols via factor analysis of aerosol mass spectrometry: a review, Anal. Bioanal. Chem., 401, 3045-3067, 2011.

Zhang, Y., Sheesley, R. J., Schauer, J. J., Lewandowski, M., Jaoui, M., Offenberg, J. H., Kleindienst, T. E., and Edney, E. O.: Source apportionment of primary and secondary organic aerosols using positive matrix factorization (PMF) of molecular markers, Atmos. Environ., 43, 5567-5574, 2009.

Zhang, Y., Tang, L., Sun, Y., Favez, O., Canonaco, F., Albinet, A., Couvidat, F., Liu, D., Jayne, J. T., Wang, Z., Croteau, P. L., Canagaratna, M. R., Zhou, H.-c., Prévôt, A. S. H., and Worsnop, D. R.: Limited formation of isoprene epoxydiols-derived secondary organic aerosol under NOx-rich environments in Eastern China, Geophys. Res. Lett., 44, 10.1002/2016GL072368, 2017.

Zhang, Y. J., Tang, L. L., Wang, Z., Yu, H. X., Sun, Y. L., Liu, D., Qin, W., Canonaco, F., Prévôt, A. S. H., Zhang, H. L., and Zhou, H. C.: Insights into characteristics, sources, and evolution of submicron aerosols during harvest seasons in the Yangtze River delta region, China, Atmos. Chem. Phys., 15, 1331-1349, 10.5194/acp-15-1331-2015, 2015.

Zhou, L., Hopke, P. K., Paatero, P., Ondov, J. M., Pancras, J. P., Pekney, N. J., and Davidson, C. I.: Advanced factor analysis for multiple time resolution aerosol composition data, Atmos. Environ., 38, 4909-4920, https://doi.org/10.1016/j.atmosenv.2004.05.040, 2004.

Zielinska, B., Sagebiel, J., Arnott, W. P., Rogers, C. F., Kelly, K. E., Wagner, D. A., Lighty, J. S., Sarofim, A. F., and Palmer, G.: Phase and Size Distribution of Polycyclic Aromatic Hydrocarbons in Diesel and Gasoline Vehicle Emissions, Environ. Sci. Technol., 38, 2557-2567, 10.1021/es030518d, 2004a.

Zielinska, B., Sagebiel, J., McDonald, J. D., Whitney, K., and Lawson, D. R.: Emission rates and comparative chemical composition from selected in-use diesel and gasoline-fueled vehicles, J. Air Waste Manage. Assoc., 54, 1138-1150, 2004b.

Ziemann, P. J., and Atkinson, R.: Kinetics, products, and mechanisms of secondary organic aerosol formation, Chem. Soc. Rev., 41, 6582-6605, 10.1039/c2cs35122f, 2012.

Zorn, S. R., Drewnick, F., Schott, M., Hoffmann, T., and Borrmann, S.: Characterization of the South Atlantic marine boundary layer aerosol using an aerodyne aerosol mass spectrometer, Atmos. Chem. Phys., 8, 4711-4728, 10.5194/acp-8-4711-2008, 2008.

Supplementary Material

Combining off-line and on-line measurements does help differentiating between the different organic aerosols fractions

D. Srivastava[1,2,3], O. Favez[1*], J-E. Petit[4], Y. Zhang[1], U. M. Sofowote[5], P.K. Hopke[6,7], N. Bonnaire[4], E. Perraudin[2,3], V. Gros[4], E. Villenave[2,3], A. Albinet[1*]

[1]INERIS, Parc Technologique Alata, BP 2, 60550 Verneuil-en-Halatte, France

[2]CNRS, EPOC, UMR 5805 CNRS, 33405 Talence, France

[3]Université de Bordeaux, EPOC, UMR 5805 CNRS, 33405 Talence, France

[4]LSCE - UMR8212, CNRS-CEA-UVSQ, Gif-sur-Yvette, France

[5]Environmental Monitoring and Reporting Branch, Ontario Ministry of the Environment and Climate Change, Toronto, Canada

[6]Center for Air Resources Engineering and Science, Clarkson University, Potsdam, NY, USA

[7]Department of Public Health Sciences, University of Rochester School of Medicine and Dentistry, Rochester, NY USA

*Correspondence to: alexandre.albinet@ineris.fr; olivier.favez@ineris.fr

In preparation for publication in Atmospheric Chemistry & Physics

Table S1. Original and adjusted instrumental detection limit (DL) (ng m^{-3}) for molecular markers (4-hr, PM_{10} filter) used in this study.

Species	Original DL	Adjusted DL
EC	$1.5\times10^{+02}$	$3.0\times10^{+02}$
Methanesulfonic acid (MSA)	4.6×10^{-01}	$1.7\times10^{+00}$
Oxalate (Ox)	4.6×10^{-01}	$4.5\times10^{+00}$
Levoglucosan (Levo)	$1.2\times10^{+00}$	$1.2\times10^{+00}$
6H-Dibenzo[b,d]pyran-6-one (6H-DPone)	1.9×10^{-04}	4.0×10^{-03}
Benzo[a]fluorenone (B[a]Fone)	2.5×10^{-05}	4.5×10^{-05}
Benzo[b]fluorenone (B[b]Fone)	5.1×10^{-05}	5.1×10^{-05}
9-Nitroanthracene (9-NA)	3.7×10^{-05}	5.0×10^{-03}
2-Nitrofluoranthene (2-Nflt)	3.8×10^{-05}	2.2×10^{-03}
1-Nitropyrene (1-NP)	2.9×10^{-05}	2.9×10^{-03}
2,3-Dihydroxy-4-oxopentanoic acid (DHOPA)	1.2×10^{-03}	7.2×10^{-03}
4-Methyl-5-Nitrocatechol (4-Me5Nc)	4.5×10^{-03}	4.5×10^{-02}
3-Methyl-5-Nitrocatechol (3-Me5Nc)	1.2×10^{-02}	1.2×10^{-02}
α-Methylglyceric acid (α-MGA)	5.7×10^{-04}	4.1×10^{-02}
2-Methylerythritol (2-MT)	1.4×10^{-03}	1.4×10^{-03}

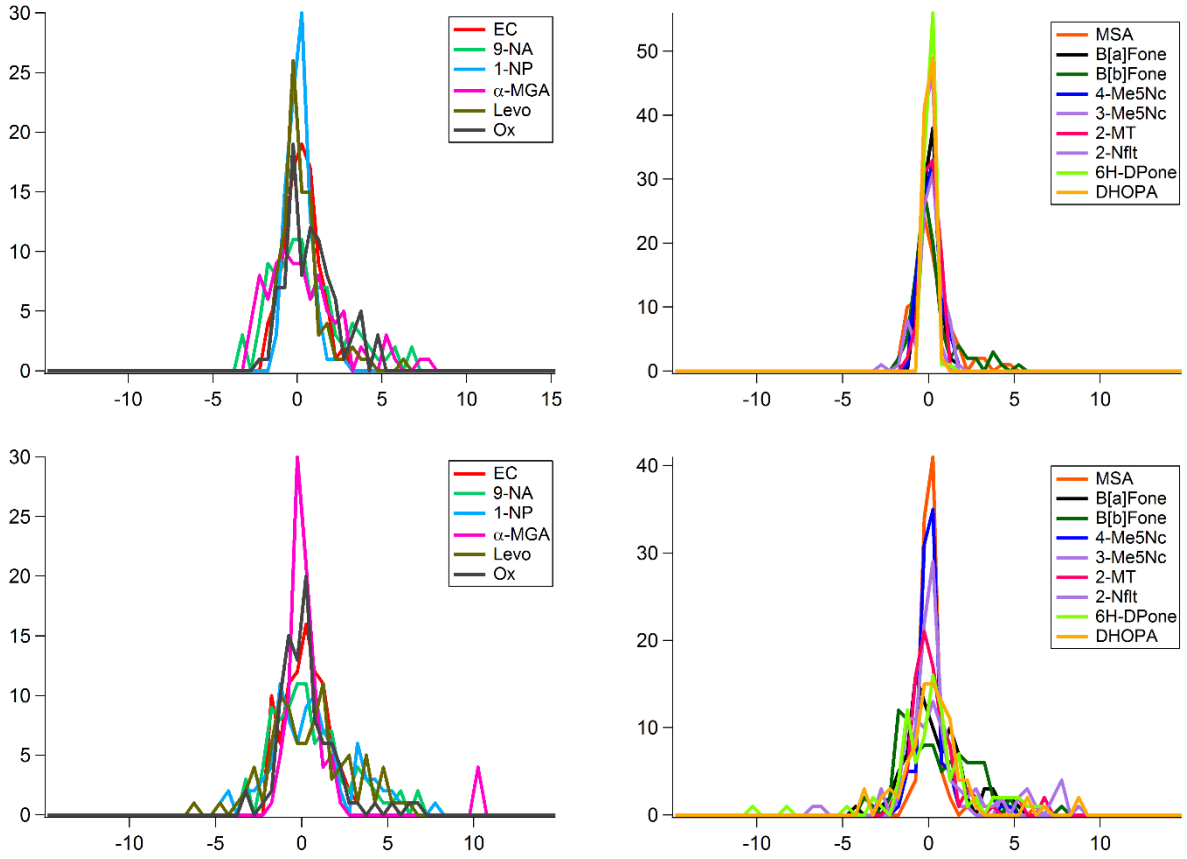

Figure S1. Residuals observed for all organic markers used in the combined ME-2 analysis. Upper panel represents the residuals linked to the optimized error values. Lower panel represents the residuals linked to the original errors without any optimization.

Table S2. Mean, min-max, concentrations (ng m^{-3}) of all organic molecular markers used in the input matrix for the ME2 analysis (n=92, PM_{10} filter samples).

Species	Mean concentrations	Min	Max
EC	$1.20\times10^{+03}$	$1.30\times10^{+02}$	$3.19\times10^{+03}$
Methanesulfonic acid (MSA)	$3.94\times10^{+01}$	9.70×10^{-01}	$1.97\times10^{+02}$
Oxalate (Ox)	$1.93\times10^{+02}$	$5.28\times10^{+01}$	$5.41\times10^{+02}$
Levoglucosan (Levo)	$2.97\times10^{+02}$	$2.00\times10^{+01}$	$1.11\times10^{+03}$
6H-Dibenzo[b,d]pyran-6-one (6H-DPone)	6.82×10^{-01}	5.58×10^{-04}	$3.14\times10^{+00}$
Benzo[a]fluorenone (B[a]Fone)	1.06×10^{-01}	1.73×10^{-02}	5.47×10^{-01}
Benzo[b]fluorenone (B[b]Fone)	1.26×10^{-01}	2.10×10^{-02}	6.36×10^{-01}
9-Nitroanthracene (9-NA)	7.34×10^{-02}	3.61×10^{-03}	5.20×10^{-01}
2-Nitrofluoranthene (2-Nflt)	9.61×10^{-02}	4.34×10^{-03}	6.39×10^{-01}
1-Nitropyrene (1-NP)	6.36×10^{-03}	1.44×10^{-03}	2.74×10^{-02}
2,3-Dihydroxy-4-oxopentanoic acid (DHOPA)	$1.49\times10^{+00}$	3.42×10^{-05}	$3.66\times10^{+00}$
4-Methyl-5-Nitrocatechol (4-Me5Nc)	$4.12\times10^{+01}$	$4.26\times10^{+00}$	$5.72\times10^{+02}$
3-Methyl-5-Nitrocatechol (3-Me5Nc)	$3.03\times10^{+01}$	$4.77\times10^{+00}$	$3.92\times10^{+02}$
α-Methylglyceric acid (α-MGA)	5.10×10^{-01}	4.08×10^{-06}	$3.98\times10^{+00}$
2-Methylerythritol (2-MT)	5.90×10^{-01}	4.43×10^{-06}	$1.32\times10^{+00}$

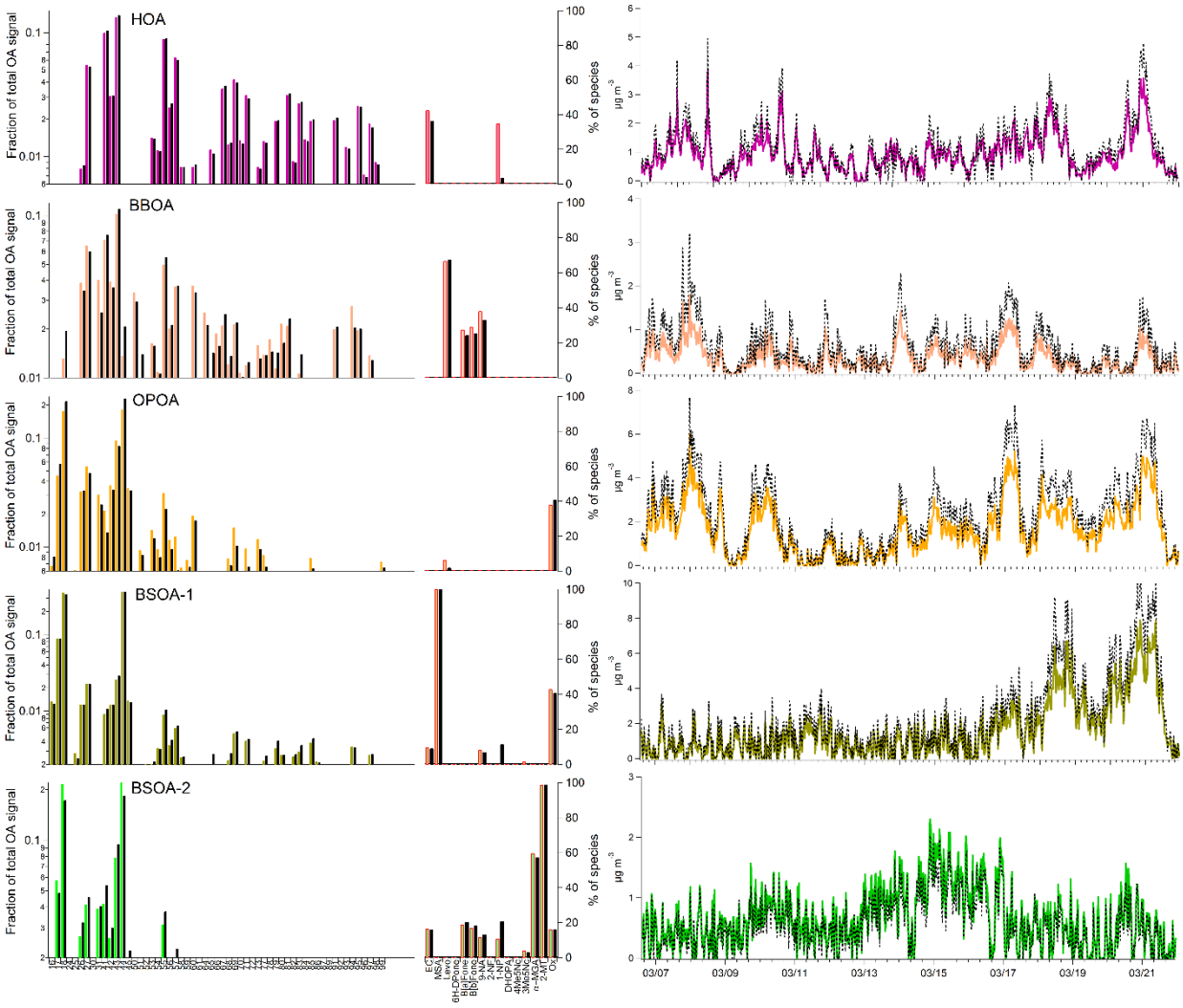

Figure S2. Source profiles and temporal evolution of HOA, BBOA, OPOA, BSOA-1 and BSOA-2 factors identified at Paris-SIRTA, France (March 2015) for base (coloured bars) and constrained (black bars) runs. Left panel: Left side; ACSM mass fragments for each factor (log scale); Right side; Contribution of organic markers in each factor. Right panel: Coloured lines; base run. Black/dashed lines; constrained run. HOA: primary traffic emissions; BBOA: biomass burning OA; OPOA: oxidized primary OA; BSOA-1: biogenic SOA-1 (marine-rich); BSOA-2: biogenic SOA-2 (isoprene oxidation).

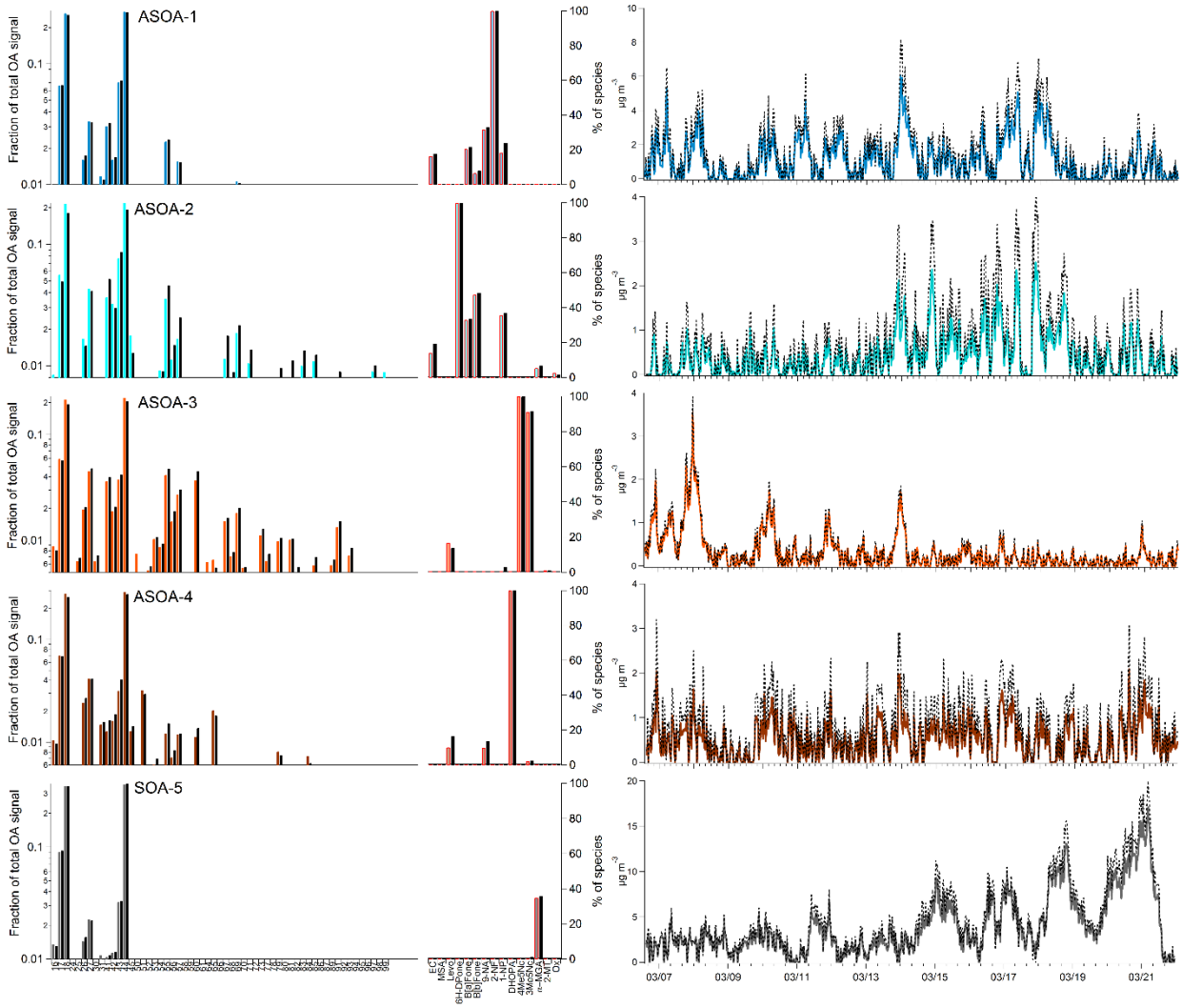

Figure S3. Source profiles and temporal evolution of ASOA-1, ASOA-2, ASOA-3, ASOA-4 and SOA-5 factors identified at Paris-SIRTA, France (March 2015) for base (coloured bars) and constrained (black bars) runs. Left panel: Left side; ACSM mass fragments for each factor (log scale); Right side; Contribution of organic markers in each factor. Right panel: Coloured lines; base run. Black/dashed lines; constrained run. ASOA-1: anthropogenic SOA-1 (oxy-PAHs); ASOA-2: anthropogenic SOA-2 (nitro-PAHs); ASOA-3: anthropogenic SOA-3 (phenolic compounds oxidation); ASOA-4: anthropogenic SOA-4 (toluene oxidation).

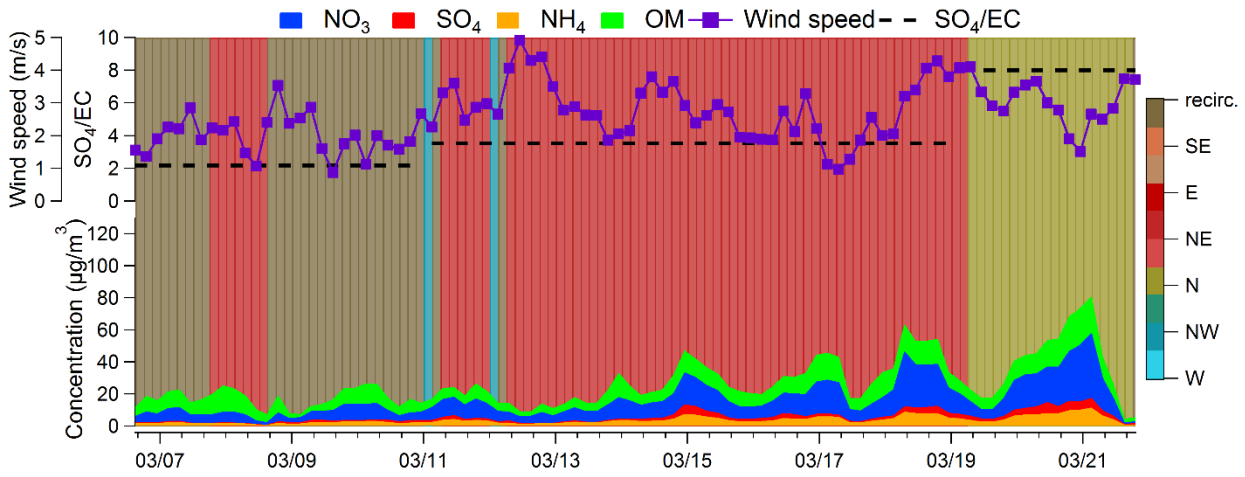

Figure S4. Temporal variation of PM_1 chemical composition, SO_4/EC ratio and wind speed observed at Paris-SIRTA, France (March 2015). Background colours refer to air mass clusters. Cluster analysis performed using ZeFir (Petit et al., 2017) based on back trajectories calculated every 3 h with HYSPLIT model (Draxler, 1999; Stein et al., 2015).

PMF analysis from the ACSM measurements

Four OA factors including two primary OA (POA) factors; HOA (hydrocarbon like OA) and BBOA (biomass burning); and two secondary OA (SOA) factors; LO-OOA (less oxidized oxygenated OA) and MO-OOA (more oxidized oxygenated OA); were resolved by PMF (Figure S8). PMF was solved using the multilinear engine (ME-2) implemented in Source Finder (SoFi) toolkit, which enables an efficient exploration of the solution space by constraining the factors elements within a certain range defined by the scalar a ($0<a<1$) (Canonaco et al., 2013).

The HOA and BBOA factors were constrained using reference mass spectra from Fröhlich et al. (2015) while the other factors were unconstrained. The HOA spectrum was characterized by peak characteristic of aliphatic hydrocarbons, including m/z 27 ($C_2H^+_3$), 41 ($C_3H^+_5$), 43 ($C_3H^+_7$), 55 ($C_4H^+_7$), 57 ($C_4H^+_9$), 69 ($C_5H^+_9$), and 71 ($C_5H^+_{11}$) (Aiken et al., 2009). The mass spectrum of BBOA was characterized by the prominent signal of m/z 60 (mainly $C_2H_4O_2^+$) and 73 ($C_3H_5O_2^+$), two markers indicative of biomass burning emissions (Lanz et al., 2007; Mohr et al., 2009). The mass spectrum of MO-OOA is characterized by a dominant peak at *m/z* 44 (CO_2^+), similar the low-volatile oxygenated OA (LV-OOA) factor determined at other urban/suburban sites (Ulbrich et al., 2009; Ng et al., 2010) The mass spectrum of LO-OOA has lower f_{44}/f_{43}. (fraction of *m/z* 43 and *m/z* 44 in the total OA signal) ratio and higher fraction of *m/z* 43 (mainly $C_2H_3O^+$) compared to MO-OOA, and similar to the semi-volatile OOA (SV-OOA) (Ng et al., 2010) (Figure S5).

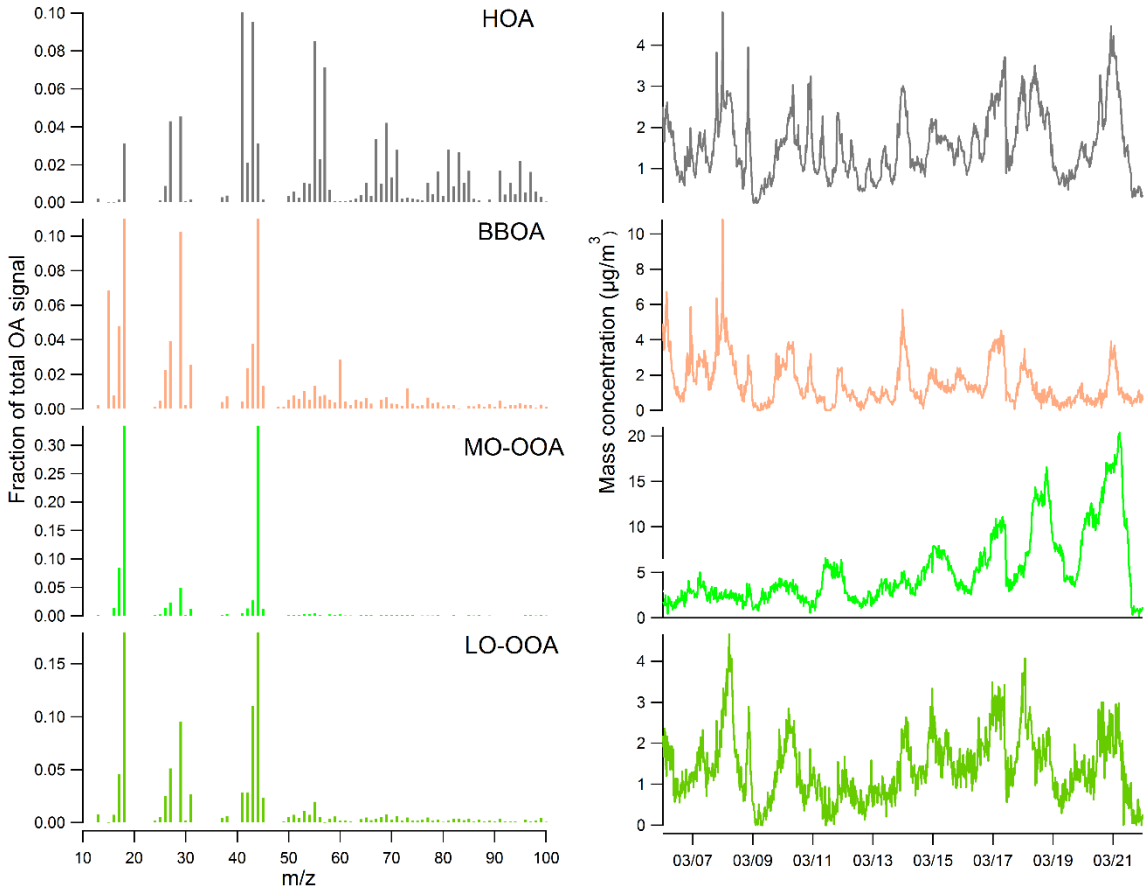

Figure S5. Chemical and temporal profiles of HOA, BBOA, MO-OOA, and LO-OOA PMF factors (from ACSM measurements) identified at Paris-SIRTA, France (March 2015). HOA (a=0.4) and BBOA (a=0.4) are constrained. HOA: hydrocarbon like OA; BBOA: biomass burning; LO-OOA: less oxidized oxygenated OA; MO-OOA: more oxidized oxygenated OA.

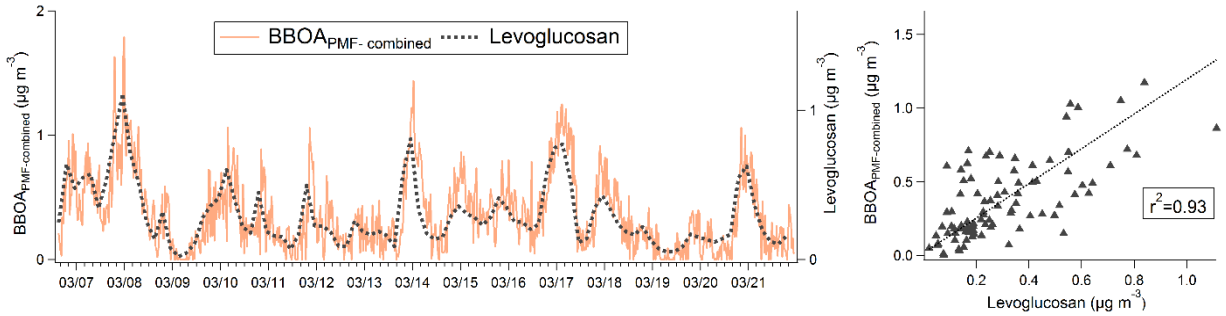

Figure S6. Temporal evolutions of $BBOA_{PMF\text{-}combined}$ and levoglucosan (left) and correlation between $BBOA_{PMF\text{-}combined}$ and levoglucosan (right) at Paris-SIRTA, France (March 2015).

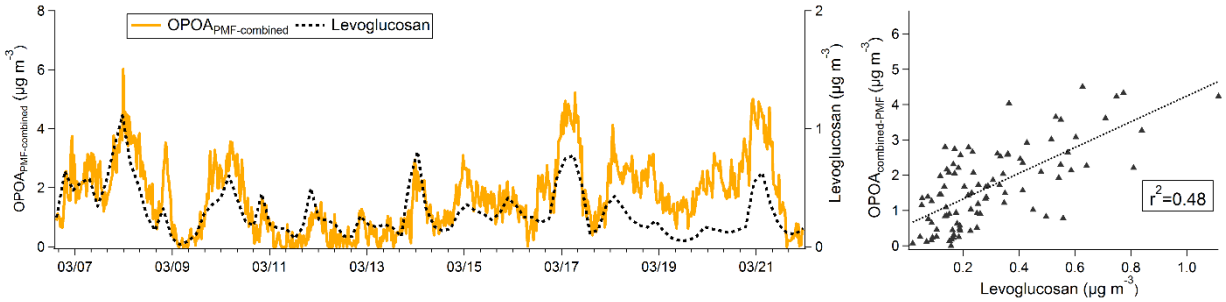

Figure S7. Temporal evolutions of $OPOA_{PMF\text{-}combined}$ and levoglucosan (left) and correlation between $OPOA_{PMF\text{-}combined}$ and levoglucosan (right) at Paris-SIRTA, France (March 2015).

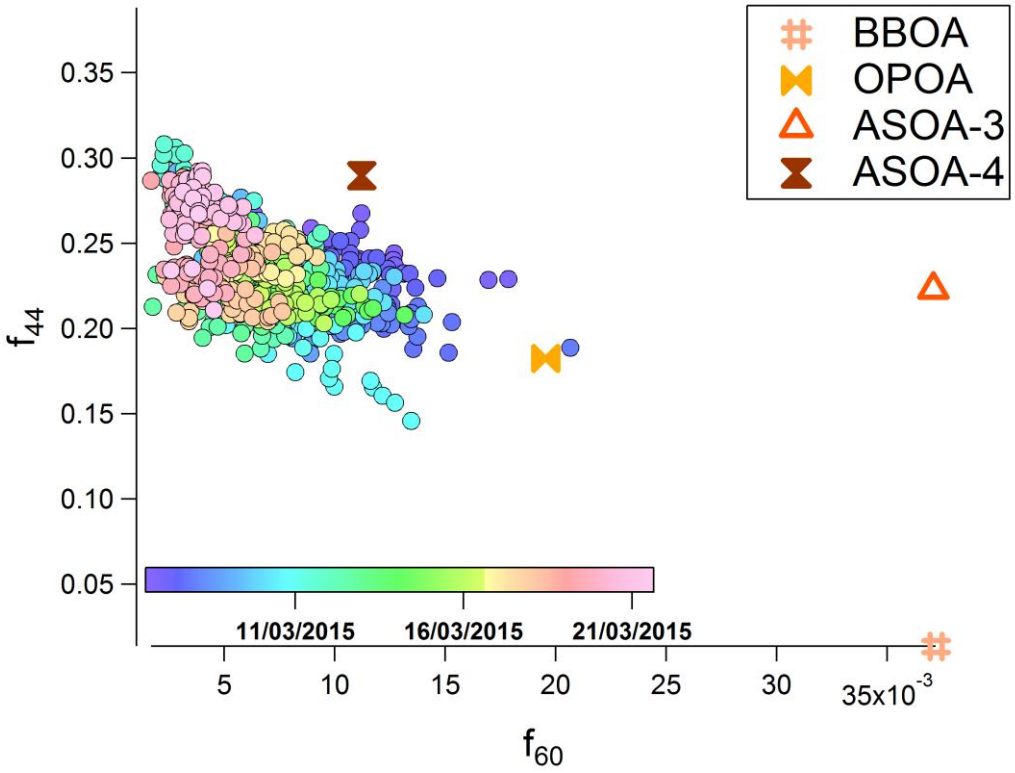

Figure S8. f_{44} vs. f_{60} triangle plot for all OA factors related to biomass burning. f_{44} and f_{60} represents the fractions of m/z 44 and m/z 60 in OA obtained from ACSM measurements, respectively. The dots are coloured according to the sampling dates. BBOA: biomass burning OA; OPOA: oxidized primary OA; ASOA-3: anthropogenic SOA-3 (phenolic compounds oxidation); ASOA-4: anthropogenic SOA-4 (toluene oxidation).

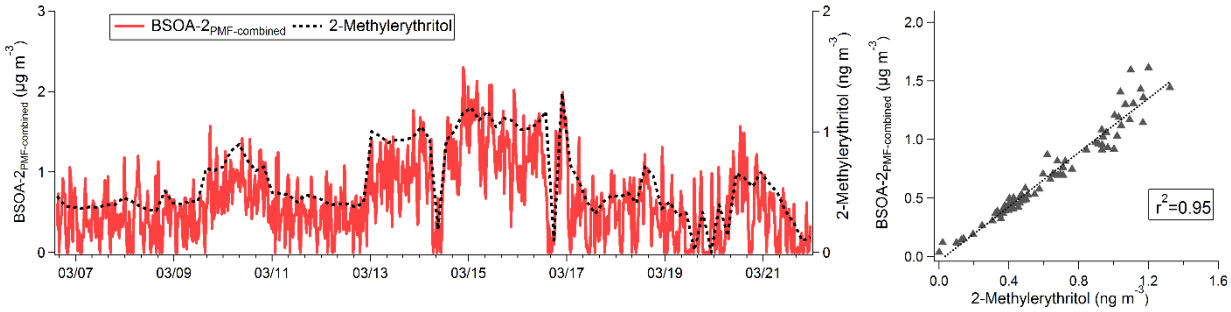

Figure S9. Temporal evolutions of BSOA-$2_{PMF\text{-}combined}$ and 2-methylerythritol (left) and correlation between BSOA-$2_{PMF\text{-}combined}$ and 2-methylerythritol (right) at Paris-SIRTA, France (March 2015). BSOA-2: biogenic SOA-2 (isoprene oxidation).

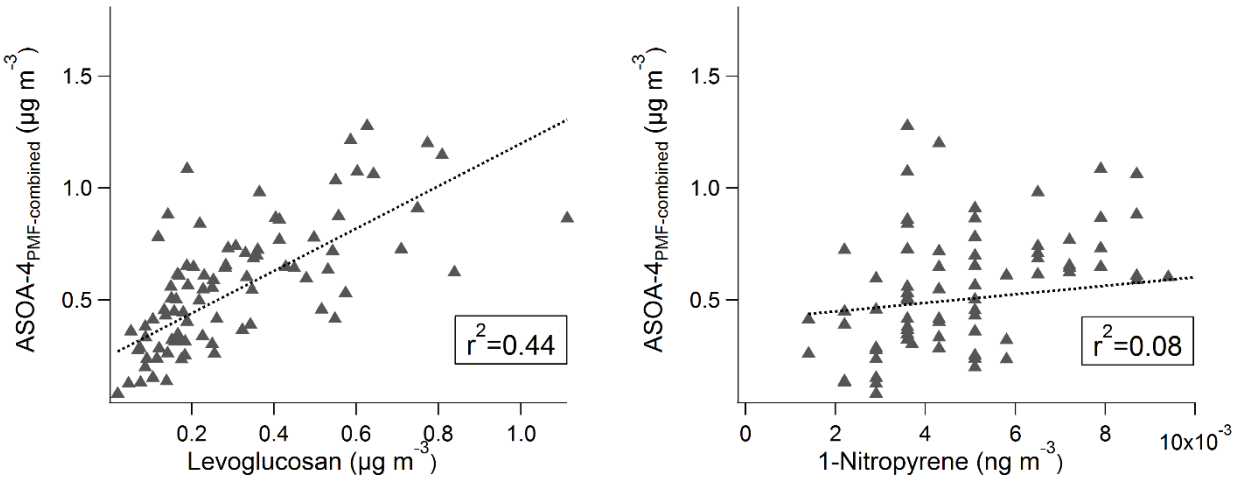

Figure S10. Correlations observed between ASOA-$4_{PMF\text{-}combined}$ and levoglucosan (left) and ASOA-$4_{PMF\text{-}combined}$ and 1-nitropyrene (right). ASOA-4: anthropogenic SOA-4 (toluene oxidation).

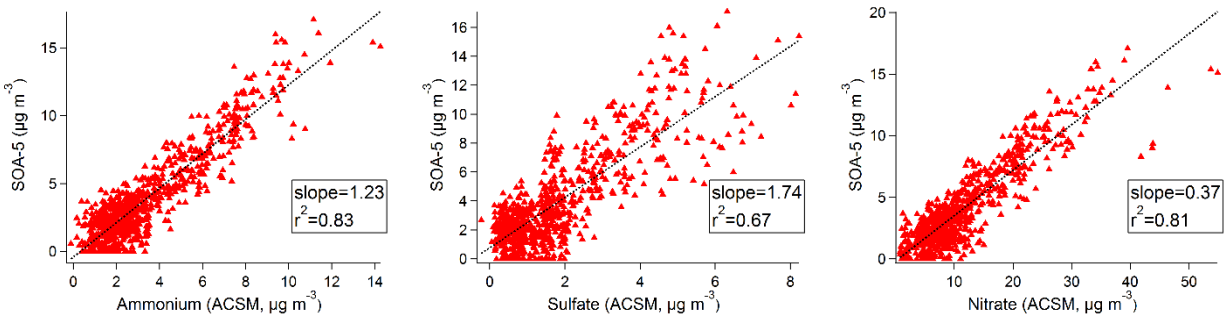

Figure S11. Correlations observed between SOA-5 and secondary inorganic species (ammonium, sulfate and nitrate).

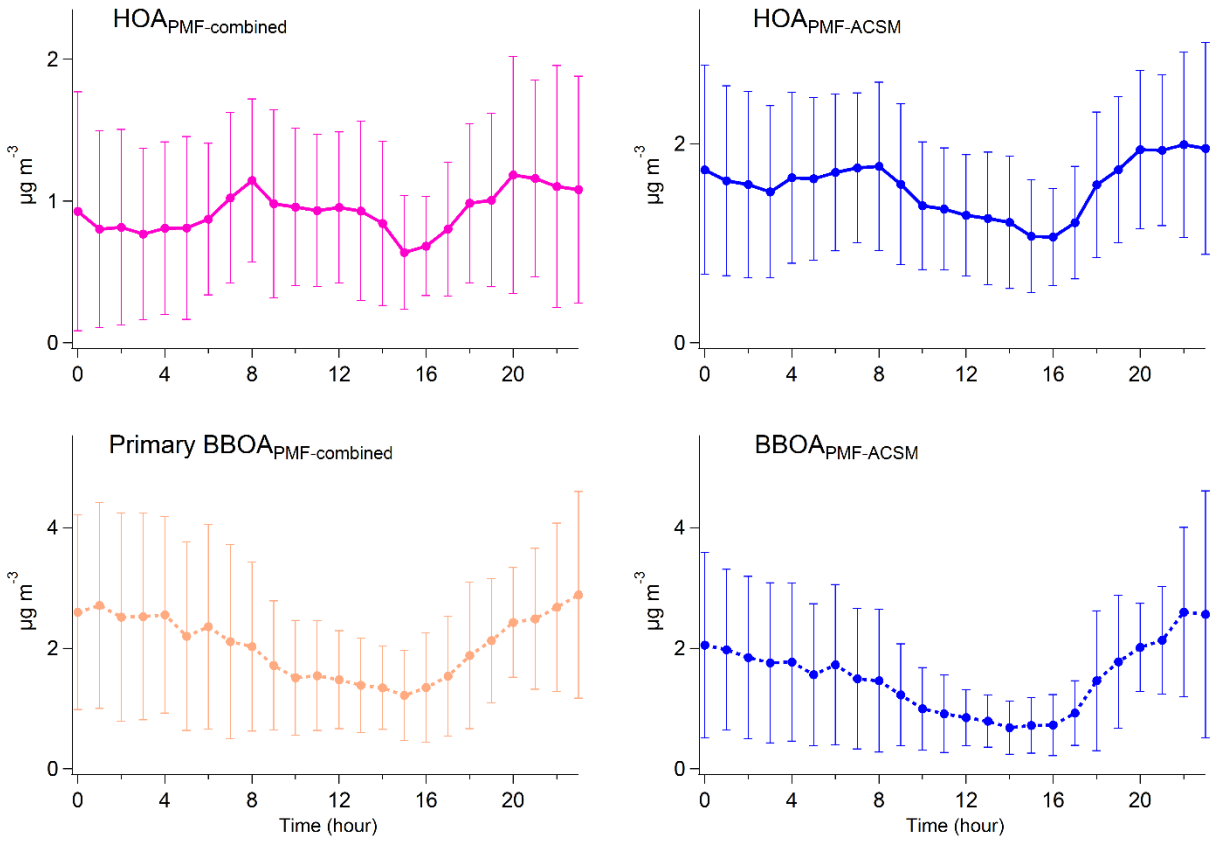

Figure S12. Diurnal profiles of HOA and BBOA sources resolved from the PMF-combined and PMF-ACSM analyses. Error bars show ± 2 SD (standard deviation).

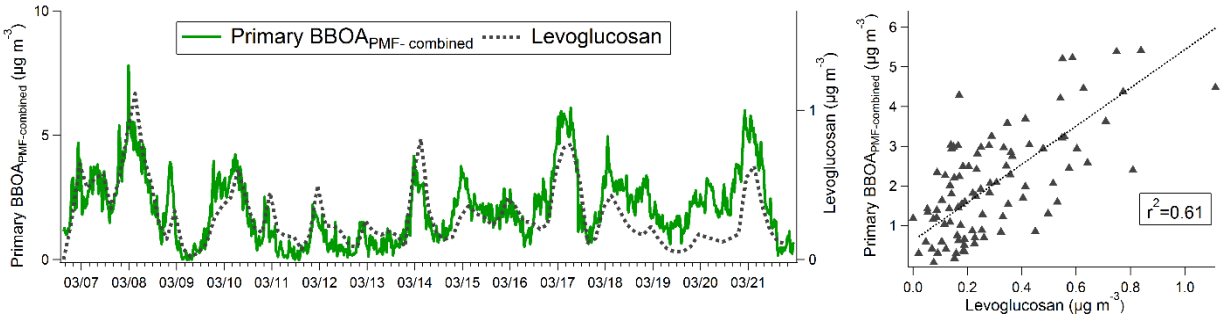

Figure S13. Temporal evolutions of primary $BBOA_{PMF\text{-}combined}$ and levoglucosan (left) and correlation between primary $BBOA_{PMF\text{-}combined}$ and levoglucosan (right) at Paris-SIRTA, France (March 2015).

Table S3. Correlations (r^2) between all SOA factors from the combined PMF and PMF-ACSM analyses. SOA factors resolved from the combined PMF analysis, BSOA-1: biogenic SOA-1 (marine-rich); BSOA-2: biogenic SOA-2 (isoprene oxidation); ASOA-1: anthropogenic SOA-1 (oxy-PAHs); ASOA-2: anthropogenic SOA-2 (nitro-PAHs); ASOA-3: anthropogenic SOA-3 (phenolic compounds oxidation); ASOA-4: anthropogenic SOA-4 (toluene oxidation). OOA factors resolved from the ACSM PMF analysis, MO-OOA: more oxidized oxygenated OA; LO-OOA: low oxidized oxygenated OA.

	BSOA-1	*BSOA-2*	*ASOA-1*	*ASOA-2*	*ASOA-3*	*ASOA-4*	*SOA-5*	*MO-OOA*	*LO-OOA*
BSOA-1	1.00								
BSOA-2	0.02	1.00							
ASOA-1	0.00	0.01	1.00						
ASOA-2	0.01	0.08	0.16	1.00					
ASOA-3	0.06	0.00	0.09	0.00	1.00				
ASOA-4	0.01	0.09	0.08	0.03	0.10	1.00			
SOA-5	0.53	0.00	0.02	0.02	0.05	0.03	1.00		
MO-OOA	0.76	0.00	0.00	0.06	0.05	0.05	0.89	1.00	
LO-OOA	0.05	0.06	0.24	0.16	0.07	0.13	0.13	0.13	1.00

References

Aiken, A. C., Salcedo, D., Cubison, M. J., Huffman, J. A., DeCarlo, P. F., Ulbrich, I. M., Docherty, K. S., Sueper, D., Kimmel, J. R., Worsnop, D. R., Trimborn, A., Northway, M., Stone, E. A., Schauer, J. J., Volkamer, R. M., Fortner, E., de Foy, B., Wang, J., Laskin, A., Shutthanandan, V., Zheng, J., Zhang, R., Gaffney, J., Marley, N. A., Paredes-Miranda, G., Arnott, W. P., Molina, L. T., Sosa, G., and Jimenez, J. L.: Mexico City aerosol analysis during MILAGRO using high resolution aerosol mass spectrometry at the urban supersite (T0) – Part 1: Fine particle composition and organic source apportionment, Atmos. Chem. Phys., 9, 6633-6653, 10.5194/acp-9-6633-2009, 2009.

Canonaco, F., Crippa, M., Slowik, J., Baltensperger, U., and Prévôt, A.: SoFi, an IGOR-based interface for the efficient use of the generalized multilinear engine (ME-2) for the source apportionment: ME-2 application to aerosol mass spectrometer data, Atmos. Meas. Tech., 6, 3649-3661, 2013.

Draxler, R.: Hysplit4 User's Guide. NOAA Tech. Memo. ERL ARL-230, 35 pp. http://www.arl.noaa.gov/documents/reports/hysplit_user_guide.pdf, 1999.

Fröhlich, R., Crenn, V., Setyan, A., Belis, C. A., Canonaco, F., Favez, O., Riffault, V., Slowik, J. G., Aas, W., Aijälä, M., Alastuey, A., Artiñano, B., Bonnaire, N., Bozzetti, C., Bressi, M., Carbone, C., Coz, E., Croteau, P. L., Cubison, M. J., Esser-Gietl, J. K., Green, D. C., Gros, V., Heikkinen, L., Herrmann, H., Jayne, J. T., Lunder, C. R., Minguillón, M. C., Močnik, G., O'Dowd, C. D., Ovadnevaite, J., Petralia, E., Poulain, L., Priestman, M., Ripoll, A., Sarda-Estève, R., Wiedensohler, A., Baltensperger, U., Sciare, J., and Prévôt, A. S. H.: ACTRIS ACSM intercomparison – Part 2: Intercomparison of ME-2 organic source apportionment results from 15 individual, co-located aerosol mass spectrometers, Atmos. Meas. Tech., 8, 2555-2576, 10.5194/amt-8-2555-2015, 2015.

Lanz, V. A., Alfarra, M. R., Baltensperger, U., Buchmann, B., Hueglin, C., and Prévôt, A. S. H.: Source apportionment of submicron organic aerosols at an urban site by factor analytical modelling of aerosol mass spectra, Atmos. Chem. Phys., 7, 1503-1522, 10.5194/acp-7-1503-2007, 2007.

Mohr, C., Huffman, J. A., Cubison, M. J., Aiken, A. C., Docherty, K. S., Kimmel, J. R., Ulbrich, I. M., Hannigan, M., and Jimenez, J. L.: Characterization of Primary Organic Aerosol Emissions from Meat Cooking, Trash Burning, and Motor Vehicles with High-Resolution Aerosol Mass Spectrometry and Comparison with Ambient and Chamber Observations, Environ. Sci. Technol., 43, 2443-2449, 10.1021/es8011518, 2009.

Ng, N. L., Canagaratna, M. R., Zhang, Q., Jimenez, J. L., Tian, J., Ulbrich, I. M., Kroll, J. H., Docherty, K. S., Chhabra, P. S., Bahreini, R., Murphy, S. M., Seinfeld, J. H., Hildebrandt, L., Donahue, N. M., DeCarlo, P. F., Lanz, V. A., Prévôt, A. S. H., Dinar, E., Rudich, Y., and Worsnop, D. R.: Organic aerosol components observed in Northern Hemispheric datasets from Aerosol Mass Spectrometry, Atmos. Chem. Phys., 10, 4625-4641, 10.5194/acp-10-4625-2010, 2010.

Petit, J. E., Favez, O., Albinet, A., and Canonaco, F.: A user-friendly tool for comprehensive evaluation of the geographical origins of atmospheric pollution: Wind and trajectory analyses, Environ. Modell. Softw., 88, 183-187, https://doi.org/10.1016/j.envsoft.2016.11.022, 2017.

Stein, A. F., Draxler, R. R., Rolph, G. D., Stunder, B. J. B., Cohen, M. D., and Ngan, F.: NOAA's HYSPLIT Atmospheric Transport and Dispersion Modeling System, Bull. Am. Meteorol. Soc., 96, 2059-2077, 10.1175/bams-d-14-00110.1, 2015.

Ulbrich, I. M., Canagaratna, M. R., Zhang, Q., Worsnop, D. R., and Jimenez, J. L.: Interpretation of organic components from Positive Matrix Factorization of aerosol mass spectrometric data, Atmos. Chem. Phys., 9, 2891-2918, 10.5194/acp-9-2891-2009, 2009.

Chapter VII

Conclusions and perspectives

The main goal of the present experimental PhD work was to investigate methodologies dedicated to the source apportionment of POA and SOA fractions. It has been accomplished following four major steps.

First, an extensive review of previous studies using common OA source apportionment methodologies was achieved to document their major benefits and limitations, and to provide a synthetic picture of POA and SOA distributions at the global scale. Those included the EC tracer method, CMB, SOA tracer method, (^{14}C) radiocarbon measurements and PMF. A comparison of the SOC estimates obtained worldwide, has been investigated with a review of the studies reported from 2006 to 2016, focusing then on the most recent information available on SOC estimations. The results reported worldwide on SOC estimates obtained by different methodologies showed that SOC constitutes a significant fraction of OC. Such methodologies witness a certain number of uncertainties but they finally provide quite consistent results especially for warm periods (spring-summer). Therefore, the appropriate methodology should be selected very carefully because each approach has its own advantages and disadvantages. The SOA tracer method tends to underestimate the SOC estimates, particularly for China. SOC from the oxidation of numerous other VOC and SVOC/IVOCS (i.e. alkanes, polycyclic aromatic compounds (PAHs), phenolic compounds….) is not considered using such methodology, only one anthropogenic marker (2,3-dihdroxy-4-oxopentanoic acid, DHOPA) from toluene photooxidation is accounted in the SOA tracer method to estimate the SOA from anthropogenic sources and could explain the observed SOC underestimation using the SOA tracer method.

Overall, the different methodologies to apportion SOC present a good agreement. This review work also highlighted that only a detailed chemical characterization at a molecular level and the use of key species, i.e. molecular markers, allow to get a definitive link between SOC content and SOA sources.

In a second step, a special attention has been put to highlight the benefits of the use of molecular markers for OA source apportionment. To do so, an experimental work, based on two field campaigns, has been conducted. They have been carried out in Grenoble (urban site) over one year in 2013 and in the Paris area (suburban site of SIRTA) during an intense PM pollution event (March 2015).

Prior to sample analyses, the procedures of quantification of PAH derivatives (oxy-and nitro-PAHs) and SOA markers have been improved and/or developed. Slight modifications have been made in the protocol used for the analyses of nitro-and oxy-PAHs of the SIRTA samples. The purification step has been improved to make it more automated and a change in the GC column used for the analysis has been made to improve the separation of key compounds such as 2- and 3-nitrofluoranthenes. The method developed for the SOA markers analysis has been applied to a standard reference material (NIST SRM1649b, urban dust) and used as validation within an inter-comparison of the results obtained from three laboratories, namely INERIS (France), NIST (USA) and LSCE (France), using different analytical procedures (GC/MS or LC/MS-MS following QuEChERS-like and/or sonication extractions). Notably the quantification has been based on authentic standards for all the SOA markers compounds. The results showed good consistency for most of the compounds except for succinic acid and 2-C-methyl-D-erythritol. The observed concentration values for these two compounds have shown large variation, making it difficult to provide any common range. Interestingly, the efficacy of both extraction procedures, sonication and QuEChERS, was similar for all the analysed SOA markers.

The identification of rarely apportioned sources in both case studies (Grenoble and SIRTA) was finally based on the use of polyols, cellulose combustion products, odd number higher alkanes, and of several SOA markers related to the oxidation of isoprene, α-pinene, toluene, phenolic compounds and PAHs. Nine OA sources were resolved at Grenoble, including sources

rarely apportioned such as primary biogenics (fungal spores + plant debris) as well as explicit SOA factors (biogenic SOA formed from α-pinene or isoprene oxidation, and anthropogenic SOA formed from precursors including PAHs and toluene oxidation). Overall, the major contributors to OC were biomass burning (25%), primary traffic (12%), mineral dust (13%), fungal spores (12%), secondary inorganics (11%) and plant debris (10%), followed by both SOA fractions (14% in total) and aged sea salt (3%). These results highlighted the large contributions of primary OA sources, namely, biomass burning, traffic and biogenic source (59% in total on an annual average). The significant impact of biomass burning within OC was in good agreement with previous findings at Grenoble.

For the first time, the use of PAH derivatives (oxy-PAHs) in the PMF model has been demonstrated to apportion anthropogenic SOA (PAH SOA) at Grenoble. This source accounted for 15% of OC in winter and up to 42% of OC (18% of PM_{10}) during an intense wintertime PM pollution event. This could be explained by the accumulation of pollutants due to specific meteorological conditions and the enhancement of SOA formation via probable Fenton-like reactions, in link with the very high concentrations of metallic species and notably the transition metals (Fe, Cu, Cr, V…) observed during this period, and self-amplification cycle of SOA formation. These results also showed that the SOA from the oxidation of PAHs could account significantly to total SOA and OA concentrations in urban influenced environments. In this PhD work, attempts were also made to investigate the origins of Humic Like Substances (HuLiS), a significant fraction of organic matter which plays an important role in the atmosphere. Overall, 22%, 22%, 15%, and 14% of HuLiS mass were respectively associated with biomass burning, secondary inorganics, mineral dust and biogenic SOA on an annual average.

Similarly, at SIRTA, eleven OA sources were identified. Besides common factors (biomass burning, traffic, dust, sea salt, secondary inorganic aerosols), 2 specific biogenic SOA (marine

+ isoprene) and 3 anthropogenic SOA (nitro-PAHs + oxy-PAHs + phenolic oxidation) factors have been resolved. Major contributors were mineral dust (representing 20% of total OC on average for the campaign), biomass burning (19%), and mixed secondary aerosols (17%), followed by primary traffic emissions (14%) and nitrate-rich factor (11%). The use of similar markers allowed the identification of PAH SOA, accounting for 24% of the total SOC. Thus, anthropogenic SOA seems to contribute significantly to OA in urban influenced environments and the results obtained suggest the use of such markers to improve the OA or PM source apportionment and should be recommended. The apportionment of anthropogenic SOA linked to biomass burning emissions using methylnitrocatechol isomers has also been implemented in the PMF model. The results obtained showed significant contribution of this source, accounting for 11% of the total SOC mass at SIRTA in March 2015. Finally, the results obtained highlighted that 1-nitropyrene (1-NP) can be used as a good marker to trace primary traffic emissions and notably diesel exhaust ones.

However, the significant amount of OA fraction was still not clearly identified at both sites and found to be associated with sulfate- and nitrate-rich factors. Future studies are still needed to focus on the identification, and then the incorporation into PMF analysis, of molecular markers from other known SOA precursors (alkanes, alkenes, mono- and polyaromatic compounds) and of class of compounds which significantly contribute to the SOC fraction (i.e., organosulfates and organonitrates) to further discriminate the nature of OA associated with secondary inorganic sources. In addition, the use of higher time-resolution measurements could allow to get the better understanding of the atmospheric processes.

As a third step, efforts have been made to compare three different source apportionment methodologies (namely, EC- and SOA-tracer method, as well as PMF) applied on different measurements (filter-based chemical speciation datasets and offline AMS mass spectra, online ACSM mass spectra). Overall, total POC and SOC concentrations obtained from the various

approaches were globally consistent between each other, except for the SOA-tracer method. The identification of more molecular markers corresponding to SOA classes, possibly such as organonitrates and/or organosulfates, unaccounted so far, and their introduction in the latter approach, is deemed necessary to fix this discrepancy.

The primary biomass burning- and traffic-related factors were further supported by their respective diurnal profiles. They displayed a rather good consistency from one methodology to the other, with however some probable mixing issues in the cases of mass spectra PMF analyses. For individual SOA factors, mixed secondary aerosols obtained from PMF-chemical data were found to correlate well with highly oxidized OA factors retrieved from mass spectra analyses, suggesting similar origins for these factors. However, none of the used approach was able to fully identify the specific formation mechanisms and/or the gaseous precursors responsible for this SOA fraction (representing here about 25% of total OA in PM_{10}).

Finally, the development of a novel methodology to refine OA sources has also been proposed in this work. In this last step, PMF was performed using time synchronization with the multilinear engine (ME-2) algorithm on the combined dataset including OA mass spectra from ACSM measurements and specific primary and secondary organic molecular markers from PM_{10} filters on their original time resolution. By comparison to the PMF-ASCM results (4 OA factors), the use of combined dataset allowed the deconvolution of ten OA factors including 3 primary OA (POA) and 7 SOA (biogenic and anthropogenic SOA) factors including common factors such as primary traffic emissions (HOA), biomass burning (BBOA), oxidized primary OA (OPOA), an undefined SOA factor (SOA-5) as well as 2 specific biogenic- and 4 anthropogenic-SOA sources.

Two primary biomass burning factors (BBOA and OPOA) were resolved using this new approach and were further supported by their expected diurnal profiles with a pronounced peak at night-time, which is consistent with the main residential heating time. The results highlighted

more than 80% of the primary BBOA fraction was dominated by OPOA, referring the fact that the BBOA in the atmosphere is more like OPOA. The new methodology also allowed the clear identification of about half of the total SOA mass (75% of OA) observed during the sampling campaign performed at SIRTA in March 2015. Of that, 28% of the total SOC fraction seemed to be related to anthropogenic SOA (4 SOA factors) from combustion sources i.e., biomass burning and traffic emissions. Valuable insights into the formation and aging processes of secondary OA components compared to "conventional approaches" were finally obtained. For instance; anthropogenic SOA related to the oxidation of PAHs (characterized by nitro-PAHs), toluene, and phenolic compounds exhibited a clear diurnal pattern with high concentrations during the night indicating the promising role of night-time chemistry. The consistency of new methodology was also investigated by comparing the results with PMF ACSM analysis. The results showed a very good agreement for both, primary and secondary fractions.

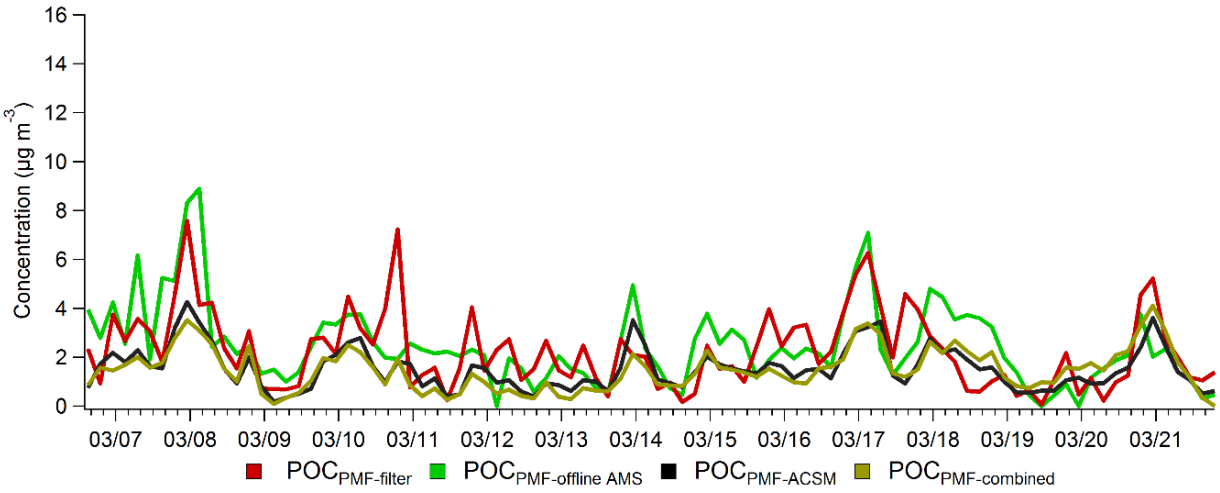

Figure VII.1. *Comparison of the total POC estimates obtained using different OA source apportionment approaches and measurements at Paris-SIRTA, France (March 2015).*

The newly developed OA apportionment methodology was also compared to different common used ones as mentioned before. The obtained results for POC estimates showed good agreement with other methodologies, almost similar to previous observations. However, filter

based POC estimations (PMF-filter and PMF-offline AMS) always exhibited higher concentration levels than the online approaches (Figure VII.1).

Finally, SOC estimates were also made to account the contribution from individual precursors using the SOA tracer method. $SOC_{SOA\ tracer}$ obtained in this study accounted for SOC formed by the photooxidation of α-pinene, isoprene, naphthalene, toluene and phenolic compounds. For the first time, attempts were made to account the contribution of anthropogenic SOA linked to biomass burning in the SOA tracer method using methylnitrocatechols, secondary photooxidation product of phenolic compounds (i.e., phenol, cresols, methoxyphenols…), mainly originating from biomass burning emissions (Bruns et al., 2016; Iinuma et al., 2010). However, all the methodologies for SOC estimates showed also a very good agreement including similar time evolutions and average concentrations throughout the sampling period except the $SOC_{SOA\ tracer}$ (Figure VII.2). These results were consistent with the observations reported in the literature comparing different SOC apportionment methodologies. Slight difference observed for the SOC estimates could be linked to the errors associated with the methodologies and measurements used.

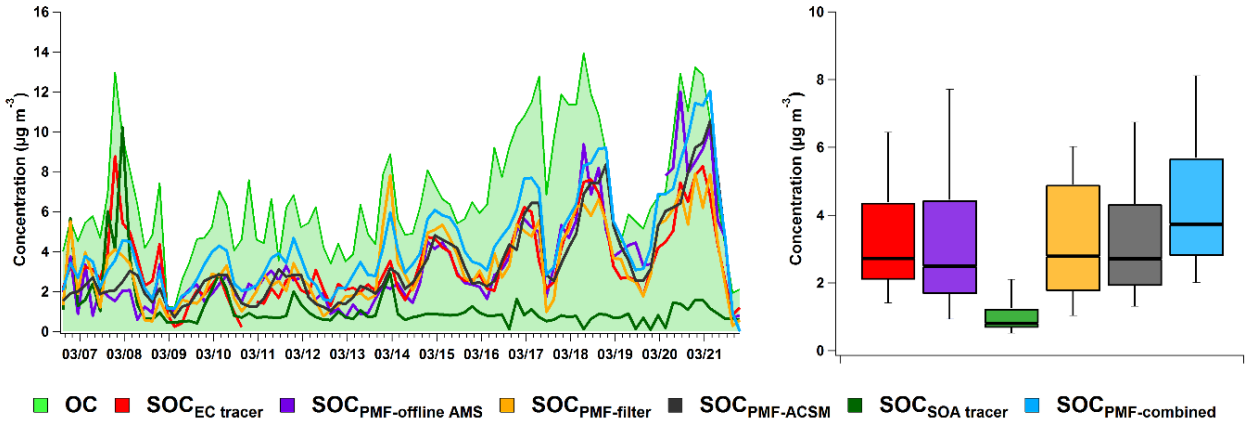

Figure VII.2. *Comparison of the SOC estimates obtained using different OA source apportionment approaches and measurements at Paris-SIRTA, France (March 2015).*

Attempts were also made to compare the more oxidized components obtained from the different OA apportionment methodologies used are presented on Figure VII.3. High concentrations of these factors were notably observed during the second half of the campaign. Along with the significance of inorganic loadings, a probable predominant long-range transport influence might be expected during this period (Srivastava et al., 2018a).

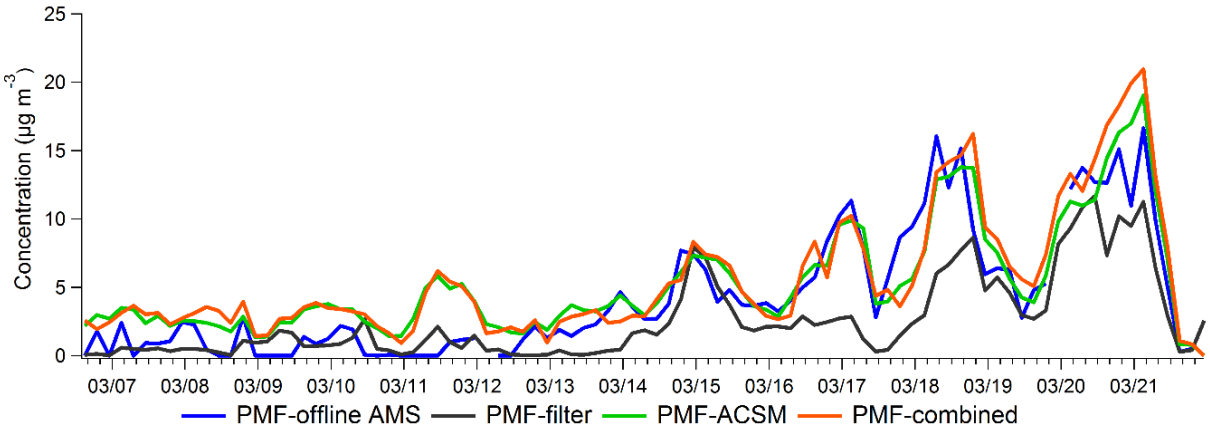

Figure VII.3. *Comparison of highly oxidized OA factors obtained from PMF-offline AMS (OOA1), PMF-ACSM (MO-OOA), the sum of the mixed secondary aerosol and marine biogenic SOA factors obtained from the PMF-filter analysis and the sum of the BSOA-1 (marine-rich) and SOA-5 SOA factors obtained from the PMF-combined analysis.*

However, the development of a proper link between the more oxidized components and the given sources are still difficult to achieve. This probably shows a clear identification of the more oxidized OOA is probably impossible as shown by its association only with quite ultimate oxidation end-products (MSA and oxalate).

Regarding the low oxidized component (LO-OOA) obtained from the different approaches, notably from the PMF offline AMS and ACSM analyses did not show any direct link with the given SOA sources. This highlights that the LO-OOA fraction does not stand for a single source, precursor or specific process. Further and more specifically-oriented studies would still

be needed to comprehensively describe the wide variety of low oxidized intermediate organic compounds in the atmosphere.

Overall, this PhD work has illustrated a better comprehension of OA sources and the complexity of the chemical processes involved, especially for secondary aerosols. More precisely, three major outcomes can be drawn from of this work:

- ✓ The use of molecular markers allow a better apportionment and discrimination of, primary or secondary anthropogenic and biogenic aerosol sources.
- ✓ Results obtained from different SOC apportionment methodologies are overall in a good agreement. However, some methods, such as EC-tracer method, show some limitations under certain conditions (season, source vicinity) and the SOA tracer method tends to underestimate the contribution of SOC to total OC. The use and comparison of different approaches are therefore to be preferred to apportion POC and SOC fractions and further validate the obtained OA fractions.
- ✓ The use of combined dataset (online (OA mass spectra) + offline measurements (organic molecular markers measured from the filter measurements)) in the PMF model provides a better discrimination and understanding of the OA sources and the chemical processes involved. This approach also offers the opportunity for a clear improvement of the conventional aerosol mass spectrometer-based source apportionment approach.

This PhD work thus demonstrates that combination of different approaches and/or measurements does enhance the understanding about the differences existing in POA and SOA contents.

Eventually, on the basis of my PhD work and related outcomes, the following prospects can be proposed for future studies:

- Further works are still needed to identify specific molecular markers (i.e. alkanes, alkenes, polycyclic aromatic compounds (PAHs), etc.) including markers for organosulfate and organonitrate formations, and in-cloud processing. The use of these markers into source receptor model (i.e., PMF) and the SOA tracer method could help to elucidate more information on OA origins (i.e., secondary inorganic sources).
    - Dedicated smog chamber/oxidant flow reactor experiments can be considered to investigate specific molecular markers based on precursors or emissions. The identification of specific markers or their chemical fingerprint can be achieved via non-target methods using liquid or gas chromatography coupled to HRMS (high-resolution mass spectrometry) (LC-HRMS, GC-HRMS).
    - The determination of SOA/SOC mass fraction from the smog chamber experiments for a given class of precursor could improve the SOC estimation.
    - Stability of organic markers is another big challenge. In general, the atmospheric lifetimes of SOA markers have been theoretically estimated based on their volatility. The exact values are just available for a few of them (e.g., cis-pinonic acid and 3-methyl-1, 2, 3-butanetricarboxylic acid). If some markers have a tendency to undergo a rapid decay in the atmosphere, yielding to a short lifetime, their use may cause a bias in the source apportionment model results. Therefore, smog chamber/ flow reactor experiments are needed to investigate the atmospheric lifetimes of SOA markers, at least those frequently used in source apportionment studies.
- The quantification of relevant molecular markers using advanced instrumentation such as TAG-AMS (thermal desorption aerosol gas chromatograph-AMS), EESI-TOF-MS

(extractive electrospray ionization-time of flight-MS), or different inlets associated to PTR-MS (proton-transfer reaction-MS) or CIMS (chemical ionization MS) such as FIGAERO (filter inlet for gases and aerosols), CHARON (chemical analysis of aerosol online) or thermo-desorption (TD) systems, and further combining them with PMF can enhance the understanding of atmospheric processes as well as their sources.

- There could be many ways to combine the different measurements. One has already been proposed during this PhD work. Another approach could combine some specific mass fragments with PM_{10} data matrix on long term dataset, allowing to help to identify some new factors based on seasonality.
- In the present scenario, processes like OPOA (significant fraction of primary biomass burning) are not included in the chemical transport models. The selected emission inventories are often issued from the measurement directly performed at the emission point. The implementation of SOA formation mechanisms for several anthropogenic and biogenic precursors and the use of advanced emission inventories including OPOA-related processes could improve the modelling of OA, especially for SOA sources. Comparing simulated concentrations to measurements or estimated ones obtained using different complementary methodologies could also facilitate to bridge the existing gap between atmospheric models and field measurements.

Annexes

Detailed list of peer-reviewed articles

Papers in Referred Journal

- **D. Srivastava**, S. Tomaz, O. Favez, G. M. Lanzafame, B. Golly, J.-L. Besombes, L. Y. Alleman, J.-L. Jaffrezo, V. Jacob, E. Perraudin, E. Villenave, A. Albinet. Speciation of organic fraction does matter for source apportionment. Part 1: one-year campaign in Grenoble (France). *Science of the Total Environment*, 624, 1598-1611, https://doi.org/10.1016/j.scitotenv.2017.12.135, **2018**.
- **D. Srivastava**, O. Favez, N. Bonnaire, F. Lucarelli, M. Haeffelin, E. Perraudin, V. Gros, E. Villenave, and A. Albinet. Speciation of organic fraction does matter for source apportionment. Part 2: Intensive short-term campaign in the Paris area (France). *Science of The Total Environment*, 634, 267-278, https://doi.org/10.1016/j.scitotenv.2018.03.296, **2018.**

Papers in preparation

- **D. Srivastava**, O. Favez. E. Perraudin, E. Villenave and A. Albinet. Comparison of methodologies based on measurement data to apportion Secondary Organic Carbon (SOC) in PM2.5: a review of recent studies, *to be submitted in Atmospheric Environment.*

- **D. Srivastava**, K. R. Daellenbach, Y. Zhang, N. Bonnaire, E. Perraudin, V. Gros, E. Villenave, A. S. H. Prévôt, I. El Haddad, O. Favez, A. Albinet. Comparison of different methodologies to discriminate primary and secondary organic aerosols, *to be submitted in Environmental Science & Technology*.

- **D. Srivastava**, O. Favez, J-E. Petit, Y. Zhang, U. M. Sofowote, P. K. Hopke, N. Bonnaire, E. Perraudin, V. Gros, E. Villenave, A. Albinet. *Combining off-line and on-line measurements does help differentiating between the different organic aerosols fractions, to be submitted in Atmospheric Chemistry & Physics*.

Communications

- **D. Srivastava**, O. Favez, J-E. Petit, Y. Zhang, U. M. Sofowote, P.K. Hopke, N. Bonnaire, E. Perraudin, V. Gros, E. Villenave, and A. Albinet. An Improved Approach to Resolve Sources of Organic Aerosol by Combining Offline and Online Measurements. *International Aerosol Research IAC, 2-7 September 2018, Saint Louis, Missouri, USA. Poster Presentation*.

- **D. Srivastava**, O. Favez, E. Perraudin, J.-L. Besombes, L. Y. Alleman, G.-M. Lanzafame, S. Tomaz, J.-L. Jaffrezo, B. Golly, N. Bonnaire, V. Gros, F. Lucarelli, E. Villenave, A. Albinet. Use of Specific Primary and Secondary Organic Markers for PM Source Apportionment Based on Positive Matrix Factorization (PMF). *International Aerosol Research IAC, 2-7 September 2018, Saint Louis, Missouri, USA. Poster Presentation*.

- G.M. Lanzafame, **D. Srivastava**, F. Couvidat, O. Favez, B. Bessagnet, and A. Albinet. One year comparison of SOA markers modelling and measurements: seasonality and gas/particle partitioning evaluation. *International Aerosol Research IAC, 2-7 September 2018, Saint Louis, Missouri, USA. Poster Presentation*.

- **D. Srivastava**, O. Favez, N. Bonnaire, E. Perraudin, V. Gros, F. Lucarelli, E. Villenave, and A. Albinet. Combinaison de mesures automatiques et manuelles pour l'étude des sources de l'aérosol organique. *French Aerosol Conference CFA, 30-31 January 2018, Paris, France. Oral Presentation.*

- **D. Srivastava**, O. Favez, E. Perraudin, J.-L. Besombes, L. Y. Alleman, G.-M. Lanzafame, S. Tomaz, J.-L. Jaffrezo, B. Golly, E. Villenave, A. Albinet. Demonstrating That Speciation of Organic Fraction Does Matter for Source Apportionment: Use of Specific Primary and Secondary Organic Markers. *American Aerosol Research AAAR, 16-20 October 2017, Raleigh, USA. Oral Presentation.*

- **D. Srivastava**, O. Favez, N. Bonnaire, E. Perraudin, V. Gros, F. Lucarelli, E. Villenave, and A. Albinet. Source Apportionment of Organic Aerosols in Paris (France) A synergic approach to perform source apportionment of organic aerosol using offline and online measurements in Positive Matrix Factorization. *American Aerosol Research AAAR, 16-20 October 2017, Raleigh, USA. Oral Presentation.*

- G.M. Lanzafame, **D. Srivastava**, N. Bonnaire, F. Couvidat, O. Favez, B. Bessagnet, and A. Albinet. Modelling of SOA markers: simulation through detailed mechanisms and validation by comparison with measurements. A new approach to understand SOA formation. *American Aerosol Research AAAR, 16-20 October 2017, Raleigh, USA. Oral Presentation.*

- A. Albinet**,** S. Tomaz, **D. Srivastava**, G.M. Lanzafame, O. Favez, J.-L. Jaffrezo, N. Bonnaire, V. Gros, L. Y. Alleman, F. Lucarelli, E. Perraudin, and E. Villenave. Understanding of the chemical processes involving nitro- and oxy-PAHs in ambient air and evaluation of SOA PAH contribution on PM via annual and intensive field campaigns. *American Aerosol Research AAAR, 16-20 October 2017, Raleigh, USA. Oral Presentation.*

- **D. Srivastava**, O. Favez, N. Bonnaire, E. Perraudin, V. Gros, F. Lucarelli, E. Villenave, and A. Albinet. A synergic approach to perform source apportionment of organic aerosol using offline and online measurements in Positive Matrix Factorization. *European Aerosol Conference EAC, 27 August-01 September 2017, Zurich, Switzerland. Oral Presentation.*

- **D. Srivastava**, O. Favez, N. Bonnaire, E. Perraudin, V. Gros, J.-L. Jaffrezo, Lucarelli, E. Villenave, and A. Albinet. Comparison of Secondary Organic Carbon (SOC) estimates made using indirect techniques in Paris (France). *European Aerosol Conference EAC, 27 August-01 September 2017, Zurich, Switzerland. Poster Presentation.*

- G. M. Lanzafame, **D. Srivastava**, N. Bonnaire, F. Couvidat, O. Favez, B. Bessagnet, and A. Albinet. Modelling of SOA markers: simulation through detailed mechanisms and validation by comparison with measurements. A new approach to understand SOA formation. *European Aerosol Conference EAC, 27 August-01 September 2017, Zurich, Switzerland.* Oral Presentation.

- A. Albinet**,** S. Tomaz, **D. Srivastava**, G.M. Lanzafame, O. Favez, J.-L. Jaffrezo, N. Bonnaire, V. Gros, L. Y. Alleman, F. Lucarelli, E. Perraudin, and E. Villenave. Understanding of the chemical processes involving nitro- and oxy-PAHs in ambient air and evaluation of SOA PAH contribution on PM via annual and intensive field campaigns**.** *European Aerosol Conference EAC, 27 August-01 September 2017, Zurich, Switzerland. Oral Presentation.*

- A. Albinet**,** S. Tomaz, **D. Srivastava**, G. M. Lanzafame, O. Favez, J.-L. Jaffrezo, N. Bonnaire, V. Gros, L. Y. Alleman, F. Lucarelli, E. Perraudin, and E. Villenave. Understanding of the

chemical processes involving nitro- and oxy-PAHs in ambient air and evaluation of SOA PAH contribution on PM via annual and intensive field campaigns. *International Conference on Chemistry and the Environment ICCE, 18-22 June 2017, Oslo, Norway.* *Oral Presentation.*

- **D. Srivastava**, O. Favez, N. Bonnaire, E. Perraudin, V. Gros, E. Villenave, and A. Albinet. Source Apportionment of Organic Aerosols in Paris (France) Using Offline-AMS Analysis and Validation of Factors Through the Use of External Markers. *American Aerosol Research AAAR, 17-21 October 2016, Portland, USA.* *Oral Presentation.*

- **D. Srivastava**, O. Favez, N. Bonnaire, E. Perraudin, V. Gros, E. Villenave, and A. Albinet. Investigation of primary and secondary processes in the formation of oxy-PAHs and nitro-PAHs in Paris (France) by conjoining on-line and off-line measurements. *American Aerosol Research AAAR, 17-21 October 2016, Portland, USA.* *Oral Presentation.*

- **D. Srivastava**, O. Favez, N. Bonnaire, E. Perraudin, V. Gros, E. Villenave, and A. Albinet. Secondary Organic Carbon (SOC) Estimation Using Several Indirect Techniques and the Evaluation of Their Uncertainties. *American Aerosol Research AAAR, 17-21 October 2016, Portland, USA. Poster Presentation.*

- **D. Srivastava**, O. Favez, N. Bonnaire, E. Perraudin, V. Gros, E. Villenave, and A. Albinet. Investigation of primary and secondary processes in the formation of oxy-PAHs and nitro-PAHs in Paris (France) by conjoining on-line and off-line measurements. *European Aerosol Conference EAC, 6-11 September 2016, Tours, France.* *Oral Presentation.*

- G. M. Lanzafame, **D. Srivastava**, F. Couvidat, O. Favez, B. Bessagnet and A. Albinet. Benefits of cross modelling and field measurement approaches on the evaluation of SOA distribution: a case study in Grenoble, France. *European Aerosol Conference EAC, 6-11 September 2016, Tours, France. Poster Presentation.*

- **D. Srivastava**, F. Masson, S. Ngo, A. Waked, J.-L. Jaffrezo, B. Golly, J.-C. Francony, J.-L. Besombes, L. Y. Alleman, C. Chabanis, E. Moussu, C. Bret, S. Tomaz, E. Perraudin, E. Villenave, N. Bocquet, R. Aujay, N. Nuttens, N. Guillaumet, O. Favez, and A. Albinet. PM source apportionment by Positive Matrix Factorization (PMF) using an extended aerosol chemical characterization including specific molecular markers. *European Aerosol Conference EAC, 6-11 September 2015, Milan, Italy. Poster Presentation.*

Abstract

Organic aerosols (OAs), originating from a wide variety of sources and atmospheric processes, have strong impacts on air quality and climate change. The present PhD thesis aimed to get a better understanding of OA origins using specific organic molecular markers together with their input into source-receptor model such as positive matrix factorization (PMF). This experimental work was based on two field campaigns, conducted in Grenoble (urban site) over the 2013 year and in the Paris region (suburban site of SIRTA, 25 km southwest of Paris) during an intense PM pollution event in March 2015. Following an extended chemical characterization (from 139 to 216 species quantified), the use of key primary and secondary organic molecular markers within the standard filter-based PMF model allowed to deconvolve 9 and 11 PM_{10} sources (Grenoble and SIRTA, respectively). These included common ones (biomass burning, traffic, dust, sea salt, secondary inorganics and nitrate), as well as uncommon resolved sources such as primary biogenic OA (fungal spores and plant debris), biogenic secondary AO (SOA) (marine, isoprene oxidation) and anthropogenic SOA (polycyclic aromatic hydrocarbons (PAHs) and/or phenolic compounds oxidation). In addition, high time-resolution filter dataset (4h-timebase) available for the Paris region also illustrated a better understanding of the diurnal profiles and the involved chemical processes. These results could be compared to outputs from other measurement techniques (online ACSM (aerosol chemical speciation monitor), offline AMS (aerosol mass spectrometer) analyses), and/or to other data treatment methodologies (EC (elemental carbon) tracer method and SOA tracer method). A good agreement was obtained between all the methods in terms of separation between primary and secondary OA fractions. Nevertheless, and whatever the method used, still about half of the SOA mass was not fully described. Therefore, a novel OA source apportionment approach has finally been developed by combining online (ACSM) and offline (organic molecular markers) measurements and using a time synchronization script. This combined PMF analysis was performed on the unified matrix. It revealed 10 OA factors, including 4 different biomass burning-related chemical profiles. Compared to conventional approaches, this new methodology provided a more comprehensive description of the atmospheric processes related to the different OA sources.

Résumé

Les aérosols organiques (AO), issus de nombreuses sources et de différents processus atmosphériques, ont un impact significatif sur la qualité de l'air et le changement climatique. L'objectif de ce travail de thèse était d'acquérir une meilleure connaissance de l'origine des AO par l'utilisation de marqueurs organiques moléculaires au sein de modèles source-récepteur de type *positive matrix factorization* (PMF). Ce travail expérimental était basé sur deux campagnes de prélèvements réalisées à Grenoble (site urbain) au cours de l'année 2013 et dans la région parisienne (site péri-urbain du SIRTA, 25 km au sud-ouest de Paris) lors d'un intense épisode de pollution aux particules (PM) en Mars 2015. Une caractérisation chimique étendue (de 139 à 216 espèces quantifiées) a été réalisée et l'utilisation de marqueurs moléculaires primaires et secondaires clés dans la PMF a permis de déconvoluer de 9 à 11 sources différentes de PM_{10} (Grenoble et SIRTA, de façon respective) incluant aussi bien des sources classiques (combustion de biomasse, trafic, poussières, sels de mer, nitrate et espèces inorganiques secondaires) que des sources non communément résolues telles que AO biogéniques primaires (spores fongiques et débris de plantes), AO secondaires (AOS) biogéniques (marin, oxydation de l'isoprène) et AOS anthropiques (oxydation des hydrocarbures aromatiques polycycliques (HAP) et/ou des composés phénoliques). En outre, le jeu de données obtenu pour la région parisienne à partir de prélèvements sur des pas de temps courts (4h) a permis d'obtenir une meilleure compréhension des profils diurnes et des processus chimiques impliquées. Ces résultats ont été comparés à ceux issus d'autres techniques de mesures (en temps réel, ACSM (aerosol chemical speciation monitor) et analyse AMS (aerosol mass spectrometer) en différée) et/ou d'autres méthodes de traitement de données (méthodes traceur EC (elemental carbon) et traceur AOS). Un bon accord a été obtenu entre toutes les méthodes en termes de séparation des fractions primaires et secondaires. Cependant, et quelle que soit l'approche utilisée, la moitié de la masse d'AOS n'était toujours pas complètement décrite. Ainsi, une nouvelle approche d'étude des sources de l'AO a été développée en combinant les mesures en temps réel (ACSM) et celles sur filtres (marqueurs moléculaires organiques) et en utilisant un script de synchronisation des données. L'analyse PMF combinée a été réalisée sur la matrice de données unifiée. 10 facteurs AO, incluant 4 profils chimiques différents en lien avec la combustion de biomasse, ont été mis en évidence. Par rapport aux approches conventionnelles, cette nouvelle méthodologie a permis d'obtenir une meilleure compréhension des processus atmosphériques liés aux différentes sources d'AO.